

Advances in Experimental Medicine and Biology 1236

Aimin Liu *Editor*

Animal Models of Human Birth Defects

 Springer

Advances in Experimental Medicine and Biology

Volume 1236

Series Editors

Wim E. Crusio, Institut de Neurosciences Cognitives et Intégratives d'Aquitaine,
CNRS and University of Bordeaux UMR 5287, Pessac Cedex, France

Heinfried H. Radeke, Institute of Pharmacology & Toxicology, Clinic of the
Goethe University Frankfurt Main, Frankfurt am Main, Germany

Nima Rezaei, Research Center for Immunodeficiencies, Children's Medical
Center, Tehran University of Medical Sciences, Tehran, Iran

Advances in Experimental Medicine and Biology provides a platform for scientific contributions in the main disciplines of the biomedicine and the life sciences. This series publishes thematic volumes on contemporary research in the areas of microbiology, immunology, neurosciences, biochemistry, biomedical engineering, genetics, physiology, and cancer research. Covering emerging topics and techniques in basic and clinical science, it brings together clinicians and researchers from various fields.

Advances in Experimental Medicine and Biology has been publishing exceptional works in the field for over 40 years, and is indexed in SCOPUS, Medline (PubMed), Journal Citation Reports/Science Edition, Science Citation Index Expanded (SciSearch, Web of Science), EMBASE, BIOSIS, Reaxys, EMBiology, the Chemical Abstracts Service (CAS), and Pathway Studio.

2018 Impact Factor: 2.126.

More information about this series at <http://www.springer.com/series/5584>

Aimin Liu
Editor

Animal Models of Human Birth Defects

 Springer

Editor

Aimin Liu

Department of Biology, Eberly College of Science and

Huck Institute of Life Sciences

The Pennsylvania State University

University Park, PA, USA

ISSN 0065-2598

ISSN 2214-8019 (electronic)

Advances in Experimental Medicine and Biology

ISBN 978-981-15-2388-5

ISBN 978-981-15-2389-2 (eBook)

<https://doi.org/10.1007/978-981-15-2389-2>

© Springer Nature Singapore Pte Ltd. 2020

This work is subject to copyright. All rights are reserved by the Publisher, whether the whole or part of the material is concerned, specifically the rights of translation, reprinting, reuse of illustrations, recitation, broadcasting, reproduction on microfilms or in any other physical way, and transmission or information storage and retrieval, electronic adaptation, computer software, or by similar or dissimilar methodology now known or hereafter developed.

The use of general descriptive names, registered names, trademarks, service marks, etc. in this publication does not imply, even in the absence of a specific statement, that such names are exempt from the relevant protective laws and regulations and therefore free for general use.

The publisher, the authors, and the editors are safe to assume that the advice and information in this book are believed to be true and accurate at the date of publication. Neither the publisher nor the authors or the editors give a warranty, expressed or implied, with respect to the material contained herein or for any errors or omissions that may have been made. The publisher remains neutral with regard to jurisdictional claims in published maps and institutional affiliations.

This Springer imprint is published by the registered company Springer Nature Singapore Pte Ltd. The registered company address is: 152 Beach Road, #21-01/04 Gateway East, Singapore 189721, Singapore

Preface

About one in every 33 babies in the United States is born with structural birth defects, according to the Center for Disease Control and Prevention. One or more organs do not form properly in these babies, leading to disfiguring and/or inconvenience in mild cases, and debilitating disability in severe cases. In addition to structural birth defects, about one in every 1000 babies is born with defects in metabolism. In severe cases, these metabolic defects lead to neurological problems and cause damages to other tissues as well. Although surgery and medication can fully or partially correct the defects in some cases, most birth defects cannot be fully corrected, leaving the patients and their families in great pain and burden. Therefore, understanding the cause of human birth defects, prevention, early detection, and intervention are the keys to reducing the occurrence and ameliorating the impact of birth defects.

As many experimental studies cannot be performed on human fetuses, we have been relying on animal models to understand the developmental mechanisms and pathogenesis of birth defects. In the early days, embryologists performed surgical manipulations using amphibians (frogs, newts, etc.) and fowls (chicken and quail) to reveal cell lineages and inductive events. Various model animals exposed to environmental insults such as alcohol and other toxic chemicals were used to study their effects on embryonic development and the potential in inducing birth defects. The advent of recombinant DNA and systematic genetic screening methods allowed an explosion of knowledge in the functions of individual genes in animal development in the late 1980s and the decades that followed. Gene-targeting and genome engineering techniques allowed production of precise models of human diseases in a variety of model systems ranging from nematodes, fruit flies to mice and even primates.

In recent years, organoids, three-dimensional miniature cellular structures mimicking internal organs have been derived from human stem cells. Useful information has been gleaned from the study of these organoids. However, these will be great supplement, but not replacement for animal model research. First, the protocols for deriving the organoids are based on our limited understanding of the organogenesis in model animals, and they are still far from becoming the true replica of the organs themselves. Second, the isolated organoids in culture lack the complexity of bodily environment which contribute greatly to phenotypical expression. Finally, potential ethical concerns may prevent us from producing and analyzing more sophisticated brain organoids or producing early embryos from man-made germ cells.

Therefore, animal models will continue to play a central role in our understanding of birth defects in the foreseeable future.

The goal of this book is to give the readers an opportunity to learn about the current status of research related to human birth defects in various tissue systems. The intended readers include senior undergraduate students of biology major who are considering a clinical or research career, or would like to extend their knowledge from the basic developmental biology or genetics courses. Starting graduate students and postdocs may also find their passion in birth defects research using animal models by reading this book. In addition, this book can also be a good start point for researchers who plan to start a project in an unfamiliar organ system, before plunging into a sea of specialized reviews and original literature.

In this book, experts actively working on the developmental mechanisms of the neural tube, heart, craniofacial structures, skeleton, digestive tract, kidney, and endocrine pancreas review the use of animal models in understanding human birth defects affecting the various organ systems. Each chapter starts with a brief introduction of the anatomy and development of the relevant organ system to familiarize readers with the biology before delving into specific examples of human birth defects and the current progress in animal model development and analyses. Therefore, readers do not need to have prior knowledge of the organ system in order to appreciate the use of animal models in the study of human birth defects affecting that system.

The last chapter focuses on the application of animal models in the study and treatment of various congenital metabolic disorders. Three examples are carefully chosen for in-depth discussion to show how conventional genetic models and sometimes serendipitously obtained models advance our understanding of these metabolic disorders.

As genetic methods employed in animal model research have become increasingly sophisticated, it may be challenging for readers of non-genetics major to fully appreciate the genetic approaches utilized in animal research. To help readers to overcome this challenge, Dr. Maria Garcia-Garcia describes in chapter one the various genetics tools and corresponding terminology frequently mentioned in the rest of the book. The chapter is also a fascinating review of the history of the house mouse as the most popular model species, thus even readers familiar with the technology may find the historical aspect of the chapter appealing.

We would like to thank Dr. Juhee Jeong of New York University College of Dentistry, Dr. Sangeeta Dhawan of Diabetes and Metabolism Research Institute, City of Hope, Dr. Paul Gadue of Children's Hospital of Philadelphia, Dr. Robert Maxson of Keck School of Medicine of USC, Dr. Megan Davey of the Roslin Institute, Dr. Nathalia Holtzman of Queens College, and Dr. Andrey Guillaume of University of Geneva Medical School, for volunteering their precious time to read the manuscripts and provide helpful feedback.

Contents

1 A History of Mouse Genetics: From Fancy Mice to Mutations in Every Gene	1
María J García-García	
2 Mouse Models of Neural Tube Defects	39
Irene E. Zohn	
3 Animal Models of Pancreas Development, Developmental Disorders, and Disease	65
David S. Lorberbaum, Fiona M. Docherty, and Lori Sussel	
4 Animal Models of Congenital Gastrointestinal Maladies	87
Ryan J. Smith, Roshane Francis, Ji-Eun Kim, and Tae-Hee Kim	
5 Mouse Models of Congenital Kidney Anomalies	109
Satu Kuure and Hannu Sariola	
6 What Do Animal Models Teach Us About Congenital Craniofacial Defects?	137
Beatriz A. Ibarra and Radhika Atit	
7 Animal Models for Understanding Human Skeletal Defects	157
Isabella Skuplik and John Cobb	
8 Using Zebrafish to Analyze the Genetic and Environmental Etiologies of Congenital Heart Defects	189
Rabina Shrestha, Jaret Lieberth, Savanna Tillman, Joseph Natalizio, and Joshua Bloomekatz	
9 Animal Model Contributions to Congenital Metabolic Disease	225
Corinna A. Moro and Wendy Hanna-Rose	



A History of Mouse Genetics: From Fancy Mice to Mutations in Every Gene

1

María J García-García

1.1 Overview

The laboratory mouse has become the model organism of choice in numerous areas of biological and biomedical research, including the study of congenital birth defects. The appeal of mice for these experimental studies stems from the similarities between the physiology, anatomy, and reproduction of these small mammals with our own, but it is also based on a number of practical reasons: mice are easy to maintain in a laboratory environment, are incredibly prolific, and have a relatively short reproductive cycle. Another compelling reason for choosing mice as research subjects is the number of tools and resources that have been developed after more than a century of working with these small rodents in laboratory environments. As will become obvious from the reading of the different chapters in this book, research in mice has already helped uncover many of the genes and processes responsible for congenital birth malformations and human diseases. In this chapter, we will provide an overview of the methods, scientific advances, and serendipitous circumstances that

have made these discoveries possible, with a special emphasis on how the use of genetics has propelled scientific progress in mouse research and paved the way for future discoveries.

1.2 Establishing the Mouse as a Mammalian Model for Research

Mice have accompanied humans since the early days of agriculture. Therefore, it is no surprise that people developed curiosity about these small mammals and even fancied them as pets [1]. Ancient Chinese and Japanese records report the domestication and breeding of many varieties of mice with different coat colors, like *albino* or *yellow*, and peculiar behaviors, such as those of “waltzing mice,” which tend to run around in circles due to mutations that affect the inner ear [2]. During the 1800s and well into the early twentieth century, these “fancy” mice gained popularity among Europeans and Americans, who imported them and set up breeding programs, showing their most fancy specimens at mouse shows and clubs. As fortune would have it, one of these “mouse fanciers,” Miss Abbie E. C. Lathrop, a retired school teacher who set up a mouse pet farm around 1900, played an important role in the establishment of mice as a model organism for research experimentation [1].

M. J. García-García (✉)
Molecular Biology and Genetics Department, Cornell
University, Ithaca, NY, USA
e-mail: garciamj@cornell.edu

1.2.1 Mendelian Genetics in Mice

The first reports of mice being used for research purposes date back to the sixteenth century, when Robert Hooke analyzed the effects of increased air pressure on mice [3]. However, it would not be until the beginning of the twentieth century that scientists unleashed the power of mouse genetics by demonstrating that Mendel's laws of inheritance are also applicable to these small mammals. In 1902, French biologist Lucien Cuénot was the first to report the use of *albino* coat-color mice to confirm Mendel's laws of inheritance. This report was quickly followed by work from additional scientists, who confirmed and extended these findings to other genetic mouse traits [2]. It would be one of these scientists, American William E. Castle, who would become recognized as the father of mammalian genetics, a merit based on his multiple research contributions, as well as his influential role as the director of the Bussey Institute of Experimental Biology at Harvard from 1909 until 1937, where many prominent scientists trained and worked under his supervision, including Clarence C. Little, Sewal Wright, Leonel Strong, George D. Snell, and Leslie C. Dunn, to name a few [4].

Miss Abbie Lathrop's mice farm, located in Granby, Massachusetts, played a critical role during these first years of research on mouse genetics. At her farm, Miss Lathrop bred several colonies of mice, either collected from the wild or imported from European "mouse fanciers," with the intention of selling them as pets. However, she unexpectedly became the supplier of mice for the Bussey Institute, as well as a few other research institutions. Many of the mice currently used in laboratories worldwide can be traced to the colonies initially established by Abbie Lathrop. However, Lathrop's contributions were not limited to being a mouse provider. She was a meticulous breeder and a perceptive observer of her mice, as attested by her careful breeding records and the multiple research papers she contributed to.

1.2.2 Inbred Mouse Strains

While the birth of mouse genetics was linked to the rediscovery of Mendel's laws, it was research on cancer that dominated during the following five decades. Through her careful breeding, Abbie Lathrop had noticed that some of her mice colonies had a propensity to develop skin lesions. In an effort to diagnose these, she sent mice to Dr. Leo Loeb, an experimental pathologist at the University of Pennsylvania, who concluded that Lathrop's mice were developing cancers [5]. This interaction marked the beginning of their collaboration, which rendered several important publications on cancer susceptibility of different mouse strains. Meanwhile, other investigators were experimenting with transplanting tumors in mice and grappling with the idea of whether cancer susceptibility was a heritable Mendelian trait. Support for this hypothesis came from early observations that tumors could be transplanted among waltzing mice, but failed to grow if transplanted onto mice of a different colony. Starting in 1909 and all the way into the 1920s, critical papers from Ernest E. Tyzzer, Leo Loeb, Maude Slye, and Halsey Bagg supported the heritability of cancer susceptibility. However, these investigators found so much variability in their data that they had problems verifying their own observations or concluding whether cancer susceptibility was a dominant or a recessive trait. Around 1909, Clarence C. Little and Leonell C. Strong postulated that the culprit of such variability was the inherent genetic heterogeneity of the mouse strains that were being used for experimentation. To solve this problem, they launched intensive breeding programs to achieve isogenic mouse strains [5]. Their thought was that by systematically performing brother-to-sister matings for more than 20 generations, the genetic constitution of the resulting mice will become homogeneous and stable (isogenic), making them ideal for research subjects (Fig. 1.1). This idea was received with great skepticism in the scientific community since inbreeding was known to be

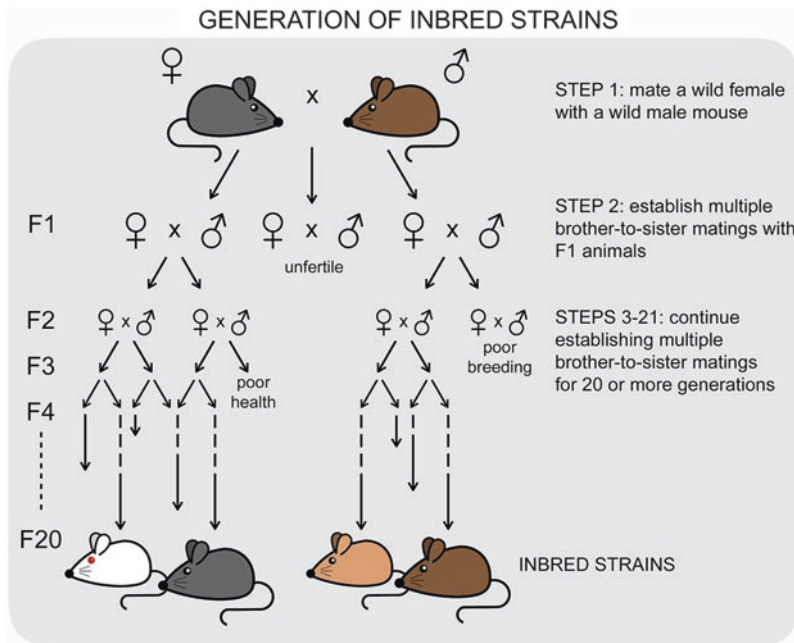


Fig. 1.1 *Inbred mouse strains.* Inbred mice are generated by crossing two wild mice, then systematically performing sister-to-brother matings for more than 20 generations. As breeding proceeds and alleles segregate, individual traits eventually reach homozygosity. Homozygosity for some traits can affect the fertility or viability of mice, compromising further breeding. In other cases, homozygosity pro-

duces distinct visible phenotypes, such as different coat colors. Selection of healthy breeders with specific characteristics is performed in each generation in order to render different isogenic mouse strains that can be easily maintained in research facilities. The genome of inbred mice is 98% identical to that of their siblings by 20 generations and 99.5% identical at 40 generations

evolutionarily discouraged, and it was feared that, as recessive factors present in wild mice populations reached homozygosity, a “sterility barrier” would be encountered. However, Little and Strong thought that it would be possible to bypass this “sterility barrier” by keeping multiple independent crosses for each generation and selecting those that did not carry factors detrimental to vigor, reproduction, or susceptibility to diseases. Years of breeding would be needed for these and a few other investigators to reach their goals and establish several viable lines of isogenic mice. Their journeys were not exempt from unexpected challenges, such as disease outbreaks and accidents, including one that decimated 80% of the ongoing crosses due to the escape of stove gases into one of the “mouse coops” [5]. The resulting colonies became known as **inbred mouse strains** and constitute the first innovation in the field of mouse genetic research. The first inbred strain, called DBA (which carries three

color-coat alleles for *dilute*, *brown*, and *non-agouti*), was established by Clarence C. Little, but many others followed. Today, there are more than 450 available inbred strains, whose genealogies can be found in the following review [6].

1.3 Getting to Know the Mouse Genome: From Inbred Lines to Genetic Maps

The establishment of inbred strains provided standardized, genetically uniform strains of mice to be used in the study of cancer. Additionally, the large breeding programs required for their generation had important ripples in the field of mouse genetics. As different inbred strains became available during the 1920s and 1930s, it was obvious that they differed in a variety of characteristics, not only cancer susceptibility, but also coat color, behavior, longevity, and many

others. At that time, it was clear that these differences were likely due to either the separation of different allele variants present in the original populations of wild mice used to generate inbred strains or to spontaneous mutations arising during breeding. The **chromosome theory of inheritance**, proposed by Walter Sutton in 1902, and the term **gene**, coined by Wilhelm Johannsen in 1909, provided a framework for understanding that the different alleles of inbred strains correlated with physical entities in chromosomes. However, it would not be until the mid-1940s that the nature of nucleic acids as carriers of genetic information would be recognized. As a consequence, during most of the first half of the twentieth century, genes were just viewed as alleles that segregated in specific ways during breeding, causing dominant or recessive phenotypes.

1.3.1 Inbred and Congenic Strains

At a time when tools to analyze the mouse genome were scarce, early mouse geneticists focused on using inbred strains to identify different alleles responsible for particular traits and follow their segregation through breeding. With the objective of applying this genetics methodology to the study of cancer in mice, Clarence C. Little founded in 1929 the Roscoe B. Jackson Memorial Laboratories in Bar Harbor, Maine. This institution would become an important center for mouse genetics, both as a research organization and, later, as a supply center for mice strains to other institutions [7]. During the first few years, research at the Jackson Labs focused on the identification of alleles that could explain the ability of inbred strains to accept or reject transplanted tumors. For this, animals from two inbred strains with different ability for accepting transplanted tumors were crossed with each other, then the resulting progeny (from F1, F2, F3, and subsequent generations) were analyzed for the inheritance of resistance to tumor transplant. By applying this, so-called **outcross-intercross method** at Jackson Labs, Clarence Little and Leonel Strong were able to deduce that transplant rejection was controlled by multiple loci, which were called *histocompatibility (H)*

loci. However, it was not until 1948 that George Snell could isolate independent alleles responsible for tumor rejection. To isolate different *histocompatibility* loci, Snell applied a new breeding scheme known as the “**outcross-backcross-intercross method**,” which entailed breeding mice from two inbred strains, one of which (recipient strain) rejected tumors from the other one (donor strain), followed by mating the F1 hybrid progeny to animals from the parental inbred donor strain, then continue backcrossing to the donor strain individuals selected from the G2, G3, G4, and subsequent generations for their ability to carry the allele causing tumor rejection (Fig. 1.2). This selection of carriers often required brother–sister intercrosses since many of the alleles for cancer rejection behaved in a recessive fashion. Snell calculated that, by backcrossing selected carriers for more than ten generations, the genome of the resulting mice will mostly originate from the donor strain, except for a small chromosomal segment containing the loci responsible for the tumor rejection phenotype [8]. Strains produced through this method, later called **congenic strains**, represent an important method for the identification of specific genetic loci [1]. Snell’s congenic strains carrying alleles for tumor rejection turned out to be critical for the analysis of the *H2 histocompatibility complex*, a work that granted him the Nobel Prize in 1980.

1.3.2 The Origins of Developmental Genetics

In 1927, Nelly Dobrovolskaia-Zavadskaia, a cancer research scientist working at the Pasteur Institute in Paris, discovered a dominant mutation in the course of an X-ray mutagenesis screen that caused animals to develop a short tail [9]. This mutation, called *Brachyury* or *T*, became one of the first developmental mutations studied in mammals. Initially, however, the interest in this mutation focused not on understanding embryology, but rather on unraveling the puzzling genetic behavior of the *T* locus, which presented several violations of Mendel’s laws. The first of these violations was an abnormal proportion of mice with short tails in the progeny of heterozygote *T*

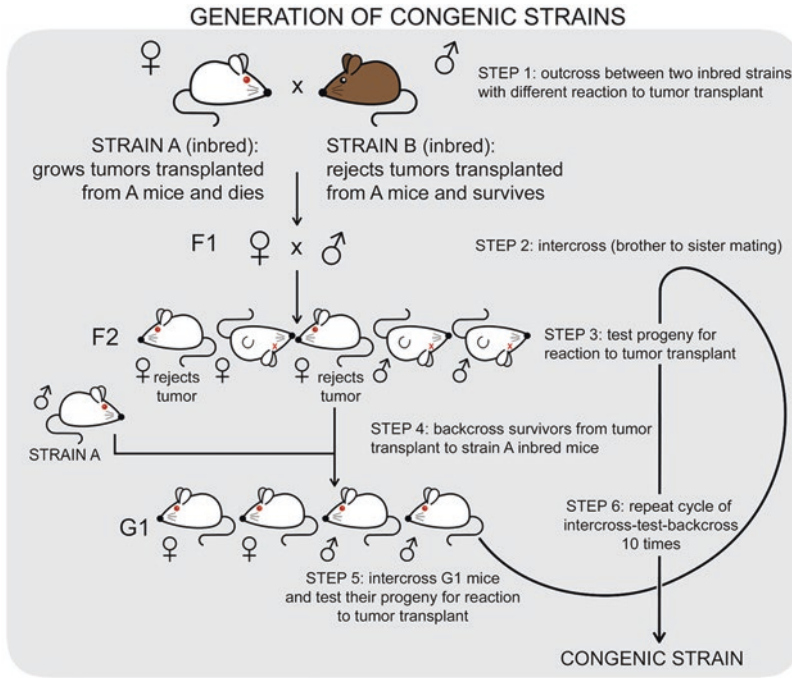


Fig. 1.2 *Congenic mouse strains.* The outcross-intercross-backcross method allows the genetic isolation and propagation of an individual genetic element responsible for a selectable trait. This method was first used by George Snell to isolate loci responsible for the rejection to tumor transplant. By backcrossing selected mice carrying the allele for tumor rejection for ten or more generations to inbred mice that lack this allele (strain A), the genome

of the resulting congenic strain originates mostly from strain A, except for a small chromosomal segment that contains the locus responsible for tumor rejection (which originated from strain B). Note that the breeding scheme in the illustration applies to the generation of congenic strains for recessive traits. For dominant traits, intercrosses are not required since selection for tumor rejection can be done directly in the progeny of each backcross

animals, a phenomenon due to the fact that homozygote *T/T* animals died in utero shortly after gastrulation. However, many other mysteries surrounded the *T* locus, including the findings that some *T* chromosomes showed puzzling genetic interactions with alleles from wild mice, could suppress recombination, and caused transmission ratio distortion in males (reviewed in [10]). The study of these anomalies revealed that the genetic behaviors of the *T* locus were in fact due to several linked loci that became known as the *t-complex*, an area later discovered to span the third distal part of chromosome 17, containing more than 500 genes. Additionally, it was found that certain allelic combinations (haplotypes) of the *t-complex* contained embryonic lethal mutations, small inversions (which were responsible for the suppressed recombination), and alleles causing male sterility (which explained the transmission ratio distortion). Sorting out these mysteries took

more than 70 years of research and the work of numerous investigators, including Leslie C. Dunn, Salome Glueckshon-Schoenheimer, Mary Lyon, Dorothea Bennett, Lee Silver and Karen Artz, to name a few. Because of the numerous embryonic lethal mutations at the *t-complex*, understanding the intricacies of this locus inspired the study of embryonic development, contributing to the identification and characterization of many mutations that disrupted development at different embryonic stages [11].

1.3.3 Linkage Analysis, Complementation Tests, and Recombination Maps

Through experiments with flies, Thomas Morgan had shown that the segregation of certain alleles violated Mendel's laws of independent assortment

and that the basis for this phenomenon was the location of cosegregating alleles in the same chromosome [12]. This principle, called **genetic linkage**, was first demonstrated in mice by John B. S. Haldane using *albino* and *pink-eyed dilution* fancy mice to show that alleles for these two loci segregated together [13]. Early mouse geneticists soon adopted linkage as a convenient tool for tracking loci of interest in inbred and congenic strains. Linkage was useful because, if dominant alleles with visible phenotypes were found linked to alleles that would otherwise only be detectable with the help of time-consuming tests, linked alleles could be used as visible markers in breeding schemes, enormously facilitating the maintenance and analysis of “invisible” interesting alleles (Fig. 1.3). The convenience of using linkage as a tool prompted the generation of inbred strains that contained different “marker” traits, such as different coat colors (albino, brown, pink-eyed dilution) or other morphological characters (i.e., the short tail of *T* mice and the kinked tail of *Fused* mice). Inbred strains simultaneously containing several of these markers, called “**linkage testing stocks**,” were especially useful, since they allowed to establish whether or not a new phenotype was linked to one of different markers in the course of a single cross strategy [14].

As more allele variants were discovered in different inbred strains, it became important to discern whether some of the observed phenotypes were controlled by the same or through different loci. For recessive alleles, this was done by crossing two mice, each heterozygote for one of the alleles to be tested, then inquiring whether the progeny showed the recessive phenotype, a breeding strategy known as **complementation test** (Fig. 1.4).

Although early mouse geneticists could not pinpoint where their alleles were exactly located within chromosomes in physical or molecular terms, linkage analysis allowed them to map their position in relationship with other known alleles. This strategy was previously exploited by fly geneticists in the early twentieth century for the generation of what became known as **recombination maps or linkage maps**. Linkage maps

relied on the facts that any two loci in close proximity within a chromosome will have a tendency to segregate together and that recombination between these loci, due to crossovers during the generation of gametes, can be used as an index of the distance between them (Fig. 1.3; [15]). In mice, recombination mapping efforts were initially limited to alleles that were interesting as based on their relevance to human disease. As a consequence, linkage maps grew very slowly. By 1941, the first edition of the *Biology of the Laboratory Mouse*, a text of reference for mouse investigators at the time [16], listed 24 independent loci, 15 of which were mapped to 7 different linkage groups. The progress of linkage maps has been captured in the regular publication of the *Mouse News Letter* (MNL), a free biannual bulletin that ran between 1949 and 1991 and was used by geneticists to report new mutants, inbred strains, as well as updates of the “*Mouse Linkage Map*.” Leslie C. Dunn, Salome Gluecksohn-Waelsch, Margaret Green, and Mary Lyon were among the first editors of the newsletter, which constituted the first “journal” on mammalian genetics until *Mouse Genome* was created [5, 10, 17]. A historical event marking the progress of linkage analysis took place in 1958 at the Tenth Congress of Genetics in Montreal, where the staff of the Jackson Laboratory put together a Live Linkage Map of the Mouse, with live mice from about 60 different strains, each in a small cage, showcased onto 18 lines that represented different linkage groups. While the exhibit proudly displayed the achievements of the scientific community at the time, it is worth mentioning that linkage groups were listed in the order in which they were discovered, since it was not yet possible to assign these groups to any chromosomal location.

1.3.4 Cytogenetics: Chromosomal Maps and Rearrangements

Around the 1920s, the use of dyes such as orcein, Giemsa, or Feulgen was used to karyotype animals of different species and determine differences in their genome organization. Using these

dyes, Theophilus S. Painter was the first one to determine that house mice contain 20 chromosome pairs (19 autosomes, plus the X and Y sex chromosomes) [18]. Proper identification of mouse chromosomes was initially challenging due to the facts that early staining protocols revealed uniformly stained chromosomes, and that all mouse chromosomes were found to be telocentric. However, advances in cytogenetics during the 1960s and 1970s led to the development of alternative staining protocols called Q, G, R, or C **banding methods**. In these new protocols, samples were subject to chromatin denaturation and/or a mild enzymatic digestion prior to staining with a DNA-binding dye. These treatments affected chromatin differently, depending on its composition and/or structure and, as a result, the dyes revealed reproducible patterns of high- and low-intensity bands that were unique to each chromosome. In this way, banding methods allowed the identification of individual chromosomes and the generation of detailed **cytogenetic or chromosomal maps** of the mouse genome [1, 5].

As different laboratory and wild mouse strains were analyzed with banding methods, differences among strains were detected in the form of chromosomal translocations, deletions, duplications, and inversions. By analyzing the banding patterns of these chromosomal rearrangements, and especially those that disrupted known loci and/or linkage relationships, investigators could determine the chromosomal location of genes. For instance, by using Q and G banding on a deletion involving the *albino* locus, it was possible to

determine its location to chromosome 7 [19]. Using this strategy, linkage groups previously identified through recombination mapping could finally be assigned to specific chromosomes, an achievement that was reflected for the first time in the 1975 issue of the Mouse News Letter [20]. By 1980, all linkage groups had been assigned to physical chromosomes (reviewed in [21]).

1.3.5 Improving Linkage Maps: New Markers, Recombinant Inbred Lines, and Interspecific Backcrosses

Because linkage maps depend on the recombination between alleles that can serve as markers, the resolution of these maps depends on two factors: the number of markers available and the number of crossover events that can be analyzed. Efforts to address these limiting factors and produce a comprehensive map of the mouse genome spanned most of the second half of the twentieth century.

Initially, linkage analysis could only be performed using a limited number of **morphological markers**, allele variants with phenotypes that could be directly observed in animals, such as coat-color variants (Fig. 1.5, top-left panel). However, advances in molecular biology allowed the development of two additional types of markers: biochemical polymorphisms and DNA polymorphisms. **Biochemical markers** became available during the 1940s and 1950s, when it was discovered that protein extracts from different inbred strains sometimes showed differences

Fig. 1.3 (continued) independent of each other, generating four types of gametes that, when randomly combined during fertilization, give rise to four different phenotypes in the F2 progeny at the indicated 9:3:3:1 ratios. Genes located on the same chromosome do not obey Mendel's law of independent assortment and, instead, segregate together in gametes (lower panel, left). In the example, the genes *H-2* and *Fused (Fu)* are genetically linked, and as a consequence, heterozygote animals at these loci only produce two types of gametes that, when randomly combined, give rise to two phenotypes in the F2 progeny at 3:1 ratios. Linkage between alleles can be used for tracking the inheritance of "invisible" traits. In this example, the morphology of the tail can be used to track the inheritance

of the ability to grow/reject tumors. During gametogenesis, the "linkage" between alleles located on the same chromosome can be disrupted in the event of chromosome recombination (lower panel, right). In this case, recombinant allelic combinations can be found in gametes, and four phenotypes can be observed in F2 progeny. While these four different phenotypes are similar to the ones expected if the genes had undergone independent assortment, their observed ratios are not 9:3:3:1. The ratio of progeny from recombinant gametes is proportional to the physical distance between the genes on the chromosomes. This principle can be used to infer the relative location of genetic elements in the genome and is the basis for the generation of genetic linkage maps

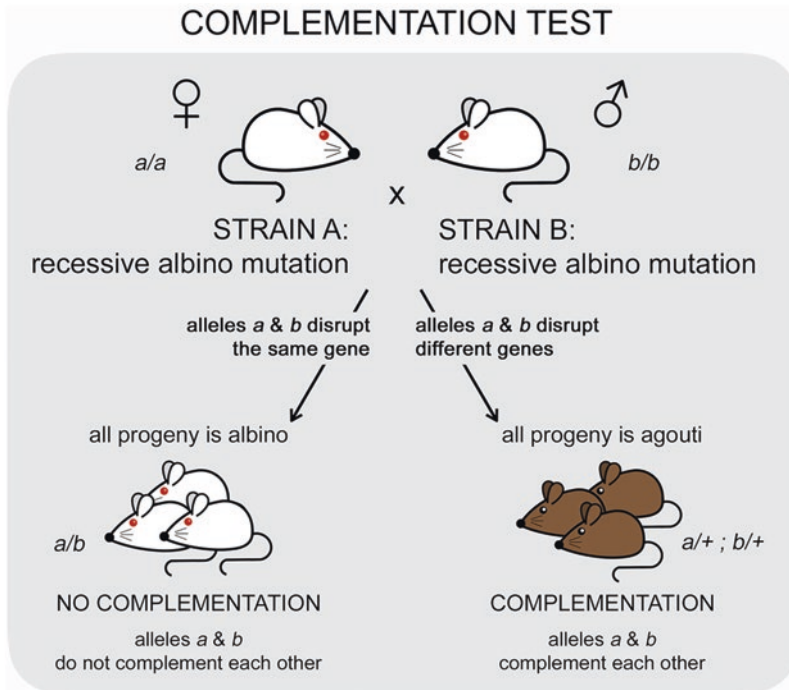


Fig. 1.4 *Complementation test.* By analyzing the F1 progeny from two animals carrying recessive alleles that cause the same phenotype, it can be determined whether the two alleles disrupt the same or different genes. In the illustrated example, if the *a* and *b* alleles causing albinism correspond to the same gene (left), albinism will be

observed in the progeny and the alleles are said to not complement. If, on the contrary, the alleles correspond to different genes (right), mice with normal coat-color pigmentation will be observed in the progeny and the alleles are said to “complement” each other

in their biochemical properties (Fig. 1.5, bottom-left panel). Differences included changes in the electrophoretic mobility of proteins, in their enzymatic activity, their solubility in certain buffers, their thermal inactivation profile, their distribution in organelles, or their immunoreactivity [1, 5]. While the basis for these protein polymorphisms was thought to reside in allele variants for the genes encoding them, the actual genes and/or nucleotide changes were in many cases unknown.

Biochemical markers contributed to improving recombination maps by providing additional anchor points in the genome for linkage analysis. However, finding novel morphological or biochemical markers for linkage studies depended on serendipitous discoveries. As a consequence, the number of available markers remained an important limiting factor toward obtaining detailed linkage maps for many years. This situation changed dramatically in the 1980s and 1990s

with the development of recombinant DNA technologies and improvements in DNA sequencing (reviewed in [1, Chapters 7 and 8]). By enabling the cloning, sequencing, and analysis of genomic sequences, these techniques led to the discovery of sequence differences between the DNA from different inbred strains (Fig. 1.5, right panel). These sequence differences, known as **DNA polymorphisms**, had two advantages over morphological and biochemical markers: they could be actively identified by comparing sequencing data between inbred strains, and they seemed to be distributed randomly throughout the genome, therefore providing a wide source of additional anchor points for linkage analysis. While DNA polymorphisms could be detected by sequencing, this approach was not practical for linkage analysis at the time, since sequencing methods were laborious and linkage analysis required testing hundreds of recombinant samples.

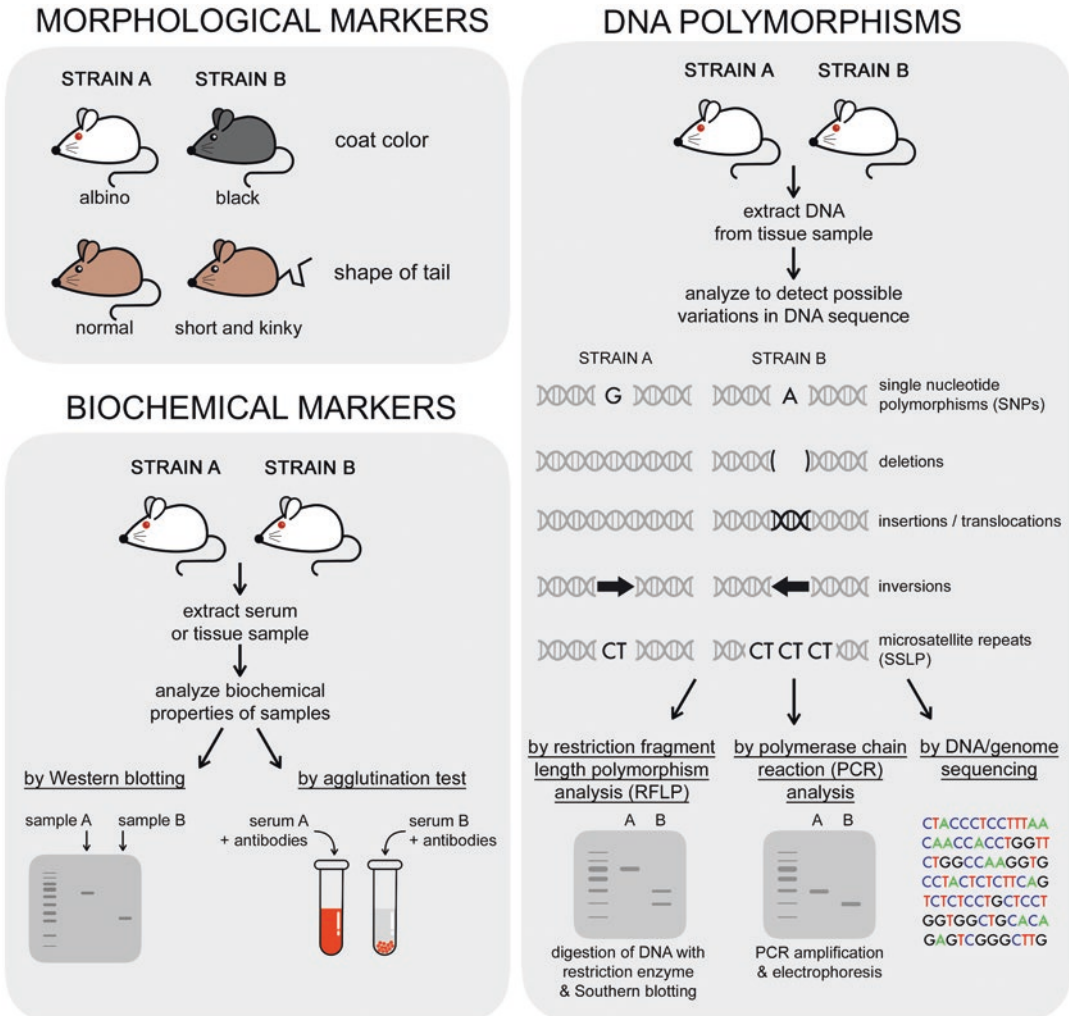


Fig. 1.5 *Markers for linkage analysis.* Linkage analysis necessitates detectable markers to establish the relative chromosomal location of genetic elements. Morphological markers (top-left panel) rely on phenotypes that can be directly observed in animals, such as coat color or the shape of the tail. Biochemical markers (bottom-left panel) are based on differences in the biochemical properties of tissue samples obtained from animals. The detection of these biochemical differences generally requires labora-

tory tests such as Western blotting or agglutination assays. DNA polymorphisms (right panel) are based on differences in the DNA sequence, such as deletions, insertions, translocations, inversions, nucleotide changes (also referred to as single-nucleotide polymorphisms (SNPs)), and variations in the number of microsatellite repeats. Detection of DNA polymorphisms can be done by direct sequencing, RFLP analysis, or PCR-based methods

One of the first practical methods developed for the detection of DNA polymorphisms made use of the ability of restriction enzymes to cut DNA at specific sequences. The principle behind this method relies on the fact that sequence differences among strains might disrupt recognition sites for certain restriction enzymes. As a consequence, DNA polymorphisms can be visualized as

restriction fragment length polymorphisms (RFLP), differences in the size of the fragments that resulted from digesting genomic DNA from different strains with restriction enzymes. This approach was laborious, since the detection of restriction fragments required the use of Southern blotting with a probe located near the position of each known DNA polymorphism, but allowed

testing multiple samples in a single experiment. Another advantage of this method is that it allowed the detection of many types of DNA polymorphisms, not only single nucleotide changes, but also a variety of chromosomal rearrangements such as deletions, insertions, or translocations. As a consequence, the use of RFLP contributed significantly to improve the resolution of linkage maps.

With the popularization of polymerase chain reaction (PCR) methods in the 1990s, the detection of RFLP was greatly facilitated by eliminating the need to use Southern blotting to identify a particular genomic region. However, around this time, the use of RFLP as markers was relegated by the discovery of a new type of DNA polymorphisms involving repetitive genome sequences, which demonstrated unmatched benefits as markers for linkage analysis [22]. The most useful of these repetitive elements were **microsatellites**, genomic elements that contain mono-, di-, tri-, or tetrameric sequences repeated in tandem multiple times at specific locations in the genome. Microsatellite repeats do not have any known function and are thought to generate from recombination or replication errors at genome areas that are not critical for gene function. As a consequence, the number of tandem repeats at a given loci tends to vary among different laboratory mouse strains, making them ideal markers for linkage analysis. Also, microsatellites seemed widely distributed across the mouse genome and therefore could provide a widespread coverage of anchor points for linkage. On the practical side, it was easy to design PCR-based methods to detect microsatellite polymorphisms, also called **simple sequence length polymorphisms (SSLP)**. Similar to RFLPs, microsatellites were also easy to identify in the data that started outpouring from the sequencing of cDNA, bacterial artificial chromosomes (BACs), yeast artificial chromosomes (YACs), and cosmid libraries. As a consequence, the number of available SSLP increased rapidly in just a few years. The Center for Genome Research at the Whitehead Institute/MIT led a systematic search for polymorphic microsatellite loci that could be used for linkage analysis [23]. The completion of this ambitious

project identified more than 6000 SSLPs and mapped them with respect to each other and with existing RFLP linkage maps, providing the first comprehensive linkage map of the mouse genome [24].

In parallel to the development of polymorphic markers, mouse geneticists worked toward finding efficient ways to test linkage and establish detailed maps. In its early days, linkage analysis entailed setting up breeding crosses between mouse strains carrying different morphological markers, then scoring the progeny for recombination events. However, a methodological breakthrough came in the 1970s, when Donald Bailey and Benjamin Taylor established **recombinant inbred (RI) strains** and conceptualized its use for linkage analysis [5, 25]. Recombinant inbred strains are obtained by crossing two known inbred strains and then establishing inbred colonies from the progeny. The resulting set of RI strains provide a collection of samples in which recombination events are preserved for future analysis through inbreeding (Fig. 1.6). Many RI strains, as well as genomic DNA samples of mice from these colonies, were maintained at Jackson Labs and were available to investigators for a small fee. Consequently, new markers could be mapped with respect to existing ones without the need to perform any breeding. Despite the convenience of RI strains, the scarcity of polymorphic markers at the time remained an important limitation to increase the resolution of existing linkage maps. In fact, almost two decades had to pass before a substantial number of DNA polymorphisms became available and RI strains could show its full potential for recombination mapping.

Meanwhile, investigators realized that the convenience of RI strains was tainted by the fact that most of the laboratory inbred strains used to generate them originated from just a few animals captured in the same geographical area and, as a consequence, their genomes were not very polymorphic. The discovery that fertile progeny could be obtained from **interspecific crosses** between laboratory strains (*Mus musculus*) and the distantly related species *M. spretus* [26] opened the possibility of using the genetic diversity between

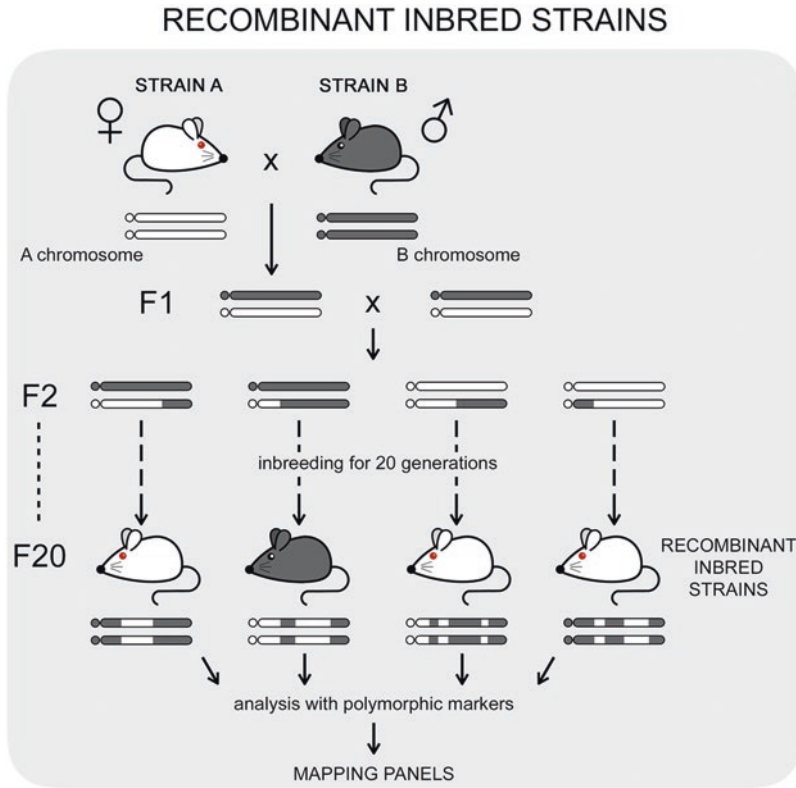


Fig. 1.6 *Recombinant inbred strains.* Recombinant inbred strains are generated by crossing mice from two previously established inbred strains, then performing brother-to-sister matings for 20 or more generations. Each of the resulting RI strains is genetically homogeneous and contains a mix of chromosome segments from the two original inbred strains. However, different RI strains differ in their genetic composition depending on the recombina-

tion history of alleles in each of the breeding lines. The collection of DNA samples from the resulting RI strains constitutes a mapping panel. These samples can be tested with markers that are polymorphic between the original inbred strains, and the linkage relationships among the alleles from the A strain and the B strain can be used to construct linkage maps

species as a source of polymorphisms for linkage analysis [27]. Unfortunately, only the F1 hybrid females from interspecific crosses were fertile, but these could be backcrossed to males from laboratory strains, and DNA from the progeny could be preserved for analysis. Using this approach, several initiatives, including one at the Jackson Labs and another one in Europe (EUCIB—European Collaborative Backcross) performed interspecific backcrosses (with *M. spretus*, *M. castaneus*, and *M. domesticus*) and generated collections of DNA samples that, together with those obtained from RI strains, became known as **mapping panels** (reviewed in [28] and [1, Chapter 9]).

Mapping panels from interspecific crosses and RI strains played an important role in achieving a high-resolution linkage map of the mouse genome. By the 1980s, the amount of linkage information grew to a point where the “index card” system initially established by Margaret Green, and periodically published in the Mouse News Letter, became impractical [17]. To adjust to the demands of this research progress, Muriel Davisson and Thomas Roderick, at Jackson Labs, compiled all the existing information by 1990 and created one of the first computer-based mouse databases, the Genomic Database of the Mouse (Gbase). In 1992, the information from Gbase and other useful databases was compiled into a single

online portal, the precursor of today's **Mouse Genome Informatics** (MGI) (<http://www.informatics.jax.org/>). Since its inception, MGI has remained the most comprehensive database serving the international research community on mouse genetics, incorporating links to many useful Internet resources [29].

1.3.6 From Linkage Maps to Physical Maps

Genetic distances in linkage maps are measured in **centimorgans** (cM), an arbitrary unit that corresponds to the distance between two loci that segregate separately in the progeny at a frequency of 1 in every 100 individuals (which represents a crossover rate of 1%). While the frequency of recombination between two loci is roughly proportional to the length of DNA that separates them, numerous factors affect the frequencies at which recombination is observed and the interpretation of the results (reviewed in [1, Chapter 7]). For instance, loci separated by 50 cM or more have recombination frequencies similar to those of loci located in different chromosomes, making them appear as unlinked. Additionally, loci located far away from each other can undergo multiple crossovers, which skew the observed ratios of recombination in the progeny (i.e., an even number of crossover events between two loci produces the same allele combination as in the parental line and is therefore undetected). Another consideration is that recombination events within a chromosome are not independent of each other since the formation of a crossover site inhibits the initiation of additional recombination events nearby, a phenomenon known as **genetic interference**. As investigators became aware of these limitations, mathematical mapping functions were developed to correct for the effects of multiple crossovers and genetic interference ([14] and references therein). Nonetheless, as more linkage, cytogenetic, and sequence data became available, additional factors influencing recombination mapping were recognized. Among these, it was found that recombination sites are not randomly distributed

across the genome: telomeric regions are more recombinogenic than are centromeric regions [30], and certain regions within chromosomes, known as **recombination hotspots**, have a higher incidence of recombination [31]. Recombination frequencies were also found to differ depending on the sex of the hybrid analyzed (recombination is higher in females than in males) and among different mouse strains [32, 33]. In recognizing these factors, it became clear that linkage and cytogenetic maps provided a comprehensive look at the mouse genome, but there were limits to their resolution, and therefore they could not substitute for a detailed physical map, where genes could be accurately placed in order onto chromosomes. As we will describe below, this accomplishment was made possible with the advent of molecular biology techniques, but would not be fully materialized until 2002, when the first draft of the mouse genome sequence was published [34].

1.4 The Molecular Biology Revolution and Mouse Genetics

The events that led to the birth of molecular biology and the publication of its central dogma in 1958 transformed the scope of genetic research [35, 36]. During the 1970s and 1980s, DNA cloning, DNA sequencing, nucleic acid hybridization, and the polymerase chain reaction made it possible to analyze the genome of any species with an unprecedented level of detail. Genes were no longer just alleles that manifested in different phenotypes; they could be identified as DNA sequences that were transcribed in specific tissues to produce proteins with specific cellular functions. As a result, natural alleles and induced mutations could now be analyzed at the molecular level as variations in the nucleotide sequence of genes that caused alterations in protein functions.

During the early years of molecular biology, libraries containing DNA fragments and complementary DNA (cDNA, DNA complementary to gene transcripts) were created in a variety of

vectors (bacterial plasmids, BACs, YACs, and cosmids), and sequences from these cloned DNAs were published in public repositories, including the European Molecular Biology Laboratory database (founded in 1980, currently part of EMBL-EBI), GenBank (founded in 1982, currently part of NCBI), and the DNA Data Bank of Japan (DDBJ) (founded in 1986), among others (reviewed in [37]). An important aspect of how these methods contributed to revolutionizing scientific research was that these repositories were all public: everyone could contribute their results to the databases, and archived sequences were available to anyone in the scientific community (although perhaps not as easily as we are used to nowadays since e-mail, the Internet, and the World Wide Web were not yet publicly available then). Also critical during these early years was the publication of the practical handbook *Molecular Cloning: A Laboratory Manual*, which, by offering detailed protocols, democratized the use of recombinant DNA techniques worldwide [38].

Sequencing information and molecular biology techniques had such a transformative impact on the field of mouse genetics that it is impossible to provide here a detailed account of the many techniques and approaches that contributed to this revolution. Nonetheless, we will mention a few highlights in the areas of linkage analysis, gene expression, and gene function. As discussed above, sequencing data provided a source of novel RFLP and SSLP polymorphisms that could be used to increase the resolution of linkage maps. Additionally, in situ hybridization techniques allowed the visualization of DNA in cytological preparations, enabling the mapping of genes and DNA sequences directly onto chromosomes [39]. As a result, these techniques made it possible to reconcile existing linkage, cytogenetic, and physical maps. Beyond linkage maps, molecular cloning and in situ hybridization techniques allowed investigators to determine that genes were transcribed in specific tissues and organs (reviewed in [40]), providing clues about their possible functions. Meanwhile, sequence comparison among different organisms revealed that many sequences and genes were evolution-

arily conserved across species, suggesting that research findings in a given organism could provide valuable information to determine gene function in another, an approach that later solidified in the creation of gene ontology databases [41]. In turn, these and other molecular biology contributions enabled the implementation of additional approaches toward the study of gene function. For instance, linkage maps became critical for the positional cloning of spontaneous and induced mutations. Additionally, the development of transgenesis and gene targeting approaches in the 1980s (see below) hinged on the ability of investigators to obtain and manipulate genomic sequences.

1.5 Manipulating the Mouse Genome: Making Mutants

Understanding the functional elements of mammalian genomes requires mechanisms to study how changes in DNA sequence and organization affect the physiology and/or reproduction of organisms. In the early years of mouse genetics, allele variants within natural populations and inbred strains were the only way to study the relationship between genes and phenotypes. Later on, the intense breeding programs carried out by mouse fanciers and research labs uncovered spontaneous mutations, providing additional genetic variants that could be correlated with disease outcomes and/or morphological differences [5]. However, investigators soon found more efficient ways to manipulate the genome by either using mutagenic agents, introducing exogenous pieces of DNA, or engineering customized changes in the genome's DNA sequence.

From a methodological perspective, two fundamental strategies have been historically used to study the effects of mutations (Fig. 1.7). **Forward genetics** is a phenotype-driven approach where naturally occurring or induced mutations are selected based on their phenotype, then further studied to determine the genetic and molecular causes for the morphological or physiological defects observed. Conversely, **reverse genetics** is

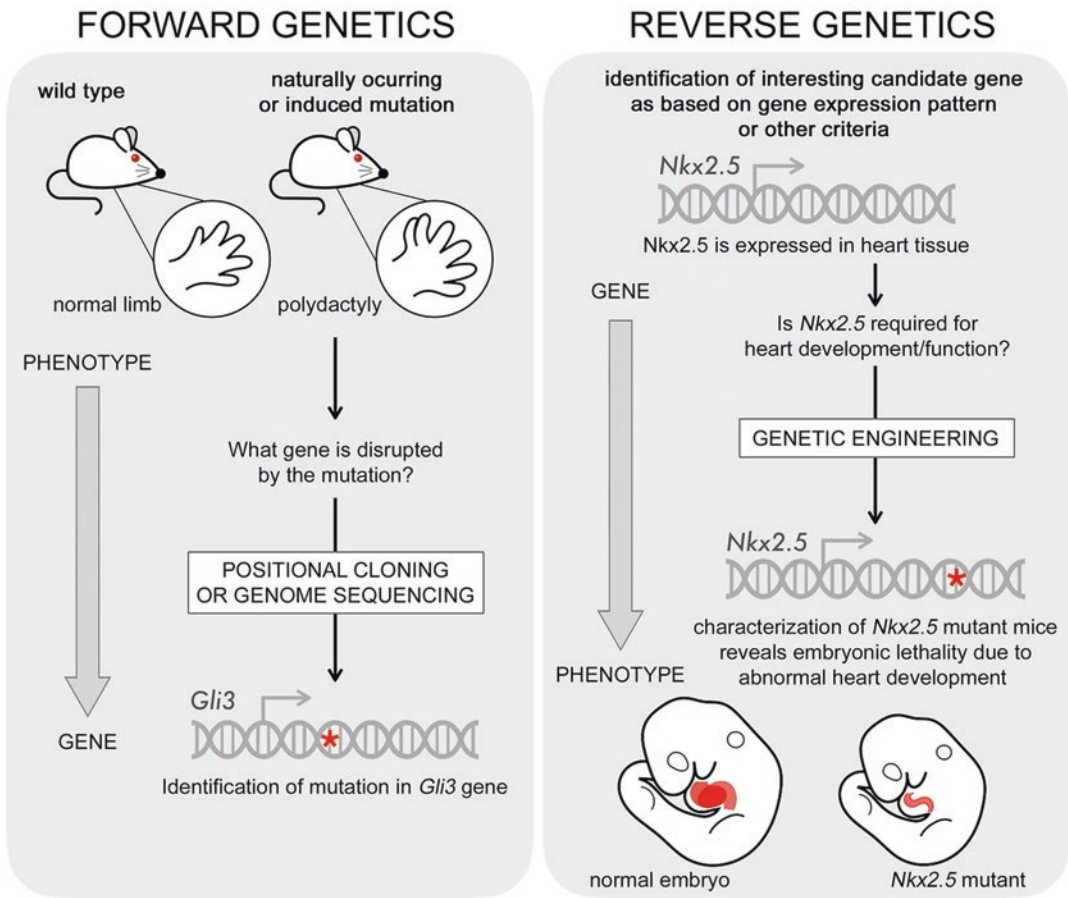


Fig. 1.7 Genetic approaches to study gene function. Genetic studies rely on the ability to link the genetic makeup of an organism (genotype) to its morphological or physiological constitution (phenotype). Forward genetic approaches (left panel) start with the analysis of naturally occurring or induced mutations that cause interesting phenotypes such as polydactyly, a condition that causes the appearance of extra digits in the extremities of mammals. Positional cloning or genome sequencing can be later used

to identify the gene/mutation linked to the phenotype observed. Reverse genetic approaches (right panel) start with a known element of the genome, such as the gene *Nkx2.5*, and use genetic engineering methods to establish the effect of mutations disrupting that genetic element. Reverse genetic approaches are used by investigators to determine the function of genes that are interesting as based on previous research results or to establish mouse models of genetic human diseases

a DNA-driven approach that starts with the targeted disruption of a specific genetic element, then follows up on the study of the effects of this mutation on the *phenotype* of an organism. Forward genetic approaches do not require any previous knowledge of what sequences in the genome might be functional. Therefore, they constitute an unbiased strategy toward the discovery of novel elements in the genome. On the other side, reverse genetic approaches are ideal

for studying previously identified elements of the genome whose functions are unknown. The development of techniques to support forward and reverse genetic approaches evolved in parallel since the 1950s, supported by discoveries in research areas as disparate as developmental biology, teratogenesis, and bacterial genomics, providing another example of how serendipity in research often promotes scientific progress in unanticipated ways.

1.5.1 The Power of Mutagens

The ability of radiation and certain chemicals to induce mutations was well known before the end of World War II from work on *Drosophila* and maize. However, bombings in Hiroshima and Nagasaki raised an interest in understanding the impact that atomic warfare and nuclear power plants could have on exposed individuals and their descendants. In the US, a big project toward this goal was initiated at the Biology Division of the Oak Ridge National Laboratories (ORNL) (reviewed in [42]). Mice offered an ideal model system for investigating the effects of radiation on mammals. Consequently, Bill Russell, who had trained with Sewall Wright studying phenotypic variability in inbred strains, was recruited to lead the operations in 1947. To test the rates of mutagenesis elicited by different mutagenic agents in germ cells, Russell introduced a methodological innovation known as the **specific locus test (SLT)**. This test involved crosses between mutagenized animals and “tester stocks” carrying alleles for seven different recessive markers with morphological phenotypes easy to distinguish by visual inspection. By scoring for the appearance of the recessive phenotypes in the F1 progeny, these crosses provided a standardized way to evaluate and compare the mutagenic rates of different types of mutagens and mutagenic regimes. In the early years, studies at ORNL centered on the effects of both external radiation sources (including X-rays, gamma rays, neutrons) and internal emitters (animals treated with radioactive isotopes such as tritium and plutonium). Later on, the successful platforms established at ORNL were also used to test the mutagenesis rates of chemicals. Studies with chemicals were initiated in the early 1960s and were greatly expanded in the 1980s, covering a wide spectrum of substances.

While the main focus of the ORNL programs was to study the effects of mutagens in female and male germ cells by using the SLT, work at ORNL spawned research in a variety of areas. Efforts to understand the effects of mutagens on testes and ovaries resulted in basic research on gametogenesis. Also, studies with embryos

revealed that the early stages of embryogenesis were especially sensitive to the effects of radiation, a result that led to clinical recommendations for the practice of radiology on women of child-bearing age. Perhaps the most influential contribution of the mutagenesis program at ORNL was that, as expected from such an intense use of mutagenic agents, lots of mutations and chromosome aberrations were obtained. From the onset, ORNL was committed to keeping mutants for their use in basic research projects. As a consequence, mouse genetics was no longer limited to the study of inbred strains and/or spontaneous mutations. Studies on some of the mutants obtained at ORNL contributed to important scientific discoveries, including the mechanism of sex determination in mice and the phenomenon of X-chromosome inactivation. Mutations obtained at ORNL were distributed to investigators worldwide for analysis and, as techniques were developed for freezing embryos and sperm [43–45], the ORNL devoted resources toward cryopreserving the entire ORNL stock collection for future investigation on the molecular effects of mutagens.

While the big genetic programs at ORNL were the first ones to be established, they were not the only ones. The United Kingdom initiated a similar mutagenesis program in the early 1950s, first located at the University of Edinburgh, then at Harwell. Focused on the analysis of chromosomal rearrangements, research at Harwell provided critical materials for cytogenetic analysis and genetic mapping [17]. Additionally, the Federal Republic of Germany recruited Udo Ehling to carry a chemical mutagenesis program at Neuherberg, near Munich in the mid-1960s [42]. Taken together, the use of mutagens represented the first methodology for investigators to manipulate the genome and generate mutations. The study of the resulting mutants highlighted the power of this approach to uncover the roles of the genome in regulating biological processes. Unfortunately, tools were not yet in place for investigators to be able to identify the genes disrupted by the mutations induced. However, once these tools became available during the 1980s and 1990s, the use of chemical mutagens for the

functional analysis of the mouse genome resurrected in the form of forward mutagenesis screens (see below).

1.5.2 Transgenesis: Introducing Exogenous DNA in the Mouse Genome

Starting in the early 1970s, a variety of methods for introducing foreign DNA into somatic and germ cell lineages of mice were developed. The first attempts used **viral DNA or retroviral particles** to infect early embryos [46], but shortly afterward techniques became available for introducing recombinant DNA into fertilized oocytes [47] and zygotic pronuclei [48]. Fundamental for the success of these techniques was the previous establishment of strategies to extract and manipulate embryos from pregnant mice, then reintroduce them into surrogate females. These strategies were developed during the 1950s and 1960s under the auspices of experimental embryologists who, motivated by their interest in understanding mammalian reproduction, required techniques to observe embryos outside of the uterus without disrupting their normal development. Thus, several developmental biologists contributed to optimizing protocols for growing two to eight cell embryos to the blastocyst stage in culture, aggregating cultured embryonic cells into chimeric embryos, and transferring cultured embryos into the oviduct of females (reviewed in [49]). Another embryonic manipulation that would become widely used for the generation of transgenic animals was **pronuclear injection**, a procedure that involved the injection of foreign genetic material directly into the pronucleus of fertilized mouse oocytes (Fig. 1.8; [50]). The success of pronuclear injection, and the exciting possibilities that transgenesis brought for genetic research, are exemplified in the fact that numerous groups adopted this technique just a year after it was first published [51–54]. Mice were the first organisms in which transgenesis was accomplished. Therefore, the establishment of these techniques constituted an important landmark that opened the door for genetic manipula-

tions in other organisms, including the generation of transgenic farm animals that could be used to produce large quantities of pharmacological compounds or that could be modified for improved agricultural productivity [55].

In mice, transgenesis provided a new tool for the analysis of gene function by allowing investigators to analyze the effects of **ectopic expression of genes** in a tissue and/or specific developmental stage. Spatial and/or temporal expression was usually accomplished by placing known enhancers or inducible promoters in transgenes [56]. Some applications of this strategy include studies on the oncogenic activity of certain genes (*Myc*, *Ras*), the analysis of immune responses to self-antigens, and the effects of developmental regulators (reviewed in [57]). In general terms, the ectopic expression of transgenic genes represents a **gain-of-function mutation**. However, transgenesis has also been used to generate **dominant negative conditions** by introducing mutated versions of genes (such as truncations or point mutations) that can sequester wild-type products in an inactive conformation (e.g., as inactive dimers; [58]). The ectopic expression of transgenes can also be used in the context of **complementation tests**, to evaluate whether candidate genes can rescue loss of function mutations [59]. Transgenesis was also used by developmental biologists in the context of **cell lineage analysis**, either by expression of reporter genes under the control of cell-/tissue-specific regulatory sequences [60]—such as the bacterial *lacZ* gene [61] or the gene encoding green fluorescent protein (GFP) [62]—or by ablation of certain cells through the controlled expression of toxic genes (e.g., diphtheria toxin; [63]).

While retroviral vectors for transgenesis have a limit to the length of the fragments that can be cloned into them, large fragments cloned in bacterial and yeast artificial chromosomes (BAC and YAC vectors) can successfully be integrated into the mouse genome through pronuclear injection (reviewed in [64, 65]). By allowing the integration of large genomic regions, transgenesis through pronuclear injection brought investigators a novel tool for the **identification of regulatory sequences**. The logic of this type of

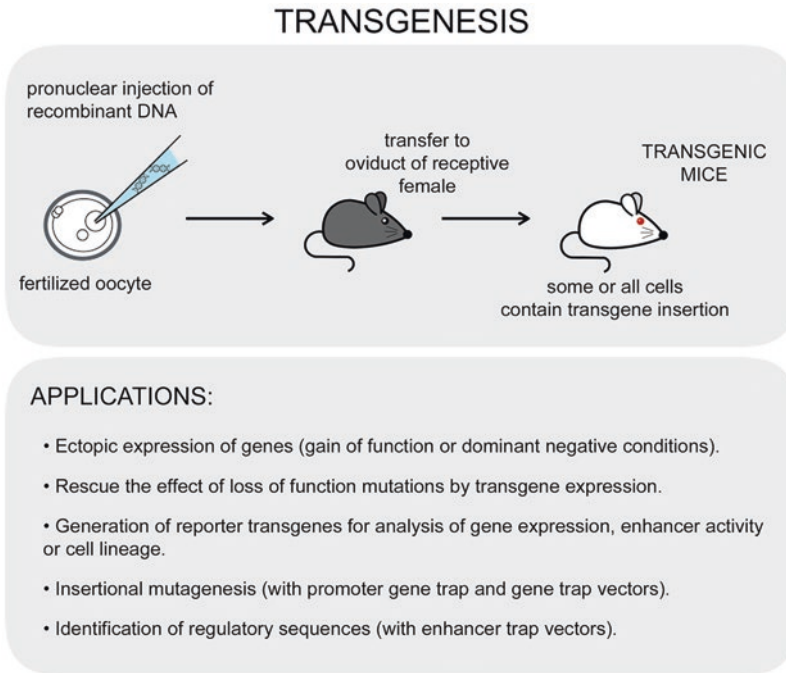


Fig. 1.8 *Transgenesis*. Efficient introduction of exogenous genetic material into the mouse genome can be accomplished by pronuclear injection of recombinant DNA into fertilized oocytes. Injected oocytes are then briefly cultured *in vitro*, then transferred to the oviduct of females that are hormonally receptive to these embryos (pseudopregnant females). The pups born from the pseudopregnant female/s will be transgenic if the injected

recombinant DNA integrated into the oocyte genome. If the integration takes place before the first mitotic division of the oocyte, then all the cells of transgenic animals would contain the transgene. If integration takes place later during embryogenesis, then the transgene might only integrate in some of the cells from the resulting transgenic animals

experiments is that if a large transgene containing a given gene of interest is expressed correctly after integrating into a random location in the genome, it can be inferred that the regulatory elements required for its expression were also present in the transgene. If so, these elements can be later localized by either deleting candidate sequences from the original BAC/YAC clone or testing the function of these candidate sequences in the context of reporter transgenes. This strategy was used extensively to identify regulatory elements conferring spatial and/or temporal transcriptional control in a variety of genes (reviewed in [65]). This type of information contributed to a better understanding of the mechanisms that regulate gene expression and identified regulatory sequences that could be used to drive ectopic gene expression in particular tissues or developmental stages.

Another important application of transgenesis related to the fact that the insertion of foreign genetic material can disrupt genes or functional elements of the genome located at the integration site. As a consequence of this effect, called **insertional mutagenesis**, many transgenesis experiments unexpectedly led to abnormal phenotypes in transgenic embryos/animals [66]. In these cases, since the mutagenic agent (the foreign DNA) remained integrated in the genome, it could be used as a tag from which to clone the genes disrupted. The overall frequency of insertional mutagenesis was found to be relatively low (7%, [65]). Nonetheless, at a time when there were few mechanisms to identify the genes disrupted by other mutagenic agents (such as radiation or chemicals), insertional mutagenesis provided investigators with a useful strategy to characterize the functional elements of the

genome. This approach was later employed as the basis for large-scale gene-trap mutagenesis screens (see below).

1.5.3 Targeted Mutagenesis Through Homologous Recombination

While mutagens, including transgenes, provided mechanisms to manipulate the genome, the location where mutations were introduced was out of the control of the investigator. This situation changed in the mid-1980s with the development of techniques that allowed the modification of a target sequence of interest in a controlled fashion. Several lines of experimentation had to merge for the development of these techniques. The first critical step was the discovery that **pluripotent embryonic stem cells (ES cells)** could be isolated from early mouse embryos [67, 68] and that, when injected into blastocysts, these cells could contribute to any cell lineage in the resulting embryos, including the germline [69]. These findings inspired experiments to generate genetically modified animals by using ES cells that had been previously manipulated in culture, either by exposure to retroviruses or by transfection of DNA [70, 71]. Meanwhile, Mario Capecchi and Oliver Smithies were experimenting with the idea of whether **homologous recombination**, a process known to promote the exchange of DNA between DNA fragments with similar sequence, could be used to modify genes in mammalian cells. In 1987, both groups reported the successful use of homologous recombination to modify genes in ES cells [72, 73]. Shortly afterward, the first gene-targeted mice were born [74–78]. At this point, advances in recombinant DNA and molecular biology techniques had provided investigators with a wealth of information about cloned mammalian genes and, in some cases, their association to human diseases. Therefore, the possibility of using targeted mutagenesis to introduce mutations in any locus of interest opened the door to interrogating the function of any known sequence in the genome and/or to generate mouse mutants

that could serve as models to study human disease (reviewed in [79, 80]). Gene targeting was soon adopted by many investigators, and the number of mouse mutants obtained through this technology, which became known as **knockout (KO) mice**, grew exponentially during the last decade of the twentieth century. In recognition of the transformative impact that gene targeting had on the field of mouse genetics, Mario R. Capecchi, Martin J. Evans, and Oliver Smithies received the Nobel Prize in Physiology or Medicine in 2007.

The generation of knockout mice starts with the design of an appropriate targeting vector containing the desired gene modifications (Fig. 1.9). The vector is then electroporated into ES cells for homologous recombination to take place. Because the efficiency of homologous recombination is very low compared to the rate of transgenesis, careful selection of ES cell clones is required to identify those in which the desired locus has been modified. This step was initially very laborious. However, smart improvements in vector design made the selection process less cumbersome by introducing sequences that allow the positive selection of the cells that have incorporated the vector through homologous recombination and the negative selection of cells in which the vector has randomly integrated in the genome. Over the years, vector design incorporated additional modifications to facilitate the selection process and eliminate undesired effects at the targeted locus (reviewed in [81]).

Targeting vectors can be designed to introduce a variety of modifications at the target locus of interest, including deletions, point mutations, insertions, and sequence substitutions. This versatility enabled the use of targeted mutagenesis for a variety of applications, including the possibility of rescuing a mutant allele by replacing the mutated gene for a wild-type copy, the generation of mouse models of human disease through the introduction of point mutations identified in humans, and the generation of knock-in mice containing reporter alleles, to name a few [56, 81]. Despite this versatility, when inquiring about the roles of a previously uncharacterized gene, investigators usually chose to design targeting vectors toward the generation of null mutations,

TARGETED MUTAGENESIS BY HOMOLOGOUS RECOMBINATION

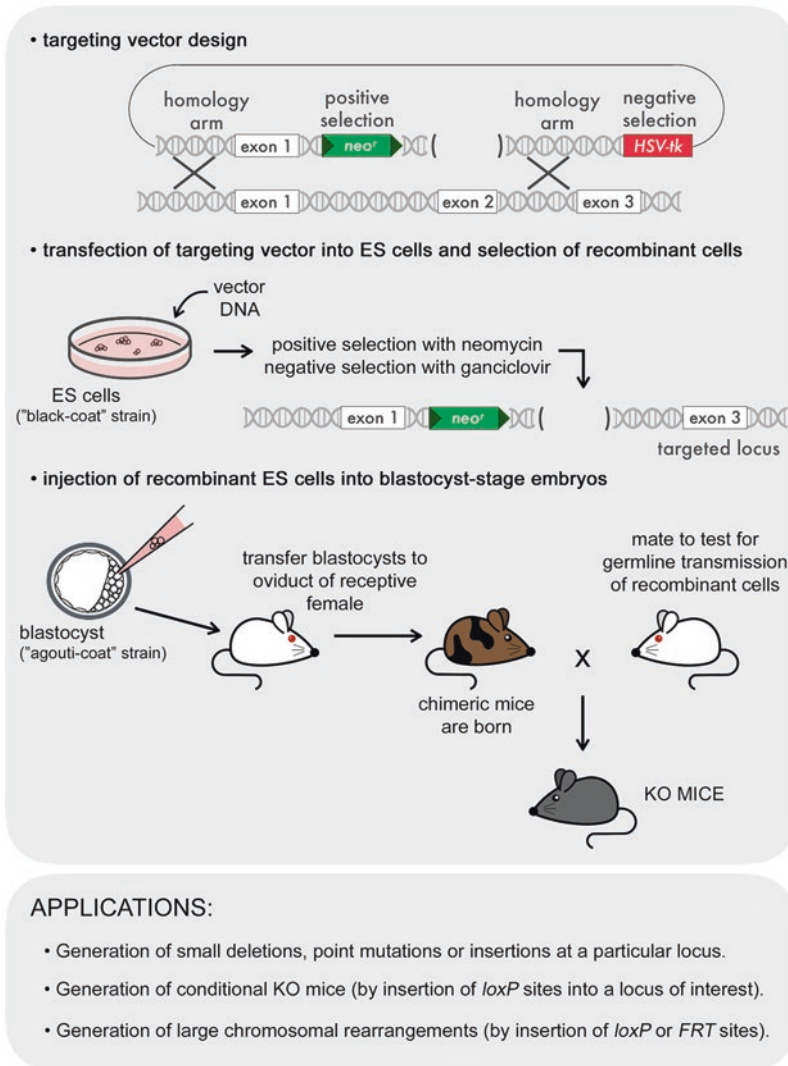


Fig. 1.9 Targeted mutagenesis by homologous recombination. The generation of KO mice starts with the design and engineering of a plasmid targeting vector containing the DNA sequence with the desired modification/mutation to be introduced and a positive selection cassette (generally *neo^r*, which confers resistance to neomycin). These elements need to be flanked by two regions with complete homology to the locus to be genetically modified (homology arms). Also, a negative selection cassette located after one of the homology arms (generally *HSV-tk*, which confers resistance to ganciclovir) is needed to select against cases where the targeting vector does not undergo homologous recombination but, instead, integrates randomly in the genome. The targeting vector is electroporated into ES cells and, after positive and negative selection, recombi-

nant ES cell clones carrying the targeting vector into the locus of interest are injected into blastocyst-stage embryos. These embryos are then transferred to pseudo-pregnant females. The pups born from these females are chimeric, bearing cells from the blastocyst that was injected and from the ES cells that were introduced. The genetic makeup of ES cells and blastocysts can be chosen to provide coat-color markers that can facilitate the assessment of chimerism and selection of KO mice. In the illustration, “black” coat color marks cells of ES cell origin, while agouti coat color marks blastocysts cells. To further study the effects of the mutation, chimeric mice must be able to transmit the modifications to their progeny (germline transmission)

generally by eliminating one or more exons of the targeted gene. The phenotypes of null mutations were often quite unexpected, offering lessons of humility to investigators who, eager to find phenotypes in tissues where the targeted gene was known to be expressed, were confronted with finding no phenotype at all or unpredicted phenotypes, such as embryonic defects and/or lethality. These unforeseen effects highlighted the fact that the function of mammalian genes is sometimes redundant with closely related genes, and therefore phenotypes are not obvious unless two or more genes are knocked out simultaneously. In other cases, mammalian genes have pleiotropic functions at different developmental stages, and therefore early phenotypes preclude the analysis of later functions.

To address the analysis of pleiotropic gene functions, the design of targeting vectors was refined such that gene function would only be altered in specific tissues and/or at precise developmental timepoints. One of these refinements was the use of the *Cre/loxP* recombinase system to generate **conditional knockout mice**. This system is based on the ability of the *Cre* recombinase from the P1 bacteriophage to excise any region of DNA placed between two recognition motifs called *loxP* sites. Consequently, the two elements of this system, *Cre* recombinase and *loxP* sites, need to be introduced into mice for the generation of conditional knockouts. On one side, homologous recombination is used to place two *loxP* sites flanking an essential exon of the gene to be knocked out. If done properly, the resulting mice would contain a “**floxed**” allele in which the *loxP* sites do not interfere with the normal transcription or splicing of the gene. Mice with a floxed allele are then mated to transgenic animals in which the *Cre* recombinase is expressed under the control of tissue-specific enhancers. As a result, excision of the floxed allele will only happen in specific tissues of the progeny. As more labs adopted this strategy to analyze the function of genes expressed in a particular tissue of interest, a variety of *Cre* lines became available. Many of these lines can now be obtained through public repositories [82]. Variations of the *Cre/loxP* approach employing other recombinases (*FLP*-

FRT system) or incorporating inducible gene expression systems (tamoxifen or tetracycline-dependent expression) provided alternative methods and additional versatility for the conditional inactivation of genes. Another interesting application of the *Cre/loxP* system was the **engineering of chromosomal rearrangements** such as large deletions, duplications, inversions, and translocations, some of which could be used as mouse balancer chromosomes [83].

1.5.4 Genome Engineering with Endonucleases: CRISPR/Cas9 Engineering

For more than 20 years, homologous recombination remained the only reverse genetic approach to purposely target a known element of the mouse genome. However, in the early years of the twenty-first century, endonucleases emerged as powerful tools for gene editing. Endonucleases work by generating double-strand breaks (DSBs) in the DNA, thereby triggering one of several DNA repair mechanisms that are endogenous to cells. Nonhomologous end joining is an error-prone repair mechanism that frequently leads to the production of small insertions or deletions (indels), which can potentially disrupt genes or other functional elements of the genome. DSBs can also be repaired through high-fidelity homology-directed repair mechanisms. In normal conditions, homology-directed repair uses a sister chromatid as template, but this repair system can be deceived to use a single-stranded or double-stranded DNA cointroduced into the cell, as long as it bears homology to the locus being repaired. Therefore, by delivering simultaneously a nuclease with an alternative repair template containing mutations, any desired sequence change, such as nucleotide substitutions, deletions, or insertions, can be introduced at or near the induced DSB. Key to the use of endonucleases for targeted mutagenesis was the development of methods to direct these enzymes to introduce DSBs exclusively at a desired locus in the genome. This has been accomplished through different strategies.

The first endonuclease systems used for gene editing were **zinc-finger nucleases (ZFNs)** and **transcription activator-like effector nucleases (TALENs)**. Both ZFNs and TALENs are modular enzymes that contain the bacterial FokI endonuclease domain fused with a DNA recognition motif that can be engineered to recognize any known sequence in the genome (reviewed in [84]). ZFNs and TALENs were successfully applied for gene editing in a variety of experimental systems. However, their use for gene editing was eclipsed by the difficulties associated with the design of specific DNA recognition motifs and the advent of a novel and more versatile gene editing system. This new gene editing method was adapted from a bacterial locus that confers adaptive immunity against bacteriophages and comprises three different elements: (1) an array of **clustered regularly interspaced short palindromic repeats (CRISPR)**, which contains sequences derived from bacteriophages or other invading genetic elements and is transcribed to produce a CRISPR RNA (crRNA); (2) a nuclease, encoded by nearby CRISPR-associated genes (**Cas**); and (3) a trans-activating crRNA sequence (tracrRNA), which is transcribed into an RNA complementary to parts of the crRNA and can recruit the Cas nuclease. These three elements form a functional Cas-crRNA-tracrRNA complex able to recognize and digest exogenous DNA with sequences complementary to those in the crRNA sequence, thereby protecting bacteria from the harmful effects of a phage infection. While three different types of CRISPR/Cas systems have been described [85], the type II **CRISPR/Cas9 system** has been adopted for gene editing due to its high efficiency and adaptability to a variety of organisms (reviewed in [86]). In 2013, the CRISPR/Cas9 system was successfully used for the first time to edit the genome of mouse and human cells [87, 88]. This was accomplished by transfecting cells with plasmids encoding the Cas9 and an engineered guiding RNA (gRNA), which contained a reprogrammed crRNA with sequence complementary to a 30 bp unique target site in the genome and an 89 bp tracrRNA (Fig. 1.10). Since then, the technique has been further developed

for its application to a wide spectrum of model organisms. Additionally, protocol improvements have been introduced to provide better efficiency, target specificity, and to favor homology-directed repair [89].

In mice, it was found that co-injecting the components of the CRISPR/Cas9 system directly into one-cell embryos can result in gene editing, either through nonhomologous end joining or through homology-dependent repair mechanisms (Fig. 1.10; [90, 91]). This finding revolutionized gene targeting in mice since it allowed the generation of CRISPR-edited animals, referred to as **CRISPRed mice**, as early as 6 weeks after embryo injections. Consequently, CRISPR/Cas9 editing offers a faster and simpler one-step protocol as compared to the process of obtaining KO mice, which takes several months of cumbersome vector design, ES cell selection and injection into blastocysts, followed by selection of animals with germ-line contribution. Also, the CRISPR system offers additional advantages over targeted mutagenesis by homologous recombination in ES cells. First, the high targeting efficiency of CRISPR/Cas9 makes it possible to edit the two homologous chromosomes in a single procedure, facilitating the analysis of recessive traits. Also, by injecting multiple gRNA constructs, CRISPR/Cas9 can be multiplexed to accomplish the simultaneous targeting of several loci, making it possible to generate double or triple mutant mice directly. While CRISPR-induced editing is not yet exempt from a few experimental pitfalls [89], its application in one-cell mouse embryos was found to be highly specific, alleviating the concerns about possible off-target effects that had been raised in other experimental settings [91, 92]. Moreover, the last few years have seen the publication of protocol variations, such as CRISPR-EZ, that continue improving the fidelity, efficiency, and versatility of this system [93]. At present, CRISPR/Cas9 has been successfully used to generate indels that disrupt gene function, to introduce subtle genomic modifications such as point mutations, to insert exogenous sequences such as those that allow to generate conditional floxed alleles or epitope tags [92, 94], and to generate relatively large deletions (up to

CRISPR/Cas9 GENOME ENGINEERING

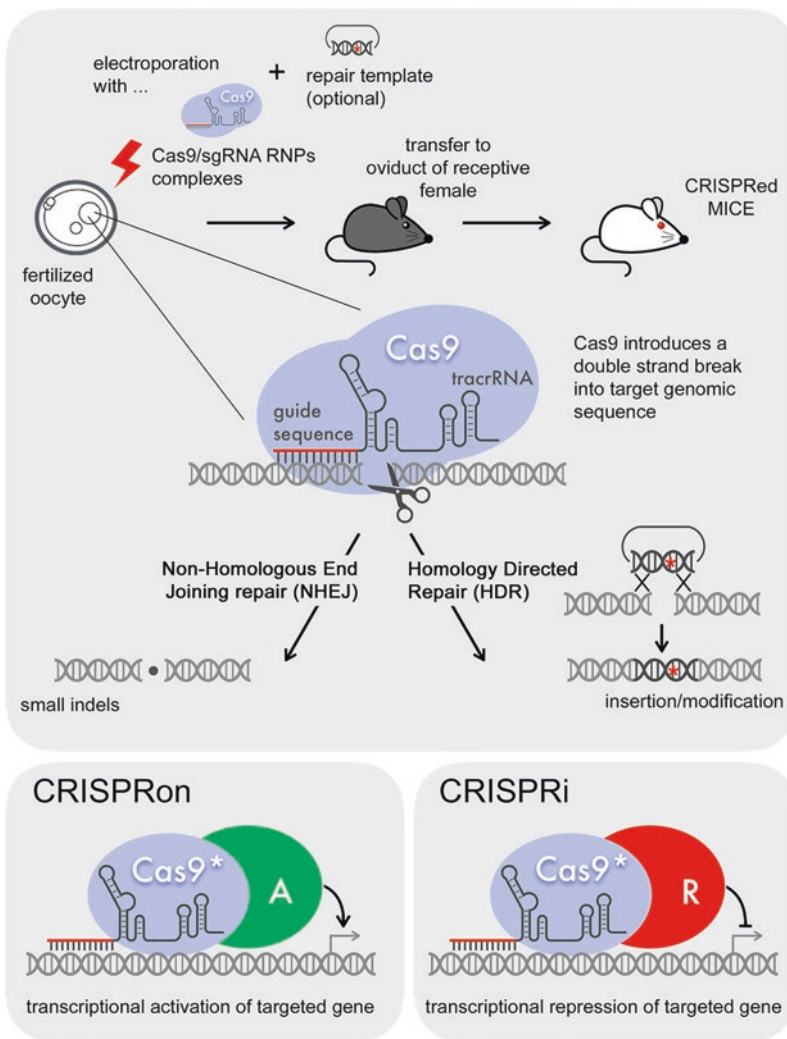


Fig. 1.10 *CRISPR/Cas9 engineering.* Adapted from a bacterial immunity system against bacteriophages, CRISPR/Cas9 genetic engineering is based on the ability of the Cas9 endonuclease to introduce double-strand breaks (DSB) into the DNA (upper panel). Cas9 (light blue) can be targeted to particular genomic loci when cotransfected with RNA molecules that contain an area of homology to the target locus (guide RNA sequence) and a specific RNA sequence able to interact with Cas9 (tracrRNA). DSB introduced by Cas9 can be repaired through one of two available repair mechanisms endogenous to cells: the nonhomologous end-joining repair (NHEJ) pathway, which frequently causes small deletions or insertions (indels) at the repaired site, or the homology-directed repair (HDR) pathway, which uses sequences with homology to the affected locus to repair the damage. Normally, homologous chromosomes serve as templates

for HDR, but alternative repair templates (plasmids containing mutations or modifications) can be provided experimentally. In mice, electroporation of Cas9/sgRNA ribonucleoprotein complexes into fertilized oocytes (with or without repair templates) can efficiently promote genome editing. Electroporated oocytes can be cultured in vitro to the blastocyst stage, then transferred to pseudo-pregnant females. Following this procedure, CRISPR-edited (CRISPRed) mice can be obtained in about 6 weeks. CRISPRon (lower left panel) and CRISPRi (lower right panel) are alternative applications of the CRISPR/Cas9 system. By using versions of Cas9 that lack endonuclease activity and are fused to a transcriptional activator (CRISPRon) or a transcriptional repressor (CRISPRi), these systems can respectively produce transcriptional activation or repression at the locus targeted by the cotransfected gRNA sequence

10 kb, [95]). Additionally, modified versions of the CRISPR system have been recently developed for applications beyond genome editing. Examples are the CRISPR-on and CRISPRi (Fig. 1.10, lower panels), which constitute tools for targeted regulation of gene expression by using Cas9 variants that lack nuclease activity and are tethered to transcriptional activator or repressor proteins [96–98].

1.6 The Mouse Genome Sequence

In 1985, a group of scientists, summoned by Robert Sinsheimer, met at the University of California Santa Cruz to discuss the feasibility of sequencing the whole human genome. This meeting was the first effort toward what ended up crystallizing in 1990 as the **International Human Genome Project**. While the ultimate goal of the project was to produce a complete assembly of the human genome, it was decided from the outset that the project should also include the analysis of other species, including mice [99]. The benefits of including other species were seen as double: on one side, sequencing smaller genomes, such as those of bacteria, yeast, *Drosophila melanogaster* (a fruit fly) and *Caenorhabditis elegans* (a nematode worm), would serve as a proof of principle that the DNA sequencing technology, as well as the computational methods required for the alignment and assembly of the resulting sequence, were ready to handle more complex genomes. On the other side, understanding the functional roles of the human genome would benefit from comparative studies among different organisms. The Human Genome Sequencing Project, which published its first complete draft in 2001, has arguably been one of the most ambitious scientific endeavors undertaken by humankind and one of exemplary international cooperation [100, 101]. Nonetheless, this ambitious project was not exempt from many scientific and political issues, which have been the topic of multiple divulgation books [102, 103].

The **Mouse Genome Sequencing Consortium** was created in 1999 and ran in par-

allel to the sequencing of other genomes. Initially, the strategy chosen for accomplishing a high-quality sequence of the mouse genome was similar to the one devised for the human genome and included two phases: in the first phase, efforts focused on improving the resolution of linkage maps with additional DNA polymorphisms and on using this information as a blueprint to map the chromosomal location of DNA fragments cloned into a variety of vectors (including expression libraries, BACs, YACs, and cosmids). A second phase comprised the sequencing of the DNA fragments in these libraries, its assembly into contigs (sets of overlapping sequences corresponding to a large genomic region), and the filling of the gaps between contigs to accomplish a contiguous sequence for each chromosome. While these were the initial plans, lessons learned from the “public” *Human Genome Project* and the “private” sequencing ventures initiated by the company *Celera Genomics* suggested that an alternative sequencing strategy known as **shotgun sequencing** could significantly accelerate genome sequencing. Shotgun sequencing relies on the use of computational approaches to align sequencing results from random clones and DNA fragments, whose location in the genome is initially unknown. By eliminating the need for mapping the location of each DNA clone within the genome, this strategy proved to be a useful method to assemble a first draft of the genome quickly. Nonetheless, it was found that the presence of highly repetitive sequences in complex genomes complicates the computational alignment of shotgun sequences. As a consequence, the mouse genome sequence was obtained through a diversified strategy that involved both shotgun sequencing and the sequencing of DNA fragments previously mapped to existing linkage maps. By combining the benefits of these two types of approaches, the first high-quality assembly of the mouse genome was accomplished in 2002 [34]. This achievement marked a new era in mouse research, facilitating the application of both forward and reverse genetic approaches toward the functional characterization of all the genes in the genome.

Following the completion of the mouse genome project, the increased availability of DNA sequence from different mouse strains led to the discovery of a new type of sequence variation among inbred strains, termed **single-nucleotide polymorphisms (SNPs)**. At present, SNPs constitute the best type of DNA polymorphic markers for linkage analysis due to their dense distribution across the genome, their high variability among mouse strains, and the availability of multiplexed genotyping platforms that simplify their detection in mouse samples [104, 105]. Because the discovery and detection of SNPs was only possible after technological advances allowed cheap and reliable genome sequencing, SNPs did not play a significant role in the initial development of accurate linkage maps. Nonetheless, the unsurpassed density of SNPs between different inbred strains made this type of polymorphisms stand out as powerful tools for the positional cloning of mouse mutations, as we will discuss below. To fully characterize molecular variations between the most common inbred strains, the **Mouse Genomes Project** was launched in 2009. Since then, sequence from more than 35 different inbred strains has provided a catalog of SNPs, as well as other genetic variants such as short indels and transposable elements [106].

1.7 A Mutant in Every Gene: Large-Scale Approaches to Study Gene Function

The use of mutagens and, later, the development of transgenesis and targeted mutagenesis accelerated the pace of mouse genetic research by giving investigators the tools required to obtain mutations that could inform about the roles of the different functional elements in mammalian genomes. However, as indicated above, each of these methods to manipulate the genome presented a different set of strengths and limitations, making it clear that understanding the functions of every gene in the genome would require complementary strategies. Up to this day, investigators have grappled with choosing the mutagenesis

method most appropriate to address their particular research goals. In the process, technical improvements in targeted mutagenesis and transgenesis, as well as progress from the mouse genome sequencing project, opened venues for large-scale mutagenesis efforts. As a consequence, the ambitious goal of obtaining mutations for each of the genes in the mouse genome became feasible. Below we review how large-scale chemical mutagenesis, transgenesis, and genetic engineering have contributed toward this goal, which is expected to be accomplished in 2020.

1.7.1 Forward Mutagenesis Screens and Positional Cloning

Results from research at ORNL identified N-ethyl-N-nitrosourea (ENU) as one of the most powerful mutagens in mice [107]. This finding raised the possibility of using ENU to perform genome-wide mutagenesis screens akin to those performed in other organisms, such as the Nüsslein-Volhard and Wieschaus screens in fruit flies, which would be later recognized with a Nobel Prize in 1995 [108]. The promise of using ENU for forward genetic approaches was initially diminished by the fact that linkage maps during the 1980s were still rudimentary, and many investigators feared that the identification of the point mutations responsible for the phenotypes recovered would be extremely difficult. Despite this, a few early investigators pioneered the use of ENU toward the identification of alleles at the *t complex* [109, 110], a genomic region that had long been subject to intense investigation due to its importance in the control of histocompatibility and embryonic development [10]. The success of these projects, together with improvements in linkage maps and the discovery of SSLP polymorphisms in the early 1990s, resurrected the enthusiasm in using **large-scale ENU-based forward genetic approaches** to uncover the functional elements of the mouse genome. This enthusiasm reinvigorated even further with the publication of a few additional successful ENU mutagenesis projects, which identified dominant-

effect point mutations causing tumorigenesis and circadian clock phenotypes [111–114]. As a consequence, several large-scale mutagenesis screens were initiated worldwide (reviewed in [115–117]).

The first large-scale ENU-based screens focused on the identification of **dominant phenotypes**, given the simpler breeding scheme required for the detection and perpetuation of dominant mutations. However, **recessive screens**, which require three generations of crosses before animals can be screened, were launched shortly afterward. Because forward genetics is a phenotype-driven approach, the establishment of reliable **phenotyping platforms** for the analysis of mutants is a must. The SHIRPA platform set the groundwork for the systematic assessment of a wide gamut of physiological and behavioral parameters [118, 119], but each project introduced its own screening protocol as based on its particular interest. In fact, individual forward mutagenesis projects focused on the identification of mutations causing particular phenotypes ranging from the identification of neurological defects to hematological conditions, behavioral anomalies, or developmental malformations (reviewed in [115, 116]). Projects also differed in their scope. Some projects run **genome-wide screens**, while others performed **focused screens** on specific areas of the genome. Focused screens were accomplished by mating mutagenized animals to mice carrying chromosomal rearrangements (deficiencies or balancer chromosomes), a strategy that allows the fast identification of mutations affecting a particular chromosome or genomic regions [120–126]. A few labs carried out **small-scale ENU screens** that, while not achieving a full saturation of the genome, proved really successful in identifying novel genes and pathways involved in specific biological processes, including embryogenesis, immunity, and neuronal development [127–135]. Other labs embarked on **sensitized screens**, mating mutagenized animals to known mutants, then screening for mutations that could either enhance or suppress their phenotypes [136, 137]. As a whole, ENU-based screens demonstrated that forward genetic

approaches, regardless of their scale, are really valuable for the unbiased discovery of genes and pathways involved in any biological process for which a reliable phenotyping method can be established.

The identification of the point mutations responsible for the phenotypes obtained in ENU screens was initially accomplished through a process known as **positional cloning** (Fig. 1.11). For this, screens used a breeding strategy that involved two different inbred strains: first, ENU was injected in mice of one strain (strain A), then these animals were mated to a different strain (strain B), and the progeny was screened for interesting phenotypes. Selected carriers for these phenotypes were then systematically outcrossed to the second strain until establishing congenic mutant lines. As a consequence of the outbreeding process, the content of DNA from strain B increases throughout the genome, except for a small chromosomal interval from the mutagenized strain (strain A) selected to carry the mutation of interest. In this way, linkage analysis to the mutagenized strain can be used to identify the chromosomal region containing the mutation. For the early pioneers of ENU mutagenesis, mapping mutations to small chromosomal intervals was extremely laborious, given the inaccuracies in linkage maps and the scarcity of polymorphic markers. Even more challenging was to identify the genes mapping to the particular chromosomal interval and to sequence candidate genes in search of ENU-induced mutations [138–140]. However, these challenges disappeared as improvements in linkage maps and in the availability of polymorphic markers, including SNPs, streamlined positional cloning. More recently, the development of next-generation sequencing methods has significantly reduced the cost of sequencing whole genomes, making it possible to sequence all transcribed sequences in samples from ENU-induced mutant animals and directly identify the causative mutations, even without the need for positional cloning [141–144].

An attractive part of ENU mutagenesis is that it introduces point mutations into DNA, and therefore, as opposed to homologous recombination or transgenesis, it can uncover hypomorphic

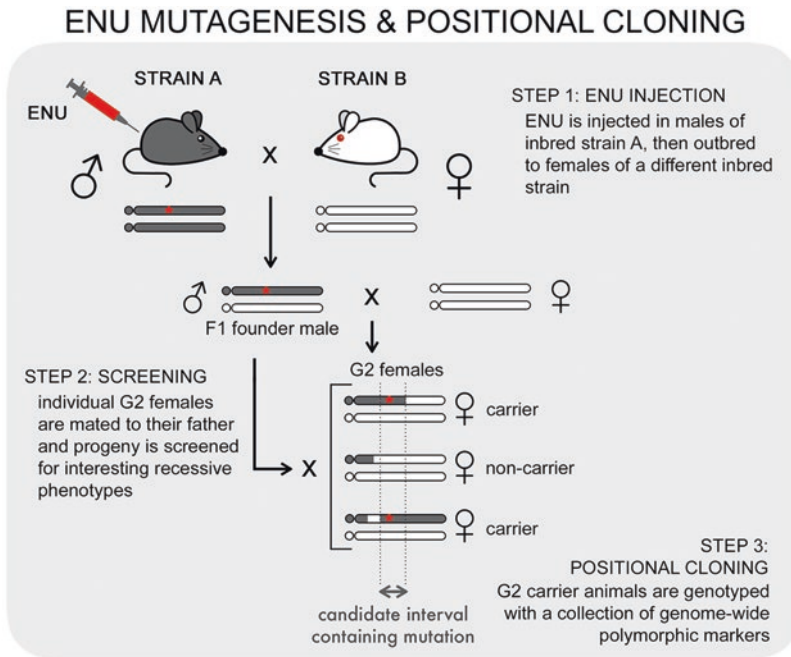


Fig. 1.11 *Large-scale ENU mutagenesis and positional cloning.* The different steps of a forward genetic chemical mutagenesis approach are illustrated for a screen aimed at identifying recessive mutations. First, a chemical mutagen, such as *N*-ethyl-*N*-nitrosourea (ENU), is injected into male mice of a particular inbred strain (strain A). Injected males are then mated to females of a different inbred strain (strain B) to propagate the germline mutations caused by ENU (red asterisk). Polymorphisms between the DNA of these inbred strains (illustrated as black and white chromosomes) will later facilitate the identification of the mutations. Males from the progeny (F1 founder males) are used to establish independent colonies and screen for interesting mutations. For this, F1 founder males are crossed to inbred females of strain B, then females from their G2 progeny are mated back to their father. The progeny from these G2 females is then screened for interesting phenotypes in embryos or adults. The logic of this breeding scheme is that if the F1 founder male is a carrier of an interesting mutation, 50% of his progeny (G2 animals) will also carry that mutation, and

when they are mated back to their father, they will produce progeny-carrying recessive traits in homozygosis. Therefore, by establishing random crosses between G2 females with their father and selecting those G2 females that produce interesting and reproducible phenotypes, a collection of G2 animals that are heterozygote carriers for the mutation can be identified. The use of different inbred strains in the breeding scheme implies that recombination in the germ line of F1 founder males (and subsequent generations) produces recombinant chromosomes that contain DNA from strains A and B. Positional cloning is based on the fact that ENU mutations will be linked to DNA originating from strain A. Therefore, DNA from selected carriers can be genotyped with a collection of genome-wide DNA polymorphic markers, and the genotype of these animals can help identify linkage of the mutation to a particular chromosomal region. Genes within this interval are candidates to contain ENU-induced mutations and can be sequenced to identify the point mutation responsible for the phenotype identified through screening

and dominant alleles, mutations more similar to those arising spontaneously in humans. ENU also has a wide spectrum of genomic targets, and although biases have been observed, including mutagenic hot spots and a preference for transcribed genomic regions [145], it can lead to the identification of genes located anywhere in the genome without prior knowledge of their exist-

tence. Consequently, the greatest advantage of ENU mutagenesis is that it provides an unbiased strategy to identify essential genes whose functions would be difficult to uncover using hypothesis-driven approaches. An example of this was the discovery of the cilium as a cellular structure required for signal transduction in mammalian cells (reviewed in [146]).

1.7.2 Gene-Trap Mutagenesis Screens

The finding that the random insertion of transgenes in the genome could disrupt gene function [66] and that the transgene insertion could facilitate the identification of the integration site [147, 148] motivated the use of transgenesis for what became known as **insertional mutagenesis**. However, as explained above, the most efficient transgenesis method initially involved pronuclear injection of exogenous DNA into fertilized oocytes, a demanding and time-consuming process that was not optimal for scaling up the generation and screening of transgene insertions. As a consequence, large-scale insertional mutagenesis was not possible until a few technical improvements came into place.

The first breakthrough that made large-scale insertional mutagenesis screens possible was the establishment of ES cells as useful platforms for transgenesis [149]. ES cells offered several advantages: first, exogenous DNA could be introduced efficiently through electroporation or retroviral infection. Second, ES cells could be grown in multiplexed platforms, facilitating the generation, screening, and characterization of new insertions. Third, transgenic ES cell lines could be kept frozen until the insertion sites could be characterized. Fourth, the identification of the insertion site for each ES cell line could be easily accomplished through procedures such as **plasmid rescue** [147] or **rapid amplification of cDNA ends** (RACE) [148], both of which used vector sequences as entry points to identify the adjacent genomic sequences. Last but not least, ES cells selected to contain interesting insertions could be injected into early blastocyst-stage embryos, allowing the analysis of the resulting chimeric embryos and/or the selection of chimeras with germ-line transmission of the transgene, ultimately making it possible to test whether the transgene insertion caused any abnormal phenotype in animals. Because of these numerous advantages, ES cells were soon adopted as platforms for large-scale insertional mutagenesis screens [150], establishing this technique as a powerful method to systematically obtain and

catalog mutations in each of the genes in the mouse genome (Fig. 1.12, upper panel).

Also critical for the success of large-scale insertional mutagenesis screens were improvements in the design of DNA vectors that could disrupt gene function with high efficiency (Fig. 1.12, lower panel; reviewed in [151]). The first vectors used for mouse insertional mutagenesis derived from plasmids originally employed for **enhancer-trap screens** in flies [152]. These enhancer-trap plasmids contained the bacterial *lacZ* reporter gene under the control of a weak promoter, plus a marker that allowed the selection of animals in which the transgene had successfully integrated into the genome. The weak promoter was insufficient for the detection of reporter gene expression, unless the plasmid integrated in the vicinity of a transcriptional regulatory element, in which case *lacZ* would be expressed with the temporal and/or spatial expression pattern dictated by the “trapped” enhancer. The use of these vectors in mice led to the identification of transgenic animals that expressed *lacZ* in a variety of tissue-specific patterns [150, 153, 154]. Similar transgenic experiments were later performed with promoter-less reporter vectors that, when inserted in frame within the exon of a gene, could simultaneously report the expression pattern of the gene and disrupt its function, either totally or partially [155]. These later **promoter-trap vectors** demonstrated a higher mutagenicity rate than enhancer-trap vectors. However, it would be a third type of vectors, called **gene-trap vectors**, that became more widely used for large-scale insertional mutagenesis screens due to their high mutagenic rate. The increased mutagenicity of gene-trap vectors relied on the presence of a splicing acceptor site in front of a promoterless *lacZ* reporter gene, followed by a strong polyadenylation signal such that, upon integration in any of the intronic sequences of a gene, the reporter would divert its normal splicing, causing protein truncations or missense transcripts, while also reporting the areas where the gene was expressed. Gene-trap vectors were not exempt from certain pitfalls, including their preference for inserting in certain genome

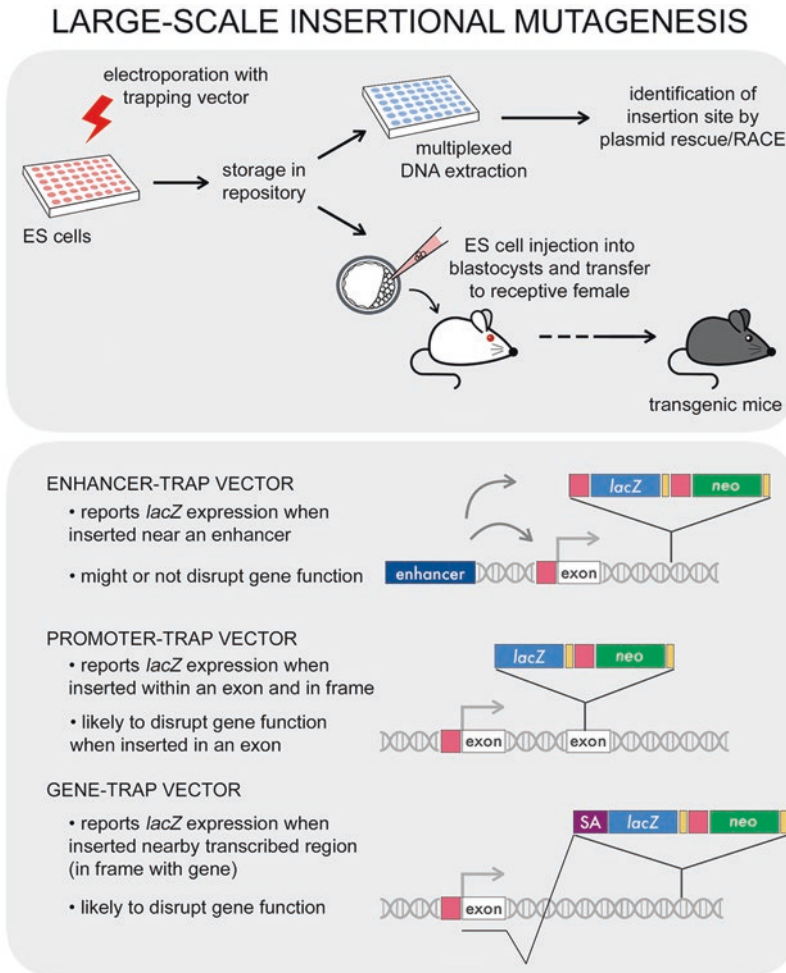


Fig. 1.12 *Large-scale insertional mutagenesis.* The possibility of electroporating vectors into ES cells opened the door to large-scale insertional mutagenesis (upper panel). After selecting for transgene insertion, ES cells can be frozen and stored until the molecular or phenotyping analysis of the insertions can be performed. The molecular characterization of the insertion site can be accomplished through plasmid rescue or RACE techniques, both of which make use of the known vector sequences to isolate the genomic areas flanking the insertion site. ES cell lines with interesting insertions can be injected into blastocysts to generate transgenic mice. All vectors contain a selection cassette that confers neomycin resistance (*neo*^r, green

box) to the ES cells that have incorporated the transgene. Other features vary among trapping vectors (lower panel). In enhancer-trap vectors, the *lacZ* reporter gene is placed downstream of a basic promoter (pink box) and upstream of a polyadenylation site (yellow box), enabling these vectors to report the expression pattern dictated by enhancers nearby the insertion site. In promoter-trap vectors, the *lacZ* reporter gene lacks a promoter and therefore can only report expression when inserted in frame within a coding sequence. In gene-trap vectors, the *lacZ* reporter is preceded by a splicing acceptor site (SA, purple box), which functions to divert the normal splicing of genes in the vicinity of the insertion site

regions [156]. However, several generations of gene-trap vectors, with increasing degrees of sophistication, were developed to bypass some of these drawbacks and to facilitate the selection of different types of insertions (reviewed in [151]).

Compared to other contemporary methods, gene-trap mutagenesis stood out as one of the most practical approaches to generating mutations in mouse genes: large-scale mutagenesis screens using chemicals were still impractical due to the hardship of identifying the genes

disrupted by the mutations, and targeted mutagenesis through homologous recombination was not yet amenable to large-scale pipelines. In contrast, gene-trap mutagenesis could be performed on ES cells in a multiplexed format, and the resulting lines could be kept frozen until the insertion sites could be further characterized. As a consequence, the use of large-scale gene-trap mutagenesis spread quickly during the mid-1980s, with multiple academic groups throughout the globe, as well as the private company Lexicon Genetics, performing screen with different vectors and diverse overall goals [147, 150, 155–166]. Together, by the early years of the twenty-first century, these initiatives contributed to trapping nearly two thirds of all genes in mice. Importantly, the public gene-trap mutagenesis efforts, united under the operational umbrella of the **International Gene Trap Consortium** (IGTC) (<https://igtc.org>), provided annotated information about each transgenic line through online databases and made frozen ES cell stocks available without restriction to investigators worldwide [167, 168].

1.7.3 The International Knockout and Phenotyping Consortia

The first drafts of the human and mouse genome sequence revealed that the total number of genes in mammalian organisms would not be as high as the 150,000 that had been initially predicted but rather be between 25,000 and 30,000 genes. This lower number raised optimism that, given the genetic tools available in mice, it would be feasible to undertake a systematic functional characterization of all the genes in the mouse genome. At the time, it was estimated that the combined efforts of the scientific community, including large-scale ENU mutagenesis screens, gene-trap insertional mutagenesis, and mouse knockouts generated by individual investigators, already accounted for functional annotations in about 5000 genes [167]. Therefore, generating mutations in an additional 20,000–25,000 genes seemed attainable. Contributing to this optimism was the fact that the scientific community was

still under the spell of the recent successes of the international genome sequencing projects and the International Gene Trap Consortium, both of which left clear that international public investments in “big science” projects can enormously facilitate scientific exploration and spark new research venues. Inspired by this positive climate, scientists worldwide initiated discussions to endorse the systematic mutagenesis of all mouse genes and to devise the best approaches to reach this goal. Pan-European discussions, sponsored by the European Commission (EC Frame Program 6), started as early as 2002 [169], and a historical international meeting, held at the Banbury Center of the Cold Spring Harbor Laboratory in September of 2003, solidified the proposal for an international resource that could generate mutations in all mouse genes and make them available to the scientific community [170]. This proposal became a reality in 2007 with the creation of the **International Knockout Mouse Consortium** (IKMC), a partnership of three different initiatives led and financed by the EU (European Conditional Mouse Mutagenesis (EUCOMM) Program, <https://www.eucomm.org>), the US (Knock Out Mouse Project (KOMP), <https://www.komp.org>), and Canada (North American Conditional Mouse Mutagenesis (NorCOMM) project, <http://www.norcomm2.org/>) [171].

From the outset, it was recognized that this ambitious enterprise will require complementary mutagenesis approaches and a coordination of all parties involved. **Large-scale gene-trap mutagenesis in ES cells** was considered the fastest and most cost-effective method to obtain gene mutations. Hence, additional gene-trap screens were launched using newest and more powerful vectors that, by including target sites for FLP and Cre recombinases, made it possible to generate conditional alleles [172]. Progress reports demonstrated the success of this strategy to obtain mutant ES cell lines [173, 174]. However, because some genes are recalcitrant to insertional mutagenesis and gene-trap strategies cannot guarantee null mutations, it was clear that targeted mutagenesis would also be needed to deliver a comprehensive catalog of mutations in

all genes [175]. Fortunately, technological innovations in bacterial recombineering [176–178], together with the introduction of robotics and computerized vector design [179], transformed the originally laborious homologous recombination protocols into streamlined high-throughput and automated processes. As a consequence, the IKMC phased out gene-trap mutagenesis and substituted this approach with automated homologous recombination ES cell pipelines [174]. These pipelines benefited from versatile new targeting vectors that, by borrowing some “tricks” from gene-trap vectors, allowed the generation of “**KO first, conditional ready**” alleles that could also report the expression pattern of the targeted genes. As a result of these combined efforts, thousands of mutant ES cell clones have become available through repositories worldwide, making it easier for individual investigators to obtain and analyze mouse mutants in their favorite genes. The number of ES cell clone requests processed by IKMC repositories attests to the impact that these resources have had in the scientific community [173].

While the first goal of the IKMC was to generate mutant ES cell lines for every gene in the genome, original discussions also recognized that the functional annotation of all of the genes in the mouse genome would also benefit from the systematic generation of live mice carrying the resulting mutations and their phenotyping through standardized tests. These second phase goals solidified in the creation of the **International Mouse Phenotyping Consortium (IMPC)** in 2010 [180]. This initiative benefited from the centers, infrastructure, and resources of the IKMC, which first used the available mutant ES cell lines to generate live mice colonies that would then be subject to standardized phenotyping. However, as of 2013, IMPC centers adopted CRISPR/Cas9 genetic engineering methods for gene targeting since this approach can be directly applied to embryos with high efficiency and specificity, bypassing the need to generate ES cell-line intermediates and, therefore, facilitating the workflow required to analyze gene function [181]. Regarding the phenotypic analysis of

mouse mutants, the IMPC benefited from the accrued experience of the European Mouse Clinics, which had been developing standardized phenotyping tests for the systematic analysis of ENU-induced mouse mutants for about a decade. Thus, initial IMPC efforts used the standardized high-throughput phenotyping pipelines defined by the European Mouse Phenotyping Resource of Standardized Screens (EMPreSS) as part of the EUMORPHIA (European Union Mouse Research for Public Health and Industrial Applications) program [182]. These pipelines include about 20 different platforms for the systematic analysis and statistical analysis of more than 400 variables relating to lethality, morphology, metabolism, skeletal and cardiovascular systems, neurobehavioral and sensory systems, hematology, biochemistry, and immunity [183, 184]. Since IMPC’s inception, additional platforms have been developed for the evaluation of additional phenotypes, such as auditory dysfunction, ophthalmic diseases, congenital disorders, and complex traits, as well as for the identification of disease susceptibility under different environmental conditions, such as diet variations or infection [185–187].

All mouse models generated by the IKMC and the IMPC are available from worldwide repositories, either as live mice or as frozen sperm or embryos. Additionally, data and conclusions from the phenotypic analysis of mouse mutants are publicly available and regularly updated at the IMPC online portal (<https://www.mousephenotype.org/>). As of the writing of this book, the last IMPC update reported that 5861 mouse genes have already been completely or partially phenotyped, resulting in 69,982 phenotype calls reported and millions of data points produced [187]. Even though the international community will still need a few more years to complete the ambitious goals established in 2007, the data so far indicate that 30% of the mutations analyzed cause embryonic lethality and, therefore, are essential for life [186, 187]. Moreover, the analysis of these data through computerized algorithms has revealed that IMPC efforts have produced mouse models for about a third of all known

human Mendelian conditions, making the IMPC catalog a critical resource for understanding the molecular and genetic basis of human diseases.

1.8 Future Perspectives

A century of research on mouse genetics has transformed fancy mice into a powerful model system for understanding human biology. From the availability of inbred strains to the sequence and functional annotation of the mouse genome, the tools and resources currently available constitute invaluable assets to the scientific community. While the research accomplishments to date are countless, we are still far from understanding how our genomes make us who we are and how mutations cause disease. Some of the mysteries still lurking in our genomes include the inheritance of complex traits, the identification of regulatory elements, as well as the mechanisms responsible for epigenetic inheritance and cellular reprogramming. Scientific advances in the areas of genomics and computational biology are already increasing the research toolbox to dissect these fascinating phenomena [188]. These and future innovations, combined with the power of mouse genetics for uncovering the functional elements of our genomes, make the future ahead nothing but exciting.

References

1. Silver LM. Mouse genetics. Oxford: Oxford University Press; 1995. 1 p.
2. Paigen K. One hundred years of mouse genetics: an intellectual history. I. The classical period (1902–1980). *Genetics*. 2003;163(1):1–7.
3. Guenet J-L, Bonhomme F. Origin of the laboratory mouse and related subspecies. The laboratory mouse: Elsevier Ltd.; 2004. 9 p.
4. Russell ES. One man's influence: a tribute to William Ernest Castle. *J Hered Narnia*. 1954;45(5):211–4.
5. Morse HCI. Origins of inbred mice [Internet]. Academic Press; 1978. 1 p. <http://www.informatics.jax.org/morsebook/frames/frame45.shtml>.
6. Beck JA, Lloyd S, Hafezparast M, Lennon-Pierce M, Eppig JT, Festing MFW, et al. Genealogies of mouse inbred strains. *Nat Genet*. 2000;24(1):23.
7. Crow JF. C. C. Little, cancer and inbred mice. *Genetics*. 2002;161(4):1357–61.
8. Klein J. George Snell's first foray into the unexplored territory of the major histocompatibility complex. *Genetics*. 2001;159:435–9.
9. Dobrovolskaia-Zavadskaia N. Sur la mortification spontanée de la queue chez la souris nouveau-née et sur l'existence d'un caractère (facteur) héréditaire "non-viable". *Contes Rendues Soc Biol Paris*. 1927;97:114–6.
10. Artzt K. Mammalian developmental genetics in the twentieth century. *Genetics*. 2012;192(4):1151–63.
11. Bennett D. Abnormalities associated with a chromosome region in the mouse. II. Embryological effects of lethal alleles in the T-region. *Science*. 1964;144(3616):263–7.
12. Morgan TH. Data for the study of sex-linked inheritance in *Drosophila*. *J Exp Zool*. 1912;13:79–101.
13. Haldane JBS, Sprunt AD, Haldane NM. Reduplication in mice (preliminary communication). *J Genet*. 1915;5(2):133–5.
14. Carter TC, Falconer DS. Stocks for detecting linkage in the mouse, and the theory of their design. *J Genet*. 1951;50(2):307–23.
15. Sturtevant AH. The linear arrangement of six sex-linked factors in *Drosophila*, as shown by their mode of association. *J Exp Zool*. 1913;14(1):43–59.
16. Snell GD. *Biology of lab mouse*; 1941. pp. 1–520.
17. Lyon MF. A personal history of the mouse genome. *Annu Rev Genome Human Genet*. 2002;3(1):1–16.
18. Painter TS. The chromosomes of rodents. *Science*. 1926;64(1657):336.
19. Miller DA, Dev VG, Tantravahi R, Miller OJ, Schiffman MB, Yates RA, et al. Cytological detection of the c-25H deletion involving the albino (c) locus on chromosome 7 in the mouse. *Genetics*. 1974;78(3):905–10.
20. Miller OJ, Miller DA. Cytogenetics of the mouse. *Annu Rev Genet*. 1975;9:285–303.
21. Eicher EM. Foundation for the future: formal genetics of the mouse. *Prog Clin Biol Res*. 1981;45:1–49.
22. Love JM, Knight AM, McAleer MA, Todd JA. Towards construction of a high resolution map of the mouse genome using PCR-analysed microsatellites. *Nucleic Acids Res*. 1990;18(14):4123–30.
23. Dietrich W, Katz H, Lincoln SE, Shin HS, Friedman J, Dracopoli NC, et al. A genetic map of the mouse suitable for typing intraspecific crosses. *Genetics*. 1992;131(2):423–47.
24. Dietrich WF, Miller J, Steen R, Merchant MA, Damron-Boles D, Husain Z, et al. A comprehensive genetic map of the mouse genome. *Nature*. 1996;380(6570):149–52.
25. Bailey DW. Recombinant-inbred strains. An aid to finding identity, linkage, and function of histocompatibility and other genes. *Transplantation*. 1971;11(3):325–7.
26. Bonhomme F, Benmehdi F, Britton-Davidian J, Martin S. [Genetic analysis of interspecific crosses *Mus musculus* L. x *Mus spretus* Lataste: linkage of *Adh-1* with *Amy-1* on chromosome 3 and *Es-14*

- with Mod-1 on chromosome 9]. *C R Acad Sci D*. 1979;289(6):545–8.
27. Avner P, Amar L, Dandolo L, Guenet JL. Genetic analysis of the mouse using interspecific crosses. *Trends Genet*. 1988;4(1):18–23.
 28. Copeland NG, Jenkins NA, Gilbert DJ, Eppig JT, Maltais LJ, Miller JC, et al. A genetic linkage map of the mouse: current applications and future prospects. *Science*. 1993;262(5130):57–66.
 29. Saunders TL. A survey of internet resources for mouse development. *Methods Enzymol*. 2010;476:3–21.
 30. de Boer P, Groen A. Fertility and meiotic behavior of male T70H tertiary trisomics of the mouse (*Mus musculus*). A case of preferential telomeric meiotic pairing in a mammal. *Cytogenet Cell Genet*. 1974;13(6):489–510.
 31. Steinmetz M, Uematsu Y, Lindahl KF. Hotspots of homologous recombination in mammalian genome. *Trends Genet*. 1987;3:7–10.
 32. Seldin MF, Howard TA, D'Eustachio P. Comparison of linkage maps of mouse chromosome 12 derived from laboratory strain intraspecific and *Mus spretus* interspecific backcrosses. *Genomics*. 1989;5(1):24–8.
 33. Reeves RH, Crowley MR, Moseley WS, Seldin MF. Comparison of interspecific to intersubspecific backcrosses demonstrates species and sex differences in recombination frequency on mouse chromosome 16. *Mamm Genome*. 1991;1(3):158–64.
 34. Mouse Genome Sequencing Consortium, Waterston RH, Lindblad-Toh K, Birney E, Rogers J, Abril JF, et al. Initial sequencing and comparative analysis of the mouse genome. *Nature*. 2002;420(6915):520–62.
 35. Morange M, Cobb M. A history of molecular biology. Cambridge: Harvard University Press; 2000. 1 p.
 36. Judson HF. The eighth day of creation; 2004. 1 p.
 37. Attwood TK, Gisel A, Bongcam-Rudloff E, Eriksson N-E. Concepts, historical milestones and the central place of bioinformatics in modern biology: a European perspective; 2011.
 38. Maniatis T, Fritsch EF, Sambrook J. *Molecular cloning*; 1982. 1 p.
 39. Gall JG, Pardue ML. Formation and detection of RNA-DNA hybrid molecules in cytological preparations. *Proc Natl Acad Sci U S A*. 1969;63(2):378–83.
 40. Gall JG. The origin of in situ hybridization—a personal history. *Methods*. 2016;98:4–9.
 41. Gene Ontology Consortium. The gene ontology project in 2008. *Nucleic Acids Res*. 2008;36(Database issue):D440–4.
 42. Russell LB. The mouse house: a brief history of the ORNL mouse-genetics program, 1947–2009. *Mutat Res*. 2013;753(2):69–90.
 43. Nakagata N. Cryopreservation of mouse spermatozoa. *Mamm Genome*. 2000;11(7):572–6.
 44. Szein JM, Takeo T, Nakagata N. History of cryobiology, with special emphasis in evolution of mouse sperm cryopreservation. *Cryobiology*. 2018;82:57–63.
 45. Whittingham DG, Leibo SP, Mazur P. Survival of mouse embryos frozen to –196 degrees and –269 degrees C. *Science*. 1972;178(4059):411–4.
 46. Jaenisch R. Germ line integration and Mendelian transmission of the exogenous Moloney leukemia virus. *Proc Natl Acad Sci U S A*. 1976;73(4):1260–4.
 47. Brinster RL, Chen HY, Trumbauer ME, Avarbock MR. Translation of globin messenger RNA by the mouse ovum. *Nature*. 1980;283(5746):499–501.
 48. Gordon JW, Ruddle FH. Integration and stable germ line transmission of genes injected into mouse pronuclei. *Science*. 1981;214(4526):1244–6.
 49. Nagy A, Behringer RR, Gertsenstein M, Vintersten K. *Manipulating the mouse embryo: a laboratory manual*. 3rd ed. New York: Cold Spring Harbor Laboratory Press; 2003.
 50. Gordon JW, Scangos GA, Plotkin DJ, Barbosa JA, Ruddle FH. Genetic transformation of mouse embryos by microinjection of purified DNA. *Proc Natl Acad Sci U S A*. 1980;77(12):7380–4.
 51. Brinster RL, Chen HY, Trumbauer M, Senear AW, Warren R, Palmiter RD. Somatic expression of herpes thymidine kinase in mice following injection of a fusion gene into eggs. *Cell*. 1981;27(1 Pt 2):223–31.
 52. Costantini F, Lacy E. Introduction of a rabbit beta-globin gene into the mouse germ line. *Nature*. 1981;294(5836):92–4.
 53. Wagner TE, Hoppe PC, Jollick JD, Scholl DR, Hodinka RL, Gault JB. Microinjection of a rabbit beta-globin gene into zygotes and its subsequent expression in adult mice and their offspring. *Proc Natl Acad Sci U S A*. 1981;78(10):6376–80.
 54. Wagner EF, Stewart TA, Mintz B. The human beta-globin gene and a functional viral thymidine kinase gene in developing mice. *Proc Natl Acad Sci U S A*. 1981;78(8):5016–20.
 55. Niemann H, Kues W, Carnwath JW. Transgenic farm animals: present and future. *Rev Sci Tech*. 2005;24(1):285–98.
 56. Lewandoski M. Conditional control of gene expression in the mouse. *Nat Rev Genet*. 2001;2(10):743–55.
 57. Hanahan D. Transgenic mice as probes into complex systems. *Science*. 1989;246(4935):1265–75.
 58. Stacey A, Bateman J, Choi T, Mascara T, Cole W, Jaenisch R. Perinatal lethal osteogenesis imperfecta in transgenic mice bearing an engineered mutant pro-alpha 1(I) collagen gene. *Nature*. 1988;332(6160):131–6.
 59. Readhead C, Popko B, Takahashi N, Shine HD, Saavedra RA, Sidman RL, et al. Expression of a myelin basic protein gene in transgenic shiverer mice: correction of the dysmyelinating phenotype. *Cell*. 1987;48(4):703–12.
 60. Lo CW, Coulling M, Kirby C. Tracking of mouse cell lineage using microinjected DNA sequences: analyses using genomic Southern blotting and

- tissue-section in situ hybridizations. *Differentiation*. 1987;35(1):37–44.
61. Goring DR, Rossant J, Clapoff S, Breitman ML, Tsui LC. In situ detection of beta-galactosidase in lenses of transgenic mice with a gamma-crystallin/lacZ gene. *Science*. 1987;235(4787):456–8.
 62. Okabe M, Ikawa M, Kominami K, Nakanishi T, Nishimune Y. “Green mice” as a source of ubiquitous green cells. *FEBS Lett*. 1997;407(3):313–9.
 63. Palmiter RD, Behringer RR, Quaife CJ, Maxwell F, Maxwell IH, Brinster RL. Cell lineage ablation in transgenic mice by cell-specific expression of a toxin gene. *Cell*. 1987;50(3):435–43.
 64. Jaenisch R. Transgenic animals. *Science*. 1988;240(4858):1468–74.
 65. Palmiter RD, Brinster RL. Germ-line transformation of mice. *Annu Rev Genet*. 1986;20(1):465–99.
 66. Soriano P, Gridley T, Jaenisch R. Retroviruses and insertional mutagenesis in mice: proviral integration at the *Mov 34* locus leads to early embryonic death. *Genes Dev*. 1987;1(4):366–75.
 67. Evans MJ, Kaufman MH. Establishment in culture of pluripotential cells from mouse embryos. *Nature*. 1981;292(5819):154–6.
 68. Martin GR. Isolation of a pluripotent cell line from early mouse embryos cultured in medium conditioned by teratocarcinoma stem cells. *Proc Natl Acad Sci U S A*. 1981;78(12):7634–8.
 69. Bradley A, Evans M, Kaufman MH, Robertson E. Formation of germ-line chimaeras from embryo-derived teratocarcinoma cell lines. *Nature*. 1984;309(5965):255–6.
 70. Robertson E, Bradley A, Kuehn M, Evans M. Germ-line transmission of genes introduced into cultured pluripotential cells by retroviral vector. *Nature*. 1986;323(6087):445–8.
 71. Gossler A, Doetschman T, Korn R, Serfling E, Kemler R. Transgenesis by means of blastocyst-derived embryonic stem cell lines. *Proc Natl Acad Sci U S A*. 1986;83(23):9065–9.
 72. Doetschman T, Gregg RG, Maeda N, Hooper ML, Melton DW, Thompson S, et al. Targetted correction of a mutant *HPRT* gene in mouse embryonic stem cells. *Nature*. 1987;330(6148):576–8.
 73. Thomas KR, Capecchi MR. Site-directed mutagenesis by gene targeting in mouse embryo-derived stem cells. *Cell*. 1987;51(3):503–12.
 74. Thompson S, Clarke AR, Pow AM, Hooper ML, Melton DW. Germ line transmission and expression of a corrected *HPRT* gene produced by gene targeting in embryonic stem cells. *Cell*. 1989;56(2):313–21.
 75. Schwartzberg PL, Goff SP, Robertson EJ. Germ-line transmission of a *c-abl* mutation produced by targeted gene disruption in ES cells. *Science*. 1989;246(4931):799–803.
 76. Thomas KR, Capecchi MR. Targetted disruption of the murine *int-1* proto-oncogene resulting in severe abnormalities in midbrain and cerebellar development. *Nature*. 1990;346(6287):847–50.
 77. Zijlstra M, Li E, Sajjadi F, Subramani S, Jaenisch R. Germ-line transmission of a disrupted beta 2-microglobulin gene produced by homologous recombination in embryonic stem cells. *Nature*. 1989;342(6248):435–8.
 78. Koller BH, Hagemann LJ, Doetschman T, Hagaman JR, Huang S, Williams PJ, et al. Germ-line transmission of a planned alteration made in a hypoxanthine phosphoribosyltransferase gene by homologous recombination in embryonic stem cells. *Proc Natl Acad Sci U S A*. 1989;86(22):8927–31.
 79. Babinet C, Cohen-Tannoudji M. Genome engineering via homologous recombination in mouse embryonic stem (ES) cells: an amazingly versatile tool for the study of mammalian biology. *An Acad Bras Cienc*. 2001;73(3):365–83.
 80. Paigen K. One hundred years of mouse genetics: an intellectual history. II. The molecular revolution (1981–2002). *Genetics*. *Genet Soc Am*. 2003;163(4):1227–35.
 81. Hall B, Limaye A, Kulkarni AB. Overview: generation of gene knockout mice. *Curr Protoc Cell Biol*. 2009; Chapter 19(1):Unit19.12.1–17.
 82. Nagy A. Cre recombinase: the universal reagent for genome tailoring. *Genesis*. 2000;26(2):99–109.
 83. Yu Y, Bradley A. Engineering chromosomal rearrangements in mice. *Nat Rev Genet*. 2001;2(10):780–90.
 84. Gaj T, Gersbach CA, Barbas CF. ZFN, TALEN, and CRISPR/Cas-based methods for genome engineering. *Trends Biotechnol*. 2013;31(7):397–405.
 85. Makarova KS, Haft DH, Barrangou R, Brouns SJJ, Charpentier E, Horvath P, et al. Evolution and classification of the CRISPR-Cas systems. *Nat Rev Micro*. 2011;9(6):467–77.
 86. Lander ES. The heroes of CRISPR. *Cell*. 2016;164(1–2):18–28.
 87. Cong L, Ran FA, Cox D, Lin S, Barretto R, Habib N, et al. Multiplex genome engineering using CRISPR/Cas systems. *Science*. 2013;339(6121):819–23.
 88. Jinek M, East A, Cheng A, Lin S, Ma E, Doudna J. RNA-programmed genome editing in human cells. *Elife*. 2013;2:e00471.
 89. Singh P, Schimenti JC, Bolcun-Filas E. A mouse geneticist’s practical guide to CRISPR applications. *Genetics*. 2015;199(1):1–15.
 90. Shen B, Zhang J, Wu H, Wang J, Ma K, Li Z, et al. Generation of gene-modified mice via Cas9/RNA-mediated gene targeting. *Cell Res*. 2013;23(5):720–3.
 91. Wang H, Yang H, Shivalila CS, Dawlaty MM, Cheng AW, Zhang F, et al. One-step generation of mice carrying mutations in multiple genes by CRISPR/Cas-mediated genome engineering. *Cell*. 2013;153(4):910–8.
 92. Yang H, Wang H, Shivalila CS, Cheng AW, Shi L, Jaenisch R. One-step generation of mice carrying reporter and conditional alleles by CRISPR/Cas-mediated genome engineering. *Cell*. 2013;154(6):1370–9.

93. Modzelewski AJ, Chen S, Willis BJ, Lloyd KCK, Wood JA, He L. Efficient mouse genome engineering by CRISPR-EZ technology. *Nat Protoc.* 2018;13(6):1253–74.
94. Yang H, Wang H, Jaenisch R. Generating genetically modified mice using CRISPR/Cas-mediated genome engineering. *Nat Protoc.* 2014;9(8):1956–68.
95. Fujii W, Kawasaki K, Sugiura K, Naito K. Efficient generation of large-scale genome-modified mice using gRNA and CAS9 endonuclease. *Nucleic Acids Res.* 2013;41:e187–e187.
96. Qi LS, Larson MH, Gilbert LA, Doudna JA, Weissman JS, Arkin AP, et al. Repurposing CRISPR as an RNA-guided platform for sequence-specific control of gene expression. *Cell.* 2013;152(5):1173–83.
97. Gilbert LA, Larson MH, Morsut L, Liu Z, Brar GA, Torres SE, et al. CRISPR-mediated modular RNA-guided regulation of transcription in eukaryotes. *Cell.* 2013;154(2):442–51.
98. Cheng AW, Wang H, Yang H, Shi L, Katz Y, Theunissen TW, et al. Multiplexed activation of endogenous genes by CRISPR-on, an RNA-guided transcriptional activator system. *Cell Res.* 2013;23(10):1163–71.
99. National Research Council, Studies DOEAL, Sciences COL, Genome COMASTH. Mapping and sequencing the human genome. National Academies Press; 1988. 1 p.
100. Lander ES, Linton LM, Birren B, Nusbaum C, Zody MC, Baldwin J, et al. Initial sequencing and analysis of the human genome. *Nature.* 2001;409(6822):860–921.
101. Venter JC, Adams MD, Myers EW, Li PW, Mural RJ, Sutton GG, et al. The sequence of the human genome. *Science.* 2001;291(5507):1304–51.
102. Ferry G, Sulston J. The common thread. Washington, DC: Joseph Henry Press; 2002. 1 p
103. Cook-Deegan RM. The gene wars. New York: W. W. Norton & Company; 1996. 1 p
104. Lindblad-Toh K, Winchester E, Daly MJ, Wang DG, Hirschhorn JN, Lavolette JP, et al. Large-scale discovery and genotyping of single-nucleotide polymorphisms in the mouse. *Nat Genet.* 2000;24(4):381–6.
105. Frazer KA, Eskin E, Kang HM, Bogue MA, Hinds DA, Beilharz EJ, et al. A sequence-based variation map of 8.27 million SNPs in inbred mouse strains. *Nature.* 2007;448(7157):1050–3.
106. Adams DJ, Doran AG, Lilue J, Keane TM. The Mouse Genomes Project: a repository of inbred laboratory mouse strain genomes. *Mamm Genome.* 2015;26(9–10):403–12.
107. Russell WL, Kelly EM, Hunsicker PR, Bangham JW, Maddux SC, Phipps EL. Specific-locus test shows ethylnitrosourea to be the most potent mutagen in the mouse. *Proc Natl Acad Sci U S A.* 1979;76(11):5818–9.
108. Nüsslein-Volhard C, Wieschaus E. Mutations affecting segment number and polarity in *Drosophila*. *Nature.* 1980;287(5785):795–801.
109. Bode VC. Ethylnitrosourea mutagenesis and the isolation of mutant alleles for specific genes located in the T region of mouse chromosome 17. *Genetics.* 1984;108(2):457–70.
110. Shedlovsky A, Guenet JL, Johnson LL, Dove WF. Induction of recessive lethal mutations in the T/t-H-2 region of the mouse genome by a point mutagen. *Genet Res.* 1986;47(2):135–42.
111. Vitaterna MH, King DP, Chang AM, Kornhauser JM, Lowrey PL, McDonald JD, et al. Mutagenesis and mapping of a mouse gene, Clock, essential for circadian behavior. *Science.* 1994;264(5159):719–25.
112. Moser AR, Pitot HC, Dove WF. A dominant mutation that predisposes to multiple intestinal neoplasia in the mouse. *Science.* 1990;247(4940):322–4.
113. King DP, Zhao Y, Sangoram AM, Wilsbacher LD, Tanaka M, Antoch MP, et al. Positional cloning of the mouse circadian clock gene. *Cell.* 1997;89(4):641–53.
114. Su LK, Kinzler KW, Vogelstein B, Preisinger AC, Moser AR, Luongo C, et al. Multiple intestinal neoplasia caused by a mutation in the murine homolog of the APC gene. *Science.* 1992;256(5057):668–70.
115. Justice MJ, Noveroske JK, Weber JS, Zheng B, Bradley A. Mouse ENU mutagenesis. *Hum Mol Genet.* 1999;8(10):1955–63.
116. Clark AT, Goldowitz D, Takahashi JS, Vitaterna MH, Siepka SM, Peters LL, et al. Implementing large-scale ENU mutagenesis screens in North America. *Genetica.* 2004;122(1):51–64.
117. Gondo Y. Trends in large-scale mouse mutagenesis: from genetics to functional genomics. *Nat Rev Genet.* 2008;9(10):803–10.
118. Rogers DC, Fisher EM, Brown SD, Peters J, Hunter AJ, Martin JE. Behavioral and functional analysis of mouse phenotype: SHIRPA, a proposed protocol for comprehensive phenotype assessment. *Mamm Genome.* 1997;8(10):711–3.
119. Hrabé de Angelis MH, Flawsinkel H, Fuchs H, Rathkolb B, Soewarto D, Marschall S, et al. Genome-wide, large-scale production of mutant mice by ENU mutagenesis. *Nat Genet.* 2000;25(4):444–7.
120. Rinchik EM, Carpenter DA. N-ethyl-N-nitrosourea mutagenesis of a 6- to 11-cM subregion of the Fah-Hbb interval of mouse chromosome 7: completed testing of 4557 gametes and deletion mapping and complementation analysis of 31 mutations. *Genetics.* 1999;152(1):373–83.
121. Schimenti J, Bucan M. Functional genomics in the mouse: phenotype-based mutagenesis screens. *Genome Res.* 1998;8(7):698–710.
122. Justice MJ, Zheng B, Woychik RP, Bradley A. Using targeted large deletions and high-efficiency N-ethyl-N-nitrosourea mutagenesis for functional analyses of the mammalian genome. *Methods.* 1997;13(4):423–36.
123. Kile BT, Hentges KE, Clark AT, Nakamura H, Salinger AP, Liu B, et al. Functional genetic analysis of mouse chromosome 11. *Nature.* 2003;425(6953):81–6.

124. Hagge-Greenberg A, Snow P, O'Brien TP. Establishing an ENU mutagenesis screen for the piebald region of mouse chromosome 14. *Mamm Genome*. 2001;12(12):938–41.
125. Boles MK, Wilkinson BM, Maxwell A, Lai L, Mills AA, Nishijima I, et al. A mouse chromosome 4 balancer ENU-mutagenesis screen isolates eleven lethal lines. *BMC Genet*. 2009;10(1):12.
126. Ching Y-H, Munroe RJ, Moran JL, Barker AK, Mauceli E, Fennell T, et al. High resolution mapping and positional cloning of ENU-induced mutations in the *Rw* region of mouse chromosome 5. *BMC Genet*. 2010;11(1):106.
127. Kasarskis A, Manova K, Anderson KV. A phenotype-based screen for embryonic lethal mutations in the mouse. *Proc Natl Acad Sci U S A*. 1998;95(13):7485–90.
128. Herron BJ, Lu W, Rao C, Liu S, Peters H, Bronson RT, et al. Efficient generation and mapping of recessive developmental mutations using ENU mutagenesis. *Nat Genet*. 2002;30(2):185–9.
129. Zarbalis K, May SR, Shen Y, Ekker M, Rubenstein JLR, Peterson AS. A focused and efficient genetic screening strategy in the mouse: identification of mutations that disrupt cortical development. *PLoS Biol*. 2004;2(8):E219. Joshua R Sanes, editor. Public Library of Science.
130. Hoebe K, Beutler B. Unraveling innate immunity using large scale N-ethyl-N-nitrosourea mutagenesis. *Tissue Antigens*. 2005;65(5):395–401.
131. García-García MJ, Eggenschwiler JT, Caspary T, Alcorn HL, Wyler MR, Huangfu D, et al. Analysis of mouse embryonic patterning and morphogenesis by forward genetics. *Proc Natl Acad Sci U S A*. 2005;102(17):5913–9.
132. Papanthasiou P, Goodnow CC. Connecting mammalian genome with phenome by ENU mouse mutagenesis: gene combinations specifying the immune system. *Annu Rev Genet*. 2005;39(1):241–62.
133. Stottmann RW, Moran JL, Turbe-Doan A, Driver E, Kelley M, Beier DR. Focusing forward genetics: a tripartite ENU screen for neurodevelopmental mutations in the mouse. *Genetics*. 2011;188(3):615–24.
134. Ha S, Stottmann RW, Furley AJ, Beier DR. A forward genetic screen in mice identifies mutants with abnormal cortical patterning. *Cereb Cortex*. 2015;25(1):167–79.
135. Hentges K, Thompson K, Peterson A. The flat-top gene is required for the expansion and regionalization of the telencephalic primordium. *Development*. 1999;126(8):1601–9.
136. Rubio-Aliaga I, Soewarto D, Wagner S, Klafthen M, Fuchs H, Kalaydjiev S, et al. A genetic screen for modifiers of the *delta1*-dependent notch signaling function in the mouse. *Genetics*. 2007;175(3):1451–63.
137. Matera I, Watkins-Chow DE, Loftus SK, Hou L, Incao A, Silver DL, et al. A sensitized mutagenesis screen identifies *Gli3* as a modifier of *Sox10* neuro-cristopathy. *Hum Mol Genet*. 2008;17(14):2118–31.
138. Horner VL, Caspary T. Creating a “hopeful monster”: mouse forward genetic screens. *Methods Mol Biol*. 2011;770:313–36.
139. Caspary T. Chapter 16—phenotype-driven mouse ENU mutagenesis screen. In: *Guide to techniques in mouse development, part B: mouse molecular genetics*, 2nd ed., vol. 477. Elsevier Inc.; 2010. 15 p.
140. Stottmann RW, Beier DR. Using ENU mutagenesis for phenotype-driven analysis of the mouse. *Meth Enzymol*. 2010;477:329–48.
141. Moresco EMY, Li X, Beutler B. Going forward with genetics. *Am J Pathol*. 2013;182(5):1462–73.
142. Sun M, Mondal K, Patel V, Horner VL, Long AB, Cutler DJ, et al. Multiplex chromosomal exome sequencing accelerates identification of ENU-induced mutations in the mouse. *G3 (Bethesda)*. 2012;2(1):143–50.
143. Gallego-Llamas J, Timms AE, Geister KA, Lindsay A, Beier DR. Variant mapping and mutation discovery in inbred mice using next-generation sequencing. *BMC Genomics*. 2015;16(1):913.
144. Geister KA, Timms AE, Beier DR. Optimizing genomic methods for mapping and identification of candidate variants in ENU mutagenesis screens using inbred mice. *G3 (Bethesda)*. 2018;8(2):401–9.
145. Takahasi KR, Sakuraba Y, Gondo Y. Mutational pattern and frequency of induced nucleotide changes in mouse ENU mutagenesis. *BMC Mol Biol*. 2007;8(1):52.
146. Eggenschwiler JT, Anderson KV. Cilia and developmental signaling. *Annu Rev Cell Dev Biol*. 2007;23(1):345–73.
147. Hicks GG, Shi EG, Li XM, Li CH, Pawlak M, Ruley HE. Functional genomics in mice by tagged sequence mutagenesis. *Nat Genet*. 1997;16(4):338–44.
148. Townley DJ, Avery BJ, Rosen B, Skarnes WC. Rapid sequence analysis of gene trap integrations to generate a resource of insertional mutations in mice. *Genome Res*. 1997;7(3):293–8.
149. Lovell-Badge RH, Bygrave AE, Bradley A, Robertson E, Evans MJ, Cheah KS. Transformation of embryonic stem cells with the human type-II collagen gene and its expression in chimeric mice. *Cold Spring Harb Symp Quant Biol*. 1985;50:707–11.
150. Gossler A, Joyner AL, Rossant J, Skarnes WC. Mouse embryonic stem cells and reporter constructs to detect developmentally regulated genes. *Science*. 1989;244(4903):463–5.
151. Stanford WL, Cohn JB, Cordes SP. Gene-trap mutagenesis: past, present and beyond. *Nat Rev Genet*. 2001;2(10):756–68.
152. O’Kane CJ, Gehring WJ. Detection in situ of genomic regulatory elements in *Drosophila*. *Proc Natl Acad Sci U S A*. 1987;84(24):9123–7.
153. Allen ND, Cran DG, Barton SC, Hettle S, Reik W, Surani MA. Transgenes as probes for active chromosomal domains in mouse development. *Nature*. 1988;333(6176):852–5.
154. Kothary R, Clapoff S, Brown A, Campbell R, Peterson A, Rossant J. A transgene containing *lacZ*

- inserted into the dystonia locus is expressed in neural tube. *Nature*. 1988;335(6189):435–7.
155. Friedrich G, Soriano P. Promoter traps in embryonic stem cells: a genetic screen to identify and mutate developmental genes in mice. *Genes Dev*. 1991;5(9):1513–23.
156. Hansen J, Floss T, Van Sloun P, Füchtbauer E-M, Vauti F, Arnold H-H, et al. A large-scale, gene-driven mutagenesis approach for the functional analysis of the mouse genome. *Proc Natl Acad Sci U S A*. 2003;100(17):9918–22.
157. Skarnes WC, Auerbach BA, Joyner AL. A gene trap approach in mouse embryonic stem cells: the lacZ reported is activated by splicing, reflects endogenous gene expression, and is mutagenic in mice. *Genes Dev*. 1992;6(6):903–18.
158. Niwa H, Araki K, Kimura S, Taniguchi S, Wakasugi S, Yamamura K. An efficient gene-trap method using poly A trap vectors and characterization of gene-trap events. *J Biochem*. 1993;113(3):343–9.
159. Skarnes WC, Moss JE, Hurtley SM, Beddington RS. Capturing genes encoding membrane and secreted proteins important for mouse development. *Proc Natl Acad Sci U S A*. 1995;92(14):6592–6.
160. Wurst W, Rossant J, Prideaux V, Kownacka M, Joyner A, Hill DP, et al. A large-scale gene-trap screen for insertional mutations in developmentally regulated genes in mice. *Genetics*. 1995;139(2):889–99.
161. Salminen M, Meyer BI, Gruss P. Efficient poly A trap approach allows the capture of genes specifically active in differentiated embryonic stem cells and in mouse embryos. *Dev Dyn*. 1998;212(2):326–33.
162. Zambrowicz BP, Friedrich GA, Buxton EC, Lilleberg SL, Person C, Sands AT. Disruption and sequence identification of 2,000 genes in mouse embryonic stem cells. *Nature*. 1998;392(6676):608–11.
163. Araki K, Imaizumi T, Sekimoto T, Yoshinobu K, Yoshimuta J, Akizuki M, et al. Exchangeable gene trap using the Cre/mutated lox system. *Cell Mol Biol (Noisy-le-grand)*. 1999;45(5):737–50.
164. Wiles MV, Vauti F, Otte J, Füchtbauer EM, Ruiz P, Füchtbauer A, et al. Establishment of a gene-trap sequence tag library to generate mutant mice from embryonic stem cells. *Nat Genet*. 2000;24(1):13–4.
165. Hardouin N, Nagy A. Gene-trap-based target site for cre-mediated transgenic insertion. *Genesis*. 2000;26(4):245–52.
166. Stryke D. BayGenomics: a resource of insertional mutations in mouse embryonic stem cells. *Nucleic Acids Res*. 2003;31(1):278–81.
167. The International Mouse Mutagenesis Consortium, Nadeau JH, Balling R, Barsh G, Beier D, SDM B, et al. Functional annotation of mouse genome sequences. *Science*. 2001;291(5507):1251–5.
168. Skarnes WC, von Melchner H, Wurst W, Hicks G, Nord AS, Cox T, et al. A public gene trap resource for mouse functional genomics. *Nat Genet*. 2004;36(6):543–4.
169. Auwerx J, Avner P, Baldock R, Ballabio A, Balling R, Barbacid M, et al. The European dimension for the mouse genome mutagenesis program. *Nat Genet*. 2004;36(9):925–7.
170. Austin CP, Battey JF, Bradley A, Bucan M, Capecchi M, Collins FS, et al. The knockout mouse project. *Nat Genet*. 2004;36(9):921–4.
171. International Mouse Knockout Consortium, Collins FS, Rossant J, Wurst W. A mouse for all reasons. *Cell*. 2007;128(1):9–13.
172. Schnütgen F, De-Zolt S, Van Sloun P, Hollatz M, Floss T, Hansen J, et al. Genomewide production of multipurpose alleles for the functional analysis of the mouse genome. *Proc Natl Acad Sci U S A*. 2005;102(20):7221–6.
173. Lloyd KCK. A knockout mouse resource for the biomedical research community. *Ann N Y Acad Sci*. 2011;1245(1):24–6.
174. Bradley A, Anastassiadis K, Ayadi A, Battey JF, Bell C, Birling M-C, et al. The mammalian gene function resource: the International Knockout Mouse Consortium. *Mamm Genome*. 2012;23(9–10):580–6.
175. Friedel RH, Seisenberger C, Kaloff C, Wurst W. EUCOMM the European conditional mouse mutagenesis program. *Brief Funct Genomic Proteomic*. 2007;6(3):180–5.
176. Angrand PO, Daigle N, van der Hoeven F, Schöler HR, Stewart AF. Simplified generation of targeting constructs using ET recombination. *Nucleic Acids Res*. 1999;27(17):e16.
177. Zhang Y, Buchholz F, Muyrers JP, Stewart AF. A new logic for DNA engineering using recombination in *Escherichia coli*. *Nat Genet*. 1998;20(2):123–8.
178. Copeland NG, Jenkins NA, Court DL. Recombineering: a powerful new tool for mouse functional genomics. *Nat Rev Genet*. 2001;2(10):769–79.
179. Valenzuela DM, Murphy AJ, Frendewey D, Gale NW, Economides AN, Auerbach W, et al. High-throughput engineering of the mouse genome coupled with high-resolution expression analysis. *Nat Biotechnol*. 2003;21(6):652–9.
180. Abbott A. Mouse project to find each gene's role. *Nature*. 2010;465(7297):410.
181. Lanza DG, Gaspero A, Lorenzo I, Liao L, Zheng P, Wang Y, et al. Comparative analysis of single-stranded DNA donors to generate conditional null mouse alleles. *BMC Biol*. 2018;16(1):69.
182. Brown SDM, Chambon P, de Angelis MH, Eumorphia Consortium. EMPReSS: standardized phenotype screens for functional annotation of the mouse genome. *Nat Genet*. 2005;37(11):1155.
183. Brown SDM, Moore MW. The International Mouse Phenotyping Consortium: past and future perspectives on mouse phenotyping. *Mamm Genome*. 2012;23(9–10):632–40.
184. de Angelis MH, Nicholson G, Selloum M, White J, Morgan H, Ramirez-Solis R, et al. Analysis of mammalian gene function through broad-based phenotypic screens across a consortium of mouse clinics. *Nature*. 2015;47(9):969–78.

185. Ayadi A, Birling M-C, Bottomley J, Bussell J, Fuchs H, Fray M, et al. Mouse large-scale phenotyping initiatives: overview of the European Mouse Disease Clinic (EUMODIC) and of the Wellcome Trust Sanger Institute Mouse Genetics Project. *Mamm Genome*. 2012;23(9–10):600–10.
186. Meehan TF, Conte N, West DB, Jacobsen JO, Mason J, Warren J, et al. Disease model discovery from 3328 gene knockouts by The International Mouse Phenotyping Consortium. *Nature*. 2017;49(8):1231–8.
187. Cacheiro P, Haendel MA, Smedley D, Meehan T, Mason J, Mashhadi HH, et al. New models for human disease from the International Mouse Phenotyping Consortium. *Mamm Genome*. 2019;30(5–6):143–50.
188. ENCODE Project Consortium. The ENCODE (ENCyclopedia Of DNA Elements) Project. *Science*. 2004;306(5696):636–40.



Mouse Models of Neural Tube Defects

2

Irene E. Zohn

2.1 Overview

During embryonic development, the central nervous system forms as the neural plate and then rolls into a tube in a complex morphogenetic process known as neurulation. Neural tube defects (NTDs) occur when neurulation fails and are among the most common structural birth defects in humans. The frequency of NTDs varies greatly anywhere from 0.5 to 10 in 1000 live births, depending on the genetic background of the population, as well as a variety of environmental factors [1–3]. The prognosis varies depending on the size and placement of the lesion and ranges from death to severe or moderate disability, and some NTDs are asymptomatic. This chapter reviews how mouse models have contributed to the elucidation of the genetic, molecular, and cellular basis of neural tube closure, as well as to our understanding of the causes and prevention of this devastating birth defect.

2.2 Types of NTDs

The neural tube initially forms as a flat epithelial plate that must roll into a tube to form the brain and spinal cord. Defects in this process result in NTDs, a constellation of malformations of the central nervous system (Fig. 2.1). The most common NTD in humans is spina bifida, which results from failure of closure in the spinal region. The consequence of spina bifida varies greatly, depending on the size and placement of the lesion, the involvement of the spinal nerves and meninges, as well as the presence of associated conditions such as hydrocephalus, Chiari malformation, genitourinary, and gastrointestinal disorders. Spina bifida can manifest as myelomeningocele, meningocele, or spina bifida occulta. Myelomeningocele is the most common and severe form of spina bifida and involves protrusion of the meninges and spinal cord through an opening in the vertebrae. Meningocele occurs when the meninges but not the spinal cord protrude. Spina bifida occulta can be asymptomatic and occurs when the dorsal part of vertebrae does not properly form. More severe open NTDs include craniorachischisis and anencephaly. Craniorachischisis is the most serious NTD, resulting from failure of neural tube closure along the entire neural plate. Exencephaly (the embryonic precursor to anencephaly) occurs when closure fails in the anterior neural plate or future brain. Anencephaly and craniorachischisis

I. E. Zohn (✉)
Center for Genetic Medicine, Children's Research
Institute, Children's National Medical Center,
Washington, DC, USA
e-mail: IZohn@childrensnational.org

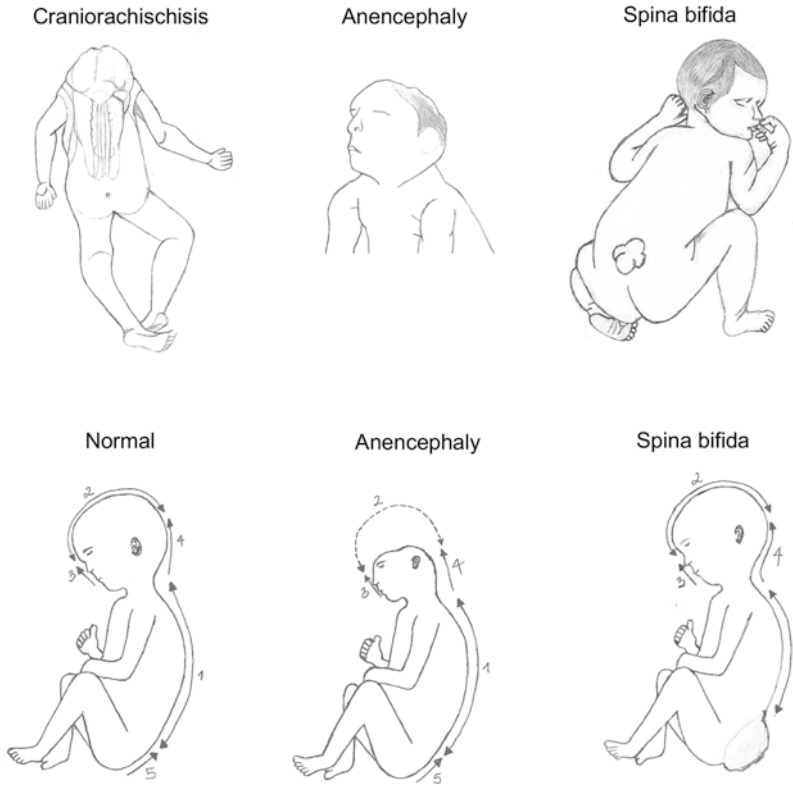


Fig. 2.1 Top panels. Types of neural tube defects that originate from failure of neural tube closure. Craniorachischisis occurs when the neural tube fails to close along the entire length of the neural plate. Anencephaly occurs when closure fails in the cranium and spina bifida at the posterior end of the neural tube. Bottom Panels. Regions of neural tube closure postulated by analysis of defects in human embryos superimposed on newborn body. During

normal neural tube formation, multiple zones of neural tube closure extend in anterior and posterior directions from distinct closure points. Zone 1 is in the spinal cord; zones 2, 3, and 4 in the cranium; and zone 5 in the most posterior of the neural tube. Anencephaly is caused by the failure of neural plate fusion in regions 2–4 and spina bifida by the failure of regions 1 and 5. Illustrations are after reference [328] and courtesy of Claris Nde

are fatal, resulting in the prenatal death or demise of the newborn shortly after birth. Spina bifida occulta and multiple abnormalities are classified clinically as NTDs; however, the developmental origins of these malformations are not due to failure of neural tube closure. Closed NTDs include encephalocele, iniencephaly, hydrocephalus, microcephaly, and holoprosencephaly. Encephalocele occurs when the cranial vault fails to form properly around a closed neural tube, leading to protrusion of the brain and meninges through an opening in the skull, whereas other NTDs such as iniencephaly, hydrocephalus, microcephaly, and holoprosencephaly result from improper growth of the closed neural tube.

2.3 Diagnosis and Treatment of NTDs

Most NTDs are diagnosed before birth by standard prenatal screening tests. High levels of alpha fetal protein (AFP) in maternal serum or in amniotic fluid are correlated with NTDs and signal the need for further testing. Most NTDs can be identified by ultrasound during the routine anatomy scan between 18 and 22 weeks. Babies with spina bifida are typically delivered by cesarean section, and the lesion is surgically corrected either in utero or shortly after birth [4, 5]. However, secondary defects frequently occur with spina bifida, including Arnold-Chiari malformations with hindbrain herniation, hydrocephalus requiring

placement of a shunt, and tethering of the spinal cord leading to progressive pain, incontinence, and weakness of the lower extremities, as well as spinal deformities [6–11]. Nerve damage can result in neurogenic bladder and bowel or paralysis of lower extremities requiring the need to use a wheelchair, braces, or crutches [5]. Because of reduced sensation to lower extremities, patients are susceptible to unrealized infections, which may necessitate amputation of damaged limbs. Other complications include learning disabilities, social issues, and latex allergies [5]. In spite of these complications, with improvements in care, the majority of patients survive well into adulthood [5, 8].

2.4 The Etiology of NTDs

While the cause of individual cases of NTDs are rarely known, the vast majority of NTDs are due to complex interactions of multiple genetic and environmental factors with an estimated 60–70% of NTDs having a genetic contribution [12–14]. Evidence for the genetic causes of NTDs comes from the finding that chromosomal abnormalities are often present in NTD-affected fetuses, and NTDs are noted in spontaneous abortions with abnormal karyotypes [15–18]. NTDs also occur at higher rates in certain genetic syndromes, including Meckel-Gruber, Waardenburg, and 22q11.2 deletion syndromes [19–33]. Finally, twin studies indicate a 5% concordance rate, and NTD risk is significantly increased in NTD patients or individuals with a previously affected pregnancy [18, 34–37]. In spite of a clear genetic component, few causative genes have been identified. This is in part due to complex etiology of the malformation, the number of genes that could cause the defect, as well as the existence of few multiplex families for genetic studies. While thus far a handful of genes associated with NTDs were identified in small cohorts of patients, few definitive causative genes are known [38]. Interestingly, the majority of variants identified to date are linked to the noncanonical Wnt pathway that controls planar cell polarity or to folic acid metabolism, implicating these as key pathways driving

NTDs in humans [39, 40]. This chapter will focus on Wnt signaling and folic acid metabolism to illustrate how the study of mouse models has been essential in elucidating the central role of these pathways in neurulation.

In addition to the large number of genes that could cause NTDs, another complicating factor in finding the genetic causes of NTDs in humans is the complex etiology of these defects. The majority of genetic mutations involved in NTDs do not likely cause a defect unless combined with other genetic or environmental factors. The multifactorial threshold model (Fig. 2.2) is proposed to account for the pattern of NTD inheritance observed in humans where multiple factors of small effect interact to cause a disease [41, 42]. This model postulates that neural tube closure is a threshold event that occurs either successfully or not, resulting in either normal neural tube closure or defects. A single genetic insult or environmental exposure might not cross the threshold to cause NTDs, but one or more factors in combination result in failure of neural tube closure. The mouse model is a tractable experimental system in which to test the multifactorial threshold model and test gene–gene, gene–environment, and environment–environment interactions [41, 43]. Digenic inheritance can be modeled in mouse in compound mutants, or modifier variants do not cause NTDs themselves but increase the penetrance and/or severity of defects in combination [42, 44–50]. Gene–environment interactions are also tractable in the mouse model. For example, the impact of alterations of either macro- or micronutrients on the incidence and severity of NTDs can be studied in models [51]. Varying macronutrients such as dietary protein, fat, and carbohydrate composition of the mouse chow can influence NTD risk [51–54]. Micronutrient supplementation with folic acid, inositol, retinoic acid, iron, as well as nutrients that feed into the folate pathway, including vitamin B12, choline, methionine, formate, and glycine, can also impact NTDs in a variety of mutant mouse models [51, 55–59]. Studies of mouse models of diabetes provide novel insight as to the genes and pathways that interact with hyperglycemia to cause NTDs [51, 60, 61]. Exposure to teratogens, including

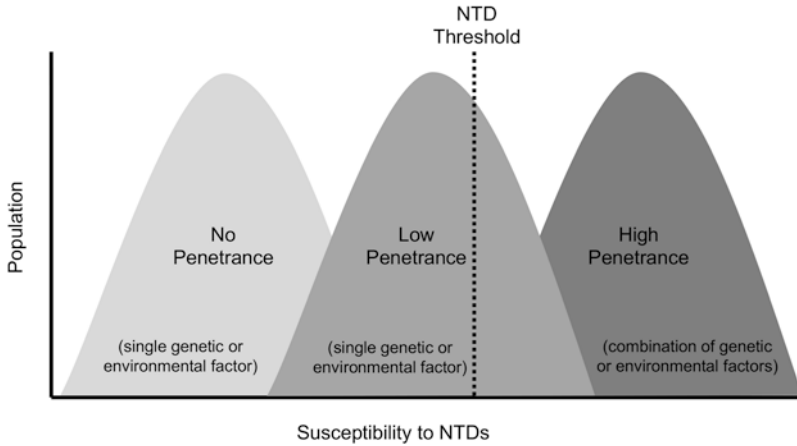


Fig. 2.2 Multifactorial threshold model illustrating the complex inheritance of NTDs. Multiple genetic and environmental factors contribute to the susceptibility for NTDs. Defects result when neurulation is significantly disrupted so that a threshold event, represented by the dotted line (NTD threshold), is surpassed. Susceptibility to NTDs

follows a normal distribution, and in isolation, factors may not be sufficient to cause NTDs (no penetrance) or only a few individuals with a particular contributing factor show NTDs (low penetrance). However, factors in combination can interact to surpass the NTD threshold, resulting in a high percentage of individuals showing NTDs

medications (e.g., valproic acid), arsenic, the mycotoxin fumonisin, or hyperthermia, as a result of hot tub usage or maternal fever can induce NTDs in mouse models [62–65].

2.5 NTDs Result from Failure of Neural Tube Closure

Primary neurulation is a complex morphogenetic process that results in the transformation of the flat neural plate into the neural tube (Fig. 2.3). Neural tube formation involves the coordinated growth and morphogenesis of multiple tissues. Forces that drive neural tube closure arise from the neural tissue itself (intrinsic forces), as well as from the adjacent surface ectoderm and underlying mesoderm (extrinsic forces; [66]). Primary neurulation begins after gastrulation as the neuroepithelium is induced from the embryonic ectoderm. Following induction, the neural plate forms as individual neuroepithelial cells elongate, resulting in a thickening of the ectoderm on the dorsal side of the embryo. Two coordinated morphogenetic movements intrinsic to the neural plate drive elevation of the neural folds by facilitating the rolling of the plate into a tube. Convergent extension (CE) movements drive

lengthening and narrowing of the neural plate and direct formation of hinge points around which the neural plate bends. A single hinge point forms in the midline of the neural plate (medial hinge point (MHP)), followed by the formation of paired dorsal lateral hinge points (DLHPs) in lateral regions. Extrinsic forces from the surface epithelium and surrounding mesenchyme also promote elevation of the neural folds. As the paired neural folds meet in the dorsal midline, they fuse and the neural and surface epithelium remodels to form two separate epithelial sheets.

Broadly speaking, two mechanisms of neurulation are employed to form a neural tube, primary and secondary neurulation. Primary neurulation is when a flat neural plate rolls into a tube, whereas secondary neurulation occurs when mesenchymal cells coalesce into a tube. In amniotes, the majority of the central nervous system is formed by primary neurulation, whereas the most posterior portion of the spine caudal to the sacral vertebrae forms by secondary neurulation [67–69]. In primary neurulation, the neural plate does not roll into a tube all at once; rather, closure is initiated at discrete points, followed by “zipping” to fuse the neural folds together (Fig. 2.1; [70]). Closure 1 initiates at the hind-

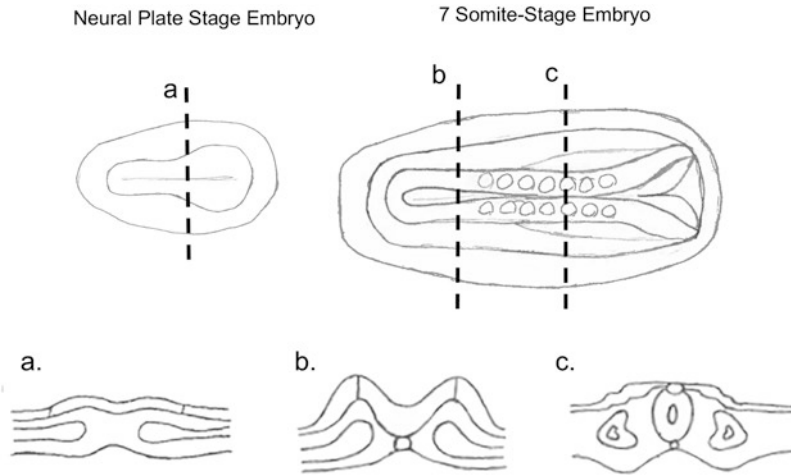


Fig. 2.3 Neural tube closure in the human embryo. The top-left panel shows an illustration of a neural plate stage embryo where the neural plate and neural groove has formed but the neural folds have not yet begun to elevate. The top-right panel shows a seven-somite stage embryo with a neural tube that has begun to form in the spinal region but the posterior neural pore is not yet closed and neural fold elevation is just beginning in the cranium. Bottom panels show cross-sectional views of the neural

plate in different stages of closure from positions delineated by the dotted lines in the top panels. (a) Cross-section of a neural plate stage embryo where the neural groove is formed but the neural folds have not elevated. (b) Cross-section of neural plate where neural folds are in the process of elevating. (c) The neural tube has closed, and the neural ectoderm and nonneural ectoderm are in the process of separating. Illustrations courtesy of Claris Nde

brain/spinal cord boundary and extends in both anterior and posterior directions. This is followed by the formation of closure points in the cranial region: Closure 2 at the midbrain/forebrain boundary and Closure 3 at the anterior aspect of the forebrain. The position of Closure 2 is variable between mouse strains, and its position is correlated with strain-specific susceptibility to exencephaly [71, 72]. Closure 2 may also be variable during human neurulation, as it has been identified in some but not other human embryo samples [73]. Another closure point then forms at the caudal end of the spine as closure of the posterior neuropore becomes imminent [74]. As primary neurulation ceases, there is a transition zone where the dorsal portion of the neural tube undergoes elevation and folding, whereas cells of the ventral neural tube delaminate and then integrate into the neural tube [75]. As neurulation proceeds further, this transition zone gives way to purely secondary neurulation where neuromesodermal progenitors undergo mesenchymal to epithelial transitions to incorporate into the forming neural tube [76]. Disruptions in any

of these processes can result in NTDs. The remainder of this chapter will review the molecular and cellular basis of these processes, illustrating how studies in animal models reveal their integration to provide a basis for the interaction of genetic lesion impacting these processes in human NTDs.

2.6 Mouse Models Have Been Instrumental in Elucidating the Mechanics of Neural Tube Closure

While multiple animal models are used to study neurulation, the mouse has several advantages. First of all, as opposed to that in frogs (African clawed frog, *Xenopus laevis*) and fish (zebrafish, *Danio rerio*), neural tube closure in chickens and mice is most similar to that in humans, where primary neurulation occurs in the majority of the neural tube. In contrast, zebrafish employs a modified secondary neurulation process along the entire neural axis in which deep and superfi-

cial mesenchymal cells converge toward the midline and coalesce into a neural keel intermediate. Deep and superficial cells then undergo radial intercalation to form an epithelial tube [77]. The *Xenopus* neural plate is also stratified into deep and superficial layers [78], and apical constriction occurs in the superficial layers to drive neural fold elevation [79]. Once the folds fuse in the dorsal midline, deep and superficial cells undergo radial intercalation to form a pseudostratified epithelium. While the pathways that control cell shape changes, such as convergent extension and apical constriction are conserved between these animal models, overall difference in morphogenesis between these models makes the mouse and chicken most broadly relevant for understanding human neural tube closure.

The mouse also has the advantage of being amenable to genetic approaches to study the genes required for neural tube closure. The availability of numerous mouse mutants with NTDs provides a rich source of diverse models for study to elucidate the genes and pathways required for neural tube closure [42, 44, 45, 59]. However, because the mouse embryo develops in utero, examination of the cell behaviors that underlie neurulation presents significant challenges compared to models that develop exteriorly. Thus, historically most of what is known about the dynamic cell movements and behaviors that drive neurulation comes from studies in the frog, fish, and chicken. Yet recent advances in live-imaging approaches combined with improved *ex utero* culture conditions are beginning to overcome these hurdles, providing new insight as to the cell and tissue movements that underlie neural tube formation in the mouse and how genetic mutations disrupt this process [74, 80–90].

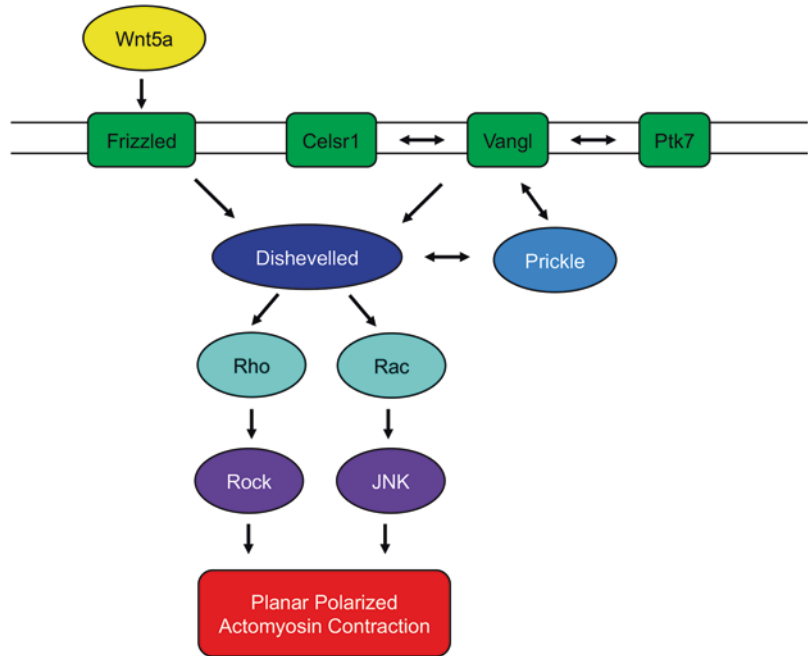
2.7 Convergent Extension Movements and the Planar Cell Polarity Pathway

Following a thickening of the neuroepithelium, the neural plate undergoes convergent extension movements, resulting in lengthening and narrowing

along the anterior-posterior and medial-lateral axes. Polarized cell behaviors that mediate convergent extension movements are controlled by the planar cell polarity (PCP) pathway [91–93]. PCP was first described in *Drosophila*, where it controls the polarity of cells within an epithelium and the positioning of asymmetrically localized structures such as wing hairs [94]. The PCP pathway is conserved in vertebrates and is controlled by the non-canonical Wnt pathway leading to asymmetrical distribution of protein complexes within an epithelium (Fig. 2.4). During neurulation, PCP regulates the polarization of mediolateral protrusions that drive convergent extension movements [95]. Best studied in the *Looptail* (*Lp*) mouse line with mutation of *Van Gogh like-2* (*Vangl2*), defective convergent extension leads to craniorachischisis, where the neural tube fails to close along the entire anterior-posterior axis accompanied by shortening of the embryo and a wider midline and floorplate [96–104]. Interestingly, human embryos with craniorachischisis are short with a broad floorplate [105], suggesting that similar mechanisms may underlie craniorachischisis in humans. *Vangl2* is necessary for convergent extension movements in the notochord and neural plate [98], and mutations in other PCP pathway genes also result in NTDs in the mouse. For example, compound mutants for the vertebrate homologues of *Disheveled* or *Frizzled* receptors show craniorachischisis [106–108], as do targeted knockouts of other PCP pathway components such as *Celsr1*, *Wnt5a*, and *Ptk7* [109–112]. Mutations of PCP genes can also result in spina bifida and exencephaly [106, 113–117].

Consistent with the multifactorial threshold model for NTDs, a number of genes can interact with *Vangl2^{Lp}* heterozygotes, resulting in NTDs in compound mutants. For example, *Vangl2^{Lp}* can genetically interact with other PCP genes, including *Wnt5a*, *Vangl1*, *Dvl2*, *Dvl3*, *Celsr1*, *Fz1*, *Fz2*, *Daam1*, and *Protein tyrosine kinase-7* (*Ptk7*) in compound mutants to cause NTDs [76, 97, 107–112, 118–121]. Additionally, *Vangl2^{Lp}* can genetically interact with mutations in genes not previously identified as regulating PCP pathways to give NTDs. These include *Grhl3*, *Bardet-Biedl syndrome-1* (*BBS1*), *BBS4*, *BBS6*, *cordon bleu* (*cobl*) and *Scribble* (*Scrbl*), *Syndecan 4*

Fig. 2.4 Key elements of the noncanonical Wnt/planar cell polarity pathway signaling pathway involved in neural tube closure in humans and mice. Wnt5a stimulates the PCP pathway by binding to Frizzled that interacts with Celsr1, Vangl, Prickle, and the coreceptor Ptk7 to recruit disheveled (Dvl). Dvl activates the small GTPases Rho and Rac, leading to planar polarized actomyosin contraction



(Sdc4), and Sec24b [121–127]. Interestingly, heterozygous *Vangl2*^{L^{pt}+} embryos show a slightly wider and shorter midline and delayed neural tube closure [98], providing the basis for the development of NTDs in heterozygous embryos and in genetic interaction experiments.

PCP genes are also associated with NTDs in humans. Thus far, multiple mutations in a variety of PCP-related genes are associated with NTDs in humans, including predicted and/or proven deleterious mutations in *CELSR1*, *CELSR3*, *FZD6*, *PRICKLE1*, *VANGL1*, *VANGL2*, *FUZ*, *SCRIB*, *PTK7*, and *DACT1* [40, 128–148]. The deleterious nature of a handful of these sequence variants has been verified in a variety of assays to test the ability to rescue PCP phenotypes in zebrafish, binding to known interacting proteins or altered localization in polarized epithelium [129, 134, 136, 137, 139, 140]. Remarkably, digenic inheritance has also been found involving PCP genes in human patients [40, 141, 142, 145, 148].

2.8 Hinge Point Formation

The medial point in the spinal cord is formed as cells of the neural epithelium become wedge shaped eliciting bending of the neural plate around these hinge points (Fig. 2.5). The pseudostratified neuroepithelium is comprised of bipolar neural progenitors with a nucleus that moves between apical and basal positions dependent upon the phase of the cell cycle. During mitosis, the nucleus is localized at the apical surface, and during other phases of the cell cycle, it is positioned more basally. As hinge points form, the cell cycle is prolonged, resulting in greater numbers of cells in the hinge point in nonmitotic phases and nuclei localized in basal positions [149–152]. The majority of cells in the MHP have basally positioned nuclei, resulting in multiple wedge-shaped cells that contribute to the bending of the epithelium. This in combination with local destabilization of adherens and tight junctions at the hinge points allows bending of the rigid neural plate at the hinge points [149–151]. The rigidity of the neural plate is maintained by apical constriction involving nonmuscle myosin that contracts the

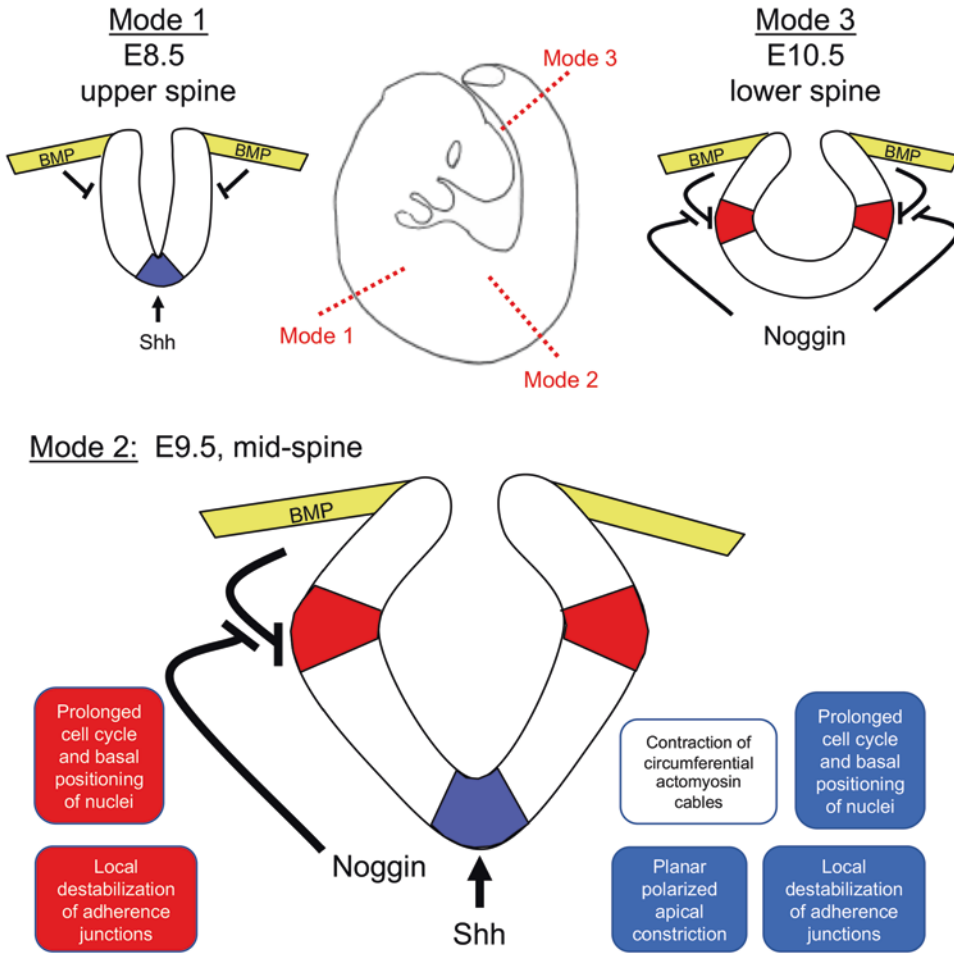


Fig. 2.5 Interaction of BMP and Shh signaling results in different modes of neurulation along the anterior-posterior axis. In the anterior spinal cord (Mode 1), only the medial hinge point (MHP) (blue) forms. In the mid-spinal cord (Mode 2), both MHP and paired dorsal lateral hinge points (DLHP) (red) form. In the posterior spinal region (Mode 3), only exaggerated DLHPs are found. The formation of the MHP is promoted by Shh from the notochord and that of DLHPs is inhibited by BMP from the nonneural ectoderm. BMP expression is consistent along the anterior/posterior axis, but Shh is not expressed in the lower spinal cord and the BMP antagonist Noggin is not expressed in the anterior spinal cord. In Mode 1 neurulation, BMP and Shh are expressed and inhibit DLHP but promote MHP formation. In the mid-spinal cord region,

Mode 2 neurulation involves both MHP and DLHPs. Here Noggin blocks the DLHP-inhibiting activity of BMP. In the posterior spinal region, Shh expression is weak or nonexistent and no MHP forms. The absence of Shh and the presence of Noggin promote the formation of prominent DLHPs. BMP and Shh influence hinge point formation by regulating cellular behaviors. In the DLHP (red) and MHP (blue), inhibition of BMP prolongs the cell cycle, resulting in increased number of cells with basal positioned nuclei, as well as local destabilization of adherence junctions, which leads to buckling of the neural plate around regions (white) where circumferential contraction of actomyosin cables promote a rigid neural plate. Planar polarized apical constriction also contributes to formation of the medial hinge point

circumferential actomyosin cables anchored at the adherens junction [153, 154].

In the cranial region, coordinated apical constriction of the neural epithelium also contributes to hinge point formation and bending of the

neural plate [149, 153]. The contractile force needed for apical constriction is also generated by myosin contracting the actin filaments, a process involving the small GTPase RhoA, ROCK, and myosin light chain kinase [155–158].

Inhibition of this kinase cascade or mutation of actin-binding proteins disrupts neural tube closure [159–164]. One of the best studied regulators of apical constriction in the cranial region is *Shroom3* [155, 156, 158, 165, 166]. Importantly, putative loss of function sequence variants in *SHROOM3* are associated with NTDs in humans [167–169].

2.9 Apical Constriction Is Coordinated with PCP Activation in the Neural Plate

Dynamic integration of PCP and apical constriction pathways drives simultaneous convergent extension and bending of the neural plate [158, 170–173]. Asymmetrical enrichment of PCP components with apical constriction pathways at the mediolateral facing edge of neuroepithelial cells results in the tightening of actomyosin cables preferentially along the mediolateral axis to allow for the rolling of the neural plate [170]. Narrowing and lengthening of the neural plate also involves the coordination of PCP and apical constriction as epithelial rosettes resolve in a preferred direction [174, 175]. This complex and intimate link between the dynamic localization of core PCP proteins, actomyosin assembly, and polarized junction shrinking during cell intercalation is key for neural tube closure [176]. This interaction also provides a basis for genetic interaction of the basal-lateral *Scribble* and the core PCP protein *Vangl2*, which results in craniorachischisis in *Vangl2^{Lpl/+};Scribl^{Ccr/+}* compound mutants [122].

2.10 Formation of Hinge Points Is Regulated by Shh and BMPs

The relative contribution of the MHP and DLHPs to neurulation differs along the anterior-posterior axis of the spinal cord (Fig. 2.5; [177]). In the anterior spinal cord, MHPs are most prominent and DLHPs fail to form, resulting in the neural plate folding over the MHP and the neural folds

meeting in the dorsal midline. This pattern of neurulation is referred to as “Mode 1.” In more caudal regions, both the MHP and paired DLHPs are prominent and the neural plate rolls around these hinge points. This is referred to as “Mode 2” neurulation. In the posterior spinal cord, “Mode 3” neurulation predominates where a prominent MHP does not form and the neural folds roll around the DLHP. In the cranial region, both MHP and DLHPs form and DLHP formation is a dynamic process, as evident in live-imaging experiments where DLHPs form, disappear, and then reform as the neural folds elevate [81].

The dynamic activity of *Shh* and BMPs along the anterior-posterior axis of the spinal cord influences the mode of neurulation (Fig. 2.5; [178]). *Shh* is expressed at highest levels in the anterior regions of the spinal cord and is almost nonexistent in the most caudal regions [178]. Moreover, *Shh* and BMPs inhibit formation of the DLHPs [178, 179]. BMPs are secreted from the surface ectoderm, and their expression remains essentially constant along the spinal neural plate. However, the BMP antagonist *Noggin* is expressed in middle and posterior regions, where it promotes DLHP formation by inhibiting BMPs and destabilizing adherens and tight junctions [149–151]. While disruption of BMP signaling results in NTDs [180–186], loss of *Shh* signaling results in exaggerated hinge points, and the neural tube still closes. On the other hand, activation of *Shh* signaling by loss of negative regulators results in failure of DLHP formation and neural tube closure in regions of the neural tube where DLHPs are critical [187]. Importantly, sequence variants in negative regulators of *Shh* signaling, including *SUFU*, *PTCH1*, *PKA*, and *GPR161*, are associated with spina bifida in humans [188–191].

2.11 PCP, Ciliogenesis, and Shh Signaling

PCP signaling also influences the positioning of cilia on the cell [192]. Many of the genes that interact with *Vangl2^{Lp}* to cause NTDs in mouse

models are involved in cilia, including BBS (Bardet–Biedl syndrome) proteins. While NTDs are not commonly described as features of BBS, mouse mutants in some of the genes that cause BBS show a low penetrance of NTDs or interact with other genes to cause NTDs [126, 193]. Similarly other ciliopathies, such as Meckel-Gruber (MKS) and Joubert syndromes are also associated with NTDs in mouse models but not the human syndrome [194–196]. Mutations of the PCP effector proteins *Fuzzy* and *Inturned* result in defects in cilia and Shh signaling and neural tube closure [115–117]. Because cilia play an essential role in the transduction of Shh signaling [197, 198], the PCP pathway can potentially interact with Shh signaling to cause NTDs.

2.12 Role of the Nonneural Ectoderm in Neural Fold Elevation and Fusion

The nonneural ectoderm is required for neural tube closure by providing an inductive signal for DLHP formation, a driving force for the elevation of the neural folds and participating in the fusion of the neural folds [199–203]. In chicken embryos, removal of the surface epithelium results in failure of DLHP formation and neural fold elevation [202]. This could reflect either an inductive or a mechanical role in DLHP formation and elevation of the neural folds. In support of an inductive role, removal of all but a small strip of surface epithelium is sufficient to induce DLHPs [202]. BMP and Noggin are expressed in the surface ectoderm, and culture with a Noggin-coated bead will induce DLHPs [179]. On the other hand, oriented cell divisions in the epidermis of the chicken embryo drive medial-lateral expansion of the tissue [204], and the surface epithelium in *Xenopus* migrates medially during neural tube closure [203], potentially providing a mechanical force for neural fold elevation. The surface ectoderm differentially contacts the neural tube along the anterior posterior neural axis and it is likely that the role of the surface ectoderm changes as well [173].

Grhl2 and *Grhl3* are expressed almost exclusively in the surface ectoderm during neurulation and are required for the proper development of the epidermis and neural tube closure [205–212]. *Grhl3* is also expressed in the hindgut epithelium, and mutation of *Grhl3^{et}* in a hypomorphic mouse line creates an imbalance in proliferation between the posterior neural tube and the underlying hindgut epithelium resulting in spina bifida [213]. *Grhl3* and *Grhl2* null mouse mutants show defects in more anterior regions of the spinal cord and failure of DLHP formation in spite of normal expression of epidermally derived factors involved in DLHP formation, such as *BMP2* and *Noggin* [205–212]. Importantly, *GRHL* genes are implicated in human NTDs [167, 168, 214].

During fusion of the neural folds, cells extend finger-like projections that contact protrusions on the opposing neural folds, intercalate, draw the folds closer, and fasten them together [81, 82]. The neural folds are comprised of neural and nonneural ectoderm, which extend different projections in regionally distinct areas of the neural tube [85, 90, 153]. Live-imaging experiments in the mouse suggest that closure in the hindbrain/midbrain region does not occur by “zipping” but rather formation of multiple intermediate closure points that “button up” the folds together [82, 89]. The tissue layer that makes initial contact differs based on the anterior-posterior level. Between closure points 1 and 2, fusion is initiated by cells of the nonneural ectoderm, followed by cells of the neural ectoderm [82, 215]. Between closure points 2 and 3, both layers contact at the same time while initiation at closure 3 is mediated by the neural ectoderm [215]. Scanning electron microscopy revealed that protrusions are predominantly filopodia during early stages of spinal neurulation, then replaced by membrane ruffles and filopodia [90, 153]. The PCP pathway is also required for directional protrusive activity of the neural epithelium during fusion [76]. *Grhl2* is also required for neural fold fusion evident in live-imaging experiments where elevation and apposition of the neural folds can occur but fusion fails [208]. As the neural folds meet in the midline, extensive tissue remodeling separates the neural and nonneural

ectoderm joining the opposing folds. Molecularly, GRHL transcription factors influence expression of multiple proteins that can influence neural fold fusion, including adherens junctions, as well as proteins that suppress EMT to reinforce the epithelial properties of the nonneural ectoderm during tissue remodeling [86].

2.13 Prevention of NTDs by Micronutrient Supplementation

Maternal diet is a key environmental factor influencing the incidence of NTDs, and by the 1960s, folic acid emerged as a key micronutrient with reports that women with NTD-affected pregnancies had reduced intake of folate, as well as lower folate levels in blood, than in normal pregnancies [216, 217]. This led to a series of clinical trials to test if folic acid supplementation could prevent NTDs [218–223]. In 1991, results of a double-blind randomized trial demonstrated a 72% reduction of NTDs in a large trial involving women with previous NTD-affected pregnancies [224]. Further trials to determine if folic acid supplementation could prevent NTDs in women of average risk demonstrated that improvement is greater depending on the initial NTD rate of the population [225]. For example, in Northern China, where the NTD rate is very high (48 in 10,000 live births), the incidence was reduced to 7 in 10,000 with supplementation. But in Southern China, the NTD rate was rather low (10 in 10,000) and was only reduced to 6 in 10,000 [226]. Many countries now fortify grains and cereals with folic acid, and in the United States, studies show that fortification results in increased folate status of the population, and an estimated 30% reduction in the incidence of NTDs [227–229]. The *MTHFR* gene encodes methylenetetrahydrofolate reductase, which is essential for the conversion of homocysteine to methionine, a key reaction in the folate pathway. Common polymorphisms in the *MTHFR* gene that reduce enzyme function are associated with increased risk of NTDs [230]. For example, 40% of the general population is heterozygous and

10% homozygous for the hypomorphic *MTHFR* 667C>T allele. Another common mechanism impacting folate metabolism is the production of function-blocking autoantibodies against the folate receptor, which are found at higher levels in maternal serum from NTD-affected pregnancies [231–234]. Folic acid supplementation can overcome the increased risk associated with *MTHFR* 667C>T polymorphism or the presence of folic acid receptor autoantibodies [235, 236]. However, folic acid supplementation does not prevent all NTDs in humans, and supplementation typically only reduces the incidence to 5–7 per 10,000 live births [225].

Folic acid supplementation can also prevent NTDs in mouse models, including lines with deletion of *Folbp1*, *Rfc1*, *Cart1*, and *Gcn5* or mutation in *Lrp6^{cd}* and *Pax3^{2H}* [237–246]. The maternal genotype also impacts the risk of NTDs and response to supplementation. For example, NTDs in the *Lrp2* mouse model are prevented by the injection of folic acid but not dietary folic acid [247]. Since *Lrp2* plays an important role in folate uptake with folate deficiency [248], this result highlights the impact of the maternal genotype on folate status. This is echoed in human data where mothers who are heterozygous for the *MTHFR* 667C>T allele have a slightly increased risk of having an NTD-affected pregnancy, whereas the risk increases to 60% for homozygous mothers and to 90% for homozygous females from homozygous mothers [230].

Similar to NTDs in humans, many mutant mouse lines are not rescued by folic acid supplementation [181, 210, 249–252]. Interestingly, this may be influenced by the impact of the particular mutant allele rather than the gene involved. For example, NTDs in the *Lrp6^{cd}* mouse line are prevented by supplementation with folic acid, whereas supplementation in the *Lrp6^{null}* mouse line results in more severe NTDs and embryo loss [253]. In fact, folic acid supplementation results in the early loss of mutant embryos in some mouse lines [253, 254]. Furthermore, high levels of dietary folic acid intake results in activation of negative feedback loops, leading to overrepression of folic acid metabolism [255, 256]. The adverse effects of folic acid supplementation are

cumulative, with long-term but not short-term supplementation being detrimental [254].

Importantly, folic acid deficiency is not sufficient to induce NTDs in humans or mouse models [257–263]. Rather, gene–environment interactions (e.g., suboptimal folate status plus a genetic predisposition) likely combine to result in NTDs. For example, folate deficiency increased the frequency of NTDs in *Pax3^{Sp}* mutants and other susceptible mouse background strains [259, 260]. Similarly, mutation of a gene required for folate metabolism (*Shmt1*) does not result in NTDs, but with folate deficiency, NTDs occur [257, 264]. Altered folate metabolism has been documented in cell lines derived from NTD-affected human fetuses, as well the *Pax3^{Sp}* and *Lrp6^{Cd}* mouse models of NTDs [243, 265, 266]. Finally, *Pax3^{Sp/+};Shmt1^{-/+}* compound mutants show increased penetrance and severity of NTDs, indicating an interaction of *Pax3* mutation with the folate pathway [264]. This may be relevant to human NTDs as spina bifida and anencephaly are associated with *PAX3* mutations in the autosomal dominant Waardenburg syndrome, as well as in nonsyndromic NTDs [22, 32, 167, 267–277].

2.14 Mechanisms by Which Folic Acid Prevents NTDs

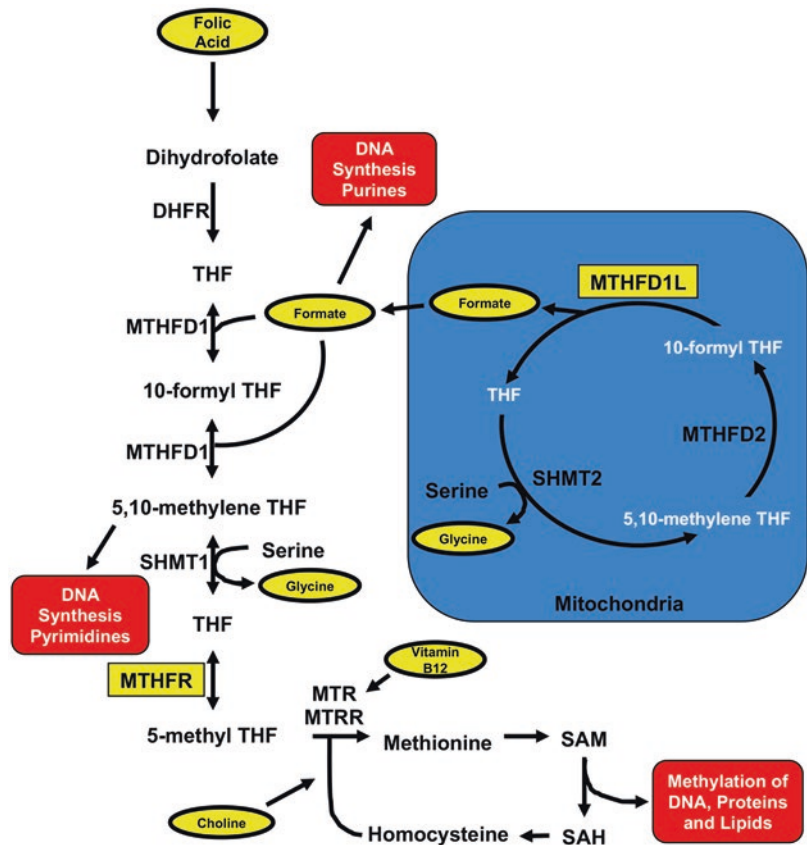
In spite of the clear benefit for folic acid supplementation, it is not clear how folic acid prevents NTDs [230]. Folates are not synthesized by the body and need to be included in the diet. Folic acid feeds into the folate one carbon metabolism pathway (Fig. 2.6), a network of interlinked reactions that generates key metabolites required for several cellular processes, including the synthesis of nucleic and amino acids; the production of methyl donor S-adenosyl methionine (SAM) used for methylation of histones, proteins, lipids, and DNA; as well as influencing homocysteine production [278–280]. These outputs can directly impact apical constriction and the cytoskeletal dynamics necessary for neural fold elevation, as well as cilia formation [281–283]. The emerging picture is that a variety of functional outputs of folate metabo-

lism are required for normal development. Impaired flux of metabolites through these reactions may be the key factor responsible for NTDs with deficiency and prevention with supplementation. The specific metabolites required are likely due to individual metabolic need based on how flux through the pathway is perturbed by genetic mutations and environmental factors.

2.15 Folate is a Cofactor Required for Synthesis of DNA, Amino Acid and Methyl Donors

The *Pax3^{Sp2H}* mutant mouse strain, which has a metabolic deficiency in the supply of folate for the biosynthesis of pyrimidine, is susceptible to NTDs with folate deficiency, and NTDs in this strain are prevented by folate supplementation [243, 264]. Either Folic acid supplementation or deficiency have measurable effects on DNA methylation impacting gene expression [284, 285]. Importantly, both global DNA hypomethylation and hypomethylation at specific genes are associated with an increased risk for NTDs [286]. One of these genes is *Pax3*, which exhibits reduced expression and altered methylation with exposure to polycyclic aromatic hydrocarbon, as well as oxidative stress in diabetic pregnancy that induces NTDs [287, 288]. Similar to the *Pax3* mutant models, supplementation of diabetic mice with folic acid can prevent NTDs [289]. The greater susceptibility of females to NTDs and prevention by folic acid supplementation suggests an epigenetic requirement for folate metabolism to provide methyl donor groups. Data from both humans and mouse demonstrate that anencephaly affects more females than males, and NTDs in females are reduced to a greater extent with folic acid supplementation [290]. Epigenetic inactivation of the X chromosome is proposed to act as a sink for methyl donors, resulting in less methyl donor groups available for other functions. Folic acid supplementation potentially increases available methyl groups and preferentially rescue NTDs in females [290–292].

Fig. 2.6 The folate pathway and neural tube defects. Schematic of the folate metabolic pathway showing key enzymes involved in the cytoplasm and mitochondria (blue). Key outputs of the folate cycle hypothesized to modulate neural tube closure are shown in red boxes and include regulation of DNA synthesis by providing the building blocks for pyrimidines and purines, as well as production of methyl donors required for methylation of DNA, proteins, and lipids. Metabolites that can prevent NTDs when supplemented in mouse models are highlighted by yellow ovals and key enzymes implicated in NTDs in humans, such as *MTHFR* and *MTHFD1L*, and are also highlighted by yellow boxes



2.16 Folate and Homocysteine

Another possible mechanism by which folic acid supplementation might prevent NTDs is by reducing homocysteine levels [293]. Elevated maternal homocysteine during pregnancy is associated with an increased risk for NTDs [294]. Homocysteine accumulation leads to homocysteinylated proteins that increase their antigenicity. Folate deficiency in a mouse model increases homocysteine levels and expression of autoantibodies against homocysteinylated proteins that was reversible with folate supplementation [295]. In humans, genotypes associated with reduced folate uptake or metabolism result in elevated antifolate receptor autoantibodies further impacting folate status of the mother [296]. Furthermore, homocysteinylated H3K79 was increased in brain tissue from NTD cases along with alterations in gene expression [297].

2.17 Studies in Mice Suggest Supplementation with Inositol or Formate May Prevent Folate-Resistant NTDs

Aside from *MTHFR*, other enzymes in the folate one carbon metabolism pathway have not consistently been associated with NTDs in human populations or in mouse models [39]. On the other hand, the glycine cleavage branch of the pathway that links folate one carbon metabolism in the mitochondria with reactions in the cytoplasm through the transfer of formate is emerging as key for NTD susceptibility in both mouse models and humans [148, 298–300]. In human populations, sequence variants in either the mitochondrial methylenetetrahydrofolate reductase (*MTHFD1L*) or the mitochondrial inner membrane folate transporter (*SLC25A32*) are associated with increased risk for NTDs [298, 299, 301, 302]. Mutation of

mouse homologues of these genes also results in NTDs [299, 300, 302–306]. Importantly, NTDs in many of these models are prevented by supplementation with formate but not folate. These findings provide important preclinical data suggesting that formate supplementation in conjunction with folate should be considered in the prevention of folate-insensitive NTDs in humans.

Another supplement with a promise to prevent folate-resistant NTDs is inositol, a simple carbohydrate naturally found in many foods [307]. Inositol acts as an insulin-sensitizing agent, and supplementation improves glucose and lipid profiles with positive effects on fertility in assisted reproduction and in women with polycystic ovary syndrome [308]. Hyperglycemia results in inositol depletion, and inositol supplementation suppresses diabetes-induced NTDs in mouse models [309, 310]. Mouse embryos grown in culture and *Grhl3^{ct}* mutants, in particular, develop NTDs with reduced inositol in the growth media, and the incidence of NTDs in *Grhl3^{ct}* mutants is reduced by inositol but not folic acid supplementation [311–315]. Additionally, mutation of genes involved in inositol metabolism results in NTDs [316, 317]. Studies in humans also provide support for inositol in the prevention of NTDs. Low serum concentrations of inositol are associated with increased NTD risk and are also found in children with spina bifida. Preliminary trials where dual supplementation of inositol and folate is given to women with previous NTD-affected pregnancies suggest that this treatment is highly effective as no NTDs have occurred in the dual supplementation group, whereas some NTDs did occur with folate supplementation alone. However, the sample size of these studies is still too low to draw definitive conclusions [318–323].

2.18 Future Directions

In recent years, next-generation sequencing approaches such as whole-genome and whole-exome sequencing, as well as targeted sequencing of extensive panels of candidate genes in large NTD patient cohorts, have been employed

to identify the genes responsible for NTDs in humans [38, 141, 142, 145, 324–326]. These approaches have the potential to identify new candidate genes, as well as multiple sequence variants, in a single individual that might contribute to NTD in a multifactorial fashion. In fact, a recent whole-genome sequencing study concluded that the genetic basis for NTD is omnigenic involving genes spread across almost the entire genome [326]. Furthermore, this study concluded that predicted loss of function variants in almost all genes had some minor impact on NTD risk, and NTD risk was associated with increased numbers of rare loss of function variants. Surprisingly, there was no significant enrichment of damaging variants in human orthologs of the 249 mouse NTD-associated genes previously implicated in NTDs [42, 44–46, 59, 327]. These findings indicate that previous efforts using targeted genomic screens that rely heavily on the candidate genes identified in animal models represent only the tip of the iceberg in terms of the genes that contribute to NTDs. As new candidate genes are identified in these human screens, the mouse model will be essential for modeling the complex interaction of variants leading to NTDs.

References

1. Gu X, Lin L, Zheng X, Zhang T, Song X, Wang J, et al. High prevalence of NTDs in Shanxi Province: a combined epidemiological approach. *Birth Defects Res A Clin Mol Teratol.* 2007;79(10):702–7.
2. Parker SE, Mai CT, Canfield MA, Rickard R, Wang Y, Meyer RE, et al. Updated national birth prevalence estimates for selected birth defects in the United States, 2004–2006. *Birth Defects Res A Clin Mol Teratol.* 2010;88(12):1008–16.
3. Copp AJ, Stanier P, Greene ND. Neural tube defects: recent advances, unsolved questions, and controversies. *Lancet Neurol.* 2013;12(8):799–810.
4. Adzick NS, Thom EA, Spong CY, Brock JW III, Burrows PK, Johnson MP, et al. A randomized trial of prenatal versus postnatal repair of myelomeningocele. *N Engl J Med.* 2011;364(11):993–1004.
5. Thompson DN. Postnatal management and outcome for neural tube defects including spina bifida and encephaloceles. *Prenat Diagn.* 2009;29(4):412–9.
6. Oakeshott P, Hunt GM. Long-term outcome in open spina bifida. *Br J Gen Pract.* 2003;53(493):632–6.

7. Dias MS, McLone DG. Hydrocephalus in the child with dysraphism. *Neurosurg Clin N Am*. 1993;4(4):715–26.
8. Adzick NS, Walsh DS. Myelomeningocele: prenatal diagnosis, pathophysiology and management. *Semin Pediatr Surg*. 2003;12(3):168–74.
9. Hertzler DA II, DePowell JJ, Stevenson CB, Mangano FT. Tethered cord syndrome: a review of the literature from embryology to adult presentation. *Neurosurg Focus*. 2010;29(1):E1.
10. Yamada S, Won DJ, Siddiqi J, Yamada SM. Tethered cord syndrome: overview of diagnosis and treatment. *Neurol Res*. 2004;26(7):719–21.
11. Hudgins RJ, Gilreath CL. Tethered spinal cord following repair of myelomeningocele. *Neurosurg Focus*. 2004;16(2):E7.
12. Copp AJ, Adzick NS, Chitty LS, Fletcher JM, Holmbeck GN, Shaw GM. Spina bifida. *Nat Rev Dis Primers*. 2015;1:15007.
13. Bassuk AG, Kibar Z. Genetic basis of neural tube defects. *Semin Pediatr Neurol*. 2009;16(3):101–10.
14. Lupo PJ, Agopian AJ, Castillo H, Castillo J, Clayton GH, Dosa NP, et al. Genetic epidemiology of neural tube defects. *J Pediatr Rehabil Med*. 2017;10(3–4):189–94.
15. Chen CP. Chromosomal abnormalities associated with neural tube defects (II): partial aneuploidy. *Taiwan J Obstet Gynecol*. 2007;46(4):336–51.
16. Chen CP. Chromosomal abnormalities associated with neural tube defects (I): full aneuploidy. *Taiwan J Obstet Gynecol*. 2007;46(4):325–35.
17. Chen CP. Prenatal sonographic features of fetuses in trisomy 13 pregnancies (II). *Taiwan J Obstet Gynecol*. 2009;48(3):218–24.
18. Detrait ER, George TM, Etchevers HC, Gilbert JR, Vekemans M, Speer MC. Human neural tube defects: developmental biology, epidemiology, and genetics. *Neurotoxicol Teratol*. 2005;27(3):515–24.
19. Kinoshita H, Kokudo T, Ide T, Kondo Y, Mori T, Homma Y, et al. A patient with DiGeorge syndrome with spina bifida and sacral myelomeningocele, who developed both hypocalcemia-induced seizure and epilepsy. *Seizure*. 2010;19(5):303–5.
20. Chen CP. Meckel syndrome: genetics, perinatal findings, and differential diagnosis. *Taiwan J Obstet Gynecol*. 2007;46(1):9–14.
21. Chen CP. Syndromes, disorders and maternal risk factors associated with neural tube defects (III). *Taiwan J Obstet Gynecol*. 2008;47(2):131–40.
22. Baldwin CT, Lipsky NR, Hoth CF, Cohen T, Mamuya W, Milunsky A. Mutations in PAX3 associated with Waardenburg syndrome type I. *Hum Mutat*. 1994;3(3):205–11.
23. Canda MT, Demir N, Bal FU, Doganay L, Sezer O. Prenatal diagnosis of a 22q11 deletion in a second-trimester fetus with conotruncal anomaly, absent thymus and meningocele: Kousseff syndrome. *J Obstet Gynaecol Res*. 2012;38(4):737–40.
24. Forrester S, Kovach MJ, Smith RE, Rimer L, Wesson M, Kimonis VE. Kousseff syndrome caused by deletion of chromosome 22q11-13. *Am J Med Genet*. 2002;112(4):338–42.
25. Kousseff BG. Sacral meningocele with conotruncal heart defects: a possible autosomal recessive trait. *Pediatrics*. 1984;74(3):395–8.
26. Logan CV, Abdel-Hamed Z, Johnson CA. Molecular genetics and pathogenic mechanisms for the severe ciliopathies: insights into neurodevelopment and pathogenesis of neural tube defects. *Mol Neurobiol*. 2011;43(1):12–26.
27. Maclean K, Field MJ, Colley AS, Mowat DR, Sparrow DB, Dunwoodie SL, et al. Kousseff syndrome: a causally heterogeneous disorder. *Am J Med Genet A*. 2004;124A(3):307–12.
28. Nickel RE, Magenis RE. Neural tube defects and deletions of 22q11. *Am J Med Genet*. 1996;66(1):25–7.
29. Nickel RE, Pillers DA, Merkens M, Magenis RE, Driscoll DA, Emanuel BS, et al. Velo-cardio-facial syndrome and DiGeorge sequence with meningocele and deletions of the 22q11 region. *Am J Med Genet*. 1994;52(4):445–9.
30. Seller MJ, Mohammed S, Russell J, Ogilvie C. Microdeletion 22q11.2, Kousseff syndrome and spina bifida. *Clin Dysmorphol*. 2002;11(2):113–5.
31. Toriello HV, Sharda JK, Beaumont EJ. Autosomal recessive syndrome of sacral and conotruncal developmental field defects (Kousseff syndrome). *Am J Med Genet*. 1985;22(2):357–60.
32. Nye JS, Balkin N, Lucas H, Knepper PA, McLone DG, Charrow J. Myelomeningocele and Waardenburg syndrome (type 3) in patients with interstitial deletions of 2q35 and the PAX3 gene: possible digenic inheritance of a neural tube defect. *Am J Med Genet*. 1998;75(4):401–8.
33. Hart J, Miriyala K. Neural tube defects in Waardenburg syndrome: a case report and review of the literature. *Am J Med Genet A*. 2017;173(9):2472–7.
34. Risch N. Linkage strategies for genetically complex traits. III. The effect of marker polymorphism on analysis of affected relative pairs. *Am J Hum Genet*. 1990;46(2):242–53.
35. Risch N. Linkage strategies for genetically complex traits. II. The power of affected relative pairs. *Am J Hum Genet*. 1990;46(2):229–41.
36. Mitchell LE. Epidemiology of neural tube defects. *Am J Med Genet C Semin Med Genet*. 2005;135C(1):88–94.
37. Mitchell LE, Adzick NS, Melchionne J, Pasquariello PS, Sutton LN, Whitehead AS. Spina bifida. *Lancet*. 2004;364(9448):1885–95.
38. Au KS, Ashley-Koch A, Northrup H. Epidemiologic and genetic aspects of spina bifida and other neural tube defects. *Dev Disabil Res Rev*. 2010;16(1):6–15.
39. Greene ND, Stanier P, Copp AJ. Genetics of human neural tube defects. *Hum Mol Genet*. 2009;18(R2):R113–29.
40. De Marco P, Merello E, Piatelli G, Cama A, Kibar Z, Capra V. Planar cell polarity gene mutations con-

- tribute to the etiology of human neural tube defects in our population. *Birth Defects Res A Clin Mol Teratol.* 2014;100(8):633–41.
41. Zohn IE, Sarkar AA. Modeling neural tube defects in the mouse. *Curr Top Dev Biol.* 2008;84:1–35.
 42. Harris MJ, Juriloff DM. Mouse mutants with neural tube closure defects and their role in understanding human neural tube defects. *Birth Defects Res A Clin Mol Teratol.* 2007;79(3):187–210.
 43. Zohn IE. Mouse as a model for multifactorial inheritance of neural tube defects. *Birth Defects Res C Embryo Today.* 2012;96(2):193–205.
 44. Harris MJ, Juriloff DM. An update to the list of mouse mutants with neural tube closure defects and advances toward a complete genetic perspective of neural tube closure. *Birth Defects Res A Clin Mol Teratol.* 2010;88(8):653–69.
 45. Juriloff DM, Harris MJ. A consideration of the evidence that genetic defects in planar cell polarity contribute to the etiology of human neural tube defects. *Birth Defects Res A Clin Mol Teratol.* 2012;94(10):824–40.
 46. Juriloff DM, Harris MJ. Insights into the etiology of mammalian neural tube closure defects from developmental, genetic and evolutionary studies. *J Dev Biol.* 2018;6(3):22.
 47. Kooistra MK, Leduc RY, Dawe CE, Fairbridge NA, Rasmussen J, Man JH, et al. Strain-specific modifier genes of *Cecr2*-associated exencephaly in mice: genetic analysis and identification of differentially expressed candidate genes. *Physiol Genomics.* 2012;44(1):35–46.
 48. Korstanje R, Desai J, Lazar G, King B, Rollins J, Spurr M, et al. Quantitative trait loci affecting phenotypic variation in the vacuolated lens mouse mutant, a multigenic mouse model of neural tube defects. *Physiol Genomics.* 2008;35(3):296–304.
 49. Letts VA, Schork NJ, Copp AJ, Bernfield M, Frankel WN. A curly-tail modifier locus, *mct1*, on mouse chromosome 17. *Genomics.* 1995;29(3):719–24.
 50. Neumann PE, Frankel WN, Letts VA, Coffin JM, Copp AJ, Bernfield M. Multifactorial inheritance of neural tube defects: localization of the major gene and recognition of modifiers in ct mutant mice. *Nat Genet.* 1994;6(4):357–62.
 51. Kappen C. Modeling anterior development in mice: diet as modulator of risk for neural tube defects. *Am J Med Genet C Semin Med Genet.* 2013;163C(4):333–56.
 52. Harris MJ, Juriloff DM. Maternal diet alters exencephaly frequency in *SELH/Bc* strain mouse embryos. *Birth Defects Res A Clin Mol Teratol.* 2005;73(8):532–40.
 53. Juriloff DM, Macdonald KB, Harris MJ. Genetic analysis of the cause of exencephaly in the *SELH/Bc* mouse stock. *Teratology.* 1989;40(4):395–405.
 54. Bentham J, Michell AC, Lockstone H, Andrew D, Schneider JE, Brown NA, et al. Maternal high-fat diet interacts with embryonic *Cited2* genotype to reduce *Pitx2c* expression and enhance penetrance of left-right patterning defects. *Hum Mol Genet.* 2010;19(17):3394–401.
 55. Greene ND, Copp AJ. Mouse models of neural tube defects: investigating preventive mechanisms. *Am J Med Genet C Semin Med Genet.* 2005;135C(1):31–41.
 56. Zohn IE, Sarkar AA. The visceral yolk sac endoderm provides for absorption of nutrients to the embryo during neurulation. *Birth Defects Res A Clin Mol Teratol.* 2010;88(8):593–600.
 57. Zeisel SH. Importance of methyl donors during reproduction. *Am J Clin Nutr.* 2009;89(2):673S–7S.
 58. Gray JD, Ross ME. Mechanistic insights into folate supplementation from Crooked tail and other NTD-prone mutant mice. *Birth Defects Res A Clin Mol Teratol.* 2009;85(4):314–21.
 59. Harris MJ. Insights into prevention of human neural tube defects by folic acid arising from consideration of mouse mutants. *Birth Defects Res A Clin Mol Teratol.* 2009;85(4):331–9.
 60. Reece EA. Diabetes-induced birth defects: what do we know? What can we do? *Curr Diab Rep.* 2012;12(1):24–32.
 61. Zabihi S, Loeken MR. Understanding diabetic teratogenesis: where are we now and where are we going? *Birth Defects Res A Clin Mol Teratol.* 2010;88(10):779–90.
 62. Cabrera RM, Hill DS, Etheredge AJ, Finnell RH. Investigations into the etiology of neural tube defects. *Birth Defects Res C Embryo Today.* 2004;72(4):330–44.
 63. Lammer EJ, Sever LE, Oakley GP Jr. Teratogen update: valproic acid. *Teratology.* 1987;35(3):465–73.
 64. Gelineau-van Waes J, Voss KA, Stevens VL, Speer MC, Riley RT. Maternal fumonisin exposure as a risk factor for neural tube defects. *Adv Food Nutr Res.* 2009;56:145–81.
 65. Wang A, Holladay SD, Wolf DC, Ahmed SA, Robertson JL. Reproductive and developmental toxicity of arsenic in rodents: a review. *Int J Toxicol.* 2006;25(5):319–31.
 66. Colas JF, Schoenwolf GC. Towards a cellular and molecular understanding of neurulation. *Dev Dyn.* 2001;221(2):117–45.
 67. Morriss-Kay G, Wood H, Chen WH. Normal neurulation in mammals. *Ciba Found Symp.* 1994;181:51–63; discussion 63–9.
 68. Schoenwolf GC. Histological and ultrastructural studies of secondary neurulation in mouse embryos. *Am J Anat.* 1984;169(4):361–76.
 69. Schoenwolf GC, Delongo J. Ultrastructure of secondary neurulation in the chick embryo. *Am J Anat.* 1980;158(1):43–63.
 70. Copp AJ, Greene ND, Murdoch JN. The genetic basis of mammalian neurulation. *Nat Rev Genet.* 2003;4(10):784–93.
 71. Fleming A, Copp AJ. A genetic risk factor for mouse neural tube defects: defining the embryonic basis. *Hum Mol Genet.* 2000;9(4):575–81.

72. Juriloff DM, Harris MJ, Tom C, MacDonald KB. Normal mouse strains differ in the site of initiation of closure of the cranial neural tube. *Teratology*. 1991;44(2):225–33.
73. Greene ND, Copp AJ. Development of the vertebrate central nervous system: formation of the neural tube. *Prenat Diagn*. 2009;29(4):303–11.
74. Galea GL, Cho YJ, Galea G, Mole MA, Rolo A, Savery D, et al. Biomechanical coupling facilitates spinal neural tube closure in mouse embryos. *Proc Natl Acad Sci U S A*. 2017;114(26):E5177–E86.
75. Dady A, Havis E, Escriou V, Catala M, Duband JL. Junctional neurulation: a unique developmental program shaping a discrete region of the spinal cord highly susceptible to neural tube defects. *J Neurosci*. 2014;34(39):13208–21.
76. Lopez-Escobar B, Caro-Vega JM, Vijayraghavan DS, Plageman TF, Sanchez-Alcazar JA, Moreno RC, et al. The non-canonical Wnt-PCP pathway shapes the mouse caudal neural plate. *Development*. 2018;145(9).
77. Harrington MJ, Chalasani K, Brewster R. Cellular mechanisms of posterior neural tube morphogenesis in the zebrafish. *Dev Dyn*. 2010;239(3):747–62.
78. Davidson LA, Keller RE. Neural tube closure in *Xenopus laevis* involves medial migration, directed protrusive activity, cell intercalation and convergent extension. *Development*. 1999;126(20):4547–56.
79. Schroeder TE. Neurulation in *Xenopus laevis*. An analysis and model based upon light and electron microscopy. *J Embryol Exp Morphol*. 1970;23(2):427–62.
80. Jones EA, Crotty D, Kulesa PM, Waters CW, Baron MH, Fraser SE, et al. Dynamic in vivo imaging of postimplantation mammalian embryos using whole embryo culture. *Genesis*. 2002;34(4):228–35.
81. Massarwa R, Niswander L. In toto live imaging of mouse morphogenesis and new insights into neural tube closure. *Development*. 2013;140(1):226–36.
82. Pyrgaki C, Trainor P, Hadjantonakis AK, Niswander L. Dynamic imaging of mammalian neural tube closure. *Dev Biol*. 2010;344(2):941–7.
83. Yamaguchi Y, Shinotsuka N, Nonomura K, Takemoto K, Kuida K, Yosida H, et al. Live imaging of apoptosis in a novel transgenic mouse highlights its role in neural tube closure. *J Cell Biol*. 2011;195(6):1047–60.
84. McDole K, Guignard L, Amat F, Berger A, Malandain G, Royer LA, et al. In toto imaging and reconstruction of post-implantation mouse development at the single-cell level. *Cell*. 2018;175(3):859–76.e33.
85. Ray HJ, Niswander LA. Dynamic behaviors of the non-neural ectoderm during mammalian cranial neural tube closure. *Dev Biol*. 2016;416(2):279–85.
86. Ray HJ, Niswander LA. Grainyhead-like 2 downstream targets act to suppress epithelial-to-mesenchymal transition during neural tube closure. *Development*. 2016;143(7):1192–204.
87. Massarwa R, Ray HJ, Niswander L. Morphogenetic movements in the neural plate and neural tube: mouse. *Wiley Interdiscip Rev Dev Biol*. 2014;3(1):59–68.
88. Galea GL, Nychyk O, Mole MA, Moulding D, Savery D, Nikolopoulou E, et al. Vangl2 disruption alters the biomechanics of late spinal neurulation leading to spina bifida in mouse embryos. *Dis Model Mech*. 2018;11(3).
89. Wang S, Garcia MD, Lopez AL III, Overbeek PA, Larin KV, Larina IV. Dynamic imaging and quantitative analysis of cranial neural tube closure in the mouse embryo using optical coherence tomography. *Biomed Opt Express*. 2017;8(1):407–19.
90. Rolo A, Savery D, Escuin S, de Castro SC, Armer HE, Munro PM, et al. Regulation of cell protrusions by small GTPases during fusion of the neural folds. *Elife*. 2016;5:e13273.
91. Heisenberg CP, Tada M, Rauch GJ, Saude L, Concha ML, Geisler R, et al. Silberblick/Wnt11 mediates convergent extension movements during zebrafish gastrulation. *Nature*. 2000;405(6782):76–81.
92. Tada M, Smith JC. Xwnt11 is a target of *Xenopus* Brachyury: regulation of gastrulation movements via Dishevelled, but not through the canonical Wnt pathway. *Development*. 2000;127(10):2227–38.
93. Wallingford JB, Rowning BA, Vogeli KM, Rothbacher U, Fraser SE, Harland RM. Dishevelled controls cell polarity during *Xenopus* gastrulation. *Nature*. 2000;405(6782):81–5.
94. Vladar EK, Antic D, Axelrod JD. Planar cell polarity signaling: the developing cell's compass. *Cold Spring Harb Perspect Biol*. 2009;1(3):a002964.
95. Wallingford JB. Planar cell polarity and the developmental control of cell behavior in vertebrate embryos. *Annu Rev Cell Dev Biol*. 2012;28:627–53.
96. Wallingford JB, Harland RM. Neural tube closure requires Dishevelled-dependent convergent extension of the midline. *Development*. 2002;129(24):5815–25.
97. Wang J, Hamblet NS, Mark S, Dickinson ME, Brinkman BC, Segil N, et al. Dishevelled genes mediate a conserved mammalian PCP pathway to regulate convergent extension during neurulation. *Development*. 2006;133(9):1767–78.
98. Ybot-Gonzalez P, Savery D, Gerrelli D, Signore M, Mitchell CE, Faux CH, et al. Convergent extension, planar-cell-polarity signalling and initiation of mouse neural tube closure. *Development*. 2007;134(4):789–99.
99. Kibar Z, Vogan KJ, Groulx N, Justice MJ, Underhill DA, Gros P. Ltap, a mammalian homolog of *Drosophila* Strabismus/Van Gogh, is altered in the mouse neural tube mutant Loop-tail. *Nat Genet*. 2001;28(3):251–5.
100. Murdoch JN, Doudney K, Paternotte C, Copp AJ, Stanier P. Severe neural tube defects in the loop-tail mouse result from mutation of *Lpp1*, a novel gene involved in floor plate specification. *Hum Mol Genet*. 2001;10(22):2593–601.

101. Wilson DB, Wyatt DP. Analysis of neurulation in a mouse model for neural dysraphism. *Exp Neurol.* 1994;127(1):154–8.
102. Smith LJ, Stein KF. Axial elongation in the mouse and its retardation in homozygous looptail mice. *J Embryol Exp Morphol.* 1962;10:73–87.
103. Gerrelli D, Copp AJ. Failure of neural tube closure in the loop-tail (Lp) mutant mouse: analysis of the embryonic mechanism. *Brain Res Dev Brain Res.* 1997;102(2):217–24.
104. Greene ND, Gerrelli D, Van Straaten HW, Copp AJ. Abnormalities of floor plate, notochord and somite differentiation in the loop-tail (Lp) mouse: a model of severe neural tube defects. *Mech Dev.* 1998;73(1):59–72.
105. Kirillova I, Novikova I, Auge J, Audollent S, Esnault D, Encha-Razavi F, et al. Expression of the sonic hedgehog gene in human embryos with neural tube defects. *Teratology.* 2000;61(5):347–54.
106. Hamblet NS, Lijam N, Ruiz-Lozano P, Wang J, Yang Y, Luo Z, et al. Dishevelled 2 is essential for cardiac outflow tract development, somite segmentation and neural tube closure. *Development.* 2002;129(24):5827–38.
107. Etheridge SL, Ray S, Li S, Hamblet NS, Lijam N, Tsang M, et al. Murine dishevelled 3 functions in redundant pathways with dishevelled 1 and 2 in normal cardiac outflow tract, cochlea, and neural tube development. *PLoS Genet.* 2008;4(11):e1000259.
108. Wang Y, Guo N, Nathans J. The role of Frizzled3 and Frizzled6 in neural tube closure and in the planar polarity of inner-ear sensory hair cells. *J Neurosci.* 2006;26(8):2147–56.
109. Curtin JA, Quint E, Tshipouri V, Arkell RM, Cattanch B, Copp AJ, et al. Mutation of Celsr1 disrupts planar polarity of inner ear hair cells and causes severe neural tube defects in the mouse. *Curr Biol.* 2003;13(13):1129–33.
110. Qian D, Jones C, Rzadzinska A, Mark S, Zhang X, Steel KP, et al. Wnt5a functions in planar cell polarity regulation in mice. *Dev Biol.* 2007;306(1):121–33.
111. Lu X, Borchers AG, Jolicoeur C, Rayburn H, Baker JC, Tessier-Lavigne M. PTK7/CCK-4 is a novel regulator of planar cell polarity in vertebrates. *Nature.* 2004;430(6995):93–8.
112. Paudyal A, Damrau C, Patterson VL, Ermakov A, Formstone C, Lalanne Z, et al. The novel mouse mutant, chuzhoi, has disruption of Ptk7 protein and exhibits defects in neural tube, heart and lung development and abnormal planar cell polarity in the ear. *BMC Dev Biol.* 2010;10:87.
113. Gray RS, Abitua PB, Wlodarczyk BJ, Szabo-Rogers HL, Blanchard O, Lee I, et al. The planar cell polarity effector Fuz is essential for targeted membrane trafficking, ciliogenesis and mouse embryonic development. *Nat Cell Biol.* 2009;11(10):1225–32.
114. Copp AJ, Checiu I, Henson JN. Developmental basis of severe neural tube defects in the loop-tail (Lp) mutant mouse: use of microsatellite DNA markers to identify embryonic genotype. *Dev Biol.* 1994;165(1):20–9.
115. Heydeck W, Liu A. PCP effector proteins inturned and fuzzy play nonredundant roles in the patterning but not convergent extension of mammalian neural tube. *Dev Dyn.* 2011;240(8):1938–48.
116. Heydeck W, Zeng H, Liu A. Planar cell polarity effector gene Fuzzy regulates cilia formation and Hedgehog signal transduction in mouse. *Dev Dyn.* 2009;238(12):3035–42.
117. Zeng H, Hoover AN, Liu A. PCP effector gene Inturned is an important regulator of cilia formation and embryonic development in mammals. *Dev Biol.* 2010;339(2):418–28.
118. Yu H, Smallwood PM, Wang Y, Vidaltamayo R, Reed R, Nathans J. Frizzled 1 and frizzled 2 genes function in palate, ventricular septum and neural tube closure: general implications for tissue fusion processes. *Development.* 2010;137(21):3707–17.
119. Torban E, Patenaude AM, Leclerc S, Rakowiecki S, Gauthier S, Andelfinger G, et al. Genetic interaction between members of the Vangl family causes neural tube defects in mice. *Proc Natl Acad Sci U S A.* 2008;105(9):3449–54.
120. Murdoch JN, Damrau C, Paudyal A, Bogani D, Wells S, Greene ND, et al. Genetic interactions between planar cell polarity genes cause diverse neural tube defects in mice. *Dis Model Mech.* 2014;7(10):1153–63.
121. De Castro SCP, Gustavsson P, Marshall AR, Gordon WM, Galea G, Nikolopoulou E, et al. Overexpression of Grainyhead-like 3 causes spina bifida and interacts genetically with mutant alleles of Grhl2 and Vangl2 in mice. *Hum Mol Genet.* 2018;27(24):4218–30.
122. Murdoch JN, Henderson DJ, Doudney K, Gaston-Massuet C, Phillips HM, Paternotte C, et al. Disruption of scribble (Scrb1) causes severe neural tube defects in the circletail mouse. *Hum Mol Genet.* 2003;12(2):87–98.
123. Carroll EA, Gerrelli D, Gasca S, Berg E, Beier DR, Copp AJ, et al. Cordon-bleu is a conserved gene involved in neural tube formation. *Dev Biol.* 2003;262(1):16–31.
124. Caddy J, Wilanowski T, Darido C, Dworkin S, Ting SB, Zhao Q, et al. Epidermal wound repair is regulated by the planar cell polarity signaling pathway. *Dev Cell.* 2010;19(1):138–47.
125. Merte J, Jensen D, Wright K, Sarsfield S, Wang Y, Schekman R, et al. Sec24b selectively sorts Vangl2 to regulate planar cell polarity during neural tube closure. *Nat Cell Biol.* 2010;12(1):41–6; sup pp 1–8.
126. Ross AJ, May-Simera H, Eichers ER, Kai M, Hill J, Jagger DJ, et al. Disruption of Bardet-Biedl syndrome ciliary proteins perturbs planar cell polarity in vertebrates. *Nat Genet.* 2005;37(10):1135–40.
127. Escobedo N, Contreras O, Munoz R, Farias M, Carrasco H, Hill C, et al. Syndecan 4 interacts genetically with Vangl2 to regulate neural tube

- closure and planar cell polarity. *Development*. 2013;140(14):3008–17.
128. Shi Y, Ding Y, Lei YP, Yang XY, Xie GM, Wen J, et al. Identification of novel rare mutations of DACT1 in human neural tube defects. *Hum Mutat*. 2012;33(10):1450–5.
 129. Bosoi CM, Capra V, Allache R, Trinh VQ, De Marco P, Merello E, et al. Identification and characterization of novel rare mutations in the planar cell polarity gene PRICKLE1 in human neural tube defects. *Hum Mutat*. 2011;32(12):1371–5.
 130. Allache R, De Marco P, Merello E, Capra V, Kibar Z. Role of the planar cell polarity gene CELSR1 in neural tube defects and caudal agenesis. *Birth Defects Res A Clin Mol Teratol*. 2012;94(3):176–81.
 131. De Marco P, Merello E, Rossi A, Piatelli G, Cama A, Kibar Z, et al. FZD6 is a novel gene for human neural tube defects. *Hum Mutat*. 2012;33(2):384–90.
 132. Doudney K, Ybot-Gonzalez P, Paternotte C, Stevenson RE, Greene ND, Moore GE, et al. Analysis of the planar cell polarity gene Vangl2 and its co-expressed paralogue Vangl1 in neural tube defect patients. *Am J Med Genet A*. 2005;136(1):90–2.
 133. Kibar Z, Salem S, Bosoi CM, Pauwels E, De Marco P, Merello E, et al. Contribution of VANGL2 mutations to isolated neural tube defects. *Clin Genet*. 2011;80(1):76–82.
 134. Kibar Z, Torban E, McDearmid JR, Reynolds A, Berghout J, Mathieu M, et al. Mutations in VANGL1 associated with neural-tube defects. *N Engl J Med*. 2007;356(14):1432–7.
 135. Lei YP, Zhang T, Li H, Wu BL, Jin L, Wang HY. VANGL2 mutations in human cranial neural-tube defects. *N Engl J Med*. 2010;362(23):2232–5.
 136. Robinson A, Escuin S, Doudney K, Vekemans M, Stevenson RE, Greene ND, et al. Mutations in the planar cell polarity genes CELSR1 and SCRIB are associated with the severe neural tube defect cranio-rachischisis. *Hum Mutat*. 2012;33(2):440–7.
 137. Seo JH, Zilber Y, Babayeveva S, Liu J, Kyriakopoulos P, De Marco P, et al. Mutations in the planar cell polarity gene, Fuzzy, are associated with neural tube defects in humans. *Hum Mol Genet*. 2011;20(22):4324–33.
 138. Lei Y, Zhu H, Duhon C, Yang W, Ross ME, Shaw GM, et al. Mutations in planar cell polarity gene SCRIB are associated with spina bifida. *PLoS One*. 2013;8(7):e69262.
 139. Reynolds A, McDearmid JR, Lachance S, De Marco P, Merello E, Capra V, et al. VANGL1 rare variants associated with neural tube defects affect convergent extension in zebrafish. *Mech Dev*. 2010;127(7-8):385–92.
 140. Kharfallah F, Guyot MC, El Hassan AR, Allache R, Merello E, De Marco P, et al. Scribble1 plays an important role in the pathogenesis of neural tube defects through its mediating effect of Par-3 and Vangl1/2 localization. *Hum Mol Genet*. 2017;26(12):2307–20.
 141. Chen Z, Lei Y, Cao X, Zheng Y, Wang F, Bao Y, et al. Genetic analysis of Wnt/PCP genes in neural tube defects. *BMC Med Genomics*. 2018;11(1):38.
 142. Beaumont M, Akloul L, Carre W, Quelin C, Journel H, Pasquier L, et al. Targeted panel sequencing establishes the implication of planar cell polarity pathway and involves new candidate genes in neural tube defect disorders. *Hum Genet*. 2019;138(4):363–74.
 143. Lei Y, Zhu H, Yang W, Ross ME, Shaw GM, Finnell RH. Identification of novel CELSR1 mutations in spina bifida. *PLoS One*. 2014;9(3):e92207.
 144. Shi OY, Yang HY, Shen YM, Sun W, Cai CY, Cai CQ. Polymorphisms in FZD3 and FZD6 genes and risk of neural tube defects in a northern Han Chinese population. *Neurol Sci*. 2014;35(11):1701–6.
 145. Wang L, Xiao Y, Tian T, Jin L, Lei Y, Finnell RH, et al. Digenic variants of planar cell polarity genes in human neural tube defect patients. *Mol Genet Metab*. 2018;124(1):94–100.
 146. Wang M, De Marco P, Merello E, Drapeau P, Capra V, Kibar Z. Role of the planar cell polarity gene Protein tyrosine kinase 7 in neural tube defects in humans. *Birth Defects Res A Clin Mol Teratol*. 2015;103(12):1021–7.
 147. Lei Y, Kim SE, Chen Z, Cao X, Zhu H, Yang W, et al. Variants identified in PTK7 associated with neural tube defects. *Mol Genet Genomic Med*. 2019;7:e584.
 148. Ishida M, Cullup T, Boustred C, James C, Docker J, English C, et al. A targeted sequencing panel identifies rare damaging variants in multiple genes in the cranial neural tube defect, anencephaly. *Clin Genet*. 2018;93(4):870–9.
 149. Eom DS, Amarnath S, Agarwala S. Apicobasal polarity and neural tube closure. *Dev Growth Differ*. 2013;55(1):164–72.
 150. Eom DS, Amarnath S, Fogel JL, Agarwala S. Bone morphogenetic proteins regulate hinge point formation during neural tube closure by dynamic modulation of apicobasal polarity. *Birth Defects Res A Clin Mol Teratol*. 2012;94(10):804–16.
 151. Eom DS, Amarnath S, Fogel JL, Agarwala S. Bone morphogenetic proteins regulate neural tube closure by interacting with the apicobasal polarity pathway. *Development*. 2011;138(15):3179–88.
 152. Smith JL, Schoenwolf GC. Cell cycle and neuroepithelial cell shape during bending of the chick neural plate. *Anat Rec*. 1987;218(2):196–206.
 153. Rolo A, Escuin S, Greene NDE, Copp AJ. Rho GTPases in mammalian spinal neural tube closure. *Small GTPases*. 2018;9(4):283–9.
 154. Escuin S, Vernay B, Savery D, Gurniak CB, Witke W, Greene ND, et al. Rho-kinase-dependent actin turnover and actomyosin disassembly are necessary for mouse spinal neural tube closure. *J Cell Sci*. 2015;128(14):2468–81.
 155. Haigo SL, Hildebrand JD, Harland RM, Wallingford JB. Shroom induces apical constriction and is required for hinge point formation during neural tube closure. *Curr Biol*. 2003;13(24):2125–37.

156. Hildebrand JD, Soriano P. Shroom, a PDZ domain-containing actin-binding protein, is required for neural tube morphogenesis in mice. *Cell*. 1999;99(5):485–97.
157. Lee JD, Silva-Gagliardi NF, Tepass U, McGlade CJ, Anderson KV. The FERM protein Epb4.115 is required for organization of the neural plate and for the epithelial-mesenchymal transition at the primitive streak of the mouse embryo. *Development*. 2007;134(11):2007–16.
158. Nishimura T, Takeichi M. Shroom3-mediated recruitment of Rho kinases to the apical cell junctions regulates epithelial and neuroepithelial planar remodeling. *Development*. 2008;135(8):1493–502.
159. Kinoshita N, Sasai N, Misaki K, Yonemura S. Apical accumulation of Rho in the neural plate is important for neural plate cell shape change and neural tube formation. *Mol Biol Cell*. 2008;19(5):2289–99.
160. Rolo A, Skoglund P, Keller R. Morphogenetic movements driving neural tube closure in *Xenopus* require myosin IIB. *Dev Biol*. 2009;327(2):327–38.
161. Gray J, Ross ME. Neural tube closure in mouse whole embryo culture. *J Vis Exp*. 2011;(56).
162. Gray JD, Kholmanskikh S, Castaldo BS, Hansler A, Chung H, Klotz B, et al. LRP6 exerts non-canonical effects on Wnt signaling during neural tube closure. *Hum Mol Genet*. 2013;22(21):4267–81.
163. Lanier LM, Gates MA, Witke W, Menzies AS, Wehman AM, Macklis JD, et al. Mena is required for neurulation and commissure formation. *Neuron*. 1999;22(2):313–25.
164. Menzies AS, Aszodi A, Williams SE, Pfeifer A, Wehman AM, Goh KL, et al. Mena and vasodilator-stimulated phosphoprotein are required for multiple actin-dependent processes that shape the vertebrate nervous system. *J Neurosci*. 2004;24(37):8029–38.
165. Plageman TF Jr, Chauhan BK, Yang C, Jaudon F, Shang X, Zheng Y, et al. A Trio-RhoA-Shroom3 pathway is required for apical constriction and epithelial invagination. *Development*. 2011;138(23):5177–88.
166. Plageman TF Jr, Chung MI, Lou M, Smith AN, Hildebrand JD, Wallingford JB, et al. Pax6-dependent Shroom3 expression regulates apical constriction during lens placode invagination. *Development*. 2010;137(3):405–15.
167. Lemay P, De Marco P, Traverso M, Merello E, Dionne-Laporte A, Spiegelman D, et al. Whole exome sequencing identifies novel predisposing genes in neural tube defects. *Mol Genet Genomic Med*. 2019;7(1):e00467.
168. Lemay P, Guyot MC, Tremblay E, Dionne-Laporte A, Spiegelman D, Henrion E, et al. Loss-of-function de novo mutations play an important role in severe human neural tube defects. *J Med Genet*. 2015;52(7):493–7.
169. Chen Z, Kuang L, Finnell RH, Wang H. Genetic and functional analysis of SHROOM1-4 in a Chinese neural tube defect cohort. *Hum Genet*. 2018;137(3):195–202.
170. Nishimura T, Honda H, Takeichi M. Planar cell polarity links axes of spatial dynamics in neural-tube closure. *Cell*. 2012;149(5):1084–97.
171. Mahaffey JP, Grego-Bessa J, Liem KF Jr, Anderson KV. Cofilin and Vangl2 cooperate in the initiation of planar cell polarity in the mouse embryo. *Development*. 2013;140(6):1262–71.
172. McGreevy EM, Vijayraghavan D, Davidson LA, Hildebrand JD. Shroom3 functions downstream of planar cell polarity to regulate myosin II distribution and cellular organization during neural tube closure. *Biol Open*. 2015;4(2):186–96.
173. Nikolopoulou E, Galea GL, Rolo A, Greene ND, Copp AJ. Neural tube closure: cellular, molecular and biomechanical mechanisms. *Development*. 2017;144(4):552–66.
174. Sutherland AE. Tissue morphodynamics shaping the early mouse embryo. *Semin Cell Dev Biol*. 2016;55:89–98.
175. Williams M, Yen W, Lu X, Sutherland A. Distinct apical and basolateral mechanisms drive planar cell polarity-dependent convergent extension of the mouse neural plate. *Dev Cell*. 2014;29(1):34–46.
176. Butler MT, Wallingford JB. Spatial and temporal analysis of PCP protein dynamics during neural tube closure. *Elife*. 2018;7.
177. Shum AS, Copp AJ. Regional differences in morphogenesis of the neuroepithelium suggest multiple mechanisms of spinal neurulation in the mouse. *Anat Embryol (Berl)*. 1996;194(1):65–73.
178. Ybot-Gonzalez P, Cogram P, Gerelli D, Copp AJ. Sonic hedgehog and the molecular regulation of mouse neural tube closure. *Development*. 2002;129(10):2507–17.
179. Ybot-Gonzalez P, Gaston-Massuet C, Girdler G, Klingensmith J, Arkell R, Greene ND, et al. Neural plate morphogenesis during mouse neurulation is regulated by antagonism of Bmp signalling. *Development*. 2007;134(17):3203–11.
180. Panchision DM, Pickel JM, Studer L, Lee SH, Turner PA, Hazel TG, et al. Sequential actions of BMP receptors control neural precursor cell production and fate. *Genes Dev*. 2001;15(16):2094–110.
181. Stottmann RW, Berrong M, Matta K, Choi M, Klingensmith J. The BMP antagonist Noggin promotes cranial and spinal neurulation by distinct mechanisms. *Dev Biol*. 2006;295(2):647–63.
182. McMahon JA, Takada S, Zimmerman LB, Fan CM, Harland RM, McMahon AP. Noggin-mediated antagonism of BMP signaling is required for growth and patterning of the neural tube and somite. *Genes Dev*. 1998;12(10):1438–52.
183. Chang H, Huylebroeck D, Verschueren K, Guo Q, Matzuk MM, Zwijsen A. Smad5 knockout mice die at mid-gestation due to multiple embryonic and extraembryonic defects. *Development*. 1999;126(8):1631–42.
184. Solloway MJ, Robertson EJ. Early embryonic lethality in *Bmp5;Bmp7* double mutant mice suggests

- functional redundancy within the 60A subgroup. *Development*. 1999;126(8):1753–68.
185. Castranio T, Mishina Y. Bmp2 is required for cephalic neural tube closure in the mouse. *Dev Dyn*. 2009;238(1):110–22.
 186. Stottmann RW, Klingensmith J. Bone morphogenetic protein signaling is required in the dorsal neural folds before neurulation for the induction of spinal neural crest cells and dorsal neurons. *Dev Dyn*. 2011;240(4):755–65.
 187. Murdoch JN, Copp AJ. The relationship between sonic Hedgehog signaling, cilia, and neural tube defects. *Birth Defects Res A Clin Mol Teratol*. 2010;88(8):633–52.
 188. Wang Z, Wang L, Shangguan S, Lu X, Chang S, Wang J, et al. Association between PTCH1 polymorphisms and risk of neural tube defects in a Chinese population. *Birth Defects Res A Clin Mol Teratol*. 2013;97(6):409–15.
 189. Wang Z, Shangguan S, Lu X, Chang S, Li R, Wu L, et al. Association of SMO polymorphisms and neural tube defects in the Chinese population from Shanxi Province. *Int J Clin Exp Med*. 2013;6(10):960–6.
 190. Wu J, Lu X, Wang Z, Shangguan S, Chang S, Li R, et al. Association between PKA gene polymorphism and NTDs in high risk Chinese population in Shanxi. *Int J Clin Exp Pathol*. 2013;6(12):2968–74.
 191. Kim SE, Lei Y, Hwang SH, Wlodarczyk BJ, Mukhopadhyay S, Shaw GM, et al. Dominant negative GPR161 rare variants are risk factors of human spina bifida. *Hum Mol Genet*. 2019;28(2):200–8.
 192. Wallingford JB, Mitchell B. Strange as it may seem: the many links between Wnt signaling, planar cell polarity, and cilia. *Genes Dev*. 2011;25(3):201–13.
 193. Eichers ER, Abd-El-Barr MM, Paylor R, Lewis RA, Bi W, Lin X, et al. Phenotypic characterization of Bbs4 null mice reveals age-dependent penetrance and variable expressivity. *Hum Genet*. 2006;120(2):211–26.
 194. Caspary T, Larkins CE, Anderson KV. The graded response to Sonic Hedgehog depends on cilia architecture. *Dev Cell*. 2007;12(5):767–78.
 195. Abdelhamed ZA, Wheway G, Szymanska K, Natarajan S, Toomes C, Inglehearn C, et al. Variable expressivity of ciliopathy neurological phenotypes that encompass Meckel-Gruber syndrome and Joubert syndrome is caused by complex de-regulated ciliogenesis, Shh and Wnt signalling defects. *Hum Mol Genet*. 2013;22(7):1358–72.
 196. Weatherbee SD, Niswander LA, Anderson KV. A mouse model for Meckel syndrome reveals Mks1 is required for ciliogenesis and Hedgehog signaling. *Hum Mol Genet*. 2009;18(23):4565–75.
 197. Bay SN, Caspary T. What are those cilia doing in the neural tube? *Cilia*. 2012;1(1):19.
 198. Briscoe J, Therond PP. The mechanisms of Hedgehog signalling and its roles in development and disease. *Nat Rev Mol Cell Biol*. 2013;14(7):416–29.
 199. Hackett DA, Smith JL, Schoenwolf GC. Epidermal ectoderm is required for full elevation and for convergence during bending of the avian neural plate. *Dev Dyn*. 1997;210(4):397–406.
 200. Alvarez IS, Schoenwolf GC. Expansion of surface epithelium provides the major extrinsic force for bending of the neural plate. *J Exp Zool*. 1992;261(3):340–8.
 201. Jacobson AG, Moury JD. Tissue boundaries and cell behavior during neurulation. *Dev Biol*. 1995;171(1):98–110.
 202. Moury JD, Schoenwolf GC. Cooperative model of epithelial shaping and bending during avian neurulation: autonomous movements of the neural plate, autonomous movements of the epidermis, and interactions in the neural plate/epidermis transition zone. *Dev Dyn*. 1995;204(3):323–37.
 203. Morita H, Kajiura-Kobayashi H, Takagi C, Yamamoto TS, Nonaka S, Ueno N. Cell movements of the deep layer of non-neural ectoderm underlie complete neural tube closure in *Xenopus*. *Development*. 2012;139(8):1417–26.
 204. Sausedo RA, Smith JL, Schoenwolf GC. Role of nonrandomly oriented cell division in shaping and bending of the neural plate. *J Comp Neurol*. 1997;381(4):473–88.
 205. Brouns MR, De Castro SC, Terwindt-Rouwenhorst EA, Massa V, Hekking JW, Hirst CS, et al. Overexpression of Grhl2 causes spina bifida in the axial defects mutant mouse. *Hum Mol Genet*. 2011;20(8):1536–46.
 206. Auden A, Caddy J, Wilanowski T, Ting SB, Cunningham JM, Jane SM. Spatial and temporal expression of the Grainyhead-like transcription factor family during murine development. *Gene Expr Patterns*. 2006;6(8):964–70.
 207. Gustavsson P, Greene ND, Lad D, Pauws E, de Castro SC, Stanier P, et al. Increased expression of Grainyhead-like-3 rescues spina bifida in a folate-resistant mouse model. *Hum Mol Genet*. 2007;16(21):2640–6.
 208. Pyrgaki C, Liu A, Niswander L. Grainyhead-like 2 regulates neural tube closure and adhesion molecule expression during neural fold fusion. *Dev Biol*. 2011;353(1):38–49.
 209. Rifat Y, Parekh V, Wilanowski T, Hislop NR, Auden A, Ting SB, et al. Regional neural tube closure defined by the Grainy head-like transcription factors. *Dev Biol*. 2010;345(2):237–45.
 210. Ting SB, Wilanowski T, Auden A, Hall M, Voss AK, Thomas T, et al. Inositol- and folate-resistant neural tube defects in mice lacking the epithelial-specific factor Grhl-3. *Nat Med*. 2003;9(12):1513–9.
 211. Werth M, Walentin K, Aue A, Schonheit J, Wuebken A, Pode-Shakked N, et al. The transcription factor grainyhead-like 2 regulates the molecular composition of the epithelial apical junctional complex. *Development*. 2010;137(22):3835–45.

212. Yu Z, Lin KK, Bhandari A, Spencer JA, Xu X, Wang N, et al. The Grainyhead-like epithelial transactivator Get-1/Grhl3 regulates epidermal terminal differentiation and interacts functionally with LMO4. *Dev Biol*. 2006;299(1):122–36.
213. Copp AJ, Brook FA, Roberts HJ. A cell-type-specific abnormality of cell proliferation in mutant (curly tail) mouse embryos developing spinal neural tube defects. *Development*. 1988;104(2):285–95.
214. Lemay P, De Marco P, Emond A, Spiegelman D, Dionne-Laporte A, Laurent S, et al. Rare deleterious variants in GRHL3 are associated with human spina bifida. *Hum Mutat*. 2017;38(6):716–24.
215. Geelen JA, Langman J. Ultrastructural observations on closure of the neural tube in the mouse. *Anat Embryol (Berl)*. 1979;156(1):73–88.
216. Smithells RW, Sheppard S, Schorah CJ. Vitamin deficiencies and neural tube defects. *Arch Dis Child*. 1976;51(12):944–50.
217. Laurence KM, Carter CO, David PA. Major central nervous system malformations in South Wales. II. Pregnancy factors, seasonal variation, and social class effects. *Br J Prev Soc Med*. 1968;22(4):212–22.
218. Holmes-Siedle M, Lindenbaum RH, Galliard A. Recurrence of neural tube defect in a group of at risk women: a 10 year study of Pregnavite Forte F. *J Med Genet*. 1992;29(2):134–5.
219. Laurence KM, James N, Miller MH, Tennant GB, Campbell H. Double-blind randomised controlled trial of folate treatment before conception to prevent recurrence of neural-tube defects. *Br Med J (Clin Res Ed)*. 1981;282(6275):1509–11.
220. Seller MJ, Nevin NC. Periconceptional vitamin supplementation and the prevention of neural tube defects in south-east England and Northern Ireland. *J Med Genet*. 1984;21(5):325–30.
221. Smithells RW, Sheppard S, Schorah CJ, Seller MJ, Nevin NC, Harris R, et al. Possible prevention of neural-tube defects by periconceptional vitamin supplementation. *Lancet*. 1980;1(8164):339–40.
222. Smithells RW, Sheppard S, Schorah CJ, Seller MJ, Nevin NC, Harris R, et al. Apparent prevention of neural tube defects by periconceptional vitamin supplementation. *Arch Dis Child*. 1981;56(12):911–8.
223. Vergel RG, Sanchez LR, Heredero BL, Rodriguez PL, Martinez AJ. Primary prevention of neural tube defects with folic acid supplementation: Cuban experience. *Prenat Diagn*. 1990;10(3):149–52.
224. Wald N, Sneddon J, Densem J, Frost C, Stone R, Group MVS. Prevention of neural tube defects: results of the Medical Research Council Vitamin Study. MRC Vitamin Study Research Group. *Lancet*. 1991;338(8760):131–7.
225. Hesecker HB, Mason JB, Selhub J, Rosenberg IH, Jacques PF. Not all cases of neural-tube defect can be prevented by increasing the intake of folic acid. *Br J Nutr*. 2009;102(2):173–80.
226. Berry RJ, Li Z, Erickson JD, Li S, Moore CA, Wang H, et al. Prevention of neural-tube defects with folic acid in China. China-U.S. Collaborative Project for Neural Tube Defect Prevention. *N Engl J Med*. 1999;341(20):1485–90.
227. Honein MA, Paulozzi LJ, Mathews TJ, Erickson JD, Wong LY. Impact of folic acid fortification of the US food supply on the occurrence of neural tube defects. *JAMA*. 2001;285(23):2981–6.
228. Williams J, Mai CT, Mulinare J, Isenburg J, Flood TJ, Ethen M, et al. Updated estimates of neural tube defects prevented by mandatory folic acid fortification—United States, 1995–2011. *MMWR Morb Mortal Wkly Rep*. 2015;64(1):1–5.
229. Mosley BS, Cleves MA, Siega-Riz AM, Shaw GM, Canfield MA, Waller DK, et al. Neural tube defects and maternal folate intake among pregnancies conceived after folic acid fortification in the United States. *Am J Epidemiol*. 2009;169(1):9–17.
230. Blom HJ, Shaw GM, den Heijer M, Finnell RH. Neural tube defects and folate: case far from closed. *Nat Rev Neurosci*. 2006;7(9):724–31.
231. Rothenberg SP, da Costa MP, Sequeira JM, Cracco J, Roberts JL, Weedon J, et al. Autoantibodies against folate receptors in women with a pregnancy complicated by a neural-tube defect. *N Engl J Med*. 2004;350(2):134–42.
232. Cabrera RM, Shaw GM, Ballard JL, Carmichael SL, Yang W, Lammer EJ, et al. Autoantibodies to folate receptor during pregnancy and neural tube defect risk. *J Reprod Immunol*. 2008;79(1):85–92.
233. Boyles AL, Ballard JL, Gorman EB, McConaughy DR, Cabrera RM, Wilcox AJ, et al. Association between inhibited binding of folic acid to folate receptor alpha in maternal serum and folate-related birth defects in Norway. *Hum Reprod*. 2011;26(8):2232–8.
234. Yang N, Wang L, Finnell RH, Li Z, Jin L, Zhang L, et al. Levels of folate receptor autoantibodies in maternal and cord blood and risk of neural tube defects in a Chinese population. *Birth Defects Res A Clin Mol Teratol*. 2016;106(8):685–95.
235. van der Linden IJ, Afman LA, Heil SG, Blom HJ. Genetic variation in genes of folate metabolism and neural-tube defect risk. *Proc Nutr Soc*. 2006;65(2):204–15.
236. Denny KJ, Jeanes A, Fathe K, Finnell RH, Taylor SM, Woodruff TM. Neural tube defects, folate, and immune modulation. *Birth Defects Res A Clin Mol Teratol*. 2013;97(9):602–9.
237. Piedrahita JA, Oetama B, Bennett GD, van Waes J, Kamen BA, Richardson J, et al. Mice lacking the folic acid-binding protein Folbp1 are defective in early embryonic development. *Nat Genet*. 1999;23(2):228–32.
238. Gelineau-van Waes J, Heller S, Bauer LK, Wilberding J, Maddox JR, Aleman F, et al. Embryonic development in the reduced folate carrier knockout mouse is modulated by maternal folate supplementation. *Birth Defects Res A Clin Mol Teratol*. 2008;82(7):494–507.
239. Zhao R, Russell RG, Wang Y, Liu L, Gao F, Kneitz B, et al. Rescue of embryonic lethality in reduced folate

- carrier-deficient mice by maternal folic acid supplementation reveals early neonatal failure of hematopoietic organs. *J Biol Chem.* 2001;276(13):10224–8.
240. Spiegelstein O, Mitchell LE, Merriweather MY, Wicker NJ, Zhang Q, Lammer EJ, et al. Embryonic development of folate binding protein-1 (Folbp1) knockout mice: effects of the chemical form, dose, and timing of maternal folate supplementation. *Dev Dyn.* 2004;231(1):221–31.
241. Zhao Q, Behringer RR, de Crombrughe B. Prenatal folic acid treatment suppresses acrania and meroencephaly in mice mutant for the *Cart1* homeobox gene. *Nat Genet.* 1996;13(3):275–83.
242. Lin W, Zhang Z, Srajer G, Chen YC, Huang M, Phan HM, et al. Proper expression of the *Gcn5* histone acetyltransferase is required for neural tube closure in mouse embryos. *Dev Dyn.* 2008;237(4):928–40.
243. Fleming A, Copp AJ. Embryonic folate metabolism and mouse neural tube defects. *Science.* 1998;280(5372):2107–9.
244. Barbera JP, Rodriguez TA, Greene ND, Weninger WJ, Simeone A, Copp AJ, et al. Folic acid prevents exencephaly in *Cited2* deficient mice. *Hum Mol Genet.* 2002;11(3):283–93.
245. Carter M, Chen X, Slowinska B, Minnerath S, Glickstein S, Shi L, et al. Crooked tail (*Cd*) model of human folate-responsive neural tube defects is mutated in *Wnt* coreceptor lipoprotein receptor-related protein 6. *Proc Natl Acad Sci U S A.* 2005;102(36):12843–8.
246. Wlodarczyk BJ, Tang LS, Triplett A, Aleman F, Finnell RH. Spontaneous neural tube defects in *splotch* mice supplemented with selected micronutrients. *Toxicol Appl Pharmacol.* 2006;213(1):55–63.
247. Sabatino JA, Stokes BA, Zohn IE. Prevention of neural tube defects in *Lrp2* mutant mouse embryos by folic acid supplementation. *Birth Defects Res.* 2017;109(1):16–26.
248. Birn H, Spiegelstein O, Christensen EI, Finnell RH. Renal tubular reabsorption of folate mediated by folate binding protein 1. *J Am Soc Nephrol.* 2005;16(3):608–15.
249. Essien FB, Wannberg SL. Methionine but not folic acid or vitamin B-12 alters the frequency of neural tube defects in *Axd* mutant mice. *J Nutr.* 1993;123(1):27–34.
250. Seller MJ. Vitamins, folic acid and the cause and prevention of neural tube defects. *Ciba Found Symp.* 1994;181:161–73; discussion 73–9.
251. Wong RL, Wlodarczyk BJ, Min KS, Scott ML, Kartiko S, Yu W, et al. Mouse *Fkbp8* activity is required to inhibit cell death and establish dorsoventral patterning in the posterior neural tube. *Hum Mol Genet.* 2008;17(4):587–601.
252. Chi H, Sarkisian MR, Rakic P, Flavell RA. Loss of mitogen-activated protein kinase kinase kinase 4 (*MEKK4*) results in enhanced apoptosis and defective neural tube development. *Proc Natl Acad Sci U S A.* 2005;102(10):3846–51.
253. Gray JD, Nakouzi G, Slowinska-Castaldo B, Dazard JE, Rao JS, Nadeau JH, et al. Functional interactions between the LRP6 WNT co-receptor and folate supplementation. *Hum Mol Genet.* 2010;19(23):4560–72.
254. Marean A, Graf A, Zhang Y, Niswander L. Folic acid supplementation can adversely affect murine neural tube closure and embryonic survival. *Hum Mol Genet.* 2011;20(18):3678–83.
255. Christensen KE, Mikael LG, Leung KY, Levesque N, Deng L, Wu Q, et al. High folic acid consumption leads to pseudo-MTHFR deficiency, altered lipid metabolism, and liver injury in mice. *Am J Clin Nutr.* 2015;101(3):646–58.
256. Bahous RH, Jadavji NM, Deng L, Cosin-Tomas M, Lu J, Malysheva O, et al. High dietary folate in pregnant mice leads to pseudo-MTHFR deficiency and altered methyl metabolism, with embryonic growth delay and short-term memory impairment in offspring. *Hum Mol Genet.* 2017;26(5):888–900.
257. Beaudin AE, Abarinov EV, Malysheva O, Perry CA, Caudill M, Stover PJ. Dietary folate, but not choline, modifies neural tube defect risk in *Shmt1* knockout mice. *Am J Clin Nutr.* 2012;95(1):109–14.
258. Burgoon JM, Selhub J, Nadeau M, Sadler TW. Investigation of the effects of folate deficiency on embryonic development through the establishment of a folate deficient mouse model. *Teratology.* 2002;65(5):219–27.
259. Burren KA, Savery D, Massa V, Kok RM, Scott JM, Blom HJ, et al. Gene-environment interactions in the causation of neural tube defects: folate deficiency increases susceptibility conferred by loss of *Pax3* function. *Hum Mol Genet.* 2008;17(23):3675–85.
260. Burren KA, Scott JM, Copp AJ, Greene ND. The genetic background of the curly tail strain confers susceptibility to folate-deficiency-induced exencephaly. *Birth Defects Res A Clin Mol Teratol.* 2010;88(2):76–83.
261. De Castro SC, Leung KY, Savery D, Burren K, Rozen R, Copp AJ, et al. Neural tube defects induced by folate deficiency in mutant curly tail (*Grhl3*) embryos are associated with alteration in folate one-carbon metabolism but are unlikely to result from diminished methylation. *Birth Defects Res A Clin Mol Teratol.* 2010;88(8):612–8.
262. Heid MK, Bills ND, Hinrichs SH, Clifford AJ. Folate deficiency alone does not produce neural tube defects in mice. *J Nutr.* 1992;122(4):888–94.
263. Kirke PN, Molloy AM, Daly LE, Burke H, Weir DG, Scott JM. Maternal plasma folate and vitamin B12 are independent risk factors for neural tube defects. *Q J Med.* 1993;86(11):703–8.
264. Beaudin AE, Abarinov EV, Noden DM, Perry CA, Chu S, Stabler SP, et al. *Shmt1* and de novo thymidylate biosynthesis underlie folate-responsive neural tube defects in mice. *Am J Clin Nutr.* 2011;93(4):789–98.

265. Dunlevy LP, Chitty LS, Burren KA, Doudney K, Stojilkovic-Mikic T, Stanier P, et al. Abnormal folate metabolism in foetuses affected by neural tube defects. *Brain*. 2007;130(Pt 4):1043–9.
266. Ernest S, Carter M, Shao H, Hosack A, Lerner N, Colmenares C, et al. Parallel changes in metabolite and expression profiles in crooked-tail mutant and folate-reduced wild-type mice. *Hum Mol Genet*. 2006;15(23):3387–93.
267. Carezani-Gavin M, Clarren SK, Steege T. Waardenburg syndrome associated with meningo-myelocele. *Am J Med Genet*. 1992;42(1):135–6.
268. Begleiter ML, Harris DJ. Waardenburg syndrome and meningocele. *Am J Med Genet*. 1992;44(4):541.
269. Chatkupt S, Chatkupt S, Johnson WG. Waardenburg syndrome and myelomeningocele in a family. *J Med Genet*. 1993;30(1):83–4.
270. da-Silva EO. Waardenburg I syndrome: a clinical and genetic study of two large Brazilian kindreds, and literature review. *Am J Med Genet*. 1991;40(1):65–74.
271. de Saxe M, Kromberg JG, Jenkins T. Waardenburg syndrome in South Africa. Part I. An evaluation of the clinical findings in 11 families. *S Afr Med J*. 1984;66(7):256–61.
272. Hol FA, Hamel BC, Geurds MP, Mullaart RA, Barr FG, Macina RA, et al. A frameshift mutation in the gene for PAX3 in a girl with spina bifida and mild signs of Waardenburg syndrome. *J Med Genet*. 1995;32(1):52–6.
273. Hoth CF, Milunsky A, Lipsky N, Sheffer R, Clarren SK, Baldwin CT. Mutations in the paired domain of the human PAX3 gene cause Klein-Waardenburg syndrome (WS-III) as well as Waardenburg syndrome type I (WS-I). *Am J Hum Genet*. 1993;52(3):455–62.
274. Kujat A, Veith VP, Faber R, Froster UG. Prenatal diagnosis and genetic counseling in a case of spina bifida in a family with Waardenburg syndrome type I. *Fetal Diagn Ther*. 2007;22(2):155–8.
275. Moline ML, Sandlin C. Waardenburg syndrome and meningo-myelocele. *Am J Med Genet*. 1993;47(1):126.
276. Pantke OA, Cohen MM Jr. The Waardenburg syndrome. *Birth Defects Orig Artic Ser*. 1971;7(7):147–52.
277. Shim SH, Wyandt HE, McDonald-McGinn DM, Zackai EZ, Milunsky A. Molecular cytogenetic characterization of multiple intrachromosomal rearrangements of chromosome 2q in a patient with Waardenburg's syndrome and other congenital defects. *Clin Genet*. 2004;66(1):46–52.
278. Beaudin AE, Stover PJ. Folate-mediated one-carbon metabolism and neural tube defects: balancing genome synthesis and gene expression. *Birth Defects Res C Embryo Today*. 2007;81(3):183–203.
279. Tibbetts AS, Appling DR. Compartmentalization of mammalian folate-mediated one-carbon metabolism. *Annu Rev Nutr*. 2010;30:57–81.
280. Ducker GS, Rabinowitz JD. One-carbon metabolism in health and disease. *Cell Metab*. 2017;25(1):27–42.
281. Martin JB, Muccioli M, Herman K, Finnell RH, Plageman TF Jr. Folic acid modifies the shape of epithelial cells during morphogenesis via a Folr1 and MLCK dependent mechanism. *Biol Open*. 2019;8(1).
282. Balashova OA, Visina O, Borodinsky LN. Folate receptor 1 is necessary for neural plate cell apical constriction during *Xenopus* neural tube formation. *Development*. 2017;144(8):1518–30.
283. Toriyama M, Toriyama M, Wallingford JB, Finnell RH. Folate-dependent methylation of septins governs ciliogenesis during neural tube closure. *FASEB J*. 2017;31(8):3622–35.
284. Li H, Niswander L. Does DNA methylation provide a link between folate and neural tube closure? *Epigenomics*. 2018;10(10):1263–5.
285. Alata Jimenez N, Torres Perez SA, Sanchez-Vasquez E, Fernandino JI, Strobl-Mazzulla PH. Folate deficiency prevents neural crest fate by disturbing the epigenetic Sox2 repression on the dorsal neural tube. *Dev Biol*. 2018;444(Suppl 1):S193–201.
286. Finnell RH, Blom HJ, Shaw GM. Does global hypomethylation contribute to susceptibility to neural tube defects? *Am J Clin Nutr*. 2010;91(5):1153–4.
287. Lin S, Ren A, Wang L, Huang Y, Wang Y, Wang C, et al. Oxidative stress and apoptosis in benzo[a]pyrene-induced neural tube defects. *Free Radic Biol Med*. 2018;116:149–58.
288. Wei D, Loeken MR. Increased DNA methyltransferase 3b (Dnmt3b)-mediated CpG island methylation stimulated by oxidative stress inhibits expression of a gene required for neural tube and neural crest development in diabetic pregnancy. *Diabetes*. 2014;63(10):3512–22.
289. Oyama K, Sugimura Y, Murase T, Uchida A, Hayasaka S, Oiso Y, et al. Folic acid prevents congenital malformations in the offspring of diabetic mice. *Endocr J*. 2009;56(1):29–37.
290. Juriloff DM, Harris MJ. Hypothesis: the female excess in cranial neural tube defects reflects an epigenetic drag of the inactivating X chromosome on the molecular mechanisms of neural fold elevation. *Birth Defects Res A Clin Mol Teratol*. 2012;94(10):849–55.
291. Poletta FA, Rittler M, Saleme C, Campana H, Gili JA, Pawluk MS, et al. Neural tube defects: sex ratio changes after fortification with folic acid. *PLoS One*. 2018;13(3):e0193127.
292. Evans JA. Comment on changes in sex ratio in neural tube defects since food fortification with folic acid: re “hypothesis: the female excess in cranial neural tube defects reflects an epigenetic drag of the inactivating X chromosome on the molecular mechanisms of neural tube fold elevation”. *Birth Defects Res A Clin Mol Teratol*. 2012;94(11):958.
293. Taparia S, Gelineau-van Waes J, Rosenquist TH, Finnell RH. Importance of folate-homocysteine homeostasis during early embryonic development. *Clin Chem Lab Med*. 2007;45(12):1717–27.

294. Yang M, Li W, Wan Z, Du Y. Elevated homocysteine levels in mothers with neural tube defects: a systematic review and meta-analysis. *J Matern Fetal Neonatal Med.* 2017;30(17):2051–7.
295. Denny KJ, Kelly CF, Kumar V, Witham KL, Cabrera RM, Finnell RH, et al. Autoantibodies against homocysteinylated protein in a mouse model of folate deficiency-induced neural tube defects. *Birth Defects Res A Clin Mol Teratol.* 2016;106(3):201–7.
296. Dong Y, Wang L, Lei Y, Yang N, Cabrera RM, Finnell RH, et al. Gene variants in the folate pathway are associated with increased levels of folate receptor autoantibodies. *Birth Defects Res.* 2018;110(12):973–81.
297. Zhang Q, Bai B, Mei X, Wan C, Cao H, Dan L, et al. Elevated H3K79 homocysteinylated causes abnormal gene expression during neural development and subsequent neural tube defects. *Nat Commun.* 2018;9(1):3436.
298. Shah RH, Northrup H, Hixson JE, Morrison AC, Au KS. Genetic association of the glycine cleavage system genes and myelomeningocele. *Birth Defects Res A Clin Mol Teratol.* 2016;106(10):847–53.
299. Narisawa A, Komatsuzaki S, Kikuchi A, Niihori T, Aoki Y, Fujiwara K, et al. Mutations in genes encoding the glycine cleavage system predispose to neural tube defects in mice and humans. *Hum Mol Genet.* 2012;21(7):1496–503.
300. Pai YJ, Leung KY, Savery D, Hutchin T, Prunty H, Heales S, et al. Glycine decarboxylase deficiency causes neural tube defects and features of non-ketotic hyperglycinemia in mice. *Nat Commun.* 2015;6:6388.
301. Parle-McDermott A, Pangilinan F, O'Brien KK, Mills JL, Magee AM, Troendle J, et al. A common variant in MTHFD1L is associated with neural tube defects and mRNA splicing efficiency. *Hum Mutat.* 2009;30(12):1650–6.
302. Kim J, Lei Y, Guo J, Kim SE, Wlodarczyk BJ, Cabrera RM, et al. Formate rescues neural tube defects caused by mutations in *Slc25a32*. *Proc Natl Acad Sci U S A.* 2018;115(18):4690–5.
303. Martiniova L, Field MS, Finkelstein JL, Perry CA, Stover PJ. Maternal dietary uridine causes, and deoxyuridine prevents, neural tube closure defects in a mouse model of folate-responsive neural tube defects. *Am J Clin Nutr.* 2015;101(4):860–9.
304. Momb J, Lewandowski JP, Bryant JD, Fitch R, Surman DR, Vokes SA, et al. Deletion of *Mthfd11* causes embryonic lethality and neural tube and craniofacial defects in mice. *Proc Natl Acad Sci U S A.* 2013;110(2):549–54.
305. Sudiwala S, De Castro SC, Leung KY, Brosnan JT, Brosnan ME, Mills K, et al. Formate supplementation enhances folate-dependent nucleotide biosynthesis and prevents spina bifida in a mouse model of folic acid-resistant neural tube defects. *Biochimie.* 2016;126:63–70.
306. Bryant JD, Sweeney SR, Sentandreu E, Shin M, Ipas H, Xhemalce B, et al. Deletion of the neural tube defect-associated gene *Mthfd11* disrupts one-carbon and central energy metabolism in mouse embryos. *J Biol Chem.* 2018;293(16):5821–33.
307. Greene ND, Leung KY, Copp AJ. Inositol, neural tube closure and the prevention of neural tube defects. *Birth Defects Res.* 2017;109(2):68–80.
308. Noventa M, Vitagliano A, Quaranta M, Borgato S, Abdulrahim B, Gizzo S. Preventive and therapeutic role of dietary inositol supplementation in periconceptional period and during pregnancy: a summary of evidences and future applications. *Reprod Sci.* 2016;23(3):278–88.
309. Khandelwal M, Reece EA, Wu YK, Borenstein M. Dietary myo-inositol therapy in hyperglycemia-induced embryopathy. *Teratology.* 1998;57(2):79–84.
310. Reece EA, Khandelwal M, Wu YK, Borenstein M. Dietary intake of myo-inositol and neural tube defects in offspring of diabetic rats. *Am J Obstet Gynecol.* 1997;176(3):536–9.
311. Greene ND, Copp AJ. Inositol prevents folate-resistant neural tube defects in the mouse. *Nat Med.* 1997;3(1):60–6.
312. van Straaten HW, Copp AJ. Curly tail: a 50-year history of the mouse spina bifida model. *Anat Embryol (Berl).* 2001;203(4):225–37.
313. Cockroft DL. Changes with gestational age in the nutritional requirements of postimplantation rat embryos in culture. *Teratology.* 1988;38(3):281–90.
314. Cockroft DL, Brook FA, Copp AJ. Inositol deficiency increases the susceptibility to neural tube defects of genetically predisposed (curly tail) mouse embryos in vitro. *Teratology.* 1992;45(2):223–32.
315. Cogram P, Tesh S, Tesh J, Wade A, Allan G, Greene ND, et al. D-chiro-inositol is more effective than myo-inositol in preventing folate-resistant mouse neural tube defects. *Hum Reprod.* 2002;17(9):2451–8.
316. Wang Y, Lian L, Golden JA, Morrissey EE, Abrams CS. PIP5KI gamma is required for cardiovascular and neuronal development. *Proc Natl Acad Sci U S A.* 2007;104(28):11748–53.
317. Wilson MP, Hugge C, Bielinska M, Nicholas P, Majerus PW, Wilson DB. Neural tube defects in mice with reduced levels of inositol 1,3,4-trisphosphate 5/6-kinase. *Proc Natl Acad Sci U S A.* 2009;106(24):9831–5.
318. Cavalli P, Copp AJ. Inositol and folate resistant neural tube defects. *J Med Genet.* 2002;39(2):E5.
319. Cavalli P, Tedoldi S, Riboli B. Inositol supplementation in pregnancies at risk of apparently folate-resistant NTDs. *Birth Defects Res A Clin Mol Teratol.* 2008;82(7):540–2.
320. Cavalli P, Tonni G, Grosso E, Poggiani C. Effects of inositol supplementation in a cohort of mothers at risk of producing an NTD pregnancy. *Birth Defects Res A Clin Mol Teratol.* 2011;91(11):962–5.
321. Cavalli P, Ronda E. Myo-inositol: the bridge (PONTI) to reach a healthy pregnancy. *Int J Endocrinol.* 2017;2017:5846286.
322. Greene ND, Leung KY, Gay V, Burren K, Mills K, Chitty LS, et al. Inositol for the prevention of neural

- tube defects: a pilot randomised controlled trial. *Br J Nutr.* 2016;115(6):974–83.
323. Groenen PM, Peer PG, Wevers RA, Swinkels DW, Franke B, Mariman EC, et al. Maternal myo-inositol, glucose, and zinc status is associated with the risk of offspring with spina bifida. *Am J Obstet Gynecol.* 2003;189(6):1713–9.
324. Lei Y, Finnell RH. New techniques for the study of neural tube defects. *Adv Tech Biol Med.* 2016;4(1).
325. Bassuk AG, Muthuswamy LB, Boland R, Smith TL, Hulstrand AM, Northrup H, et al. Copy number variation analysis implicates the cell polarity gene glypican 5 as a human spina bifida candidate gene. *Hum Mol Genet.* 2013;22(6):1097–111.
326. Chen Z, Lei Y, Zheng Y, Aguiar-Pulido V, Ross ME, Peng R, et al. Threshold for neural tube defect risk by accumulated singleton loss-of-function variants. *Cell Res.* 2018;28(10):1039–41.
327. Wilde JJ, Petersen JR, Niswander L. Genetic, epigenetic, and environmental contributions to neural tube closure. *Annu Rev Genet.* 2014;48:583–611.
328. Van Allen MI, Kalousek DK, Chernoff GF, Juriloff D, Harris M, McGillivray BC, et al. Evidence for multi-site closure of the neural tube in humans. *Am J Med Genet.* 1993;47(5):723–43.



Animal Models of Pancreas Development, Developmental Disorders, and Disease

3

David S. Lorberbaum, Fiona M. Docherty,
and Lori Sussel

3.1 Overview

The pancreas is a glandular organ responsible for diverse homeostatic functions, including hormone production from the endocrine islet cells to regulate blood sugar levels and enzyme secretion from the exocrine acinar cells to facilitate food digestion. These pancreatic functions are essential for life; therefore, preserving pancreatic function is of utmost importance. Pancreas dysfunction can arise either from developmental disorders or adult onset disease, both of which are caused by defects in shared molecular pathways. In this chapter, we discuss what is known about the molecular mechanisms controlling pancreas development, how disruption of these mechanisms can lead to developmental defects and disease, and how essential pancreas functions can be modeled using human pluripotent stem cells. At the core of understanding of these molecular processes are animal model studies that continue to be essential for elucidating the mechanisms underlying human pancreatic functions and diseases.

D. S. Lorberbaum · F. M. Docherty · L. Sussel (✉)
Barbara Davis Center, University of Colorado
Anschutz Medical Center, Aurora, CO, USA
e-mail: DAVID.LORBERBAUM@UCDENVER.EDU;
FIONA.DOCHERTY@UCDENVER.EDU;
Lori.Sussel@ucdenver.edu

3.2 Introduction

The pancreas is a multipurpose glandular organ consisting of exocrine acinar cells dedicated to secreting digestive enzymes and endocrine islet cells that produce critical hormones to regulate glucose homeostasis. Both of these functions can be disrupted by genetic mutations that lead to a wide range of developmental defects and postnatal complications that can drastically affect the life of afflicted individuals. The most severe developmental defects are often incompatible with life unless treated at birth, whereas subtler defects are often not manifested until adulthood. One of the more common diseases associated with pancreatic defects is diabetes mellitus, which is characterized by an inability to regulate blood glucose levels, leading to hyperglycemia. Over the years, significant effort and resources have been dedicated to elucidating the etiology of pancreatic diseases, including understanding the underlying congenital defects. To develop treatments for diseases of the pancreas, including diabetes, it will be important to characterize the development of the organ and determine how the highly specialized pancreatic cell types are specified and function. A complete understanding of pancreas development and function will help identify genetic risk factors and facilitate the implementation of improved therapies that could eventually cure rare and common diseases of the pancreas. Furthermore, developmental studies in

animal models have greatly informed efforts to directly differentiate functional islet cell populations from human stem cells in vitro. In this chapter, we will predominantly describe what is known from rodent studies but will also highlight contributions from other model organisms and indicate when human studies have confirmed the findings from these animal models.

Most of what is known about embryonic pancreas development has been gleaned from studies in several model organisms, including mice (*Mus musculus*), zebrafish (*Danio rerio*), and frogs (*Xenopus laevis*). Each of these model organisms has its own unique benefits and shortcomings, but the integrated discoveries have significantly advanced our knowledge of pancreas development and its associated dysfunctions. Until recently, the most commonly used model of human pancreas development and disease has been the house mouse due to the high degree of genomic conservation between the two species, shared developmental processes, and amenability to genetic manipulations. Studies in rats (*Rattus norvegicus*) have also been used to characterize pancreas physiology since many physiological and metabolic responses to stress and external stimuli are more easily monitored in the rat model [1]. Although it has traditionally been more difficult to manipulate rat genomes, recent technological advances in gene editing have largely overcome these barriers, causing a recent resurgence in using rat as a model system for both physiological and developmental analyses. In addition to rodents, organisms such as chicken, zebrafish, and frogs have also provided valuable knowledge and insights into the mechanisms of pancreas development and beta cell dysfunction [2–4]. Although these models are less evolutionarily related to humans, they each have unique assets that have provided critical insights into the more fundamental questions about developmental processes. These model systems have provided information about the mechanisms of gene regulation, cell communication, and the signaling pathways that influence cellular function and contribute to congenital diseases. These studies in model organisms have also paved the way for

human stem cell-derived models of pancreas development and disease, which will be discussed at the end of the chapter.

3.2.1 Overview of Pancreas Development

The pancreas is specified at embryonic days 8–9 (E8.0–9.0) in mice, which corresponds to approximately 29–31 days post conception (dpc) in humans [5]. This multifunctional organ is derived from the foregut endoderm in response to critical signals from surrounding tissues, as demonstrated in coculture experiments using ex vivo mouse tissue [6]. These early experiments were not able to identify the exact molecular pathways in play [7]; however, subsequent experiments across several model systems have provided a wealth of information regarding the molecular regulation of these early stages of pancreas development [8]. Briefly, in both mice and humans, the pancreas initially forms as two spatially distinct buds on the dorsal and ventral sides of the endodermal gut tube posterior to the lungs and anterior to the intestine (Fig. 3.1). The dorsally derived bud receives signals from the notochord and dorsal aorta, whereas the ventral bud receives signals from the septum transversum mesenchyme and cardiac mesoderm. Much of what is known about dorsal pancreas induction derives from elegant studies in chicken embryos [9]. These experiments highlighted the importance of the notochord as a signaling hub for dorsal pancreas induction. The same group of investigators went on to identify activin and FGF as the secreted notochord factors that were responsible for repressing Sonic hedgehog (Shh) signaling within the underlying foregut endoderm. Furthermore, they demonstrated that repression of Shh signaling within the prepancreatic foregut endoderm was critical for promoting pancreas induction [10]. Alternatively, the ventral pancreas develops in a noncontiguous region of the foregut endoderm in close proximity to the liver. In experiments performed predominantly in mice, it was demonstrated that BMP and FGF signaling from the adjacent septum transversum mesenchyme and

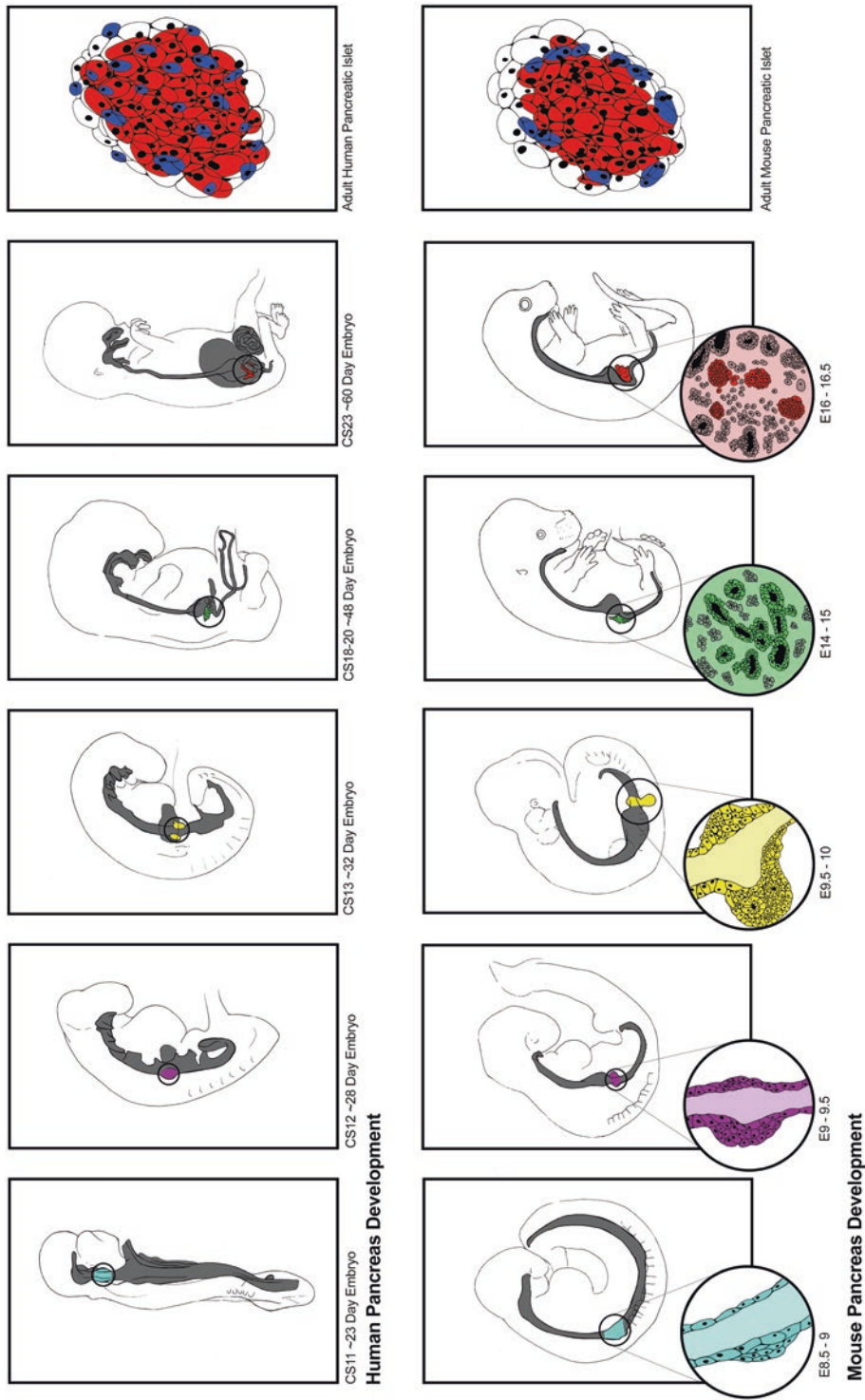


Fig. 3.1 Human and mouse pancreas development. Pancreas developmental programs in humans and mice, top and bottom, respectively, are highly conserved, as shown in the panels correlating similar time points across species. Starting about 23 days after conception in humans (~CS11) and 8.5–9 days in mice (E8.5–E9) the dorsal pancreatic bud emerges from the endodermal gut tube. Several stages of development are depicted across each row demonstrating similar morphological changes occurring in both humans and mice over about 60 days in humans and 16.5 days in mice, at which point immature endocrine cells are present and producing hormones. Over the next few months in humans and weeks in mice, these endocrine cells mature as islets that contain the same cell types but in different ratios and distribution within the islet in each species

Fig. 3.1 Human and mouse pancreas development. Pancreas developmental programs in humans and mice, top and bottom, respectively, are highly conserved, as shown in the panels correlating similar time points across species. Starting about 23 days after conception in humans (~CS11) and 8.5–9 days in mice (E8.5–E9) the dorsal pancreatic bud emerges from the endodermal gut tube. Several stages of development are depicted across each row demonstrating similar morphological changes occurring in both humans and mice over about 60 days in humans and 16.5 days in mice, at which point immature endocrine cells are present and producing hormones. Over the next few months in humans and weeks in mice, these endocrine cells mature as islets that contain the same cell types but in different ratios and distribution within the islet in each species

cardiac mesoderm specified the ventral pancreatic bud while simultaneously repressing the liver primordium [11]. Although there are still many gaps in our understanding of these earliest events in pancreas specification and development, these studies provided a comprehensive analysis of the early tissue interactions and signaling pathways that are important for the primary steps of pancreas induction. Furthermore, many of the developmental events that have been characterized in these animal model systems have recently been shown to be conserved in human pancreas development [12, 13].

Following initial pancreas specification, the dorsal and ventral buds independently grow, branch, and initiate parallel cellular differentiation pathways in what has been referred to as the *primary transition* stage in mice. Between E12.5 and E15.5 (40–48 dpc in human), the two buds are brought into close proximity through morphological movements inherent to the rotating gut tube and fuse to form a single organ (Fig. 3.1). Although each anlage gives rise to the same complement of adult pancreatic cell types, they delineate distinguishable regions of the adult organ as the pancreatic head (ventrally derived, attached to the duodenum and intestines) and tail (dorsally derived, attached to the spleen and stomach). Between approximately E14.5–E16.5, FGF10 induces Notch and a cascade of unknown signaling events [12, 14, 15] to initiate the formation of exocrine lineage progenitors at the tip of the elongating branches and the emergence of endocrine progenitors in the central core of the organ. At this stage, there is a major wave of islet cell differentiation and expansion, which is referred to as the *secondary transition*. By birth, each of the exocrine and endocrine cell lineages have been fully specified and continues to mature and proliferate for approximately 2 weeks postnatally. Several extensive reviews describe many additional intrinsic and extrinsic signaling pathways that have been implicated at several stages of pancreatic differentiation, maturation, and expansion [14, 15].

In adults, the pancreas is comprised of three major tissues: exocrine, endocrine, and ductal epithelium. The majority (>90–95%) of the pancreas is made up of exocrine tissue, which is made up of acinar cells that secrete digestive

enzymes through the pancreatic ducts into the intestine. Most of the remaining pancreatic tissue (~5–10%) is composed of endocrine cells, which are organized into mini-organs known as islets of Langerhans. The islets are responsible for supplying the body with hormones to control blood sugar levels. There are four major endocrine cell types found in mouse and human adult islets: alpha, beta, delta, and PP cells, each of which produces a unique hormone: glucagon, insulin, somatostatin, and pancreatic polypeptide, respectively (Fig. 3.2). Although the same four endocrine cell populations exist in mice and humans, they are present in different relative ratios and with dissimilar spatial distribution within islets of the two species [16] (Fig. 3.2). Both mouse and human endocrine cells predominantly differentiate from an endocrine progenitor population as single hormone-expressing cells, although a subset of endocrine cells within the human embryonic pancreas are polyhormonal [17]. By birth, the polyhormonal populations are no longer present; however, it is unclear whether they have resolved into monohormonal cells or have undergone cell death. Both species also form small populations of ghrelin-producing epsilon cells and gastrin-producing cells in the embryonic pancreas, but these cell types disappear during postnatal stages of pancreatic maturation [18–20].

3.2.2 Molecular Regulation of Pancreas Development

Like all developmental processes, pancreas induction, morphogenesis, and cellular differentiation require a carefully orchestrated series of developmental events that rely on the integration of many different signaling pathways and transcriptional regulators. Studies in animal models have identified several signaling pathways that are crucial for pancreagenesis and have laid the foundation for the successful *in vitro* differentiation of pancreatic progenitors and immature islet populations from human stem cells [21] (see below). Although many of these critical cell signaling pathways are conserved in human pancreas development, they

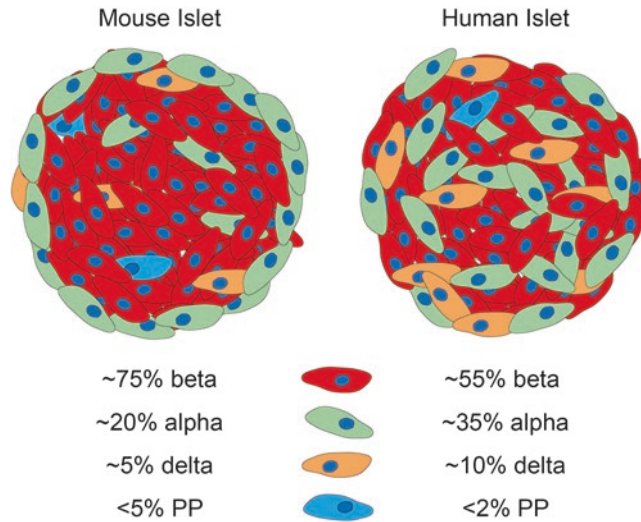


Fig. 3.2 Similarities and differences between mouse and human islets. The same endocrine cell types are present in both human and mouse islets but are spatially distinct and present in different ratios in each organism. All percentages are averages and represent a range of endocrine cell

composition, especially in human alpha and beta cells, which can vary greatly from islet to islet. Red represent insulin (beta cells), green represents glucagon (alpha cells), orange is somatostatin (delta cells), and blue is pancreatic polypeptide (PP cells)

have not been directly implicated in human pancreatic developmental defects and disease. This is likely because the majority of these pathways are globally required during development, and inactivation of such regulatory mechanisms would be incompatible with life.

While there are still open questions about the precise signaling mechanisms regulating pancreas development, animal models have provided substantial information about how transcription factors regulate pancreas development, including evidence demonstrating their functional conservation and importance in disease [22–26]. One of the first and most critical transcription factors identified in pancreas specification is pancreatic and duodenal homeobox 1 (PDX1, also known as IPF1 and STF1). PDX1 was first identified and characterized in *Xenopus* [27, 28] and has conserved expression in all model organisms studied to date, and in human. PDX1 is expressed in the pancreas, duodenum, and stomach shortly after there is morphological evidence of each respective tissue within the foregut endoderm. Within the developing pancreas, PDX1 is initially expressed throughout the pancreatic progenitor population but ultimately becomes restricted to

beta and delta cells of the islet [29]. Because of its initially broad expression, global deletion of *Pdx1* in mice leads to pancreas agenesis, a disease also associated with *PDX1* mutations in humans (Table 3.1). Shortly following pancreas specification, PDX1 becomes coexpressed with another early transcription factor—pancreas transcription factor 1a (PTF1A) within the earliest pancreatic progenitor population [56]. Deletion of *Ptf1A* also leads to partial pancreas agenesis, characterized by the absence of acinar tissue and a reduced number of endocrine cells [57]. Although PDX1 and PTF1a are the first tissue-restricted transcription factors known to be expressed at the onset of pancreas specification, a rudimentary pancreatic bud still forms when either factor is deleted, suggesting that there are as yet unidentified upstream factors that initiate pancreas specification [56].

Additional early players in pancreas development are the GATA4 and GATA6 transcription factors. These factors are broadly expressed in the foregut endoderm, prior to pancreagenesis, but become more specifically restricted to the pancreatic anlagen [58]. While whole-body knockouts of these transcription factors lead to

Table 3.1 Conserved transcription factors essential for pancreas development contributing to human and mouse pancreatic defects and disease

Transcription factor	Human disease	Mouse defect	References
PDX1	Pancreatic agenesis	Pancreatic agenesis	De Franco et al. [30]
	PNDM		Stoffers et al. [31]
	MODY4 (het)		Jonsson et al. [32]
HNF1B	Pancreatic hypoplasia	Pancreatic agenesis (Hz)	Haumaitre et al. [33]
	MODY5		Haumaitre et al. [34]
GLIS3	PNDM	Neonatal diabetes, loss of beta cells	Rubio-Cabezas et al. [35]
			Senée et al. [36]
			Kang et al. [37]
NEUROD1	PNDM (hz)	Postnatal death diabetes	Rubio-Cabezas et al. [38]
	MODY6 (het)		Malecki et al. [39]
	T2DM		Naya et al. [40]
NKX2.2	PNDM	Postnatal death—no beta cells	Flanagan et al. [41]
			Sussel et al. [42]
MNX1	PNDM	Dorsal pancreas agenesis	Flanagan et al. [41]
			Harrison et al. [43]
			Li et al. [44]
PAX6	PNDM	No alpha cells, reduced beta cells	Solomon et al. [45]
			St-Onge et al. [46]
PTF1A	Pancreatic agenesis	Pancreatic agenesis	Sellick et al. [47]
	PNDM		Weedon et al. [48]
			Kawaguchi et al. [49]
			Krapp et al. [50]
GATA6	Pancreatic agenesis (het)	None, but pancreatic agenesis in G6/G4 double knockout	De Franco et al. [30]
	PNDM		Allen et al. [51]
	Adult onset diabetes		Shaw-Smith et al. [52]
			Xuan et al. [53]
NEUROG3	Adult onset diabetes (hypomorphic mutation)	Perinatal death, no endocrine cells	Carrasco et al. [54]
	PNDM (biallelic mutations)		Rubio-Cabezas et al. [35]
			Gradwohl et al. [55]

early embryonic lethality prior to pancreas formation due to extraembryonic endoderm and heart defects, deletion of both factors simultaneously within the pancreas progenitor population causes pancreas agenesis [53, 54]. Molecular analysis of these mutants revealed that deletion of *Gata4* and *Gata6* in the foregut endoderm causes ectopic expression of the hedgehog signaling pathway and respecification of the pancreas into intestine and stomach fates [59]. Studies are currently ongoing to determine the function of the GATA factors during pancreas development since interesting differences exist between human and mice (see human pancreas agenesis section below).

The pancreatic progenitor population gives rise to the three major cell lineages in the pancreas, including the islet endocrine cells. At the onset of the secondary transition, the transient expression of the transcription factor Neurogenin3 (NEUROG3) marks a critical molecular event that defines the endocrine progenitor population. NEUROG3 is expressed in both pancreas and intestinal endocrine progenitor populations. In the pancreas, NEUROG3 expression spikes just prior to the secondary transition to delineate the endocrine progenitor cell population [60]. In mice, global deletion of *Neurog3* results in the complete absence of all pancreatic and intestinal endocrine populations [55, 61]. However, individuals with

loss of function alleles of *NEUROG3* appear to have normal islet endocrine function but suffer from severe diarrhea due to the lack of intestinal endocrine cells, suggesting that *NEUROG3* may have a lesser or redundant role in human endocrine cell development [35].

Within and downstream of the *NEUROG3* endocrine progenitor cell population, dozens of conserved transcription factors have been shown to regulate subsequent stages of endocrine cell type differentiation [26] (Fig. 3.3). This includes two members of the *NKX* family of transcription factors, *NKX2.2* and *NKX6.1*. Although *NKX2.2* and *NKX6.1* are initially expressed throughout the pancreas progenitor population, they eventually become restricted to the *NEUROG3* endocrine progenitor cells and continue to be expressed in subsets of endocrine lineages, where they function. *NKX2.2* becomes restricted to alpha, beta, and PP cells, whereas *NKX6.1* is specifically expressed in the beta cell lineage [42, 62]. Despite their widespread expression early in pancreas development, both factors predominantly function to specify the islet cell lineages: *NKX2.2* functions upstream of *NKX6.1* and is essential for the differentiation of several islet cell lineages, whereas *NKX6.1* only affects the formation and function of the beta cell lineage. Both factors continue to be expressed in the adult islet; expression of *NKX6.1* is essential for appropriate beta cell functional maturation, and *NKX2.2* is necessary for the maintenance of beta cell identity [63, 64].

NEUROD1 is another essential transcription factor that is broadly expressed in the pancreas at several developmental stages and in all islet lineages, but functions predominantly downstream of *NKX2.2* and *NEUROG3* to regulate islet cell development and survival [40, 65, 66]. *Neurod1* null mice die just after birth from severe diabetes or survive and develop hyperglycemia later in life, depending on the mouse strain background [40, 67]. Finally, *GLIS3* is a functionally conserved transcription factor that is coexpressed with *NEUROG3* and then becomes more specific to beta and PP

cells. Global deletion of *Glis3* in mice results in greatly reduced beta and PP cell numbers, and *Glis3* mutant mice often develop neonatal diabetes [68]. Consistently, humans carrying mutations in *GLIS3* can develop permanent neonatal diabetes and/or have an increased risk of developing both type 1 and type 2 diabetes [69, 70].

Genetic studies in mice have identified a large cohort of transcriptional regulators, of which only a subset have been discussed above, that are essential for pancreas development and function [22, 23]. Importantly, the identification of these conserved factors has guided targeted sequencing of patients with defective pancreas development to identify corresponding functions in human. Furthermore, with the advent of whole genome sequencing in patients suffering from pancreas-related diseases, there is increasing evidence that many human developmental disorders are caused by the mis-expression or dysregulation of specific transcription factors critical for healthy pancreas development in mice. Many of these diseases can now be traced to disrupted developmental processes or genetic mutations (see OMIM, <https://www.omim.org/>), while several others still remain uncharacterized [71].

3.2.3 Developmental Defects and Their Impact on Pancreatic Function and Disease

During the past ~20 years, there have been significant advancements in our understanding of the molecular pathways underlying pancreas development. Importantly, studies in human fetal pancreatic tissue have confirmed that there are conserved expression patterns for many of the aforementioned transcription factors and signaling molecules in humans [5, 12, 13, 26, 72, 73]. Furthermore, mutational analyses in mice have greatly contributed to our understanding of the developmental defects that can arise when these regulatory pathways are disrupted. As described

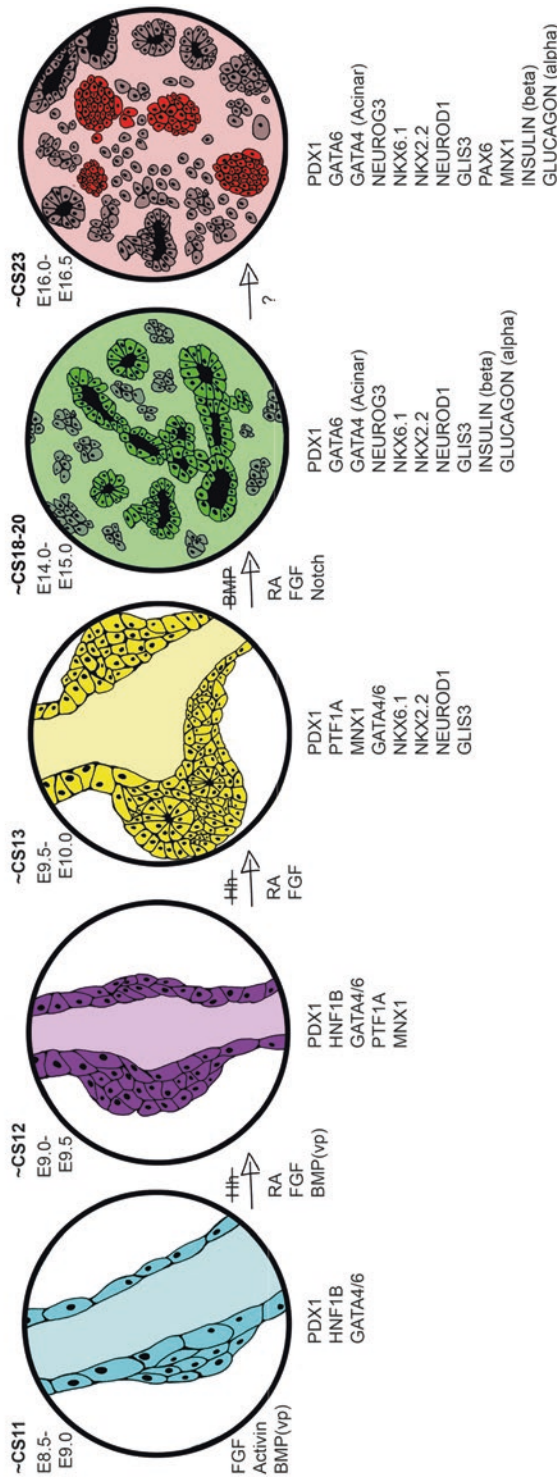


Fig. 3.3 Molecular mechanisms of pancreas development in mice and humans. A selection of transcription factors and cell signaling pathways define the transition from gut endoderm to immature pancreas, which takes place in about 37 days in humans (CS labels in bold) and about 8 days in mice (E labels). While much is known about the cell signaling pathways early on, less is known about the key signaling events later in this development scheme (~E16.0–E16.5). VP represents the contribution of BMP signaling specifically to the ventral pancreatic bud, but not the dorsal bud, at this stage of development

below, genetic studies in mice have also helped identify many of the human genetic mutations that are responsible for congenital defects that lead to neonatal and adult pancreas-related diseases. It is important to note that unlike many other organs, the pancreas is not required for gestational development. However, a functioning pancreas, and specifically insulin-producing beta cells, are critical for survival after birth. Therefore, mutations that impair aspects of pancreas development can result in a range of mild-to-severe phenotypes, depending on the nature of the genetic mutation and/or where the affected gene product functions.

Pancreas agenesis Pancreas agenesis is defined in patients who have either an incompletely formed or completely absent pancreas. The most severe cases are rare and nearly always fatal since the disrupted developmental processes often affect the formation of other tissues and are not compatible with survival. However, there are several cases of human pancreas agenesis that arise from mutations in transcription factor genes that have been characterized in mouse genetic models. For example, several cases of pancreas agenesis have been associated with mutations in *PDX1* and *PTF1a*, two of the most critical factors for early pancreas development in mice [31, 47, 49, 57, 74]. Mice lacking either *Pdx1* or *Ptf1a* form only the initial pancreatic rudiments and die shortly after birth due to severe hyperglycemia [32, 75, 76]. Despite PDX1 and PTF1a being two of the earliest and most critical transcription factors involved in pancreas organogenesis, mutations in these genes only account for a low percentage of pancreas agenesis patients, suggesting that mutations in other factors are responsible for the majority cases of this disease. One compelling study that examined the genomes of 27 agenesis patients showed that 56% of these cases could be attributed to haploinsufficient *GATA6* mutations [77]. Studies in mice have shown that *GATA6* is a critical regulator of early embryonic development—mice lacking *Gata6* die between embryonic day 5.5 and embryonic day 7.5 due to early endodermal defects [78].

Surprisingly, however, pancreas specific deletion of *Gata6* in mice had minor effects on pancreas development. Only when *Gata6* and another family member, *Gata4*, were deleted from the developing pancreas simultaneously did complete agenesis occur [53, 54]. This discrepancy between the roles of GATA factors in mouse and human development is not completely understood but does suggest that there might be background genetic modifiers or nonautonomous environmental defects contributing to the pancreas agenesis phenotypes seen in humans. Although additional genetic mutations or modifiers that might contribute to the pancreas agenesis phenotype observed in patients with *GATA6* mutations have not been identified, when heterozygous loss of *GATA6* is modeled in a system of human pluripotent stem cell-derived pancreas differentiation (see Sect. 3.4), pancreas and beta-like cells are still able to form. However, when *GATA6* mutations are combined with the inhibition of retinoic acid signaling, pancreas development is impaired. These data highlight the importance of cross-talk between signaling pathways and transcription factors that are essential for understanding the mechanisms of pancreas agenesis and other diseases [79, 80].

In many agenesis cases, patients can survive with very small rudiments of a pancreas, making it possible to live with the disease. These cases have been primarily documented as dorsal pancreas agenesis and are classified as missing the neck, body, and tail of the pancreas, which are all derived from the dorsal anlage. In some instances, these disorders are referred to as pancreatic hypoplasia. The first instance of this disease was described in 1911, and approximately 100 additional cases have been reported since then [81]. Most of these patients were surprisingly asymptomatic until they developed a secondary complication, such as diabetes mellitus or pancreatitis. The origins of pancreatic hypoplasia are also multifactorial, but there are several mouse models that develop this phenotype and could provide insight into the human defects. For example, when a key enzyme in the retinoic acid signaling

pathway, RALDH2, is deleted, mice die during gestation with apparent dorsal-specific pancreas agenesis [82]. Dorsal agenesis is also observed in mice deficient in *N-cadherin*, *MNX1*, and the *activin receptor* [43, 44, 83, 84]. A comprehensive list of mouse models that result in aspects of pancreatic agenesis has been previously documented [24]. There are many additional case studies in humans that describe pancreas hypoplasia, although most of them have not identified the causal genetic defect [85, 86]. With technological advances allowing cheaper, faster, and more efficient whole genome sequencing available, it is likely that we will soon have a more comprehensive list of mutations that contribute to pancreas agenesis, many of which are likely to have already been described in mice and other model organisms.

Annular pancreas Annular pancreas is another pancreatic defect with developmental origins. It was first described as early as the nineteenth century, when a physician noticed an extension of the pancreas, which was described as a connective tissue wrapped around the duodenum of a deceased individual during an autopsy. Some of the earliest reports of this disease suggested that it was extremely rare; random examination of cadavers for the abnormality estimated its incidence at about 3 in 20,000. However, with modern technological advances, such as endoscopies, magnetic resonance imaging (MRI), and computed tomography (CT) scans that allow physicians to identify the disorder in living patients, incidence is now estimated to be as high as 1 in 1000 [87]. Although there is currently a lack of consensus on the actual number of cases, recent work from Lim et al. 2017 estimates an occurrence of only 1 in 20,000 [88]. Some of this controversy is due to a lack of consensus regarding diagnoses. While it is generally accepted that the cause of annular pancreas is due to the inappropriate development of the ventral pancreatic bud, the pathogenesis is still not completely clear. One theory is that a free end of the ventral bud fuses to the duodenum during development and grows around the duodenum as it rotates, although it has

also been proposed that the ventral pancreas inappropriately develops as a bilobed organ, and one of the lobes grows around the duodenum [71, 87]. With a handful of exceptions, the majority of human cases are sporadic and have not been linked to genetic mutations [89]. Annular pancreas has also been observed in mouse models of pancreas development when Indian Hedgehog (*Ihh*), a ligand in the Hedgehog (*Hh*) signaling family, is inhibited. This leads to ectopic branching of the ventral pancreas, causing an annular pancreatic phenotype [90]. Interestingly, similar mutations in *Hh* pathway components have not been identified in patients with annular pancreas, suggesting that other pathways regulating *Hh* signaling contribute to the development of the disease. Further work is required to better understand the mechanisms underlying annular pancreas, and models in mice hold the most promise for elucidating those mechanisms.

Neonatal diabetes mellitus (NDM) Neonatal diabetes mellitus is a rare form of diabetes that is usually diagnosed in infants at 6 months of age or younger. NDM is often confused with type 1 diabetes, the more common autoimmune form of diabetes that can also occur in young children, but patients with NDM are distinguished by their lack of autoantibodies. Young patients are diagnosed with NDM because of their inability to regulate blood glucose levels. They present at birth with severe hyperglycemia, a life-threatening condition caused by the absence of insulin production from the endocrine pancreas. NDM is rare, with estimated cases of ~1:400,000 [91]. Roughly half of the cases are transient neonatal diabetes mellitus (TNDM), and although they often resolve, many individuals become diabetic later in life, suggesting the existence of an unresolved developmental defect. The remaining cases are referred to as permanent neonatal diabetes mellitus (PNDM) and result in lifelong diabetic conditions that require continual treatment with exogenous insulin, similar to the adult onset diabetes. A subset of both PNDM and TNDM have also been shown to result from specific mutations in genes for ATP-sensitive potassium

channels, which are critical for regulating beta cell function [92].

Several studies have identified single-gene mutations in patients with NDM largely based on targeted sequencing of transcription factor genes known to be important for pancreas development in mice. One study in particular examined the sequenced genomes of 37 patients with NDM and identified mutations in seven of the 29 candidate genes tested. Five of the genes (*GLIS3*, *NEUROD1*, *PDX1*, *PTF1a*, *RFX6*) had been previously implicated in PDM, while mutations in two additional genes (*MNX1* and *NKX2.2*) were also identified [41]. Notably, all of these transcription factors have been studied extensively in mice, where they are known to cause severe pancreatic defects and perinatal lethality when mutated [22, 42, 93], once again highlighting the importance of animal models in providing critical information about genetic defects causing human developmental diseases.

Diffuse congenital hyperinsulinism in infancy (CHI-D) CHI-D is the most frequent cause of severe, persistent hypoglycemia in newborns and infants. The majority (60%) of babies are diagnosed during the first month of life and the remainder diagnosed within the first year. Genetic analyses have linked hyperinsulinemia to rare mutations in genes encoding the transcription factors *HNF1A* and *HNF4A*; however, the majority of CHI-D cases are caused by mutations that specifically inactivate the critical K_{ATP} channel necessary for nutrient sensing and insulin secretion [94]. Interestingly, this defect does not fully explain the phenotype since a recent histological study of postmortem CHI-D pancreatic islets suggested that individuals with CHI-D displayed additional defects in the somatostatin-producing delta cell population [95]. Of particular interest was the discovery of aberrant expression of *NKX2.2* in delta cells; both mouse and human studies have demonstrated that *NKX2.2* is normally excluded from this endocrine population. In the future, experimental studies in mice to

induce ectopic expression of *NKX2.2* in delta cells would clarify whether *NKX2.2* misexpression is a causative factor of the disease.

Maturity-onset diabetes of the young (MODY) MODY is a monogenic form of diabetes and comprises about 2% of cases of diabetes in people under 20 years old, making this disease much more common than NDM [96]. Because MODY is broadly characterized by beta cell dysfunction, it is often misdiagnosed as type 1 diabetes. Currently, mutations in 11 different MODY genes have been described, the majority of which were identified by sequencing genes known to cause pancreatic islet defects when mutated in mouse models. Furthermore, most of the affected genes encode transcription factors that are expressed in the developing pancreas and in adult beta cells, including *PDX1*, *NEUROD1*, *HNF4A*, and *HNF1B* [31, 39, 97–99]; however, there are also a subset of nontranscription factor MODY genes (<https://www.omim.org/entry/606391>) that lead to diabetes as well. Since nearly all of these genes encode proteins that are critical for important developmental process during embryogenesis, MODY mutations are predominantly point mutations that cause autosomal dominant alleles. Interestingly, similar to what was observed with the *GATA6* mutations in pancreas agenesis, heterozygous dominant alleles of several MODY genes, including *HNF1alpha* and *HNF3beta* in mice, do not generally cause disease [100]. This could be due to the absence of additional genetic modifiers in the inbred animal models used for these studies or nonconserved mechanisms of disease progression. To clarify whether there are underlying genetic or environmental causes for these discrepancies between human and animal models, new genomic engineering technologies such as CRISPR/Cas9 have facilitated disease modeling in human stem cell-derived beta cells (see stem cell section below). The combination of these two disease modeling approaches will significantly improve our ability to identify and characterize genes responsible for developmental diseases of the pancreas.

3.3 Juvenile and Adult Diseases of the Pancreas

While the aforementioned pancreas disorders are rare and generally monogenic in origin, there are multiple disorders of the pancreas that are much more common and result from a combination of genetic mutations and environmental influences. The most prevalent of these more common disorders is broadly classified as diabetes mellitus (DM). This polygenic disease is extremely widespread, affecting nearly 10% of the United States population or 30.3 million people. Remarkably, an additional 84.1 million people are estimated to have prediabetes, a condition that indicates a high likelihood to develop full diabetes in a person's lifetime [101]. There is currently no cure for diabetes, which is part of the reason that it was the seventh leading cause of death in the US in 2015 (American Diabetes Association, <http://www.diabetes.org/diabetes-basics/statistics/>). Although the designation of DM represents many different diseases, nearly all of these statistics are summations of the two main types of diabetes mellitus, type 1 and type 2. In the following section, animal models of these diseases will be explored, compared, and contrasted in relation to current treatments for each disorder. Although these adult diseases are generally not considered to be "birth defects," there are strong genetic components underlying both diseases, and many of the genetic mutations are in genes previously characterized in developmental processes.

3.3.1 Type 1 Diabetes Mellitus (T1DM)

Type 1 diabetes mellitus is a multifactorial autoimmune disease characterized by the destruction of insulin-producing beta cells in the pancreatic islet, leading to severe hyperglycemia in affected individuals. T1DM is prevalent in children; however, individuals of all ages can develop the disease. As of 2015, there have been an estimated account of 542,000 children with the disease, and the incidence appears to be increasing every decade (International Diabetes Federation, [\[www.diabetesatlas.org/\]\(http://www.diabetesatlas.org/\)\). In humans, approximately 20–40 different genes have been linked to T1DM, including strong linkage to particular alleles of the major histocompatibility complex \(MHC\) II region, which accounts for approximately 40% of the hereditary cause of T1DM. Despite the important genetic component of the disease, not all individuals with genetic risk factors develop T1DM, suggesting a role for environmental factors. The disease generally progresses through several well-defined stages. The presence of autoantibodies is the main classifier of stage 1 of disease progression and will persist throughout the life of the patient. Loss of beta cell mass also begins during stage 1. Stage 2 coincides with the advent of hyperglycemia due to further loss of beta cells, which are being destroyed by the autoimmune attack. Finally, stage 3 is defined by even further loss of beta cells past a critical threshold, as well as presentation of clinical symptoms such as polyuria, thirst, hunger, and weight loss associated with severe hyperglycemia. More serious complications of chronic hyperglycemia include retinopathies, neuropathies, nephropathies, and cardiovascular diseases. All of these serious complications warrant further study and highlight a need for even better treatments and eventually a cure for the disease.](http://</p></div><div data-bbox=)

Models of T1DM There are several rodent models of T1DM that have greatly facilitated our understanding of disease onset and progression, despite some inherent limitations regarding how these models were generated and how their immune systems function as compared to humans. The most common murine model of T1DM is the nonobese diabetic (NOD) mouse. Created in Osaka, Japan, in the 1970s, these mice develop insulinitis as early as 3–4 weeks of age leading to the destruction of beta cells, mimicking T1DM progression in humans [102]. Importantly, many of the T1DM alleles and biological pathways are shared by humans and NOD mice. Furthermore, the MHCII locus is similar in structure in NOD mice and humans [103]. While NOD mice have proven to be an extremely useful model for understanding the progression of T1D,

recent access to human T1DM pancreatic tissue has revealed some important differences in immune infiltration and disease pathology between the species [104]. Furthermore, it has been relatively easy to treat NOD mice with immunotherapies and drug treatments that unfortunately have not been recapitulated in human trials [105].

Another rodent model of spontaneous autoimmune-induced T1DM are BB rats, which were named for the founder colonies: BBdp/Wor (inbred from Worcester, MA, USA) and BBdp (outbred from Ottawa, Canada) [106]. Male and female mice from both strains initially develop pancreatic insulinitis, and the beta cells are destroyed between 50 and 90 days of life. Interestingly, persistent immune cell infiltration does not occur in these animals' islets, which is consistent with patients with T1DM [106]. While these rats are clearly useful for modeling T1DM and the associated effects of the disease like neuropathies [107], a major drawback is that they almost always develop lymphopenia, a disorder in which individuals have very low levels of lymphocytes or white blood cells. While lymphopenia happens in nearly all BB rats, the condition is not normally associated with people who have T1DM. This additional immunological complication has affected the interpretation of many studies using BB rats and is an important reminder that animal models of disease are not exact replicas of human disease and should be used in conjunction with one another to make informed conclusions about the disease.

3.3.2 Type 2 Diabetes Mellitus (T2DM)

Unlike the types of diabetes mellitus discussed above, T2DM is frequently linked to the metabolic syndrome and the obesity epidemic rather than developmental mutations, although there is often a genetic component to this highly multifactorial disease. T2DM is the most common form of diabetes, accounting for more than 90% of cases. T2DM is characterized by metabolic

dysfunction, impaired insulin secretion, and insulin resistance, alone or in combination [101]. There are approximately five stages or phases of diabetes: prediabetes and phases 1–4, each marked by a particular set of symptoms. Prediabetes and phase 1 are mainly characterized by glucose intolerance in which an afflicted individual is unable to properly clear glucose after eating, which leads to hyperglycemia. In addition, prediabetics begin to lose sensitivity to insulin, even though their beta cells are still fully functional. Phase 2 is marked by basal hyperglycemia in addition to glucose intolerance. At this phase of the disease, patients may also experience insulin resistance. In phase 3, afflicted individuals generally have fasting hyperglycemia, along with some functional beta cell loss. In phase 4, patients often require exogenous insulin due to severe loss of functional beta cells, which fail to produce sufficient amounts of insulin to regulate blood glucose levels. Complications from this late phase can also, in rare cases, lead to what some describe as phase 5 and is characterized by ketoacidosis as the body begins to look for other sources of fuel. As the disease progresses, a multitude of serious secondary health complications occur, including cardiovascular disease, neuropathies (numbness, particularly in extremities), nephropathy, retinopathy, stroke, and high blood pressure [108].

Models of T2DM In humans, T2DM represents a heterogeneous set of complex polygenic diseases; therefore, choosing the right rodent T2DM model is critical. Rodent models have been traditionally classified as spontaneous or induced, and vary greatly in the severity and phase of diabetes they represent. The most common models are monogenic or diet induced, and each has advantages and disadvantages [109]. Here, we describe a subset of these models in more detail and explain how each model is used to further understand and treat T2DM.

Lep^{OB/OB} and Lep^{r^{DB/DB}} mice are two related monogenic models of obesity-induced T2DM that affect the function of the leptin hormone, which regulates appetite, and the receptor through

which it signals, respectively. The inability to regulate feeding occurs when either of these critical components does not function normally. The Lep^{OB/OB} model was discovered as a spontaneously occurring mutation in 1949 at the Jackson Laboratories, but the genetic mutation was not identified as leptin until the mid-1990s [110]. The Lep^{OB/OB} mice generally start gaining weight around 2 weeks of age and are hyperglycemic by about 4 weeks. While these mice are characterized as having diabetes due to this hyperglycemia and impaired insulin release, they generally do not progress to stage 3 of T2DM, unless they are bred to be on the C57BLKS/J background [111]. The Lep^{DB/DB} mice were similarly discovered as a spontaneous mutation in the 1960s, again at Jackson labs, but the mutation was not linked to the leptin receptor until years later [112]. The development of diabetes occurs in a similar fashion to the Lep^{OB/OB} model, but when placed on the C57BLKS/J, these mice will develop full-blown, late-stage T2DM, often leading to ketoacidosis and death after just a few months. Interestingly, depending on the strain background, each of these models can produce either hyper- or hypotrophic beta cells and can both be hyper- and hypoinsulinemic. Phenotypic variability that depends on strain background is analogous to the differences in disease progression and severity seen in patients with leptin-related deficiencies.

Named after the city in Japan where these mice were created, the AKITA mouse is another mouse model used to study T2DM. The origins of this model's disease are rooted in a spontaneous mutation in the *INS2* gene inhibiting normal processing of insulin in the beta cell. The inappropriate accumulation of misfolded insulin protein leads to ER stress, which results in severe insulin-dependent diabetes. This generally occurs in 3–4 weeks and is accompanied by some of the symptoms of T2DM, like polyuria and hyperglycemia resulting from loss of beta cell mass, although this mouse is not obese. Furthermore, Akita mice have also been used to study diabetes complications, like neuropathies or cardiovascular defects, and have served as a reliable model to test the utility of exogenous beta cell sources to supplement beta cell deficits [113, 114].

In addition to these common mouse models of T2DM, there are also several rat models available, each with its own unique benefits and caveats [109]. The Otsuka Long Evans Tokushima Fatty (OLETF) rat has been used as a model for late-onset T2DM since the early 1990s [115]. These rats are unable to restrict their appetite and become obese with age. With obesity, they develop the inability to regulate their blood glucose levels and become insulin resistant, leading to diabetes onset [116]. Similar to humans, the age of disease onset and severity of disease varies widely in OLEFT rats; however, this also makes it a difficult model to study. Another popular rat model of T2DM is the Zucker Diabetic Fatty (ZDF) rats. Developed in the mid-1980s, ZDF rats have dysfunctional leptin receptor, similar to the Lep^{DB/DB} mice. They are frequently used to study the transition from prediabetes to early-onset diabetes and become fully diabetic by about 12 weeks of age. While they serve as a good model to study this important transition, the Zucker rats are genetically predisposed to acquiring defects in beta cell transcription factors that also contribute to their diabetic phenotype independent of leptin signaling defects, which can complicate analyses [117]. The Goto-Kakizaki (GK) rat provides a nonobese model to study mild T2DM characterized by hyperglycemia and insulin resistance largely linked to neonatal beta cell developmental defects [118, 119]. Similar to all disease models, the correct choice of the animal model depends on the type of diabetes and questions being explored.

3.4 Human Models of Pancreas Development

While mice, rats, and other animal models have been invaluable in furthering our knowledge of pancreas development, as well as pancreatic disease onset and pathogenesis, the fact remains that they differ substantially from humans. Apart from the obvious differences, mice also exhibit subtle but fundamental differences from humans in terms of their beta cell development, beta cell mass, islet organization, and blood glucose

tolerance. These differences mean that although mice and other model organisms provide a great preliminary model for human development and disease research, they are not sufficient for complete insight into the complex pathologies that affect the human pancreas.

3.4.1 Modeling Human Pancreas and Islet Development In Vitro

Studying human pancreas development is fraught with challenges, both technical and ethical. Much of our current knowledge comes from pancreatic tissues taken from aborted human fetuses at various stages of early development—up to 22 weeks [5, 120]. These tissues are generally sectioned and examined by antibody staining to reveal insights into pancreas and islet morphology, appearance and relative ratios of pancreatic cell types, and islet cell organization during fetal development. While these methods have provided some insights into human pancreas development and highlighted similarities and differences between mice and humans, they only provide a static view of developmental processes in an unperturbed state. The analysis is further complicated by the extreme sample variability that exists between different patient donors. Due to the inherent limitations associated with studying human development and the corresponding defects that lead to disease, the ability to recapitulate human development in a dish by differentiating human pluripotent stem cells (hPSC), including hESCs and hiPSCs (embryonic and induced pluripotent stem cells, respectively), represents an exciting new avenue of research. Furthermore, the advent of gene editing technologies, such as TALENs and CRISPR/Cas9, which allow researchers to induce putative human disease-causing mutations into the hPSC differentiation system, has revolutionized our ability to characterize the intrinsic contribution of particular genetic mutations to developmental defects and disease. However, to truly harness the potential of hPSCs, we need efficient protocols that allow their directed differentiation to organs and

cell types of interest, including stem cell-derived pancreas and beta-like cells (SBCs).

One key approach to differentiating hPSC toward a specific cell type is to faithfully recapitulate the developmental cues in vitro that the cells would “experience” during in vivo development. As our understanding of human development is limited, directed differentiation of hPSC to SBCs is largely based on knowledge derived from animal models of development and disease that were outlined previously in this chapter. A number of protocols currently exist for the differentiation of hPSCs to pancreas and beta-like cells [121–125]. Although all of the protocols are able to accurately mimic the earliest stages of pancreas development, through to the generation of endocrine progenitor cells, the directed differentiation of the mature exocrine and islet cell types has proven more challenging. This is in part due to the relative paucity of information related to the signaling pathways that are involved in these later stages of development and differentiation.

In general, pancreas differentiation protocols can be broken down into the developmental stages defined in mice (Figs. 3.3 and 3.4). Since we know that pancreas is derived from endoderm and, in particular, foregut endoderm, the first few differentiation steps are not specific to the pancreas but are shared by all endodermally derived tissues (Fig. 3.4). First, hPSCs must transition to a definitive endoderm cell fate, which is driven by activation of the WNT and TGF beta pathways. Following 2 days of differentiation, the cells express transcription factors specific to the definitive endoderm stage of development, including SOX17. The definitive endoderm cells are then differentiated toward primitive gut tube by activation of the FGF signaling pathway. After approximately 3 days, the cells have switched on primary gut tube markers, including HNF1A, FOXA2, and HNF6. At this point, the pancreatic cell fate, which is marked by PDX1 expression, is induced by retinoic acid and the inhibition of hedgehog signaling, similar to what occurs during mouse dorsal pancreas induction. Inhibition of the BMP signaling pathway is also necessary

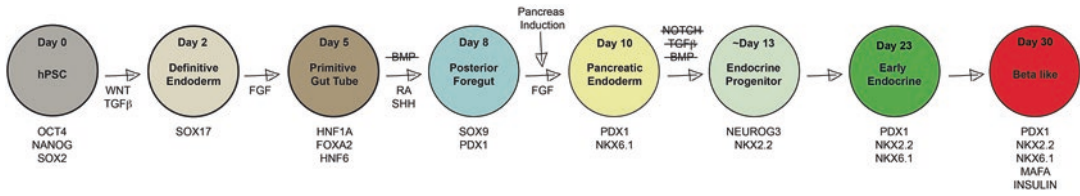


Fig. 3.4 Directed differentiation of hPSCs to beta-like cells in a dish. Based largely on knowledge gleaned from animal models of pancreas development, the stepwise addition of chemicals and small molecules to human pluripotent stem cells leads to the activation and inhibition of many of the cell signaling pathways required for differen-

tiation into insulin-producing beta-like cells. A selection of the critical transcription factors expressed at each stage is noted underneath each time point, noted by day of differentiation and largely corresponds to the same transcription factors found at similar stages of mouse development (Fig. 3.3)

to block the differentiation of pancreatic foregut cells toward liver lineages, similar to ventral pancreas formation in the mouse (Figs. 3.3 and 3.4, matching colors).

Once pancreatic cell fates have been specified (corresponding to approximately E9.5 of mouse pancreas development,) the PDX1 positive pancreatic foregut cells are then differentiated into pancreatic endoderm cells that continue to express PDX1 and have also activated NKX6.1 via FGF signaling. These cells undergo endocrine differentiation and are subsequently exposed to a cocktail of empirically defined signals that drive them toward pancreatic beta cells while blocking differentiation to other pancreatic cell types. Similar to the differentiation of mouse pancreatic endocrine cells, the pancreatic endoderm cells will transiently express the transcription factor NEUROG3 and then NKX2.2 to delineate the endocrine progenitor population around day 13 of the differentiation protocol. After approximately 10 more days of endocrine differentiation, the early endocrine cell population emerges, classified by the expression of key beta cell markers. While these cells do begin to produce the insulin hormone, they are not yet functional as they do not regulate insulin secretion in response to glucose stimulation. A further 7 days of maturation in a minimal media is required to allow the cells to become functional beta-like cells. While 95% of cells reach the NKX2.2 stage, only 20–40% go on to become insulin positive SBCs, indicating that additional research is needed both in mice and in the hPSC system to optimize the pancreas differentiation protocol.

3.4.2 Disease Modeling with Stem Cell-Derived Pancreatic Cells

Although the hPSC pancreatic differentiation protocol still needs to be refined, it has already proven to be extremely useful for validating conserved gene functions in human pancreas development. For example, in a *tour de force* study by the Huangfu group, TALEN and CRISPR/Cas-mediated gene editing was used to analyze the role of eight essential pancreatic transcription factors (PDX1, RFX6, PTF1A, GLIS3, MNX1, NEUROG3, HES1, and ARX) in the hPSC-directed differentiation of pancreas [80]. These studies not only verified conserved gene requirements between mice and humans but also revealed a number of previously unsuspected developmental mechanisms with implications for type 2 diabetes. Similar studies were also instrumental in addressing potential discrepancies between mouse and human gene functions. Using gene-edited hESCs and patient-specific iPSCs, two groups were able to partially resolve the discrepancy between mouse and human phenotypes caused by mutations in GATA6 by implicating the contribution of genetic modifiers and nonautonomous cell defects to the pancreas agenesis phenotype seen in human patients [79, 80]. Similarly, McGrath and colleagues used hESC-derived pancreatic cells to confirm that NEUROG3 had similar essential roles in mouse and human pancreas endocrine cell development but determined that patients with mutations in NEUROG3 retained sufficient functional protein to avoid disease

[126]. These are just a small number of studies that demonstrate the utility of stem cell-derived pancreas tissue to model development and disease. With increasing technological advances and a better understanding of pancreas development from animal models, these in vitro differentiation models hold great potential for making even greater strides in elucidating outstanding questions about human pancreas development and disease.

Acknowledgement Illustrations in this chapter were drawn by Jennifer Colquhoun.

References

1. Dolgin E. The knockout rat pack. *Nat Med.* 2010;16:254–7.
2. Kim SK, Hebrok M, Melton DA. Pancreas development in the chick embryo. *Cold Spring Harb Symp Quant Biol.* 1997;62:377–83.
3. Matsuda H. Zebrafish as a model for studying functional pancreatic β cells development and regeneration. *Dev Growth Differ.* 2018;60(6):393–9.
4. Chalmers AD, Slack JM. Development of the gut in *Xenopus laevis*. *Dev Dyn.* 1998;212(4):509–21.
5. Jennings RE, Berry AA, Kirkwood-Wilson R, Roberts NA, Hearn T, Salisbury RJ, et al. Development of the human pancreas from foregut to endocrine commitment. *Diabetes.* 2013;62(10):3514–22.
6. Wessells NK, Cohen JH. Early pancreas organogenesis: morphogenesis, tissue interactions, and mass effects. *Dev Biol.* 1967;15(3):237–70.
7. Slack JM. Developmental biology of the pancreas. *Development.* 1995;121(6):1569–80.
8. Zorn AM, Wells JM. Vertebrate endoderm development and organ formation. *Annu Rev Cell Dev Biol.* 2009;25(1):221–51.
9. Kim SK, Hebrok M, Melton DA. Notochord to endoderm signaling is required for pancreas development. *Development.* 1997;124(21):4243–52.
10. Hebrok M, Kim SK, Melton DA. Notochord repression of endodermal Sonic hedgehog permits pancreas development. *Genes Dev.* 1998;12(11):1705–13.
11. Wandzioch E, Zaret KS. Dynamic signaling network for the specification of embryonic pancreas and liver progenitors. *Science.* 2009;324(5935):1707–10.
12. Pan FC, Brissova M. Pancreas development in humans. *Curr Opin Endocrinol Diabetes Obes.* 2014;21(2):77–82.
13. Jennings RE, Berry AA, Strutt JP, Gerrard DT, Hanley NA. Human pancreas development. *Development.* 2015;142(18):3126–37.
14. Gittes GK. Developmental biology of the pancreas: a comprehensive review. *Dev Biol.* 2009;326(1):4–35.
15. Serup P. Signaling pathways regulating murine pancreatic development. *Semin Cell Dev Biol.* 2012;23(6):663–72.
16. Hart NJ, Powers AC. Use of human islets to understand islet biology and diabetes: progress, challenges and suggestions. *Diabetologia.* 2019;62(2):212–22.
17. Riopel M, Li J, Fellows GF, Goodyer CG, Wang R. Ultrastructural and immunohistochemical analysis of the 8–20 week human fetal pancreas. *Islets.* 2014;6(4):e982949.
18. Arnes L, Hill JT, Gross S, Magnuson MA, Sussel L. Ghrelin expression in the mouse pancreas defines a unique multipotent progenitor population. *PLoS One.* 2012;7(12):e52026.
19. Prado CL, Pugh-Bernard AE, Elghazi L, Sosa-Pineda B, Sussel L. Ghrelin cells replace insulin-producing beta cells in two mouse models of pancreas development. *Proc Natl Acad Sci U S A.* 2004;101(9):2924–9.
20. Suissa Y, Magenheimer J, Stolovich-Rain M, Hija A, Collombat P, Mansouri A, et al. Gastrin: a distinct fate of neurogenin3 positive progenitor cells in the embryonic pancreas. *PLoS One.* 2013;8(8):e70397.
21. Krentz NAJ, Lee MYY, Xu EE, Sproul SLJ, Maslova A, Sasaki S, et al. Single-cell transcriptome profiling of mouse and hESC-derived pancreatic progenitors. *Stem Cell Reports.* 2018;11(6):1551–64.
22. Jørgensen MC, Ahnfelt-Rønne J, Hald J, Madsen OD, Serup P, Hecksher-Sørensen J. An illustrated review of early pancreas development in the mouse. *Endocr Rev.* 2007;28(6):685–705.
23. Pan FC, Wright C. Pancreas organogenesis: from bud to plexus to gland. *Dev Dyn.* 2011;240(3):530–65.
24. Mastracci TL, Sussel L. The endocrine pancreas: insights into development, differentiation, and diabetes. *Wiley Interdiscip Rev Dev Biol.* 2012;1(5):609–28.
25. Cano DA, Soria B, Martín F, Rojas A. Transcriptional control of mammalian pancreas organogenesis. *Cell Mol Life Sci.* 2013;71(13):2383–402.
26. Hanley N. Closing in on pancreatic beta cells. *Nat Biotechnol.* 2014;32(11):1100–2.
27. Peshavaria M, Gamer L, Henderson E, Teitelman G, Wright CV, Stein R. XIHbox 8, an endoderm-specific *Xenopus* homeodomain protein, is closely related to a mammalian insulin gene transcription factor. *Mol Endocrinol.* 1994;8(6):806–16.
28. Gamer LW, Wright CV. Autonomous endodermal determination in *Xenopus*: regulation of expression of the pancreatic gene XIHbox 8. *Dev Biol.* 1995;171(1):240–51.
29. Potter LA, Choi E, Hipkens SB, Wright CVE, Magnuson MA. A recombinase-mediated cassette exchange-derived cyan fluorescent protein reporter allele for Pdx1. *Genesis.* 2012;50(4):384–92.
30. De Franco E, Shaw-Smith C, Flanagan SE, et al. Biallelic PDX1 (insulin promoter factor 1) mutations causing neonatal diabetes without exocrine pancreatic insufficiency. *Diabet Med.* 2013;30(5):e197–200.

31. Stoffers DA, Ferrer J, Clarke WL, Habener JF. Early-onset type-II diabetes mellitus (MODY4) linked to IPF1. *Nat Genet.* 1997;17(2):138–9.
32. Jonsson J, Carlsson L, Edlund T, Edlund H. Insulin-promoter-factor 1 is required for pancreas development in mice. *Nature.* 1994;371(6498):606–9.
33. Haumaitre C, Fabre M, Cormier S, Baumann C, Delezoide AL, Cereghini S. Severe pancreas hypoplasia and multicystic renal dysplasia in two human fetuses carrying novel HNF1beta/MODY5 mutations. *Hum Mol Genet.* 2006;15(15):2363–75.
34. Haumaitre C, Barbacci E, Jenny M, Ott MO, Gradwohl G, Cereghini S. Lack of TCF2/vHNF1 in mice leads to pancreas agenesis. *Proc Natl Acad Sci U S A.* 2005;102(5):1490–5.
35. Rubio-Cabezas O, Jensen JN, Hodgson MI, Codner E, Ellard S, Serup P, et al. Permanent neonatal diabetes and enteric anendocrinosis associated with biallelic mutations in NEUROG3. *Diabetes.* 2011;60(4):1349–53.
36. Senée V, Chelala C, Duchatelet S, et al. Mutations in GLIS3 are responsible for a rare syndrome with neonatal diabetes mellitus and congenital hypothyroidism. *Nat Genet.* 2006;38(6):682–7.
37. Kang HS, Kim YS, ZeRuth G, et al. Transcription factor Glis3, a novel critical player in the regulation of pancreatic beta-cell development and insulin gene expression. *Mol Cell Biol.* 2009;29(24):6366–79.
38. Rubio-Cabezas O, Minton JA, Kantor I, Williams D, Ellard S, Hattersley AT. Homozygous mutations in NEUROD1 are responsible for a novel syndrome of permanent neonatal diabetes and neurological abnormalities. *Diabetes.* 2010;59(9):2326–31.
39. Malecki MT, Jhala US, Antonellis A, Fields L, Doria A, Orban T, et al. Mutations in NEUROD1 are associated with the development of type 2 diabetes mellitus. *Nat Genet.* 1999;23(3):323–8.
40. Naya FJ, Huang HP, Qiu Y, Mutoh H, DeMayo FJ, Leiter AB, et al. Diabetes, defective pancreatic morphogenesis, and abnormal enteroendocrine differentiation in BETA2/neuroD-deficient mice. *Genes Dev.* 1997;11(18):2323–34.
41. Flanagan SE, De Franco E, Lango Allen H, Zerah M, Abdul-Rasoul MM, Edge JA, et al. Analysis of transcription factors key for mouse pancreatic development establishes NKX2-2 and MNX1 mutations as causes of neonatal diabetes in man. *Cell Metab.* 2014;19(1):146–54.
42. Sussel L, Kalamaras J, Hartigan-O'Connor DJ, Meneses JJ, Pedersen RA, Rubenstein JL, et al. Mice lacking the homeodomain transcription factor Nkx2.2 have diabetes due to arrested differentiation of pancreatic beta cells. *Development.* 1998;125(12):2213–21.
43. Harrison KA, Thaler J, Pfaff SL, Gu H, Kehrl JH. Pancreas dorsal lobe agenesis and abnormal islets of Langerhans in Hlxb9-deficient mice. *Nat Genet.* 1999;23(1):71–5.
44. Li H, Arber S, Jessell TM, Edlund H. Selective agenesis of the dorsal pancreas in mice lacking homeobox gene Hlxb9. *Nat Genet.* 1999;23(1):67–70.
45. Solomon BD, Pineda-Alvarez DE, Balog JZ, et al. Compound heterozygosity for mutations in PAX6 in a patient with complex brain anomaly, neonatal diabetes mellitus, and microphthalmia. *Am J Med Genet A.* 2009;149A(11):2543–6.
46. St-Onge L, Sosa-Pineda B, Chowdhury K, Mansouri A, Gruss P. Pax6 is required for differentiation of glucagon-producing alpha-cells in mouse pancreas. *Nature.* 1997;387(6631):406–9.
47. Sellick GS, Barker KT, Stolte-Dijkstra I, Fleischmann C, Coleman RJ, Garrett C, et al. Mutations in PTF1A cause pancreatic and cerebellar agenesis. *Nat Genet.* 2004;36(12):1301–5.
48. Weedon MN, Cebola I, Patch AM, et al. Recessive mutations in a distal PTF1A enhancer cause isolated pancreatic agenesis. *Nat Genet.* 2014;46(1):61–4.
49. Kawaguchi Y, Cooper B, Gannon M, Ray M, MacDonald RJ, Wright CV. The role of the transcriptional regulator Ptf1a in converting intestinal to pancreatic progenitors. *Nat Genet.* 2002;32(1):128–34.
50. Krapp A, Knofler M, Frutiger S, Hughes GJ, Hagenbuchle O, Wellauer PK. The p48 DNA-binding subunit of transcription factor PTF1 is a new exocrine pancreas-specific basic helix-loop-helix protein. *EMBO J.* 1996;15(16):4317–29.
51. Allen HL, Flanagan SE, Shaw-Smith C, et al. GATA6 haploinsufficiency causes pancreatic agenesis in humans. *Nat Genet.* 2011;44(1):20–2.
52. Shaw-Smith C, De Franco E, Lango Allen H, et al. GATA4 mutations are a cause of neonatal and childhood-onset diabetes. *Diabetes.* 2014;63(8):2888–94.
53. Xuan S, Borok MJ, Decker KJ, Battle MA, Duncan SA, Hale MA, et al. Pancreas-specific deletion of mouse Gata4 and Gata6 causes pancreatic agenesis. *J Clin Invest.* 2012;122(10):3516–28.
54. Carrasco M, Delgado I, Soria B, Martín F, Rojas A. GATA4 and GATA6 control mouse pancreas organogenesis. *J Clin Invest.* 2012;122(10):3504–15.
55. Gradwohl G, Dierich A, LeMeur M, Guillemot F. Neurogenin3 is required for the development of the four endocrine cell lineages of the pancreas. *Proc Natl Acad Sci U S A.* 2000;97(4):1607–11.
56. Burlison JS, Long Q, Fujitani Y, et al. Pdx-1 and Ptf1a concurrently determine fate specification of pancreatic multipotent progenitor cells. *Dev Biol.* 2008;316(1):74–86.
57. Krapp A, Knöfler M, Ledermann B, Bürki K, Berney C, Zoerkler N, et al. The bHLH protein PTF1-p48 is essential for the formation of the exocrine and the correct spatial organization of the endocrine pancreas. *Genes Dev.* 1998;12(23):3752–63.
58. Decker K, Goldman DC, Grasch CL, Sussel L. Gata6 is an important regulator of mouse pancreas development. *Dev Biol.* 2006;298(2):415–29.
59. Xuan S, Sussel L. GATA4 and GATA6 regulate pancreatic endoderm identity through inhibition of hedgehog signaling. *Development.* 2016;143(5):780–6.

60. Villasenor A, Chong DC, Cleaver O. Biphasic Ngn3 expression in the developing pancreas. *Dev Dyn*. 2008;237(11):3270–9.
61. Lee CS, Perreault N, Brestelli JE, Kaestner KH. Neurogenin 3 is essential for the proper specification of gastric enteroendocrine cells and the maintenance of gastric epithelial cell identity. *Genes Dev*. 2002;16(12):1488–97.
62. Sander M, Sussel L, Connors J, Scheel D, Kalamaras J, Cruz Dela F, et al. Homeobox gene Nkx6.1 lies downstream of Nkx2.2 in the major pathway of beta-cell formation in the pancreas. *Development*. 2000;127(24):5533–40.
63. Schaffer AE, Taylor BL, Benthuysen JR, Liu J, Thorel F, Yuan W, et al. Nkx6.1 controls a gene regulatory network required for establishing and maintaining pancreatic Beta cell identity. *PLoS Genet*. 2013;9(1):e1003274.
64. Gutiérrez GD, Bender AS, Cirulli V, Mastracci TL, Kelly SM, Tsirigos A, et al. Pancreatic β cell identity requires continual repression of non- β cell programs. *J Clin Invest*. 2017;127(1):244–59.
65. Anderson KR, Torres CA, Solomon K, Becker TC, Newgard CB, Wright CV, et al. Cooperative transcriptional regulation of the essential pancreatic islet gene NeuroD1 (beta2) by Nkx2.2 and neurogenin 3. *J Biol Chem*. 2009;284(45):31236–48.
66. Chao CS, Loomis ZL, Lee JE, Sussel L. Genetic identification of a novel NeuroD1 function in the early differentiation of islet alpha, PP and epsilon cells. *Dev Biol*. 2007;312(2):523–32.
67. Huang H-P, Chu K, Nemoz-Gaillard E, Elberg D, Tsai M-J. Neogenesis of beta-cells in adult BETA2/NeuroD-deficient mice. *Mol Endocrinol*. 2002;16(3):541–51.
68. Kang HS, Takeda Y, Jeon K, Jetten AM. The spatio-temporal pattern of Glis3 expression indicates a regulatory function in bipotent and endocrine progenitors during early pancreatic development and in beta, PP and ductal cells. *PLoS One*. 2016;11(6):e0157138.
69. Barrett JC, Clayton DG, Concannon P, Akolkar B, Cooper JD, Erlich HA, et al. Genome-wide association study and meta-analysis find that over 40 loci affect risk of type 1 diabetes. *Nat Genet*. 2009;41(6):703–7.
70. Dupuis J, Langenberg C, Prokopenko I, Saxena R, Soranzo N, Jackson AU, et al. New genetic loci implicated in fasting glucose homeostasis and their impact on type 2 diabetes risk. *Nat Genet*. 2010;42(2):105–16.
71. Cano DA, Hebrok M, Zenker M. Pancreatic development and disease. *Gastroenterology*. 2007;132(2):745–62.
72. Piper K, Brickwood S, Turnpenny LW, Cameron IT, Ball SG, Wilson DI, et al. Beta cell differentiation during early human pancreas development. *J Endocrinol*. 2004;181(1):11–23.
73. Jennings RE, Berry AA, Gerrard DT, Wearne SJ, Strutt J, Withey S, et al. Laser capture and deep sequencing reveals the transcriptomic programmes regulating the onset of pancreas and liver differentiation in human embryos. *Stem Cell Reports*. 2017;9(5):1387–94.
74. Schwitzgebel VM, Mamin A, Brun T, Ritz-Laser B, Zaiko M, Maret A, et al. Agenesis of human pancreas due to decreased half-life of insulin promoter factor 1. *J Clin Endocrinol Metab*. 2003;88(9):4398–406.
75. Guz Y, Montminy MR, Stein R, Leonard J, Gamer LW, Wright CV, et al. Expression of murine STF-1, a putative insulin gene transcription factor, in beta cells of pancreas, duodenal epithelium and pancreatic exocrine and endocrine progenitors during ontogeny. *Development*. 1995;121(1):11–8.
76. Offield MF, Jetton TL, Labosky PA, Ray M, Stein RW, Magnuson MA, et al. PDX-1 is required for pancreatic outgrowth and differentiation of the rostral duodenum. *Development*. 1996;122(3):983–95.
77. Allen HL, Flanagan SE, Shaw-Smith C, De Franco E, Akerman I, Caswell R, et al. GATA6 haploinsufficiency causes pancreatic agenesis in humans. *Nat Genet*. 2011;44(1):20–2.
78. Morrissey EE, Tang Z, Sigrist K, Lu MM, Jiang F, Ip HS, et al. GATA6 regulates HNF4 and is required for differentiation of visceral endoderm in the mouse embryo. *Genes Dev*. 1998;12(22):3579–90.
79. Tiyaboonchai A, Cardenas-Diaz FL, Ying L, Maguire JA, Sim X, Jobaliya C, et al. GATA6 plays an important role in the induction of human definitive endoderm, development of the pancreas, and functionality of pancreatic β cells. *Stem Cell Reports*. 2017;8(3):589–604.
80. Shi Z-D, Lee K, Yang D, Amin S, Verma N, Li QV, et al. Genome editing in hPSCs reveals GATA6 haploinsufficiency and a genetic interaction with GATA4 in human pancreatic development. *Cell Stem Cell*. 2017;20(5):675–88.
81. Robert AP, Iqbal S, John M. Complete agenesis of the dorsal pancreas: a rare clinical entity. *Int J Appl Basic Med Res*. 2016;6(4):290–2.
82. Molotkov A, Molotkova N, Duester G. Retinoic acid generated by Raldh2 in mesoderm is required for mouse dorsal endodermal pancreas development. *Dev Dyn*. 2005;232(4):950–7.
83. Esni F, Johansson BR, Radice GL, Semb H. Dorsal pancreas agenesis in N-cadherin-deficient mice. *Dev Biol*. 2001;238(1):202–12.
84. Kim SK, Hebrok M, Li E, et al. Activin receptor patterning of foregut organogenesis. *Genes Dev*. 2000;14(15):1866–71.
85. Jain A, Singh M, Dey S, Kaura A, Diwakar G. A rare case of complete agenesis of dorsal pancreas. *Euroasian J Hepatogastroenterol*. 2017;7(2):183–4.
86. Erotokritou A, Gerharz CD, Sagir A. Agenesis of dorsal pancreas associated with pancreatic neuroendocrine tumor: a case report and review of the literature. *J Med Case Rep*. 2018;12(1):185.
87. Etienne D, John A, Menias CO, Ward R, Tubbs RS, Loukas M. Annular pancreas: a review of its molecular embryology, genetic basis and clinical considerations. *Ann Anat*. 2012;194(5):422–8.

88. Lim J, Porter J, Varia H, Pettit S. Annular pancreas causing duodenal obstruction in an adult. *BMJ Case Rep.* 2017;2017.
89. Lainakis N, Antypas S, Panagidis A, Alexandrou I, Kambouri K, Kyriazis C, et al. Annular pancreas in two consecutive siblings: an extremely rare case. *Eur J Pediatr Surg.* 2005;15(5):364–8.
90. Hebrok M, Kim SK, St Jacques B, McMahon AP, Melton DA. Regulation of pancreas development by hedgehog signaling. *Development.* 2000;127(22):4905–13.
91. Kanakatti Shankar R, Pihoker C, Dolan LM, Standiford D, Badaru A, Dabelea D, et al. Permanent neonatal diabetes mellitus: prevalence and genetic diagnosis in the SEARCH for Diabetes in Youth Study. *Pediatr Diabetes.* 2013;14(3):174–80.
92. Flanagan SE, Patch A-M, Mackay DJG, Edghill EL, Gloyn AL, Robinson D, et al. Mutations in ATP-sensitive K⁺ channel genes cause transient neonatal diabetes and permanent diabetes in childhood or adulthood. *Diabetes.* 2007;56(7):1930–7.
93. Li H, Edlund H. Persistent expression of Hlxb9 in the pancreatic epithelium impairs pancreatic development. *Dev Biol.* 2001;240(1):247–53.
94. Demirbilek H, Hussain K. Congenital hyperinsulinism: diagnosis and treatment update. *J Clin Res Pediatr Endocrinol.* 2017;9(Suppl 2):69–87.
95. Salisbury RJ, Han B, Jennings RE, Berry AA, Stevens A, Mohamed Z, et al. Altered phenotype of β -cells and other pancreatic cell lineages in patients with diffuse congenital hyperinsulinism in infancy caused by mutations in the ATP-sensitive K-channel. *Diabetes.* 2015;64(9):3182–8.
96. Pihoker C, Gilliam LK, Ellard S, Dabelea D, Davis C, Dolan LM, et al. Prevalence, characteristics and clinical diagnosis of maturity onset diabetes of the young due to mutations in HNF1A, HNF4A, and glucokinase: results from the SEARCH for Diabetes in Youth. *J Clin Endocrinol Metab.* 2013;98(10):4055–62.
97. Stoffel M, Le Beau MM, Espinosa R, Bohlander SF, Le Paslier D, Cohen D, et al. A yeast artificial chromosome-based map of the region of chromosome 20 containing the diabetes-susceptibility gene, MODY1, and a myeloid leukemia related gene. *Proc Natl Acad Sci U S A.* 1996;93(9):3937–41.
98. Vaxillaire M, Boccio V, Philippi A, Vigouroux C, Terwilliger J, Passa P, et al. A gene for maturity onset diabetes of the young (MODY) maps to chromosome 12q. *Nat Genet.* 1995;9(4):418–23.
99. Horikawa Y, Iwasaki N, Hara M, Furuta H, Hinokio Y, Cockburn BN, et al. Mutation in hepatocyte nuclear factor-1 beta gene (TCF2) associated with MODY. *Nat Genet.* 1997;17(4):384–5.
100. Shih DQ, Heimesaat M, Kuwajima S, Stein R, Wright CVE, Stoffel M. Profound defects in pancreatic beta-cell function in mice with combined heterozygous mutations in Pdx-1, Hnf-1alpha, and Hnf-3beta. *Proc Natl Acad Sci U S A.* 2002;99(6):3818–23.
101. Centers for Disease Control and Prevention (CDC). National Diabetes Statistics Report, 2017; 2017. p. 1–20.
102. Makino S, Kunimoto K, Muraoka Y, Mizushima Y, Katagiri K, Tochino Y. Breeding of a non-obese, diabetic strain of mice. *Jikken Dobutsu.* 1980;29(1):1–13.
103. Wicker LS, Clark J, Fraser HI, Garner VES, Gonzalez-Munoz A, Healy B, et al. Type 1 diabetes genes and pathways shared by humans and NOD mice. *J Autoimmun.* 2005;25(Suppl):29–33.
104. Katsarou A, Gudbjörnsdóttir S, Rawshani A, Dabelea D, Bonifacio E, Anderson BJ, et al. Type 1 diabetes mellitus. *Nat Rev Dis Primers.* 2017;3:17016.
105. Roep BO. Are insights gained from NOD mice sufficient to guide clinical translation? Another inconvenient truth. *Ann NY Acad Sci.* 2007;1103(1):1–10.
106. Mordes JP, Bortell R, Blankenhorn EP, Rossini AA, Greiner DL. Rat models of type 1 diabetes: genetics, environment, and autoimmunity. *ILAR J.* 2004;45(3):278–91.
107. Zhang W, Kamiya H, Ekberg K, Wahren J, Sima AAF. C-peptide improves neuropathy in type 1 diabetic BB/Wor-rats. *Diabetes Metab Res Rev.* 2006;23(1):63–70.
108. DeFronzo RA, Ferrannini E, Groop L, Henry RR, Herman WH, Holst JJ, et al. Type 2 diabetes mellitus. *Nat Rev Dis Primers.* 2015;1:15019.
109. Chen D, Wang M-W. Development and application of rodent models for type 2 diabetes. *Diabetes Obes Metab.* 2005;7(4):307–17.
110. Zhang Y, Proenca R, Maffei M, Barone M, Leopold L, Friedman JM. Positional cloning of the mouse obese gene and its human homologue. *Nature.* 1994;372(6505):425–32.
111. Lindström P. The physiology of obese-hyperglycemic mice [ob/ob mice]. *ScientificWorldJournal.* 2007; 7:666–85.
112. Chen H, Charlat O, Tartaglia LA, Woolf EA, Weng X, Ellis SJ, et al. Evidence that the diabetes gene encodes the leptin receptor: identification of a mutation in the leptin receptor gene in db/db mice. *Cell.* 1996;84(3):491–5.
113. Drel VR, Pacher P, Stavniichuk R, Xu W, Zhang J, Kuchmerovska TM, et al. Poly(ADP-ribose) polymerase inhibition counteracts renal hypertrophy and multiple manifestations of peripheral neuropathy in diabetic Akita mice. *Int J Mol Med.* 2011;28(4):629–35.
114. Chen H, Zheng C, Zhang X, Li J, Li J, Zheng L, et al. Apelin alleviates diabetes-associated endoplasmic reticulum stress in the pancreas of Akita mice. *Peptides.* 2011;32(8):1634–9.
115. Kawano K, Hirashima T, Mori S, Natori T. OLETF (Otsuka Long-Evans Tokushima Fatty) rat: a new NIDDM rat strain. *Diabetes Res Clin Pract.* 1994;24(Suppl):S317–20.
116. Bi S, Moran TH. Obesity in the Otsuka Long Evans Tokushima Fatty rat: mechanisms and discoveries. *Front Nutr.* 2016;3:21.

117. Tokuyama Y, Sturis J, DePaoli AM, Diabetes JT. Evolution of β -cell dysfunction in the male Zucker diabetic fatty rat. *Diabetes*. 1995;44(12):1447–57.
118. Gauguier D, Froguel P, Parent V, Bernard C, Bihoreau MT, Portha B, et al. Chromosomal mapping of genetic loci associated with non-insulin dependent diabetes in the GK rat. *Nat Genet*. 1996;12(1):38–43.
119. Kuwabara WMT, Panveloski-Costa AC, Yokota CNF, Pereira JNB, Filho JM, Torres RP, et al. Comparison of Goto-Kakizaki rats and high fat diet-induced obese rats: are they reliable models to study Type 2 Diabetes mellitus? *PLoS One*. 2017;12(12):e0189622.
120. Meier JJ, Butler AE, Saisho Y, Monchamp T, Galasso R, Bhushan A, et al. Beta-cell replication is the primary mechanism subserving the postnatal expansion of beta-cell mass in humans. *Diabetes*. 2008;57(6):1584–94.
121. Pagliuca FW, Millman JR, Gürtler M, Segel M, Van Dervort A, Ryu JH, et al. Generation of functional human pancreatic β cells. *Cells*. 2014;159(2): 428–39.
122. Rezanian A, Bruin JE, Arora P, Rubin A, Batushansky I, Asadi A, et al. Reversal of diabetes with insulin-producing cells derived in vitro from human pluripotent stem cells. *Nat Biotechnol*. 2014;32(11):1121–33.
123. Nostro MC, Sarangi F, Yang C, Holland A, Elefanty AG, Stanley EG, et al. Efficient generation of NKX6-1+ pancreatic progenitors from multiple human pluripotent stem cell lines. *Stem Cell Reports*. 2015;4(4):591–604.
124. Russ HA, Parent AV, Ringler JJ, Hennings TG, Nair GG, Shveygert M, et al. Controlled induction of human pancreatic progenitors produces functional beta-like cells in vitro. *EMBO J*. 2015;34(13):1759–72.
125. Zhu S, Russ HA, Wang X, Zhang M, Ma T, Xu T, et al. Human pancreatic beta-like cells converted from fibroblasts. *Nat Commun*. 2016;7:10080.
126. McGrath PS, Watson CL, Ingram C, Helmrath MA, Wells JM. The basic helix-loop-helix transcription factor NEUROG3 is required for development of the human endocrine pancreas. *Diabetes*. 2015;64(7):2497–505.



Animal Models of Congenital Gastrointestinal Maladies

4

Ryan J. Smith, Roshane Francis, Ji-Eun Kim,
and Tae-Hee Kim

4.1 Overview

The gastrointestinal (GI) tract consists of a remarkable series of organs that spatially and temporally coordinate the vital process of digestion to extract key nutrients required to sustain our day-to-day functions. During development, it undergoes complex and highly specialized morphogenetic events to form functionally distinct organs. Its failure to develop properly leads to serious congenital diseases, which if left untreated are particularly devastating and often result in premature death. These GI diseases have been estimated to impact approximately 8–16 of every 10,000 newborns [1, 2]. Importantly, the clinical manifestations of these diseases are severe, with untreated cases having high mortality rates. While some disorders, such as Hirschsprung's disease, can be treated effectively with surgery, the efficacy of this management strategy is far lower for other diseases, such as necrotizing enterocolitis. Moreover, children often face complications from these surgical procedures, leading to secondary ailments. Consequently, a better understanding of gastrointestinal development is fundamental to the treatment and prevention of

congenital GI maladies. This chapter will explore some of the most prevalent and biologically complex congenital diseases of the GI system, with emphasis on animal models that both elucidate their underlying causes and lay the essential groundwork for the advancement of translational medicine.

4.2 Development of the Gastrointestinal System

To understand how GI maladies impact the health of an individual, a foundational knowledge in the structure, function, and development of the GI tract is crucial. In humans, the GI tract is divided into several morphologically distinct regions, each of which performs a unique role in digestion (Fig. 4.1). At the rostral end is the esophagus, the primary function of which is to pass partially digested food from the mouth to the stomach [3]. The stomach is a cavernous structure that performs several duties, the foremost being the chemical breakdown of food via the secretion of hydrochloric acid. Additionally, the stomach secretes hormones that regulate appetite and stores digested food before passing it to the small intestine [4]. The small intestine comprises three major regions: the duodenum, jejunum, and ileum. A coordinated effort between these three regions enhances the breakdown of stomach contents, allowing for the

R. J. Smith · R. Francis · J.-E. Kim · T.-H. Kim (✉)
The Hospital for Sick Children and University of
Toronto, Toronto, ON, Canada
e-mail: rj.smith@mail.utoronto.ca;
roshane.francis@mail.utoronto.ca;
tae-hee.kim@sickkids.ca

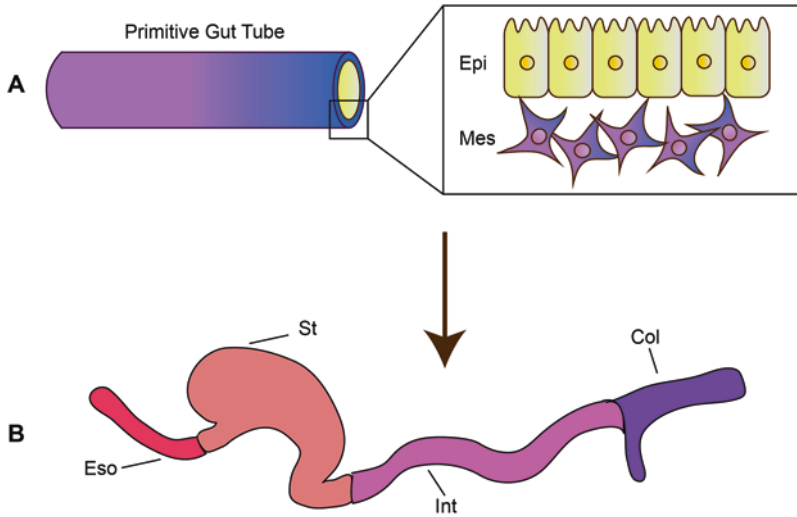


Fig. 4.1 Diagrammatic representation of gastrointestinal maturation. The primitive gut tube (a) is composed of two primary germ layers: endoderm (which will give rise to epithelial cells) and mesoderm (which will develop into supporting structures along the gut). As the gut develops

and undergoes regionalization, this featureless tube grows into several functionally and morphologically distinct organs, including the esophagus, stomach, intestine, and colon (b). *Epi* epithelium, *Mes* mesenchyme, *Eso* esophagus, *St* stomach, *Int* intestine, *Col* colon

absorption of fats, carbohydrates, and proteins through its large, finger-like epithelial projections known as villi [5, 6]. Finally, the large intestine exists at the most caudal end of the GI system. The large intestine, or colon, is devoid of villi, having instead a flat surface that absorbs water from luminal contents and contributes to the excretion of waste [7].

The GI system begins as a simple, featureless tube extending the length of the embryo. Known as the primitive gut tube, this cylindrical structure forms during gastrulation and is composed of cells from two primary germ layers. The outer layer of the tube is derived from mesodermal cells, which will eventually give rise to the muscle, vascular system, and stromal cells. The cells facing the inner lumen are of endodermal origin, eventually differentiating into the various epithelial cells that provide the GI tract with its core functions [8–11]. In humans, the primitive gut tube closes at approximately the fourth week of pregnancy, with divisions occurring over time into morphologically distinct regions, known as the foregut, midgut, and hindgut. The foregut structure is the precursor to several distinct organs, including the esophagus, stomach, proximal intestine, pancreas, liver, and

gallbladder. The midgut will eventually grow to form the small intestine, and a portion of the colon, while the hindgut gives rise to the descending colon and rectum [12, 13]. The enteric nervous system also begins to form during the third week of gestation, with neural crest cells invading the mesodermal lining. This process begins at the rostral (proximal) end of the gut, innervating the foregut at week 3 and the distal (caudal) hindgut at week 7 [14, 15]. The featureless primitive gut tube eventually gains functionally distinct regions, beginning at approximately day 51, with epithelial protrusions (villi) forming in the proximal intestine, growing in a proximal-distal wave until the 54th day. Likewise, the gastric epithelium undergoes patterning and differentiation, establishing the sharp boundaries that wall this organ off from the esophagus and intestine [10]. Development of the gut continues in this fashion, with the growth and development of unique cell types and morphologies, even after birth.

Notably, organisms commonly used to model the GI system have evolved their own unique gastrointestinal architecture, making them distinct from humans. For example, the keratinized layer of the murine esophagus extends into the stomach,

creating a region known as the “forestomach,” acting as another region to mechanically break down food [11]. Likewise, the chicken does not have a stomach per se, but rather has an analogous structure termed “gizzard.” This structure is much more muscular than a stomach and contains small, ingested stones that serve to grind food rather than digest it chemically [16]. Further, the mouse intestine fully matures after birth, finishing at about postnatal day 15 [17, 18]. However, humans establish fully defined villi embryonically [10]. Understandably, the structural and functional differences from models to humans limits the utility of models. However, much of the developmental machinery remains intact despite these differences, establishing these animal models as highly useful approximations of their human counterparts. For this reason, animal models of GI disorders play an indispensable role in defining the mechanisms that function in human disease.

4.3 Esophageal Morphogenesis and Disease

Located dorsally to the trachea, the esophagus is a muscular tube lined with stratified, squamous epithelium, connecting the oral cavity to the stomach. Mucus secreted by submucosal glands and peristaltic contractions by underlying smooth musculature drives the passage of consumed substances into the stomach. In humans, the adult esophagus is approximately 18–25 cm in length and is demarcated by the upper and lower sphincters, which ensure the unidirectional flow of food and liquid [19].

During embryonic development, a sheet of endodermal cells rearranges to form the primitive gut tube, marking the onset of gut organogenesis. This process begins 26–28 days post fertilization in humans and 8.5 days (E8.5) post fertilization in mice. Specifically, the esophagus derives from the anterior portion of the foregut. Cellular and molecular events coordinated by converging signaling pathways lead to the polarized separation of the single lumen gut tube into the ventrally located trachea and the dorsally located esophagus. This process occurs from E9.5 to E11 in

mice and between 28 and 42 days post fertilization in humans [20]. Consequently, congenital esophageal defects are primarily caused by dysregulated signaling pathways, which activate a cascade of transcriptional programs, leading to disrupted gut tube polarization and morphogenesis. Ultimately, the loss of proper dorsal-ventral patterning in the gut tube culminates in the improper separation of the trachea and esophagus, leading to life-threatening defects in newborns (Fig. 4.2).

4.3.1 Esophageal Atresia and Fistula

Affecting one in 3500–4000 births in the United States, congenital defects of the esophagus include esophageal atresia (EA) with and without trachea-esophageal fistula (TEF) [21, 22]. Pure EA is characterized by the abrupt sac-like termination of the true esophagus that disrupts the connection to the stomach. However, in most fetal patients, EA occurs in conjunction with TEF, where an ectopic pseudo-esophagus, or “fistula,” will branch from the trachea and connect to the stomach. EA/TEF phenotypes can manifest in various forms, potentially due to gene dosage effects [23], environmental factors, and/or the presence of modifier loci [24]. Clinically, five types of EA/TEF categories have been observed: type A) pure EA with no TEF, type 2) EA with proximal TEF, type C) EA with distal TEF, type D) EA with proximal and distal TEF, and lastly, type E) H-shaped TEF with no EA. Notably, type C is the most common form of EA/TEF, with 84% of affected newborns presenting with this variant. It must be noted that EA/TEF rarely occurs as the sole disorder in patients; it rather usually occurs in conjunction with abnormalities in other organs. The observed variation in EA type and disease pathology enforces the concept that EA/TEF is a complex disease, potentially influenced by multiple genetic and environmental interactions (Fig. 4.2).

Mouse knockout models demonstrate the critical roles of epithelial and mesenchymal transcription factors (TFs) in permitting tracheal-

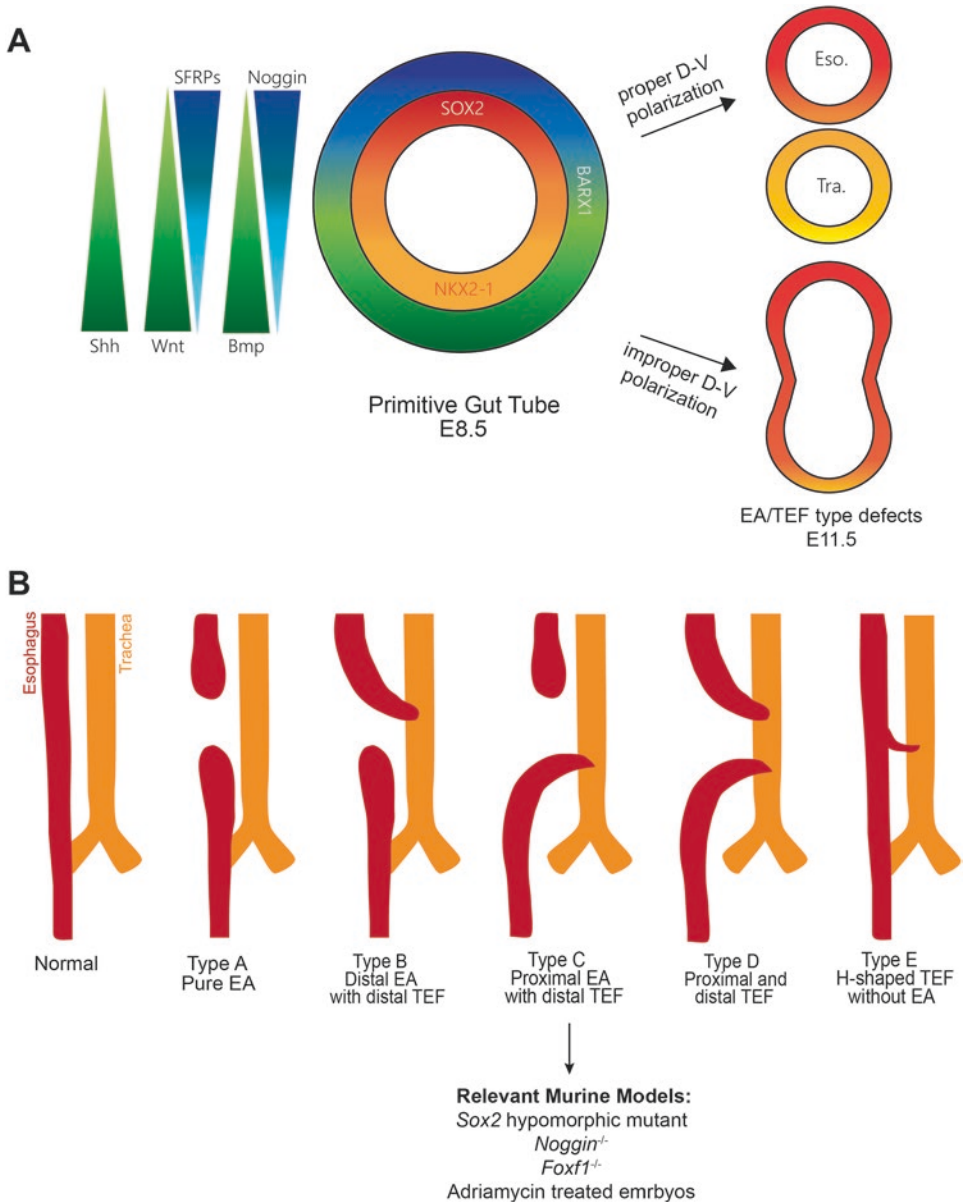


Fig. 4.2 Developmental cascades and diagrammatic representations of EA/TF. (a) Cross sectional view of the primitive foregut demonstrating TFs and signaling pathways enriched in the dorsal and ventral regions. The putative esophageal region contains high levels of SOX2, NOGGIN, and BMP7, while the opposing future tracheal epithelium contains NKX2.1, SHH, and WNT7b. BARX1, a mesenchymal factor expressed in the boundary between the early esophagus and trachea, attenuates Wnt signaling in the dorsal esophageal region. Dysregulation of these

expression patterns impairs esophageal-tracheal separation, leading to EA/TEF type defects. (b) Clinical representations of EA/TEF categories. EA/TEF can occur along a spectrum of phenotypes, with different combinations of EA with and without proximal or distal fistula formation. Type C is the most common form of EA/TEF (87% of affected patients): *Sox2* hypomorphic mutants, *Noggin*^{-/-}, Adriamycin-treated embryos, *Foxf1*^{-/-} all display type C EA/TEF and are relevant models to study this type of EA

esophageal separation. TFs are DNA-binding proteins that are known to be critical in regulating tissue-specific programs in a spatial and temporal fashion. SOX2, a key member of the SRY family of TFs, is abnormally expressed in a host of esophageal disorders such as EA/TEF, anophthalmia-esophageal-genital (AEG) syndrome [25], and esophageal cancer [26]. During murine esophageal development, SOX2 is enriched in the dorsal epithelium of the gut tube (the putative esophagus), while a homeobox containing TF NKX2.1 is enriched in the ventral epithelium (the future trachea). In murine embryos, the loss or reduction of either TF ectopically activates the reciprocal factor, disrupting the dorsal-ventral polarization and subsequently resulting in EA/TEF phenotypes. Specifically, hypomorphic *Sox2* mutants with varying levels of *Sox2* depletion exhibit increasingly severe EA/TEF phenotypes and an expanded *Nkx2.1* expression domain [23]. In contrast, *Nkx2.1* knockout mutants exhibit an overexpression of *Sox2*, but these mice still recapitulate TEF defects [27]. These findings corroborate rare EA/TEF phenotypes seen in AEG syndrome patients with heterozygous, inactivating *SOX2* mutations [25]. Given the conservation of the SOX2 function in murine and human esophageal development, these mouse models highlight the importance of dorsal-ventral patterning via TFs during tracheal-esophageal separation.

In conjunction with epithelium-specific factors, mesenchymal TFs also play a critical role during tracheal-esophageal separation. Heterozygous deletion of the mesenchymal TF, *Foxf1*, in murine embryos attenuates Sonic hedgehog (Shh) signaling, causing TEF defects [28]. Similarly, patients with deletions spanning the *FOXF1* cluster at 16q24.1 also display EA/TEF defects, emphasizing the importance of both mesenchymal TFs and Shh signaling in esophageal-tracheal separation. While *Foxf1* heterozygous mouse mutants do not display EA like the human counterparts [29], these differences can be explained by the additionally deleted loci within the *FOXF1* cluster in humans (i.e., modifier loci) and/or *FOXF1* gene dosage effects. BARX1, like

FOXF1, is a mesenchymal TF that influences esophageal development. BARX1 is a homeobox TF enriched in the dorsal foregut mesenchyme and functions to restrict Wnt signaling by promoting the expression of the Wnt antagonists (sFRP1 and sFRP2) [30]. In developing mice, deletion of *Barx1* expands the Wnt expression domain into the dorsal foregut, resulting in EA/TEF, which was visualized using TOPGAL, a reporter of Wnt activity (which marks activation of the canonical Wnt target *Tcf3/Lef1*) [31]. These models highlight the importance of TFs in establishing dorsal-ventral patterning during foregut tube separation. Ultimately, more studies are required to investigate how these TFs interact with signaling pathways to establish dorsal-ventral polarization.

In addition to TFs, key developmental pathways coordinate tracheal-esophageal separation via epithelial-mesenchymal cross-talk. Wnt, Bmp, Shh, and retinoic acid (RA) signaling pathways aid in the differentiation of respiratory and esophageal fate, ensuring the generation of two diverse tubes from one simple endodermal intermediate.

As previously mentioned, Wnt signaling is specifically active in the ventral (or putative tracheal) foregut, while in the dorsal domain this cascade is inhibited by SFRPs. Deletion of *β-catenin*, the main Wnt signaling effector, in the mouse endodermal epithelium (*Shh^{Cre}, β-catenin^{fl/fl}*) causes loss of *Nkx2.1* expression and expansion of the *Sox2* domain, leading to EA/TEF defects [32]. In addition, loss of *Wnt2* and *Wnt2b* in the developing foregut causes complete lung agenesis, while esophageal specification is unimpaired [33]. These results together demonstrate that Wnt signaling is critical for tracheal-esophageal separation but dispensable for esophageal fate specification.

Bmp signaling is critical for specifying tracheal fate and for the suppression of esophageal identity. The Bmp ligands BMP4 and BMP7 are expressed in the primitive gut tube epithelium (ventrally and dorsally, respectively) [34, 35]. However, the Bmp antagonist *Noggin* is restricted to the dorsal side. This leads to the selective activation of Bmp signaling in the ventral tracheal region, adding another

level of dorsal-ventral patterning. Relatedly, murine embryos lacking *Noggin* (*Noggin*^{-/-}) displayed EA/TEF defects, which are rescued upon loss of *Bmp4* or *Bmp7* [24]. Loss of one copy of *Bmp4* or deletion of *Bmp7* in the *Noggin*-null background rescued the EA/TEF phenotype by attenuating overactive Bmp signaling [24, 36]. In addition, loss of Bmp receptors in epithelial cells (*Shh*^{Cve}, *Bmpr1a*^{fl/-}, *Bmpr1b*^{-/-}) also developed EA/TEF defects due to loss of gut tube polarization via ventral expansion of the dorsal SOX2⁺ domain [37]. Jointly, these studies demonstrate the importance of tightly regulated Bmp signaling during esophageal-tracheal separation. In humans, loss of the locus containing *NOG* recapitulates the murine EA/TEF phenotype, validating the *Noggin* knockout mutants as a model for EA/TEF [38].

Shh signaling has also proven to be a vital regulator of tracheal-esophageal development. *Shh* is first expressed in the ventral foregut endoderm prior to tracheal organogenesis and is later expressed in the ventral esophageal epithelium. After the esophageal-tracheal separation, *Shh* expression shifts to the dorsal portion of the esophagus, while expression elsewhere is reduced. In mice, the loss of *Shh* or its downstream effectors, *Gli2* and *Gli3*, leads to EA/TEF through decreased expression of tracheal specifying factors such as NKX2.1, WNT2/2b, and BMP4 [39]. Similarly, a subset of patients with mutations in *SHH* (*SHH*^{+/-}) and *GLI3* also display the EA/TEF phenotype [39–41], demonstrating the importance of murine systems in modeling human EA/TEF.

Finally, RA signaling has been shown to function upstream of Bmp, Shh, and Wnt signaling and is thus a critical initiating factor of events leading to tracheal-esophageal separation. To dissect the sequence of signaling induction, two different animal models were employed by Rankin et al.: RA signaling was attenuated in *Xenopus* embryos using morpholinos and in E7.5 mouse embryos ex vivo using RA signaling antagonists. Both models demonstrated that the ablation of RA signaling dysregulates the downstream expression of Shh, Bmp, and Wnt effectors [42]. Corroborating these data, knockout mice of RA signaling receptors present with EA/TEF [43].

Although genetic manipulation of rodent models has been critical in defining the molecular mechanisms underlying foregut morphogenesis and EA/TEF development, key mechanistic questions remain unanswered. The incorporation of advanced live-cell imaging, TF chromatin immunoprecipitation sequencing, and mouse genetics will further our understanding of how foregut cells establish dorsal-ventral patterning and distribute themselves appropriately to achieve proper esophageal-tracheal separation. In addition, 93% of patients with EA/TEF have associated defects in vertebral, anorectal, cardiac, tracheal, esophageal, renal, and limb (VACTERL) structures [19]. Given that these structures share early developmental origins (for instance, the anus and rectum are both primitive gut tube derivatives), it may be beneficial to revisit straight deletions of common, early development genes shown to be critical for the VACTERL development and potential EA/TEF-like phenotypes.

It is important to note that mouse models, while highly useful, do have limitations when it comes to studying esophageal morphogenesis. Structural differences in esophagi between mice and humans limit the use of these animals in identifying secondary disease mechanisms related to esophageal versus tracheal fate specification during EA/TEF pathology. As such, organoids derived from human pluripotent stem cells would be highly beneficial for understanding human-specific disease mechanisms [44]. In addition, the early postnatal lethality of current EA/TEF mouse models complicates the study of potential treatment options for newborns with surgically corrected EA/TEF. In order to generate a clinically relevant animal model that can be utilized to study the feasibility of potential surgical treatments, the first porcine model of type A or pure EA has been generated by surgically attenuating the esophagus, in a procedure known as esophagectomy. These minipigs were used in a follow-up surgical procedure to study potential treatment options for pure EA phenotypes [45]. Building upon existing mouse models, alternate surgically induced EA/TEF animal models such as porcine, canine, and nonhuman primates would therefore advance the prospects of disease treatment and/or management.

4.4 Gastric Structure, Function, and Disease

The stomach plays a critical role in the digestion process. Through secretion of hydrochloric acid and enzymes, it is the site of chemical decomposition of ingested food. The stomach also regulates the sensation of hunger through the production of satiety-inducing hormones. Further, the stomach acts as a holding cell for digested food (chyme) to permit efficient digestion and nutrient absorption by the small intestine. Disruptions in these core functions ultimately impairs nutrient absorption [11, 46, 47].

In humans, the stomach is divided into several functionally distinct units. At the most rostral point lies the cardia, wherein the cardiac sphincter joins the esophagus to the stomach to prevent stomach contents from entering the esophagus. Caudally from this junction, the stomach widens, with the leftmost curvature (residing below the diaphragm) being termed the fundus. Food begins its chemical breakdown process in the body of the stomach, which lies caudally to both the cardia and fundus, via mixing with acid and enzymes. Digested food then collects in the fundus of the stomach, where it awaits passage into the small intestine through the pylorus. The pylorus houses the pyloric sphincter, a thick, muscular layer that carefully regulates the passage of chyme into the duodenum (proximal small intestine) for nutrient absorption [48, 49] (Fig. 4.3).

Given the unique roles of stomach compartments, it is no surprise that each of these regions comprises functionally distinct epithelial cell types that become specified throughout development. These cells are the functional units of the stomach and, as such, play a diverse set of roles. Gastric epithelial cells are arranged into glandular units, column-shaped invaginations into the surrounding stromal tissue, with each region of the stomach retaining its own unique gland type. While each type varies in its composition, the major cell types include: parietal cells, which secrete gastric acid and intrinsic factor, chief cells (or zymogenic cells), which secrete the enzyme pepsinogen (responsible for the breakdown of proteins into smaller peptides), and

enteroendocrine cells, which secrete a number of hormones such as gastrin and cholecystokinin [11, 50, 51].

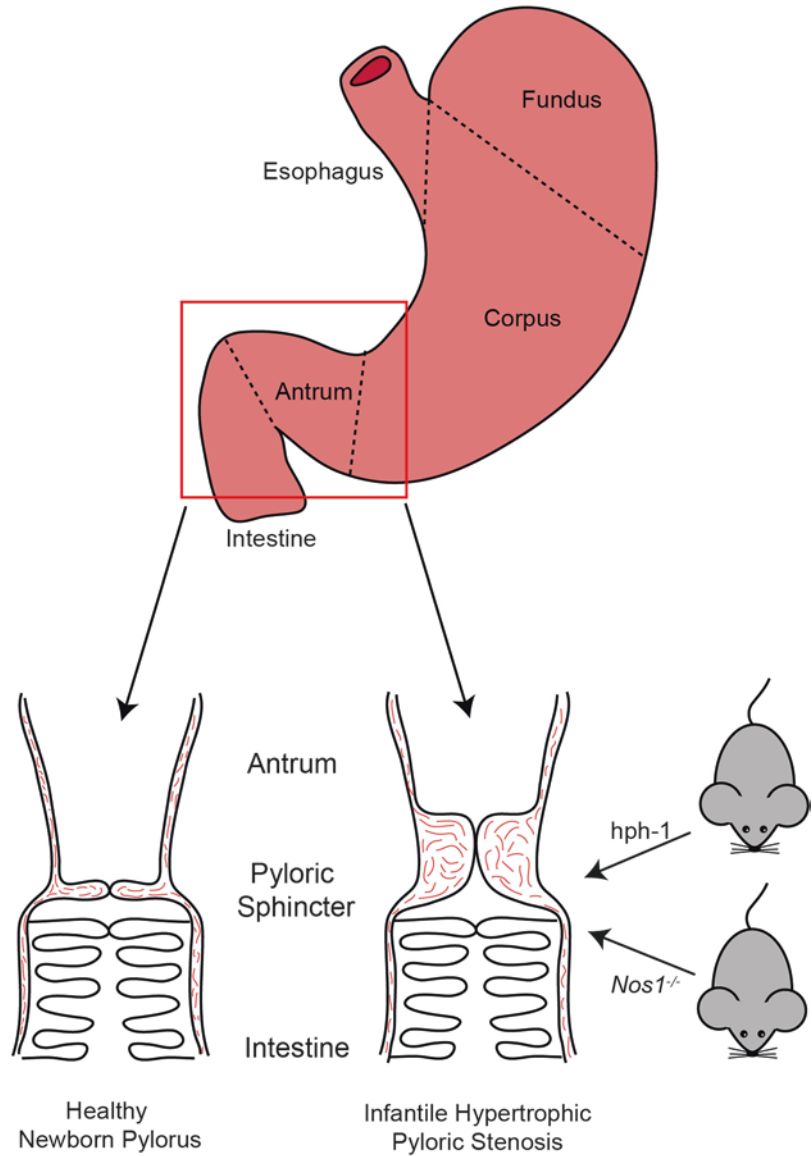
Congenital disorders of the stomach are rare but can have serious implications for an individual's quality of life. Often these disorders disrupt the flow of chyme from the stomach to the intestine, leading to severe blockages and ultimately malnutrition in neonates. Clearly, a better understanding of these disorders will be crucial in alleviating this medical burden. Below we will discuss infantile hypertrophic pyloric stenosis, one of the most common congenital gastric disorders, and highlight recent advances in the employment of new animal models.

4.4.1 Infantile Hypertrophic Pyloric Stenosis

Infantile hypertrophic pyloric stenosis (IHPS) is a relatively uncommon disorder of the gastric pylorus region, affecting 1–4/1000 newborns, and its severity differs significantly by race, geographical location, and sex [52–54]. As its name suggests, individuals afflicted with this illness experience a weakening of the pyloric muscle layers. However, individuals also experience hyperplasia and thickening of the muscle layer, leading to severe obstruction of the gastric outlet. The clinical presentation begins between one and 12 weeks of age, with initial presentations being mild, infrequent vomiting of small volumes. However, as the disease progresses, infants present with projectile vomiting, a direct consequence of gastric outlet obstruction [55]. Advancements in surgical remediation have improved the outcome of IHPS dramatically, with significantly reduced mortality rates [56], but the cause of this disorder remains up for debate (Fig. 4.3).

It is theorized that this disorder is multifaceted, being shaped by both genetic and environmental forces. Evidence of this stems from epidemiological studies. One such study noted a 200-fold increase in the likelihood of IHPS development among monozygotic twins and a 40- to 50-fold increase among dizygotic twins [57]. Further, studies have demonstrated that

Fig. 4.3 Morphological changes of the stomach in models of infantile hypertrophic pyloric stenosis (IHPS). The stomach is divided into structurally and functionally distinct regions: the corpus, fundus, and pylorus. The esophagus is located at the rostral end of the stomach, and the small intestine is attached to the caudal end of the stomach through the pyloric sphincter. Mouse models of IHPS (*hph-1* and *Nos1^{-/-}*) present with an abnormally thickened muscle layer of the pyloric sphincter, visually recapitulating gastric blockages seen in human infants



males are four- to fivefold more likely to develop IHPS than are females. Collectively, these studies suggest a strong genetic component in IHPS formation, ultimately driving investigations into the underlying genetic mechanisms.

In the early stages of its investigation, several studies noted the presence of pyloric spasms in newborns, who later developed IHPS. It was therefore theorized that improper innervation of the pylorus may be an underlying cause of this disease. Two mouse models have thus been developed to investigate the role of the enteric

nervous system in IHPS development, converging on the nitric oxide (NO) synthesis pathway, a critical mediator of muscle relaxation.

The first model, termed *hph-1* [58], is deficient in GTP cyclohydrolase (GTPCH) activity, which is required for the metabolism of BH₄, a cofactor of NO synthase activity. In this model, NO production is diminished, and the mice present with temporary IHPS symptoms, including a thickening of longitudinal and circular muscle layers that persist for approximately 6 months [59]. While GTPCH activity is diminished, it is

unclear whether the mutation is directly disrupting the *Gtpch* gene. The *hph-1* mouse model was first identified through a forward-genetics screen aimed at locating deficiencies in phenylalanine hydroxylase function, but subsequent sequencing of *Gtpch* [60] and its 5' flank [61] was unable to identify functional mutations.

Recent work has questioned the canonical framework of IHPS development in *hph-1* mice, noting that BH₄-mediated reduction of NO also results in the production of reactive oxygen species (ROS) [62]. It was found that ROS accumulation activated ROCK-2, a protein traditionally involved in smooth muscle contraction, ultimately increasing pyloric thickness in *hph-1* mice. These findings suggest that pyloric contraction, rather than relaxation, is culpable in IHPS development.

Further, a recent study examined the regression of IHPS symptoms in adult *hph-1* mice. The authors of this study noted that adult mice display no symptoms of IHPS and that these mice were no longer deficient in BH₄. This group reasoned that exogenous sources of BH₄ could contribute to the regression of IHPS symptoms over time. Ultimately, this study identified a commensal BH₄-producing bacterial population in adult mice, which is absent in newborns. This team therefore concludes that in the absence of endogenous BH₄ production, bacteria act as a critical reservoir to ensure proper postnatal pyloric development [63].

The second model of IHPS again converges on the NO synthesis pathway. The *Nos1* mouse model harbors a targeted disruption of exon 1 in the *Nos1* gene, leading to a specific inhibition of NO synthesis. These mice have large distended stomachs and, as a result, pyloric hypertrophy, reminiscent of the human condition [64]. Interestingly, the previous genome-wide SNP association study revealed no significant variations within the coding region of *NOS1* in IHPS patients, suggesting that altered epigenetic regulation of this gene might be involved in the disease pathogenesis [65].

While it is well understood that disruptions in muscle function, stemming from disrupted NO synthesis and ROS production, are causative fac-

tors in IHPS pathogenesis, the exact pathways and the identity of genes involved are unknown. Consistent with the critical roles of developmental TFs in esophageal development, a recent mouse genetic study has demonstrated that *Nkx2-5* and *Gata3* are required for the development of a pyloric outer longitudinal muscle fascicle during pyloric sphincter morphogenesis [66] (Fig. 4.3).

Clearly, many questions regarding the pathology of IHPS remain. While NO synthesis and gastric-specific transcription factors seem to play crucial roles in stomach muscle development, the clinical causes of IHPS are still unclear. However, recent work has made progress on this front, with a genome-wide association study identifying IHPS-associated variants near the *NKX2-5* locus, corroborating findings in mice [67]. Accordingly, future work should focus on establishing novel mouse models based on clinically relevant mutations. A recent study took a strong bioinformatic approach, wherein the use of over 1600 cases of IHPS identified a series of novel SNPs. In this study, the team focused on their most significant hit, a SNP located 301 bases downstream of *APOA1* (a gene associated with circulating cholesterol). Interestingly, this team discovered that reduction in circulating cholesterol correlated with both the *APOA1* SNP and an increased risk of IHPS [68]. These results indicate that much more work needs to be done to understand the etiology of IHPS, which will require novel and fully characterized models of this disease.

4.5 Neonatal Intestine and Disease

The neonatal intestine is exposed to an extremely different environment soon after birth. The immune response must begin to distinguish between self and nonself, differentiating food antigens and commensal microbiota from pathogenic species. This highly complicated and regulated process is perturbed in premature infants exposed to broad-spectrum antibiotics. Antibiotics disrupt the bacterial diversity of the newborn intestinal tract, subsequently impairing normal intestinal immune system development

[69]. Additionally, immature intestinal epithelial cells exhibit a compromised physical barrier, allowing the translocation of pathogens, and express high levels of *TLR4*, which activate abnormal immune responses [70]. These events ultimately lead to intestinal inflammation.

The small intestinal gland unit consists of the villus and crypt. *Lgr5*-expressing intestinal stem cells located at the bottom of the crypt give rise to two major cell types, enterocytes and secretory (endocrine, goblet, and Paneth cells) lineages [71]. Each cell lineage plays a unique and important role in maintaining barrier integrity [72]. Goblet cells arise in embryonic stages of gut development. These cells secrete mucin glycoproteins, which generate the mucus layer of the intestine to protect against the harsh environment of the intestinal lumen [73]. Animal studies showed that mucus gene expression is influenced by bacterial colonization, demonstrating that glycosylation alters interactions with bacterial pathogens [74, 75]. Paneth cells, a secretory cell type found at the base of the intestinal crypts, secrete antimicrobial peptides to guard against pathogenic species [76]. Studies comparing germ-free mice to conventionally raised mice demonstrated a reduced number of goblet cells and impaired expression of Paneth cell lectin, suggesting a microbial influence on the differentiation of goblet cells and Paneth cells [77, 78].

4.5.1 Necrotizing Enterocolitis (NEC)

Necrotizing enterocolitis (NEC) is an inflammatory intestinal disease occurring mainly in the ileum and colon of neonates, leading to intestinal necrosis, systemic sepsis, and multiorgan failure [79]. NEC is one of the most prevalent and life-threatening gastrointestinal diseases in preterm infants with low birth weight (<1500 g) [80]. In North America, approximately 5–10% of preterm neonates are afflicted with NEC, with an approximately 30% mortality rate [81, 82]. NEC survivors have poor neurodevelopmental outcomes, and the average annual cost of caring for these infants ranges from 500 million to 1 billion dol-

lars [69]. NEC is considered a multifactorial disease associated with prematurity of the intestinal epithelium, enteral feeding, use of antibiotics, and abnormal bacterial colonization [83–87]. Despite decades of studies examining the pathogenesis of NEC, its complex etiology remains poorly understood, and effective treatment options have yet to emerge, with mortality rates remaining stagnant. Consequently, developing reliable and reproducible animal models for the study of NEC is crucial to advance the state of knowledge in this field.

Several models have been developed to evaluate specific facets of this disease in isolation and in combination with therapeutic treatment [88, 89]. A widely cited murine model of NEC makes use of a hypoxia/hypothermia/formula feeding (HHF) regimen to induce NEC-like symptoms, which include necrosis, hypoxic stress, and severe ileum histopathology. Based on this, various new NEC models have been proposed: administration of platelet-activating factor (PAF), Paneth cell depletion, infection, and chemical injury [88]. This section will highlight the various strengths and weaknesses of these models and discuss potential directions for the development of new models.

The rat model of NEC was developed in the early 1970s by Dr. Barlow and colleagues in New York. This model makes use of formula feeding and bacterial colonization to demonstrate that rat breast milk feedings completely protect against NEC development compared to pups receiving formula feedings. This result suggests that breast milk may support mucosal immunity and facilitate commensal gut flora, thus promoting intestinal epithelial repair and regeneration [90]. Building on this idea, the same research group then developed a new model, which includes hypoxia, hypothermia, and formula feeding (HHF), demonstrating that any stress that decreases mesenteric blood flow can promote NEC [91]. Reflecting physiological and histopathological changes observed in human NEC, this model has become the gold standard of NEC model systems [89]. Today, the histologic grading standard devised by Dr. Barlow remains in use for NEC confirmation in all current rodent models.

Variations of the rat HHF experimental strategy have since been employed by investigators to address novel questions. Caplan et al. used the rat HHF NEC model to compare full-term with premature newborn rats, revealing that hypoxia is a crucial instigating factor of NEC [92]. Interestingly, enteral treatment of the PAF-degrading enzyme acetylhydrolase (PAF-AH) is sufficient to reduce NEC incidence. Further supporting the role of PAF in NEC pathogenesis, direct injection of PAF with LPS can induce NEC-like symptoms in rats [93].

Compared to the rat NEC model, establishing a mouse model of NEC has been challenging due to their small size and the frailty of transgenic pups. However, the use of mice to model NEC has the potential to produce novel, highly impactful insights into NEC pathogenesis due to the tractability of mouse genetics. The earliest attempt to use mice in NEC research was actually a temporary intestinal ischemia model achieved by occluding both superior mesenteric vessels with a bulldog clamp [94]. However, the first true neonatal mouse NEC model was established in 2006, when the rat HHF NEC model was adapted to mice [70]. In this model, mice were delivered by cesarean section before term and subjected to gavage feeding with puppy formula every 2 h from postnatal day 0 (P0) using a small orogastric feeding catheter. These mice were also exposed to both hypoxic conditions (100% N₂ for 1 min) and cold stress (4 °C for 10 min), twice daily for total of 72 h (Fig. 4.4). Using the *Tlr4* mutant mice, the authors demonstrated that *Tlr4* mutant mice are protected from NEC-like pathology, revealing its role in NEC pathogenesis [70].

While the HHF mouse model of NEC is now widely employed, some studies have made use of chemical stress factors to induce this disease in mouse pups. Ginzl et al. [95] demonstrated that dextran sodium sulfate (DSS) is sufficient to induce NEC in formula-fed neonatal mice, causing NEC-like lesions with humoral and cellular immune responses in the small and large intestines. This NEC model has the advantage of avoiding physical stressors for animals, such as hypoxia and hypothermia [95]. Trinitrobenzenesulfonic

acid (TNBS) has also been used to instigate NEC phenotypes in 10-day-old mice. TNBS acts as a hapten, generating an immune response that induces macrophage-dominated mucosal lesions, similar to that of human NEC [96].

Paneth cell (PC) elimination is another interesting method used to induce NEC in mouse pups. Paneth cells are epithelial cells that secrete antimicrobial peptides. The heavy-metal chelator dithizone reacts with the zinc contained in Paneth cells to produce zinc-dithizonate complexes, which impairs Paneth cell function [97]. Zhang et al. [98] reported that P14–P16 mice subjected to intraperitoneal injection of dithizone and administered *Klebsiella pneumoniae* (a gram negative bacteria), developed NEC within 10 h. This implies a central role of Paneth cells in mitigating pathogen-induced NEC initiation.

In addition to rats and mice, rabbits, quail, and hamsters have also been used in the study of NEC pathogenesis [99–101]. Functionally, many of these models are variations of the HHF model employed in rats and mice. However, several models have been created to address unique facets of NEC etiology. For instance, mechanical models of NEC exist for rabbits, wherein the application of tissue adhesive to anal openings and formula feeding with *Enterobacter cloacae* can recapitulate the intestinal dysmotility observed in human patients [99]. Further, the contribution of individual bacterial species in the pathophysiology of NEC also has been delineated using a gnotobiotic quail model [100]. In this instance, inoculation of germ-free quail with bacteria of interest led to an improved understanding of iNOS pathway activation in early-stage NEC. Similarly, administration of *Clostridium butyricum* elucidated the roles of butyric acid in NEC formation, demonstrating the importance of germ-free models in understanding NEC initiation [102, 103]. Finally, models of NEC have extended to nonhuman primates. The preterm baboon (*Papio cynocephalus anubis/P. cynocephalus cynocephalus*) has also proven itself invaluable in understanding NEC etiology. Baboons delivered via cesarean section at 125 days gestation (67% gestation, term being 185 days, equivalent to 27-week gestation in

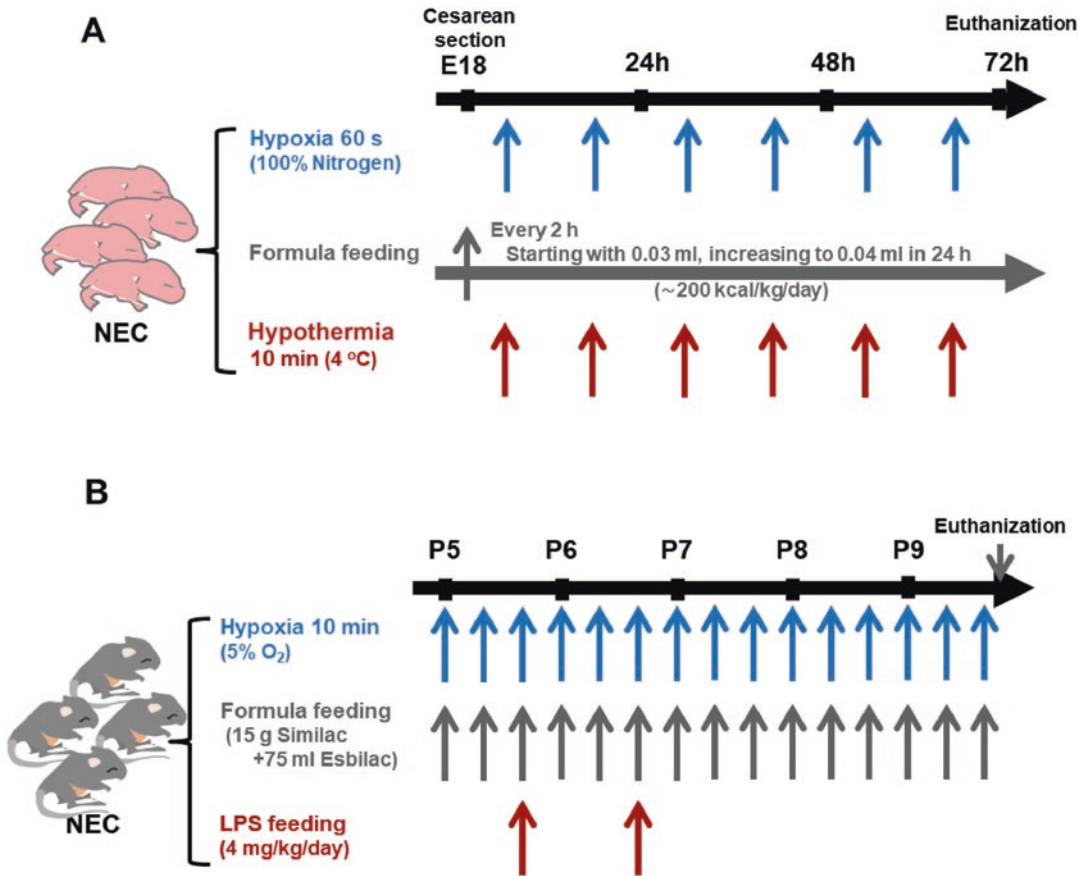


Fig. 4.4 Representative mouse NEC models. (a) Conventional HHF model described by Caplan et al. [70, 92]. Cesarean section was performed between E18 and E19. Pups were allowed to recover for 2 h, then fed every 2 h starting with 0.03 mL of formula, increasing to 0.04 mL in the subsequent 24 h (to deliver ~200 kcal/kg/day). Hypoxia stress was accomplished by exposure to 100% nitrogen for 60 s, followed by exposure to hypothermic

conditions (4 °C) for 10 min twice daily. (b) NEC model proposed by Zani et al. [140]. NEC induction starts from postnatal day 5 (P5). Mice are formula fed by gavage (15 g Similac+75 mL Esbilac) and subjected to hypoxia (5% O₂ for 10 min, three times a day). Oral administration of 4 mg/kg/day of LPS (lipopolysaccharide from *Escherichia coli* 0111:B4) is done on the first and second day of NEC induction in combination with formula feeding

humans) [104] were provided treatment similar to that employed for neonatal humans with sepsis, including mechanical ventilation, antibiotics, and enteral feeds. Interestingly, this study demonstrated that the premature intestine increases levels of *Smad7* expression, which inhibits the autocrine expression of TGF- β 2 in epithelial cells, resulting in increased macrophage inflammatory responses, resembling human NEC [104, 105].

Animal NEC models have made great strides over the past 40 years, encompassing numerous species to answer diverse and distinct questions of NEC etiology (Table 4.1). Although no model

perfectly replicates human NEC, each model has greatly improved our understanding of the immature intestinal tract and the pathophysiology of NEC. However, it is also clear that an animal model more accurately representing human NEC will be required for elevating the management protocol of NEC patients and developing therapeutics to improve patient outcomes. Future work could utilize recently developed humanized mouse models such as xenobiotic receptor humanized mice [106] and TLR4 humanized mice [107]. By simulating the human condition with great accuracy, these models could significantly advance human NEC research.

Table 4.1 Costs and benefits of NEC animal models

Model species	Advantages	Disadvantages
Rat	– Low cost	– Few transgenic models available
	– Easy breeding	– Resilience to stress which results in high tolerance to bacterial infection and endotoxins, relative to humans
	– Easy to formula feed	– Limited commercially available antibodies
Mouse	– Low cost	– Technical challenging of gavage feeding due to small size of the pups
	– Easy breeding	– Short-term model due to the fragility of pups
	– Accessibility of knockout and transgenic animal models	
Others	– Piglet, baboon	– High cost
	– Anatomical similarities with preterm human intestine	– Scarcity of genetic models
	– Pathological similarities with human NEC	– Few commercially available antibodies

Summary of the major benefits and drawbacks of species as models of NEC

4.6 Colonic Structure, Function, and Disease

The colon (or large intestine) is the most distal region of the gastrointestinal system. Its main function is to remove and absorb water from digested food. Similar to its small intestinal counterpart, the colon is arranged into repeated epithelial structures along its length. However, unlike the small intestine, the colon lacks villi. Instead, it is fully composed of crypts, in a physical structure reminiscent of gastric glands. Colonic crypts house stem cells at the base of the crypt, where they give rise to absorptive enterocytes, as well as goblet cells and enteroendocrine cells of the

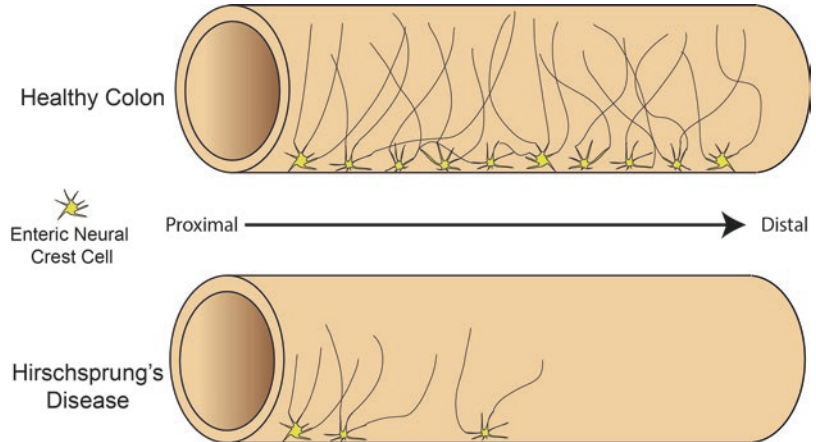
secretory lineage (notably, Paneth cells are not present in the colon). The colon develops similarly to the small intestine, in a wave-like pattern of growth. This results in a gradient of colonic crypt depth, with the most shallow crypts present in the proximal colon and the deepest in the distal colon [7, 108]. Newborn diseases of the colon are relatively common, as far as GI disorders go, and life-threatening if left untreated. Preclinical models of colonic diseases are therefore imperative to improve survival rates, as well as the quality of life in those who survive.

4.6.1 Hirschsprung's Disease

Hirschsprung's disease (HD) is primarily a disorder of the enteric nervous system (ENS). Characterized by the absence of ganglion cells from the distal colon, it ultimately causes prolonged muscle contraction and colonic obstruction (Fig. 4.5). Patients present with distended abdomens, often accompanied by severe vomiting and an inability to pass stool. This disease occurs in about 1:5000 newborns, with males being four times more likely than females to present with HD [109, 110]. When left untreated, newborn survival is dramatically reduced due to enterocolitis (bacterial infection and inflammation) [111]. Colonic resection, the primary treatment of HD, significantly reduces mortality rates, but patients often have complications from infection after surgery. A recent summary of HD explores this topic in great depth [110]. Given its varied penetrance and range of severity among patients, it is difficult to discern the underlying mechanisms of HD. It is therefore crucial to establish animal models that will recapitulate the etiology of this disease.

A number of animal models have been established to study the complexities of HD. Mouse models of HD have previously been discussed at length [112], so this section aims to summarize the most prevalent models and highlight recent advancements and insights. These models can be divided into two classifications: genetic and environmental. Genetic models examine various individual aspects of this disease, including clinical heterogeneity and cellular

Fig. 4.5 Aganglionosis of the colon in models of Hirschsprung's disease. Enteric neural crest cell (ENCCs) migration occurs in a proximal-to-distal wave during gastrointestinal development. Disruption of ENCC migration and proliferation impairs innervation, and consequently function of the colon



alterations. Environmental models have been used to explore preventative therapies and to examine gene–environment interactions.

RET proto-oncogene (RET) is a receptor tyrosine kinase specific to glial-cell-line-derived neurotrophic factor (GDNF) ligands. Similar to other receptor tyrosine kinases [113], RET activation influences a number of signaling paths, including Ras/MAP kinase, phospholipase C- γ , and PI3 kinase/AKT. Its function has been documented throughout nervous system development, notably in the enteric nervous system. RET mutations are relatively common in HD patients [114]. As might be expected, many mouse models of RET mutations have emerged, ranging from isoform variants to point mutations [115–121]. Collectively, these models have been incredibly useful in elucidating the molecular mechanisms underpinning ENS development, defining a clear role for RET in ENS proliferation, differentiation, growth, survival, and migration. Each of these models recapitulates the aganglionosis described in HD patients, albeit to varying degrees. Mice with complete null mutations of *Ret* experience complete aganglionosis in the intestine and ultimately die of kidney defects at birth [117]. Consequently, subsequent *Ret* models have focused on diminishing (rather than ablating) RET function to explore later stages of development. Interestingly, conditional ablation of *Ret* after neural crest cell colonization of the intestine determined that RET is crucial in maintaining ENS survival [118]. RET has also been

found to have indirect effects on colonic health, specifically contributing to epithelial barrier function. A recent study discovered that *Ret* expression also occurs in Group 3 innate lymphoid cells and is not limited to the ENS. GDNFs from the neighboring ENS were found to bind RET in the innate lymphoid cells, activating the p38 MAPK/ERK-AKT cascade to stimulate IL22, ultimately contributing to colonic epithelial health [122].

Animal models disrupting the endothelin 3 (EDN3) cascade have also been shown to develop aganglionosis of the distal colon, resembling RET models and HD patients. Specifically, mice with these deletions experienced delayed enteric neural crest cell (ENCC) migration into the colon, with patches completely devoid of ganglionic cells [123–127]. EDN3 is an endothelium-derived peptide, part of a family of peptides that have a wide range of functions. Mouse models ablating EDN3 function, as well as its canonical receptor, EDN3R, were used to elucidate the functions of ENCC; these studies demonstrated that this EDN3-EDN3R axis is critical for glial cell proliferation and glial stem cell progenitor maintenance [128, 129]. In an especially interesting study, *EdnrB* knockout mice were used to advance regenerative medicine in the colon. In this study, induced pluripotent stem cells were transplanted into *EdnrB* knockout mice exhibiting aganglionosis, resulting in extensive ENCC colonization [130]. This study also demonstrated that pluripotent stem cells are able to influence

migration patterns of ENCCs in the developing chick, suggesting that these models might be used as preclinical models for regenerative medicine. However, it is important to recall that the mechanisms through which EDN3 exerts its influence are still unknown. The models discussed here offer an excellent opportunity to identify downstream components of this cascade, which could provide novel therapeutic targets for treating and managing the effects of HD.

In addition to signaling cascades, a number of TFs have been examined in animal models of HD. The best studied HD-associated TF is SOX10. In mice, haploinsufficiency of *Sox10* is sufficient to drive aganglionosis and megacolon phenotypes, phenocopying HD patient pathology. This is unsurprising, given that SOX10 is a master regulator of ENCC fate, governing the expression of genes such as *Ret* and *EdnrB* (often in concert with other TFs, such as PAX3 [131]), and mutations in *SOX10* were found in syndromic cases of HD [132]. At a cellular level, SOX10 works to maintain the pluripotency of ENCCs. Loss of *Sox10* function results in proper migration but premature differentiation and loss of the progenitor pool, thus leading to reduced overall ENCC numbers [133]. A novel mouse model has been used to further elucidate the function of SOX10 in ENCCs. The *Sox10-H2B*Venus line allowed spatial and temporal visualization of *Sox10* expression, leading to the finding that this gene controls ENCC migration [134]. A second reporter strain, *Sox10^{lacZ/+}*, was used to demonstrate the importance of this gene in the cell adhesion properties of ENCCs [135]. Taken together, it is clear that novel genetic models of ENCC development and maturation can lead to unexpected findings regarding the etiology of HD. Future work should expand upon these molecular mechanisms, investigating the translation of these findings to their human counterparts.

HD patients experience a wide and varied range of penetrance and severity, suggesting that genetic and environmental factors influence complex disease outcomes. Next, we will examine some models of environmental stimulants of HD.

Two studies led by Dr. Heuckeroth have taken a broad, unbiased approach to understanding

environmental triggers of HD. Using zebrafish, they screened over 1500 drugs and identified nine that significantly disrupted ENS development. Mycophenolic acid (MPA) caused the most striking phenotypic change in fish and was subsequently investigated in wild-type mouse embryos. Surprisingly, MPA treatment disrupted ENCC colonization of the colon, suggesting that this compound might influence HD development. Interestingly, MPA alone is incapable of causing aganglionosis, but the authors determined that treatment of *Sox10* and *Ret* mutant mice with MPA caused enhanced aganglionosis, again highlighting the complexity of HD penetrance. MPA is a commonly used immunosuppressant that impairs GMP synthesis by blocking inosine monophosphate dehydrogenase (IMPDH). In essence, MPA is able to block the proliferation of ENCC cells, leading to decreased ENCC colonization. The authors therefore theorized that disruption of ENCC proliferation would increase the susceptibility of mice, and potentially humans, to HD development [136]. This team went on to create a genetic model that recaptures the effects seen as the result of MPA treatment, creating a conditional knockout of the IMPDH isoform *Impdh2* under the control of Wnt1-Cre [137].

This same group approached this question in a similar manner to establish a novel developmental impact of the widely used nonsteroidal anti-inflammatory Ibuprofen [138]. The additional screening for ENCC colonization in zebrafish performed by this team identified hits for both Ibuprofen and acetylsalicylic acid (however, the latter caused the fish to die, so Ibuprofen was the focus of the study). These findings were translated to the mouse, where again maternal ingestion of this drug slowed ENCC colonization in embryos. Most strikingly, experiments in chicks demonstrated that Ibuprofen treatment completely impaired this colonization process, suggesting that the likelihood of HD is increased in pregnant mothers who ingest Ibuprofen. It is important to note that no human studies have examined this topic to date, but this study clearly demonstrates the utility of preclinical models in understanding, and perhaps preventing, complex disorders.

Finally, a recent model has been established specifically to address nongenetic contributors to the aganglionosis phenotype of HD. In this model, chickens were treated with phosphoramidon at embryonic day 10. Phosphoramidon is an inhibitor of endothelin-converting enzyme 1 (ECE1), which is required for the production of EDN1, EDN2, and EDN3. As noted above, the EDN family of molecules is critical to the growth and maturation of ENCCs in the colon, while disruptions in EDN3 and its receptor, EDNRB, result in impaired ENCC proliferation and migration. As expected, phosphoramidon-mediated inhibition of ECE1 impairs the EDN-EDNRB signaling axis, reducing proliferation, accelerating differentiation, and ultimately mimicking HD aganglionosis phenotypes [139]. This model is especially suited to the examination of environmental modifiers of HD penetrance and severity. The specific utility of this model will permit the determination of environmental stressors and their individual contributions to HD progression.

Hirschsprung's disease, while phenotypically simple, appears to result from the complex interplay of genes and the environment. Consequently, the development of clinically relevant models has been a challenge. Many models have focused solely on the genetic contributions to disease initiation, defining key regulators such as EDN3, SOX10, and RET. While these models have provided unprecedented progress in our understanding of HD, future research should further explore genetic-environmental interactions.

4.7 Concluding Remarks

Congenital gastrointestinal diseases have long-lasting and severe consequences on the well-being of individuals. An understanding of the initiation and progression of these diseases is therefore fundamental to the development of novel therapeutics and treatment practices to improve patient outcomes. Animal models of GI disorders vary widely in their prevalence, complexity, and ability to recapitulate human diseases, as presented here. Notably, mouse models are the most widely used system to model human

disorders, likely due to the extent of genetic tools available for their manipulation. In this chapter, we have also discussed how other models such as chick and quail, rats, and pigs can offer valuable insight into the pathogenesis of human illness.

Human GI diseases are often multifactorial, and their underlying genetic and environmental causes still remain poorly understood. While recent work has made substantial progress in exploring these intricacies, it is apparent that many current animal models do not precisely replicate human disease. Recent studies reveal several recurrent themes, including the importance of high-throughput sequencing of patients to develop clinically relevant models and the interactions of genes and environmental forces. Accordingly, future work in understanding congenital GI diseases therefore presents a great challenge—to mine large volumes of patient data with the goal of developing novel animal models encompassing the complexities of genetic and environmental interactions faced by human patients.

References

1. Asindi AA, Al-Daama SA, Zayed MS, Fatinni YA. Congenital malformation of the gastrointestinal tract in Aseer region, Saudi Arabia. *Saudi Med J*. 2002;23(9):1078–82.
2. Public Health Infobase: Congenital Anomalies in Canada [Internet]. Public Health Infobase. 2017. <https://infobase.phac-aspc.gc.ca/congenital-anomalies/data-tool/>.
3. Oezcelik A, DeMeester SR. General anatomy of the esophagus. *Thorac Surg Clin*. 2011;21(2):289–97.
4. O'Connor A, O'Morain C. Digestive function of the stomach. *Dig Dis*. 2014;32(3):186–91.
5. Helander HF, Fändriks L. Surface area of the digestive tract—revisited. 2014;49(6):681–9. <https://doi.org/10.3109/003655212014898326>.
6. Okumura R, Takeda K. Roles of intestinal epithelial cells in the maintenance of gut homeostasis. *Exp Mol Med*. 2017;49(5):e338.
7. Sandle G. Salt and water absorption in the human colon: a modern appraisal. *Gut*. 1998;43(2):294–9.
8. Zorn AM, Wells JM. Vertebrate endoderm development and organ formation. *Annu Rev Cell Dev Biol*. 2009;25:221–51.
9. Spence JR, Lauf R, Shroyer NF. Vertebrate intestinal endoderm development. *Dev Dyn*. 2011;240(3):501–20.

10. Chin AM, Hill DR, Aurora M, Spence JR. Morphogenesis and maturation of the embryonic and postnatal intestine. *Semin Cell Dev Biol.* 2017;66:81–93.
11. Kim TH, Shivdasani RA. Stomach development, stem cells and disease. *Development.* 2016;143(4):554–65.
12. Raghoebir L, Bakker ER, Mills JC, Swagemakers S, Kempen M, Munck A, et al. SOX2 redirects the developmental fate of the intestinal epithelium toward a premature gastric phenotype. *J Mol Cell Biol.* 2012;4(6):377–85.
13. Dufort D, Schwartz L, Harpal K, Rossant J. The transcription factor HNF3beta is required in visceral endoderm for normal primitive streak morphogenesis. *Development.* 1998;125(16):3015–25.
14. Tourneur E, Chassin C. Neonatal immune adaptation of the gut and its role during infections. *Clin Dev Immunol.* 2013;2013:270301.
15. Nagy N, Goldstein AM. Enteric nervous system development: a crest cell's journey from neural tube to colon. *Semin Cell Dev Biol.* 2017;66:94–106.
16. Svihus B. The gizzard: function, influence of diet structure and effects on nutrient availability. *Worlds Poult Sci J.* 2011;67(2):207–23.
17. Schmidt GH, Winton DJ, Ponder BA. Development of the pattern of cell renewal in the crypt-villus unit of chimaeric mouse small intestine. *Development.* 1988;103(4):785–90.
18. Calvert R, Pothier P. Migration of fetal intestinal intervillous cells in neonatal mice. *Anat Rec.* 1990;227(2):199–206.
19. Kuo B, Urma D. Esophagus—anatomy and development. *GI Motility online.* 2006.
20. Que J. The initial establishment and epithelial morphogenesis of the esophagus: a new model of tracheal-esophageal separation and transition of simple columnar into stratified squamous epithelium in the developing esophagus. *Wiley Interdiscip Rev Dev Biol.* 2015;4(4):419–30.
21. Esophageal Atresia and/or Tracheoesophageal Fistula—NORD (National Organization for Rare Disorders). 2019. <https://rarediseases.org/rare-diseases/esophageal-atresia-and-or-tracheoesophageal-fistula/>.
22. Ioannides AS, Massa V, Ferraro E, Cecconi F, Spitz L, Henderson DJ, Copp AJ. Foregut separation and tracheo-oesophageal malformations: the role of tracheal outgrowth, dorso-ventral patterning and programmed cell death. *Dev Biol.* 2010;337(2):351–62.
23. Que J, Okubo T, Goldenring JR, Nam K-T, Kurotani R, Morrisey EE, Taranova O, Pevny LH, Hogan BLM. Multiple dose-dependent roles for Sox2 in the patterning and differentiation of anterior foregut endoderm. *Development.* 2007;134(13):2521–31.
24. Que J, Choi M, Ziel JW, Klingensmith J, Hogan BL. Morphogenesis of the trachea and esophagus: current players and new roles for noggin and Bmps. *Differentiation.* 2006;74(7):422–37.
25. Williamson KA, Hever AM, Rainger J, Rogers RC, Magee A, Fiedler Z, et al. Mutations in SOX2 cause anophthalmia-esophageal-genital (AEG) syndrome. *Hum Mol Genet.* 2006;15(9):1413–22.
26. Liu K, Lin B, Zhao M, Yang X, Chen M, Gao A, Liu F, Que J, Lan X. The multiple roles for Sox2 in stem cell maintenance and tumorigenesis. *Cell Signal.* 2019;25(5):1264–71.
27. Minoo P, Su G, Drum H, Bringas P, Kimura S. Defects in tracheoesophageal and lung morphogenesis in Nkx2.1(-/-) mouse embryos. *Dev Biol.* 2019;209(1):60–71.
28. Mahlapuu M, Enerbäck S, Carlsson P. Haploinsufficiency of the forkhead gene Foxf1, a target for sonic hedgehog signaling, causes lung and foregut malformations. *Development.* 2019;12.
29. Stankiewicz P, Sen P, Bhatt SS, Storer M, Xia Z, Bejjani BA, et al. Genomic and genic deletions of the FOX gene cluster on 16q24.1 and inactivating mutations of FOXF1 cause alveolar capillary dysplasia and other malformations. *Am J Hum Genet.* 2009;84(6):780–91.
30. Kim BM, Buchner G, Miletich I, Sharpe PT, Shivdasani RA. The stomach mesenchymal transcription factor Barx1 specifies gastric epithelial identity through inhibition of transient Wnt signaling. *Dev Cell.* 2005;8(4):611–22.
31. Woo J, Miletich I, Kim BM, Sharpe PT, Shivdasani RA. Barx1-mediated inhibition of Wnt signaling in the mouse thoracic foregut controls tracheo-esophageal septation and epithelial differentiation. *PLoS One.* 2019;6(7):e22493.
32. Harris-Johnson KS, Domyan ET, Vezina CM, Sun X. beta-Catenin promotes respiratory progenitor identity in mouse foregut. *Proc Natl Acad Sci U S A.* 2009;106(38):16287–92.
33. Goss AM, Tian Y, Tsukiyama T, Cohen ED, Zhou D, Lu MM, Yamaguchi TP, Morrisey EE. Wnt2/2b and beta-catenin signaling are necessary and sufficient to specify lung progenitors in the foregut. *Dev Cell.* 2019;17(2):290–8.
34. Li Y, Gordon J, Manley NR, Litingtung Y, Chiang C. Bmp4 is required for tracheal formation: a novel mouse model for tracheal agenesis. *Dev Biol.* 2008;322(1):145–55.
35. Rodriguez P, Da Silva S, Oxburgh L, Wang F, Hogan BL, Que J. BMP signaling in the development of the mouse esophagus and forestomach. *Development.* 2010;137(24):4171–6.
36. Li Y, Litingtung Y, Ten Dijke P, Chiang C. Aberrant Bmp signaling and notochord delamination in the pathogenesis of esophageal atresia. *Dev Dyn.* 2007;236(3):746–54.
37. Domyan ET, Ferretti E, Throckmorton K, Mishina Y, Nicolis SK, Sun X. Signaling through BMP receptors promotes respiratory identity in the foregut via repression of Sox2. *Development.* 2019;1385(5):971–81.
38. Marsh AJ, et al. Interstitial deletion of chromosome 17 (del(17)(q22q23.3)) confirms a link with oesophageal atresia. *J Med Genet.* 2000;37(9):701–4.

39. Motoyama J, Liu J, Mo R, Ding Q, Post M, Hui CC. Essential function of Gli2 and Gli3 in the formation of lung, trachea and oesophagus. *Nat Genet.* 2019;20(1):54–7.
40. Motoyama J, Liu J, Mo R, Ding Q, Post M, Hui CC. Essential function of Gli2 and Gli3 in the formation of lung, trachea and oesophagus. *Nat Genet.* 1998;20(1):54–7.
41. Spilde T, Bhatia A, Ostlie D, Marosky J, Holcomb G III, Snyder C, et al. A role for sonic hedgehog signaling in the pathogenesis of human tracheoesophageal fistula. *J Pediatr Surg.* 2003;38(3):465–8.
42. Rankin SA, Han L, McCracken KW, Kenny AP, Anglin CT, Grigg EA, Crawford CM, Wells JM, Shannon JM, Zorn AM. A retinoic acid-hedgehog cascade coordinates mesoderm-inducing signals and endoderm competence during lung specification. *Cell Rep.* 2016;16(1):66–78.
43. Luo J, Sucov HM, Bader JA, Evans RM, Giguère V. Compound mutants for retinoic acid receptor (RAR) beta and RAR alpha 1 reveal developmental functions for multiple RAR beta isoforms. *Mech Dev.* 2019;55(1):33–44.
44. Trisno SL, Philo KED, McCracken KW, Catá EM, Ruiz-Torres S, Rankin SA, et al. Esophageal organoids from human pluripotent stem cells delineate Sox2 functions during esophageal specification. *Cell Stem Cell.* 2018;23(4):501–15.e7.
45. Glenn IC, Bruns NE, Schomisch SJ, Ponsky TA. Creation of an esophageal atresia animal model using a bifurcated esophagus to maintain digestive tract continuity. *J Laparoendosc Adv Surg Tech A.* 2017;27(10):1079–84.
46. McCracken KW, Wells JM. Mechanisms of embryonic stomach development. *Semin Cell Dev Biol.* 2017;66:36–42.
47. Han ME, Oh SO. Gastric stem cells and gastric cancer stem cells. *Anat Cell Biol.* 2013;46(1):8–18.
48. Chaudhry SR, Bhimji SS. *Anatomy, abdomen and pelvis, stomach.* StatPearls Publishing; 2018.
49. Soybel DI. *Anatomy and physiology of the stomach.* *Surg Clin North Am.* 2005;85(5):875–94.
50. Lloyd KC. Gut hormones in gastric function. *Baillieres Clin Endocrinol Metab.* 1994;8(1):111–36.
51. Schubert ML. Functional anatomy and physiology of gastric secretion. *Curr Opin Gastroenterol.* 2015;31(6):479–85.
52. To T, Wajja A, Wales PW, Langer JC. Population demographic indicators associated with incidence of pyloric stenosis. *Arch Pediatr Adolesc Med.* 2005;159(6):520–5.
53. Sommerfield T, Chalmers J, Youngson G, Heeley C, Fleming M, Thomson G. The changing epidemiology of infantile hypertrophic pyloric stenosis in Scotland. *Arch Dis Child.* 2008;93(12):1007–11.
54. Krogh C, Fischer TK, Skotte L, Biggar RJ, Oyen N, Skythe A, et al. Familial aggregation and heritability of pyloric stenosis. *JAMA.* 2010;303(23):2393–9.
55. Aboagye J, Goldstein SD, Salazar JH, Papandria D, Okoye MT, Al-Omar K, et al. Age at presentation of common pediatric surgical conditions: reexamining dogma. *J Pediatr Surg.* 2014;49(6):995–9.
56. Peters B, Oomen MW, Bakx R, Benninga MA. Advances in infantile hypertrophic pyloric stenosis. *Expert Rev Gastroenterol Hepatol.* 2014;8(5):533–41.
57. Schechter R, Torfs CP, Bateson TF. The epidemiology of infantile hypertrophic pyloric stenosis. *Paediatr Perinat Epidemiol.* 1997;11(4):407–27.
58. Bode VC, McDonald JD, Guenet JL, Simon D. hph-1: a mouse mutant with hereditary hyperphenylalaninemia induced by ethylnitrosourea mutagenesis. *Genetics.* 1988;118(2):299–305.
59. Abel RM, Dore CJ, Bishop AE, Facer P, Polak JM, Spitz L. A histological study of the hph-1 mouse mutant: an animal model of phenylketonuria and infantile hypertrophic pyloric stenosis. *Anat Histol Embryol.* 2004;33(3):125–30.
60. Gutlich M, Ziegler I, Witter K, Hemmens B, Hultner L, McDonald JD, et al. Molecular characterization of HPH-1: a mouse mutant deficient in GTP cyclohydrolase I activity. *Biochem Biophys Res Commun.* 1994;203(3):1675–81.
61. Shimoji M, Hirayama K, Hyland K, Kapatos G. GTP cyclohydrolase I gene expression in the brains of male and female hph-1 mice. *J Neurochem.* 1999;72(2):757–64.
62. Welsh C, Shifrin Y, Pan J, Belik J. Infantile hypertrophic pyloric stenosis (IHPS): a study of its pathophysiology utilizing the newborn hph-1 mouse model of the disease. *Am J Physiol Gastrointest Liver Physiol.* 2014;307(12):G1198–206.
63. Belik J, Shifrin Y, Arning E, Bottiglieri T, Pan J, Daigneault MC, et al. Intestinal microbiota as a tetrahydrobiopterin exogenous source in hph-1 mice. *Sci Rep.* 2017;7:44161.
64. Huang PL, Dawson TM, Brecht DS, Snyder SH, Fishman MC. Targeted disruption of the neuronal nitric oxide synthase gene. *Cell.* 1993;75(7):1273–86.
65. Everett KV, Chioza BA, Georgoula C, Reece A, Capon F, Parker KA, et al. Genome-wide high-density SNP-based linkage analysis of infantile hypertrophic pyloric stenosis identifies loci on chromosomes 11q14-q22 and Xq23. *Am J Hum Genet.* 2008;82(3):756–62.
66. Udager AM, Prakash A, Saenz DA, Schinke M, Moriguchi T, Jay PY, et al. Proper development of the outer longitudinal smooth muscle of the mouse pylorus requires Nkx2-5 and Gata3. *Gastroenterology.* 2014;146(1):157–65.e10.
67. Feenstra B, Geller F, Krogh C, Hollegaard MV, Gørtz S, Boyd HA, et al. Common variants near MBNL1 and NKX2-5 are associated with infantile hypertrophic pyloric stenosis. *Nat Genet.* 2012;44(3):334–7.
68. Feenstra B, Geller F, Carstensen L, Romitti PA, Korberg IB, Bedell B, et al. Plasma lipids, genetic variants near APOA1, and the risk of infantile hypertrophic pyloric stenosis. *JAMA.* 2013;310(7):714–21.

69. Neu J, Walker WA. Necrotizing enterocolitis. *N Engl J Med*. 2011;364(3):255–64.
70. Jilling T, Simon D, Lu J, Meng FJ, Li D, Schy R, et al. The roles of bacteria and TLR4 in rat and murine models of necrotizing enterocolitis. *J Immunol*. 2006;177(5):3273–82.
71. van der Flier LG, Clevers H. Stem cells, self-renewal, and differentiation in the intestinal epithelium. *Annu Rev Physiol*. 2009;71:241–60.
72. Peterson LW, Artis D. Intestinal epithelial cells: regulators of barrier function and immune homeostasis. *Nat Rev Immunol*. 2014;14(3):141–53.
73. Kim YS, Ho SB. Intestinal goblet cells and mucins in health and disease: recent insights and progress. *Curr Gastroenterol Rep*. 2010;12(5):319–30.
74. Chu SH, Walker WA. Developmental changes in the activities of sialyl- and fucosyltransferases in rat small intestine. *Biochim Biophys Acta*. 1986;883(3):496–500.
75. Bergström A, Kristensen MB, Bahl MI, Metzendorf SB, Fink LN, Frøkiaer H, et al. Nature of bacterial colonization influences transcription of mucin genes in mice during the first week of life. *BMC Res Notes*. 2012;5:402.
76. Clevers HC, Bevins CL. Paneth cells: maestros of the small intestinal crypts. *Annu Rev Physiol*. 2013;75:289–311.
77. Deplancke B, Gaskins HR. Microbial modulation of innate defense: goblet cells and the intestinal mucus layer. *Am J Clin Nutr*. 2001;73(6):1131S–41S.
78. Bry L, Falk P, Huttner K, Ouellette A, Midtvedt T, Gordon JI. Paneth cell differentiation in the developing intestine of normal and transgenic mice. *Proc Natl Acad Sci U S A*. 1994;91(22):10335–9.
79. Lin PW, Stoll BJ. Necrotising enterocolitis. *Lancet*. 2006;368(9543):1271–83.
80. Uauy RD, Fanaroff AA, Korones SB, Phillips EA, Phillips JB, Wright LL. Necrotizing enterocolitis in very low birth weight infants: biodemographic and clinical correlates. National Institute of Child Health and Human Development Neonatal Research Network. *J Pediatr*. 1991;119(4):630–8.
81. Stoll BJ, Hansen NI, Bell EF, Walsh MC, Carlo WA, Shankaran S, et al. Trends in care practices, morbidity, and mortality of extremely preterm neonates, 1993–2012. *JAMA*. 2015;314(10):1039–51.
82. Papillon S, Castle SL, Gayer CP, Ford HR. Necrotizing enterocolitis: contemporary management and outcomes. *Adv Pediatr*. 2013;60(1):263–79.
83. Leaphart CL, Cavallo J, Gribar SC, Cetin S, Li J, Branca MF, et al. A critical role for TLR4 in the pathogenesis of necrotizing enterocolitis by modulating intestinal injury and repair. *J Immunol*. 2007;179(7):4808–20.
84. White JR, Gong H, Pope B, Schlievert P, McElroy SJ. Paneth-cell-disruption-induced necrotizing enterocolitis in mice requires live bacteria and occurs independently of TLR4 signaling. *Dis Model Mech*. 2017;10(6):727–36.
85. Wu RY, Li B, Koike Y, Määttänen P, Miyake H, Cadete M, et al. Human milk oligosaccharides increase mucin expression in experimental necrotizing enterocolitis. *Mol Nutr Food Res*. 2019;63(3):e1800658.
86. Sturm R, Staneck JL, Stauffer LR, Neblett WW. Neonatal necrotizing enterocolitis associated with penicillin-resistant, toxigenic *Clostridium butyricum*. *Pediatrics*. 1980;66(6):928–31.
87. Coggins SA, Wynn JL, Weitkamp JH. Infectious causes of necrotizing enterocolitis. *Clin Perinatol*. 2015;42(1):133–54, ix.
88. Tanner SM, Berryhill TF, Ellenburg JL, Jilling T, Cleveland DS, Lorenz RG, et al. Pathogenesis of necrotizing enterocolitis: modeling the innate immune response. *Am J Pathol*. 2015;185(1):4–16.
89. Sodhi C, Richardson W, Gribar S, Hackam DJ. The development of animal models for the study of necrotizing enterocolitis. *Dis Model Mech*. 2008;1(2-3):94–8.
90. Barlow B, Santulli TV, Heird WC, Pitt J, Blanc WA, Schullinger JN. An experimental study of acute neonatal enterocolitis—the importance of breast milk. *J Pediatr Surg*. 1974;9(5):587–95.
91. Barlow B, Santulli TV. Importance of multiple episodes of hypoxia or cold stress on the development of enterocolitis in an animal model. *Surgery*. 1975;77(5):687–90.
92. Caplan MS, Hedlund E, Adler L, Hsueh W. Role of asphyxia and feeding in a neonatal rat model of necrotizing enterocolitis. *Pediatr Pathol*. 1994;14(6):1017–28.
93. Gonzalez-Crussi F, Hsueh W. Experimental model of ischemic bowel necrosis. The role of platelet-activating factor and endotoxin. *Am J Pathol*. 1983;112(1):127–35.
94. Krasna IH, Howell C, Vega A, Ziegler M, Koop CE. A mouse model for the study of necrotizing enterocolitis. *J Pediatr Surg*. 1986;21(1):26–9.
95. Ginzel M, Feng X, Kuebler JF, Klemann C, Yu Y, von Wasielewski R, et al. Dextran sodium sulfate (DSS) induces necrotizing enterocolitis-like lesions in neonatal mice. *PLoS One*. 2017;12(8):e0182732.
96. MohanKumar K, Kaza N, Jagadeeswaran R, Garzon SA, Bansal A, Kurundkar AR, et al. Gut mucosal injury in neonates is marked by macrophage infiltration in contrast to pleomorphic infiltrates in adult: evidence from an animal model. *Am J Physiol Gastrointest Liver Physiol*. 2012;303(1):G93–102.
97. Sawada M, Takahashi K, Sawada S, Midorikawa O. Selective killing of Paneth cells by intravenous administration of dithizone in rats. *Int J Exp Pathol*. 1991;72(4):407–21.
98. Zhang C, Sherman MP, Prince LS, Bader D, Weitkamp JH, Slaughter JC, et al. Paneth cell ablation in the presence of *Klebsiella pneumoniae* induces necrotizing enterocolitis (NEC)-like injury

- in the small intestine of immature mice. *Dis Model Mech.* 2012;5(4):522–32.
99. Bozeman AP, Dassinger MS, Birusingh RJ, Burford JM, Smith SD. An animal model of necrotizing enterocolitis (NEC) in preterm rabbits. *Fetal Pediatr Pathol.* 2013;32(2):113–22.
 100. Waligora-Dupriet AJ, Dugay A, Auzeil N, Huerre M, Butel MJ. Evidence for clostridial implication in necrotizing enterocolitis through bacterial fermentation in a gnotobiotic quail model. *Pediatr Res.* 2005;58(4):629–35.
 101. Cassutto BH, Misra HP, Pfeiffer CJ. Intestinal post-ischemic reperfusion injury: studies with neonatal necrotizing enterocolitis. *Acta Physiol Hung.* 1989;73(2–3):363–9.
 102. Waligora-Dupriet AJ, Dugay A, Auzeil N, Nicolis I, Rabot S, Huerre MR, et al. Short-chain fatty acids and polyamines in the pathogenesis of necrotizing enterocolitis: kinetics aspects in gnotobiotic quails. *Anaerobe.* 2009;15(4):138–44.
 103. Butel MJ, Roland N, Hibert A, Popot F, Favre A, Tessedre AC, et al. Clostridial pathogenicity in experimental necrotizing enterocolitis in gnotobiotic quails and protective role of bifidobacteria. *J Med Microbiol.* 1998;47(5):391–9.
 104. Namachivayam K, Blanco CL, MohanKumar K, Jagadeeswaran R, Vasquez M, McGill-Vargas L, et al. Smad7 inhibits autocrine expression of TGF- β 2 in intestinal epithelial cells in baboon necrotizing enterocolitis. *Am J Physiol Gastrointest Liver Physiol.* 2013;304(2):G167–80.
 105. Maheshwari A, Kelly DR, Nicola T, Ambalavanan N, Jain SK, Murphy-Ullrich J, et al. TGF- β 2 suppresses macrophage cytokine production and mucosal inflammatory responses in the developing intestine. *Gastroenterology.* 2011;140(1):242–53.
 106. Scheer N, Roland Wolf C. Xenobiotic receptor humanized mice and their utility. *Drug Metab Rev.* 2013;45(1):110–21.
 107. Hajjar AM, Ernst RK, Fortuno ES, Brasfield AS, Yam CS, Newlon LA, et al. Humanized TLR4/MD-2 mice reveal LPS recognition differentially impacts susceptibility to *Yersinia pestis* and *Salmonella enterica*. *PLoS Pathog.* 2012;8(10):e1002963.
 108. Azzouz LL, Sharma S. Physiology, large intestine. *StatPearls Publishing*; 2018.
 109. Kenny SE, Tam PK, Garcia-Barcelo M. Hirschsprung's disease. *Semin Pediatr Surg.* 2010;19(3):194–200.
 110. Heuckeroth RO. Hirschsprung disease—integrating basic science and clinical medicine to improve outcomes. *Nat Rev Gastroenterol Hepatol.* 2018;15(3):152–67.
 111. Vieten D, Spicer R. Enterocolitis complicating Hirschsprung's disease. *Semin Pediatr Surg.* 2004;13(4):263–72.
 112. Bondurand N, Southard-Smith EM. Mouse models of Hirschsprung disease and other developmental disorders of the enteric nervous system: old and new players. *Dev Biol.* 2016;417(2):139–57.
 113. Ibanez CF. Structure and physiology of the RET receptor tyrosine kinase. *Cold Spring Harb Perspect Biol.* 2013;5(2).
 114. Burzynski GM, Nolte IM, Bronda A, Bos KK, Osinga J, Twigt B, et al. Identifying candidate Hirschsprung disease-associated RET variants. *Am J Hum Genet.* 2005;76(5):850–8.
 115. de Graaff E, Srinivas S, Kilkenny C, D'Agati V, Mankoo BS, Costantini F, et al. Differential activities of the RET tyrosine kinase receptor isoforms during mammalian embryogenesis. *Genes Dev.* 2001;15(18):2433–44.
 116. Gianino S, Grider JR, Cresswell J, Enomoto H, Heuckeroth RO. GDNF availability determines enteric neuron number by controlling precursor proliferation. *Development.* 2003;130(10):2187–98.
 117. Schuchardt A, D'Agati V, Larsson-Blomberg L, Costantini F, Pachnis V. Defects in the kidney and enteric nervous system of mice lacking the tyrosine kinase receptor Ret. *Nature.* 1994;367(6461):380–3.
 118. Uesaka T, Nagashimada M, Yonemura S, Enomoto H. Diminished Ret expression compromises neuronal survival in the colon and causes intestinal aganglionosis in mice. *J Clin Invest.* 2008;118(5):1890–8.
 119. Jain S, Naughton CK, Yang M, Strickland A, Vij K, Encinas M, et al. Mice expressing a dominant-negative Ret mutation phenocopy human Hirschsprung disease and delineate a direct role of Ret in spermatogenesis. *Development.* 2004;131(21):5503–13.
 120. Carniti C, Belluco S, Riccardi E, Cranston AN, Mondellini P, Ponder BA, et al. The RetC620R mutation affects renal and enteric development in a mouse model of Hirschsprung's disease. *Am J Pathol.* 2006;168(4):1262–75.
 121. Asai N, Fukuda T, Wu Z, Enomoto A, Pachnis V, Takahashi M, et al. Targeted mutation of serine 697 in the Ret tyrosine kinase causes migration defect of enteric neural crest cells. *Development.* 2006;133(22):4507–16.
 122. Ibiza S, García-Cassani B, Ribeiro H, Carvalho T, Almeida L, Marques R, et al. Glial-cell-derived neuroregulators control type 3 innate lymphoid cells and gut defence. *Nature.* 2016;535(7612):440.
 123. Baynash AG, Hosoda K, Gaiad A, Richardson JA, Emoto N, Hammer RE, et al. Interaction of endothelin-3 with endothelin-B receptor is essential for development of epidermal melanocytes and enteric neurons. *Cell.* 1994;79(7):1277–85.
 124. Coventry S, Yost C, Palmiter RD, Kapur RP. Migration of ganglion cell precursors in the ileoceca of normal and lethal spotted embryos, a murine model for Hirschsprung disease. *Lab Invest.* 1994;71(1):82–93.
 125. McCallion AS, Stames E, Conlon RA, Chakravarti A. Phenotype variation in two-locus mouse models of Hirschsprung disease: tissue-specific interaction between Ret and Ednrb. *Proc Natl Acad Sci U S A.* 2003;100(4):1826–31.

126. Fujimoto T. Natural history and pathophysiology of enterocolitis in the piebald lethal mouse model of Hirschsprung's disease. *J Pediatr Surg.* 1988;23(3):237–42.
127. Hosoda K, Hammer RE, Richardson JA, Baynash AG, Cheung JC, Giaid A, et al. Targeted and natural (piebald-lethal) mutations of endothelin-B receptor gene produce megacolon associated with spotted coat color in mice. *Cell.* 1994;79(7):1267–76.
128. Nagy N, Goldstein AM. Endothelin-3 regulates neural crest cell proliferation and differentiation in the hindgut enteric nervous system. *Dev Biol.* 2006;293(1):203–17.
129. Nagy N, Mwiszerwa O, Yaniv K, Carmel L, Pieretti-Vanmarcke R, Weinstein BM, et al. Endothelial cells promote migration and proliferation of enteric neural crest cells via beta1 integrin signaling. *Dev Biol.* 2009;330(2):263–72.
130. Fattahi F, Steinbeck JA, Kriks S, Tchieu J, Zimmer B, Kishinevsky S, et al. Deriving human ENS lineages for cell therapy and drug discovery in Hirschsprung disease. *Nature.* 2016;531(7592):105.
131. Lang D, Epstein JA. Sox10 and Pax3 physically interact to mediate activation of a conserved c-RET enhancer. *Hum Mol Genet.* 2003;12(8):937–45.
132. Sánchez-Mejías A, Watanabe Y, Fernández RM, López-Alonso M, Antiñolo G, Bondurand N, et al. Involvement of SOX10 in the pathogenesis of Hirschsprung disease: report of a truncating mutation in an isolated patient. *J Mol Med (Berl).* 2010;88(5):507–14.
133. Paratore C, Eichenberger C, Suter U, Sommer L. Sox10 haploinsufficiency affects maintenance of progenitor cells in a mouse model of Hirschsprung disease. *Hum Mol Genet.* 2002;11(24):3075–85.
134. Corpening JC, Deal KK, Cantrell VA, Skelton SB, Buehler DP, Southard-Smith EM. Isolation and live imaging of enteric progenitors based on Sox10-Histone2BVenus transgene expression. *Genesis.* 2011;49(7):599–618.
135. Watanabe Y, Broders-Bondon F, Baral V, Paul-Gilloteaux P, Pingault V, Dufour S, et al. Sox10 and Itgb1 interaction in enteric neural crest cell migration. *Dev Biol.* 2013;379(1):92–106.
136. Lake JI, Tusheva OA, Graham BL, Heuckeroth RO. Hirschsprung-like disease is exacerbated by reduced de novo GMP synthesis. *J Clin Invest.* 2013;123(11):4875–87.
137. Lake JI, Avetisyan M, Zimmermann AG, Heuckeroth RO. Neural crest requires Impdh2 for development of the enteric nervous system, great vessels, and craniofacial skeleton. *Dev Biol.* 2016;409(1):152–65.
138. Schill EM, Lake JI, Tusheva OA, Nagy N, Bery SK, Foster L, et al. Ibuprofen slows migration and inhibits bowel colonization by enteric nervous system precursors in zebrafish, chick and mouse. *Dev Biol.* 2016;409(2):473–88.
139. Gasc JM, Clemessy M, Corvol P, Kempf H. A chicken model of pharmacologically-induced Hirschsprung disease reveals an unexpected role of glucocorticoids in enteric aganglionosis. *Biol Open.* 2015;4(5):666–71.
140. Zani A, Zani-Ruttenstock E, Peyvandi F, Lee C, Li B, Pierro A. A spectrum of intestinal injury models in neonatal mice. *Pediatr Surg Int.* 2016;32(1):65–70.



Mouse Models of Congenital Kidney Anomalies

5

Satu Kuure and Hannu Sariola

5.1 Overview

Congenital anomalies of the kidney and urinary tract (CAKUT) are common birth defects, which cause the majority of chronic kidney diseases in children. CAKUT covers a wide range of malformations that derive from deficiencies in embryonic kidney and lower urinary tract development, including renal aplasia, hypodysplasia, hypoplasia, ectopia, and different forms of ureter abnormalities. The majority of the genetic causes of CAKUT remain unknown. Research on mutant mice has identified multiple genes that critically regulate renal differentiation. The data generated from this research have served as an excellent resource to identify the genetic bases of human

kidney defects and have led to significantly improved diagnostics. Furthermore, genetic data from human CAKUT studies have also revealed novel genes regulating kidney differentiation.

5.2 Introduction

Congenital anomalies of the kidney and lower urinary tract (CAKUT) are caused by inborn defects in the differentiation of the organs, including the kidneys as well as the urine excretion organs. In order to understand the potential genetic, molecular, and cellular bases of these malformations, it is essential to comprehend how these organs normally develop.

A large part of our understanding of mammalian kidney formation comes from the early inductive studies carried out by Clifford Grobstein and Lauri Saxén. It rapidly became evident that the development of the kidney is controlled through reciprocal inductive tissue interactions [1–3]. Since then, we have learned that the interacting tissues in the kidney rudiment are the ureteric bud (UB) epithelium, derived from the Wolffian duct (WD, also known as nephric duct), the metanephric mesenchyme (MM, also called renal mesenchyme) in close proximity to the UB, and the stromal cells surrounding the MM. The inductive interplay between these tissues results in developmental changes in the nascent tissue, which reciprocally affects the signal-sending tissue.

S. Kuure (✉)
GM-Unit, Helsinki Institute of Life Science,
University of Helsinki, Helsinki, Finland

Stem Cells and Metabolism Research Program,
Faculty of Medicine, University of Helsinki,
Helsinki, Finland

Medicum, Faculty of Medicine, University of
Helsinki, Helsinki, Finland
e-mail: satu.kuure@helsinki.fi

H. Sariola
Medicum, Faculty of Medicine, University of
Helsinki, Helsinki, Finland

Paediatric Pathology, HUSLAB, Helsinki University
Central Hospital, Helsinki, Finland
e-mail: hannu.sariola@helsinki.fi

These interactions are largely mediated by direct cell-cell contacts, secreted paracrine morphogens, and other as-yet-unknown mechanisms.

5.3 Renal Differentiation

5.3.1 Origin of the Kidneys

The kidneys originate from the intermediate mesoderm (IM). Recent advances in understanding the early specification of kidney precursors revealed that IM is temporally regionalized, and the interacting tissues of the developing kidney are derived from its distinct subpopulations [4, 5]. The most anterior IM is the first to form and gives rise to the WD and its derivatives, whereas the posterior IM differentiates into the MM and stroma. Initially, the IM undergoes mesenchyme-to-epithelium transition (MET) to generate the WD, which begins to grow posteriorly simultaneously to MM specification in the leading front of the WD.

Mammalian kidney differentiation involves the formation of three sets of sequentially formed distinct kidneys [6, 7]. During the posterior growth of the WD, the first kidneys to form are the pronephroi, which are transient organs with no known function in mammals (Fig. 5.1a). The next kidneys to develop are the mesonephroi. Each mesonephros in humans contains a total of 34 mesonephric tubules all connected to the WD and is functional during the early phases of fetal life (Fig. 5.1b). They secrete urine and form the aorta-gonad-mesonephros region, which hosts hematopoietic stem cells [8]. In mouse, where the mesonephroi are nonfunctional organs, there are two distinct sets of mesonephric tubules of which the 4–6 cranial pairs are connected to the WD while the majority of the caudal tubules remain without direct connection to the WD [9]. The last kidneys are the metanephroi, the permanent kidneys, which start functioning after mid-gestation and play an important role in fetal health by excreting primary urine to become the amniotic fluid (Fig. 5.1c). In fact, one phenotypic change in newborns with defective kidney function is the so-called Potter's sequence (oligohydramnion

sequence). Here, a reduced amount of amniotic fluid caused by minimal urine production gives rise to the characteristic fetal features including flattened nose and abnormalities around the eyes and ears, clubfeet, and small lungs (pulmonary hypoplasia) resulting in respiratory insufficiency.

5.3.2 Development of the Permanent Kidney (Metanephros)

The development of the permanent kidney, the metanephros, begins at approximately embryonic day 30–32 (E30–32) in humans and at E10.5 in mice when the caudal end of the WD has made contact with the cloaca, the future bladder, and bulges towards the medial-dorsally located MM [10]. The initial bulge then rapidly elongates and invades the MM to form the UB. The bud at this stage is already divided into the tip and trunk regions, which bear divergent molecular signatures and show different cellular behaviors (Fig. 5.2). The UB tip, which is intimately surrounded by MM, is highly proliferative, includes actively moving individual cells, and is surrounded by discontinuous and scarce extracellular matrix. The UB trunk, on the other hand, shows a significantly lower rate of cell division as its elongation is dominated by convergent extensions. It also begins to build up distinct, continuous extracellular matrix characteristic of the collecting ducts and ureter.

5.3.2.1 Branching Morphogenesis

The UB tip is surrounded by the MM, which is more tightly packed near the UB epithelium than the more distally located stromal mesenchyme in the outermost layer of the developing kidney (Fig. 5.2). After its formation, the UB starts dichotomous branching morphogenesis, instructed by signals derived from the MM [11]. First, an existing tip balloons to form an ampulla, which then bifurcates into two new tips that thereafter elongate to generate new trunks [12, 13]. Genetic labeling experiments together with live imaging of cultured kidneys at the single-cell level have revealed that some tip cells are maintained within

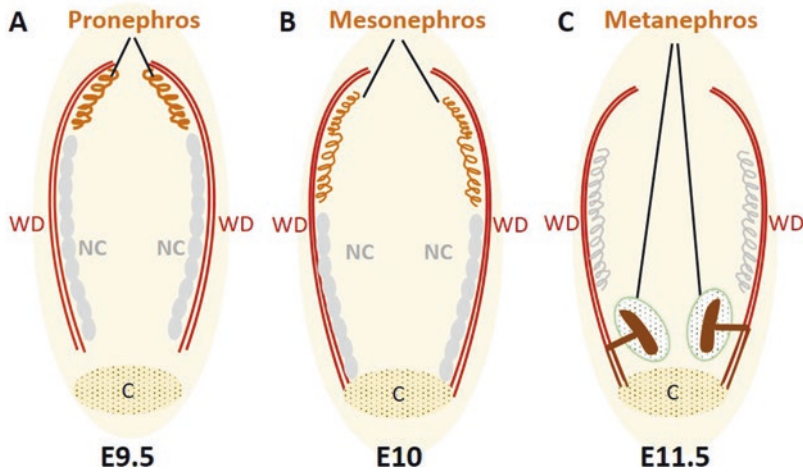


Fig. 5.1 Illustration of the three developmental stages of kidney morphogenesis. (a) Pronephros, the first kidney to form, is present in the fetus before the Wolffian duct (WD) makes the connection to the cloaca (C), approximately at embryonic day 9.5 (E9.5). The nephrogenic cord (NC) is formed together with the WD and is depicted in light gray. (b) Mesonephros development follows the pronephros

and takes place concomitantly with WD fusion to the cloaca (C). (c) The last kidney to form is the metanephros or permanent kidney, which begins to develop when the NC has differentiated into metanephric mesenchyme (light green) and induces the WD epithelium to bulge and form the ureteric bud (brown)

the tips while others are left behind in trunk regions [14–17]. This has led to a relatively well-proven model where the UB tips host progenitor cells for the entire collecting duct, composed of intercalated and principal cells. Currently, the molecular regulation and cell-specific gene signatures to distinguish progenitors from the cells destined for differentiation are missing, but improvements in single-cell transcriptomic techniques together with the possibility to spatially map multiple gene expressions simultaneously are expected to shed light on this currently stochastic-seeming process [18, 19]. Finally, it has been estimated that the mouse UB undergoes some 11–12 rounds of repeated branching events to finally generate the shape of the organ with collecting ductal system of an appropriate complexity [20]. In addition to branching, the collecting ducts undergo complex reorganization at mid-gestation to form the pelvis and distinct medulla-cortex compartmentalization [21].

5.3.2.2 Nephrogenesis

Nephron differentiation begins simultaneously at the start of branching morphogenesis (Fig. 5.2). Nephrons are derived from the subpopulation of

metanephric mesenchyme called cap mesenchyme, which is defined by its tight and oriented arrangement of mesenchymal cells around UB tips [13, 22–24]. These nephron progenitors both self-renew to maintain the cap mesenchyme until cessation of nephrogenesis and differentiate through MET into specialized epithelial cells of all nephron segments [25–27]. Nephron progenitors (NPs) are maintained in the cap mesenchyme surrounding each newly formed UB tip, while their differentiation takes place in the nascent mesenchyme of the same tip. The molecular regulation of NP specification and maintenance involves both intrinsic (cell autonomous) and UB-derived paracrine pathways, which merge to balance between self-renewal and differentiation. Nephrogenesis begins by the compaction of NP cells into the armpits of the T-shaped UB, after which this so-called pretubular aggregate epithelializes via the characteristic morphological stages of the renal vesicle and comma-shaped and S-shaped bodies to form a secretory nephron (Fig. 5.2). Thus, the final nephron number in each individual closely reflects the extent of UB branching [3, 20]. Each nephron segment, namely the podocytes of glomeruli, Bowman’s capsule,

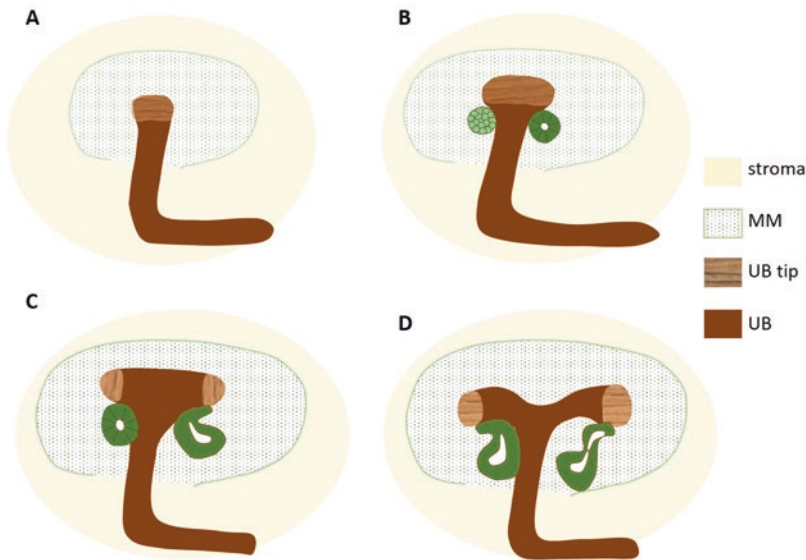


Fig. 5.2 Schematic view of metanephros development. (a) The ureteric bud (UB) is divided into the trunk (dark brown) and tip (light brown) regions, which are already defined at the initial bud stage. The UB is surrounded by the metanephric mesenchyme (MM) while spindle cell stroma (S) encircles the MM. (b) The UB branching begins with the formation of an ampulla at the tip of the UB. Simultaneously, the UB induces the MM to condense and form a pretubular aggregate (left of the UB tip, light green cells), which begins epithelialization into the nephron by forming the renal vesicle (right of the UB tip, green vesicle). (c) The UB

ampulla extends to develop two new tips while the renal vesicle further differentiates into comma-shaped body (right of the UB). (d) UB tips continue to branch out with concurrent further connection of the comma-shaped body to the UB tips. Nephrogenesis continues by differentiation of the comma-shaped body into the S-shaped body (right of the UB). These events are reiterated until the end of branching morphogenesis when the final nephron differentiation burst uses up all remaining nephron progenitors in the metanephric mesenchyme, and in this way, each kidney attains its final nephron count

the proximal tubules, the loop of Henle, the distal tubules, and the connecting piece joining the nephron to the collecting duct system, derives from the same NP pool. The causes of NP exhaustion and the end of nephrogenesis at late gestation in humans (week 36) or at early postnatal days in mice (P3) [28, 29] are not known.

5.4 Mouse as a Mannequin of Renal Disease in Man: Inborn Errors and Effective Dissimilarities

Different animals have been used to aid the understanding of the mechanisms guiding differentiation since the early days of developmental biology studies. Modern research largely relies on rodents as mammalian models, and due to the development of genetic manipulation techniques

(see below) specific for house mouse, *Mus musculus*, it has become the predominant animal model in kidney development.

The mouse as an experimental animal comes in various different flavors. The fact that over 450 inbred mouse strains exist translates into a wealth of different genotypes and phenotypes for those utilizing the mouse as a model of diseases in human [30]. Moreover, laboratory mice are also maintained as outbred strains, expanding the complexity even further. In reality, researchers worldwide focus on using many of the same inbred strains, which are employed in experiments with genetically modified mouse models (see below). For the purpose of renal diseases, it is important to remember that both gender and genetic variations in the inbred strains very much influence, e.g., predisposition to kidney damage. In other words, some strains, like C57BL/6, are rather resistant to kidney damage and develop

proteinuria, glomerulosclerosis, and/or hypertension only when highly damaged [31]. This likely derives from the different accumulation of genetic aberrations between the strains as, e.g., C57BL/6 only has one functional gene for renin, resulting in a decreased renin-angiotensin-aldosterone system as compared to, e.g., 129/Sv substrains [32]. Moreover, female mice in general better tolerate ischemic renal damage and chemically induced diabetic nephropathy than male mice.

5.4.1 Spontaneous Mouse Models

Mice with inborn errors in kidney differentiation resulting in renal aplasia [33], lupus nephritis, polycystic kidney disease, interstitial disease, hypertension, and diabetes-induced nephropathy have greatly facilitated our understanding of the pathogenesis and mechanisms of renal diseases [34]. Classical mutations such as *Danforth's short tail (Sd)* and *limb deformity (ld)* cause renal aplasia due to failure to induce UB formation and growth [35]. The first model of autosomal polycystic kidney disease, the *cpk/cpk* mouse, represents an aggressive, early-onset renal disease, especially in the DBA/2J strain [36]. Similarly, *bpk/bpk* and *pcy/pcy* mice show inherited proximal tubule cystogenesis, which eventually spreads into all nephron segments. Though great models for diabetic nephropathy are still to come, NOD mice have been widely used for type I diabetes-associated nephropathy, while the corresponding model for type II diabetic nephropathy are the *db/db* mice [37].

5.4.2 Genetically Modified Mouse Models

The mouse became the most popular species in genetic engineering due to the early availability of its genome sequence, the possibility to derive and successfully culture its embryonic stem (ES) cells, and its relative similarity to human physiology. Previously, the possibilities to manipulate mammalian genomes were limited to chemically

induced random mutagenesis (forward genetic approach such as ENU mutagenesis), radiation, and nontargeted integration of foreign DNA (transgenesis). Though rather imperfect, these strategies have provided not only the basis for the more modern techniques currently in use but also advanced our understanding of many complex biological processes. Due to the current predominance of targeted genome editing approaches (reverse genetics), these techniques, which are utilized to produce point mutations, large deletions, and conventional and conditional knockout mouse lines, are shortly described below.

5.4.2.1 Targeting in ES Cells

Genetic engineering of mouse ES cells in combination with the techniques allowing aggregation of mutated and wild-type ES cells to generate chimeric embryos has been the basis for the generation of gene knockouts and conditional alleles for the last two decades [38]. The key requirement is that the locus of the gene of interest is known and cloned, as this is utilized to build a targeting vector, which includes not only the disrupted gene of interest, but also 5' and 3' sequences around it. The surrounding sequences, known as homology arms, anneal to the corresponding region of the genome in ES cells and allow replacement of the endogenous gene through homologous recombination.

Classically, a neomycin resistance gene in the targeting vector is used to inactivate the gene of interest. Alternatively, the generation of point mutations and conditional alleles requires insertion of a desired genetic alteration, e.g., the nucleotide change or loxP sequences, to the targeting vector [39]. As homologous recombination is a rare event in any cell, neomycin resistance and thymidine kinase genes in the targeting vector are used to identify those ES cells where the endogenous gene is replaced with the targeted gene [40]. After confirming the successful targeting by sequencing, the ES cells are introduced into wild-type morulae or blastocysts by aggregation or injections, respectively. Host embryos typically originate from a different mouse strain than the targeted ES cells, allowing identification of the genetically engineered pups

by their chimeric coat color. The final requirement for the establishment of a new genetically engineered mouse line is that the chimeric founder transmits the desired gene editing to its offspring. In general, the traditional targeting strategy is a lengthy and expensive procedure where the generation of gene-modified mouse line typically takes 18–24 months.

5.4.2.2 CRISPR/Cas9-Mediated Targeting

The revolution of genetic engineering began with the development of programmable, highly specific DNA nucleases of which the first ones, zinc finger nucleases (ZFN) and transcription activator-like effector nucleases (TALEN), were based on modifiable DNA domains that guide the FokI nuclease to a specific genomic location [41]. Next-generation genome editing now utilizes short RNA guides to specifically locate CAS9 endonuclease (originating from the bacterial immune system) to the desired site in the genome. All these editing systems are ideologically similar as they are based on nuclease function, which cuts DNA to generate double-strand breaks that activate the endogenous repair systems in any given cell type [42]. The predominant repair system is nonhomologous end joining, which is error-prone and results in inactivation of the gene of interest by introducing small nucleotide insertions and deletions that disrupt the normal reading frame. In animal model generation, this is achieved through injection of RNA guides together with CAS9 (mRNA or protein) into the fertilized oocyte. Injected zygotes then develop into conventional knockout founders, each with a slightly different disruption in the gene of interest. The CRISPR/CAS9-based gene inactivation is applicable not only in mice but also in many other species. It has proven to be an efficient and inexpensive method that is an extremely attractive and useful tool for genome editing in the development of different disease models.

Opposed to the ease of generating knockouts with CRISPR/CAS9, targeted insertion of additional genetic material into the host genome is more difficult. Targeted insertion is necessary

when the goal is to faithfully mimic human diseases, like those caused by congenital kidney defects as the result of point mutations or short deletions. Similar to ES cell targeting, this requires the engagement of homologous recombination, which is inefficient due to its uncommon occurrence. Additional challenges in the generation of knock-in models come from the fact that CRISPR/CAS9 is particularly efficient in genome editing through nonhomologous end joining, which is activated simultaneously to homologous recombination. This unfortunately results in additional, undesired editing near the point mutation containing template DNA. Careful design, use of control animals, and genotyping of the founder animals as well as F1 offspring by sequencing are needed to ascertain that possible phenotypic alterations derive from the anticipated edit and not from the extra editing in an undesired locus [43].

5.5 Common Renal Malformations in Human Fetal Autopsies and Their Analogous Mouse Models

5.5.1 Oligohydramnion Sequence

The founder of pediatric pathology in the USA, Edith Potter (1901–1993), first described the oligohydramnion sequence. It is caused by the lack of amniotic fluid, a condition called oligohydramnion. Amniotic fluid is predominantly urine, and oligohydramnion is thus caused by the lack of the kidneys (bilateral renal aplasia), urethral valve (thin membrane blocking the urethra) preventing urination, or premature rupture of the fetal membranes (PROM). Placental insufficiency, for instance, in pre-eclampsia, can also cause oligohydramnion. Amniotic fluid contains a number of growth factors, and as the fetus inhales amniotic fluid, the factors promote the growth and maturation of the lungs. Oligohydramnion sequence is characterized by typical external features and small lungs (pulmonary hypoplasia), which can cause postnatal respiratory insufficiency and high neonatal mortality rates.

5.5.2 Aplasia and Hypoplasia

Lack of one or both kidneys is referred to as uni- or bilateral renal aplasia. If the kidneys are smaller than expected for the developmental or newborn stage, they are hypoplastic. The genetic causes of renal aplasia have been only partially resolved, but a common environmental cause for renal hypoplasia is the lack of vitamin A [44, 45]. The biologically inactive vitamin A is locally activated to become retinoic acid by the retinaldehyde dehydrogenase 2 enzyme (RALDH2, also known as ALDH2) synthesized by the renal interstitial or stromal cells [46].

5.5.2.1 Mouse Models of Renal Aplasia

Analysis of spontaneous and knockout mouse models has revealed several causes of renal aplasia and thus has helped understanding of the mechanisms leading to congenital absence of kidneys in humans [33]. Among the first aplasia models are *Danforth's short tail (sd)* spontaneous mouse mutant, which is caused by disruption of *pancreas-specific transcription factor 1a (Ptf1a)*, with transposon insertion [47], and *formin* mutation resulting in *limb deformity (ld)* model [48]. Genetic inactivation of a single mouse gene, such as the transcription factor *Pax2* [49], *Osr1* [50, 51], *Gata1* [52], *Lhx1* [53, 54], *Wt1* [55], *Hox11* [56, 57], *Eya1* [58], *Six1* [59], or *Sall1* [60], arrests renal differentiation due to defects in early specification of intermediate mesoderm (*Osr1*), formation of WD (*Gata3* and *Lhx1*), or induction of the kidney itself. The lack of kidney induction is typically caused by either the failure to induce primary UB formation (*Eya1*, *Hox11*, *Pax2*, *Six1*, *Sall1*) leading to subsequent apoptosis of the MM or the inability of the MM to survive (*Wt1*).

In addition to transcription factors, deletion of the specific components in key growth factor signaling pathways causes renal aplasia [25]. Characterization of mouse mutants lacking genes for glial-cell-line-derived neurotrophic factor (*Gdnf* [61–63]) or its receptor complex (*Ret* [64, 65] and co-receptor *Gfral* [66, 67]) revealed renal aplasia due to impaired UB formation [68]. Also, simultaneous deletion of *Etv4* and *Etv5*, the first identified GDNF/RET-dependent transcription

factors, causes renal aplasia [16, 69]. GDNF belongs to transforming growth factor beta (TGF β) superfamily, and unlike the TGF β genes themselves, another TGF β superfamily member, growth/differentiation factor 11 (GDF11), is necessary for normal UB formation [70–73]. Deletion of *Gdf11* results in a spectrum of renal abnormalities with bilateral aplasia being the most frequent [70]. Interestingly, several genetic studies in mice imply that the level of bone morphogenetic protein (BMP) signaling, also belonging to the TGF β superfamily, is essential for normal UB outgrowth and early organogenesis of the kidney. Not only is too little or missing signaling harmful, but enhanced levels also result in abnormalities, as shown by renal aplasia in mice with knockout of BMP antagonist *Gremlin1* [74–76].

The fibroblast growth factor (FGF) cascade works parallel to GDNF/RET signaling as shown by the conditional deletion of FGF receptors 1 and 2 with *Pax3Cre* [77]. The UB forms in the absence of the FGF receptors, but its subsequent elongation and branching are arrested leading to renal aplasia. Many FGF ligands are expressed in the developing kidney, suggesting redundancy in their signaling. Accordingly, inactivation of one FGF receptor, but not a single FGF ligand, causes renal aplasia, supporting the essential functional importance of FGF signaling for kidney differentiation [78]. Furthermore, simultaneous disruption of *Fgf9* and *Fgf20* results in renal aplasia, likely due to deficiency in UB formation, although, this is not experimentally confirmed [79].

Inactivation of wingless-type MMTV integration site family (WNT) signaling by deleting *Wnt9b* results in renal aplasia in mouse [80]. Unlike many other aplasia models with early UB arrest, the loss of *Wnt9b* primarily affects the MM, which fails to maintain nephron progenitors and induce them for differentiation [81, 82]. Canonical WNT signaling is mediated by inactivation of glycogen synthase 3 (GSK3) and causes stabilization of cytoplasmic β -catenin, which leads to activation of TCF/LEF1 transcription factors. Numerous experiments have demonstrated that canonical WNT signaling is essential for UB branching, collecting duct morphogenesis, and

nephron induction as well as differentiation [83] (for details, see the section on Mouse models of hypoplasia). Of note, simultaneous deletion of *Gsk3a* and *Gsk3b* specifically in the collecting duct results in renal aplasia (ASN Kidney Week 2011, <https://www.asn-online.org/abstracts/>), unlike similar deletion of β -catenin, which usually causes hypodysplasia [84].

Genes encoding essential structural proteins, such as those related to cell adhesion and extracellular matrix, are also vital for early kidney specification and induction. A good example is integrin-linked kinase (ILK), which binds the cytoplasmic domains of β -integrin to regulate actin dynamics and, when deleted, results in renal aplasia [85]. However, a single gene deletion of a structural protein often appears without a phenotype, probably because of compensation or redundancy by another family member, or results in an incompletely penetrant renal aplasia [86]. This is exemplified by inactivation of the Fraser syndrome gene, Fraser extracellular matrix complex subunit 1 (*Fras1*) [87, 88], integrin alpha 8 (*Itga8*) [89], and nidogens 1 and 2 (simultaneously) [90], which all cause incompletely penetrant kidney development failure.

5.5.2.2 Mutations Identified in Human Renal Aplasia

Sequencing of human CAKUT samples has confirmed that several genes identified as essential regulators of early kidney induction in mice are also mutated in human patients [91]. As in mice, mutations in transcription factors *HOX11* [92], *PAX8* [93], *SALL1* [94], and *WT1* [95], as well as in signaling pathways such as *FGFR1* [96] (syndromic; renal agenesis in Kallmann syndrome), *FGF20* [79], *GREM1* [97], and *RET* [94, 98], cause renal aplasia in humans. Moreover, *FRAS1* [88] (syndromic; renal agenesis in Fraser syndrome) and *Fras1*-related extracellular matrix protein 2 (*FREM2*) [92, 99], as well as integrin alpha 8 (*ITGA8*) [100], mutations are associated with renal aplasia in CAKUT patients. Other genes not previously identified in animal models cause not only renal aplasia but also other kidney defects in humans. These include WAP four-disulfide core domain 18 [101, 102] (also known

as *KALI*), cell division cycle 5 like (*CDC5L*) [94], establishment of sister chromatid cohesion N-acetyltransferase 2 (*ESCO2*) [103] (syndromic; included in the Roberts syndrome spectrum), and dual serine/threonine and tyrosine protein kinase (*DSTYK*), which is a positive regulator of extracellular signal-regulated kinase (ERK) that colocalizes with FGF receptors in the UB and MM and may perturb FGF signaling [104].

The vast majority of CAKUT-causing gene mutations are heterozygous. In general, homozygous mutations of key regulators may result in early miscarriage or abortion of the fetus rather than cause a disease syndrome or single-organ defect. It is also possible that multiplied members of a gene family in humans can substitute for the loss of a single member (redundancy), or that modifier aberrations in other genes are required for CAKUT manifestation.

5.5.2.3 Mutations in Human Renal Hypoplasia and Hypodysplasia

Many genes causing renal aplasia in mice are not associated with renal aplasia in human, but rather, when mutated in human, cause an explicitly less severe renal phenotype, such as hypoplasia (small kidney with normal morphology) or hypodysplasia (small kidney with abnormal differentiation). Such genes include *EYAI* [94, 105], *OSRI* [106], *PAX2* [94, 107], *SALL1* [94, 105], and *GRFAL* [108, 109]. Mutations in additional genes associated with human renal hypoplasia or hypodysplasia are transcription factors hepatocyte nuclear factor 1 B [94, 110] (*HNF1B*) and sine oculis-related homeobox 2 [111] (*SIX2*); signaling molecules uroplakin 3A [112] (*UPK3A*), *WNT4* [94], and *BMP4* [113]; and planar polarity gene EGF LAG seven-pass G-type receptor 1 (*CELSRI*) [114]. It is likely that renal hypoplasia is an underdiagnosed subcategory of CAKUT as patients with hypoplastic kidneys, which mostly function normally and do not develop renal disease, remain unrecognized unless the individual does develop related complications like hypertension. This is different in genetically modified experimental models, which are carefully analyzed for renal defects both during embryogenesis and adulthood [115].

5.5.2.4 Mouse Models of Hypo(dys)plasia

A huge number of mouse mutants display either hypoplasia only or in combination with dysplasia. Due to the scope of this chapter, we focus on genes that associate with human CAKUT genes and their signaling cascades.

Mutations in transcription factors HNF1B and PAX2 are the most common causes of renal hypodysplasia in children [105, 116]. This is reflected in mouse where the full inactivation of *Pax2* causes aplasia, while its heterozygous deletion alone causes no phenotype, but simultaneous compound heterozygosity for *Hnf1b* results in renal hypodysplasia [117]. Homozygous deletion of *Hnf1b* on the other hand results in embryonic lethality before gastrulation [118]. However, tetraploid embryo complementation and tissue-specific inactivation studies have demonstrated the requirement of *Hnf1b* for at least growth and integrity of the UB, early nephrogenesis, differentiation of the proximal nephron segment, and differentiation of the renal medulla [119–121]. In addition, deletion of transcription factor *Etv4* or *Etv5* results in renal hypodysplasia though their distinct and joint tissue-specific functions are not fully revealed [16, 69]. Also *Sox8* and *Sox9* act together downstream of GDNF/RET signaling, and their inactivation in the developing kidney causes renal defects varying from aplasia to mild hypoplasia [122]. Interestingly, SOX9 appears to mediate important responses to acute kidney injury, at least as identified in mouse with ischemia-reperfusion-induced injury [123, 124].

Renal hypodysplasia in mice without *B cell leukemia/lymphoma 2 (Bcl2)* factor is caused by an unusual mechanism as its inactivation allows normal renal differentiation until embryonic day 13, after which the nephron progenitors disappear due to increased apoptosis [125]. Similarly, inactivation of *Six2* causes renal hypoplasia due to early loss of nephron progenitors, but in this case through their premature differentiation and exhaustion at mid-gestation [22, 126].

Vitamin A deficiency has been experimentally shown to control nephron number as mice with inactivated *Raldh1a2* (also known as *Aldh1a1*)

have small kidneys due to a UB branching defect [127]. Genetic experiments have also revealed strong involvement of BMP and WNT signaling in guiding embryonic kidney growth and differentiation [128–131]. The involvement of BMP signaling is exemplified by deletion of *Bmp7*, which results in severe renal hypoplasia with virtually no glomeruli due to a defect in survival of nephron progenitors [132–135]. Further studies have shown redundant functions for BMP4 and BMP7; genetic substitution of *Bmp7* by *Bmp4* in mice rescues renal defects [136]. Furthermore, deletion of either ligand in a *Grem1*-null background, which causes renal aplasia on its own [75], restores normal kidney differentiation [137]. High redundancy in BMP signaling, as suggested by ligand deletions, is also obvious at the receptor level because deletion of BMP receptors has either no impact on kidney development or results in hypodysplasia in the renal medulla (*Bmpr1a*) [128, 138]. The phosphatase *Dullard*, a recently identified negative BMP signaling modulator, on the other hand is required for maintenance of postnatal nephrons [139]. Deletion of another BMP signaling modulator, *Crossveinless2*, which likely amplifies signal strength, results in multi-organ defects including renal hypoplasia due to impaired nephrogenesis [140, 141]. Signaling downstream of BMP receptors phosphorylates Smad1/5/8 and/or induces TAK1, which can activate p38/mitogen-activated protein kinase (MAPK), JNK/c-Jun, and NF- κ B cascades. Inactivation of either *Tak1* or *Jun* tissue specifically in nephron progenitors causes their premature depletion and results in mild renal hypoplasia [142].

The importance of WNT signaling for renal differentiation, and especially for nephron induction, was originally revealed by classical induction experiments performed with isolated mouse MM in tissue culture. Initially, these experiments showed that in the absence of a heterologous inducer, such as spinal cord, the MM underwent rapid apoptosis and failed to survive [1, 143]. Soon it was discovered that embryonic spinal cord is rich in WNT proteins. When WNT proteins were expressed in cultured cells and placed in contact with MM, they also induced tubulogenesis [144]. Inactivation of *Wnt4* in mouse

verified the essential function of WNT activation as a nephron inducer, as nephrogenesis failed to progress beyond the pretubular aggregate stage in this model [145]. Consequent tissue-specific deletion [146] and activation [147] of β -catenin in the MM verified the requirement for the canonical WNT pathway. Similarly, β -catenin is required for keeping the UB actively branching as shown by the loss- [84, 148] and gain-of-function [149] strategies that both result in renal hypoplasia due to defects in maintaining the balance of self-renewal and differentiation.

As shown by deletion of receptor tyrosine kinases *Ret* or *Fgf* receptors and their ligands, these signaling pathways are essential for initiation of kidney development and, when fully inactivated, most often cause renal aplasia [150]. However, mutations introduced in the specific tyrosine domains of *Ret* responsible for the distinct intracellular pathway activation cause phenotypes varying from mild hypoplasia to severe hypodysplasia [151–154]. These models together with chemical inhibition experiments in cultured mouse kidney explants have demonstrated that MAPK/ERK, PI3K/AKT, and PLC γ cascades mediate the downstream effects of RTK signaling in developing kidneys [12, 155, 156]. Furthermore, tissue-specific inactivation of tyrosine phosphatase *Shp2*, which functions downstream of RTK and hormone receptors, as well as MAPK/ERK in the UB, results in renal hypodysplasia [157, 158]. The latter model also revealed a specific requirement for MAPK/ERK activity in kidney growth where it promotes UB arborization via novel branch formation [158]. Inactivation of MAPK/ERK activity in the MM, on the other hand, results in slightly less severe renal hypodysplasia and demonstrates that the MAPK/ERK pathway maintains nephron progenitors while also being crucial for their normal differentiation beyond the comma-shaped body stage [23]. UB-specific genetic disruption of another intracellular cascade, the PI3K/AKT pathway, suggests that it is important for shaping the UB branching pattern [159].

Hippo signaling regulates the growth and size of organs in insects and mammals and has

recently been implicated in the guidance of kidney morphogenesis [160]. In mammals, the Hippo pathway involves the kinases MST1/2 and LATS1/2, and their functions are mediated by the transcriptional co-activators YAP and TAZ. Genetic studies have revealed that *Lats1* and *Lats2* are critically required for UB branching as their tissue-specific deletion results in renal aplasia [161]. Interestingly, experiments with the mutant UB also revealed an unexpected interaction between *Nf2* (also known as Merlin) and Hippo signaling, as genetic overexpression of either *Yap* or *Taz* fully rescues severe renal hypodysplasia in the kidneys with UB-specific *Nf2* deletion [161]. In the MM, *Lats1* and *Lats2* together promote differentiation of nephron progenitors [162], while *Yap* and *Taz* appear to have distinct functions in the developing mouse kidney. Similarly to the upstream kinases, *Yap* promotes nephrogenesis [163], while *Taz* is needed for prevention of cyst formation [164, 165].

Cell polarity is an important feature of the functional kidney. Inactivation of either of the planar cell polarity genes *Celsr1* [114] or *Vangl1* [166] causes renal hypodysplasia in mice as both genes are required for normal growth and branch patterning in the developing kidney. Tissue-specific deletion of structural proteins, such as actin remodeling factors destrin (*Dstn*) and cofilin (*Cfl1*) [167], and adhesion proteins like p120 [168] also serve as excellent models of renal hypodysplasia. Instead of halting organogenesis at its earliest stage, these models allow formation of the UB, some degree of branching, and induction of nephrogenesis, thus enabling experimentation that facilitates understanding of kidney differentiation at the cellular level.

5.5.3 Ectopia

The kidneys are normally located in the retroperitoneal space (behind the abdominal cavity) at the level of the stomach. The most common ectopic location of the kidney is in the pelvis. Ectopia can be associated with vesicourinary reflux and mislocation of the ureteric opening in the wall of the

urinary bladder, where the normal location is close to the urethral orifice in the so-called triangle area of the urinary bladder.

5.5.3.1 Mouse Models of Ectopia

Experimental models of ectopia are rare despite its relatively common prevalence in humans. The etiology of ectopia was originally hypothesized by Mackie and Stephens (1975) to derive from aberrant initial ureteric budding site [169] and has since been proven by, e.g., genetic reduction of *Bmp4* dosage, which results in hydronephrosis and ectopia of the ureterovesical orifice [170]. Similarly, defective RET signaling results in ectopic connection of the ureter to bladder [46, 171–173], and recent findings show that dosage of *Gdnf* critically regulates the initial UB budding site and width. As shown in recent study, GDNF positively regulates self-renewal of collecting duct progenitors, which in the genetic excess of *Gdnf* expand abnormally resulting in failure of UB trunk elongation [174, 175]. Consequently, a phenotype very much resembling human pelvic kidney develops due to short ureter length caused by imbalanced progenitor self-renewal and differentiation. Kidney ectopia may also arise through a different mechanism involving deficiency in retinoic acid receptors [176] and defects in the differentiation of smooth muscle cells around the ureter itself as seen in mice with deleted transcription factors *Sox9* [177], *Sox11* [178], or *Tbx18* [179] that all have abnormally positioned kidneys.

5.5.3.2 Mutations Identified in Human Renal Ectopia

Aberrations in *SOX11* [178] and *TBX18* [180] have been identified in patients with varying renal defects that include posterior urethral valves, ureteropelvic junction obstructions, ureterovesical junction obstruction, and vesicoureteral reflux. Rare mutations in genes encoding *RET* and *GFRal* were also identified in CAKUT fetuses and patients with urinary tract malformations, while only one patient with combined unilateral agenesis and ectopic kidney so far has been identified with a *GDNF*-only mutation [109, 181].

5.5.4 Ureteral Duplication

Ureteral duplication is a common form of CAKUT. It can be complete, resulting in two pelvises and two separate ureters in one kidney. Alternatively, one ureter can be divided into two branches with two distinct orifices in the urinary bladder. Ureteral duplication is associated with many complications of which vesicoureteral reflux and ureteropelvic junction obstruction are most often found in patients with incomplete duplication. Complete duplication, which most often associates with vesicoureteral reflux, ectopic ureterocele, or ectopic ureteral insertion, shows a gender bias as all of the associated complications are more common in girls than in boys [182].

5.5.4.1 Mouse Models of Ureteral Duplication

Supernumerary ureteric buds are experimentally promoted in mouse by transgenic GDNF overexpression [183] or in kidney culture by GDNF-releasing beads [184]. Inactivation of genes that restrict *Gdnf* expression (*Robo2/Slit2* [185, 186], *FoxC* [187]) or regulate GDNF/RET signaling activity (*Sprouty1* [188, 189]) causes extra UB formation and exhibits defects commonly associated with duplicated ureters. Interestingly, endogenous overexpression of *Gdnf* by disruption of its 5' untranslated region does not induce extra ureteric budding even though both mRNA and protein levels are significantly increased [174]. Quite unexpectedly, inactivating mutations in the RET docking site responsible for PLCY activation also cause supernumerary budding similar to that seen with exogenous GDNF [151, 184]. These somewhat confusing results from different genetic mouse models of the same signaling pathway can be interpreted in a way that a single UB formation is an absolutely essential requirement for normal renal morphogenesis. Thus, multiple molecular mechanisms, several different genes, and many pathways at distinct levels are engaged to secure the single UB formation. In support of this are the findings demonstrating that simultaneous inactivation of *Spry1* and *Gdnf* or *Ret* allows functional kidney formation, but

additional deletion of a single allele of *Fgf8* results in failure to form kidneys [190, 191]. Furthermore, exogenous application of FGF together with activin A induces supernumerary ureter budding in cultured kidneys even in the absence of GDNF/RET signaling [192].

Disruption of other genes not directly linked to GDNF or FGF signaling also causes ureteral duplication. Deletion of leucine zipper putative tumor suppressor 2 (*Lzts2*), which modulates transcription and regulates cell cycle, results in ureteral duplication due to ectopic UB formation [193]. Genetic experiments have shown that BMP4 is an essential molecule assuring that a single UB forms as mice heterozygous for *Bmp4* loss show multiple UBs [111]. Conditional deletion of transcription factor *Isl1* resulted in reduced *Bmp4* expression and multiple UBs mimicking the *Bmp4* heterozygote phenotype [194].

5.5.4.2 Mutations Identified in Human Ureteral Duplications

Roughly the same genes are involved in ureteral duplication as in renal ectopia. In addition to those mentioned previously for ectopic kidneys, mutations in *BMP4* [111, 195], *SIX2* [111], *SOX17* [196], and glypican 1 (*GPC1*) [197] and variations in *ROBO2* associate with vesicoureteral reflux and/or duplex kidneys [198–200].

5.5.5 Horseshoe Kidneys/Renal Fusion

Fusion of the lower parts of two kidneys results in a horseshoe kidney that is commonly seen in trisomy 18 (also known as Edward's syndrome; see Fig. 5.3) and Turner syndrome patients. Its incidence is likewise slightly increased in trisomy 21 (Down's syndrome). Horseshoe kidneys furthermore occur sporadically without any associated syndromes or functional disturbances. Etiology of this anomaly derives from abnormal migration of nephrogenic cells across the primitive streak and general structural changes caused by midline fusion, flexion/rotation of the caudal spine, and narrowed arterial forks during migration. Fusion typically occurs between weeks 4

and 6 of human development. The rare late fusions occur through fibrous isthmus rather than renal parenchyma [201].

5.5.5.1 Mouse Models of Horseshoe Kidney

Disruption of functional sonic hedgehog (*Shh*) signaling causes midline defects and inactivation of *Shh* specifically in the notochord and the floor plate causes fusion of the kidneys [202]. Similarly, horseshoe kidneys are seen in mice with mild aberrations in retinoic acid signaling, such as those caused by deletion of *Cyp26a*, which is required for the inactivation of retinoic acid [203, 204]. Deletion of transcription factor *Foxd1* results in a range of renal defects, which include fusion of maturing kidneys that remain in the pelvic position [205]. A follow-up study focused on analyzing causes of kidney fusion in *Foxd1* mutant kidneys. This revealed the presence of ectopic cell types in the renal capsule, which leads to its maturation defect and pelvic horseshoe kidneys [206].

5.5.5.2 Mutations Identified in Human Horseshoe Kidneys

Regardless of familial clustering of horseshoe kidney in certain cases, its genetic causes remain largely unidentified. Potential deleterious variations have been identified in Dachsous cadherin-related 2 (*DCHS2*) and leucine-rich repeat-containing G protein-coupled receptor 4 (*LGR4*) [207]. Genome-wide association studies identified *CYP26A* together with *CYP24A* and *BMP4* as potential disease-causing mutations in CAKUT, but their association specifically to horseshoe kidney is not reported [208]. Thus, according to current knowledge, large chromosomal aberrations rather than single gene mutations associate with fused kidney in humans.

5.5.6 Renal Multicystic Dysplasia and Polycystic Kidney Disease

Renal multicystic dysplasia is characterized by variable numbers of cysts in either one or both kidneys or only in a segment of a kidney (Fig. 5.3). The pathogenesis is not yet completely resolved,

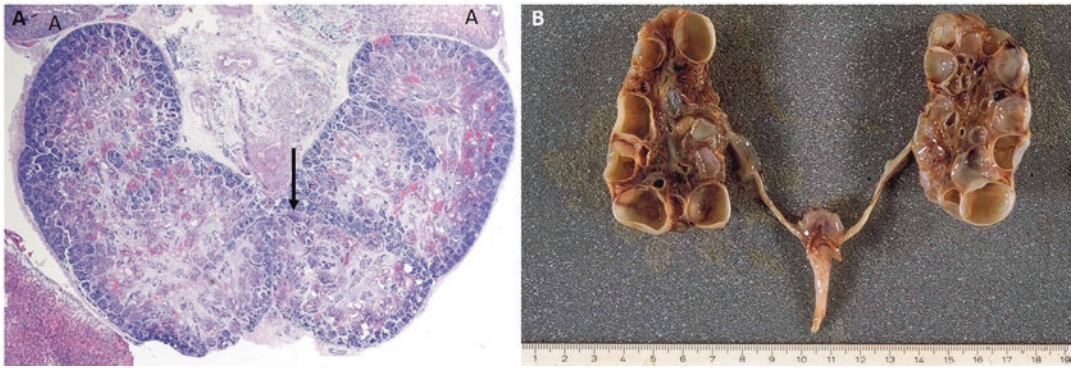


Fig. 5.3 Horseshoe kidney/renal fusion and multicystic dysplasia. **(a)** A human horseshoe kidney at gestational week 13 (equal to 11 weeks of fetal development). The genetic cause for the horseshoe kidney in this fetus is trisomy 18. Fusion is always seen in the caudal part of the

kidneys (arrow). **(b)** Multicystic renal dysplasia is characterized by large cysts surrounded by clear cytoplasmic stromal cells. The cysts can be either in a segment of a kidney, in one whole kidney, or in both kidneys. A adrenal gland

but experimental studies with rabbits have shown that ligation of the ureter causes similar cyst formation and differentiation defect [209].

There are two types of polycystic kidney diseases (PKD), the infantile (early-onset recessive) and adult (late-onset dominant) polycystic kidney diseases. Infantile PKD manifests at birth or soon after and is associated with high mortality if renal transplantation is not performed. Adult PKD manifests at any age of adulthood and has a less severe outcome. These two most common forms of PKD show autosomal recessive and autosomal dominant inheritance, respectively. The later-onset autosomal dominant PKD is one of the most common genetic diseases with an incidence of 1:500 to 1:1000, while the early-onset autosomal recessive form is much rarer [210].

5.5.6.1 Mutations Identified in Humans with Renal Cysts

Although renal multicystic dysplasia is less abundant in humans than PKD, mutations in BicC family RNA binding protein 1 (*BICCI*) [97, 211], *CDC5L* [212], dachshund family transcription factor 1 (*DACHI*) [213], *HNF1B* [110, 214, 215], and upstream transcription factor 2 (*USF2*) [216] all associate with cystic dysplasia. Autosomal dominant PKD mainly derives from mutations in polycystin (*PKD*) genes [217]. The majority of the mutations (~85%) are in *PKD1*, which encodes a large receptor-like protein (polycystin 1)

that interacts with *PKD2* gene product polycystin 2 [218]. Mutations in *PKD2* account for ~15% of autosomal dominant PKD cases, while recently a new causative gene, glucosidase II alpha subunit (*GANAB*), was identified in rare patients who are negative for *PKD1* and *PKD2* mutations [217, 219]. Autosomal recessive PKD was long considered a genetically homogenous disease. Mutations in *PKHD1*, which encodes fibrocystin localizing to the primary cilia to modulate Shh and Wnt activities, cause the majority of these cases [220]. Aberrations in yet another ciliary protein encoded by *DZIP1L* [221] were recently identified in patients with moderate clinical symptoms of autosomal recessive PKD, affecting also liver function. Mutated *HNF1B* in some patients also causes cystic kidneys, while its aberrations are associated with hypodysplasia and diabetes syndrome [110, 222].

5.5.6.2 Mouse Models of Cystic Kidney and Polycystic Kidney Disease

The mouse models of polycystic kidney disease have revealed that defects in genes encoding primary cilia-located proteins are responsible for abnormal cellular proliferation and fluid accumulation that jointly lead to the formation of numerous cysts in renal tubules. Deletion of either *Pkd1* [223] or *Pkd2* [224, 225] best models the human PKD, while inactivation of *Pkhd1* [226] in rats and inhibition of ciliogenesis by loss of *Kif3a* in mouse

[227] also result in a phenotype very reminiscent of human PKD. In mouse models of inactivated *glucosidase II β* and *Sec63p*, which exhibit mild kidney cysts on their own, reduced *Pkd1* sensitizes kidneys for cystogenesis further highlighting its essential role in PKD pathogenesis [228].

Genetic disruption of genes regulating ureter morphogenesis and/or connection to the bladder may cause renal multicystic dysplasia. As examples, atypical cadherin *Fat4* [229], its interacting partner four-jointed box 1 (*Fjx1*) [229], cadherin-related dachshous genes (*Dchs1* and *Dchs2*) [229, 230], and other adhesion-related molecules like *Dlg5*, which is required for the delivery of adhesive complex components [231], *Frem2* [99] and *Glc3* [232], all cause cystic kidneys when inactivated in mice. Also, *Lzts2* mutant embryos, which exhibit duplex ureters, show other defects such as hydroureters and hydronephrosis accompanied with renal multicystic dysplasia [193].

5.5.7 Congenital Nephrosis

Congenital nephrosis is a condition under which the glomeruli leak protein into the urine during pregnancy. It is caused by the defects of the glomerular filtration barrier, which is composed of the slit diaphragm connecting adjacent podocyte foot processes, the glomerular basement membrane, and the fenestrated endothelium of the capillary loops. Congenital nephrosis is characterized by excess of amniotic fluid or polyhydramnion and enlarged placenta, which weighs more than 50 percent of the fetal weight. Renal symptoms are typically caused by impaired podocyte physiology that derives from mutations in gene encoding proteins of the slit diaphragm [233]. The congenital nephrotic syndrome is a rare form of nephrosis, which is highly enriched in the Finnish population with occasional cases reported all over the world [234].

5.5.7.1 Mutations Causing Congenital Nephrotic Syndrome in Humans

Kestilä et al. identified the causative mutation for congenital nephrotic syndrome of the Finnish type in a gene encoding the slit diaphragm protein nephrin (*NPHS1*) [235]. Originally, two founder

mutations were identified but since then more than 20 additional mutations have been shown to cause this syndrome. Although approximately 98% of Finnish and 38–90% of non-Finnish congenital nephrotic syndrome patients carry mutations in *NPHS1* [236–238], mutations in other genes encoding podocin (*NPHS2*), phospholipase C epsilon-1 (*PLCE1*), *WT1*, and laminin beta 2 (*LAMB2*) have been identified. Genetic diagnosis is important for designing patient treatment plans, as steroid-resistant nephrotic syndrome typically derives from the defects in *NPHS2* [238, 239]. Moreover, mutations in *PLCE1* [240] and *WT1* [238, 241], like in *FAT1* [242], cause a more diffuse mesangial sclerosis type of phenotype while *LAMB2* [238, 243] mutations give rise to microcoria. Finally, mutations in genes encoding collagen IV (*COL4A3*, *COL4A4*, and *COL4A5*), which is the major form of collagen present in the glomerulus, also cause congenital nephrosis due to characteristic abnormalities in the glomerular basement membrane [244].

5.5.7.2 Mouse Models of Congenital Nephrotic Syndrome

Characteristic of congenital nephrotic syndrome studies is that the human mutations were often identified prior to the generation of their genetic animal models. The mouse models where the major syndrome-causing genes, *Nphs1* [245], *Nphs2* [246], *Lamb2* [247, 248], or *Col4a3* [249], were knocked out recapitulate the renal symptoms quite well and have been valuable tools for understanding the cellular and molecular mechanisms of these pathologies. Manipulation of other genes encoding slit diaphragm components, like inactivation of CD2-associated protein (*Cd2ap*) [250], often compromises podocyte function and may recapitulate specific features of congenital nephrosis [251].

5.5.8 Nephroblastomatosis (Nephrogenic Rests) and Wilms' Tumor

Nephroblastomatosis is a condition where islands of the nephrogenic blastema remain in the kidney postnatally (Fig. 5.4). These islands are also

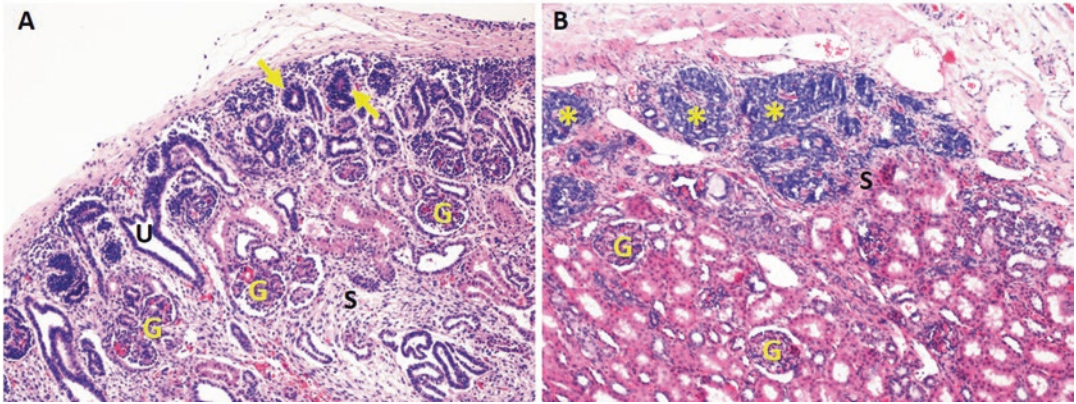


Fig. 5.4 Nephroblastomatosis/nephrogenic rests. (a) Normal human kidney at gestational week 12. Arrows point to differentiating nephron precursors. (b) Nephrogenic rests are the dark blue, highly cellular islands in the subcortical or perilobar areas. They repre-

sent persistent foci of nephrogenic blastema in the postnatal kidney in a 1-year-old child. Because he had multiple foci of nephrogenic rests (white asterisks), the condition is called nephroblastomatosis. *G* glomerulus, *U* ureteric bud, *S* stroma

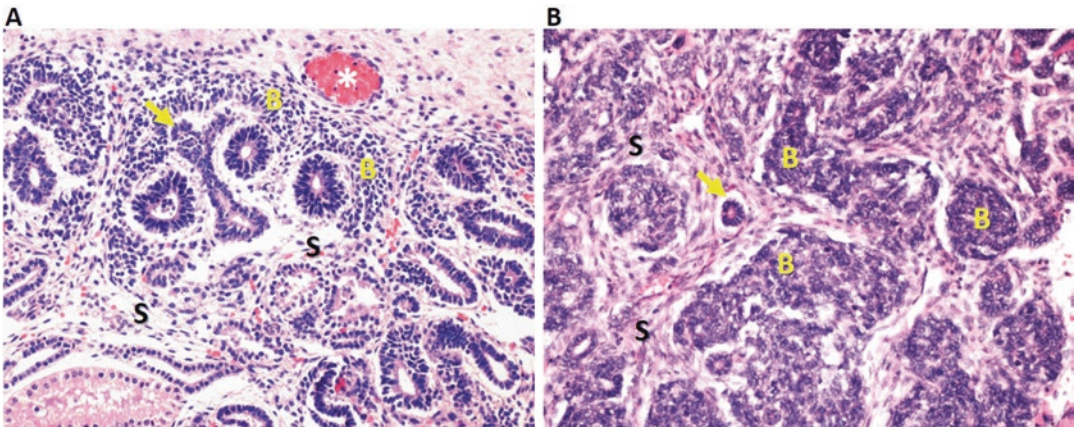


Fig. 5.5 Wilms' tumor or nephroblastoma. (a) Normal human kidney at gestational week 12. Arrow points to a ureteric bud, B marks blastema (the metanephric mesenchyme), and S is the stroma. (b) The morphology of the

classic Wilms' tumor (also called nephroblastoma) mimics that of embryonic kidneys showing blastemal (B), stromal (S), and epithelial cells (arrow) but in a disorganized manner

called nephrogenic rests and may reside either intra- or perilobarly. Intralobar rests arise early in renal development, while perilobar rests are in the renal cortex, which is the active differentiating zone. They either spontaneously regress or progress, and finally become malignant tumors called nephroblastomas, also known as Wilms' tumors (Fig. 5.5). It is impossible to distinguish between regressive and progressive nephroblastomas by any morphological or immunohistochemical means.

5.5.8.1 Mutations and Syndromes Associated with Wilms' Tumor in Humans

Despite being the most common pediatric renal cancer, the prevalence of Wilms' tumor is generally low (1:10,000 children). Its incidence is significantly increased in syndromes like Wilms' tumor, aniridia, genitourinary anomalies, and mental retardation (WAGR), Beckwith-Wiedemann (BWS), hemihypertrophy, Denys-Drash, and Perlman. Hemihypertrophy is a condition where

the left and right sides of the body show clear growth differences, while Beckwith-Wiedemann syndrome is a congenital overgrowth syndrome, where the organs are bigger than expected for the age of the child. Tuberous sclerosis, a highly variable disorder typically diagnosed soon after birth, associates with the development of benign tumors in different organs, including the kidneys [252]. Although otherwise harmless, the benign tumors may interfere with the normal function of the affected organ. Tuberous sclerosis causes cystic kidneys in approximately 20–30% of individuals, but their renal function is rarely compromised.

The most commonly altered genetic locus causing Wilms' tumor is the one disturbing *insulin-like growth factor 2 (IGF2)*, which is one of the imprinted genes and normally expressed only when paternally derived. In approximately 70% of all Wilms' tumors, biallelic IGF2 expression results in tumorigenesis [253]. Genetic analysis of WAGR and Denys-Drash revealed an association of germline mutations in *WT1*, and later, somatic mutations were identified in many Wilms' tumors [254]. These somatic-inactivating mutations associate with intralobar nephrotic rests and thus could be responsible for early defects in renal differentiation leading to tumor development [255]. Other mutations have been identified in the β -catenin encoding *CTNNB1* gene [256], often together with a *WT1* mutation [257], and in Wilms' tumor on chromosome X (*WTX*) gene [258], which couples *WT1* to β -catenin as it negatively regulates Wnt signaling and participates in the control of *WT1* transcription [259, 260]. Also, mutations in the microRNA-processing genes that derepress IGF2 levels via its regulator *PLAG1* have been identified. This further underlines the importance of the IGF2 signaling dosage in tissue homeostasis during kidney differentiation [261]. Interestingly, a long-sought Wilms' tumor cancer stem cell, double positive for *NCAM1* and *RALDH1*, was identified [262]. This may help the future aims of revealing the relationship between cancer stem cells and other stem cell types in the kidney, namely, nephron and collecting ductal progenitors.

5.5.8.2 Mouse Models of Nephroblastomatosis and Wilms' Tumor

The genes associated with Wilms' tumor in humans are required for the early steps of embryogenesis and renal development. *Wt1* deletion in mouse results in complete failure of kidney induction [55, 263]. *Ctnnb1* expressed by the UB is required for branching morphogenesis and in the MM for normal nephrogenesis [84, 149]. Thus, the proteins encoded by these genes are crucial for normal organogenesis, and their null mutant mice fail to serve as models for nephrogenic rests or Wilms' tumor. Mosaic inactivation of *Wt1* together with constantly increased *Igf2* rescues mice from perinatal death caused by complete inactivation of *Wt1* and results in nephron progenitor-derived renal tumors that resemble a certain subtype of human tumors [264, 265]. Moreover, inactivation of *Wt1* at different nephron differentiation stages and comparison of the resulting RNA signature in mutant kidneys with different subtypes of human Wilms' tumor revealed a correlation supporting the view that the disturbed nephrogenesis is an important contributor of tumorigenesis [263]. Interestingly, kidneys in the mouse model of excess endogenous *Gdnf* [174] show structures reminiscent of perilobar nephrogenic rests, but these disappear by spontaneous differentiation during early postnatal life (our unpublished results). To our knowledge, the field still lacks a proper genetic model of pediatric renal cancer that could serve as a preclinical model and facilitate understanding of the mechanisms of tumor growth and the role of kidney cancer stem cells.

5.5.9 Renal Disease in Syndromes

In addition to the syndromes mentioned in the previous sections, Alagille, branchio-oto-renal (BOR), Fraser, Kallmann, Meckel, Pallister-Hall, renal coloboma, and Townes-Brocks syndromes are all associated with renal anomalies.

Alagille syndrome is caused by defective Notch signaling. It is characterized by defects in the liver, heart, skeleton, eyes, and kidneys.

The kidneys are most often affected in individuals with NOTCH2 mutations and include hypodysplasia and cysts, which compromise renal function [266]. The majority of Alagille patients, though, have mutations in NOTCH ligand Jagged1 (JAG1). Despite a suggested function in the maintenance of UB tip identity, very little is known about the function of *Jag1* in renal differentiation [267]. Inactivation of *Notch2* in mouse recapitulates renal defects and has revealed the importance of this signaling pathway in fate determination of distinct nephron segments [268, 269].

Branchio-oto-renal syndrome is an inherited autosomal dominant disorder, which, according to its name, exhibits defects in a variety of organs, including a spectrum of kidney defects ranging from mild to very severe (aplasia). The causative mutations of BOR have been identified in *EYA1*, *SIX5*, and *SIX1* genes, along with *SALL1* mutations, which cause a BOR-related disorder, Townes-Brocks syndrome. See Sect. 5.5.2 for details of these genes and their functions.

Fraser syndrome The spectrum of renal defects in Fraser syndrome include hypo(dys)plasia and uni- or bilateral agenesis. Human mutations have been identified in *FRAS1* and *FREM2*, which were discussed previously (Sect. 5.5.2), as well as in glutamate receptor-interacting protein 1 (*GRIPI*) gene [270, 271].

Kallmann syndrome The most typical feature of Kallmann syndrome is delayed or absence of sexual development. The renal manifestation is relatively rare in Kallmann patients, but it may appear as the absence of one kidney. Kallmann syndrome mutations have been identified in *FGFR1*, *FGF8* (discussed earlier), WAP four-disulfide core domain 18 (*WFDC18*, also known as *ANOS1* and *KALI*) [272], *SOX10* [273], and semaphorin *SEMA3A* [274].

Meckel syndrome (also known as Gruber-Meckel syndrome) consists of a posterior encephalocele, where the dorsal parts of the brain expand backwards and are only covered by skin. The patients also show postaxial polydactyly (duplicated little finger and/or toe) and cystic renal disease that somewhat morphologically resembles polycystic renal disease with liver cysts.

Meckel syndrome, similar to congenital nephrosis of the Finnish type, is greatly enriched in the Finnish population due to the founder effect, which enriches disease inheritance and manifestation in isolated populations typically due to a major mutation distribution among a small number of individuals living within the population. Identification of mutations in Meckel syndrome, type 1 (*MKS1*) gene, encoding a protein required for the normal function of primary cilia [275], was a landmark for understanding the cellular mechanisms leading to Meckel syndrome and other ciliopathies. Since then, mutations in at least 12 more genes have been associated with Meckel syndrome [276]. Despite an obvious genetic heterogeneity, the major Meckel syndrome-causing mutations are in *MKS1*, *MKS3/TMEM67*, and *MKS6/CC2D2A*.

Pallister-Hall syndrome derives from defects in hedgehog signaling manifested as mutations in *GLI3* effector gene [277]. The manifold abnormalities in Pallister-Hall patients are often not life-threatening, unlike, e.g., deletion of *Gli3* in mice, which causes renal aplasia [278]. Associated kidney abnormalities of Pallister-Hall syndrome are rare, but typically manifest as renal dysplasia.

Renal coloboma syndrome The characteristic defects of renal coloboma syndrome, also known as papillorenal syndrome, include optic nerve dysplasia and renal hypodysplasia. It is a rare autosomal dominant disorder, which is caused by mutations in *PAX2* [279]. Defects caused by *Pax2* inactivation in mouse have been discussed in Sect. 5.5.2.

5.6 Conclusions

Mouse models have greatly facilitated our understanding of renal differentiation and its molecular regulation. The benefit for genetics and diagnosis of congenital kidney anomalies is also obvious. However, the majority of human CAKUT cases are idiopathic, and their causes remain unknown despite the strong familial aggregation in approximated 15% of patients [91, 280]. In addition to genetic causes, environmental and epigenetic

factors are also involved, while only approximately 5–20% of CAKUT are considered monogenic disease [281–283]. The two challenges in modeling congenital kidney anomalies in experimental animals are the lack of knowledge of causative gene mutation and use of inappropriate strategy to mimic given human disease in mouse. The first of these may derive from the fact that large portions of genome (GC-rich and other repetitive or difficult-to-reach regions) are not covered in whole-genome sequencing experiments. Potential aberrations in these noncoding genomic regions may be considered epigenetic causes of CAKUT, and they remain unexplored until better knowledge and methodologies are available for their exploration. The second challenge refers to the fact that mouse models of CAKUT so far have largely been made by complete inactivation of the entire gene. The next task for the scientific community is to utilize CRISPR/CAS9 methodology to mimic specific human CAKUT mutations in mice, a strategy which is expected to much better phenocopy the given anomaly it associates with in human patients.

Acknowledgements We would like to thank Dr. Carlton Bates, Dr. Cristina Cebrian, and Dr. Peter Hohenstein for insightful discussions and MSc Kristen Kurtzeborn for reviewing the manuscript for English language.

References

- Saxen L. Failure to demonstrate tubule induction in a heterologous mesenchyme. *Devel Biol.* 1970;23:511–23.
- Wartiovaara J, Nordling S, Lehtonen E, Saxen L. Transfilter induction of kidney tubules: correlation with cytoplasmic penetration into Nucleopore filters. *J Embryol Exp Morphol.* 1974;31:667–82.
- Saxen L. *Organogenesis of the kidney.* Cambridge: Cambridge University Press; 1987.
- Takasato M, Little MH. The origin of the mammalian kidney: implications for recreating the kidney in vitro. *Development.* 2015;142(11):1937–47.
- Taguchi A, Kaku Y, Ohmori T, Sharmin S, Ogawa M, Sasaki H, et al. Redefining the in vivo origin of metanephric nephron progenitors enables generation of complex kidney structures from pluripotent stem cells. *Cell Stem Cell.* 2014;14(1):53–67.
- Davidson AJ. *Mouse kidney development.* Cambridge, MA: StemBook; 2008.
- Davidson AJ, Lewis P, Przepiorski A, Sander V. Turning mesoderm into kidney. *Semin Cell Dev Biol.* 2019;91:86–93.
- de Bruijn MF, Speck NA, Peeters MC, Dzierzak E. Definitive hematopoietic stem cells first develop within the major arterial regions of the mouse embryo. *EMBO J.* 2000;19(11):2465–74.
- Sainio K, Hellstedt P, Kreidberg JA, Saxen L, Sariola H. Differential regulation of two sets of mesonephric tubules by WT-1. *Development.* 1997;124(7):1293–9.
- Woolf AS, Winyard PJD, Hermanns MM, Welham SJM. Maldevelopment of the human kidney and lower urinary tract: an overview. In: Vize PD, Woolf AS, Bard JBL, editors. *The kidney: from normal development to congenital disease.* London: Academic Press; 2003. p. 377.
- Costantini F. Genetic controls and cellular behaviors in branching morphogenesis of the renal collecting system. *Wiley Interdiscip Rev Dev Biol.* 2012;1(5):693–713.
- Watanabe T, Costantini F. Real-time analysis of ureteric bud branching morphogenesis in vitro. *Dev Biol.* 2004;271(1):98–108.
- Short KM, Combes AN, Lefevre J, Ju AL, Georgas KM, Lamberton T, et al. Global quantification of tissue dynamics in the developing mouse kidney. *Dev Cell.* 2014;29(2):188–202.
- Shakya R, Watanabe T, Costantini F. The role of GDNF/Ret signaling in ureteric bud cell fate and branching morphogenesis. *Dev Cell.* 2005;8(1):65–74.
- Chi X, Michos O, Shakya R, Riccio P, Enomoto H, Licht JD, et al. Ret-dependent cell rearrangements in the Wolffian duct epithelium initiate ureteric bud morphogenesis. *Dev Cell.* 2009;17(2):199–209.
- Kuure S, Chi X, Lu B, Costantini F. The transcription factors Etv4 and Etv5 mediate formation of the ureteric bud tip domain during kidney development. *Development.* 2010;137(12):1975–9.
- Riccio P, Cebrian C, Zong H, Hippenmeyer S, Costantini F. Ret and Etv4 promote directed movements of progenitor cells during renal branching morphogenesis. *PLoS Biol.* 2016;14(2):e1002382.
- Potter SS. Single-cell RNA sequencing for the study of development, physiology and disease. *Nat Rev Nephrol.* 2018;14(8):479–92.
- Lignell A, Kerosuo L, Streichan SJ, Cai L, Bronner ME. Identification of a neural crest stem cell niche by spatial genomic analysis. *Nat Commun.* 2017;8(1):1830.
- Cebrian C, Borodo K, Charles N, Herzlinger DA. Morphometric index of the developing murine kidney. *Dev Dyn.* 2004;231(3):601–8.
- Nagalakshmi VK, Yu J. The ureteric bud epithelium: morphogenesis and roles in metanephric kidney patterning. *Mol Reprod Dev.* 2015;82(3):151–66.

22. Kobayashi A, Valerius MT, Mugford JW, Carroll TJ, Self M, Oliver G, et al. Six2 defines and regulates a multipotent self-renewing nephron progenitor population throughout mammalian kidney development. *Cell Stem Cell*. 2008;3(2):169–81.
23. Ihermann-Hella A, Hirashima T, Kupari J, Kurtzeborn K, Li H, Kwon HN, et al. Dynamic MAPK/ERK activity sustains nephron progenitors through niche regulation and primes precursors for differentiation. *Stem Cell Reports*. 2018;11(4):912–28.
24. Sariola H. Nephron induction revisited: from caps to condensates. *Curr Opin Nephrol Hypertens*. 2002;11(1):17–21.
25. Kurtzeborn K, Cebrian C, Kuure S. Regulation of renal differentiation by trophic factors. *Front Physiol*. 2018. <https://doi.org/10.3389/fphys.2018.01588>.
26. O'Brien LL. Nephron progenitor cell commitment: striking the right balance. *Semin Cell Dev Biol*. 2019;91:94–103.
27. Costantini F, Kopan R. Patterning a complex organ: branching morphogenesis and nephron segmentation in kidney development. *Dev Cell*. 2010;18(5):698–712.
28. Hartman HA, Lai HL, Patterson LT. Cessation of renal morphogenesis in mice. *Dev Biol*. 2007;310(2):379–87.
29. Cebrian C, Asai N, D'Agati V, Costantini F. The number of fetal nephron progenitor cells limits ureteric branching and adult nephron endowment. *Cell Rep*. 2014;7(1):127–37.
30. Beck JA, Lloyd S, Hafezparast M, Lennon-Pierce M, Eppig JT, Festing MF, et al. Genealogies of mouse inbred strains. *Nat Genet*. 2000;24(1):23–5.
31. Rabe M, Schaefer F. Non-transgenic mouse models of kidney disease. *Nephron*. 2016;133(1):53–61.
32. Wang Q, Hummler E, Nussberger J, Clement S, Gabbiani G, Brunner HR, et al. Blood pressure, cardiac, and renal responses to salt and deoxycorticosterone acetate in mice: role of renin genes. *J Am Soc Nephrol*. 2002;13(6):1509–16.
33. Kuure S, Vuolteenaho R, Vainio S. Kidney morphogenesis: cellular and molecular regulation. *Mech Dev*. 2000;92(1):31–45.
34. Anders H, Schlondorff D. Murine models of renal disease: possibilities and problems in studies using mutant mice. *Exp Nephrol*. 2000;8(4-5):181–93.
35. Lyon MF, Rastan S, Brown SDM, editors. Genetic variants and strains of the laboratory mouse. 3rd ed. Oxford: Oxford University Press; 1996.
36. Schieren G, Pey R, Bach J, Hafner M, Gretz N. Murine models of polycystic kidney disease. *Nephrol Dial Transplant*. 1996;11(Suppl 6):38–45.
37. Alpers CE, Hudkins KL. Mouse models of diabetic nephropathy. *Curr Opin Nephrol Hypertens*. 2011;20(3):278–84.
38. Capecchi MR. Altering the genome by homologous recombination. *Science*. 1989;244(4910):1288–92.
39. Stricklett PK, Nelson RD, Kohan DE. The Cre/loxP system and gene targeting in the kidney. *Am J Physiol*. 1999;276(5 Pt 2):F651–7.
40. Silver LM. Mouse genetics: concepts and applications. New York: Oxford University Press; 1995.
41. WareJoncas Z, Campbell JM, Martinez-Galvez G, Gendron WAC, Barry MA, Harris PC, et al. Precision gene editing technology and applications in nephrology. *Nat Rev Nephrol*. 2018;14(11):663–77.
42. Fernandez A, Josa S, Montoliu L. A history of genome editing in mammals. *Mamm Genome*. 2017;28(7-8):237–46.
43. Mianne J, Codner GF, Caulder A, Fell R, Hutchison M, King R, et al. Analysing the outcome of CRISPR-aided genome editing in embryos: Screening, genotyping and quality control. *Methods*. 2017;121–122:68–76.
44. Wilson JG, Roth CB, Warkany J. An analysis of the syndrome of malformations induced by maternal vitamin A deficiency. Effects of restoration of vitamin A at various times during gestation. *Am J Anat*. 1953;92(2):189–217.
45. El Kares R, Manolescu DC, Lakhal-Chaieb L, Montpetit A, Zhang Z, Bhat PV, et al. A human ALDH1A2 gene variant is associated with increased newborn kidney size and serum retinoic acid. *Kidney Int*. 2010;78(1):96–102.
46. Batourina E, Gim S, Bello N, Shy M, Clagett-Dame M, Srinivas S, et al. Vitamin A controls epithelial/mesenchymal interactions through Ret expression. *Nat Genet*. 2001;27(1):74–8.
47. Vlangos CN, Siuniak AN, Robinson D, Chinnaiyan AM, Lyons RH Jr, Cavalcoli JD, et al. Next-generation sequencing identifies the Danforth's short tail mouse mutation as a retrotransposon insertion affecting Ptf1a expression. *PLoS Genet*. 2013;9(2):e1003205.
48. Maas R, Elfering S, Glaser T, Jepeal L. Deficient outgrowth of the ureteric bud underlies the renal agenesis phenotype in mice manifesting the *limb deformity (ld)* mutation. *Devel Dyn*. 1994;199:214–28.
49. Torres M, Gomez-Pardo E, Dressler GR, Gruss P. Pax-2 controls multiple steps of urogenital development. *Development*. 1995;121(12):4057–65.
50. James RG, Kamei CN, Wang Q, Jiang R, Schultheiss TM. Odd-skipped related 1 is required for development of the metanephric kidney and regulates formation and differentiation of kidney precursor cells. *Development*. 2006;133(15):2995–3004.
51. Wang Q, Lan Y, Cho ES, Maltby KM, Jiang R. Odd-skipped related 1 (Odd 1) is an essential regulator of heart and urogenital development. *Dev Biol*. 2005;288(2):582–94.
52. Lim KC, Lakshmanan G, Crawford SE, Gu Y, Grosveld F, Engel JD. Gata3 loss leads to embryonic lethality due to noradrenaline deficiency of the sympathetic nervous system. *Nat Genet*. 2000;25(2):209–12.

53. Shawlot W, Behringer RR. Requirement for *Lim1* in head-organizer function. *Nature*. 1995;374(6521):425–30.
54. Tsang TE, Shawlot W, Kinder SJ, Kobayashi A, Kwan KM, Schughart K, et al. *Lim1* activity is required for intermediate mesoderm differentiation in the mouse embryo. *Dev Biol*. 2000;223(1):77–90.
55. Kreidberg JA, Sariola H, Loring JM, Maeda M, Pelletier J, Housman D, et al. *WT-1* is required for early kidney development. *Cell*. 1993;74:679–91.
56. Patterson LT, Pembaur M, Potter SS. *Hoxa11* and *Hoxd11* regulate branching morphogenesis of the ureteric bud in the developing kidney. *Development*. 2001;128(11):2153–61.
57. Patterson LT, Potter SS. Hox genes and kidney patterning. *Curr Opin Nephrol Hypertens*. 2003;12(1):19–23.
58. Xu PX, Adams J, Peters H, Brown MC, Heaney S, Maas R. *Eya1*-deficient mice lack ears and kidneys and show abnormal apoptosis of organ primordia. *Nat Genet*. 1999;23(1):113–7.
59. Xu PX, Zheng W, Huang L, Maire P, Laclef C, Silvius D. *Six1* is required for the early organogenesis of mammalian kidney. *Development*. 2003;130(14):3085–94.
60. Nishinakamura R, Matsumoto Y, Nakao K, Nakamura K, Sato A, Copeland NG, et al. Murine homolog of *SALL1* is essential for ureteric bud invasion in kidney development. *Development*. 2001;128(16):3105–15.
61. Moore MW, Klein RD, Farinas I, Sauer H, Armanini M, Phillips H, et al. Renal and neuronal abnormalities in mice lacking GDNF. *Nature*. 1996;382(6586):76–9.
62. Pichel JG, Shen L, Sheng HZ, Granholm AC, Drago J, Grinberg A, et al. Defects in enteric innervation and kidney development in mice lacking GDNF. *Nature*. 1996;382(6586):73–6.
63. Sanchez MP, Silos-Santiago I, Frisen J, He B, Lira SA, Barbacid M. Renal agenesis and the absence of enteric neurons in mice lacking GDNF. *Nature*. 1996;382(6586):70–3.
64. Schuchardt A, D'Agati V, Larsson-Blomberg L, Costantini F, Pachnis V. Defects in the kidney and enteric nervous system of mice lacking the tyrosine kinase receptor *Ret*. *Nature*. 1994;367(6461):380–3.
65. Schuchardt A, D'Agati V, Pachnis V, Costantini F. Renal agenesis and hypodysplasia in *ret-k*-mutant mice result from defects in ureteric bud development. *Development*. 1996;122(6):1919–29.
66. Cacalano G, Farinas I, Wang LC, Hagler K, Forgie A, Moore M, et al. *GFRalpha1* is an essential receptor component for GDNF in the developing nervous system and kidney. *Neuron*. 1998;21(1):53–62.
67. Enomoto H, Araki T, Jackman A, Heuckeroth RO, Snider WD, Johnson EMJ, et al. *GFRalpha1*-deficient mice have deficits in the enteric nervous system and kidneys. *Neuron*. 1998;21(2):317–24.
68. Costantini F. GDNF/*Ret* signaling and renal branching morphogenesis: from mesenchymal signals to epithelial cell behaviors. *Organogenesis*. 2010;6(4):252–62.
69. Lu BC, Cebrian C, Chi X, Kuure S, Kuo R, Bates CM, et al. *Etv4* and *Etv5* are required downstream of GDNF and *Ret* for kidney branching morphogenesis. *Nat Genet*. 2009;41(12):1295–302.
70. Esquela AF, Lee SJ. Regulation of metanephric kidney development by growth/differentiation factor 11. *Dev Biol*. 2003;257(2):356–70.
71. Sanford LP, Ormsby I, Gittenberger-de Groot AC, Sariola H, Friedman R, Boivin GP, et al. *TGFbeta2* knockout mice have multiple developmental defects that are non-overlapping with other *TGFbeta* knockout phenotypes. *Development*. 1997;124(13):2659–70.
72. Shull MM, Ormsby I, Kier AB, Pawlowski S, Diebold RJ, Yin M, et al. Targeted disruption of the mouse transforming growth factor-beta 1 gene results in multifocal inflammatory disease. *Nature*. 1992;359(6397):693–9.
73. Kaartinen V, Voncken JW, Shuler C, Warburton D, Bu D, Heisterkamp N, et al. Abnormal lung development and cleft palate in mice lacking *TGF-beta 3* indicates defects of epithelial-mesenchymal interaction. *Nat Genet*. 1995;11(4):415–21.
74. Hsu DR, Economides AN, Wang X, Eimon PM, Harland RM. The *Xenopus* dorsalizing factor Gremlin identifies a novel family of secreted proteins that antagonize BMP activities. *Mol Cell*. 1998;1(5):673–83.
75. Michos O, Panman L, Vintersten K, Beier K, Zeller R, Zuniga A. Gremlin-mediated BMP antagonism induces the epithelial-mesenchymal feedback signaling controlling metanephric kidney and limb organogenesis. *Development*. 2004;131(14):3401–10.
76. Michos O, Goncalves A, Lopez-Rios J, Tiecke E, Naillat F, Beier K, et al. Reduction of BMP4 activity by gremlin 1 enables ureteric bud outgrowth and GDNF/*WNT11* feedback signalling during kidney branching morphogenesis. *Development*. 2007;134(13):2397–405.
77. Poladia DP, Kish K, Kutay B, Hains D, Kegg H, Zhao H, et al. Role of fibroblast growth factor receptors 1 and 2 in the metanephric mesenchyme. *Dev Biol*. 2006;291(2):325–39.
78. Walker KA, Sims-Lucas S, Bates CM. Fibroblast growth factor receptor signaling in kidney and lower urinary tract development. *Pediatr Nephrol*. 2016;31(6):885–95.
79. Barak H, Huh SH, Chen S, Jeanpierre C, Martinovic J, Parisot M, et al. *FGF9* and *FGF20* maintain the stemness of nephron progenitors in mice and man. *Dev Cell*. 2012;22(6):1191–207.
80. Carroll TJ, Park JS, Hayashi S, Majumdar A, McMahon AP. *Wnt9b* plays a central role in the regulation of mesenchymal to epithelial transitions underlying organogenesis of the Mammalian urogenital system. *Dev Cell*. 2005;9(2):283–92.
81. Karner CM, Das A, Ma Z, Self M, Chen C, Lum L, et al. Canonical *Wnt9b* signaling balances progeni-

- tor cell expansion and differentiation during kidney development. *Development*. 2011;138(7):1247–57.
82. Kiefer SM, Robbins L, Rauchman M. Conditional expression of *Wnt9b* in *Six2*-positive cells disrupts stomach and kidney function. *PLoS One*. 2012;7(8):e43098.
 83. Boivin FJ, Sarin S, Evans JC, Bridgewater D. The good and bad of beta-catenin in kidney development and renal dysplasia. *Front Cell Dev Biol*. 2015;3:81.
 84. Bridgewater D, Cox B, Cain J, Lau A, Athaide V, Gill PS, et al. Canonical WNT/beta-catenin signaling is required for ureteric branching. *Dev Biol*. 2008;317(1):83–94.
 85. Lange A, Wickstrom SA, Jakobson M, Zent R, Sainio K, Fassler R. Integrin-linked kinase is an adaptor with essential functions during mouse development. *Nature*. 2009;461(7266):1002–6.
 86. Mathew S, Chen X, Pozzi A, Zent R. Integrins in renal development. *Pediatr Nephrol*. 2012;27(6):891–900.
 87. Vrontou S, Petrou P, Meyer BI, Galanopoulos VK, Imai K, Yanagi M, et al. *Fras1* deficiency results in cryptophthalmos, renal agenesis and blebbed phenotype in mice. *Nat Genet*. 2003;34(2):209–14.
 88. McGregor L, Makela V, Darling SM, Vrontou S, Chalepakis G, Roberts C, et al. Fraser syndrome and mouse blebbed phenotype caused by mutations in *FRAS1/Fras1* encoding a putative extracellular matrix protein. *Nat Genet*. 2003;34(2):203–8.
 89. Muller U, Wang D, Denda S, Meneses JJ, Pedersen RA, Reichardt LF. Integrin alpha8beta1 is critically important for epithelial-mesenchymal interactions during kidney morphogenesis. *Cell*. 1997;88(5):603–13.
 90. Bader BL, Smyth N, Nedbal S, Miosge N, Baranowsky A, Mokkupati S, et al. Compound genetic ablation of nidogen 1 and 2 causes basement membrane defects and perinatal lethality in mice. *Mol Cell Biol*. 2005;25(15):6846–56.
 91. Nigam A, Knoers N, Renkema KY. Impact of next generation sequencing on our understanding of CAKUT. *Semin Cell Dev Biol*. 2019;91:104–10.
 92. Saisawat P, Tasic V, Vega-Warner V, Kehinde EO, Gunther B, Airik R, et al. Identification of two novel CAKUT-causing genes by massively parallel exon resequencing of candidate genes in patients with unilateral renal agenesis. *Kidney Int*. 2012;81(2):196–200.
 93. Meeus L, Gilbert B, Rydlewski C, Parma J, Roussie AL, Abramowicz M, et al. Characterization of a novel loss of function mutation of *PAX8* in a familial case of congenital hypothyroidism with in-place, normal-sized thyroid. *J Clin Endocrinol Metab*. 2004;89(9):4285–91.
 94. Hwang DY, Dworschak GC, Kohl S, Saisawat P, Vivante A, Hilger AC, et al. Mutations in 12 known dominant disease-causing genes clarify many congenital anomalies of the kidney and urinary tract. *Kidney Int*. 2014;85(6):1429–33.
 95. Little SE, Hanks SP, King-Underwood L, Jones C, Rapley EA, Rahman N, et al. Frequency and heritability of *WT1* mutations in nonsyndromic Wilms' tumor patients: a UK Children's Cancer Study Group Study. *J Clin Oncol*. 2004;22(20):4140–6.
 96. Dode C, Levilliers J, Dupont JM, De Paepe A, Le Du N, Soussi-Yanicostas N, et al. Loss-of-function mutations in *FGFR1* cause autosomal dominant Kallmann syndrome. *Nat Genet*. 2003;33(4):463–5.
 97. Kohl S, Hwang DY, Dworschak GC, Hilger AC, Saisawat P, Vivante A, et al. Mild recessive mutations in six Fraser syndrome-related genes cause isolated congenital anomalies of the kidney and urinary tract. *J Am Soc Nephrol*. 2014;25(9):1917–22.
 98. Skinner MA, Safford SD, Reeves JG, Jackson ME, Freemerman AJ. Renal aplasia in humans is associated with *RET* mutations. *Am J Hum Genet*. 2008;82(2):344–51.
 99. Jadeja S, Smyth I, Pitera JE, Taylor MS, van Haelst M, Bentley E, et al. Identification of a new gene mutated in Fraser syndrome and mouse myelencephalic blebs. *Nat Genet*. 2005;37(5):520–5.
 100. Humbert C, Silbermann F, Morar B, Parisot M, Zarhrate M, Masson C, et al. Integrin alpha 8 recessive mutations are responsible for bilateral renal agenesis in humans. *Am J Hum Genet*. 2014;94(2):288–94.
 101. Albuissou J, Pecheux C, Carel JC, Lacombe D, Leheup B, Lapuzina P, et al. Kallmann syndrome: 14 novel mutations in *KAL1* and *FGFR1* (*KAL2*). *Hum Mutat*. 2005;25(1):98–9.
 102. Heidet L, Moriniere V, Henry C, De Tomasi L, Reilly ML, Humbert C, et al. Targeted exome sequencing identifies *PBX1* as involved in monogenic congenital anomalies of the kidney and urinary tract. *J Am Soc Nephrol*. 2017;28(10):2901–14.
 103. Uy N, Reidy K. Developmental genetics and congenital anomalies of the kidney and urinary tract. *J Pediatr Genet*. 2016;5(1):51–60.
 104. Sanna-Cherchi S, Sampogna RV, Papeta N, Burgess KE, Nees SN, Perry BJ, et al. Mutations in *DSTYK* and dominant urinary tract malformations. *N Engl J Med*. 2013;369(7):621–9.
 105. Weber S, Moriniere V, Knuppel T, Charbit M, Dusek J, Ghiggeri GM, et al. Prevalence of mutations in renal developmental genes in children with renal hypodysplasia: results of the ESCAPE study. *J Am Soc Nephrol*. 2006;17(10):2864–70.
 106. Zhang Z, Iglesias D, Eliopoulos N, El Kares R, Chu L, Romagnani P, et al. A variant *OSR1* allele which disturbs *OSR1* mRNA expression in renal progenitor cells is associated with reduction of newborn kidney size and function. *Hum Mol Genet*. 2011;20(21):4167–74.
 107. Favor J, Sandulache R, Neuhauser-Klaus A, Pretsch W, Chatterjee B, Senft E, et al. The mouse *Pax2*(1^{Neu}) mutation is identical to a human *PAX2* mutation in a family with renal-coloboma syndrome and results in developmental defects of the brain, ear, eye, and kidney. *Proc Natl Acad Sci U S A*. 1996;93(24):13870–5.

108. Zhang Z, Quinlan J, Hoy W, Hughson MD, Lemire M, Hudson T, et al. A common RET variant is associated with reduced newborn kidney size and function. *J Am Soc Nephrol.* 2008;19(10):2027-34.
109. Chatterjee R, Ramos E, Hoffman M, VanWinkle J, Martin DR, Davis TK, et al. Traditional and targeted exome sequencing reveals common, rare and novel functional deleterious variants in RET-signaling complex in a cohort of living US patients with urinary tract malformations. *Hum Genet.* 2012;131(11):1725-38.
110. Barbacci E, Chalkiadaki A, Masdeu C, Haumaitre C, Lokmane L, Loirat C, et al. HNF1beta/TCF2 mutations impair transactivation potential through altered co-regulator recruitment. *Hum Mol Genet.* 2004;13(24):3139-49.
111. Weber S, Taylor JC, Winyard P, Baker KF, Sullivan-Brown J, Schild R, et al. SIX2 and BMP4 mutations associate with anomalous kidney development. *J Am Soc Nephrol.* 2008;19(5):891-903.
112. Jenkins D, Bitner-Glindzicz M, Malcolm S, Hu CC, Allison J, Winyard PJ, et al. De novo Uroplakin IIIa heterozygous mutations cause human renal adysplasia leading to severe kidney failure. *J Am Soc Nephrol.* 2005;16(7):2141-9.
113. Nixon TRW, Richards A, Towns LK, Fuller G, Abbs S, Alexander P, et al. Bone morphogenetic protein 4 (BMP4) loss-of-function variant associated with autosomal dominant Stickler syndrome and renal dysplasia. *Eur J Hum Genet.* 2019;27(3):369-77.
114. Brzoska HL, d'Esposito AM, Kolatsi-Joannou M, Patel V, Igarashi P, Lei Y, et al. Planar cell polarity genes *Celsr1* and *Vangl2* are necessary for kidney growth, differentiation, and rostrocaudal patterning. *Kidney Int.* 2016;90(6):1274-84.
115. Schedl A. Renal abnormalities and their developmental origin. *Nat Rev Genet.* 2007;8(10):791-802.
116. Thomas R, Sanna-Cherchi S, Warady BA, Furth SL, Kaskel FJ, Gharavi AG. HNF1B and PAX2 mutations are a common cause of renal hypodysplasia in the CKiD cohort. *Pediatr Nephrol.* 2011;26(6):897-903.
117. Paces-Fessy M, Fabre M, Lesaulnier C, Cereghini S. *Hnf1b* and *Pax2* cooperate to control different pathways in kidney and ureter morphogenesis. *Hum Mol Genet.* 2012;21(14):3143-55.
118. Barbacci E, Reber M, Ott MO, Breillat C, Huetz F, Cereghini S. Variant hepatocyte nuclear factor 1 is required for visceral endoderm specification. *Development.* 1999;126(21):4795-805.
119. Lokmane L, Heliot C, Garcia-Villalba P, Fabre M, Cereghini S. vHNF1 functions in distinct regulatory circuits to control ureteric bud branching and early nephrogenesis. *Development.* 2010;137(2):347-57.
120. Heliot C, Desgrange A, Buisson I, Prunskaitė-Hyyryläinen R, Shan J, Vainio S, et al. HNF1B controls proximal-intermediate nephron segment identity in vertebrates by regulating Notch signalling components and *Irx1/2*. *Development.* 2013;140(4):873-85.
121. Desgrange A, Heliot C, Skovorodkin I, Akram SU, Heikkilä J, Ronkainen VP, et al. HNF1B controls epithelial organization and cell polarity during ureteric bud branching and collecting duct morphogenesis. *Development.* 2017;144(24):4704-19.
122. Reginensi A, Clarkson M, Neirijnck Y, Lu B, Ohyama T, Groves AK, et al. SOX9 controls epithelial branching by activating RET effector genes during kidney development. *Hum Mol Genet.* 2011;20(6):1143-53.
123. Liu J, Krautzberger AM, Sui SH, Hofmann OM, Chen Y, Baetscher M, et al. Cell-specific translational profiling in acute kidney injury. *J Clin Invest.* 2014;124(3):1242-54.
124. Kumar S, Liu J, Pang P, Krautzberger AM, Reginensi A, Akiyama H, et al. Sox9 activation highlights a cellular pathway of renal repair in the acutely injured mammalian kidney. *Cell Rep.* 2015;12(8):1325-38.
125. Nagata M, Nakauchi H, Nakayama K, Nakayama K, Loh D, Watanabe T. Apoptosis during an early stage of nephrogenesis induces renal hypoplasia in *bcl-2*-deficient mice. *Am J Pathol.* 1996;148(5):1601-11.
126. Self M, Lagutin OV, Bowling B, Hendrix J, Cai Y, Dressler GR, et al. *Six2* is required for suppression of nephrogenesis and progenitor renewal in the developing kidney. *EMBO J.* 2006;25(21):5214-28.
127. Rosselot C, Spraggon L, Chia I, Batourina E, Riccio P, Lu B, et al. Non-cell-autonomous retinoid signaling is crucial for renal development. *Development.* 2010;137(2):283-92.
128. Nishinakamura R, Sakaguchi M. BMP signaling and its modifiers in kidney development. *Pediatr Nephrol.* 2014;29(4):681-6.
129. Oxburgh L, Brown AC, Muthukrishnan SD, Fetting JL. Bone morphogenetic protein signaling in nephron progenitor cells. *Pediatr Nephrol.* 2014;29(4):531-6.
130. Wang Y, Zhou CJ, Liu Y. Wnt signaling in kidney development and disease. *Prog Mol Biol Transl Sci.* 2018;153:181-207.
131. Halt K, Vainio S. Coordination of kidney organogenesis by Wnt signaling. *Pediatr Nephrol.* 2014;29(4):737-44.
132. Brown AC, Muthukrishnan SD, Guay JA, Adams DC, Schafer DA, Fetting JL, et al. Role for compartmentalization in nephron progenitor differentiation. *Proc Natl Acad Sci U S A.* 2013;110(12):4640-5.
133. Dudley AT, Lyons KM, Robertson EJ. A requirement for bone morphogenetic protein-7 during development of the mammalian kidney and eye. *Genes Dev.* 1995;9:2795-807.
134. Luo G, Hofmann C, Bronckers AL, Sohocki M, Bradley A, Karsenty G. BMP-7 is an inducer of nephrogenesis, and is also required for eye development and skeletal patterning. *Genes Dev.* 1995;9(22):2808-20.
135. Tomita M, Asada M, Asada N, Nakamura J, Oguchi A, Higashi AY, et al. *Bmp7* maintains undiffer-

- entiated kidney progenitor population and determines nephron numbers at birth. *PLoS One*. 2013; 8(8):e73554.
136. Oxburgh L, Dudley AT, Godin RE, Koonce CH, Islam A, Anderson DC, et al. BMP4 substitutes for loss of BMP7 during kidney development. *Dev Biol*. 2005;286(2):637–46.
 137. Goncalves A, Zeller R. Genetic analysis reveals an unexpected role of BMP7 in initiation of ureteric bud outgrowth in mouse embryos. *PLoS One*. 2011;6(4):e19370.
 138. Hartwig S, Bridgewater D, Di Giovanni V, Cain J, Mishina Y, Rosenblum ND. BMP receptor ALK3 controls collecting system development. *J Am Soc Nephrol*. 2008;19(1):117–24.
 139. Sakaguchi M, Sharmin S, Taguchi A, Ohmori T, Fujimura S, Abe T, et al. The phosphatase Dullard negatively regulates BMP signalling and is essential for nephron maintenance after birth. *Nat Commun*. 2013;4:1398.
 140. Ikeya M, Kawada M, Kiyonari H, Sasai N, Nakao K, Furuta Y, et al. Essential pro-Bmp roles of cross-veinless 2 in mouse organogenesis. *Development*. 2006;133(22):4463–73.
 141. Ikeya M, Fukushima K, Kawada M, Onishi S, Furuta Y, Yonemura S, et al. Cv2, functioning as a pro-BMP factor via twisted gastrulation, is required for early development of nephron precursors. *Dev Biol*. 2010;337(2):405–14.
 142. Muthukrishnan SD, Yang X, Friesel R, Oxburgh L. Concurrent BMP7 and FGF9 signalling governs AP-1 function to promote self-renewal of nephron progenitor cells. *Nat Commun*. 2015;6:10027.
 143. Saxen L, Lehtonen E. Transfilter induction of kidney tubules as a function of the extent and duration of intercellular contacts. *J Embryol Exp Morphol*. 1978;47:97–109.
 144. Itaranta P, Lin Y, Perasaari J, Roel G, Destree O, Vainio S. Wnt-6 is expressed in the ureter bud and induces kidney tubule development in vitro. *Genesis*. 2002;32(4):259–68.
 145. Stark K, Vainio S, Vassileva G, McMahon AP. Epithelial transformation of metanephric mesenchyme in the developing kidney regulated by Wnt-4. *Nature*. 1994;372(6507):679–83.
 146. Park JS, Valerius MT, McMahon AP. Wnt/beta-catenin signaling regulates nephron induction during mouse kidney development. *Development*. 2007;134(13):2533–9.
 147. Kuure S, Popsueva A, Jakobson M, Sainio K, Sariola H. Glycogen synthase kinase-3 inactivation and stabilization of beta-catenin induce nephron differentiation in isolated mouse and rat kidney mesenchymes. *J Am Soc Nephrol*. 2007;18(4):1130–9.
 148. Marose TD, Merkel CE, McMahon AP, Carroll TJ. Beta-catenin is necessary to keep cells of ureteric bud/Wolffian duct epithelium in a precursor state. *Dev Biol*. 2008;314(1):112–26.
 149. Bridgewater D, Di Giovanni V, Cain JE, Cox B, Jakobson M, Sainio K, et al. beta-catenin causes renal dysplasia via upregulation of Tgfbeta2 and Dkk1. *J Am Soc Nephrol*. 2011;22(4):718–31.
 150. Song R, El-Dahr SS, Yosypiv IV. Receptor tyrosine kinases in kidney development. *J Signal Transduct*. 2011;2011:869281.
 151. Jain S, Encinas M, Johnson EM Jr, Milbrandt J. Critical and distinct roles for key RET tyrosine docking sites in renal development. *Genes Dev*. 2006;20(3):321–33.
 152. Jain S, Knoten A, Hoshi M, Wang H, Vohra B, Heuckeroth RO, et al. Organotypic specificity of key RET adaptor-docking sites in the pathogenesis of neurocristopathies and renal malformations in mice. *J Clin Invest*. 2010;120(3):778–90.
 153. de Graaff E, Srinivas S, Kilkenny C, D'Agati V, Mankoo BS, Costantini F, et al. Differential activities of the RET tyrosine kinase receptor isoforms during mammalian embryogenesis. *Genes Dev*. 2001;15(18):2433–44.
 154. Jijiwa M, Fukuda T, Kawai K, Nakamura A, Kurokawa K, Murakumo Y, et al. A targeting mutation of tyrosine 1062 in Ret causes a marked decrease of enteric neurons and renal hypoplasia. *Mol Cell Biol*. 2004;24(18):8026–36.
 155. Fisher CE, Michael L, Barnett MW, Davies JA. Erk MAP kinase regulates branching morphogenesis in the developing mouse kidney. *Development*. 2001;128(21):4329–38.
 156. Tang MJ, Cai Y, Tsai SJ, Wang YK, Dressler GR. Ureteric bud outgrowth in response to RET activation is mediated by phosphatidylinositol 3-kinase. *Dev Biol*. 2002;243(1):128–36.
 157. Willecke R, Heuberger J, Grossmann K, Michos O, Schmidt-Ott K, Walentin K, et al. The tyrosine phosphatase Shp2 acts downstream of GDNF/Ret in branching morphogenesis of the developing mouse kidney. *Dev Biol*. 2011;360(2):310–7.
 158. Ihermann-Hella A, Lume M, Miinalainen IJ, Pirttiniemi A, Gui Y, Peranen J, et al. Mitogen-activated protein kinase (MAPK) pathway regulates branching by remodeling epithelial cell adhesion. *PLoS Genet*. 2014;10(3):e1004193.
 159. Kim D, Dressler GR. PTEN modulates GDNF/RET mediated chemotaxis and branching morphogenesis in the developing kidney. *Dev Biol*. 2007;307(2):290–9.
 160. Enderle L, McNeill H. Hippo gains weight: added insights and complexity to pathway control. *Sci Signal*. 2013;6(296):re7.
 161. Reginensi A, Enderle L, Gregorieff A, Johnson RL, Wrana JL, McNeill H. A critical role for NF2 and the Hippo pathway in branching morphogenesis. *Nat Commun*. 2016;7:12309.
 162. McNeill H, Reginensi A. Lats1/2 regulate Yap/Taz to control nephron progenitor epithelialization and inhibit myofibroblast formation. *J Am Soc Nephrol*. 2017;28(3):852–61.
 163. Reginensi A, Scott RP, Gregorieff A, Bagherie-Lachidan M, Chung C, Lim DS, et al. Yap- and Cdc42-dependent nephrogenesis and morphogenesis

- during mouse kidney development. *PLoS Genet.* 2013;9(3):e1003380.
164. Hossain Z, Ali SM, Ko HL, Xu J, Ng CP, Guo K, et al. Glomerulocystic kidney disease in mice with a targeted inactivation of *Wwtr1*. *Proc Natl Acad Sci U S A.* 2007;104(5):1631–6.
 165. Makita R, Uchijima Y, Nishiyama K, Amano T, Chen Q, Takeuchi T, et al. Multiple renal cysts, urinary concentration defects, and pulmonary emphysematous changes in mice lacking *TAZ*. *Am J Physiol Renal Physiol.* 2008;294(3):F542–53.
 166. Yates LL, Papakrivopoulou J, Long DA, Goggolidou P, Connolly JO, Woolf AS, et al. The planar cell polarity gene *Vangl2* is required for mammalian kidney-branching morphogenesis and glomerular maturation. *Hum Mol Genet.* 2010;19(23):4663–76.
 167. Kuure S, Cebrian C, Machingo Q, Lu BC, Chi X, Hyink D, et al. Actin depolymerizing factors *cofilin1* and *destrin* are required for ureteric bud branching morphogenesis. *PLoS Genet.* 2010;6(10):e1001176.
 168. Marciano DK, Brakeman PR, Lee CZ, Spivak N, Eastburn DJ, Bryant DM, et al. *p120* catenin is required for normal renal tubulogenesis and glomerulogenesis. *Development.* 2011;138(10):2099–109.
 169. Mackie GG, Stephens FD. Duplex kidneys: a correlation of renal dysplasia with position of the ureteral orifice. *J Urol.* 1975;114(2):274–80.
 170. Miyazaki Y, Oshima K, Fogo A, Hogan BL, Ichikawa I. Bone morphogenetic protein 4 regulates the budding site and elongation of the mouse ureter. *J Clin Invest.* 2000;105(7):863–73.
 171. Bataourina E, Choi C, Paragas N, Bello N, Hensle T, Costantini FD, et al. Distal ureter morphogenesis depends on epithelial cell remodeling mediated by vitamin A and *Ret*. *Nat Genet.* 2002;32(1):109–15.
 172. Bataourina E, Tsai S, Lambert S, Sprenkle P, Viana R, Dutta S, et al. Apoptosis induced by vitamin A signaling is crucial for connecting the ureters to the bladder. *Nat Genet.* 2005;37(10):1082–9.
 173. Chia I, Grote D, Marcotte M, Bataourina E, Mendelsohn C, Bouchard M. Nephric duct insertion is a crucial step in urinary tract maturation that is regulated by a *Gata3-Raldh2-Ret* molecular network in mice. *Development.* 2011;138(10):2089–97.
 174. Kumar A, Kopra J, Varendi K, Porokuokka LL, Panhelainen A, Kuure S, et al. *GDNF* overexpression from the native locus reveals its role in the nigrostriatal dopaminergic system function. *PLoS Genet.* 2015;11(12):e1005710.
 175. Li H, Jakobson M, Ola R, Gui Y, Kumar A, Sipilä P, Sariola H, Kuure S, Andressoo JO. Development of the urogenital system is regulated via the 3'UTR of *GDNF*. *Sci Rep.* 2019;9(1):5302.
 176. Mendelsohn C, Lohnes D, Decimo D, Lufkin T, LeMeur M, Chambon P, et al. Function of the retinoic acid receptors (RARs) during development (II). Multiple abnormalities at various stages of organogenesis in RAR double mutants. *Development.* 1994;120(10):2749–71.
 177. Airik R, Trowe MO, Foik A, Farin HF, Petry M, Schuster-Gossler K, et al. Hydrourteronephrosis due to loss of *Sox9*-regulated smooth muscle cell differentiation of the ureteric mesenchyme. *Hum Mol Genet.* 2010;19(24):4918–29.
 178. Neirijnck Y, Reginensi A, Renkema KY, Massa F, Kozlov VM, Dhib H, et al. *Sox11* gene disruption causes congenital anomalies of the kidney and urinary tract (CAKUT). *Kidney Int.* 2018;93(5):1142–53.
 179. Airik R, Bussen M, Singh MK, Petry M, Kispert A. *Tbx18* regulates the development of the ureteral mesenchyme. *J Clin Invest.* 2006;116(3):663–74.
 180. Vivante A, Kleppa MJ, Schulz J, Kohl S, Sharma A, Chen J, et al. Mutations in *TBX18* cause dominant urinary tract malformations via transcriptional dysregulation of ureter development. *Am J Hum Genet.* 2015;97(2):291–301.
 181. Jeanpierre C, Mace G, Parisot M, Moriniere V, Pawtowsky A, Benabou M, et al. *RET* and *GDNF* mutations are rare in fetuses with renal agenesis or other severe kidney development defects. *J Med Genet.* 2011;48(7):497–504.
 182. Fernbach SK, Feinstein KA, Spencer K, Lindstrom CA. Ureteral duplication and its complications. *Radiographics.* 1997;17(1):109–27.
 183. Shakya R, Jho EH, Kotka P, Wu Z, Kholodilov N, Burke R, et al. The role of *GDNF* in patterning the excretory system. *Dev Biol.* 2005;283:70–84.
 184. Sainio K, Suvanto P, Davies J, Wartiovaara J, Wartiovaara K, Saarna M, et al. Glial-cell-line-derived neurotrophic factor is required for bud initiation from ureteric epithelium. *Development.* 1997;124(20):4077–87.
 185. Grieshammer U, Le M, Plump AS, Wang F, Tessier-Lavigne M, Martin GR. *SLIT2*-mediated *ROBO2* signaling restricts kidney induction to a single site. *Dev Cell.* 2004;6(5):709–17.
 186. Wainwright EN, Wilhelm D, Combes AN, Little MH, Koopman P. *ROBO2* restricts the nephrogenic field and regulates Wolffian duct-nephrogenic cord separation. *Dev Biol.* 2015;404(2):88–102.
 187. Kume T, Deng K, Hogan BL. Murine forkhead/winged helix genes *Foxc1* (*Mf1*) and *Foxc2* (*Mfh1*) are required for the early organogenesis of the kidney and urinary tract. *Development.* 2000;127(7):1387–95.
 188. Chi L, Zhang S, Lin Y, Prunskaitė-Hyyryläinen R, Vuolteenaho R, Itaranta P, et al. *Sprouty* proteins regulate ureteric branching by coordinating reciprocal epithelial *Wnt11*, mesenchymal *Gdnf* and stromal *Fgf7* signalling during kidney development. *Development.* 2004;131(14):3345–56.
 189. Basson MA, Akbulut S, Watson-Johnson J, Simon R, Carroll TJ, Shakya R, et al. *Sprouty1* is a critical regulator of *GDNF/RET*-mediated kidney induction. *Dev Cell.* 2005;8(2):229–39.
 190. Rozen EJ, Schmidt H, Dolcet X, Basson MA, Jain S, Encinas M. Loss of *Sprouty1* rescues renal agenesis caused by *Ret* mutation. *J Am Soc Nephrol.* 2009;20(2):255–9.

191. Michos O, Cebrian C, Hyink D, Grieshammer U, Williams L, D'Agati V, et al. Kidney development in the absence of Gdnf and Spry1 requires Fgf10. *PLoS Genet.* 2010;6(1):e1000809.
192. Maeshima A, Sakurai H, Choi Y, Kitamura S, Vaughn DA, Tee JB, et al. Glial cell-derived neurotrophic factor independent ureteric bud outgrowth from the Wolffian duct. *J Am Soc Nephrol.* 2007;18(12):3147–55.
193. Peng Y, Clark C, Luong R, Tu WH, Lee J, Johnson DT, et al. The leucine zipper putative tumor suppressor 2 protein LZTS2 regulates kidney development. *J Biol Chem.* 2011;286(46):40331–42.
194. Kaku Y, Ohmori T, Kudo K, Fujimura S, Suzuki K, Evans SM, et al. Islet1 deletion causes kidney agenesis and hydronephrosis resembling CAKUT. *J Am Soc Nephrol.* 2013;24(8):1242–9.
195. Tabatabaeifar M, Schlingmann KP, Litwin M, Emre S, Bakkaloglu A, Mehls O, et al. Functional analysis of BMP4 mutations identified in pediatric CAKUT patients. *Pediatr Nephrol.* 2009;24(12):2361–8.
196. Gimelli S, Caridi G, Beri S, McCracken K, Bocciardi R, Zordan P, et al. Mutations in SOX17 are associated with congenital anomalies of the kidney and the urinary tract. *Hum Mutat.* 2010;31(12):1352–9.
197. Weber S, Landwehr C, Renkert M, Hoischen A, Wuhl E, Denecke J, et al. Mapping candidate regions and genes for congenital anomalies of the kidneys and urinary tract (CAKUT) by array-based comparative genomic hybridization. *Nephrol Dial Transplant.* 2011;26(1):136–43.
198. Bertoli-Avella AM, Conte ML, Punzo F, de Graaf BM, Lama G, La Manna A, et al. ROBO2 gene variants are associated with familial vesicoureteral reflux. *J Am Soc Nephrol.* 2008;19(4):825–31.
199. Lu W, van Eerde AM, Fan X, Quintero-Rivera F, Kulkarni S, Ferguson H, et al. Disruption of ROBO2 is associated with urinary tract anomalies and confers risk of vesicoureteral reflux. *Am J Hum Genet.* 2007;80(4):616–32.
200. van Eerde AM, Duran K, van Riel E, de Kovel CG, Koeleman BP, Knoers NV, et al. Genes in the ureteric budding pathway: association study on vesico-ureteral reflux patients. *PLoS One.* 2012;7(4):e31327.
201. Siebert JR. Perinatal, fetal and embryonic autopsy. In: Gilbert-Barness E, editor. *Potter's pathology of the fetus, infant and child.* 2nd ed. Philadelphia: Elsevier; 2007. p. 695–736.
202. Tripathi P, Guo Q, Wang Y, Coussens M, Liapis H, Jain S, et al. Midline signaling regulates kidney positioning but not nephrogenesis through Shh. *Dev Biol.* 2010;340(2):518–27.
203. Abu-Abed S, Dolle P, Metzger D, Beckett B, Chambon P, Petkovich M. The retinoic acid-metabolizing enzyme, CYP26A1, is essential for normal hindbrain patterning, vertebral identity, and development of posterior structures. *Genes Dev.* 2001;15(2):226–40.
204. Sakai Y, Meno C, Fujii H, Nishino J, Shiratori H, Saijoh Y, et al. The retinoic acid-inactivating enzyme CYP26 is essential for establishing an uneven distribution of retinoic acid along the antero-posterior axis within the mouse embryo. *Genes Dev.* 2001;15(2):213–25.
205. Hatini V, Huh SO, Herzlinger D, Soares VC, Lai E. Essential role of stromal mesenchyme in kidney morphogenesis revealed by targeted disruption of Winged Helix transcription factor BF-2. *Genes Dev.* 1996;10(12):1467–78.
206. Levinson RS, Batourina E, Choi C, Vorontchikhina M, Kitajewski J, Mendelsohn CL. Foxd1-dependent signals control cellularity in the renal capsule, a structure required for normal renal development. *Development.* 2005;132(3):529–39.
207. Nicolaou N, Pulit SL, Nijman IJ, Monroe GR, Feitz WF, Schreuder MF, et al. Prioritization and burden analysis of rare variants in 208 candidate genes suggest they do not play a major role in CAKUT. *Kidney Int.* 2016;89(2):476–86.
208. Jing J, Pattaro C, Hoppmann A, Okada Y, Consortium CK, Fox CS, et al. Combination of mouse models and genomewide association studies highlights novel genes associated with human kidney function. *Kidney Int.* 2016;90(4):764–73.
209. Fetterman GH, Ravitch MM, Sherman FE. Cystic changes in fetal kidneys following ureteral ligation: studies by microdissection. *Kidney Int.* 1974;5(2):111–21.
210. Bergmann C, Guay-Woodford LM, Harris PC, Horie S, Peters DJM, Torres VE. Polycystic kidney disease. *Nat Rev Dis Primers.* 2018;4(1):50.
211. Kraus MR, Claudin S, Pfister Y, Di Maio M, Ulinski T, Constam D, et al. Two mutations in human BICC1 resulting in Wnt pathway hyperactivity associated with cystic renal dysplasia. *Hum Mutat.* 2012;33(1):86–90.
212. Groenen PM, Vanderlinden G, Devriendt K, Fryns JP, Van de Ven WJ. Rearrangement of the human CDC5L gene by a t(6;19)(p21;q13.1) in a patient with multicystic renal dysplasia. *Genomics.* 1998;49(2):218–29.
213. Schild R, Knuppel T, Konrad M, Bergmann C, Trautmann A, Kemper MJ, et al. Double homozygous missense mutations in DACH1 and BMP4 in a patient with bilateral cystic renal dysplasia. *Nephrol Dial Transplant.* 2013;28(1):227–32.
214. Verdeguer F, Le Corre S, Fischer E, Callens C, Garbay S, Doyen A, et al. A mitotic transcriptional switch in polycystic kidney disease. *Nat Med.* 2010;16(1):106–10.
215. Heidet L, Decramer S, Pawtowski A, Moriniere V, Bandin F, Knebelmann B, et al. Spectrum of HNF1B mutations in a large cohort of patients who harbor renal diseases. *Clin J Am Soc Nephrol.* 2010;5(6):1079–90.
216. Groenen PM, Garcia E, Debeer P, Devriendt K, Fryns JP, Van de Ven WJ. Structure, sequence, and chromosome 19 localization of human USF2 and

- its rearrangement in a patient with multicystic renal dysplasia. *Genomics*. 1996;38(2):141–8.
217. Cordido A, Besada-Cerecedo L, Garcia-Gonzalez MA. The genetic and cellular basis of autosomal dominant polycystic kidney disease—a primer for clinicians. *Front Pediatr*. 2017;5:279.
 218. Nagao S, Kugita M, Yoshihara D, Yamaguchi T. Animal models for human polycystic kidney disease. *Exp Anim*. 2012;61(5):477–88.
 219. Porath B, Gainullin VG, Cornec-Le Gall E, Dillinger EK, Heyer CM, Hopp K, et al. Mutations in GANAB, encoding the glucosidase IIalpha subunit, cause autosomal-dominant polycystic kidney and liver disease. *Am J Hum Genet*. 2016;98(6):1193–207.
 220. Bergmann C. Genetics of autosomal recessive polycystic kidney disease and its differential diagnoses. *Front Pediatr*. 2017;5:221.
 221. Lu H, Galeano MCR, Ott E, Kaeslin G, Kausalya PJ, Kramer C, et al. Mutations in DZIP1L, which encodes a ciliary-transition-zone protein, cause autosomal recessive polycystic kidney disease. *Nat Genet*. 2017;49(7):1025–34.
 222. Horikawa Y, Iwasaki N, Hara M, Furuta H, Hinokio Y, Cockburn BN, et al. Mutation in hepatocyte nuclear factor-1 beta gene (TCF2) associated with MODY. *Nat Genet*. 1997;17(4):384–5.
 223. Lantinga-van Leeuwen IS, Leonhard WN, van der Wal A, Breuning MH, de Heer E, Peters DJ. Kidney-specific inactivation of the Pkd1 gene induces rapid cyst formation in developing kidneys and a slow onset of disease in adult mice. *Hum Mol Genet*. 2007;16(24):3188–96.
 224. Mochizuki T, Wu G, Hayashi T, Xenophontos SL, Veldhuisen B, Saris JJ, et al. PKD2, a gene for polycystic kidney disease that encodes an integral membrane protein. *Science*. 1996;272(5266):1339–42.
 225. Wu G, D'Agati V, Cai Y, Markowitz G, Park JH, Reynolds DM, et al. Somatic inactivation of Pkd2 results in polycystic kidney disease. *Cell*. 1998;93(2):177–88.
 226. Ward CJ, Hogan MC, Rossetti S, Walker D, Sneddon T, Wang X, et al. The gene mutated in autosomal recessive polycystic kidney disease encodes a large, receptor-like protein. *Nat Genet*. 2002;30(3):259–69.
 227. Lin F, Hiesberger T, Cordes K, Sinclair AM, Goldstein LS, Somlo S, et al. Kidney-specific inactivation of the KIF3A subunit of kinesin-II inhibits renal ciliogenesis and produces polycystic kidney disease. *Proc Natl Acad Sci U S A*. 2003;100(9):5286–91.
 228. Fedeles SV, Tian X, Gallagher AR, Mitobe M, Nishio S, Lee SH, et al. A genetic interaction network of five genes for human polycystic kidney and liver diseases defines polycystin-1 as the central determinant of cyst formation. *Nat Genet*. 2011;43(7):639–47.
 229. Saburi S, Hester I, Fischer E, Pontoglio M, Eremina V, Gessler M, et al. Loss of Fat4 disrupts PCP signaling and oriented cell division and leads to cystic kidney disease. *Nat Genet*. 2008;40(8):1010–5.
 230. Mao Y, Mulvaney J, Zakaria S, Yu T, Morgan KM, Allen S, et al. Characterization of a Dchs1 mutant mouse reveals requirements for Dchs1-Fat4 signaling during mammalian development. *Development*. 2011;138(5):947–57.
 231. Nechiporuk T, Fernandez TE, Vasioukhin V. Failure of epithelial tube maintenance causes hydrocephalus and renal cysts in Dlg5^{-/-} mice. *Dev Cell*. 2007;13(3):338–50.
 232. Cano-Gauci DF, Song HH, Yang H, McKerlie C, Choo B, Shi W, et al. Glypican-3-deficient mice exhibit developmental overgrowth and some of the abnormalities typical of Simpson-Golabi-Behmel syndrome. *J Cell Biol*. 1999;146(1):255–64.
 233. Holmberg C, Jalanko H. Congenital nephrotic syndrome and recurrence of proteinuria after renal transplantation. *Pediatr Nephrol*. 2014;29(12):2309–17.
 234. Spahiu L, Merovci B, Jashari H, Kepuska AB, Rugova BE. Congenital nephrotic syndrome—Finish type. *Med Arch*. 2016;70(3):232–4.
 235. Kestila M, Lenkkeri U, Mannikko M, Lamerdin J, McCready P, Putaala H, et al. Positionally cloned gene for a novel glomerular protein—nephrin—is mutated in congenital nephrotic syndrome. *Mol Cell*. 1998;1(4):575–82.
 236. Lenkkeri U, Mannikko M, McCready P, Lamerdin J, Gribouval O, Niaudet PM, et al. Structure of the gene for congenital nephrotic syndrome of the Finnish type (NPHS1) and characterization of mutations. *Am J Hum Genet*. 1999;64(1):51–61.
 237. Hinkes BG, Mucha B, Vlangos CN, Gbadegesin R, Liu J, Hasselbacher K, et al. Nephrotic syndrome in the first year of life: two thirds of cases are caused by mutations in 4 genes (NPHS1, NPHS2, WT1, and LAMB2). *Pediatrics*. 2007;119(4):e907–19.
 238. Cil O, Besbas N, Duzova A, Topaloglu R, Peco-Antic A, Korkmaz E, et al. Genetic abnormalities and prognosis in patients with congenital and infantile nephrotic syndrome. *Pediatr Nephrol*. 2015;30(8):1279–87.
 239. Boute N, Gribouval O, Roselli S, Benessy F, Lee H, Fuchshuber A, et al. NPHS2, encoding the glomerular protein podocin, is mutated in autosomal recessive steroid-resistant nephrotic syndrome. *Nat Genet*. 2000;24(4):349–54.
 240. Gbadegesin R, Hinkes BG, Hoskins BE, Vlangos CN, Heeringa SF, Liu J, et al. Mutations in PLCE1 are a major cause of isolated diffuse mesangial sclerosis (IDMS). *Nephrol Dial Transplant*. 2008;23(4):1291–7.
 241. Jeanpierre C, Denamur E, Henry I, Cabanis MO, Luce S, Cecille A, et al. Identification of constitutional WT1 mutations, in patients with isolated diffuse mesangial sclerosis, and analysis of genotype/phenotype correlations by use of a computerized mutation database. *Am J Hum Genet*. 1998;62(4):824–33.
 242. Gee HY, Sadowski CE, Aggarwal PK, Porath JD, Yakulov TA, Schueler M, et al. FAT1 muta-

- tions cause a glomerulotubular nephropathy. *Nat Commun.* 2016;7:10822.
243. Zenker M, Aigner T, Wendler O, Tralau T, Muntefering H, Fenski R, et al. Human laminin beta2 deficiency causes congenital nephrosis with mesangial sclerosis and distinct eye abnormalities. *Hum Mol Genet.* 2004;13(21):2625–32.
 244. Kashtan CE, Ding J, Garosi G, Heidet L, Massella L, Nakanishi K, et al. Alport syndrome: a unified classification of genetic disorders of collagen IV alpha345: a position paper of the Alport Syndrome Classification Working Group. *Kidney Int.* 2018;93(5):1045–51.
 245. Putaala H, Soininen R, Kilpelainen P, Wartiovaara J, Tryggvason K. The murine nephrin gene is specifically expressed in kidney, brain and pancreas: inactivation of the gene leads to massive proteinuria and neonatal death. *Hum Mol Genet.* 2001;10(1):1–8.
 246. Ratelade J, Lavin TA, Muda AO, Morisset L, Mollet G, Boyer O, et al. Maternal environment interacts with modifier genes to influence progression of nephrotic syndrome. *J Am Soc Nephrol.* 2008;19(8):1491–9.
 247. Noakes PG, Miner JH, Gautam M, Cunningham JM, Sanes JR, Merlie JP. The renal glomerulus of mice lacking s-laminin/laminin beta 2: nephrosis despite molecular compensation by laminin beta 1. *Nat Genet.* 1995;10(4):400–6.
 248. Jarad G, Cunningham J, Shaw AS, Miner JH. Proteinuria precedes podocyte abnormalities in *Lamb2*^{-/-} mice, implicating the glomerular basement membrane as an albumin barrier. *J Clin Invest.* 2006;116(8):2272–9.
 249. Kang JS, Wang XP, Miner JH, Morello R, Sado Y, Abrahamson DR, et al. Loss of alpha3/alpha4(IV) collagen from the glomerular basement membrane induces a strain-dependent isoform switch to alpha5alpha6(IV) collagen associated with longer renal survival in *Col4a3*^{-/-} Alport mice. *J Am Soc Nephrol.* 2006;17(7):1962–9.
 250. Kim JM, Wu H, Green G, Winkler CA, Kopp JB, Miner JH, et al. CD2-associated protein haploinsufficiency is linked to glomerular disease susceptibility. *Science.* 2003;300(5623):1298–300.
 251. Machuca E, Benoit G, Antignac C. Genetics of nephrotic syndrome: connecting molecular genetics to podocyte physiology. *Hum Mol Genet.* 2009;18(R2):R185–94.
 252. Caban C, Khan N, Hasbani DM, Crino PB. Genetics of tuberous sclerosis complex: implications for clinical practice. *Appl Clin Genet.* 2017;10:1–8.
 253. Ogawa O, Eccles MR, Szeto J, McNoe LA, Yun K, Maw MA, et al. Relaxation of insulin-like growth factor II gene imprinting implicated in Wilms' tumour. *Nature.* 1993;362(6422):749–51.
 254. Hohenstein P, Pritchard-Jones K, Charlton J. The yin and yang of kidney development and Wilms' tumors. *Genes Dev.* 2015;29(5):467–82.
 255. Park S, Bernard A, Bove KE, Sens DA, Hazen-Martin DJ, Garvin AJ, et al. Inactivation of WT1 in nephrogenic rests, genetic precursors to Wilms' tumour. *Nat Genet.* 1993;5(4):363–7.
 256. Koesters R, Ridder R, Kopp-Schneider A, Betts D, Adams V, Niggl F, et al. Mutational activation of the beta-catenin proto-oncogene is a common event in the development of Wilms' tumors. *Cancer Res.* 1999;59(16):3880–2.
 257. Maiti S, Alam R, Amos CI, Huff V. Frequent association of beta-catenin and WT1 mutations in Wilms tumors. *Cancer Res.* 2000;60(22):6288–92.
 258. Rivera MN, Kim WJ, Wells J, Driscoll DR, Brannigan BW, Han M, et al. An X chromosome gene, WTX, is commonly inactivated in Wilms tumor. *Science.* 2007;315(5812):642–5.
 259. Major MB, Camp ND, Berndt JD, Yi X, Goldenberg SJ, Hubbert C, et al. Wilms tumor suppressor WTX negatively regulates WNT/beta-catenin signaling. *Science.* 2007;316(5827):1043–6.
 260. Rivera MN, Kim WJ, Wells J, Stone A, Burger A, Coffman EJ, et al. The tumor suppressor WTX shuttles to the nucleus and modulates WT1 activity. *Proc Natl Acad Sci U S A.* 2009;106(20):8338–43.
 261. Chen KS, Stroup EK, Budhipramono A, Rakheja D, Nichols-Vinueza D, Xu L, et al. Mutations in microRNA processing genes in Wilms tumors derepress the IGF2 regulator PLAG1. *Genes Dev.* 2018;32(15–16):996–1007.
 262. Pode-Shakked N, Shukrun R, Mark-Danieli M, Tsvetkov P, Bahar S, Pri-Chen S, et al. The isolation and characterization of renal cancer initiating cells from human Wilms' tumour xenografts unveils new therapeutic targets. *EMBO Mol Med.* 2013;5(1):18–37.
 263. Berry RL, Ozdemir DD, Aronow B, Lindstrom NO, Dudnakova T, Thornburn A, et al. Deducing the stage of origin of Wilms' tumours from a developmental series of *Wt1*-mutant mice. *Dis Model Mech.* 2015;8(8):903–17.
 264. Hu Q, Gao F, Tian W, Ruteshouser EC, Wang Y, Lazar A, et al. *Wt1* ablation and *Igf2* upregulation in mice result in Wilms tumors with elevated ERK1/2 phosphorylation. *J Clin Invest.* 2011;121(1):174–83.
 265. Huang L, Mokkaipati S, Hu Q, Ruteshouser EC, Hicks MJ, Huff V. Nephron progenitor but not stromal progenitor cells give rise to Wilms tumors in mouse models with beta-catenin activation or *Wt1* ablation and *Igf2* upregulation. *Neoplasia.* 2016;18(2):71–81.
 266. McDaniell R, Warthen DM, Sanchez-Lara PA, Pai A, Krantz ID, Piccoli DA, et al. NOTCH2 mutations cause Alagille syndrome, a heterogeneous disorder of the notch signaling pathway. *Am J Hum Genet.* 2006;79(1):169–73.
 267. Kuure S, Sainio K, Vuolteenaho R, Ilves M, Wartiovaara K, Immonen T, et al. Crosstalk between Jagged1 and GDNF/Ret/GFRalpha1 signalling regu-

- lates ureteric budding and branching. *Mech Dev.* 2005;122(6):765–80.
268. Cheng HT, Kim M, Valerius MT, Surendran K, Schuster-Gossler K, Gossler A, et al. Notch2, but not Notch1, is required for proximal fate acquisition in the mammalian nephron. *Development.* 2007;134(4):801–11.
269. McCright B, Gao X, Shen L, Lozier J, Lan Y, Maguire M, et al. Defects in development of the kidney, heart and eye vasculature in mice homozygous for a hypomorphic Notch2 mutation. *Development.* 2001;128(4):491–502.
270. Takamiya K, Kostourou V, Adams S, Jadeja S, Chalepakis G, Scambler PJ, et al. A direct functional link between the multi-PDZ domain protein GRIP1 and the Fraser syndrome protein Fras1. *Nat Genet.* 2004;36(2):172–7.
271. Vogel MJ, van Zon P, Brueton L, Gijzen M, van Tuil MC, Cox P, et al. Mutations in GRIP1 cause Fraser syndrome. *J Med Genet.* 2012;49(5):303–6.
272. Bick D, Franco B, Sherins RJ, Heye B, Pike L, Crawford J, et al. Brief report: intragenic deletion of the KALIG-1 gene in Kallmann's syndrome. *N Engl J Med.* 1992;326(26):1752–5.
273. Pingault V, Bodereau V, Baral V, Marcos S, Watanabe Y, Chaoui A, et al. Loss-of-function mutations in SOX10 cause Kallmann syndrome with deafness. *Am J Hum Genet.* 2013;92(5):707–24.
274. Young J, Metay C, Bouligand J, Tou B, Francou B, Maione L, et al. SEMA3A deletion in a family with Kallmann syndrome validates the role of semaphorin 3A in human puberty and olfactory system development. *Hum Reprod.* 2012;27(5):1460–5.
275. Kyttala M, Tallila J, Salonen R, Kopra O, Kohlschmidt N, Paavola-Sakki P, et al. MKS1, encoding a component of the flagellar apparatus basal body proteome, is mutated in Meckel syndrome. *Nat Genet.* 2006;38(2):155–7.
276. Bergmann C, Frank V, Salonen R. Clinical utility gene card for: Meckel syndrome—update 2016. *Eur J Hum Genet.* 2016;24(8).
277. Kang S, Graham JM Jr, Olney AH, Biesecker LG. GLI3 frameshift mutations cause autosomal dominant Pallister-Hall syndrome. *Nat Genet.* 1997;15(3):266–8.
278. Cain JE, Islam E, Haxho F, Chen L, Bridgewater D, Nieuwenhuis E, et al. GLI3 repressor controls nephron number via regulation of Wnt11 and Ret in ureteric tip cells. *PLoS One.* 2009;4(10):e7313.
279. Sanyanusin P, Schimmenti LA, McNoe LA, Ward TA, Pierpont ME, Sullivan MJ, et al. Mutation of the PAX2 gene in a family with optic nerve colobomas, renal anomalies and vesicoureteral reflux. *Nat Genet.* 1995;9(4):358–64.
280. Bulum B, Ozcakar ZB, Ustuner E, Dusunceli E, Kavaz A, Duman D, et al. High frequency of kidney and urinary tract anomalies in asymptomatic first-degree relatives of patients with CAKUT. *Pediatr Nephrol.* 2013;28(11):2143–7.
281. Nicolaou N, Renkema KY, Bongers EM, Giles RH, Knoers NV. Genetic, environmental, and epigenetic factors involved in CAKUT. *Nat Rev Nephrol.* 2015;11(12):720–31.
282. van der Ven AT, Vivante A, Hildebrandt F. Novel insights into the pathogenesis of monogenic congenital anomalies of the kidney and urinary tract. *J Am Soc Nephrol.* 2018;29(1):36–50.
283. dos Santos Junior AC, de Miranda DM, Simoes e Silva AC. Congenital anomalies of the kidney and urinary tract: an embryogenetic review. *Birth Defects Res C Embryo Today.* 2014;102(4):374–81.



What Do Animal Models Teach Us About Congenital Craniofacial Defects?

6

Beatriz A. Ibarra and Radhika Atit

6.1 Overview

The formation of the head and face is a complex process which involves many different signaling cues regulating the migration, differentiation, and proliferation of the neural crest. This highly complex process is very error-prone, resulting in craniofacial defects in nearly 10,000 births in the United States annually. Due to the highly conserved mechanisms of craniofacial development, animal models are widely used to understand the pathogenesis of various human diseases and assist in the diagnosis and generation of preventative therapies and treatments. Here, we provide a brief background of craniofacial development and discuss several rare diseases affecting craniofacial bone development. We focus on rare congenital diseases of the cranial bone, facial jaw bones, and two classes of diseases, ciliopathies and RASopathies. Studying the animal models of

these rare diseases sheds light not only on the etiology and pathology of each disease, but also provides meaningful insights towards the mechanisms which regulate normal development of the head and face.

6.2 Significance

Craniofacial defects are complex and often impact multiple structures of the head and face. One of the most severe craniofacial defects is craniosynostosis, or premature fusion of the skull bones, that occurs in 1/2500 births with detrimental consequences for brain and sensory organ development [1, 2]. The only current treatment for craniosynostosis is surgical separation of the sutures, and in some cases, the sutures become fused again over time requiring additional surgeries [1]. Similar survival treatments are available for many craniofacial disorders; however, these treatments are often limited to repeated surgical intervention and can result in lifelong economic burden to the patient's family or community. One example of such a financial burden stems from analysis of the treatment cost for the repair of cleft lip and/or cleft palate, estimated to be nearly \$700 million dollars just within the United States each year [3]. Rare genetic diseases affect a smaller proportion of the population occurring in less than 1 in 2000 births annually [4]. For example, only 1 in 500,000 individuals have been diagnosed with Robinow syndrome, described

B. A. Ibarra
Department of Biology, Case Western Reserve
University, Cleveland, OH, USA
e-mail: bai9@case.edu

R. Atit (✉)
Department of Biology, Case Western Reserve
University, Cleveland, OH, USA

Department of Genetics, Case Western Reserve
University, Cleveland, OH, USA

Department of Dermatology, Case Western Reserve
University, Cleveland, OH, USA
e-mail: rpa5@case.edu

below [5]. Over 700 rare craniofacial disorders have been categorized and thus encompass a large percentage of the patients born each year with craniofacial defects [3, 4, 6]. Mouse models are valuable to understand rare human craniofacial defects because they have comparative anatomy and physiology and a complex assortment of genetic tools to study the function of genes in spatiotemporal manner. Animal models of rare diseases improve our understanding of disease etiology and pathology and oftentimes can result in the identification of novel treatment options, as we discuss below.

6.3 Introduction into Craniofacial Development

6.3.1 Conservation of Craniofacial Development

During embryonic development across many species, the regulatory mechanisms that govern pattern formation and mechanisms of development are highly conserved [7]. An example of this highly conserved phenomenon can be observed when analyzing embryo patterning across highly diverse organisms. The Hox gene cluster, originally identified for its role in *Drosophila* body patterning, is also required for vertebrate patterning of the axial skeleton [8]. Across vertebrate model organisms, craniofacial development is highly conserved at the molecular and morphological levels [9, 10]. For this reason, animal models are critical for our understanding of many aspects of human biology. Much of our understanding of human craniofacial development came from studying various embryonic models of mouse, frog, and chick [11]. Here we focus on the insights obtained from genetic mouse models of rare craniofacial defects affecting craniofacial bone development.

6.3.2 Craniofacial Development Is Highly Error-Prone

Craniofacial development begins with the migration of cranial neural crest cells (CNCC), a cell population unique to vertebrates [12, 13], from

the neural tube to the frontonasal process (FNP), first branchial arch, and supraorbital arch (SOA) [1, 3, 4, 13, 14] (Fig. 6.1, and described in detail below). Many signaling pathways are vital for maintaining cellular and tissue movements and cell fate specification. These processes are dependent on specific signaling cues at specific spatial and temporal intervals to properly form the various structures of the head and face. For this reason, normal craniofacial development culminates from a series of events, beginning with initiation and migration and ending with differentiation of specialized cell types dependent on crucial spatiotemporal signaling [15]. If any of the steps of these events are altered, the result would be detrimental for normal development; thus, the process of craniofacial development is highly error-prone. In fact, one-third of all congenital defects result in craniofacial anomalies [3]. The precise timing of these various cellular mechanisms is not fully understood. However, the mechanisms that regulate the morphogenesis of various facial and cranial structures are still being investigated and our understanding of these pathways is rapidly expanding as new animal models emerge.

6.3.3 The Need for Animal Models of Craniofacial Defects

Due to the high prevalence of congenital craniofacial defects, there is a demand for an improved understanding of their etiology to enable proper diagnosis and discovery of therapeutic or preventative treatments [16, 17]. To this end, researchers rely on the use of animal models for a variety of reasons. First, testing various treatments and therapies is not ethically feasible in humans in most cases. Second, we are able to genetically and chemically model human diseases effectively and affordably in an animal model to understand the molecular basis of a disease and to test the aforementioned treatments *in vivo*. Third, because of the highly conserved nature of craniofacial development, there is a wide variety of vertebrate species that can be utilized to understand not only disease mechanisms, but also the mechanisms and processes that lead to normal craniofacial development.

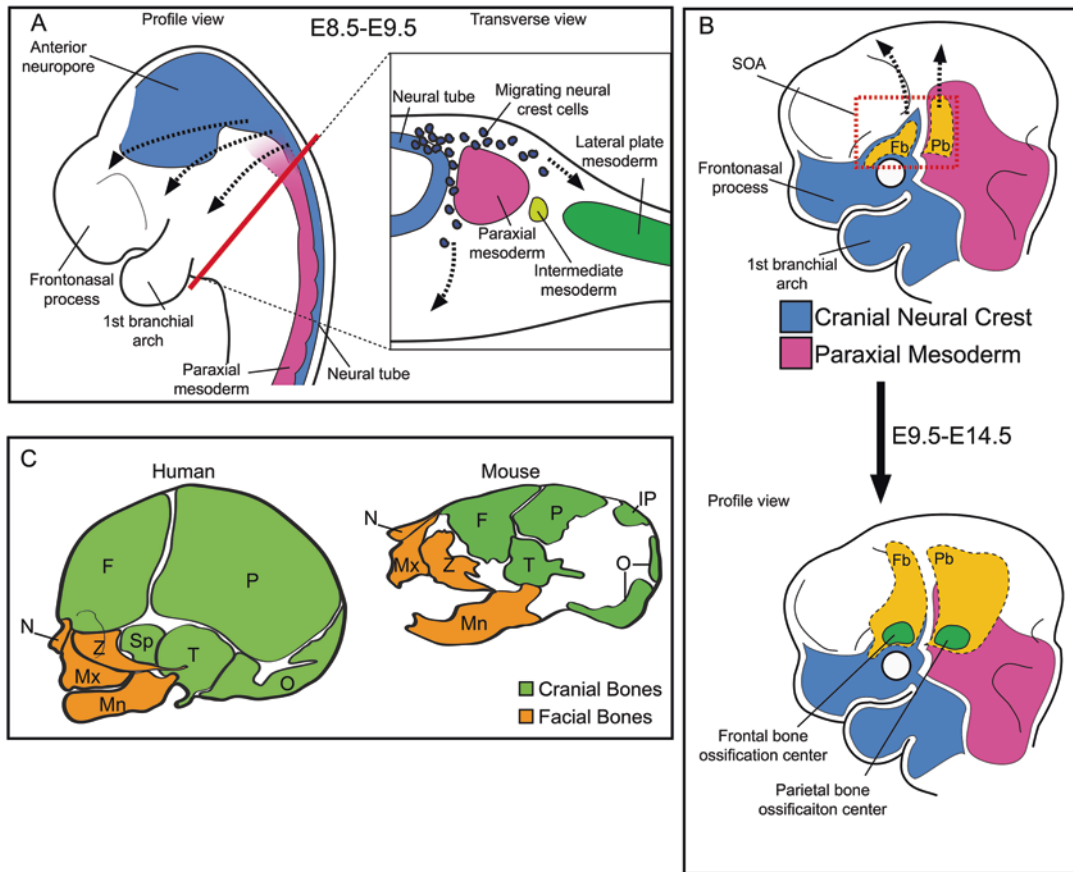


Fig. 6.1 Craniofacial bones are derived from cranial neural crest and paraxial mesoderm. (a) Cranial neural crest and paraxial mesoderm migrate from adjacent to the neural tube into the frontonasal process and first branchial arch. (b) Schematic delineating the direction of differentiation and ossification from basal to apical to form the frontal

(Fb) and parietal bones (Pb). (c) Schematic comparing the cranial and facial bones in a newborn human and mouse skull (*F* frontal, *P* parietal, *N* nasal, *Mx* maxilla, *Z* zygoid, *Sp* sphenoid, *T* temporal, *O* occipital, *IP* interparietal, *Mn* mandibular). (Panels (a) and (b) are reprinted and adapted from Ferguson and Atit 2018 with permission)

In this review, we focus on three regions of the head and face and describe findings from recent studies that illuminate the etiology of several craniofacial defects. We first focus on cranial bone development and two rare cranial bone diseases, progressive osseous heteroplasia (POH) and fibrous dysplasia (FD). Second, we review the development of facial structures and etiology of micrognathia within Robinow syndrome and Nager syndrome. Finally, we will discuss two categories of rare diseases, ciliopathies and RASopathies. While there are many useful and relevant animal models, we have limited our discussions to focus on mouse genetic models. This is due to the high conservation of signaling pathways that regulate craniofacial structures between

humans and mice and the ability to spatiotemporally test gene function in specific tissue and adequately model therapeutic treatments in mammalian models.

6.4 Defects in Cranial Bone

6.4.1 Brief Introduction to Calvarial Bone Development

6.4.1.1 Origins of Calvarial Bones

The calvaria consists of the skull bones that cover and protect the brain and other sensory organs. Mammalian skull bones are derived from cranial NCC and the paraxial mesoderm (PM) [1, 18, 19].

The CNCC give rise to the frontal bones while the PM gives rise to the parietal, squamous part of the temporal and occipital bones. Both contribute to the formation of the interparietal bones [12, 14, 19, 20] (Fig. 6.1).

6.4.1.2 Calvarial Bone Morphogenesis

In mice, the frontal and parietal bone precursors originate in the CNCC and PM mesenchyme and then migrate into the supraorbital arch (SOA) between embryonic day 9.5 (E9.5) and E12.5 [1, 19–22]. Morphogenesis of the frontal and parietal bones begins at E12.5 when the SOA mesenchyme begins to condense [23]. This condensation is pivotal to the formation of the progenitors/rudiments of the cranial bones and specification towards an osteogenic lineage [23, 24]. Upon specification, the calvarial bone progenitors express bone lineage-specific markers, such as runt-related transcription factor 2 (RUNX2) and alkaline phosphatase (AP) [25, 26]. From E13.5, the calvarial bone progenitors differentiate into committed calvarial bone osteoblasts and the cells expand apically and laterally until reaching the apex through mechanisms that remain to be defined [18, 21, 27, 28]. Unlike long bones of the body, calvarial bones form by intramembranous ossification. The condensed SOA mesenchyme directly differentiates into committed calvarial bone osteoblasts to form mineralized bone beginning at E12.5. This is in contrast to endochondral ossification of long bones, which requires formation of a cartilage template prior to mineralization and formation of mature bone. The calvarial bone mineralization for the frontal and parietal bone initiates in the SOA at approximately E14.5 and progresses apically following the wave of differentiation laid out by the osteogenic front [14, 29] (Fig. 6.1). Normal development of calvarial bones requires complex cellular signaling for proper cell differentiation and growth [20, 30]. This process is highly regulated and defects in cell signaling or cell migration results in various cranial defects including craniosynostosis [1, 27] and various skeletal dysplasias [31] (see below). Thus, it is important to understand the biological mechanisms that regulate normal morphogenesis of the cranial bones.

6.4.1.3 Bone Transcription Program

Upon migrating from the neural tube at E9.5, a subpopulation of the cranial mesenchyme in the SOA is fated to become calvarial bone progenitors and begin to express osteogenic genes from E11.5 onwards [14]. There are a growing number of genes and signaling pathways that are reported to govern this cell fate decision, and the transcription cascade that is involved in the specification of cranial bone progenitors is well understood [14, 20, 32]. The “skull bone initiation program” consists of a cascade of three major transcription factors, *Msh homeobox 1 and 2* (*Msx1* and *Msx2*), *Runx2*, and *Osterix* (*Osx/Sp7*) [14, 20]. *Msx1* and *Msx2* are expressed in the early migrating cranial mesenchyme at E10.5 and the calvarial bone precursors by E12.5 [28]. *Runx2* expression requires expression of MSX proteins and is required for establishment of calvarial bone progenitors. As the calvarial bone precursors differentiate into calvarial bone progenitors, *Runx2* expression is decreased and expression of *Osx* is increased. *Osx* is required for ossification of intramembranous bone. The function of these transcription factors has been well-studied using conditional mouse models with targeted genetic deletions of each gene [20, 32]. The bone morphogenetic protein (BMP), Wnt, Hedgehog (Hh), and Notch signaling pathways, among others, have been shown to regulate various aspects of cranial bone development and have been reviewed elsewhere [14, 20, 32, 33].

6.4.2 Rare Cranial Bone Defects

6.4.2.1 Rationale

There is a high prevalence of craniofacial defects and disease, in part due to the complexity of the many processes involved in normal skull bone development [11]. Collectively, craniofacial defects comprise one-third of all congenital defects and there are relatively few known preventative treatments or therapies [3]. Understanding the etiology of rare genetic diseases may elucidate new mechanisms of development and help to identify new therapeutic targets [17]. Here, we will explore two rare bone

disorders to demonstrate the value of utilizing animal models in our endeavor to understand the cellular mechanisms of cranial bone defects in humans.

Heterotopic ossification refers to the ectopic formation of bone in soft tissues [34, 35]. This can occur as a result of trauma, cerebral injury or surgery, or more rarely an underlying genetic disorder. One type of hereditary heterotopic ossification is progressive osseous heteroplasia (POH). On the other end of this type of abnormal bone growth is fibrous dysplasia (FD). FD is characterized as the growth of fibrous tissue in place of normal bone [36, 37]. FD presents across multiple bones, including cranial bones, in McCune-Albright syndrome (MAS) [36, 37].

Here we will discuss the current understanding of the genetic and molecular mechanisms governing these diseases. We will also review how animal models have helped to advance the clinical understanding of POH and FD and how these models have provided new insights into normal intramembranous bone development.

6.4.2.2 Progressive Osseous Heteroplasia

Etiology and Molecular Mechanisms of POH

POH (OMIM: #166350) is an autosomal dominant disease linked to loss-of-function mutations in the *GNAS* gene [34, 35, 38, 39]. The disease presents as ectopic formation of intramembranous bone in the dermis and underlying subcutaneous tissues.

GNAS encodes the alpha subunit of the G-protein complex, *G α s* [40–42]. G-protein signaling begins when a G-protein ligand binds to G-protein-coupled receptors (GPCRs) at the cell membrane. Different G-protein subunits bind to specific GPCRs to elicit a variety of cellular responses. In the context of osteogenic differentiation, *G α s* binding to the receptor results in upregulation of cAMP/PKA signaling which inhibits Hh signaling by preventing nuclear translocation of GLI (Fig. 6.2) [39, 42]. When *G α s* is lost, Hh signaling is no longer inhibited and thus there is increased ossification of cranial bone

[43]. Outlined below are the animal models which delineated the mechanism and etiology of *G α s* in POH.

Insights from Animal Models of POH

The first animal model of POH was established in heterozygous null *Gnas* mice [43]; however, this model did not fully recapitulate the unique phenotype observed in human patients with POH. First, while the heterozygous mouse models present heterotopic ossification in the dermis, there is no ossification present in the deeper subcutaneous cell populations, including muscle and connective tissues, and onset of heterotopic ossification occurred late in life, whereas POH in human patients normally presents during infancy [34, 41, 44–46]. Second, POH patients tend to exhibit heterotopic ossification biased laterally, in some cases the observed ossification failed to cross the midline—this pattern was not observed in the previously described heterozygous *Gnas* mouse models [43, 45].

Cairns et al. utilized a chick model to more accurately represent the human disease [45]. By injecting a dominant negative form of *GNAS* into specific somites, the authors demonstrated a mosaic effect of ectopic ossification similar to that observed in clinical patients of POH. Within this model, the authors were able to glean new mechanistic insight on the etiology of POH in humans. They determined that the likely mechanism of inheritance of *GNAS* mutations is dependent on a stem cell population, or nearby adjacent niche cells, which results in a mosaic distribution of ectopic bone. However, the source of the cell population responsible for driving the ectopic formation of intramembranous bone within dermal cell population is not known.

Conditional deletion of *Gnas* in specific murine tissues provided new insights into the mechanisms of osteoblast differentiation during embryonic development. Tissue-specific deletion of *Gnas* in limb mesenchyme using *Prx1-cre* resulted in efficient deletion of *Gnas* by mouse embryonic day 14.5 (E14.5) and heterotopic ossification as early as E16.5 which progressed through postnatal day 20 (P20), by which time most mutant animals died [47]. Similar levels of

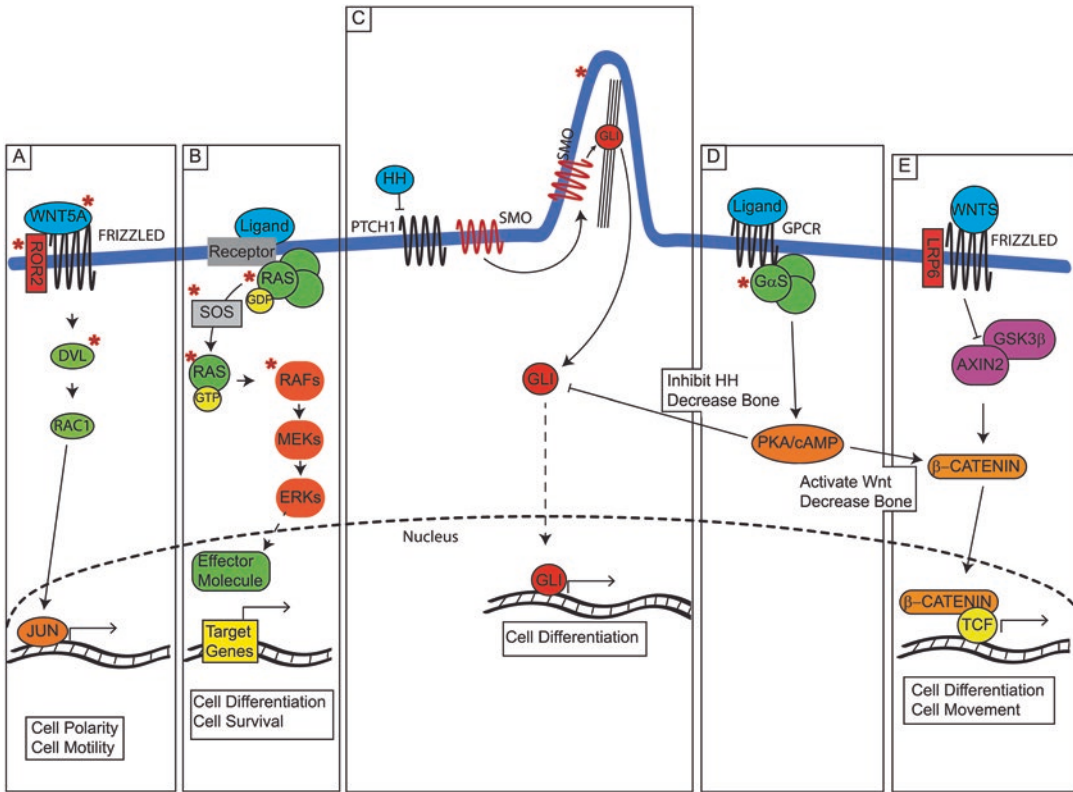


Fig. 6.2 Overview of signaling pathways linked with rare craniofacial diseases. (a) Noncanonical Wnt signaling (Robinson syndrome), (b) MAPK signaling (RASopathies), (c) Hh signaling in primary cilia (ciliopathies), (d) Gαs signaling (progressive osseous heteroplasia and Fibrous dysplasia). (e) Canonical Wnt/β-catenin signaling (FD) increase or decrease in β-catenin leads to dysregulated bone differentiation. Red asterisks indicate disease associated proteins

ing (progressive osseous heteroplasia and Fibrous dysplasia). (e) Canonical Wnt/β-catenin signaling (FD) increase or decrease in β-catenin leads to dysregulated bone differentiation. Red asterisks indicate disease associated proteins

heterotopic ossification occurred in two different models targeting *Gnas* in mesenchyme more broadly using *Dermo1-cre* and *Ap2-cre* and in adult dermis and subcutaneous tissues following injection of adenovirus-*Cre* in *Gnas^{fl/fl}* animals [47]. The introduction of mesenchyme-specific deletion of *Gnas* provided unique opportunities to elucidate the mechanism that drives the ectopic formation of intramembranous bone. Regard et al. used the *Prx1-cre Gnas* mutants to demonstrate that heterotopic ossification in the mesenchyme was a result of dysregulated Hh signaling downstream of decreased cAMP/PKA signaling [47]. Their studies established the paradigm that Hh signaling is necessary and sufficient to induce ectopic intramembranous ossification similar to that observed in POH patients. Furthermore, *Gαs*, encoded by *GNAS*, is necessary to regulate levels of Hh signaling during development and into adulthood [47]. These findings were pivotal

in developing an understanding of the etiology and pathology of POH, which could lead towards the development of new therapeutic targets.

New Therapeutic Targets

Understanding the mechanisms behind disease states can also lead to new insights towards normal cranial development. Considering that heterotopic ossification forms through intramembranous ossification of mesenchymal cells, it stands to reason that this signaling pathway may be conserved during normal development of cranial intramembranous bone. Xu et al. hypothesized that the signaling pathway implicated in POH heterotopic ossification is conserved during normal cranial intramembranous bone ossification [40]. By using comprehensive mouse genetics targeting *Gnas* and Hh signaling effectors *Smoothened (Smo)* and *Gli* and small-molecule inhibitors of Hh signaling, Xu et al. were able to

partially rescue the increased intramembranous bone formation observed in *Gnas* loss-of-function mutants [40]. These data indicate that Hh signaling inhibition may serve as a therapeutic target towards treatments of diseases such as POH and possibly similar diseases demonstrating increased intramembranous bone formation, such as craniosynostosis.

6.4.2.3 Fibrous Dysplasia

Etiology

Similar to POH, FD is caused by a somatic mutation in *GNAS* during early development [36]. This is an activating missense mutation that occurs in a somatic cell in a post-zygotic embryo [36]. FD can affect a single bone (monostotic) or multiple bones (polyostotic) [37]. Mutations leading to polyostotic FD are thought to occur pre-gastrulation as the affected bones consist of both neural crest and mesoderm-derived populations [36]. McCune-Albright syndrome (MAS) (OMIM: #174800) is a form of polyostotic FD that spans multiple bones and organs. More than half of all MAS cases include craniofacial bone defects [36]. FD lesions consist of mesenchyme-like mutated cells and normal osteoblasts resulting in deficient mineralization.

The missense mutation in *GNAS* results in a selective inhibition of its GTPase activity, leading to increased activity of PKA signaling pathways. *Gαs* has been demonstrated to regulate Wnt signaling in many contexts [48]. Wnt/ β -catenin signaling is required for normal cranial bone development [21, 49, 50]. Loss of canonical Wnt signaling in early cranial mesenchyme results in diminished skull bone formation [21, 50, 51]. However, in mature osteoblast cells, Wnt/ β -catenin signaling prevents bone mineralization and maturation [52]. Loss of *Gαs* results in increased Wnt/ β -catenin signaling in affected tissues, which inhibits osteoblast maturation (Fig. 6.2) [48, 53].

New Insights from Animal Models of FD

Bianco et al. first used mice to study the pathology of FD by transplanting human bone marrow cells from FD lesions into immunocompromised mice and observed similar lesions as to those

observed in human FD/MAS affected bone [54]. Their techniques were pivotal in understanding the role of mosaicism in FD bone lesions [54, 55]. One of the earliest genetic mouse models of FD was characterized in 2014 by Saggio et al. [56]. This mouse model was able to recapitulate some aspects of the human phenotype by overexpressing *Gnas* using viral vectors to model the most common genetic mutations observed in humans [56]. The authors described a unique pattern of bone lesion formation consisting of three phases beginning with excess bone formation, followed by bone remodeling, and culminating in fibrotic bone lesions. They identified unique histological patterns for each phase of lesion development and postulate that different stages require different treatment regimens. Although humans begin presenting pathological symptoms beginning in childhood [36], Saggio et al. described the formation of bone lesions occurring in mice aged beyond 1 year [56]. This suggests that the mechanisms elucidated in this model are not significant during juvenile stages of bone development. There may be some undescribed human mechanism resulting in the age discrepancies between the onset of FD in humans and the model described above.

More recently, a new mouse model has been developed that provides new insight into FD using a *Prx1-Cre*-activated tetracycline inducible system to conditionally activate *Gnas* in skeletal stem cells [57]. Activating this system resulted in FD lesion presentation within 2 weeks of doxycycline exposure, which improved following doxycycline withdrawal. Khan et al. utilized two different *Cre* lineages, *Prx1-Cre* and *Osx-Cre*, and determined that activation of *Gnas* led to an increase in Wnt signaling and a decrease in Hh signaling [53]. This study more completely defines a mechanism of pathology of FD in a mouse model and highlight potential therapies more relevant to the defects observed in patients with FD.

New Therapeutic Targets

Currently, there is no cure for FD/MAS, and treatments are limited to surgical intervention for extreme cases [36, 53, 57]. However, the use of animal models has provided valuable insight into the pathophysiology of FD/MAS. The unique

mouse model characterized by Zhao et al. demonstrated reversal of FD bone lesions following reduction in ectopic *Gnas* expression [57]. The authors postulate that inhibition of $G\alpha_s$ may serve as a new therapeutic outlet in the treatment of FD/MAS. Khan et al. demonstrated that inhibition of Wnt signaling in their *Gnas* mouse models also attenuates FD symptoms, highlighting yet another biological mechanism of FD and possible therapeutic target of FD/MAS [53]. Xu et al. demonstrate that inhibition of Wnt signaling using a chemical inhibitor, LGK-974, and genetic ablation of a single *Lrp6* allele can partially rescue the effects of FD in a mouse model of craniofacial FD [40].

6.4.3 Summary

In this section, we have discussed two rare craniofacial diseases that involve abnormal $G\alpha_s$ signaling in the cranial bones. These diseases result from defects in cranial bone ossification that is dependent on a balance of $G\alpha_s$ signaling to differentiate into normal cranial bone. This process seems to be dependent on two downstream signaling pathways that are differentially regulated by $G\alpha_s$ signaling, Hh and Wnt signaling. With various animal models, researchers have been able to identify the mechanisms by which $G\alpha_s$ regulates these two developmentally important signaling pathways. In some instances, putative treatments and therapies have been proposed and tested in a mouse model, demonstrating clear benefits of animal models of disease [40, 53, 57]. Next, we will discuss defects in the facial region focusing on one particular phenotype, micrognathia, across two rare genetic disorders.

6.5 Facial Defects

6.5.1 Facial Outgrowth and Patterning

The facial skeleton is derived from the mesenchymal cells that populate the frontonasal process (FNP) and first branchial arch (Fig. 6.1). The

FNP consists of NCC and head mesoderm and is divided into the medial and lateral nasal processes [58]. Alongside the FNP are the maxillary (MXP) and mandibular (MNP) processes. Together the FNP, MXP, and MNP give rise to facial primordia [4, 58, 59]. The facial prominences are observed as facial swellings by mouse embryonic day 9.5 (E9.5). By E11.5, the medial and lateral nasal processes and MXP fuse to form the upper lip and initiate primary palate development [59]. The medial nasal processes meet at the midline to form the nasal septum, which can regulate facial outgrowth (Fig. 6.3) [59]. Secondary palatogenesis is dependent on the mandibular and maxillary prominences. Finally, the jaw is derived from the first branchial arch. The branchial arches are tissue structures with an outer ectodermal layer and inner endodermal layer with a mesodermal core, surrounded by neural-crest-derived mesenchyme. Many complex signaling pathways regulate the formation of these major facial structures. Abnormal signaling, cell growth, and cell differentiation can lead to a variety of facial defects including cleft lip and palate and micrognathia, among others. Here we will describe the processes that regulate facial morphogenesis and two human diseases that result in abnormal craniofacial development.

6.5.1.1 Palate Development

The FNP is formed from migrating NCC originating from the caudal forebrain/midbrain by E9.5 [13, 59, 60]. By E10.5 the cells of the FNP have been divided into the medial and lateral nasal processes which begin to fuse with the MXP by E11.5 to form the upper lip and primary palate (Fig. 6.3) [61, 62]. Following formation of the primary palate (palatogenesis) is secondary palatogenesis. The palatal shelves arise from the MXP and grow vertically and laterally adjacent to the tongue. Prior to palatal shelf fusion, the tongue descends and the palatal shelves rotate and expand towards the midline where they fuse by E15.5 [59]. The molecular mechanisms that govern palate development have been reviewed extensively [58–60]. The normal formation of lip, primary palate, and secondary palate is heavily dependent on normal cell movements, cell

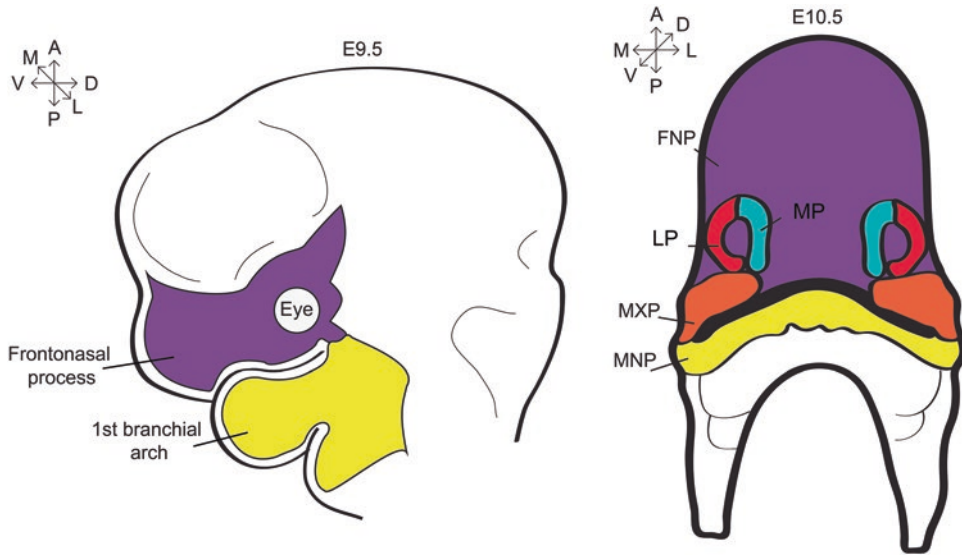


Fig. 6.3 Facial structures derived from the frontonasal process and first branchial arch. Schematic delineating the frontonasal process and first branchial arch at E9.5 (left) and the structures derived from these two cell populations that make up the facial primordia by E10.5 (right). *FNP*

frontonasal process, *MP* medial nasal process, *LP* lateral nasal process, *MXP* maxillary process, *MNP* mandibular process. (E9.5 embryo adapted with permission from Ferguson and Atit 2018)

differentiation, programmed cell death, and concerted actions across multiple adjacent tissues and cell populations. Cleft lip and cleft palate can occur when any of these processes is dysregulated during development [3, 6, 58]. The etiology and pathophysiology of cleft lip and cleft palate have been reviewed extensively [62–65] and thus will not be reviewed here.

6.5.1.2 Transcriptional Control of Jaw Development

The first branchial arch is subdivided into maxilla and mandibular prominences through pattern-specific expression of key *Dlx* (*distal-less*) genes [66]. Expression of *DLX1/2* corresponds to MXP, while expression of *DLX1/2/5/6* correlates with the MNP. The MNP is further patterned into an oral-aboral axis dependent on signaling from Lim-homeobox (*Lhx*) genes and *gooseoid* expression. Prior to formation of the mandibular bones, the formation of a specialized cartilage structure, Meckel's cartilage (MC), is required. The formation of MC begins with condensation of CNC mesenchyme at E12.5, which then differentiates into chondrocytes forming the

template for the future jaw [66]. MC expands outwards first ventromedially and then dorsolaterally until they fuse at the most distal tip. The posterior regions of MC ultimately develop into the malleus and incus bones of the middle ear, while the intermediate MC is degraded and differentiated to form connective tissues of the jaw [60, 66]. Intramembranous ossification of the jaw is driven through expression of *Dlx5*, which is required for the upregulation of the bone marker *Runx2* [66]. Ossification of the lower jaw bone begins with the formation of a primary ossification center lateral to the MC at stage E13.5 [60, 66]. The upper jawbones are derived from the MXP and are physically unique from the lower jawbones. Recent work in zebrafish has identified two novel identity markers of the upper and lower jaw. The upper jaw requires expression of the *nuclear receptor subfamily 2 group F*, *Nrf2*, nuclear receptors, while the lower jaw requires *endothelin 1* (*Edn1*) to repress expression of *Nrf2* and maintain proper lower jaw identity [67].

The size and shape of the lower jaw bones are dependent on the underlying MC, and abnormal development of the MC or ossification of the

mandibular bone presents as micrognathia, a shortened/decreased jaw, or macrognathia, an oversized/lengthened jaw. Several side effects can occur as a result from micrognathia including feeding disturbances in infants [68]. Here, we will describe the occurrence of two rare craniofacial disorders which present as syndromes including micrognathia and other facial defects.

6.5.2 Robinow Syndrome

6.5.2.1 Etiology

Robinow syndrome (RS) (OMIM: #180700, #268310, #616894, #616331) is a genetic disease that manifests as skeletal dysplasia with distinct craniofacial defects [5]. RS results from mutations in components of the noncanonical Wnt and planar cell polarity (PCP) signaling pathways. The most common mutations resulting in RS are located within the *Wnt family member 5a* (*WNT5A*) or *Receptor Tyrosine Kinase-like Orphan Receptor 2* (*ROR2*) loci [5, 69]. However, mutations in other pathway components, such as *Disheveled* (*DVL*) proteins, have also been identified [70, 71]. Apart from skeletal phenotypes such as short stature, the craniofacial defects are described as “fetal facies” which include but are not limited to macrocephaly, micrognathia, and midface hypoplasia [69, 72]. There are a high amount of genetic heterogeneity surrounding this disease owing to the large number of mutations across multiple genes that vary in the level of inheritance across patients. However, despite this RS remains a rare disorder affecting only 1 in 500,000 individuals [5].

WNT5a is a secreted protein that regulates cellular patterning and morphology through non-canonical Wnt signaling. During noncanonical signaling, *ROR2* acts as a coreceptor for frizzled receptors of *WNT5a* [73]. Binding of the ligand to the receptor results in signaling cascades involving the cellular effector *DVL*, ultimately directing cellular outgrowth, planar cell polarity, and cell migration (Fig. 6.2) [74]. It is hypothesized that heterozygous missense mutations result in loss of function of the affected *WNT5A*

allele [75]. Alternatively, homozygous *ROR2* mutations leading to decreased *ROR2* activity also result in RS [76, 77]. Finally, mutations in *DVL1* or *DVL3* also result in autosomal dominant RS [70, 71].

6.5.2.2 New Insights from Animal Models

The first animal model of RS characterized the recessive mutations in *Ror2* using a knockout mouse model [69]. They identified several defects in the craniofacial region of the developing mouse embryo. Most notably, they identified a defect in craniofacial outgrowth including smaller mandible and associated defects in Meckel’s cartilage. Person et al. described a similarity in the phenotypes of *Ror2* and *Wnt5a* null mice and identified key missense mutations in *WNT5A* in human patients of RS presenting autosomal dominant inheritance [75]. They confirmed the role of human *WNT5A* missense mutations in RS by selectively inactivating *wnt5a* alleles in zebrafish and *Xenopus* embryos. Their work linked *WNT5A* and *ROR2* in a functional pathway that is highly regulated and involved in normal craniofacial outgrowth and development [75]. The role of specific missense mutations of human *WNT5A* in RS was further delineated in another vertebrate model using chick embryos [5]. Here, the authors utilized retroviral injections into the developing chick mandible to highlight the specific effect of a human C83S *WNT5a* missense mutation on outgrowth of the vertebrate jaw and formation of normal Meckel’s cartilage. The effect of the C83S *WNT5a* missense mutations resulted in micrognathia in the chick embryos, resembling the *Ror2* and *Wnt5a* null mice described by Person et al. [75]. However, their data did not highlight a definitive loss-of-function effect of C83S *WNT5A* on the resulting micrognathia as previously hypothesized. Instead, they postulate that the specific C83S *WNT5A* mutations identified in RS patients have neither a gain nor loss-of-function effect and ultimately result in diversion of *WNT5A* towards an unknown, alternative signaling pathway, independent and separate from noncanonical Wnt signaling, thus

improving upon the current etiology of micrognathia in RS patients.

These experiments in mouse and chick highlighted the importance of balance in noncanonical Wnt signaling pathways during normal craniofacial development. Due to the genetic heterogeneity of noncanonical Wnt signaling, it was hypothesized that dysregulation in other aspects of this key WNT5a-ROR2 signaling pathway may also account for the occurrence of Robinow syndrome in humans that has not been associated with mutations in *WNT5A* or *ROR2* [78]. More recently, frameshift mutations in *DVL1* and *DVL3* have been identified in patients of dominant RS [70, 71]. DVL proteins are involved in both canonical and noncanonical Wnt signaling, and in the case of RS, it is hypothesized that the mutations in DVL proteins exist within the WNT5a-ROR2-DVL noncanonical Wnt signaling pathway. A recent genome-wide association study (GWAS) identified a variant in *Dvl2* in bulldog breeds associated with widened skull shape and decreased snout length, reminiscent of RS defects [79]. This unique animal model can provide insights into the etiology of distinct craniofacial defects associated with RS and highlights the need for further research into the molecular mechanisms of the WNT5a-ROR2-DVL pathways. Interestingly, Mansour et al. hypothesized that the *Dvl2* mutations are hypomorphic in the context of the vertebral phenotypes characterized in the dog model, similar to the conclusions of Hosseini-Farahabadi et al. regarding Wnt5a mutations with respect to mandible outgrowth in chick [5, 79]. New biophysical approaches to understand the cellular basis of Robinow syndrome has shed light on the complex etiology. Recent studies with live *Wnt5a*^{-/-} mouse embryos reveal that cell movement and cytoskeletal organization during branchial arch morphogenesis are disrupted leading to misshapen arches and diminished MXP [80]. Understanding the molecular mechanisms of WNT5a/ROR2/DVL can provide insights into the etiology of RS and normal development of the head and face.

6.5.3 Nager Syndrome

6.5.3.1 Etiology

Nager syndrome (OMIM: #154400) is a rare genetic disease reported in only 100 individuals as of 2017 [81, 82]. First identified in 1948 [83], Nager syndrome presents with facial defects, including midface retrusion and severe micrognathia, and distinct limb phenotypes unique from other types of face and limb bone diseases [81, 84, 85]. Similar to RS, Nager syndrome has been reported to be inherited as either an autosomal recessive or autosomal dominant disease. Mutations of *SF3B4*, *splicing factor 3B subunit 4*, resulting in heterozygous loss of function, have been identified in 57–64% patients with Nager syndrome [81, 86]. Patients with Nager syndrome primarily present de novo mutations of *SF3B4*; however, there have been observed instances of both autosomal dominant and autosomal recessive inheritance [81, 82, 84, 85]. *SF3B4* encodes a spliceosomal protein which has been reported to directly interact with BMP proteins to inhibit osteogenic and chondrogenic differentiation in vitro [87]. Current understanding of the etiology of this disease is limited due to the small number of affected individuals and genetic heterogeneity of individuals affected [82].

6.5.3.2 Insights from Animal Models

Thus far there has only been one characterized animal model of Nager syndrome [88]. Devotta et al. utilize morpholinos to inhibit *SF3B4* function during early development in *Xenopus* embryos [88]. The authors first demonstrated a requirement of *sf3b4* in normal neural crest development. In addition to regulating the differentiation of neural crest during early development, the authors have also characterized craniofacial defects similar to those observed in Nager syndrome patients, including decreased formation of Meckel's cartilage, among other key facial cartilage structures [88]. This was accompanied by decreased levels of *sox10* mRNA, but researchers saw no evidence of interaction with the BMP signaling pathway. The authors hypothesize a spatiotemporal requirement for spliceo-

some mechanisms during early neural crest cell specification [88]. There is still a necessity for the development of appropriate animal models of Nager syndrome to fully understand the etiology of this rare congenital disease. Understanding the etiology of this and other rare facial defects can inform our understanding of normal facial outgrowth and morphology during early embryonic development.

6.6 Ciliopathies/RASopathies

6.6.1 What Are Ciliopathies?

Ciliopathies are a group of diseases classified by defects in the function or formation of primary cilia [4]. Primary cilia are complex organelles found in all vertebrate cell types [4, 89, 90] and are required for many basic cellular processes, including transduction of major signaling pathways either by housing receptors or transducing signaling ligands. Cilia comprise three major functional domains, the axoneme, basal body, and ciliary membrane. Each domain is critical for the overall function of the cilium and its role in signal transduction. The axoneme is composed of microtubules and extends the cilium into the extracellular space [4, 90]. The axoneme builds from the basal body, a specialized centrosome structure that connects the axoneme to the cell. Intraflagellar transport (IFT) is required for the assembly of the axoneme as well as the transport of signal transduction proteins in a functioning cilium [4]. A specialized membrane encompasses the fully formed cilium where various signal transduction receptors are located.

Several key developmental signaling pathways are regulated by cilia, including Hh, Wnt, and platelet-derived growth factor- α (PDGFR α). Sonic Hedgehog (SHH) has been extensively reported to be regulated by primary cilia during development [4, 16, 90–92]. SHH receptors are localized to the ciliary membrane, and upon binding of a Hh ligand, SMO can enter the ciliary axoneme [16, 92]. Additionally, the transcription factor GLI is trafficked through the

ciliary axoneme which is believed to process GLI into a transcriptional activator or transcriptional repressor (Fig. 6.2) [16, 92]. PDGFR α signaling is required during normal cell migration and proliferation of mesenchyme during development and is localized to primary cilia [93, 94]. Loss of *Pdgfra* in mouse neural crest results in several craniofacial defects, including cleft palate and decreased formation of cranial bone [93, 95, 96]. There are many different ciliopathies that have been described in recent years [4, 16]. Here we will describe one type of ciliopathy, oral-facial-digital syndrome (OFDS) type-1, as the molecular etiology and pathologies are not well understood and there are new insights from animal models.

6.6.2 Oral-Facial-Digital Syndrome (OFDS)

6.6.2.1 Etiology

OFDS-1 (OMIM: #311200) is a ciliopathic disease linked with varying craniofacial defects, including cleft palate and micrognathia, as well as digit defects such as syndactyly and brachydactyly, and occasionally kidney defects [97]. OFDS-1 is an X-linked dominant disorder that is embryonically lethal in males and occurs in 1 of every 50–250,000 births [4, 98]. Ferrante et al. identified a variety of mutations in the *OFDI* gene resulting in loss of protein function [97]. *OFDI* encodes a protein found in the basal bodies of primary cilia that is required for normal ciliary function [98–100]. Interestingly, mutations in *OFDI* have been identified in other ciliopathies including Meckel-Gruber syndrome (OMIM: #249000) and Joubert syndrome (OMIM: # 213300) [99]. This suggests that *OFDI* is important for normal primary cilia function and that there may be multiple genes involved across these ciliopathic syndromes to account for the variability in presented phenotypes. The range and severity of defect types in individuals with OFDS-1 is variable even across familial inheritance, suggesting a complex etiology of OFDS-1 in humans that has yet to be fully defined.

6.6.2.2 New Insights from Animal Models

Ferrante et al. generated a mouse model of OFDS-1 by targeted deletion of *Ofdl* during the four-cell stage of development [100]. Mutant mice presented with severe craniofacial defects including shortened skull and facial regions and cleft palate, polysyndactyly, cystic kidney, and death at birth [100]. Similar to OFDS-1 in humans, deletion of *Ofdl* in male mice was embryonically lethal. Analysis of affected male embryos indicated a loss of primary cilia in the node and coinciding loss in left-right asymmetry. Furthermore, *Shh* and *Shh* signaling targets, *Ptch1* and *Gli1*, were decreased in the neural tube following loss of *Ofdl* correlating with the observed neural tube defects in mutant embryos [100]. These results highlighted the requirement of cilia in normal craniofacial development and specifically linked the observed defects to decreased *Shh* signaling in murine development.

A later study conducted by Ferrante et al. elucidated a novel function of *ofdl* in zebrafish linking primary cilia to noncanonical Wnt/PCP signaling [101]. Using morpholinos to block expression of *ofdl* in zebrafish in vivo, the authors observed delayed cellular migration and decreased body axis length. The cell migration phenotypes were exacerbated with simultaneous injection of a *wnt11* morpholino. WNT11 is a noncanonical Wnt/PCP ligand that is required for normal cell migration and convergent extension [101]. Van Gogh-like protein 2, *VANGL2*, is a PCP receptor protein [101]. When the authors co-injected morpholinos for *vangl2* alongside *ofdl*, they observed a significantly decreased body axis relative to single injected mutants and uninjected controls. Delayed cell migration and shortened body lengths are indicative of defects in convergent extension, and Wnt/PCP signaling is required for normal convergent extension in vertebrates during early development [101].

Both of these studies have begun to elucidate the role of *Ofdl* on ciliary function and have identified two key developmental signaling path-

ways, HH and Wnt/PCP, which are regulated by normal cilia function. The results from these studies helped to classify OFDS-1 as a ciliopathy and have begun to fill in the blanks of the etiology of this disease. Furthermore, these animal models can be used to address other questions on other types of ciliopathies. Mutations in *Ofdl* have been identified in other ciliopathies including Joubert syndrome, a ciliopathy that presents with craniofacial anomalies and neural disorders. To better understand the etiology of OFDS-1 and other ciliopathies, more studies to elucidate novel binding partners and genetic interaction with major signaling pathways will be useful. At the clinical level, identification of other genes involved in either ciliary morphogenesis, or ciliary signaling that are impacted in patients, will help to further define the complex genetic heterogeneity and pathophysiology of various ciliopathies.

6.6.3 What Are RASopathies?

RASopathies are a group of disorders caused by mutations in genes within the RAS/MAPK (mitogen-activated protein kinase) signaling pathways. RAS proteins are small GTPases that are activated in response to growth factors binding to a receptor protein [6, 103]. Activation of RAS leads to a signaling cascade first by activation of RAF, a MAPK kinase, which phosphorylates and activates MEK (mitogen-activated protein kinase kinase, which then phosphorylates and activates Erk. Activated ERK (extracellular signal-related kinase) proteins can then function on a variety of cellular processes including cell differentiation and cell cycle regulation (Fig. 6.2) [103–105]. Each RASopathy presents with its own unique phenotypes; however, they typically present with craniofacial defects, cardiac malformations, and musculoskeletal defects [6]. Here, we will discuss Noonan syndrome and recent advances made with animal models towards the understanding of this specific RASopathy and other RASopathies in general.

6.6.4 Noonan Syndrome

6.6.4.1 Etiology

Noonan syndrome (NS) is an autosomal dominant disorder that presents with short stature and craniofacial dysmorphologies including broad forehead, hypertelorism (increased distance between the eyes), and high arched palate [6, 103]. NS affects 1 in every 1000–2500 individuals [106]. At least 50% of these individuals have missense mutations in the gene *PTPN11* leading to increased phosphatase activity [6, 106]. *PTPN11* encodes a tyrosine phosphatase protein that is required for normal activation of RAS/ERK cascades [107]. Mutations have been identified in numerous other genes involved in the RAS/MAPK signaling pathway including *KRAS*, *SOS1*, *RAF1*, *NRAS*, *BRAF*, and *RITI* among others [6, 106]. Each mutation is characterized into one of ten subtypes of NS currently being defined. *KRAS* and *NRAS* are two types of *RAS* genes, and *RAF1* and *BRAF* encode *RAF* genes. *SOS* and *RITI* encode proteins required for normal signal transduction of the RAS/RAF/MAPK cascade.

6.6.4.2 New Insights from Animal Models

Araki et al. generated a mouse model of NS using an activating gain-of-function mutation of *Ptpn11* [107]. Homozygous activation of *Ptpn11* was embryonically lethal and heterozygous activation resulted in increased *Ptpn11* activation in vitro and in vivo. Heterozygous mutants presented facial phenotypes similar to those observed in humans including triangular facial features such as a wider and more blunt snout. Interestingly, the authors report increased ERK activation only in a subset of tissues indicating tissue-specific effects of *Ptpn11* activation.

Recently, several new animal models have targeted different genes affected in NS. Chen et al. characterized a gain-of-function mutation in *Sos1*, a gene required for activation of RAS, in a mouse model [108]. *Sos1* homozygous and heterozygous mutants exhibited short stature and triangular facial features, similar to those in patients with NS and in mice with *Ptpn11* muta-

tions. Homozygous mice typically died in utero; however, some were reported to be born and survive. Prenatal treatment with PD0325901, a small-molecule inhibitor of MEK, resulted in increased survival of the *Sos1* homozygous mutants and improved stature and facial feature of *Sos1* homozygous and heterozygous mutants [108, 109].

Wu et al. generated an overexpression *Raf1* mouse model which recapitulates many of the phenotypes associated with NS, including short stature and craniofacial dysmorphology [104]. Postnatal inhibition of MEK/ERK signaling using PD0325901 over the course of 6 weeks was sufficient to rescue the growth defects and craniofacial abnormalities observed in *Raf1* mutants.

Hernández-Porras et al. observed characteristic NS phenotypes, including short stature and craniofacial dysmorphology in a mouse model of *KRAS* gain of function [110]. Similarly to Chen et al. and Wu et al. [104, 108, 110], they observed significant improvement of growth and craniofacial defects in *KRAS* mutants when rescued prenatally with MEK inhibitor PD0325901. In contrast to observations in the *Raf1* model, MEK inhibition postnatally in juvenile or adult mice did not ameliorate any physical defects, although it did improve survivability by 40% [110].

These data are among the first to elucidate the pathology of MEK/ERK signaling in NS and to identify a potential treatment mechanism for patients. In addition to determining the pathology of various distinct gene mutations involved in NS, these studies have determined the role of RAF/MEK/ERK signaling in craniofacial defects across multiple experiments and furthermore elucidated potential therapies to rescue the craniofacial and growth defects associated with NS. Future studies should focus on identifying the downstream factors that are functionally important to normal craniofacial development. Specifically, understanding how MAPK signaling changes result in the observed phenotypes associated with NS will help to understand the etiology of the disease and may also inform researchers on new pathways that are relevant during normal craniofacial development.

6.7 Concluding Remarks

In this chapter, we have discussed several animal models of various craniofacial diseases and their associated defects. While we have focused primarily on mouse models, other vertebrate systems are valuable for studying craniofacial development. There are non-model organisms that are being used currently to address many unanswered questions of craniofacial development. For instance, Werren et al. utilize a unique invertebrate system, the *Nasonia* wasps, to study the genetics of craniofacial development [111]. These authors study two hybrid male species and identify quantitative trait loci that are associated with cranial morphology and identify several cranial anomalies among hybrids including cleft palate. The blind Mexican cavefish, *Astyanax mexicanus*, is used to study the natural genetic and environmental causes that result in various craniofacial anomalies, including craniosynostosis [112].

Beyond understanding the basis of normal craniofacial development and the etiology of various human diseases, animal models are also pivotal in the search for preventative treatments and cures. Various animal models, especially mice and rats, are often poised to test different therapies and treatments due to the high levels of conservation among disease pathways. Here, we have identified several research strategies for identifying cures or treatments of various craniofacial diseases such as Hh inhibition in progressive osseous heteroplasia [40], Wnt inhibition in fibrous dysplasia [40, 53], and ERK inhibition in Noonan syndrome [104, 108, 110].

Furthermore, the use of animal models has allowed for the development of many biological tools that can be utilized to understand developmental processes and help to define etiologies of various developmental diseases. While there has been considerable progress towards understanding craniofacial diseases with various animal models, there is still more to be learned for therapeutic development. Novel technologies, such as in utero stem cell transplantation, have been utilized to treat genetic disorders [113], but their potential is limited by our understanding of the

genetic causes of the many syndromes associated with craniofacial defects. Understanding the biophysical and cellular basis of craniofacial development will reveal new etiologies of craniofacial disorders. As we have discussed, many craniofacial diseases are associated with genetic heterogeneity and the high number of genetic isoforms within the human genome is just one possible explanation for this [5, 78, 82]. Advancements in sequencing technologies have allowed researchers to gather high-throughput molecular information during early development to make conclusions about cell fate and lineage decisions in early development. Hooper et al. have mapped out tissue-specific genetic programs that regulate facial morphogenesis in early mouse embryo [114]. There have been several studies that have highlighted the importance of epigenetic variation in normal craniofacial development and efforts to characterize the epigenome during development [115–118]. A greater understanding of the etiology of the various craniofacial diseases will emerge as analyses of the different genetic and epigenetic variations are identified within human patients and as animal models are developed to assess the complex signaling pathways associated with craniofacial defects and ultimately will improve our understanding of normal craniofacial development [17].

References

1. Morriss-Kay GM, Wilkie AOM. Growth of the normal skull vault and its alteration in craniosynostosis: insights from human genetics and experimental studies. *J Anat.* 2005;207(5):637–53.
2. Wilkie A. Craniosynostosis: genes and mechanisms. *Hum Mol Genet.* 1997;6(10):1647–56.
3. Trainor PA. Craniofacial birth defects: the role of neural crest cells in the etiology and pathogenesis of Treacher Collins syndrome and the potential for prevention. *Am J Med Genet Part A.* 2010;152A(12):2984–94.
4. Achilleos A, Trainor PA. Mouse models of rare craniofacial disorders. *Curr Top Dev Biol.* 2015;115:413–58.
5. Hosseini-Farahabadi S, Gignac SJ, Danescu A, Fu K, Richman JM. Abnormal WNT5A signaling causes mandibular hypoplasia in Robinow syndrome. *J Dent Res.* 2017;96(11):1265–72.

6. Goodwin AF, Kim R, Bush JO, Klein OD. From bench to bedside and back: improving diagnosis and treatment of craniofacial malformations utilizing animal models. *Curr Top Dev Biol.* 2015;115:459–92.
7. Hu D, Marcucio RS, Helms JA. A zone of frontonasal ectoderm regulates patterning and growth in the face D. *Development.* 2003;130:1749–58.
8. Mallo M. Reassessing the role of Hox genes during vertebrate development and evolution. *Trends Genet.* 2018;34(3):209–17.
9. Mork L, Crump G. Zebrafish craniofacial development: a window into early patterning. *Curr Top Dev Biol.* 2015;115:235–69.
10. Schneider RA, Hu D, Helms JA. From head to toe: conservation of molecular signals regulating limb and craniofacial morphogenesis. *Cell Tissue Res.* 1999;296:103–9.
11. Van Otterloo E, Williams T, Artinger KB. The old and new face of craniofacial research: how animal models inform human craniofacial genetic and clinical data. *Dev Biol.* 2016;415(2):171–87.
12. Frisdal A, Trainor PA. Development and evolution of the pharyngeal apparatus. *Wiley Interdiscip Rev Dev Biol.* 2014;3(6):403–18.
13. Minoux M, Rijli FM, Paleari L, Zerega B, Postiglione MP, Mantero S, et al. Molecular mechanisms of cranial neural crest cell migration and patterning in craniofacial development. *Development.* 2010;137(16):2605–21.
14. Ferguson JW, Atit RP. A tale of two cities: the genetic mechanisms governing calvarial bone development. *Genesis.* 2019;57(1):e23246.
15. Evans DJR, Francis-West PH. Craniofacial development: making faces. *J Anat.* 2005;207(5):435–6.
16. Schock EN, Brugmann SA. Discovery, diagnosis, and etiology of craniofacial ciliopathies. *Cold Spring Harb Perspect Biol.* 2017;9(9):a028258.
17. Zelzer E, Olsen BR. The genetic basis for skeletal diseases. *Nature.* 2003;423:343–8.
18. Yoshida T, Vivatbutsiri P, Morriss-Kay G, Saga Y, Iseki S. Cell lineage in mammalian craniofacial mesenchyme. *Mech Dev.* 2008;125(9–10):797–808.
19. Jiang X, Iseki S, Maxson RE, Sucov HM, Morriss-Kay GM. Tissue origins and interactions in the mammalian skull vault. *Dev Biol.* 2002;241(1):106–16.
20. Ishii M, Sun J, Ting M-C, Maxson RE. The development of the calvarial bones and sutures and the pathophysiology of craniosynostosis. *Curr Top Dev Biol.* 2015;115:131–56.
21. Tran TH, Jarrell A, Zentner GE, Welsh A, Brownell I, Scacheri PC, et al. Role of canonical Wnt signaling/ β -catenin via Dermo1 in cranial dermal cell development. *Development.* 2010;137:3973–84.
22. Deckelbaum RA, Majithia A, Booker T, Henderson JE, Loomis CA. The homeoprotein engrailed 1 has pleiotropic functions in calvarial intramembranous bone formation and remodeling. *Development.* 2006;133:63–74.
23. Goodnough LH, Dinuoscio GJ, Atit RP. Twist1 contributes to cranial bone initiation and dermal condensation by maintaining Wnt signaling responsiveness. *Dev Dyn.* 2016;245(2):144–56.
24. Dunlop LL, Hall BK. Relationships between cellular condensation, preosteoblast formation and epithelial-mesenchymal interactions in initiation of osteogenesis. *Int J Dev Biol.* 1995;39(2):357–71.
25. Han J, Ishii M, Bringas P Jr, Maas RL, Maxson RE Jr, Chai Y. Concerted action of Msx1 and Msx2 in regulating cranial neural crest cell differentiation during frontal bone development. *Mech Dev.* 2007;124:729–45.
26. Ishii M, Merrill AE, Chan Y-S, Gitelman I, Rice DPC, Sucov HM, et al. Msx2 and Twist cooperatively control the development of the neural crest-derived skeletogenic mesenchyme of the murine skull vault. *Development.* 2003;130(24):6131–42.
27. Ting M-C, Wu NL, Roybal PG, Sun J, Liu L, Yen Y, et al. EphA4 as an effector of Twist1 in the guidance of osteogenic precursor cells during calvarial bone growth and in craniosynostosis. *Development.* 2009;136(5):855–64.
28. Roybal PG, Wu NL, Sun J, Ting M, Schafer CA, Maxson RE. Inactivation of Msx1 and Msx2 in neural crest reveals an unexpected role in suppressing heterotopic bone formation in the head. *Dev Biol.* 2010;343(1–2):28–39.
29. Cesario JM, Landin Malt A, Chung JU, Khairallah MP, Dasgupta K, Asam K, et al. Anti-osteogenic function of a LIM-homeodomain transcription factor LMX1B is essential to early patterning of the calvaria. *Dev Biol.* 2018;443(2):103–16.
30. Twigg SRF, Wilkie AOM. New insights into craniofacial malformations. *Hum Mol Genet.* 2015;24(R1):R50–9.
31. Krakow D, Rimoin DL. The skeletal dysplasias. *Genet Med.* 2010;12(6):327–41.
32. Fan X, Loebel DAF, Bildsoe H, Wilkie EE, Tam PPL, Qin J, et al. Tissue interactions, cell signaling and transcriptional control in the cranial mesoderm during craniofacial development. *AIMS Genet.* 2016;3(1):74–98.
33. Pan A, Chang L, Nguyen A, James AW. A review of hedgehog signaling in cranial bone development. *Front Physiol.* 2013;4:61.
34. Kaplan FS, Hahn GV, Zasloff MA. Heterotopic ossification: two rare forms and what they can teach us. *J Am Acad Orthop Surg.* 1994;2(5):288–96.
35. Meyers C, Lisiecki J, Miller S, Levin A, Fayad L, Ding C, et al. Heterotopic ossification: a comprehensive review. *JBMR Plus.* 2019;3(4):e10172.
36. Feller L, Wood NH, Khammissa RAG, Lemmer J, Raubenheimer EJ. The nature of fibrous dysplasia. *Head Face Med.* 2009;5:22.
37. Hakim DN, Pelly T, Kulendran M, Caris JA. Benign tumours of the bone: a review. *J Bone Oncol.* 2015;4(2):37–41.
38. Kaplan FS, Pignolo RJ, Al Mukaddam M, Shore EM. Genetic disorders of heterotopic ossification. In: *Primer on the metabolic bone diseases and disorders of mineral metabolism.* Wiley; 2018. p. 865–70.

39. Pignolo RJ, Ramaswamy G, Fong JT, Shore EM, Kaplan FS. Progressive osseous heteroplasia: diagnosis, treatment, and prognosis. *Appl Clin Genet*. 2015;8:37–48.
40. Xu R, Khan SK, Zhou T, Gao B, Zhou Y, Zhou X, et al. G α s signaling controls intramembranous ossification during cranial bone development by regulating both Hedgehog and Wnt/ β -catenin signaling. *Bone Res*. 2018;6(1):33.
41. Bastepe M. GNAS mutations and heterotopic ossification. *Bone*. 2018;109:80–5.
42. Cong Q, Xu R, Yang Y. G α s signaling in skeletal development, homeostasis and diseases. *Curr Top Dev Biol*. 2019;133:281–307.
43. Pignolo RJ, Xu M, Russell E, Richardson A, Kaplan J, Billings PC, et al. Heterozygous inactivation of Gnas in adipose-derived mesenchymal progenitor cells enhances osteoblast differentiation and promotes heterotopic ossification. *J Bone Miner Res*. 2011;26(11):2647–55.
44. Happle R. Progressive osseous heteroplasia is not a Mendelian trait but a type 2 segmental manifestation of GNAS inactivation disorders: a hypothesis. *Eur J Med Genet*. 2016;59(5):290–4.
45. Cairns DM, Pignolo RJ, Uchimura T, Brennan TA, Lindborg CM, Xu M, et al. Somitic disruption of GNAS in chick embryos mimics progressive osseous heteroplasia. *J Clin Invest*. 2013;123(8):3624–33.
46. Shore EM, Kaplan FS. Inherited human diseases of heterotopic bone formation. *Nat Rev Rheumatol*. 2010;6(9):518–27.
47. Regard JB, Malhotra D, Gvozdenovic-Jeremic J, Josey M, Chen M, Weinstein LS, et al. Activation of Hedgehog signaling by loss of GNAS causes heterotopic ossification. *Nat Med*. 2013;19(11):1505–12.
48. Regard JB, Cherman N, Palmer D, Kuznetsov SA, Celi FS, Guettier J-M, et al. Wnt/ β -catenin signaling is differentially regulated by G α proteins and contributes to fibrous dysplasia. *Proc Natl Acad Sci U S A*. 2011;108(50):20101–6.
49. Day TF, Guo X, Garrett-Beal L, Yang Y. Wnt/ β -catenin signaling in mesenchymal progenitors controls osteoblast and chondrocyte differentiation during vertebrate skeletogenesis. *Dev Cell*. 2005;8(5):739–50.
50. Hill TP, Später D, Taketo MM, Birchmeier W, Hartmann C. Canonical Wnt/ β -catenin signaling prevents osteoblasts from differentiating into chondrocytes. *Dev Cell*. 2005;8(5):727–38.
51. Goodnough LH, DiNucosio GJ, Ferguson JW, Williams T, Lang RAR, Atit RP, et al. Distinct requirements for cranial ectoderm and mesenchyme-derived Wnts in specification and differentiation of osteoblast and dermal progenitors. *PLoS Genet*. 2014;10(2):e1004152. Barsh GS, editor.
52. Kahler RA, Galindo M, Lian J, Stein GS, Van Wijnen AJ, Westendorf JJ. Lymphocyte enhancer-binding factor 1 (Lef1) inhibits terminal differentiation of osteoblasts. *J Cell Biochem*. 2006;97:969–83.
53. Khan SK, Yadav PS, Elliott G, Hu DZ, Xu R, Yang Y. Induced Gnas R201H expression from the endogenous Gnas locus causes fibrous dysplasia by up-regulating Wnt/ β -catenin signaling. *Proc Natl Acad Sci U S A*. 2018;115(3):E418–27.
54. Bianco P, Kuznetsov SA, Riminucci M, Fisher LW, Spiegel AM, Robey PG. Reproduction of human fibrous dysplasia of bone in immunocompromised mice by transplanted mosaics of normal and G α -mutated skeletal progenitor cells. *J Clin Invest*. 1998;101(8):1737–44.
55. Robinson C, Collins MT, Boyce AM. Fibrous dysplasia/McCune-Albright syndrome: clinical and translational perspectives. *Curr Osteoporos Rep*. 2016;14(5):178–86.
56. Saggio I, Remoli C, Spica E, Cersosimo S, Sacchetti B, Robey PG, et al. Constitutive expression of Gs α (R201C) in mice produces a heritable, direct replica of human fibrous dysplasia bone pathology and demonstrates its natural history. *J Bone Miner Res*. 2014;29(11):2357–68.
57. Zhao X, Deng P, Iglesias-Bartolom R, Amornphimoltham P, Steffen DJ, Jin Y, et al. Expression of an active G α s mutant in skeletal stem cells is sufficient and necessary for fibrous dysplasia initiation and maintenance. *Proc Natl Acad Sci U S A*. 2018;115(3):E428–37.
58. Lan Y, Xu J, Jiang R. Cellular and molecular mechanisms of palatogenesis. *Curr Top Dev Biol*. 2015;115:59–84.
59. Szabo-Rogers HL, Smithers LE, Yakob W, Liu KJ. New directions in craniofacial morphogenesis. *Dev Biol*. 2010;341(1):84–94.
60. Bumann EE, Kaartinen V. Craniofacial morphogenesis. In: *Primer on the metabolic bone diseases and disorders of mineral metabolism*. Wiley; 2018. p. 891–900.
61. Losa M, Risolino M, Li B, Hart J, Quintana L, Grishina I, et al. Face morphogenesis is promoted by Pbx-dependent EMT via regulation of Snail1 during frontonasal prominence fusion. *Development*. 2018;145(5):dev157628.
62. Jiang R, Bush JO, Lidral AC. Development of the upper lip: morphogenetic and molecular mechanisms. *Dev Dyn*. 2006;235(5):1152–66.
63. Marcucio R, Hallgrímsson B, Young NM. Facial morphogenesis: physical and molecular interactions between the brain and the face. *Curr Top Dev Biol*. 2015;115:299–320.
64. Shkroukani MA, Chen M, Vong A. Cleft lip—a comprehensive review. *Front Pediatr*. 2013;1:53.
65. Vanderas AP. Incidence of cleft lip, cleft palate, and cleft lip and palate among races: a review. *Cleft Palate J*. 1987;24(3):216–25.
66. Parada C, Chai Y. Mandible and tongue development. *Curr Top Dev Biol*. 2015;115:31–58.
67. Barske L, Rataud P, Behizad K, Del Rio L, Cox SG, Crump JG. Essential role of Nr2f nuclear receptors in patterning the vertebrate upper jaw. *Dev Cell*. 2018;44(3):337–347.e5.
68. Tan TY, Farlie PG. Rare syndromes of the head and face—Pierre Robin sequence. *Wiley Interdiscip Rev Dev Biol*. 2013;2(3):369–77.

69. Schwabe GC, Trepczik B, Süring K, Brieske N, Tucker AS, Sharpe PT, et al. *Ror2* knockout mouse as a model for the developmental pathology of autosomal recessive Robinow syndrome. *Dev Dyn*. 2004;229(2):400–10.
70. White J, Mazzeu JF, Hoischen A, Jhangiani SN, Gambin T, Alcino MC, et al. DVL1 frameshift mutations clustering in the penultimate exon cause autosomal-dominant Robinow syndrome. *Am J Hum Genet*. 2015;96(4):612–22.
71. White JJ, Mazzeu JF, Hoischen A, Bayram Y, Withers M, Gezdirici A, et al. DVL3 alleles resulting in a -1 frameshift of the last exon mediate autosomal-dominant Robinow syndrome. *Am J Hum Genet*. 2016;98(3):553–61.
72. Spranger JW, Brill PW, Hall C, Nishimura G, Superti-Furga A, Unger S. Bone dysplasias: an atlas of genetic disorders of skeletal development. 4th ed. New York: Oxford University Press; 2018. p. 412–8.
73. Oishi I, Suzuki H, Onishi N, Takada R, Kani S, Ohkawara B, et al. The receptor tyrosine kinase *Ror2* is involved in non-canonical Wnt5a/JNK signalling pathway. *Genes to Cells*. 2003;8(7):645–54.
74. Yamaguchi TP, Bradley A, McMahon AP, Jones SA. Wnt5a pathway underlies outgrowth of multiple structures in the vertebrate embryo. *Development*. 1999;126:1211–23.
75. Person AD, Beiraghi S, Sieben CM, Hermanson S, Neumann AN, Robu ME, et al. WNT5A mutations in patients with autosomal dominant Robinow syndrome. *Dev Dyn*. 2009;239(1):327–37.
76. Afzal AR, Rajab A, Fenske CD, Oldridge M, Elanko N, Ternes-Pereira E, et al. Recessive Robinow syndrome, allelic to dominant brachydactyly type B, is caused by mutation of ROR2. *Nat Genet*. 2000;25(4):419–22.
77. Wang B, Sinha T, Jiao K, Serra R, Wang J. Disruption of PCP signaling causes limb morphogenesis and skeletal defects and may underlie Robinow syndrome and brachydactyly type B. *Hum Mol Genet*. 2011;20(2):271–85.
78. White JJ, Mazzeu JF, Coban-Akdemir Z, Bayram Y, Bahrambeigi V, Hoischen A, et al. WNT signaling perturbations underlie the genetic heterogeneity of Robinow syndrome. *Am J Hum Genet*. 2018;102(1):27–43.
79. Mansour TA, Lucot K, Konopelski SE, Dickinson PJ, Sturges BK, Vernau KL, et al. Whole genome variant association across 100 dogs identifies a frame shift mutation in DISHEVELLED 2 which contributes to Robinow-like syndrome in Bulldogs and related screw tail dog breeds. *PLOS Genet*. 2018;14(12):e1007850. Leeb T, editor.
80. Tao H, Zhu M, Lau K, Whitley O, Samani M, Xiao X, et al. Oscillatory cortical forces promote three dimensional cell intercalations that shape the mandibular arch. *bioRxiv*. 2018;309120.
81. Bernier FP, Caluseriu O, Ng S, Schwartzentruber J, Buckingham KJ, Innes AM, et al. Haploinsufficiency of SF3B4, a component of the pre-mRNA spliceosomal complex, causes Nager syndrome. *Am J Hum Genet*. 2012;90(5):925–33.
82. Terrazas K, Dixon J, Trainor PA, Dixon MJ. Rare syndromes of the head and face: mandibulofacial and acrofacial dysostoses. *Wiley Interdiscip Rev Dev Biol*. 2017;6(3):e263.
83. Kennedy SJ, Teebi AS. Newly recognized autosomal recessive acrofacial dysostosis syndrome resembling Nager syndrome. *Am J Med Genet*. 2004;129A(1):73–6.
84. Hall BD. Nager acrofacial dysostosis: autosomal dominant inheritance in mild to moderately affected mother and lethally affected phocomelic son. *Am J Med Genet*. 1989;33(3):394–7.
85. Chemke J, Mogilner BM, Ben-Itzhak I, Zurkowski L, Ophir D. Autosomal recessive inheritance of Nager acrofacial dysostosis. *J Med Genet*. 1988;25(4):230–2.
86. Petit F, Escande F, Jourdain AS, Porchet N, Amiel J, Doray B, et al. Nager syndrome: confirmation of *SF3B4* haploinsufficiency as the major cause. *Clin Genet*. 2014;86(3):246–51.
87. Watanabe H, Shionyu M, Kimura T, Kimata K, Watanabe H. Splicing factor 3b subunit 4 binds BMPR-IA and inhibits osteochondral cell differentiation. *J Biol Chem*. 2007;282(28):20728–38.
88. Devotta A, Juraver-Geslin H, Gonzalez JA, Hong C-S, Saint-Jeannet J-P. Sf3b4-depleted Xenopus embryos: a model to study the pathogenesis of craniofacial defects in Nager syndrome. *Dev Biol*. 2016;415(2):371–82.
89. Liu KJ. Craniofacial ciliopathies and the interpretation of Hedgehog signal transduction. *PLoS Genet*. 2016;12(12):e1006460.
90. Eggenschwiler JT, Anderson KV. Cilia and developmental signaling. *Annu Rev Cell Dev Biol*. 2007;23:345–73.
91. Corbit KC, Aanstad P, Singla V, Norman AR, Stainier DYR, Reiter JF. Vertebrate Smoothed functions at the primary cilium. *Nature*. 2005;437(7061):1018–21.
92. Lui JC, Garrison P, Nguyen Q, Ad M, Keembiyehetty C, Chen W, et al. EZH1 and EZH2 promote skeletal growth by repressing inhibitors of chondrocyte proliferation and hypertrophy. *Nat Commun*. 2016;7:13685.
93. Hoch RV, Soriano P. Roles of PDGF in animal development. *Development*. 2003;130:4769–84.
94. Schneider L, Clement CA, Teilmann SC, Pazour GJ, Hoffmann EK, Satir P, et al. PDGFR α signaling is regulated through the primary cilium in fibroblasts. *Curr Biol*. 2005;15(20):1861–6.
95. Soriano P. The PDGF alpha receptor is required for neural crest cell development and for normal patterning of the somites. *Development*. 1997;124:2691–700.
96. Tallquist MD, Soriano P. Cell autonomous requirement for PDGFR α in populations of cranial and cardiac neural crest cells. *Development*. 2003;130:507–18.

97. Ferrante MI, Feather SA, Bulfone A, Wright V, Ghiani M, Selicorni A, et al. Identification of the gene for oral-facial-digital type I syndrome. *Am J Hum Genet.* 2001;68(3):569–76.
98. Ferrante MI, Romio L, Castro S, Collins JE, Goulding DA, Stemple DL, et al. Convergent extension movements and ciliary function are mediated by *ofd1*, a zebrafish orthologue of the human oral-facial-digital type I syndrome gene. *Hum Mol Genet.* 2009;18(2):289–303.
99. Bruel A-L, Franco B, Duffourd Y, Thevenon J, Jegou L, Lopez E, et al. Fifteen years of research on oral-facial-digital syndromes: from 1 to 16 causal genes. *J Med Genet.* 2017;54(6):371–80.
100. Ferrante MI, Zullo A, Barra A, Bimonte S, Messaddeq N, Studer M, et al. Oral-facial-digital type I protein is required for primary cilia formation and left-right axis specification. *Nat Genet.* 2006;38(1):112–7.
101. Ferrante MI, Zullo A, Barra A, Bimonte S, Messaddeq N, Studer M, et al. Oral-facial-digital type I protein is required for primary cilia formation and left-right axis specification. *Nat Genet.* 2006 Jan 27;38(1):112–7.
102. Torban E, Kor C, Gros P, Van Gogh-like2 (*Strabismus*) and its role in planar cell polarity and convergent extension in vertebrates. *Trends Genet.* 2004;20(11):570–7.
103. Tidyman WE, Rauhen KA. The RASopathies: developmental syndromes of Ras/MAPK pathway dysregulation. *Curr Opin Genet Dev.* 2009;19(3):230–6.
104. Wu X, Simpson J, Hong JH, Kim K-H, Thavarajah NK, Backx PH, et al. MEK-ERK pathway modulation ameliorates disease phenotypes in a mouse model of Noonan syndrome associated with the *Raf1(L613V)* mutation. *J Clin Invest.* 2011;121(3):1009–25.
105. Zhang Y, Pizzute T, Pei M. A review of cross-talk between MAPK and Wnt signals and its impact on cartilage regeneration. *Cell Tissue Res.* 2014;358:633–49.
106. Tartaglia M, Mehler EL, Goldberg R, Zampino G, Brunner HG, Kremer H, et al. Mutations in *PTPN11*, encoding the protein tyrosine phosphatase SHP-2, cause Noonan syndrome. *Nat Genet.* 2001;29(4):465–8.
107. Araki T, Mohi MG, Ismat FA, Bronson RT, Williams IR, Kutok JL, et al. Mouse model of Noonan syndrome reveals cell type- and gene dosage-dependent effects of *Ptpn11* mutation. *Nat Med.* 2004;10(8):849–57.
108. Chen P-C, Wakimoto H, Conner D, Araki T, Yuan T, Roberts A, et al. Activation of multiple signaling pathways causes developmental defects in mice with a Noonan syndrome-associated *Sos1* mutation. *J Clin Invest.* 2010;120(12):4353–65.
109. Tatum R, Zhang Y, Salleng K, Lu Z, Lin J-J, Lu Q, et al. Renal salt wasting and chronic dehydration in claudin-7-deficient mice. *Am J Physiol Renal Physiol.* 2010;298(1):F24–34.
110. Hernández-Porrás I, Fabbiano S, Schuhmacher AJ, Aicher A, Cañamero M, Cámara JA, et al. *K-RasV14I* recapitulates Noonan syndrome in mice. *Proc Natl Acad Sci U S A.* 2014;111(46):16395–400.
111. Werren JH, Cohen LB, Gadau J, Ponce R, Baudry E, Lynch JA. Dissection of the complex genetic basis of craniofacial anomalies using haploid genetics and interspecies hybrids in *Nasonia* wasps. *Dev Biol.* 2016;415(2):391–405.
112. Gross JB, Powers AK. A natural animal model system of craniofacial anomalies: the blind Mexican cavefish. *Anat Rec.* 2020;303(1):24–9.
113. Chowdhury N, Asakura A. In utero stem cell transplantation: potential therapeutic application for muscle diseases. *Stem Cells Int.* 2017;2017:3027520.
114. Hooper JE, Feng W, Li H, Leach SM, Phang T, Siska C, et al. Systems biology of facial development: contributions of ectoderm and mesenchyme. *Dev Biol.* 2017;426(1):97–114.
115. Wilderman A, VanOudenhove J, Kron J, Noonan JP, Cotney J. High-resolution epigenomic atlas of human embryonic craniofacial development. *Cell Rep.* 2018;23(5):1581–97.
116. Minoux M, Holwerda S, Vitobello A, Kitazawa T, Kohler H, Stadler MB, et al. Gene bivalency at Polycomb domains regulates cranial neural crest positional identity. *Science.* 2017;355(6332):eaal2913.
117. Brinkley JF, Fisher S, Harris MP, Holmes G, Hooper JE, Jabs EW, et al. The FaceBase Consortium: a comprehensive resource for craniofacial researchers. *Development.* 2016;143(14):2677–88.
118. Weinberg SM, Cornell R, Leslie EJ. Craniofacial genetics: where have we been and where are we going? *PLoS Genet.* 2018;14(6):e1007438.



Animal Models for Understanding Human Skeletal Defects

7

Isabella Skuplik and John Cobb

7.1 Overview

Skeletal defects, such as cleft palate, scoliosis, and shortening of the limb bones, are common in the human population. Animal models have been essential for characterizing the molecular and cellular mechanisms that underlie these and other skeletal disorders. This chapter will explore the cellular origins of the vertebrate skeleton and introduce a selection of animal models for human disorders of the skull and facial bones, spinal column, and limbs. The common genetic pathways that build the skeleton of various vertebrate species and how these similarities facilitate the study of human developmental processes in laboratory animals will be a focus of discussion. This chapter will also highlight how current genome editing technologies can be applied to model various perturbations of human chromatin structure in laboratory animals.

7.2 Introduction

Skeletal malformations are among the most common birth defects in humans, affecting up to 1/3000 individuals [1]. Together, there are over

400 disorders of the skeletal system and more than 300 genes implicated in their etiology [2]. The genetic basis for many of these disorders has been elucidated through the combination of mapping and sequencing approaches and the use of animal models to characterize the roles of genes during embryonic or postnatal development. Indeed, animal models have been critical for determining the effects of specific mutations at multiple levels, from immediate changes to protein or RNA function, to the coordination of cellular processes and the morphogenesis of entire tissues and organs. Understanding the genetic pathways that build the skeleton and, in particular, understanding their constraints can guide potential therapies and inform patient outcomes. For example, the structure and size of skeletal elements is controlled by strict regulatory frameworks that dictate the timing and location(s) of gene expression during development. Animal models can often reveal the constraints on gene expression and the associated methods of gene regulation.

Before the development of gene targeting techniques, the generation of animal models of heritable human skeletal defects depended on forward genetic screens or the fortuitous appearance of mutations among breeding stocks. Early mouse models established homology to human mutations by careful morphological and physiological comparison, such as the hypophosphatemia mutant that spontaneously appeared in

I. Skuplik · J. Cobb (✉)
Department of Biological Sciences, University of
Calgary, Calgary, AB, Canada
e-mail: ioskupli@ucalgary.ca; jacobb@ucalgary.ca

Jackson Laboratory stocks and serves as a model for human X-linked hypophosphatemia [3]. Mutagenesis screens using ionizing radiation were particularly effective at generating numerous mouse mutations causing dominantly inherited skeletal defects [4]. One notable example is the gamma-ray-induced cleidocranial dysplasia (*Ccd*) mutation that causes hypoplasia of the clavicle and delayed fontanelle closure in mice, malformations that are homologous to those of humans with cleidocranial dysplasia [5]. Later, the *Ccd* mutations were found to inactivate the orthologous *Runx2* (*Cbfa1*) gene, a “master regulator” of bone development in both humans and mice, confirming the homology of the mouse model [6, 7].

Chemical mutagenesis screens were similarly effective in identifying genes required for skeletal development in zebrafish. In 1996, the Nüsslein-Volhard (Tübingen) and Driever (Boston) research groups completed parallel forward genetic screens using the mutagen ENU (ethylnitrosourea) [8, 9]. In both cases, embryonic and larval fish were observed for deformities under a basic dissecting microscope and categorized according to their phenotypes, for example, the presence of fin or jaw defects. Together, over 6000 mutations were generated and over 1200 were characterized. The Tübingen screen alone identified 372 loci uniquely required for development, including 40 that led to defects in somitogenesis, fin, jaw, or gill arch development when mutated [8–13]. The Boston group concurrently identified 220 loci, and among these, 34 were required for the formation of the craniofacial skeleton [9, 14]. Although a considerable number of mutations remain unmapped (*zhivago*, *postdoc* and *howler* are among the unmapped skeletal mutants [10, 14, 15]), those that have been are largely orthologous to human disease loci. The zebrafish mutants *choker* (*meox1*), *lockjaw* and *mont blanc* (*tfap2a*) have all been mapped to genes implicated in skeletal development and will be discussed as models for human skeletal defects later in this chapter.

As positional cloning of human disease genes expanded rapidly in the mid-1990s, many mutations that cause human skeletal defects were

identified [16]. These included, among many others, the *FGFR3* mutations that cause achondroplasia and thanatophoric dysplasia; the *FGFR2* mutations resulting in Apert, Crouzon, and Pfeiffer syndromes; and the *SOX9* mutations causing campomelic dysplasia [17–22]. While the identification of these genes established a link between certain loci and abnormal skeletal phenotypes in humans, they did not reveal the underlying molecular and cellular mechanisms. To fill this need, orthologous genes had to be identified and selectively disrupted in animal models in order to characterize their precise roles in development. Since gene targeting in the mouse was being developed at the same time as positional cloning of human disease genes, mice were largely the models of choice.

The first knockout mice were generated in 1989, soon after the discovery that modified DNA sequences could be introduced into targeted regions of the genome through homologous recombination in embryonic stem cells [23–25]. Successful germline transmission of a modified allele was first reported for the *Hprt1* locus [26, 27], followed by *c-Abl* and *β 2m* [28, 29]. These experiments set the stage for the next decade of mouse reverse genetics and implicated numerous genes as key regulators of skeletal development. For instance, the first mouse *Hox* knockout (*Hoxa3* [30]) and the many that followed revealed critical roles for *Hox* genes in patterning the axial and limb skeletons [31–34]. Mouse knockouts of *Runx2* and *Sox9* revealed that these genes are absolutely required for bone and cartilage development, osteogenesis and chondrogenesis, respectively [6, 35]. Importantly, some of these early knockouts also became models for rare human diseases, such as the *Twist1* heterozygous knockout mice that are used as a model for Saethre-Chotzen syndrome and display similar limb phenotypes and skull fusions [36–38], or the *Mesp2* and lunatic fringe (*Lfng*) knockout mice that phenocopy the vertebral defects of spondylocostal dysostosis [39–42].

However, the standard knockouts were frequently embryonically lethal, precluding the study of the gene’s function at later stages of development and the elucidation of its molecular

mechanism. Approximately 30% of mouse genes are considered to be essential for development because their homozygous null mutations are lethal [43, 44]. This is particularly relevant for pleiotropic genes that function in different tissue types or at multiple developmental stages. For example, the bone morphogenetic protein BMP4 is required for the development of early embryonic and extraembryonic tissues, such as the atrioventricular septum of the heart [45] and the allantois [46]. Homozygous *Bmp4* knockout mice die around the onset of gastrulation [47]; however, *Bmp4* also has later roles in digit patterning and craniofacial development that cannot be characterized in the standard knockout [48, 49]. Similarly, mice null for Indian hedgehog (*Ihh*) do not survive beyond birth, impeding the study of *Ihh*'s postnatal function in long bones [50, 51].

The development of the Cre-loxP system for generating conditional knockouts circumvented some of these barriers. Driven by a tissue-specific promoter, the Cre recombinase enzyme is able to excise DNA sequences surrounded by specific 34 basepair sequences, called loxP sites. Therefore, when mice carry the Cre driver together with an endogenous gene flanked by loxP sites, the function of the “floxed” gene is removed from the tissue or population of cells where the Cre is expressed. The inclusion of a modified estrogen receptor (ER) domain on the Cre recombinase can additionally be used to achieve temporal control of gene excision [52]. Importantly for this chapter, conditional knockouts can be used to remove the function of a gene in various parts of the developing skeleton, bypassing early lethality or focusing on the function of a gene in a specific cell type. Relevant drivers include *Prrx1-Cre*, *Col2a1-Cre*, and *Osx1-Cre*, targeting the limb and craniofacial mesenchyme, chondrocytes, or osteoblasts, respectively [53]. In the case of *Bmp4*, conditional knockouts with *Prrx1-Cre* demonstrated that its expression in the limb bud mesenchyme helps to regulate the number of digits [48], and eliminating *Ihh* expression with an inducible *Col2a1-Cre* (*col2a1-Cre ER**) demonstrated its continued requirement for the growth of long bones in juvenile mice [51].

More recently, CRISPR-Cas9 technology has opened the door to the efficient modeling of clinically relevant sequence changes and large-scale structural rearrangements in a variety of model organisms. Since the discovery of its mechanism of action in bacterial innate immunity [54], CRISPR (clustered regularly interspaced palindromic repeats)-Cas9 has been used to generate targeted changes in many species, including those poorly amenable to genomic manipulation. Reverse genetics in zebrafish previously relied on expensive engineered nucleases (ZFNs and TALENs) to generate knockouts [55–57], causing researchers to opt for cheaper and simpler knockdown approaches. In chickens, viral transduction was used to express dominant-negative proteins [58, 59]. Now with the efficacy of CRISPR-Cas9, specific nucleotide changes can be performed in these and a handful of other vertebrate and invertebrate species [60].

Furthermore, large deletions, duplications, and inversions can be engineered within chromosomes by the simultaneous injection of multiple guide RNAs that target DNA cleavage to specific regions of the genome [61].

The variety of modifications possible with this system allows for the generation of numerous animal models engineered to mimic human genetic diseases. In the CRISPR-era, research projects are often designed based on the following steps. First, either sequencing of the exome, whole-genome, or a clinically relevant panel of genes or a microarray-based comparative genome hybridization (CGH) approach is used to identify potential disease-causing variants in patient cohorts [62, 63]. Then, CRISPR is used to efficiently generate similar sequence changes in animal models to determine the functional consequences of the mutations on development. For example, Spielmann et al. recently demonstrated how CRISPR could be used to model a human mutation in mice, obtaining a phenotype in less than 10 weeks and confirming the detrimental effect of the mutation in the context of limb development [62].

This chapter will present a selection of animal models for human skeletal defects, including classical models such as the polydactylous *extra*

toes (Xt) mouse and the *talpid* chicken lines, as well as emerging models utilizing CRISPR technology to model specific human mutations. Importantly, the chapter will also discuss how animal models have allowed researchers to uncover networks of gene regulation and gain an understanding of developmental gene function that would not be possible from the sole study of skeletal malformations in humans.

7.2.1 The Structure and Cellular Origins of the Vertebrate Skeleton

The vertebrate skeleton can be subdivided into craniofacial, lower axial (vertebrae and ribs), and appendicular (limb/fin/wing) components. Cells contributing to each part of the skeleton are specified early during development, originating from diverse populations of mesodermal and ectodermal progenitors (Fig. 7.1).

The craniofacial skeleton consists of 14 facial bones (the viscerocranium) and 8 cranial bones (the neurocranium). Facial bones are derived from neural crest cells, which originate at the dorsal edge of the neural tube and migrate into the future facial prominences [64]. These cells form the nasal, zygomatic (cheek), maxillary, and

mandibular (jaw) bones, among others, thereby creating the structure of the face [64]. Cranial bones are derived from a mixture of ectodermal neural crest cells and head mesoderm. These cells form the bones at the top and back of the skull, including the frontal, parietal, and occipital bones [64].

The axial skeleton extends from the base of the skull and comprises the vertebral column and ribs; both structures are formed from the cells of the paraxial mesoderm (Fig. 7.1). Early in development, the paraxial mesoderm becomes transiently segmented into compartments called somites [65]. A group of cells within each somite is then specified—by signals from the adjacent notochord and neural tube—to form the sclerotome. This cell layer will ultimately give rise to the cartilage and bone of the vertebrae and ribs [66]. In addition to the sclerotome, cells from the notochord also contribute to the axial skeleton by forming the nucleus pulposus of the intervertebral discs [66].

The appendicular skeleton is composed of the bones of the fore- and hindlimbs, or wings/fins in other species, as well as the pectoral and pelvic girdles. Bones of the limb can be further regionalized into the proximal stylopod (humerus in the arm, femur in the leg), middle zeugopod (radius/ulna in the arm, tibia/fibula in the leg), and distal

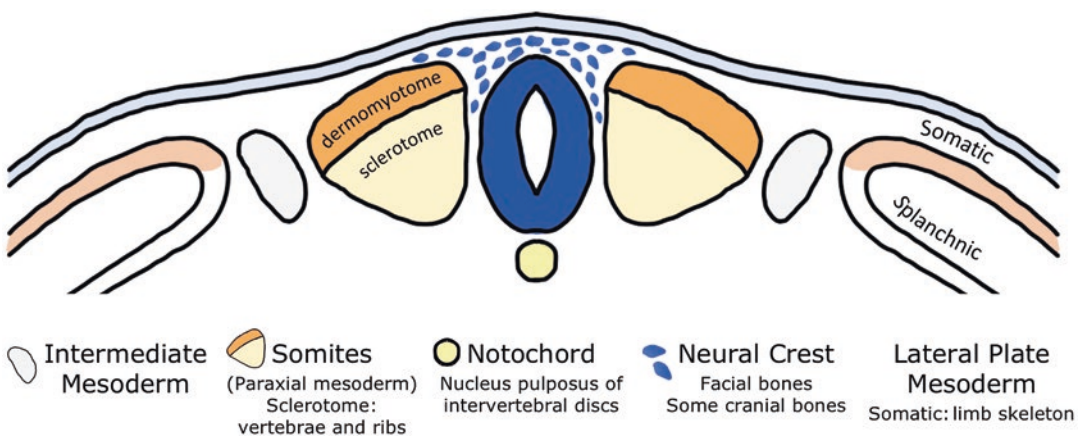


Fig. 7.1 The cellular origins of the vertebrate skeleton. At the anterior of the embryo, craniofacial bones are formed by neural crest cells originating dorsolateral to the neural tube (dark blue) and head mesoderm (not shown). More posteriorly, the axial skeleton (vertebrae

and ribs) is formed from cells of the sclerotome layer of the somites. The notochord (yellow) contributes cells to the nucleus pulposus of the intervertebral discs. The limb skeleton is derived from cells of the somatic lateral plate mesoderm

autopod (bones of the wrist and digits). The appendicular skeleton is formed from cells of the somatic lateral plate mesoderm (Fig. 7.1), through the process of endochondral ossification. Briefly, undifferentiated mesenchymal cells from the lateral plate migrate into the limb fields where they condense and differentiate to yield a cartilaginous template of each skeletal element [67]. Eventually, the cartilage cells (chondrocytes) are replaced by bone, so that each element becomes ossified.

Endochondral ossification is also used to generate the bones of the lower axial skeleton (vertebral column and ribs). In contrast, the majority of bones in the craniofacial skeleton are formed through the process of intramembranous ossification, whereby neural crest or mesodermal progenitors differentiate directly into osteoblasts (immature bone cells) without a cartilage intermediate [64].

Development of the skeleton requires coordination at multiple levels. Finely tuned molecular networks of gene activation and repression coordinate cellular processes, such as migration, proliferation, differentiation, and apoptosis, which in turn guide the morphogenesis of individual bones to assemble the over 200 bones of the human skeleton. Due to the large constraints that are placed on levels, locations, and time-limited periods of gene expression, it is not surprising that skeletal malformations are among the most common birth defects in humans.

7.3 Models for Orofacial Clefting and Other Defects of the Craniofacial Skeleton

Conducting a literature search for models of craniofacial defects makes one thing very clear; classical models continue to provide new and important insights into the etiology of rare diseases. In this section, the classic *talpid* chicken mutants, *talpid*² and *talpid*³, will be discussed alongside mouse models for oral-facial-digital syndrome (OFDS) and Joubert syndrome, respectively. Between 1936 and 1964, three separate *talpid* lines were described; each one arose as a

spontaneous mutation and was characterized by a combination of craniofacial deformities and polydactyly (extra digits), as well as an autosomal recessive inheritance pattern [68–71]. The *talpid*² and *talpid*³ mutations are now known to disrupt two proteins, C2CD3 and KIAA0586, involved in primary cilia formation and cell signaling [72, 73], providing a basis for the two diseases. Additionally, two classic zebrafish mutants, *lockjaw* and *mont blanc*, will be discussed as models for human branchio-oculo-facial syndrome (BOFS). These mutants were isolated from the Tübingen and Boston forward genetic screens and were more recently shown to disrupt *tfap2a*, a gene implicated in the formation of neural crest-derived tissues in fish, frogs, mice, and humans [74–78].

7.3.1 C2cd3 Mouse Mutants and the *talpid*² Chicken Implicate Hedgehog Signaling, Primary Cilia, and Cranial Neural Crest Cells in the Etiology of Oral-Facial-Digital Syndrome XIV

There are 14 classes of oral-facial-digital (OFD) syndromes affecting at least 11 genetic loci (reviewed in [79, 80]). Minimally, these classes share malformations in three areas: the oral cavity, face, and digits (Fig. 7.2a, b) [79]. Affected individuals may present with a cleft tongue, palate, and/or lip, together with facial features such as wide-set eyes (hypertelorism), a small jaw, or broad nasal bridge [80–82]. The appendicular skeleton is also frequently affected, with a range of possible digit patterning defects such as polydactyly, syndactyly (incomplete separation of the digits), and brachydactyly (short digits) [80, 81]. Interestingly, many of the OFD subclasses are caused by mutations that disrupt the formation or transport processes of primary cilia, suggesting a common mechanism of disease (reviewed in [80, 83]). The first subclass results from mutations in a gene encoding a centriolar protein called OFD1 [84, 85]. Two centrioles, a mother and daughter, localize to the base of the primary cilium, and the

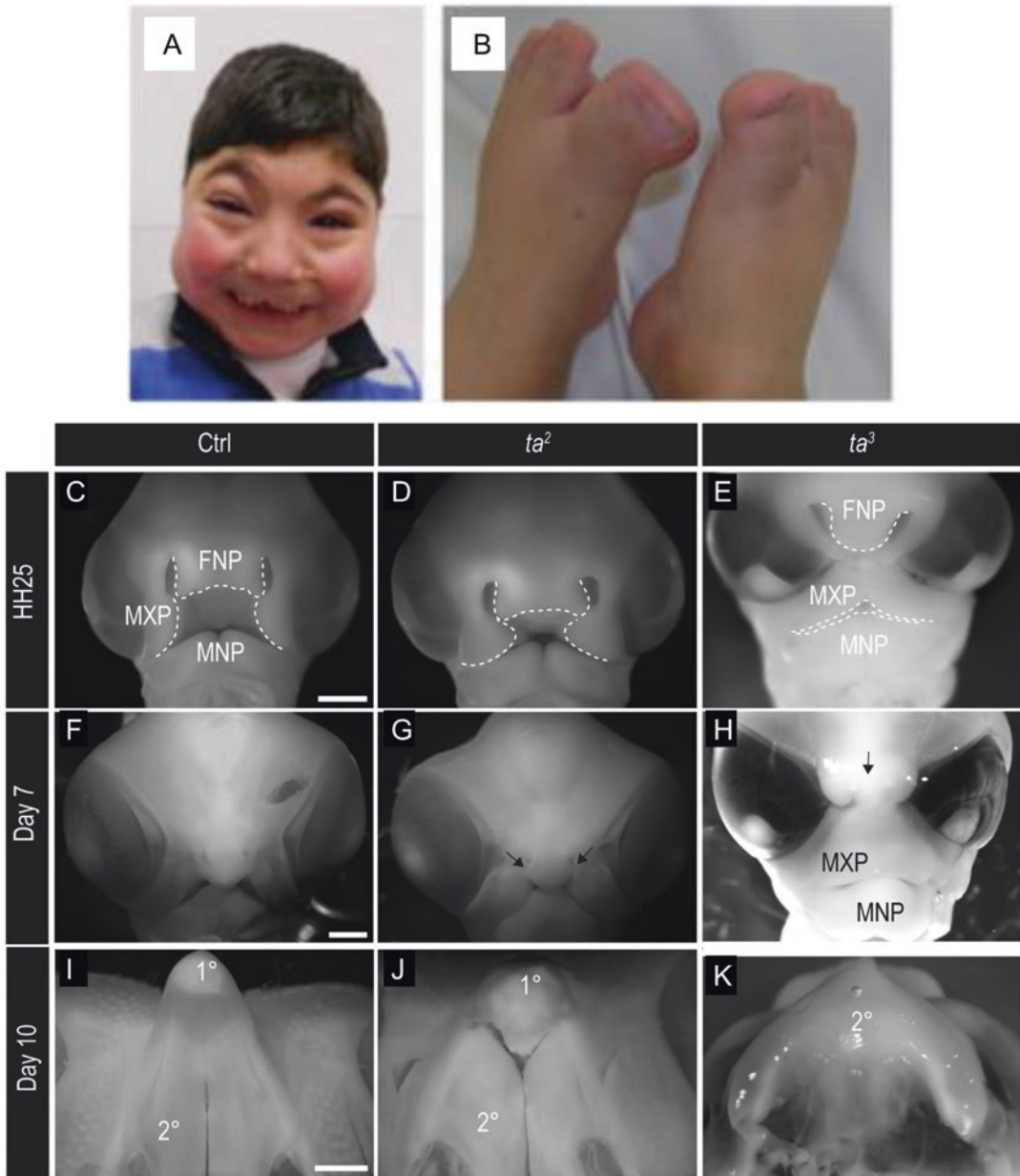


Fig. 7.2 (a, b) A child with oral-facial-digital syndrome and syndactyly. Control (c, f, i), *talpid²* (d, g, j) and *talpid³* (e, h, k) chicken lines at three developmental stages. Panel (g) indicates a facial cleft. Panels (i, j, k) compare the primary (1°) and secondary (2°) palate defects in the *talpid* lines. *FNP* frontonasal process, *MXP* maxillary process, *MNP* mandibular process. ((a, b) Reprinted with permission from Springer Nature Customer Service Centre GmbH: Springer Nature; Journal: Nature Genetics, Article: The oral-facial-digital syndrome gene C2CD3

encodes a positive regulator of centriole elongation. Christel Thauvin-Robinet, Jaelyn S Lee, Estelle Lopez, Vicente Herranz-Pérez, Toshinobu Shida et al. (2014). (c–k) Reprinted from *Developmental Biology*, 415(2), Elizabeth N. Schock, Ching-Fang Chang, Ingrid A. Youngworth, Megan G. Davey, Mary E. Delany, Samantha A. Brugmann, Utilizing the chicken as an animal model for human craniofacial ciliopathies, p326–327, (2016), with permission from Elsevier)

mother centriole forms the microtubule-organizing center or basal body of the primary cilium. OFD1 localizes to the distal end of the basal body and interacts with the C2 calcium-dependent domain-containing protein, C2CD3 [86]. Nonsense and missense mutations in *C2CD3* were recently determined to be the cause of OFD subtype XIV [86].

Importantly, animal models have demonstrated the requirement for *C2CD3* in ciliogenesis. Two mouse mutants with a loss of C2CD3 function, *Hearty (Hty)* and *C2cd3^{GT}*, had a significant reduction in the number of cells extending primary cilia at embryonic stages [87]. They also displayed phenotypes associated with defective cilia, including left-right asymmetry reversal, polydactyly, and neural tube defects [87]. Later studies using cells derived from the mouse mutants, in addition to mouse and human cell lines, showed that C2CD3 may counter the role of OFD1 and promote centriole elongation [86]. In support of this, a protein that forms a centriolar cap and is normally removed during the initiation of ciliogenesis, CP110, remained at the mother centriole in *C2cd3^{GT}* mutant cells [88]. C2CD3 was also needed to localize proteins that are involved in transport processes within the primary cilium [88]. The failure to remove CP110 and recruit intraflagellar transport proteins was recently confirmed in OFDXIV patient fibroblasts with *C2CD3* mutations, demonstrating the utility of the animal model [89].

A classic chicken mutant, *talpid²*, has also been useful for understanding OFD syndromes (Fig. 7.2d, g, j). The *talpid²* mutation arose spontaneously during an 18-year-long selection experiment for longer shank length in chickens, carried out by I. Michael Lerner between 1938 and 1956 [90–92]. The phenotype was initially described by Abbott et al. as a lethal mutation with craniofacial defects including a small and/or crossed beak, a shortened vertebral column, shortened long bones, and extra digits that were also fused (synpolydactyly) [69, 92]. Similar to OFDXIV patients, *talpid²* mutants also have facial and palatal clefting (Fig. 7.2g, j), midline defects, and polydactyly [72, 93, 94]. In 2014, a 19-bp deletion in the chicken *C2CD3* gene was

found to be the cause of the *talpid²* phenotype [72]. Therefore, *talpid²* is currently being used as a model to study the basis of skeletal defects in OFDS.

Similar to the mouse mutants, *talpid²* embryos have a significant reduction in the number of cells with primary cilia, notably within the cranial neural crest [93], and in embryonic fibroblasts derived from the limb and facial prominences [72]. Schock et al. observed defects in directional migration and increased dispersal of cranial neural crest cells in *talpid²* mutants [94]. Cranial neural crest cells populate the facial prominences and effectively create the shape and structure of the face; therefore, their disruption has been suggested to underlie a subset of the skeletal defects in *talpid²* chickens and OFDS patients [94]. *Talpid²* mutants also had increased expression of genes that modulate cartilage development (*Sox9* and *Fgf8*) in the facial prominences [94, 95], in addition to changes in hedgehog pathway components (*Shh/Gli*) that can influence cell proliferation and facial midline spacing [72, 93, 95]. Indeed, the facial and limb phenotypes of *talpid²* and OFDXIV were noted to be similar to models with increased sonic hedgehog (*Shh*) signaling [83, 96]. Primary cilia are known to be important for mediating the response to hedgehog signaling through the localization of effectors and processing of GLI transcription factors, so changes in the levels or expression domains of these proteins in *talpid²* mutants are in agreement with the phenotype of disrupted ciliogenesis.

In the absence of hedgehog signaling, Patched receptors inhibit Smoothed transmembrane proteins such that they are excluded from the primary cilium [97]. GLI proteins remain bound to the pathway antagonist, suppressor of fused (SuFu), and are processed into transcriptional repressors in the cytoplasm [97]. In the presence of a ligand, Patched is removed from the membrane and Smoothed is able to enter the cilium and promote the release of GLI from SuFu, thereby preventing its processing into a repressor [97]. Activated GLI proteins are then transported out of the cilium and into the nucleus where they can activate transcription. Interestingly, both

the *talpid²* chicken and mouse *C2cd3* mutants had increased levels of GLI3 activators in their frontonasal, maxillary, and mandibular prominences [72, 87]. Therefore, Schock et al. proposed that increased levels of GLI activators or the concurrent reduction of repressor proteins could contribute to the facial phenotypes of *talpid²* chickens, perhaps by derepressing *Fgf8* or other chondrogenesis targets [83, 94]. Evidence for the latter scenario comes from the observed reduction in GLI3 repressor binding near four of its target genes in *talpid²* mutants [98]; however, the exact consequences of the altered GLI protein ratio remain uncertain. Future studies with *talpid²* may elucidate the role of hedgehog signaling in this process and in the facial phenotypes of OFDXIV patients.

Finally, C2CD3 has been shown to interact with or recruit other centriole-associated proteins involved in oral-facial-digital syndromes, including SCLT1 [86, 88], while other OFD subtypes implicate proteins involved in downstream ciliary processes such as intraflagellar transport and signaling (reviewed in [80]). Therefore, from animal models and patient samples, we have learned that disruption at potentially multiple stages of ciliogenesis may contribute to OFD syndromes. In addition, changes to neural crest cell migration, the availability or activity of key transcription factors, and the expression of chondrogenesis genes are potential modulators of OFD phenotypes.

7.3.2 Joubert Syndrome Is Caused by Mutations in the Ciliary Protein KIAA0586

Similar to OFDS, Joubert syndrome also arises from mutations in genes encoding components of the primary cilium [99]. Indeed, overlapping sets of genes are implicated in OFDS and Joubert syndrome (reviewed in [79]). Joubert syndrome is primarily characterized by brain abnormalities and developmental delay, but it can also be associated with craniofacial malformations and polydactyly [83, 100]. In 2015, the gene *KIAA0586* was found to be disrupted in a subset of individuals

with Joubert syndrome [99, 101]. Mutations in the chicken ortholog had previously been shown to be responsible for the *talpid³* mutant [73], which has a combination of midline defects including eye fusions and a missing upper beak (Fig. 7.2e, h, k), brain abnormalities, a short vertebral column and polydactyly [70, 71]. Similar to *talpid²*, the *talpid³* mutant was found to have altered hedgehog signaling and processing of GLI proteins [73, 102–104]; however, disruptions in planar polarity and cell polarity were also observed, implicating Wnt/PCP and potentially other pathways in the development of Joubert syndrome [99].

Interestingly—like C2CD3—the KIAA0586 protein is localized to the distal ends of centrioles and is required for ciliogenesis [105, 106]. KIAA0586 also interacts with CP110 [106], the capping protein that fails to be removed in *talpid²* chicken mutants and individuals with OFDSXIV. Furthermore, a recent study demonstrated that the two *talpid* proteins, C2CD3 (*talpid²*) and KIAA0586 (*talpid³*), can physically interact in a human cell line, and a complex of KIAA0586, C2CD3, and OFD1 has been proposed to coordinate multiple aspects of ciliogenesis, such as centriole maturation and the recruitment of intraflagellar transport proteins [107]. Therefore, it is likely that these proteins work together to direct aspects of ciliogenesis and morphogenesis of the facial skeleton during development.

7.3.3 Models for Branchio-Oculo-Facial Syndrome (BOFS)

Branchio-oculo-facial syndrome (BOFS) is a rare craniofacial disease caused by defects in the first two branchial (pharyngeal) arches [78]. Affected individuals can have a cleft lip and palate, eye defects including microphthalmia, impaired hearing, and facial features such as a high forehead and small malar (cheek) [108]. Some of the hearing deficits have been attributed to malformed or fused ossicles—three small bones (malleus, incus, and stapes) in the middle ear [109, 110]. BOFS results from heterozygous

mutations in the gene *TFAP2A* and is inherited in an autosomal dominant manner [78, 108]. The *TFAP2A* gene encodes a transcription factor called AP-2, and most mutations disrupt the DNA binding domain of the protein [111]. Reported BOFS mutations are thought to produce either a partial or complete loss of protein function, or in more severe cases, a dominant-negative mutation that can interfere with the activity of normal AP-2 proteins generated from the other allele [111].

Through animal models, we have learned about the important role that *TFAP2A* has in neural crest lineages. Neural crest cells are a multipotent cell type that is specified in a region of ectoderm lateral to the neural plate, or dorsolateral to the neural tube (Fig. 7.1). Cells that are specified as neural crest undergo an epithelial-to-mesenchymal transition and migrate along specific paths to reach different destinations in the body. Different streams of crest are exposed to different environmental factors and are consequently committed to different fates, giving rise to bones, cartilage, melanocytes, neurons, glia, and other cell types [112]. Cranial neural crest cells that populate the frontonasal process and first two pharyngeal arches differentiate to form the bones and cartilage elements of the face [64].

Zebrafish were among the first animal models to implicate *TFAP2A* in neural crest cell development and survival. In 1996, the Tübingen and Boston screens generated two zebrafish mutants, *lockjaw (low)* and *mont blanc (mob)*, whose mutations were mapped to the *tfap2a* gene in 2003 [10, 14, 74, 75]. *Mob* was characterized by undergrowth of the facial skeleton, including components of the hyoid and more posterior branchial arches [14]. Similar phenotypes were observed for *low*—missing arch derivatives, a displaced jaw, and other smaller or inappropriately fused elements [10]. Particularly relevant to BOFS, the ethmoid plate and trabeculae of *low* and *mob* mutants, which are derived from the cranial neural crest, were malformed [10, 14]. These are structures within the zebrafish neurocranium that have similar developmental origins to the mammalian palate and can be used as models for human palatal defects [113, 114]. Specifically, the ethmoid plate of *low* fish was split at the middle

and sometimes absent in *mob*, and both *low* and *mob* mutants had smaller or thinner trabeculae [10, 14, 75]. This is akin to the cleft palate phenotype of BOFS patients, and at the cellular level, both structures arise from populations of neural crest cells that contribute to the frontonasal and maxillary prominences, the latter arising from the first pharyngeal arch ([75, 113]; reviewed in [114]).

The zebrafish jaw and mammalian ear also have similar origins from the first and second pharyngeal arches [114, 115]. Although not particularly severe phenotypes, *low* and *mob* fish had changes in the positioning or structure of Meckel's cartilages, the quadrates and hyosymplectics [10, 14]. These elements are equivalent to the malleus, incus, and stapes bones of the mammalian middle ear, which are malformed and/or fused in some BOFS patients with hearing deficits [109, 110, 114]. These commonalities therefore implicate a subset of neural crest cells in the craniofacial defects of BOFS and *low/mob* zebrafish.

Indeed, in 2003, two groups confirmed that *tfap2a* is required for the survival and specification of certain neural crest lineages in zebrafish, including the craniofacial cartilage and melanocytes [74, 75]. These studies showed contradicting requirements for *tfap2a* in early crest specification; however, later research indicated that *tfap2a* may have roles at multiple stages of development [116, 117]. At early stages, *tfap2a* appears to function together or upstream of *foxd3* to induce neural crest formation in zebrafish, perhaps by modulating Wnt and BMP signals in the ectoderm [116]. Similar findings were observed in *Xenopus laevis* frogs, demonstrating conserved and early functions for *tfap2a* in neural crest induction [117]. Later in development, *tfap2a* appears to regulate cell survival and differentiation along certain lineages [75].

Mouse models have also contributed to our understanding of *Tfap2a* gene function during development. Standard knockout mice were generated around the same time as *low* and *mob* zebrafish and were similarly observed to have craniofacial defects, although the phenotypes were much more severe [118, 119]. Several facial

prominences did not fuse and others were missing entirely in homozygous null mice, which also had open neural tubes and abdominal cavities and died around birth [118, 119]. Interestingly, heterozygous mice appeared mostly normal [119], suggesting that the human craniofacial skeleton is more sensitive to changes in *TFAP2A* dosage. Later studies demonstrated both autonomous and nonautonomous roles for *Tfap2a* in the cranial neural crest, as conditional knockout mice lacking *Tfap2a* in neural crest cells (Wnt1-Cre driver) displayed only a subset of the defects of standard knockout mice [77]. Of benefit to BOFS modeling, less severe phenotypes such as a cleft secondary palate presented in conditional knockouts, indicating defects in first arch-derived neural crest and confirming a role for *Tfap2a* in palate development [77]. The middle ear bones were also malformed, in particular the stapes, which is derived from the second arch and whose equivalent structure was disrupted in zebrafish *tfap2a* mutants and individuals with BOFS [10, 14, 109]. In the future, this model could be especially useful for characterizing the gene regulatory networks that are disrupted and lead to clefting and hearing defects in BOFS.

Recently, aberrant growth of the maxillary and nasal prominence was found to underlie the cleft palate defect in mice with reduced *Tfap2a* dosage [120]. By lowering the expression of *Fgf8*, the authors were able to reduce the penetrance of bilateral clefting, suggesting that the genes act in a common pathway to direct certain aspects of facial morphogenesis [120].

Together, animal models have demonstrated the necessity of *TFAP2A* for neural crest cell development and survival. They have provided a basis for several of the craniofacial defects in BOFS and will likely continue to inform our understanding of the molecular networks that are perturbed in this and other syndromes involving facial clefting and auditory defects. From this and other research, *TFAP2A* has been incorporated into multiple gene regulatory networks governing early neural crest processes, as well as later genetic interactions within the developing craniofacial skeleton [76, 112, 120].

Taken together, the mutants described in this section illustrate the utility of chick, mouse, and zebrafish models in revealing the gene expression, protein processing, cell migration, ciliary, and morphogenesis defects underlying human craniofacial defects. Such mechanistic insight is only possible with the availability of a time series of mutant animal embryos.

7.4 Approaches to Modeling Defects of the Axial Skeleton

The axial skeleton extends from the base of the skull forming the backbone (vertebral column) and ribs of the animal. The organization and number of vertebrae dictate the anterior-posterior body plan of the organism while providing structural support for the body and protecting vital organs of the respiratory and circulatory systems. The vertebral column also encases the spinal cord and, together with the skull, is critical for protecting the central nervous system. A number of developmental processes can affect the formation of the axial skeleton. Defects in the formation of somite boundaries during the segmentation of the paraxial mesoderm, or in the specification and reorganization of the sclerotome cell layer, can lead to vertebral and rib fusions and irregularly shaped vertebral bodies [40, 42, 121]. These phenotypes are often observed in human spondylocostal dysostosis as a result of mutations in the Notch signaling pathway or its downstream targets, which are required for proper somite segmentation (reviewed in [122]).

The incorrect specification or patterning of the sclerotome can also lead to vertebral and rib malformations, and mutations in the *sonic hedgehog* (*SHH*), *PAX1*, and *MEOX1* genes have been implicated in these processes [123]. Two of these genes will be discussed in the etiology of Klippel-Feil syndrome and its animal models, later in the chapter.

Portions of sclerotomes of adjacent somites eventually combine, and the cells differentiate to form the cartilage and bone of the vertebrae and ribs [66]. After birth, the vertebral bodies and ribs

continue to grow, and these later developmental processes continue to modulate the structure of the axial skeleton [124–126]. For instance, the vertebral column can become increasingly curved into adulthood. Scoliosis is a curvature of the spine of more than 10° that can present at birth (congenital scoliosis) as a result of vertebral defects, or later during postnatal development [127, 128]. If scoliosis is independent of a syndrome or a patent structural deformity, it is called idiopathic scoliosis [128, 129]. This form of scoliosis arises most frequently during adolescence and affects up to 5% of the population, with a strong female sex bias for incidence and severity [127]. In this section, a zebrafish mutant with defects in Wnt signaling will be discussed as a model for human idiopathic scoliosis [129, 130]. Furthermore, a recent CRISPR-generated *TBX6* hypomorphic mouse will be described as a model for congenital vertebral defects [131].

7.4.1 Zebrafish Models of Spinal Curvature Implicate Wnt Signaling, Cerebrospinal Fluid Flow, and Cilia in Idiopathic Scoliosis

Studies on spinal curvature in fish have raised an interesting point that rodents may not be the most suitable models for human idiopathic scoliosis (IS), because the center of mass is different in quadrupeds compared to humans [129, 130]. As fish swim, they generate head-to-tail forces that are thought to affect the spine similarly to humans standing upright [130, 132]. Therefore, if mechanical forces on the spine contribute to scoliosis development, fish may be the superior laboratory model to study this process. Indeed, juvenile-onset spinal curvatures have been detected in both zebrafish and guppies [130, 133].

The Ciruna group was the first to create a genetic model for idiopathic scoliosis (IS) in zebrafish [130]. By inactivating the zebrafish *ptk7* gene with zinc finger nucleases (ZFNs), they generated a progressive spinal curve in juvenile fish that increased in severity during the “growth

spurt” phase around 28 days of age (Fig. 7.3) [130, 134]. Like in human cases of IS, vertebral malformations were not detected until juvenile stages, with females again being more severely affected [130]. The *ptk7* gene encodes a transmembrane protein with an inactive tyrosine kinase domain that can modulate both canonical Wnt and noncanonical Wnt/PCP signaling and form complexes with several Wnt receptors [134–137]. In mice, a loss of *Ptk7* prevents the neural tube from closing and disrupts the polarization of hair cells in the inner ear, while *Xenopus* deficient for *ptk7* have problems with neural tube closure and convergent-extension movements [135, 138]; these are phenotypes associated with PCP defects. PTK7 has also been found to interact with Wnt co-receptor LRP6 and recruit the pathway effector Dishevelled [136]. However, it had not been previously implicated in scoliosis. Hayes et al. identified a heterozygous sequence change in a patient with IS affecting an extracellular domain of the PTK7 protein (patient shown in Fig. 7.3g) [130]. In *ptk7* mutant zebrafish, mRNA with the human mutation could not rescue phenotypes associated with defective Wnt/PCP signaling or a gain of canonical Wnt signaling, while wild-type human *PTK7* mRNA could [130]. It is therefore possible that changes in Wnt signaling contribute to the scoliosis phenotypes of humans as well as zebrafish; however, this remains to be established [130].

Interestingly, zebrafish lacking both zygotic and maternal *ptk7* had more serious phenotypes, namely congenital vertebral defects, convergent-extension and neurulation problems, and early death [130, 134]. Thus, it may be that *PTK7* is also required for earlier embryonic processes in humans. In support of this, two recent studies identified *PTK7* mutations in human neural tube closure defects, including in one individual with a form of spina bifida resulting from a substitution at the same position (proline 545) as the IS patient identified by Hayes et al. [139, 140]. Both mutations are predicted to disrupt an extracellular immunoglobulin-like domain and function as hypomorphs [130, 139], but it may be that the amino acid substitution causing neural tube

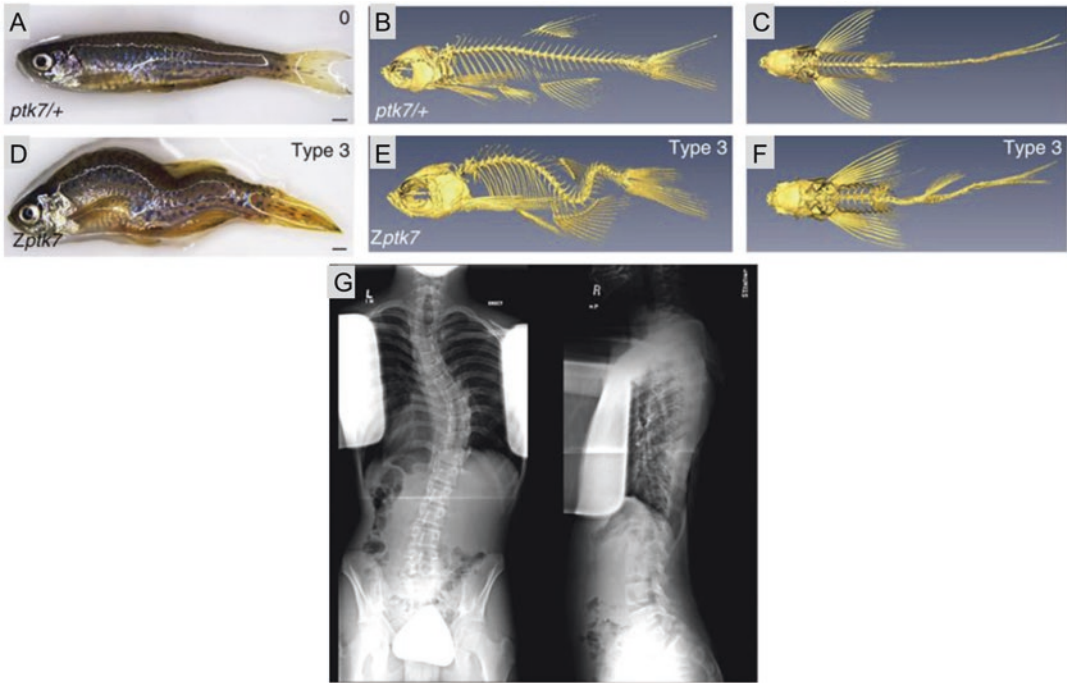


Fig. 7.3 Zebrafish with mutations in *ptk7* display spinal curvatures (d–f) similar to humans with idiopathic scoliosis (g). Panels (a–c) are heterozygous fish, used as controls. The individual in panel (g) has a heterozygous mutation in the *PTK7* gene. (Reprinted with permission from Springer Nature Customer Service Centre GmbH:

Springer Nature; Journal: Nature Genetics, Article: *ptk7* mutant zebrafish models of congenital and idiopathic scoliosis implicate dysregulated Wnt signalling in disease. Madeline Hayes, Xiaochong Gao, Lisa X Yu, Nandina Paria, R. Mark Henkelman et al. (2014))

defects has a greater disruption to protein function than the IS substitution. In this regard, *PTK7* mutations could yield a spectrum of phenotypes, from mild spinal curvatures to more serious conditions affecting the brain and spinal cord. IS has also been proposed to arise secondarily to mild neural tube defects or changes in the flow of cerebrospinal fluid (CSF) within the brain and spinal cord [129, 141]. One study found that individuals with the neural tube defect spina bifida and hydrocephalus (excess cerebrospinal fluid in the brain) were more likely to be diagnosed with scoliosis that required corrective surgery [142]. Similarly, in *ptk7* mutant zebrafish, hydrocephalus often accompanied spinal curvature [141]. Therefore, the Ciruna group investigated whether changes in CSF flow and distribution could be responsible for these pleiotropic phenotypes [141].

The CSF is created in regions of the brain called the choroid plexus and is circulated within

the brain's ventricles and central canal of the spinal cord by ependymal cells (reviewed in [143, 144]). Ependymal cells (ECs) are derived from specific ventral domains of the developing spinal cord and from radial glia in the brain [145–147]. Importantly, ECs contain microvilli and multiple motile cilia, the latter of which beat in a coordinated manner to circulate the CSF [144, 148]. The motile cilia are highly polarized on each cell and across the epithelium, and the Wnt/PCP pathway has been implicated in this polarization, which subsequently affects CSF flow velocity [149, 150]. If the motility of these cilia is disrupted, CSF flow is hindered and hydrocephaly can arise (reviewed in [151]). Because of the connection between *PTK7*, Wnt/PCP, and CSF, the Ciruna lab questioned whether aberrant CSF flow as a result of disrupted EC cilia was the cellular defect responsible for scoliosis in zebrafish [129, 141].

In support of this hypothesis, *ptk7* mutant zebrafish had fewer and more disorganized cilia on ECs within the ventricles, implying defects in both ciliogenesis and polarization [141]. Furthermore, the CSF flow was markedly slower and less directed. Expressing *ptk7* in cells with motile cilia, including ECs, rescued all of these defects and prevented scoliosis in *ptk7* mutant fish, indicating that *ptk7* expression in these cells was sufficient for maintaining CSF flow and spinal structure [141]. The authors further determined that ciliary motion was required within a specific developmental time frame that overlapped with the juvenile growth spurt, in order to maintain a straight spine. Although this study demonstrated that ciliary motion and—likely—proper CSF flow are needed to maintain normal spinal curvature, it did not establish how these dynamics relay signals that influence the vertebral bone and cartilage. The missing link might be a population of mechanosensory neurons within the spinal cord, called CSF-contacting neurons [152, 153]. These neurons have microvilli and a motile cilium and form synapses with interneurons that feed into neuronal networks for locomotion [152, 154, 155]. In zebrafish, CSF-contacting neurons are activated when the spine is bent actively or passively at the site of spinal curvature, suggesting that they may be relaying positional information about the body axis [152, 153]. Furthermore, CSF-contacting neurons contain Pkd211 ion channels that are required for neuronal activation during movement of the spine and so could potentially modulate the signal relay [153]. Zebrafish lacking *Pkd211* also develop spinal curvature, and because this marker seems to be specific to these neurons in the spinal cord, it is possible that they have a role in sensing changes in CSF dynamics and relaying this to higher neural networks [153].

This leads to a possible model for spinal curvature, where defects in the generation (ECs) or sensing (CSF-contacting neurons) of CSF flow may ultimately lead to scoliosis [129]. How exactly aberrant CSF flow and alterations to neuronal networks lead the body to modify the skeleton at particular levels along the anterior-posterior axis is still unknown [129, 156].

However, the *ptk7* zebrafish appears to be a unique and informative model to address these questions.

7.4.2 Animal Models for Klippel-Feil Syndrome: From Mouse Mutants to Emerging Models in the Field

Klippel-Feil syndrome is a congenital vertebral deformity characterized by fusions of the cervical vertebrae and, frequently, an elevated scapula (Sprengel's deformity) [157, 158]. The syndrome is associated with mutations in *MEOX1*, *GDF6*, and *PAX1* genes [158–160]. *MEOX1* encodes a homeodomain-containing transcription factor that is expressed in mesodermal derivatives along with another member of the mesenchyme homeobox gene family, *MEOX2* [161, 162]. In mice, *Meox1* is expressed within the dermomyotome and sclerotome of the somites and is partially redundant with *Meox2* in early somitogenesis [162–164]. Mice lacking both copies of *Meox1* have defects in the axial skeleton, including fusions of the cervical vertebrae and basal skull bones, while *Meox2* knockout mice have defects in muscle development [162, 164, 165]. In *Meox1* null mice, the neural arches (components of vertebrae that surround the spinal cord) of the second and third, or third and fourth, cervical vertebrae are sometimes fused [164]. In addition, the first cervical vertebra (the atlas) is variably combined with the occipital bones of the skull, a defect that is sometimes also observed in individuals with Klippel-Feil syndrome [164, 166, 167].

Besides recapitulating a subset of Klippel-Feil syndrome phenotypes, the *Meox1* mouse has been helpful for identifying cellular processes and genetic interactions that inform the syndrome's etiology. Skuntz et al. observed reduced expression levels of several sclerotome genes in *Meox1* mutant mice, particularly in the anterior somites corresponding to the cervical vertebrae and base of the skull [164]. One of these genes, *Bapx1*, is required for chondrogenesis and, in particular, for the formation of the vertebral bodies and intervertebral discs [168, 169]. Mice lacking this

transcription factor have decreased proliferation of sclerotome cells and fail to upregulate genes involved in endochondral ossification, such as collagens, *Sox9*, and osteopontin (*Spp1*) [169–171]. Interestingly, changes in the proliferation rates of sclerotome cells were also observed in *Meox1* null mice [164]. Like the *Meox1* mutant mice, *Bapx1* mutants also have defects in occipital bone formation [168]. The reduced expression of *Bapx1* in *Meox1* mutants and previous studies demonstrating that MEOX1 can bind to and activate the *Bapx1* promoter in cell culture [172] suggest that *Bapx1* may be a direct target of MEOX1 within the anterior somites and is therefore likely to contribute to the axial defects of Klippel-Feil syndrome.

Notably, *PAX1*, another gene expressed in the sclerotome, is also implicated in Klippel-Feil syndrome and other congenital vertebral defects [159, 173]. *PAX1* expression in the sclerotome is activated by sonic hedgehog signals from the notochord and floor plate of the neural tube [66]. Mice lacking *Pax1* and *Pax9* genes do not form vertebral bodies and intervertebral discs and lose the expression of *Bapx1* in the sclerotome, while *Meox1* expression remains normal [174]. Although *Pax1* and *Pax9* levels have not been observed to be reduced in *Meox1* mutant sclerotomes, they are reduced in *Meox1:Meox2* combined mutant mice [162]. Therefore, animal models have provided a rudimentary genetic pathway, where *Meox1*, *Pax1*, and *Pax9* are upstream of the chondrogenic regulator *Bapx1*, and *Meox1* may function either in concert with *Pax1* or upstream to promote sclerotome development. The aforementioned mouse mutants have been invaluable for characterizing the timing and locations of expression of Klippel-Feil candidate genes and will likely continue to inform the molecular and cellular basis of human vertebral defects.

In 2018, a zebrafish model for Klippel-Feil syndrome was described [175]. The *meox1* mutant *choker* was generated by the Tübingen genetic screen and, like the mouse model, displayed anterior vertebral fusions [13, 175].

Interestingly, the zebrafish model had an equivalent defect to Sprengel's deformity, where the left pectoral girdle of *choker* mutants was often more anteriorly displaced than the right [175]. Future studies with *choker* may help to elucidate the cause of Sprengel's deformity in patients with Klippel-Feil syndrome and solidify the gene regulatory networks underlying sclerotome differentiation in humans and other vertebrates.

Finally, mutations in the growth/differentiation factor gene *GDF6* have also been identified in Klippel-Feil syndrome [160]. *GDF6* is a member of the BMP family of signaling molecules and is important for the formation of various joints and ligaments within the body [176]. Mice lacking *Gdf6* have fused carpals and tarsals, but combined *Gdf5/Gdf6* mutants also have defects in the axial skeleton [176]. A recent study demonstrated that *GDF6* is expressed in the cartilage of vertebral bodies and intervertebral discs of human fetuses [177]. As development proceeds, *GDF6* is downregulated in ossification centers and maintained around chondrocytes, suggesting that it is important for cartilage development [177]. With regards to Klippel-Feil syndrome, a loss of functional *GDF6* may contribute to vertebral fusions by hindering the proper formation of joints between contiguous vertebrae [160, 177]. Future studies with *Gdf5* and *Gdf6* knockout mice may prove to be useful for elucidating the precise role and regulation of members of this gene family in vertebral joint formation. For instance, *Gdf5* is now known to be regulated by a number of modular enhancers that activate its expression in various joints within the mouse body [178]; therefore, it will be interesting to learn if *Gdf6* regulation is similarly modular and whether the mutation of specific noncoding sequences contributes to a subset of Klippel-Feil cases. This is especially relevant because cases resembling Klippel-Feil syndrome have been identified that lack a clear molecular cause [179], suggesting that there are yet additional genes or regulatory sequences involved in this developmental process whose roles have not been fully characterized.

7.4.3 Rapid Modeling of a Human *TBX6* Mutation in Mice Using CRISPR/Cas9 Editing

Several studies have reported an incidence of approximately 10% for *TBX6* compound heterozygous mutations in cohorts with congenital vertebral malformations [131, 180]. *TBX6* is a T-box transcription factor that is involved in specifying the paraxial mesoderm, the precursor of the somites, by repressing neural fates and activating presomitic mesoderm (PSM) genes such as mesogenin 1 (*Msgn1*) [181–183]. Mice that are completely null for *Tbx6* incorrectly activate *Sox2* expression in the paraxial mesoderm and form ectopic neural tubes in place of the somites [181, 184]. Animal models have shown that *Tbx6* also feeds into the Notch segmentation pathway that directs somitogenesis, by maintaining the expression of the Notch ligand *Dll1* [185] and the segmentation gene *Mesp2* [186, 187]. Within the presomitic mesoderm, *TBX6* expression is repeatedly restricted through protein degradation [187]. The regressing anterior limit of *TBX6* sets the boundary of the next forming somite (reviewed in [65]). While a complete loss of *Tbx6* leads to a switch from mesodermal to neural fate at the level of the PSM and early embryonic lethality [181], a substantial reduction in *Tbx6* levels appears to prevent proper segmentation or differentiation of the somites [131]. In 2019, Yang et al. identified ten patients with misshapen or improperly segmented vertebra that had a deletion of *TBX6* at one allele and hypomorphic variant in the noncoding region of the other allele [131]. Using CRISPR/Cas9 genome editing, they created a mouse model with similar genetic changes leading to a greater than 50% reduction in *Tbx6* levels. Only the mice with a combination of null and hypomorphic alleles had overt vertebral defects [131]. Because the authors did not describe any other malformations in the mice, the results would indicate that maintaining sub-heterozygous levels of *TBX6* is sufficient to specify the PSM and limit the neurectoderm, as PSM derivatives (including vertebrae and ribs) still developed along the entire anterior-posterior axis and there was no mention of ectopic neural

tissue. However, these reduced levels are not sufficient for normal vertebral development. This new model will hopefully lead to a better understanding of the molecular mechanisms underlying these congenital vertebral defects, for example, by evaluating changes in the spatiotemporal expression of *TBX6* targets *Msgn1*, *Dll1* or *Mesp2*, or in the proliferation, migration, survival, or differentiation of somite cells destined to become the vertebral bodies and arches of the axial skeleton.

In summary, the zebrafish and mouse mutants described in this section have begun to reveal how perturbation of ciliary fluid flow dynamics, WNT signaling, and transcription factor hierarchies may interfere with vertebral segmentation processes to cause skeletal defects in humans.

7.5 Animal Models of Human Limb Malformations

The limb skeleton is derived from the lateral plate mesoderm (LPM) (Fig. 7.1). Cells from the somatic LPM undergo a localized epithelial-to-mesenchymal transition at the level of the presumptive limb buds, generating a population of mesenchymal limb progenitors [188]. The cells then proliferate and—under the influence of feedback loops and graded morphogen signals—acquire specific positional identities along multiple axes. Initiation of the forelimb and hindlimb buds differs slightly during early stages, but both processes culminate in the activation of a key growth factor in the limb mesenchyme. In the forelimb field, retinoic acid from the flank mesoderm, together with other signals (Wnt/ β -catenin, Hox), activates the expression of the T-box transcription factor *TBX5*, to specify and initiate the forelimb [189, 190]. *TBX5* promotes the expression of fibroblast growth factor *FGF10*, switching on a feedback loop that drives limb outgrowth [58, 191, 192]. In the hindlimb, *Pitx1*, *Islet1*, Wnt/ β -catenin, and *Tbx4* form the early initiation network and activate *FGF10* expression [58, 193–195]. Once *FGF10* is expressed, it signals to the overlying ectoderm to form a signaling center called the apical ectodermal ridge (AER) and,

through canonical Wnt signaling, activates *FGF8* expression (reviewed in [196]). *FGF8* secreted by the AER maintains the expression of *FGF10* in the underlying mesenchyme [196]. This feedback loop promotes the proliferation of the LPM mesenchyme, driving outgrowth of the limb bud. Regional identities are established as differentiation proceeds in a proximal to distal sequence. Briefly, the P/D limb axis is patterned by *HOX* genes that—for the most part—are within the *HOXA* and *HOXD* clusters. Proximal limb cells express *HOX9* and *HOX10* paralogs and form the stylopod (humerus/femur) [34]. More distally, cells are patterned by *HOX11* and form the zeugopod (radius/ulna or tibia/fibula), while the autopod (digits and articulating bones) requires the expression of the most distal, *HOX13* paralogs [34].

Shortly after the outgrowth phase is initiated, *SHH* is activated in a posterior region of the limb bud called the zone of polarizing activity (ZPA). *SHH* secreted by the ZPA forms a gradient of *GLI3R* protein that is highest at the anterior and decreases toward the posterior of the limb bud [197]. *SHH/GLI3R* gradients provide the cells with positional information along the A/P axis and, together with *HOX* genes, eventually pattern the digits of the limb [34, 197]. *SHH* also indirectly maintains the *FGF/AER* feedback loop to ensure that limb outgrowth and patterning proceeds.

Finally, dorsal-ventral specification relies on the Wnt and BMP signaling pathways, resulting in the polarized expression of transcription factor *LMX1B* in the dorsal mesenchyme [198]. Disruption of this polarity results in limbs lacking dorsal features like the knee cap and nails on the digits, manifesting as nail-patella syndrome in humans [199].

The following pages will explore animal models that recapitulate human developmental limb defects. First, models for polydactyly resulting from altered *SHH* signaling within the limb will be described, followed by Holt-Oram syndrome, a dominant limb and heart disorder caused by mutations in *TBX5* [200]. Finally, the role of a Wnt signaling agonist, *RSPO2*, will be explored within the context of a rare human condition

called tetra-amelia [201]. Limb defects resulting from changes in chromatin organization will be explored in the next section.

7.5.1 Altered Expression of *SHH* Pathway Genes Is Responsible for a Subset of Polydactyly Cases

Within the developing limb, *Shh* expression is controlled by a long-range enhancer called the ZPA regulatory sequence (ZRS) that is located approximately 1 Mb upstream of the gene promoter, within the fifth intron of the *Lmbr1* gene [202]. The sequence and function of the ZRS enhancer is highly conserved across vertebrate species. For example, the ZRS sequence of coelacanth fish can functionally substitute for the mouse ZRS during limb development and produce complete limbs [203]. Importantly, the characterization of the ZRS enhancer in 2003 provided an explanation for a subset of cases of human polydactyly [202], and its perturbation is the likely cause of acheiropodia [204]. Lettice et al. identified a minimal active enhancer sequence that drove reporter gene expression specifically within the ZPA and which was well-conserved from human to pufferfish [202]. Two polydactylous mouse mutants, Sasquatch (*Ssq*) and hemimelic extra toes (*Hx*), were further found to disrupt the ZRS locus, resulting in a gain of *Shh* expression at the anterior of the developing limb bud [202, 205, 206]. The consequences of ectopic *Shh* expression were already understood from previous animal models. First, experiments using chicken embryos demonstrated that a gradient of *SHH* was sufficient to polarize the limb along the anterior-posterior axis and, in the presence of a normally functioning ZPA, ectopic anterior *Shh* expression in the limb would cause a mirror-image duplication of the digits [207]. These and later studies solidified the role of *SHH* as a morphogen within the early limb bud, by differentially specifying cell fates at different concentrations and durations of *SHH* signaling—with posterior digits forming in the presence of high and sustained signaling [208]. Changes to the

ZRS sequence that yield an additional domain of *Shh* expression in the anterior of the limb bud would be similarly predicted to form a secondary polarizing region (ZPA) and result in polydactyly. This was indeed the case for the *Ssq* and *Hx* mice [202]. The subsequent analysis of human families with polydactyly identified similar mutations in the ZRS sequence that were later confirmed to activate ectopic *Shh* limb expression when tested in transgenic mice [205, 209, 210].

However, not all mutations that cause polydactyly disrupt the ZRS. Loss-of-function mutations in a transcriptional effector of SHH signaling, *Gli3*, also cause polydactyly in animal models, such as the *extra toes (Xt)* mouse [211], and in humans as part of a syndrome called Greig cephalopolysyndactyly [212, 213]. Within the limb bud, GLI3 predominantly functions as a transcriptional repressor and opposes the gradient of SHH (reviewed in [196]). In the presence of active SHH signaling at the posterior of the limb bud, GLI3 is not cleaved into its repressor form (while certain SHH target genes are transcriptionally activated by other GLI effector proteins). Mutations causing the loss of *GLI3* result in the derepression of cell signaling and patterning genes, concomitant with a disruption of anterior-posterior polarity and the subsequent loss of digit identities [196, 211, 214].

Mutations that ablate ZRS activity, and therefore *Shh* expression at the posterior of the limb bud, prevent the formation of distal limb structures [216]. This was extensively characterized in the mouse model, whereby either knockouts of *Shh* [215] or deletions of the ZRS limb enhancer [216] resulted in a failure to activate *Shh* expression in the ZPA. Accordingly, GLI3 repressor proteins were not restricted to the anterior of the limb bud, causing the repression of *Shh* target genes including *Hox13* paralogs and a subsequent loss of the digits dependent on SHH signaling (all but digit one) [214–216]. The absence of SHH also caused a breakdown of AER-FGF signaling, hindering limb outgrowth [196, 214]. These models provide a potential explanation for human acheiropodia, a condition characterized by the absence of distal structures in the arm and leg, phenocopying a ZRS loss of function [204].

Acheiropodia segregates with deletions in the human *LMBR1* gene [204]; however, because these deletions do not remove the ZRS sequence from the genome, their pathogenicity is not well understood. Others have proposed that acheiropodia deletions alter the activity of the ZRS within its endogenous context [205]. Future studies generating equivalent, targeted deletions in mice could provide an answer to this question.

Together, the aforementioned models defined the role of SHH as the ZPA morphogen and the ZRS as the critical *Shh* limb enhancer. Decades of animal research on SHH signaling within the limb contributed to the elucidation of core gene regulatory networks that integrate outgrowth and patterning along the proximal-distal, anterior-posterior, and dorsal-ventral axes [196]. More recent studies on SHH function have also expanded our understanding of gene regulation through the elucidation of transcription factor binding sites within the ZRS [210]. Importantly for this chapter, animal models have accurately demonstrated the consequences of the misregulation of developmental genes and provided an explanation for a subset of human polydactyly cases.

7.5.2 Animal Models Recapitulate Phenotypes of Holt-Oram Syndrome

Holt-Oram syndrome (HOS) is an autosomal dominant disorder of the forelimbs and heart, affecting up to 1:100,000 individuals [217]. Forelimb defects can vary in severity from a deformed thumb, to shortened or missing long bones of the zeugopod and stylopod [218, 219], while congenital heart defects in HOS include atrial and, less frequently, ventricular septal defects [220]. HOS is caused by haploinsufficiency of the *TBX5* gene, and distinct mutations have been found to cause either more severe cardiac or limb phenotypes, the latter being correlated with mutations at the C-terminal end of the DNA-binding domain [221, 222]. Studies in mice, fish, and chickens have shown that *TBX5* plays a critical role in forelimb initiation by

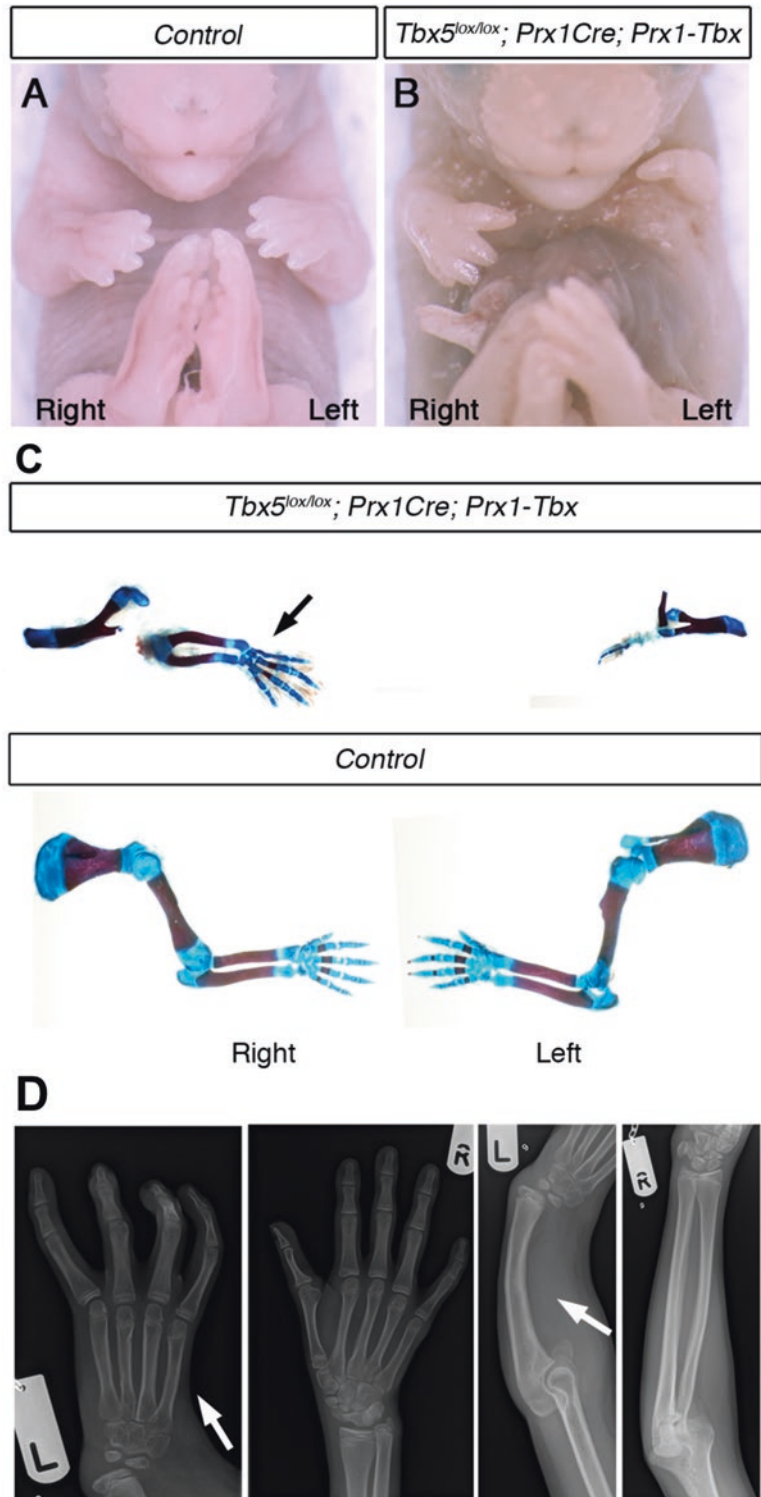
activating the transcription of *FGF10*, thereby promoting forelimb outgrowth [58, 59, 191, 192]. Indeed, *Tbx5* homozygous knockout mice [59, 223], zebrafish mutants [224], chickens expressing a dominant-negative protein [58], and frogs with targeted *Tbx5* mutations [225] completely fail to develop forelimbs. However, animal models with heterozygous *Tbx5* mutations often have normal or mostly normal forelimbs, suggesting that the human forelimb is more sensitive to reductions in *TBX5* dosage as HOS is typically caused by heterozygous mutations [223–225].

Recently, a mouse model was created to specifically investigate the limb defects of HOS. Sulaiman et al. noted that forelimb defects in HOS are often more severe on the left side (Fig. 7.4d), but the source of this left bias was not well understood or modeled in previous *Tbx5* loss-of-function mice [200]. The authors combined a *Tbx5* conditional knockout with a transgene to establish hypomorphic levels of *Tbx5* in the limb, in addition to a mosaic knockout approach [200]. Mice with reduced *Tbx5* dosage developed a range of forelimb defects and, like human HOS patients, the left forelimbs were more strongly affected than the right (Fig. 7.4). The hypomorphic levels of *Tbx5* also disrupted the expression of *Fgf10* and *Fgf8* to a greater extent in the left limb field, suggesting that outgrowth was especially hindered on this side [200]. Together, the results indicated that the left and right LPMs/limb fields are not equivalent within the context of limb development and that the left LPM is more sensitive to reductions in *Tbx5* dosage. The authors proposed that *TBX5* may normally function to equalize this asymmetry, in order to form symmetric limbs. To evaluate whether limb asymmetry in *Tbx5* hypomorphic mice was linked to the pathway establishing left-right asymmetry in the body axis (allowing the heart to be situated on the left and other organs to develop asymmetrically), they crossed the mice into a line predisposed to L/R asymmetry reversal [226]. In mice where the left-right axis was flipped, for example, where the heart and spleen developed on the right, LPM asymmetry also appeared to be flipped [200]. Accordingly, in the

presence of reduced *Tbx5* levels, the right limb was more deformed in this genetic background. Finally, Sulaiman et al. demonstrated that limb asymmetry is at least partially independent of the *FGF10/FGF8* outgrowth loop that is downstream of *TBX5*, as restoring *Fgf10* expression in the *Tbx5* hypomorphic mice did not fully rescue the left-biased limb defects [200]. The findings of this study led the authors to propose a model where the left and right LPMs are initially asymmetric, and the left LPM needs to surpass a minimal threshold level of *TBX5* in order to compensate for the asymmetric state and develop symmetric limbs. Importantly, this model can also provide an explanation for the left-biased limb defects in HOS patients.

In a different vertebrate model, the western clawed frog *Xenopus tropicalis*, a base-editing approach was recently found to be successful for recreating specific mutations associated with HOS [225]. *Xenopus tropicalis* has a diploid genome, unlike the common tetraploid lab model *Xenopus laevis*, and is amenable to genome manipulation [227, 228]. Shi et al. microinjected a modified Cas9 fusion protein, called BE3, into 1-cell stage *X. tropicalis* embryos along with a guide RNA to introduce a specific cytosine to thymine base change in a proposed pathogenic location of the *Tbx5* gene [225]. Unlike the regular Cas9 protein, BE3 is composed of a Cas9 nickase fused to DNA base modifiers including a cytidine deaminase, which promotes the conversion of C-G base-pairs into T-A [225, 229]. The first-generation injected embryos were mosaic for the C>T mutation and had a range of forelimb defects reminiscent of HOS [225]. Individuals with an equivalent mutation have more severe limb defects than heart defects, compared to other HOS mutations [222], and the same phenotype was observed in the frogs, with some missing an entire forelimb but lacking obvious heart problems. In the future, this system may help to solidify mutation-phenotype correlations and provide a better understanding of *TBX5* protein structure and function in an in vivo HOS model.

Fig. 7.4 (a–c) Mice with hypomorphic levels of *Tbx5* in the limbs have forelimb defects that are more severe on the left. (d) A patient with Holt-Oram syndrome displaying left-biased limb defects. Arrows point to a missing thumb and radius on the left hand and forearm, respectively. (Adapted from Panels of Figure 1 of Sulaiman FA, Nishimoto S, Murphy GR, Kucharska A, Butterfield NC, Newbury-Ecob R, Logan MP. *Tbx5* Buffers Inherent Left/Right Asymmetry Ensuring Symmetric Forelimb Formation. *PLoS Genet.* 2016 Dec 19;12(12):e1006521. Content used according to terms of a [Creative Commons Attribution License](#))



7.5.3 Animal Models Elucidate Components of the Signaling Pathways Disrupted in Tetra-Amelia

Tetra-amelia syndrome (TETAMS) is a very rare recessive disorder in which fetuses develop with no arms or legs [230]. Since this syndrome results in a complete failure of limb morphogenesis, understanding its molecular origins should give fundamental insight into limb initiation and outgrowth. A homozygous nonsense mutation of the *WNT3* gene was the first genetic cause of TETAMS identified [231]. This was not surprising since WNT signaling is known to be necessary for the formation of the AER, and *Wnt3* is specifically required for this function in a mouse model [232]. Together these results showed that *WNT3* has a similar function in human and mouse limb development. However, no mutations of *WNT3* were found in some fetuses with tetra-amelia, specifically those that also had lung agenesis [233] (designated TETAMS2 by OMIM). Recently, homozygous mutations of a gene called *RSPO2* were found in fetuses with TETAMS2 [201]. The *RSPO2* gene codes for one of the four R-spondin proteins (RSPO1-4), which are important positive modulators of canonical WNT/ β -catenin signaling. Secreted RSPOs are ligands for the LGR4/5/6 transmembrane receptor proteins that associate with the WNT LRP/Frizzled co-receptors to potentiate downstream signaling. RSPOs enhance WNT signaling by binding and inhibiting the transmembrane E3 ubiquitin ligases RNF43 and ZNRF3, which mediate the degradation of the LRP/Frizzled/WNT complexes [234].

Szenker-Ravi et al. described four families with fetuses displaying TETAMS2 [201]. The affected fetuses in each family had distinct homozygous changes in the coding sequence of *RSPO2*—deletions, nonsense, or frameshift mutations resulting in a severely truncated protein that is predicted to be nonfunctional. These results established a clear link between a loss of *RSPO2* function and tetra-amelia. Mouse and frog models were subsequently used in this study

to elucidate the function of the individual components of the RSPO2 signaling pathway in limb formation [201]. First, mouse fetuses were produced that were homozygous-null for all three of the RSPO receptor genes (*Lgr4/5/6*). Surprisingly the limbs of these mice developed normally, even though *Rspo2*-mutant mice have truncated limbs. This result indicates that RSPO2 does not require the LGR4/5/6 proteins for its function in limb development, implying that alternative receptors mediate RSPO2 function in this context.

Although the mouse model revealed that the function of RSPO2 in limb development is apparently independent of the LGR proteins, *Rspo2*-mutant mice are not an exact model for human tetra-amelia since these mice exhibit significant limb development. Indeed, four separate studies showed that mice null for *Rspo2* have only relatively minor defects of forelimb development while having more severe truncations of the hindlimbs [235–238]. Therefore, the absolute requirement for *Rspo2* in limb initiation may vary between species, perhaps reflecting different degrees of redundancy among RSPO proteins. An alternative *Rspo2*-null model, also described by Szenker-Ravi et al., addressed this issue. They found that inactivation of *Rspo2* in one cell of two-cell stage *Xenopus tropicalis* embryos resulted in a complete loss of limb development on the mutant side of the resulting crispant animal (Fig. 7.5a, b), effectively mirroring the human *RSPO2*-mutant phenotype. In a complementary approach, the authors simultaneously inactivated the *rnf43* and *znrf3* genes to create double-mutant frogs (on one side of the animal) using TALEN gene editing. Remarkably, *rnf43/znrf3* mutants developed ectopic limbs, therefore displaying an opposite phenotype from the *rspo2* mutant, confirming the antagonistic function of *rnf43/znrf3* versus *rspo2* in dramatic fashion (Fig. 7.5c). These studies demonstrate how combining results from multiple animal models can reveal the function of components of a signaling pathway that is disrupted in a human skeletal deformity. Notably, these models are only possible with the emergence of gene editing technologies.

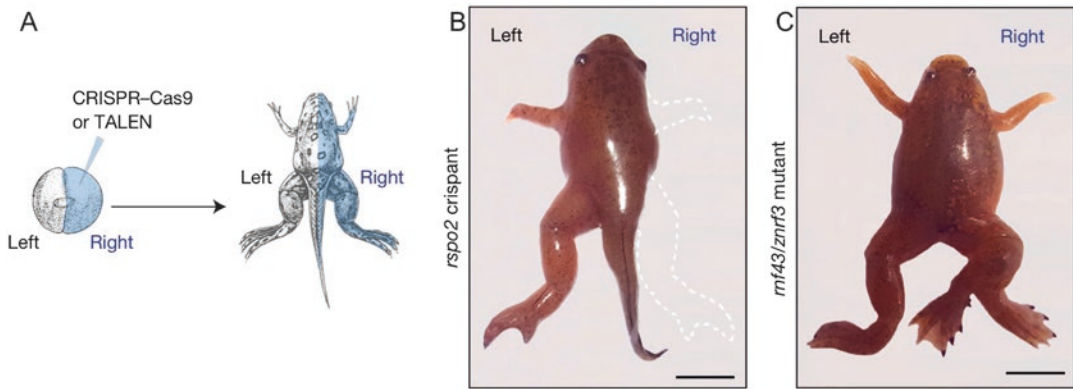


Fig. 7.5 Gene editing in frogs identifies roles for *rspo2*, *mf43*, and *znr3* in limb development. (a) CRISPR-Cas9 or TALENs are injected into one cell of a two-cell stage embryo. (b) No limbs develop in the absence of *rspo2* (right side of frog), while extra limbs develop in the absence of *mf43/znr3* (c). (Reprinted with permission

from Springer Nature Customer Service Centre GmbH: Springer Nature; Journal:Nature, Article: RSPO2 inhibition of RNF43 and ZNRF3 governs limb development independently of LGR4/5/6. Emmanuelle Szenker-Ravi, Umut Altunoglu, Marc Leushacke, Céilia Bosso-Lefèvre, Muznah Khatoo et al. (2018))

7.6 Mechanisms of Gene Regulation Are Revealed by Modeling Alterations to Chromosome Conformation in Mice

Mutations of coding and regulatory sequences are well-established mechanisms of disease, but in the last decade, advances in chromosome conformation capture and genome editing technology have demonstrated that structural variations can have equally significant effects on gene expression (reviewed in [239]). The genome is now known to be compartmentalized into ~1-Mb units called topologically associating domains (TADs) [240], in which enhancer-promoter interactions are self-contained. Within the boundaries of a single TAD, a gene is accessible to its regulatory elements. The boundary prevents ectopic interactions between the gene's promoter and enhancers located in neighboring TADs that have their own targets. TADs are depicted as heatmaps of chromatin interactions that are generated by Hi-C, a chromosome conformation capture technique that quantifies the frequency of sequence interactions across the genome [240, 241]. Interactions between genes

and promoters are revealed through 3C, a one-to-one approach, or, more commonly, 4C (circular chromosome conformation capture), a one-to-all approach that can reveal potentially all sequences interacting with a specific target in a given tissue or timepoint during development [242–244]. For a review of the different chromosome capture techniques, please see reference [245]. A number of recent studies have shown that the disruption of TAD boundaries can change the interaction profiles of genes and their surrounding enhancers, in some cases leading to aberrant chromatin contacts and misexpression of the affected gene(s) [63, 246, 247]. This section will highlight two cases where structural variations were found to cause human skeletal defects and explore how CRISPR/Cas9 was used to model these changes in mice.

7.6.1 Changes in TAD Structure Can Lead to Enhancer Adoption and the Misexpression of Developmental Genes

In 2015, the limb malformations brachydactyly (shortened digits) and polydactyly and a skeletal syndrome involving digital fusions (F-syndrome)

[248] were linked to structural variations around the *EPHA4* locus [63]. Brachydactyly was observed in three families with deletions of a putative telomeric *EPHA4* TAD boundary, including the *EPHA4* gene itself [63]. Conversely, polydactyly and F-syndrome were observed in families with duplications or inversions spanning the centromeric TAD boundary. These structural variations were predicted to disrupt the normal chromatin architecture, placing genes in the neighboring TADs (*WNT6*, *IHH* or *PAX3*) in the proximity and, potentially, under the influence of *EPHA4* enhancers [63]. By comparing human and mouse Hi-C data generated by Dixon et al. [240] with 4C-Seq data from human fibroblasts and wild-type mouse limb buds that were generated in this study, Lupiáñez et al. confirmed that *WNT6* and *IHH* normally interact with sequences restricted to the centromeric TAD, *EPHA4* interacts with sequences in its own TAD, and *PAX3* interactions are largely limited to the telomeric TAD [63]. The authors then created mutations that mirrored the human rearrangements in mice, using CRISPR/Cas9 editing in embryonic stem cells prior to establishing mutant lines. Targeting a Cas9/guide RNA complex to either side of the TAD boundary produces a double-stranded break at each location [61]. In the absence of a repair template, the two lesions are repaired through nonhomologous end joining processes that can either bring the two chromosomal ends together while excising the central fragment, or the fragment can be reintroduced in its original or reversed orientation, with some loss of sequence fidelity at the fragment ends [61]. This strategy allowed the authors to generate a deletion of the telomeric TAD boundary including the mouse *Epha4* gene, and an inversion of the centromeric boundary mirroring one rearrangement seen in an F-syndrome patient [63]. A mouse mutant called *doublefoot* was also used to model human polydactyly, as it was similarly predicted to alter the accessibility of the *Ihh* gene to sequences in the neighboring *Epha4* TAD and had a similar limb phenotype. Using embryonic limb tissue from each of the mutant mouse lines for 4C-Seq, the authors confirmed the presence of new ectopic interactions between the mouse *Pax3*, *Wnt6*, or *Ihh* gene and

sequences in the *Epha4* TAD, in the mouse lines corresponding to each human condition. Very similar contacts were detected in fibroblasts derived from the various human patients, demonstrating that the mouse is an appropriate model for structural rearrangements at this locus. Furthermore, in the mutant mouse lines, the genes forming ectopic contacts became expressed in a domain similar to *Epha4* within the developing limb bud, suggesting the co-option of *Epha4* regulatory elements [63]. Several enhancer candidates were identified that established ectopic gene contacts in both humans and mice. These enhancers drove an *Epha4*-like pattern of reporter gene expression in transgenic mice, suggesting they may also contribute to the misexpression of *PAX3*, *IHH*, and *WNT6* genes and the subsequent development of limb deformities in humans with brachydactyly, polydactyly, and F-syndrome [63].

This study was an important stepping stone in the growing field of research on enhancer-promoter interactions and how these can be perturbed through changes to chromosome structure, in this case, resulting in gene misexpression and human disease.

7.6.2 Different Chromatin States Modulate *PITX1* Expression During Forelimb and Hindlimb Development

PITX1 encodes a transcription factor that is normally expressed and functions within the developing hindlimb [194]. A loss of *Pitx1* gene function perturbs hindlimb development in mice, causing a reduction in *Tbx4* expression, shortening of the long bones, and a loss of the patella (knee cap) [249, 250]. These changes and others result in a hindlimb with forelimb-like features [249, 250]. Mice that are heterozygous for *Pitx1* variably display a foot deformity called “clubfoot,” which perturbs the alignment of the foot, ankle, and lower leg [251] (reviewed in [252]). Similar phenotypes have been observed in humans with *PITX1* deletions, including shortened long bones in the leg and the clubfoot phenotype [251, 253, 254]. Conversely, ectopic *Pitx1*

expression in the forelimbs leads to the development of hindlimb-like features and the expression of hindlimb-associated genes, including *Tbx4* [255–257]. In humans, structural chromosome variations at the *PITX1* locus cause similar transformations in Liebenberg syndrome, such as the formation of an ectopic patella at the elbow and wrist bone fusions that resemble the ankle [257, 258]. These variations were proposed to alter the position of the *PITX1* gene relative to regulatory elements that are telomeric to the gene, causing its misexpression [247, 257].

In mice, a modified chromosome capture technique (Capture Hi-C) was used to probe the interactions of *Pitx1* during embryonic limb development [247]. A strong enhancer candidate, *Pen*, was found to interact with *Pitx1* and contribute to its expression in the hindlimb, and mice with CRISPR-induced deletions of *Pen* variably developed clubfoot. Interestingly, this enhancer was able to drive the expression of a reporter gene in both the fore- and hindlimbs of transgenic mice, indicating that there is likely a mechanism that prevents *Pen* from incorrectly activating *Pitx1* in the forelimb [247]. Capture Hi-C data sets comparing the two sets of limbs supported this theory, as *Pitx1* made more frequent contacts with *Pen* in the developing hindlimb than in the forelimb. Using a polymer-based modeling tool (PRISMR) [259] to predict the 3D structure of the *Pitx1* locus, Kragesteen et al. were able to resolve chromatin domains that differed in their organization in the forelimbs and hindlimbs, based on Capture Hi-C data from each tissue [247]. Notably, *Pitx1* and *Pen* were on adjacent surfaces on two domains in the hindlimb, but were separated from each other in the forelimbs. To determine if these conformations regulate *Pitx1* expression during development, the authors created two structural variations in mice; the first was an inversion predicted to bring the *Pen* enhancer into closer 3D proximity to *Pitx1*, and the second was a deletion observed in a patient with Liebenberg syndrome. Both rearrangements caused a significant upregulation of *Pitx1* in the developing forelimb, and the inversion induced hindlimb features including an ectopic patella [247]. Therefore, the authors proposed that the pathogenesis of Liebenberg syndrome stems

from the rearrangement of chromatin architecture at the *Pitx1* locus, placing an enhancer in a spatial context where it can activate its own target gene in the wrong tissue (forelimb), where this interaction is not normally permitted.

Interestingly, a study in 2019 identified the promoter of *H2AFY* as a candidate region for insulating the *Pen* enhancer from *Pitx1* in the forelimbs, because a small deletion involving this promoter presented in a family with Liebenberg syndrome [260]. Although the mechanism is not yet clear, transcription of *H2AFY* may play a role in modulating the different chromatin states in mouse and human fore/hindlimbs, as similar promoter deletions increase *Pitx1* forelimb expression in mice [260].

7.7 Conclusion

In this chapter, we have described classical and emerging animal models for a small subset of the hundreds of human skeletal disorders. Many of the newest models described here would have been considered impossible or extremely laborious to generate less than 10 years ago. The use of animals to study human skeletal defects has entered a new era as gene editing techniques such as CRISPR-Cas9 have made it possible to rapidly generate mutant animals in previously intractable species. Meanwhile, next-generation sequencing and techniques such as chromosome conformation capture are being used to efficiently characterize the molecular causes of skeletal defects that can then be modeled by gene editing. The synergy of these techniques will make the coming years an extraordinarily exciting and productive time for studying skeletal biology.

References

1. Calder AD, Foley P. Skeletal dysplasias: an overview. *Paediatr Child Health (Oxford)*. 2018;28(2): 84–92.
2. Bonafe L, Cormier-Daire V, Hall C, Lachman R, Mortier G, Mundlos S, et al. Nosology and classification of genetic skeletal disorders: 2015 revision. *Am J Med Genet Part A*. 2015;167(12):2869–92.

3. Eicher EM, Southard JL, Scriver CR, Glorieux FH. Hypophosphatemia: mouse model for human familial hypophosphatemic (vitamin D-resistant) rickets. *Proc Natl Acad Sci U S A*. 1976;73(12):4667–71.
4. Selby PB, Selby PR. Gamma-ray-induced dominant mutations that cause skeletal abnormalities in mice I. Plan, summary of results and discussion. *Mutat Res Mol Mech Mutagen*. 1977;43(3):357–75.
5. Silience DO, Ritchie HE, Selby PB, Prieur DJ. Animal model: skeletal anomalies in mice with cleidocranial dysplasia. *Am J Med Genet*. 1987;27(1):75–85.
6. Otto F, Thornell AP, Crompton T, Denzel A, Gilmour KC, Rosewell IR, et al. *Cbfa1*, a candidate gene for cleidocranial dysplasia syndrome, is essential for osteoblast differentiation and bone development. *Cell*. 1997;89(5):765–71.
7. Mundlos S, Otto F, Mundlos C, Mulliken J, Aylsworth A, Albright S, et al. Mutations involving the transcription factor *CBFA1* cause cleidocranial dysplasia. *Cell*. 1997;89(5):773–9.
8. Haffter P, Granato M, Brand M, Mullins MC, Hammerschmidt M, Kane DA, et al. The identification of genes with unique and essential functions in the development of the zebrafish, *Danio rerio*. *Development*. 1996;123(1).
9. Driever W, Solnica-Krezel L, Schier AF, Neuhauss SC, Malicki J, Stemple DL, et al. A genetic screen for mutations affecting embryogenesis in zebrafish. *Development*. 1996;123:37–46.
10. Schilling TF, Piotrowski T, Grandel H, Brand M, Heisenberg CP, Jiang YJ, et al. Jaw and branchial arch mutants in zebrafish I: branchial arches. *Development*. 1996;123:329–44.
11. Piotrowski T, Schilling TF, Brand M, Jiang YJ, Heisenberg CP, Beuchle D, et al. Jaw and branchial arch mutants in zebrafish II: anterior arches and cartilage differentiation. *Development*. 1996;123:345–56.
12. van Eeden FJ, Granato M, Schach U, Brand M, Furutani-Seiki M, Haffter P, et al. Genetic analysis of fin formation in the zebrafish, *Danio rerio*. *Development*. 1996;123:255–62.
13. van Eeden FJ, Granato M, Schach U, Brand M, Furutani-Seiki M, Haffter P, et al. Mutations affecting somite formation and patterning in the zebrafish, *Danio rerio*. *Development*. 1996;123(1):153–64.
14. Neuhauss SC, Solnica-Krezel L, Schier AF, Zwartkuis F, Stemple DL, Malicki J, et al. Mutations affecting craniofacial development in zebrafish. *Development*. 1996;123:357–67.
15. Howe DG, Bradford YM, Conlin T, Eagle AE, Fashena D, Frazer K, Knight J, Mani P, Martin R, Moxon SA, Paddock H, Pich C, Ramachandran S, Ruef BJ, Ruzicka L, Schaper K, Shao X, Singer A, Sprunger B, Van Slyke CE, Westerfield M. ZFIN, the Zebrafish Model Organism Database: increased support for mutants and transgenics. *Nucleic Acids Res*. 2013;41(Database issue):D854–60.
16. Muenke M. Finding genes involved in human developmental disorders. *Curr Opin Genet Dev*. 1995;5(3):354–61.
17. Shiang R, Thompson LM, Zhu Y-Z, Church DM, Fielder TJ, Bocian M, et al. Mutations in the transmembrane domain of *FGFR3* cause the most common genetic form of dwarfism, achondroplasia. *Cell*. 1994;78(2):335–42.
18. Tavormina PL, Shiang R, Thompson LM, Zhu Y-Z, Wilkin DJ, Lachman RS, et al. Thanatophoric dysplasia (types I and II) caused by distinct mutations in fibroblast growth factor receptor 3. *Nat Genet*. 1995;9(3):321–8.
19. Wilkie AOM, Slaney SF, Oldridge M, Poole MD, Ashworth GJ, Hockley AD, et al. Apert syndrome results from localized mutations of *FGFR2* and is allelic with Crouzon syndrome. *Nat Genet*. 1995;9(2):165–72.
20. Reardon W, Winter RM, Rutland P, Pulley LJ, Jones BM, Malcolm S. Mutations in the fibroblast growth factor receptor 2 gene cause Crouzon syndrome. *Nat Genet*. 1994;8(1):98–103.
21. Schell U, Hehr A, Feldman GJ, Robin NH, Zackai EH, de Die-Smulders C, et al. Mutations in *FGFR1* and *FGFR2* cause familial and sporadic Pfeiffer syndrome. *Hum Mol Genet*. 1995;4(3):323–8.
22. Wagner T, Wirth J, Meyer J, Zabel B, Held M, Zimmer J, et al. Autosomal sex reversal and campomelic dysplasia are caused by mutations in and around the *SRY*-related gene *SOX9*. *Cell*. 1994;79(6):1111–20.
23. Thomas KR, Capecchi MR. Site-directed mutagenesis by gene targeting in mouse embryo-derived stem cells. *Cell*. 1987;51(3):503–12.
24. Mansour SL, Thomas KR, Capecchi MR. Disruption of the proto-oncogene *int-2* in mouse embryo-derived stem cells: a general strategy for targeting mutations to non-selectable genes. *Nature*. 1988;336(6197):348–52.
25. Doetschman T, Maeda N, Smithies O. Targeted mutation of the *Hprt* gene in mouse embryonic stem cells. *Proc Natl Acad Sci U S A*. 1988;85(22):8583–7.
26. Thompson S, Clarke AR, Pow AM, Hooper ML, Melton DW. Germ line transmission and expression of a corrected *HPRT* gene produced by gene targeting in embryonic stem cells. *Cell*. 1989;56(2):313–21.
27. Koller BH, Hagemann LJ, Doetschman T, Hagemann JR, Huang S, Williams PJ, et al. Germ-line transmission of a planned alteration made in a hypoxanthine phosphoribosyltransferase gene by homologous recombination in embryonic stem cells. *Proc Natl Acad Sci U S A*. 1989;86(22):8927–31.
28. Schwartzberg PL, Goff SP, Robertson EJ. Germ-line transmission of a *c-abl* mutation produced by targeted gene disruption in ES cells. *Science*. 1989;246(4931):799–803.
29. Koller BH, Marrack P, Kappler JW, Smithies O. Normal development of mice deficient in beta 2M, MHC class I proteins, and CD8+ T cells. *Science*. 1990;248(4960):1227–30.

30. Chisaka O, Capecchi MR. Regionally restricted developmental defects resulting from targeted disruption of the mouse homeobox gene *hox-1.5*. *Nature*. 1991;350(6318):473–9.
31. Davis AP, Witte DP, Hsieh-Li HM, Potter SS, Capecchi MR. Absence of radius and ulna in mice lacking *hoxa-11* and *hoxd-11*. *Nature*. 1995;375(6534):791–5.
32. Kostic D, Capecchi MR. Targeted disruptions of the murine *Hoxa-4* and *Hoxa-6* genes result in homeotic transformations of components of the vertebral column. *Mech Dev*. 1994;46(3):231–47.
33. Fromental-Ramain C, Warot X, Lakkaraju S, Favier B, Haack H, Birling C, et al. Specific and redundant functions of the paralogous *Hoxa-9* and *Hoxd-9* genes in forelimb and axial skeleton patterning. *Development*. 1996;122(2):461–72.
34. Zakany J, Duboule D. The role of Hox genes during vertebrate limb development. *Curr Opin Genet Dev*. 2007;17(4):359–66.
35. Bi W, Deng JM, Zhang Z, Behringer RR, de Crombrughe B. *Sox9* is required for cartilage formation. *Nat Genet*. 1999;22(1):85–9.
36. Chen ZF, Behringer RR. *twist* is required in head mesenchyme for cranial neural tube morphogenesis. *Genes Dev*. 1995;9(6):686–99.
37. Bourgeois P, Bolcato-Bellemin AL, Danse JM, Bloch-Zupan A, Yoshihara K, Stoetzel C, et al. The variable expressivity and incomplete penetrance of the *twist*-null heterozygous mouse phenotype resemble those of human Saethre-Chotzen syndrome. *Hum Mol Genet*. 1998;7(6):945–57.
38. Carver EA, Oram KF, Gridley T. Craniosynostosis in *Twist* heterozygous mice: a model for Saethre-Chotzen syndrome. *Anat Rec*. 2002;268(2):90–2.
39. Saga Y, Hata N, Koseki H, Taketo MM. *Mesp2*: a novel mouse gene expressed in the presegmented mesoderm and essential for segmentation initiation. *Genes Dev*. 1997;11(14):1827–39.
40. Evrard YA, Lun Y, Aulehla A, Gan L, Johnson RL. *lunatic fringe* is an essential mediator of somite segmentation and patterning. *Nature*. 1998;394(6691):377–81.
41. Whittock NV, Sparrow DB, Wouters MA, Sillence D, Ellard S, Dunwoodie SL, et al. Mutated *MESP2* causes spondylocostal dysostosis in humans. *Am J Hum Genet*. 2004;74(6):1249.
42. Sparrow DB, Chapman G, Wouters MA, Whittock NV, Ellard S, Fatkin D, et al. Mutation of the *LUNATIC FRINGE* gene in humans causes spondylocostal dysostosis with a severe vertebral phenotype. *Am J Hum Genet*. 2006;78(1):28–37.
43. Ayadi A, Birling M-C, Bottomley J, Bussell J, Fuchs H, Fray M, et al. Mouse large-scale phenotyping initiatives: overview of the European Mouse Disease Clinic (EUMODIC) and of the Wellcome Trust Sanger Institute Mouse Genetics Project. *Mamm Genome*. 2012;23(9–10):600–10.
44. Kabir M, Barradas A, Tzotzos GT, Hentges KE, Doig AJ. Properties of genes essential for mouse development. *PLoS One*. 2017;12(5):e0178273. Zou Q, editor.
45. Jiao K, Kulesa H, Tompkins K, Zhou Y, Batts L, Baldwin HS, et al. An essential role of *Bmp4* in the atrioventricular septation of the mouse heart. *Genes Dev*. 2003;17(19):2362–7.
46. Fujiwara T, Dunn NR, Hogan BLM. Bone morphogenetic protein 4 in the extraembryonic mesoderm is required for allantois development and the localization and survival of primordial germ cells in the mouse. *Proc Natl Acad Sci U S A*. 2001;98(24):13739–44.
47. Winnier G, Blessing M, Labosky PA, Hogan BL. Bone morphogenetic protein-4 is required for mesoderm formation and patterning in the mouse. *Genes Dev*. 1995;9(17):2105–16.
48. Selever J, Liu W, Lu M-F, Behringer RR, Martin JF. *Bmp4* in limb bud mesoderm regulates digit pattern by controlling AER development. *Dev Biol*. 2004;276(2):268–79.
49. Liu W, Selever J, Murali D, Sun X, Brugger SM, Ma L, et al. Threshold-specific requirements for *Bmp4* in mandibular development. *Dev Biol*. 2005;283(2):282–93.
50. St-Jacques B, Hammerschmidt M, McMahon AP. Indian hedgehog signaling regulates proliferation and differentiation of chondrocytes and is essential for bone formation. *Genes Dev*. 1999;13(16):2072–86.
51. Maeda Y, Nakamura E, Nguyen M-T, Suva LJ, Swain FL, Razzaque MS, et al. Indian Hedgehog produced by postnatal chondrocytes is essential for maintaining a growth plate and trabecular bone. *Proc Natl Acad Sci U S A*. 2007;104(15):6382–7.
52. Feil R, Brocard J, Mascrez B, LeMeur M, Metzger D, Chambon P. Ligand-activated site-specific recombination in mice. *Proc Natl Acad Sci U S A*. 1996;93(20):10887–90.
53. Eleftheriou F, Yang X. Genetic mouse models for bone studies—strengths and limitations. *Bone*. 2011;49(6):1242–54.
54. Jinek M, Chylinski K, Fonfara I, Hauer M, Doudna JA, Charpentier E. A programmable dual-RNA-guided DNA endonuclease in adaptive bacterial immunity. *Science*. 2012;337(6096):816–21.
55. Doyon Y, McCammon JM, Miller JC, Faraji F, Ngo C, Katibah GE, et al. Heritable targeted gene disruption in zebrafish using designed zinc-finger nucleases. *Nat Biotechnol*. 2008;26(6):702–8.
56. Meng X, Noyes MB, Zhu LJ, Lawson ND, Wolfe SA. Targeted gene inactivation in zebrafish using engineered zinc-finger nucleases. *Nat Biotechnol*. 2008;26(6):695–701.
57. Huang P, Xiao A, Zhou M, Zhu Z, Lin S, Zhang B. Heritable gene targeting in zebrafish using customized TALENs. *Nat Biotechnol*. 2011;29(8):699–700.
58. Takeuchi JK, Koshihara-Takeuchi K, Suzuki T, Kamimura M, Ogura K, Ogura T. *Tbx5* and *Tbx4* trigger limb initiation through activation

- of the Wnt/Fgf signaling cascade. *Development*. 2003;130(12):2729–39.
59. Rallis C, Bruneau BG, Del Buono J, Seidman CE, Seidman JG, Nissim S, et al. *Tbx5* is required for forelimb bud formation and continued outgrowth. *Development*. 2003;130(12):2741–51.
 60. Roy B, Zhao J, Yang C, Luo W, Xiong T, Li Y, et al. CRISPR/Cas9-mediated genome editing-challenges and opportunities. *Front Genet*. 2018;9:240.
 61. Kraft K, Geuer S, Will AJ, Chan WL, Paliou C, Borschiwer M, et al. Deletions, inversions, duplications: engineering of structural variants using CRISPR/Cas in mice. *Cell Rep*. 2015;10(5):833–9.
 62. Spielmann M, Kakar N, Tayebi N, Leettola C, Nürnberg G, Sowada N, et al. Exome sequencing and CRISPR/Cas genome editing identify mutations of *ZAK* as a cause of limb defects in humans and mice. *Genome Res*. 2016;26(2):183–91.
 63. Lupianez DG, Kraft K, Heinrich V, Krawitz P, Brancati F, Klopocki E, et al. Disruptions of topological chromatin domains cause pathogenic rewiring of gene-enhancer interactions. *Cell*. 2015;161(5):1012–25.
 64. D'Souza RN, Ruest L-B, Hinton RJ, Svoboda KKH. *Development of the craniofacial complex*. In: *Bone and development*. London: Springer; 2010. p. 153–81.
 65. Hubaud A, Pourquié O. Signalling dynamics in vertebrate segmentation. *Nat Rev Mol Cell Biol*. 2014;15(11):709–21.
 66. Scaal M. Early development of the vertebral column. *Semin Cell Dev Biol*. 2016;49:83–91.
 67. Kozhemyakina E, Lassar AB, Zelzer E. A pathway to bone: signaling molecules and transcription factors involved in chondrocyte development and maturation. *Development*. 2015;142(5):817–31.
 68. Cole RK. The “talpid lethal” in the domestic fowl. *J Hered*. 1942;33(3):83–6.
 69. Abbott UK, Taylor LW, Abplanalp H. A second talpid-like mutation in the fowl. *Poult Sci*. 1959;38:1185.
 70. Ede DA, Kelly WA. Developmental abnormalities in the head region of the Talpid mutant of the fowl. *J Embryol Exp Morphol*. 1964;12:161–82.
 71. Ede DA, Kelly WA. Developmental abnormalities in the trunk and limbs of the Talpid3 mutant of the fowl. *J Embryol Exp Morphol*. 1964;12:339–56.
 72. Chang C-F, Schock EN, O'Hare EA, Dodgson J, Cheng HH, Muir WM, et al. The cellular and molecular etiology of the craniofacial defects in the avian ciliopathic mutant talpid2. *Development*. 2014;141(15):3003–12.
 73. Davey MG, Paton IR, Yin Y, Schmidt M, Bangs FK, Morrice DR, et al. The chicken talpid3 gene encodes a novel protein essential for Hedgehog signaling. *Genes Dev*. 2006;20(10):1365–77.
 74. Knight RD, Nair S, Nelson SS, Afshar A, Javidan Y, Geisler R, et al. *lockjaw* encodes a zebrafish *tfap2a* required for early neural crest development. *Development*. 2003;130(23):5755–68.
 75. Barrallo-Gimeno A, Holzschuh J, Driever W, Knapik EW. Neural crest survival and differentiation in zebrafish depends on *mont blanc/tfap2a* gene function. *Development*. 2004;131(7):1463–77.
 76. Luo T, Lee Y-H, Saint-Jeannet J-P, Sargent TD. Induction of neural crest in *Xenopus* by transcription factor AP2alpha. *Proc Natl Acad Sci U S A*. 2003;100(2):532–7.
 77. Brewer S, Feng W, Huang J, Sullivan S, Williams T. Wnt1-Cre-mediated deletion of AP-2alpha causes multiple neural crest-related defects. *Dev Biol*. 2004;267(1):135–52.
 78. Milunsky JM, Maher TA, Zhao G, Roberts AE, Stalker HJ, Zori RT, et al. TFAP2A mutations result in branchio-oculo-facial syndrome. *Am J Hum Genet*. 2008;82(5):1171–7.
 79. Franco B, Thauvin-Robinet C. Update on oral-facial-digital syndromes (OFDS). *Cilia*. 2016;5:12.
 80. Bruel A-L, Franco B, Duffourd Y, Thevenon J, Jegou L, Lopez E, et al. Fifteen years of research on oral-facial-digital syndromes: from 1 to 16 causal genes. *J Med Genet*. 2017;54(6):371–80.
 81. Gurrieri F, Franco B, Toriello H, Neri G. Oral-facial-digital syndromes: review and diagnostic guidelines. *Am J Med Genet Part A*. 2007;143A(24):3314–23.
 82. Thauvin-Robinet C, Cossée M, Cormier-Daire V, Van Maldergem L, Toutain A, Alembik Y, et al. Clinical, molecular, and genotype-phenotype correlation studies from 25 cases of oral-facial-digital syndrome type 1: a French and Belgian collaborative study. *J Med Genet*. 2005;43(1):54–61.
 83. Schock EN, Chang C-F, Youngworth IA, Davey MG, Delany ME, Brugmann SA. Utilizing the chicken as an animal model for human craniofacial ciliopathies. *Dev Biol*. 2016;415(2):326–37.
 84. Ferrante MI, Giorgio G, Feather SA, Bulfone A, Wright V, Ghiani M, et al. Identification of the gene for oral-facial-digital type I syndrome. *Am J Hum Genet*. 2001;68(3):569–76.
 85. Romio L, Fry AM, Winyard PJD, Malcolm S, Woolf AS, Feather SA. OFD1 is a centrosomal/basal body protein expressed during mesenchymal-epithelial transition in human nephrogenesis. *J Am Soc Nephrol*. 2004;15(10):2556–68.
 86. Thauvin-Robinet C, Lee JS, Lopez E, Herranz-Pérez V, Shida T, Franco B, et al. The oral-facial-digital syndrome gene *C2CD3* encodes a positive regulator of centriole elongation. *Nat Genet*. 2014;46(8):905–11.
 87. Hoover AN, Wynkoop A, Zeng H, Jia J, Niswander LA, Liu A. *C2cd3* is required for cilia formation and Hedgehog signaling in mouse. *Development*. 2008;135(24):4049–58.
 88. Ye X, Zeng H, Ning G, Reiter JF, Liu A. *C2cd3* is critical for centriolar distal appendage assembly and ciliary vesicle docking in mammals. *Proc Natl Acad Sci U S A*. 2014;111(6):2164–9.
 89. Cortés CR, McInerney-Leo AM, Vogel I, Rondón Galeano MC, Leo PJ, Harris JE, et al. Mutations

- in human C2CD3 cause skeletal dysplasia and provide new insights into phenotypic and cellular consequences of altered C2CD3 function. *Sci Rep*. 2016;6:24083.
90. Lerner IM. Genetic homeostasis. New York: Wiley; 1954.
 91. Lerner IM. The genetic basis of selection. New York: Wiley; 1958.
 92. Abbott UK, Taylor LW, Abplanalp H. Studies with Talpid2, an embryonic lethal of the fowl. *J Hered*. 1960;51(5):195–202.
 93. Brugmann SA, Allen NC, James AW, Mekonnen Z, Madan E, Helms JA. A primary cilia-dependent etiology for midline facial disorders. *Hum Mol Genet*. 2010;19(8):1577–92.
 94. Schock EN, Chang C-F, Struve JN, Chang Y-T, Chang J, Delany ME, et al. Using the avian mutant talpid2 as a disease model for understanding the oral-facial phenotypes of oral-facial-digital syndrome. *Dis Model Mech*. 2015;8(8):855–66.
 95. Schneider RA, Hu D, Helms JA. From head to toe: conservation of molecular signals regulating limb and craniofacial morphogenesis. *Cell Tissue Res*. 1999;296(1):103–9.
 96. Caruccio NC, Martinez-Lopez A, Harris M, Dvorak L, Bitgood J, Simandl BK, et al. Constitutive activation of sonic Hedgehog signaling in the chicken mutant talpid2: Shh-independent outgrowth and polarizing activity. *Dev Biol*. 1999;212(1):137–49.
 97. Pak E, Segal RA. Hedgehog signal transduction: key players, oncogenic drivers, and cancer therapy. *Dev Cell*. 2016;38(4):333–44.
 98. Chang Y-T, Chaturvedi P, Schock EN, Brugmann SA. Understanding mechanisms of GLI-mediated transcription during craniofacial development and disease using the ciliopathic mutant, talpid2. *Front Physiol*. 2016;7:468.
 99. Stephen LA, Tawamie H, Davis GM, Tebbe L, Nürnberg P, Nürnberg G, et al. TALPID3 controls centrosome and cell polarity and the human ortholog KIAA0586 is mutated in Joubert syndrome (JBTS23). *Elife*. 2015;4:e08077.
 100. Parisi MA. Clinical and molecular features of Joubert syndrome and related disorders. *Am J Med Genet Part C Semin Med Genet*. 2009;151C(4):326–40.
 101. Bachmann-Gagescu R, Phelps IG, Dempsey JC, Sharma VA, Ishak GE, Boyle EA, et al. KIAA0586 is mutated in Joubert syndrome. *Hum Mutat*. 2015;36(9):831–5.
 102. Lewis KE, Drossopoulou G, Paton IR, Morrice DR, Robertson KE, Burt DW, et al. Expression of ptc and gli genes in talpid3 suggests bifurcation in Shh pathway. *Development*. 1999;126(11):2397–407.
 103. Buxton P, Francis-West PH, Davey MG, Tickle C, Paton IR, Morrice DR, et al. Craniofacial development in the talpid3 chicken mutant. *Differentiation*. 2004;72(7):348–62.
 104. Li J, Wang C, Wu C, Cao T, Xu G, Meng Q, et al. PKA-mediated Gli2 and Gli3 phosphorylation is inhibited by Hedgehog signaling in cilia and reduced in Talpid3 mutant. *Dev Biol*. 2017;429(1):147–57.
 105. Yin Y, Bangs F, Paton IR, Prescott A, James J, Davey MG, et al. The Talpid3 gene (KIAA0586) encodes a centrosomal protein that is essential for primary cilia formation. *Development*. 2009;136(4):655–64.
 106. Kobayashi T, Kim S, Lin Y-C, Inoue T, Dynlacht BD. The CP110-interacting proteins Talpid3 and Cep290 play overlapping and distinct roles in cilia assembly. *J Cell Biol*. 2014;204(2):215–29.
 107. Wang L, Failler M, Fu W, Dynlacht BD. A distal centriolar protein network controls organelle maturation and asymmetry. *Nat Commun*. 2018;9(1):3938.
 108. Lin AE, Gorlin RJ, Lurie IW, Brunner HG, van der Burgt I, Naumchik IV, et al. Further delineation of the branchio-oculo-facial syndrome. *Am J Med Genet*. 1995;56(1):42–59.
 109. Stoetzel C, Riehm S, Bennouna Greene V, Pelletier V, Vigneron J, Leheup B, et al. Confirmation of TFAP2A gene involvement in branchio-oculo-facial syndrome (BOFS) and report of temporal bone anomalies. *Am J Med Genet Part A*. 2009;149A(10):2141–6.
 110. Carter MT, Blaser S, Papsin B, Meschino W, Reardon W, Klatt R, et al. Middle and inner ear malformations in mutation-proven branchio-oculo-facial (BOF) syndrome: case series and review of the literature. *Am J Med Genet Part A*. 2012;158A(8):1977–81.
 111. Li H, Sheridan R, Williams T. Analysis of TFAP2A mutations in branchio-oculo-facial syndrome indicates functional complexity within the AP-2 α DNA-binding domain. *Hum Mol Genet*. 2013;22(16):3195–206.
 112. Simoes-Costa M, Bronner ME. Establishing neural crest identity: a gene regulatory recipe. *Development*. 2015;142(2):242–57.
 113. Swartz ME, Sheehan-Rooney K, Dixon MJ, Eberhart JK. Examination of a palatogenic gene program in zebrafish. *Dev Dyn*. 2011;240(9):2204–20.
 114. Mork L, Crump G. Zebrafish craniofacial development: a window into early patterning. *Curr Top Dev Biol*. 2015;115:235–69.
 115. Frisdal A, Trainor PA. Development and evolution of the pharyngeal apparatus. *Wiley Interdiscip Rev Dev Biol*. 2014;3(6):403–18.
 116. Wang W-D, Melville DB, Montero-Balaguer M, Hatzopoulos AK, Knapik EW. Tfap2a and Foxd3 regulate early steps in the development of the neural crest progenitor population. *Dev Biol*. 2011;360(1):173–85.
 117. de Crozé N, Maczkowiak F, Monsoro-Burq AH. Reiterative AP2a activity controls sequential steps in the neural crest gene regulatory network. *Proc Natl Acad Sci U S A*. 2011;108(1):155–60.
 118. Schorle H, Meier P, Buchert M, Jaenisch R, Mitchell PJ. Transcription factor AP-2 essential for cranial closure and craniofacial development. *Nature*. 1996;381(6579):235–8.
 119. Zhang J, Hagopian-Donaldson S, Serbedzija G, Elsemore J, Plehn-Dujowich D, McMahon AP,

- et al. Neural tube, skeletal and body wall defects in mice lacking transcription factor AP-2. *Nature*. 1996;381(6579):238–41.
120. Green RM, Feng W, Phang T, Fish JL, Li H, Spritz RA, et al. Tfp2a-dependent changes in mouse facial morphology result in clefting that can be ameliorated by a reduction in Fgf8 gene dosage. *Dis Model Mech*. 2015;8(1):31–43.
 121. Dunwoodie SL, Clements M, Sparrow DB, Sa X, Conlon RA, Beddington RSP. Axial skeletal defects caused by mutation in the spondylocostal dysplasia/pudgy gene Dll3 are associated with disruption of the segmentation clock within the presomitic mesoderm. *Development*. 2002;129(7):1795–806.
 122. Penton AL, Leonard LD, Spinner NB. Notch signaling in human development and disease. *Semin Cell Dev Biol*. 2012;23(4):450–7.
 123. Giampietro PF, Dunwoodie SL, Kusumi K, Pourquie O, Tassy O, Offiah AC, et al. Progress in the understanding of the genetic etiology of vertebral segmentation disorders in humans. *Ann N Y Acad Sci*. 2009;1151(1):38–67.
 124. Hoppenfeld S, Lonner B, Murthy V, Gu Y. The rib epiphysis and other growth centers as indicators of the end of spinal growth. *Spine (Phila Pa 1976)*. 2004;29(1):47–50.
 125. Wang S, Qiu Y, Zhu Z, Ma Z, Xia C, Zhu F. Histomorphological study of the spinal growth plates from the convex side and the concave side in adolescent idiopathic scoliosis. *J Orthop Surg Res*. 2007;2(1):19.
 126. Day G, Frawley K, Phillips G, McPhee IB, Labrom R, Askin G, et al. The vertebral body growth plate in scoliosis: a primary disturbance of growth? *Scoliosis*. 2008;3(1):3.
 127. Konieczny MR, Senyurt H, Krauspe R. Epidemiology of adolescent idiopathic scoliosis. *J Child Orthop*. 2013;7(1):3–9.
 128. Jada A, Mackel CE, Hwang SW, Samdani AF, Stephen JH, Bennett JT, et al. Evaluation and management of adolescent idiopathic scoliosis: a review. *Neurosurg Focus*. 2017;43(4):E2.
 129. Boswell CW, Ciruna B. Understanding idiopathic scoliosis: a new zebrafish school of thought. *Trends Genet*. 2017;33(3):183–96.
 130. Hayes M, Gao X, Yu LX, Paria N, Henkelman RM, Wise CA, et al. ptk7 mutant zebrafish models of congenital and idiopathic scoliosis implicate dysregulated Wnt signalling in disease. *Nat Commun*. 2014;5(1):4777.
 131. Yang N, Wu N, Zhang L, Zhao Y, Liu J, Liang X, et al. TBX6 compound inheritance leads to congenital vertebral malformations in humans and mice. *Hum Mol Genet*. 2019;28(4):539–47.
 132. Gorman KF, Breden F. Idiopathic-type scoliosis is not exclusive to bipedalism. *Med Hypotheses*. 2009;72(3):348–52.
 133. Gorman KF, Tredwell SJ, Breden F. The mutant guppy syndrome curveback as a model for human heritable spinal curvature. *Spine (Phila Pa 1976)*. 2007;32(7):735–41.
 134. Hayes M, Naito M, Daulat A, Angers S, Ciruna B. Ptk7 promotes non-canonical Wnt/PCP-mediated morphogenesis and inhibits Wnt/ β -catenin-dependent cell fate decisions during vertebrate development. *Development*. 2013;140(8):1807–18.
 135. Lu X, Borchers AGM, Jolicœur C, Rayburn H, Baker JC, Tessier-Lavigne M. PTK7/CCK-4 is a novel regulator of planar cell polarity in vertebrates. *Nature*. 2004;430(6995):93–8.
 136. Shnitsar I, Borchers A. PTK7 recruits dsh to regulate neural crest migration. *Development*. 2008;135(24):4015–24.
 137. Bin-Nun N, Lichtig H, Malyarova A, Levy M, Elias S, Frank D. PTK7 modulates Wnt signaling activity via LRP6. *Development*. 2014;141(2):410–21.
 138. Berger H, Wodarz A, Borchers A. PTK7 faces the Wnt in development and disease. *Front Cell Dev Biol*. 2017;5:31.
 139. Wang M, De Marco P, Merello E, Drapeau P, Capra V, Kibar Z. Role of the planar cell polarity gene *Protein tyrosine kinase 7* in neural tube defects in humans. *Birth Defects Res Part A Clin Mol Teratol*. 2015;103(12):1021–7.
 140. Lei Y, Kim S, Chen Z, Cao X, Zhu H, Yang W, et al. Variants identified in *PTK7* associated with neural tube defects. *Mol Genet Genomic Med*. 2019;7(4):e00584.
 141. Grimes DT, Boswell CW, Morante NFC, Henkelman RM, Burdine RD, Ciruna B. Zebrafish models of idiopathic scoliosis link cerebrospinal fluid flow defects to spine curvature. *Science*. 2016;352(6291):1341–4.
 142. Verhoef M, Barf H, Post M, van Asbeck F, Gooskens R, Prevo A. Secondary impairments in young adults with spina bifida. *Dev Med Child Neurol*. 2004;46(6):420–7.
 143. Brinker T, Stopa E, Morrison J, Klinge P. A new look at cerebrospinal fluid circulation. *Fluids Barriers CNS*. 2014;11(1):10.
 144. Guérout N, Li X, Barnabé-Heider F. Cell fate control in the developing central nervous system. *Exp Cell Res*. 2014;321(1):77–83.
 145. Fu H, Qi Y, Tan M, Cai J, Hu X, Liu Z, et al. Molecular mapping of the origin of postnatal spinal cord ependymal cells: evidence that adult ependymal cells are derived from Nkx6.1+ ventral neural progenitor cells. *J Comp Neurol*. 2003;456(3):237–44.
 146. Spassky N, Merkle FT, Flames N, Tramontin AD, García-Verdugo JM, Alvarez-Buylla A. Adult ependymal cells are postmitotic and are derived from radial glial cells during embryogenesis. *J Neurosci*. 2005;25(1):10–8.
 147. Yu K, McGlynn S, Matise MP. Floor plate-derived sonic hedgehog regulates glial and ependymal cell fates in the developing spinal cord. *Development*. 2013;140(7):1594–604.

148. Olstad EW, Ringers C, Hansen JN, Wens A, Brandt C, Wachten D, et al. Ciliary beating compartmentalizes cerebrospinal fluid flow in the brain and regulates ventricular development. *Curr Biol*. 2019;29(2):229–241.e6.
149. Mirzadeh Z, Han Y-G, Soriano-Navarro M, Garcia-Verdugo JM, Alvarez-Buylla A. Cilia organize ependymal planar polarity. *J Neurosci*. 2010;30(7):2600–10.
150. Kishimoto N, Sawamoto K. Planar polarity of ependymal cilia. *Differentiation*. 2012;83(2):S86–90.
151. Lee L. Riding the wave of ependymal cilia: genetic susceptibility to hydrocephalus in primary ciliary dyskinesia. *J Neurosci Res*. 2013;91(9):1117–32.
152. Böhm UL, Prendergast A, Djenoune L, Nunes Figueiredo S, Gomez J, Stokes C, et al. CSF-contacting neurons regulate locomotion by relaying mechanical stimuli to spinal circuits. *Nat Commun*. 2016;7(1):10866.
153. Sternberg JR, Prendergast AE, Brosse L, Cantaut-Belarif Y, Thouvenin O, Orts-Del'Immagine A, et al. Pkd211 is required for mechanoreception in cerebrospinal fluid-contacting neurons and maintenance of spine curvature. *Nat Commun*. 2018;9(1):3804.
154. Guertin PA. Central pattern generator for locomotion: anatomical, physiological, and pathophysiological considerations. *Front Neurol*. 2012;3:183.
155. Fidelin K, Djenoune L, Stokes C, Prendergast A, Gomez J, Baradel A, et al. State-dependent modulation of locomotion by GABAergic spinal sensory neurons. *Curr Biol*. 2015;25(23):3035–47.
156. Van Gennip JLM, Boswell CW, Ciruna B. Neuroinflammatory signals drive spinal curve formation in zebrafish models of idiopathic scoliosis. *Sci Adv*. 2018;4(12):eaav1781.
157. Tracy MR, Dormans JP, Kusumi K. Klippel-Feil syndrome: clinical features and current understanding of etiology. *Clin Orthop Relat Res*. 2004;424:183–90.
158. Mohamed JY, Faeih E, Alsiddiqi A, Alshammari MJ, Ibrahim NA, Alkuraya FS. Mutations in MEOX1, encoding mesenchyme homeobox 1, cause Klippel-Feil anomaly. *Am J Hum Genet*. 2013;92(1):157–61.
159. McGaughran JM, Oates A, Donnai D, Read AP, Tassabehji M. Mutations in PAX1 may be associated with Klippel-Feil syndrome. *Eur J Hum Genet*. 2003;11(6):468–74.
160. Tassabehji M, Fang ZM, Hilton EN, McGaughran J, Zhao Z, de Bock CE, et al. Mutations in GDF6 are associated with vertebral segmentation defects in Klippel-Feil syndrome. *Hum Mutat*. 2008;29(8):1017–27.
161. Candia AF, Hu J, Crosby J, Lalley PA, Noden D, Nadeau JH, et al. Mox-1 and Mox-2 define a novel homeobox gene subfamily and are differentially expressed during early mesodermal patterning in mouse embryos. *Development*. 1992;116(4):1123–36.
162. Mankoo BS, Skuntz S, Harrigan I, Grigorieva E, Candia A, Wright CVE, et al. The concerted action of Meox homeobox genes is required upstream of genetic pathways essential for the formation, patterning and differentiation of somites. *Development*. 2003;130(19):4655–64.
163. Candia AF, Wright CV. Differential localization of Mox-1 and Mox-2 proteins indicates distinct roles during development. *Int J Dev Biol*. 1996;40(6):1179–84.
164. Skuntz S, Mankoo B, Nguyen M-TT, Hustert E, Nakayama A, Tournier-Lasserre E, et al. Lack of the mesodermal homeodomain protein MEOX1 disrupts sclerotome polarity and leads to a remodeling of the cranio-cervical joints of the axial skeleton. *Dev Biol*. 2009;332(2):383–95.
165. Mankoo BS, Collins NS, Ashby P, Grigorieva E, Pevny LH, Candia A, et al. Mox2 is a component of the genetic hierarchy controlling limb muscle development. *Nature*. 1999;400(6739):69–73.
166. Bayrakli F, Guclu B, Yalcikier C, Balaban H, Kartal U, Erguner B, et al. Mutation in MEOX1 gene causes a recessive Klippel-Feil syndrome subtype. *BMC Genet*. 2013;14(1):95.
167. Mubarak AI, Morani AC. Anomalous vertebral arteries in Klippel-Feil syndrome with occipitalized atlas: CT angiography. *Radiol Case Rep*. 2018;13(2):434–6.
168. Lettice LA, Purdie LA, Carlson GJ, Kilanowski F, Dorin J, Hill RE. The mouse bagpipe gene controls development of axial skeleton, skull, and spleen. *Proc Natl Acad Sci U S A*. 1999;96(17):9695–700.
169. Tribioli C, Lufkin T. The murine Bapx1 homeobox gene plays a critical role in embryonic development of the axial skeleton and spleen. *Development*. 1999;126(24):5699–711.
170. Akazawa H, Komuro I, Sugitani Y, Yazaki Y, Nagai R, Noda T. Targeted disruption of the homeobox transcription factor Bapx1 results in lethal skeletal dysplasia with asplenia and gastroduodenal malformation. *Genes Cells*. 2000;5(6):499–513.
171. Lettice L, Hecksher-Sørensen J, Hill R. The role of Bapx1 (Nkx3.2) in the development and evolution of the axial skeleton. *J Anat*. 2001;199(Pt 1–2):181–7.
172. Rodrigo I, Bovolenta P, Mankoo BS, Imai K. Meox homeodomain proteins are required for Bapx1 expression in the sclerotome and activate its transcription by direct binding to its promoter. *Mol Cell Biol*. 2004;24(7):2757–66.
173. Giampietro P, Raggio C, Reynolds C, Shukla S, McPherson E, Ghebranious N, et al. An analysis of PAX1 in the development of vertebral malformations. *Clin Genet*. 2005;68(5):448–53.
174. Peters H, Wilm B, Sakai N, Imai K, Maas R, Balling R. Pax1 and Pax9 synergistically regulate vertebral column development. *Development*. 1999;126(23):5399–408.
175. Dauer MVP, Currie PD, Berger J. Skeletal malformations of Meox1-deficient zebrafish resemble human Klippel-Feil syndrome. *J Anat*. 2018;233(6):687–95.
176. Settle SH, Rountree RB, Sinha A, Thacker A, Higgins K, Kingsley DM. Multiple joint and skel-

- etal patterning defects caused by single and double mutations in the mouse *Gdf6* and *Gdf5* genes. *Dev Biol.* 2003;254(1):116–30.
177. Wei A, Shen B, Williams LA, Bhargav D, Gulati T, Fang Z, et al. Expression of growth differentiation factor 6 in the human developing fetal spine retreats from vertebral ossifying regions and is restricted to cartilaginous tissues. *J Orthop Res.* 2016;34(2):279–89.
 178. Chen H, Capellini TD, Schoor M, Mortlock DP, Reddi AH, Kingsley DM. Heads, shoulders, elbows, knees, and toes: modular *Gdf5* enhancers control different joints in the vertebrate skeleton. *PLOS Genet.* 2016;12(11):e1006454. Long F, editor.
 179. Isidor B, David A. Two girls with short stature, short neck, vertebral anomalies, Sprengel deformity and intellectual disability. *Eur J Med Genet.* 2015;58(1):47–50.
 180. Wu N, Ming X, Xiao J, Wu Z, Chen X, Shinawi M, et al. *TBX6* null variants and a common hypomorphic allele in congenital scoliosis. *N Engl J Med.* 2015;372(4):341–50.
 181. Chapman DL, Papaioannou VE. Three neural tubes in mouse embryos with mutations in the T-box gene *Tbx6*. *Nature.* 1998;391(6668):695–7.
 182. Chapman DL, Cooper-Morgan A, Harrelson Z, Papaioannou VE. Critical role for *Tbx6* in mesoderm specification in the mouse embryo. *Mech Dev.* 2003;120(7):837–47.
 183. Wittler L, Shin E, Grote P, Kispert A, Beckers A, Gossler A, et al. Expression of *Msn1* in the presomitic mesoderm is controlled by synergism of WNT signalling and *Tbx6*. *EMBO Rep.* 2007;8(8):784–9.
 184. Takemoto T, Uchikawa M, Yoshida M, Bell DM, Lovell-Badge R, Papaioannou VE, et al. *Tbx6*-dependent *Sox2* regulation determines neural or mesodermal fate in axial stem cells. *Nature.* 2011;470(7334):394–8.
 185. White PH, Chapman DL. *Dll1* is a downstream target of *Tbx6* in the paraxial mesoderm. *Genesis.* 2005;42(3):193–202.
 186. Yasuhiko Y, Haraguchi S, Kitajima S, Takahashi Y, Kanno J, Saga Y. *Tbx6*-mediated Notch signaling controls somite-specific *Mesp2* expression. *Proc Natl Acad Sci U S A.* 2006;103(10):3651–6.
 187. Oginuma M, Niwa Y, Chapman DL, Saga Y. *Mesp2* and *Tbx6* cooperatively create periodic patterns coupled with the clock machinery during mouse somitogenesis. *Development.* 2008;135(15):2555–62.
 188. Gros J, Tabin CJ. Vertebrate limb bud formation is initiated by localized epithelial-to-mesenchymal transition. *Science.* 2014;343(6176):1253–6.
 189. Nishimoto S, Wilde SM, Wood S, Logan MPO. *RA* acts in a coherent feed-forward mechanism with *Tbx5* to control limb bud induction and initiation. *Cell Rep.* 2015;12(5):879–91.
 190. Tanaka M, Zappavigna V, Conway SJ. Developmental mechanism of limb field specification along the anterior-posterior axis during vertebrate evolution. *J Dev Biol.* 2016;4(2):18.
 191. Ng JK, Kawakami Y, Büscher D, Raya A, Itoh T, Koth CM, et al. The limb identity gene *Tbx5* promotes limb initiation by interacting with *Wnt2b* and *Fgf10*. *Development.* 2002;129(22):5161–70.
 192. Agarwal P, Wylie JN, Galceran J, Arkhitko O, Li C, Deng C, et al. *Tbx5* is essential for forelimb bud initiation following patterning of the limb field in the mouse embryo. *Development.* 2003;130(3):623–33.
 193. Naiche LA, Papaioannou VE. *Tbx4* is not required for hindlimb identity or post-bud hindlimb outgrowth. *Development.* 2007;134(1):93–103.
 194. Duboc V, Logan MPO. *Pitx1* is necessary for normal initiation of hindlimb outgrowth through regulation of *Tbx4* expression and shapes hindlimb morphologies via targeted growth control. *Development.* 2011;138(24):5301–9.
 195. Kawakami Y, Marti M, Kawakami H, Itou J, Quach T, Johnson A, et al. *Islet1*-mediated activation of the B-catenin pathway is necessary for hindlimb initiation in mice. *Development.* 2011;138(20):4465–73.
 196. Zuniga A. Next generation limb development and evolution: old questions, new perspectives. *Development.* 2015;142(22):3810–20.
 197. Bénazet J-D, Zeller R. Vertebrate limb development: moving from classical morphogen gradients to an integrated 4-dimensional patterning system. *Cold Spring Harb Perspect Biol.* 2009;1(4):a001339.
 198. Niswander L. Pattern formation: old models out on a limb. *Nat Rev Genet.* 2003;4(2):133–43.
 199. Dreyer SD, Zhou G, Baldini A, Winterpacht A, Zabel B, Cole W, et al. Mutations in *LMX1B* cause abnormal skeletal patterning and renal dysplasia in nail patella syndrome. *Nat Genet.* 1998;19(1):47–50.
 200. Sulaiman FA, Nishimoto S, Murphy GRF, Kucharska A, Butterfield NC, Newbury-Ecob R, et al. *Tbx5* Buffers Inherent Left/Right Asymmetry Ensuring Symmetric Forelimb Formation. Barsh GS. *PLOS Genet.* 2016;12(12):e1006521.
 201. Szenker-Ravi E, Altunoglu U, Leushacke M, Bosso-Lefèvre C, Khatoor M, Thi Tran H, et al. *RSPO2* inhibition of *RNF43* and *ZNRF3* governs limb development independently of *LGR4/5/6*. *Nature.* 2018;557(7706):564–9.
 202. Lettice LA, Heaney SJ, Purdie LA, Li L, de Beer P, Oostra BA, et al. A long-range *Shh* enhancer regulates expression in the developing limb and fin and is associated with preaxial polydactyly. *Hum Mol Genet.* 2003;12(14):1725–35.
 203. Kvon EZ, Kamneva OK, Melo US, Barozzi I, Osterwalder M, Mannion BJ, et al. Progressive loss of function in a limb enhancer during snake evolution. *Cell.* 2016;167(3):633–642.e11.
 204. Ianakiev P, van Baren MJ, Daly MJ, Toledo SP, Cavalcanti MG, Neto JC, et al. Acheiropodia is caused by a genomic deletion in *C7orf2*, the human orthologue of the *Lmbr1* gene. *Am J Hum Genet.* 2001;68(1):38–45.
 205. Lettice LA, Hill AE, Devenney PS, Hill RE. Point mutations in a distant sonic hedgehog cis-regulator

- generate a variable regulatory output responsive for preaxial polydactyly. *Hum Mol Genet.* 2008;17(7):978–85.
206. Blanc I, Bach A, Robert B. Unusual pattern of Sonic hedgehog expression in the polydactylous mouse mutant Hemimelic extra-toes. *Int J Dev Biol.* 2002;46(7):969–74.
 207. Riddle RD, Johnson RL, Laufer E, Tabin C. Sonic hedgehog mediates the polarizing activity of the ZPA. *Cell.* 1993;75(7):1401–16.
 208. Harfe BD, Scherz PJ, Nissim S, Tian H, McMahon AP, Tabin CJ. Evidence for an expansion-based temporal Shh gradient in specifying vertebrate digit identities. *Cell.* 2004;118(4):517–28.
 209. Gurnett CA, Bowcock AM, Dietz FR, Morcuende JA, Murray JC, Dobbs MB. Two novel point mutations in the long-range SHH enhancer in three families with triphalangeal thumb and preaxial polydactyly. *Am J Med Genet Part A.* 2007;143A(1):27–32.
 210. Lettice LA, Devenney P, De Angelis C, Hill RE. The conserved sonic Hedgehog limb enhancer consists of discrete functional elements that regulate precise spatial expression. *Cell Rep.* 2017;20(6):1396–408.
 211. Hui CC, Joyner AL. A mouse model of greig cephalopolysyndactyly syndrome: the extra-toes1 mutation contains an intragenic deletion of the *Gli3* gene. *Nat Genet.* 1993;3(3):241–6.
 212. Vortkamp A, Gessler M, Grzeschik KH. *GLI3* zinc-finger gene interrupted by translocations in Greig syndrome families. *Nature.* 1991;352(6335):539–40.
 213. Vortkamp A, Franz T, Gessler M, Grzeschik KH. Deletion of *GLI3* supports the homology of the human Greig cephalopolysyndactyly syndrome (GCPS) and the mouse mutant extra toes (Xt). *Mamm Genome.* 1992;3(8):461–3.
 214. Te Welscher P, Zuniga A, Kuijper S, Drenth T, Goedemans HJ, Meijlink F, et al. Progression of vertebrate limb development through SHH-mediated counteraction of *GLI3*. *Science.* 2002;298(5594):827–30.
 215. Chiang C, Litingtung Y, Harris MP, Simandl BK, Li Y, Beachy PA, et al. Manifestation of the limb pre-pattern: limb development in the absence of sonic hedgehog function. *Dev Biol.* 2001;236(2):421–35.
 216. Sagai T. Elimination of a long-range cis-regulatory module causes complete loss of limb-specific Shh expression and truncation of the mouse limb. *Development.* 2005;132(4):797–803.
 217. Barisic I, Boban L, Greenlees R, Garne E, Wellesley D, Calzolari E, et al. Holt Oram syndrome: a registry-based study in Europe. *Orphanet J Rare Dis.* 2014;9(1):156.
 218. McDermott DA, Fong JC, Basson CT. Holt-Oram syndrome. In: Adam MP, Ardinger HH, Pagon RA, et al., editors. *GeneReviews*®. Seattle: University of Washington.
 219. Wall LB, Piper SL, Habenicht R, Oishi SN, Ezaki M, Goldfarb CA. Defining features of the upper extremity in Holt-Oram syndrome. *J Hand Surg Am.* 2015;40(9):1764–8.
 220. Vanlerberghe C, Jourdain A-S, Ghoumid J, Frenois F, Mezel A, Vaksman G, et al. Holt-Oram syndrome: clinical and molecular description of 78 patients with *TBX5* variants. *Eur J Hum Genet.* 2019;27(3):360–8.
 221. Li QY, Newbury-Ecob RA, Terrett JA, Wilson DI, Curtis ARJ, Yi CH, et al. Holt-Oram syndrome is caused by mutations in *TBX5*, a member of the Brachyury (T) gene family. *Nat Genet.* 1997;15(1):21–9.
 222. Basson CT, Huang T, Lin RC, Bachinsky DR, Weremowicz S, Vaglio A, et al. Different *TBX5* interactions in heart and limb defined by Holt-Oram syndrome mutations. *Proc Natl Acad Sci U S A.* 1999;96(6):2919–24.
 223. Bruneau BG, Nemer G, Schmitt JP, Charron F, Robitaille L, Caron S, et al. A murine model of Holt-Oram syndrome defines roles of the T-box transcription factor *Tbx5* in cardiogenesis and disease. *Cell.* 2001;106(6):709–21.
 224. Garrity DM, Childs S, Fishman MC. The heartstrings mutation in zebrafish causes heart/fin *Tbx5* deficiency syndrome. *Development.* 2002;129(19):4635–45.
 225. Shi Z, Xin H, Tian D, Lian J, Wang J, Liu G, et al. Modeling human point mutation diseases in *Xenopus tropicalis* with a modified CRISPR/Cas9 system. *FASEB J.* 2019;fj.201802661R.
 226. Yokoyama T, Copeland NG, Jenkins NA, Montgomery CA, Elder FF, Overbeek PA. Reversal of left-right asymmetry: a situs inversus mutation. *Science.* 1993;260(5108):679–82.
 227. Tymowska J. Karyotype analysis of *Xenopus tropicalis* Gray, Pipidae. *Cytogenet Genome Res.* 1973;12(5):297–304.
 228. Tandon P, Conlon F, Furlow JD, Horb ME. Expanding the genetic toolkit in *Xenopus*: approaches and opportunities for human disease modeling. *Dev Biol.* 2017;426(2):325–35.
 229. Komor AC, Kim YB, Packer MS, Zuris JA, Liu DR. Programmable editing of a target base in genomic DNA without double-stranded DNA cleavage. *Nature.* 2016;533(7603):420–4.
 230. Niemann S. Tetra-Amelia syndrome. *GeneReviews*®. Seattle: University of Washington; 2007.
 231. Niemann S, Zhao C, Pascu F, Stahl U, Aulepp U, Niswander L, et al. Homozygous *WNT3* mutation causes tetra-amelia in a large consanguineous family. *Am J Hum Genet.* 2004;74(3):558–63.
 232. Barrow JR, Thomas KR, Boussadia-Zahui O, Moore R, Kemler R, Capecchi MR, et al. Ectodermal *Wnt3*/beta-catenin signaling is required for the establishment and maintenance of the apical ectodermal ridge. *Genes Dev.* 2003;17(3):394–409.
 233. Sousa SB, Pina R, Ramos L, Pereira N, Krahn M, Borozdin W, et al. Tetra-amelia and lung hypo/aplasia syndrome: new case report and review. *Am J Med Genet Part A.* 2008;146A(21):2799–803.
 234. Hao H-X, Xie Y, Zhang Y, Charlat O, Oster E, Avello M, et al. *ZNRf3* promotes Wnt receptor turnover in an R-spondin-sensitive manner. *Nature.* 2012;485(7397):195–200.

235. Nam J-S, Park E, Turcotte TJ, Palencia S, Zhan X, Lee J, et al. Mouse R-spondin2 is required for apical ectodermal ridge maintenance in the hindlimb. *Dev Biol.* 2007;311(1):124–35.
236. Aoki M, Kiyonari H, Nakamura H, Okamoto H. R-spondin2 expression in the apical ectodermal ridge is essential for outgrowth and patterning in mouse limb development. *Dev Growth Differ.* 2007;50(2):85–95.
237. Bell SM, Schreiner CM, Wert SE, Mucenski ML, Scott WJ, Whitsett JA. R-spondin 2 is required for normal laryngeal-tracheal, lung and limb morphogenesis. *Development.* 2008;135(6):1049–58.
238. Yamada W, Nagao K, Horikoshi K, Fujikura A, Ikeda E, Inagaki Y, et al. Craniofacial malformation in R-spondin2 knockout mice. *Biochem Biophys Res Commun.* 2009;381(3):453–8.
239. Spielmann M, Lupiáñez DG, Mundlos S. Structural variation in the 3D genome. *Nat Rev Genet.* 2018;19(7):453–67.
240. Dixon JR, Selvaraj S, Yue F, Kim A, Li Y, Shen Y, et al. Topological domains in mammalian genomes identified by analysis of chromatin interactions. *Nature.* 2012;485(7398):376–80.
241. Lieberman-Aiden E, van Berkum NL, Williams L, Imakaev M, Ragoczy T, Telling A, et al. Comprehensive mapping of long-range interactions reveals folding principles of the human genome. *Science.* 2009;326(5950):289–93.
242. Dekker J, Rippe K, Dekker M, Kleckner N. Capturing chromosome conformation. *Science.* 2002;295(5558):1306–11.
243. Simonis M, Klous P, Splinter E, Moshkin Y, Willemsen R, de Wit E, et al. Nuclear organization of active and inactive chromatin domains uncovered by chromosome conformation capture–on-chip (4C). *Nat Genet.* 2006;38(11):1348–54.
244. Zhao Z, Tavoosidana G, Sjölander M, Göndör A, Mariano P, Wang S, et al. Circular chromosome conformation capture (4C) uncovers extensive networks of epigenetically regulated intra- and interchromosomal interactions. *Nat Genet.* 2006;38(11):1341–7.
245. de Wit E, de Laat W. A decade of 3C technologies: insights into nuclear organization. *Genes Dev.* 2012;26(1):11–24.
246. Franke M, Ibrahim DM, Andrey G, Schwarzer W, Heinrich V, Schöpflin R, et al. Formation of new chromatin domains determines pathogenicity of genomic duplications. *Nature.* 2016;538(7624):265–9.
247. Kragsteven BK, Spielmann M, Paliou C, Heinrich V, Schöpflin R, Esposito A, et al. Dynamic 3D chromatin architecture contributes to enhancer specificity and limb morphogenesis. *Nat Genet.* 2018;50(10):1463–73.
248. Thiele H, McCann C, van't Padje S, Schwabe GC, Hennies HC, Camera G, et al. Acropectorovertebral dysgenesis (F syndrome) maps to chromosome 2q36. *J Med Genet.* 2004;41(3):213–8.
249. Szeto DP, Rodriguez-Esteban C, Ryan AK, O'Connell SM, Liu F, Kioussi C, et al. Role of the Bicoid-related homeodomain factor Pitx1 in specifying hindlimb morphogenesis and pituitary development. *Genes Dev.* 1999;13(4):484–94.
250. Lanctôt C, Moreau A, Chamberland M, Tremblay ML, Drouin J. Hindlimb patterning and mandible development require the Ptx1 gene. *Development.* 1999;126(9):1805–10.
251. Alvarado DM, McCall K, Aferol H, Silva MJ, Garbow JR, Spees WM, et al. Pitx1 haploinsufficiency causes clubfoot in humans and a clubfoot-like phenotype in mice. *Hum Mol Genet.* 2011;20(20):3943–52.
252. Basit S, Khoshhal KI. Genetics of clubfoot; recent progress and future perspectives. *Eur J Med Genet.* 2018;61(2):107–13.
253. Gurnett CA, Alae F, Kruse LM, Desruisseau DM, Hecht JT, Wise CA, et al. Asymmetric lower-limb malformations in individuals with homeobox PITX1 gene mutation. *Am J Hum Genet.* 2008;83(5):616–22.
254. Klopocki E, Kähler C, Foulds N, Shah H, Joseph B, Vogel H, et al. Deletions in PITX1 cause a spectrum of lower-limb malformations including mirror-image polydactyly. *Eur J Hum Genet.* 2012;20(6):705–8.
255. Minguillon C, Del Buono J, Logan MP. Tbx5 and Tbx4 are not sufficient to determine limb-specific morphologies but have common roles in initiating limb outgrowth. *Dev Cell.* 2005;8(1):75–84.
256. DeLaurier A, Schweitzer R, Logan M. Pitx1 determines the morphology of muscle, tendon, and bones of the hindlimb. *Dev Biol.* 2006;299(1):22–34.
257. Spielmann M, Brancati F, Krawitz PM, Robinson PN, Ibrahim DM, Franke M, et al. Homeotic arm-to-leg transformation associated with genomic rearrangements at the PITX1 locus. *Am J Hum Genet.* 2012;91(4):629–35.
258. Al-Qattan MM, Al-Thunayan A, AlAbdulkareem I, Al Balwi M. Liebenberg syndrome is caused by a deletion upstream to the PITX1 gene resulting in transformation of the upper limbs to reflect lower limb characteristics. *Gene.* 2013;524(1):65–71.
259. Bianco S, Lupiáñez DG, Chiariello AM, Annunziatella C, Kraft K, Schöpflin R, et al. Polymer physics predicts the effects of structural variants on chromatin architecture. *Nat Genet.* 2018;50(5):662–7.
260. Kragsteven BK, Brancati F, Digilio MC, Mundlos S, Spielmann M. *H2AFY* promoter deletion causes *PITX1* endoactivation and Liebenberg syndrome. *J Med Genet.* 2019;56(4):246–51.



Using Zebrafish to Analyze the Genetic and Environmental Etiologies of Congenital Heart Defects

Rabina Shrestha, Jaret Lieberth, Savanna Tillman, Joseph Natalizio, and Joshua Bloomekatz

8.1 Overview

Congenital heart defects (CHDs) are among the most common human birth defects. However, the etiology of a large proportion of CHDs remains undefined. Studies identifying the molecular and cellular mechanisms that underlie cardiac development have been critical to elucidating the origin of CHDs. Building upon this knowledge to understand the pathogenesis of CHDs requires examining how genetic or environmental stress changes normal cardiac development. Due to strong molecular conservation to humans and unique technical advantages, studies using zebrafish have elucidated both fundamental principles of cardiac development and have been used to create cardiac disease models. In this chapter we examine the unique toolset available to zebrafish researchers and how those tools are used to interrogate the genetic and environmental contributions to CHDs.

“If life is a continuous struggle against the inexorable march of entropy, then the heartbeat is at the core of that conflict. By purveying energy to our

cells, it counteracts our tendency toward dissipation and disarray.”

Sandeep Jauhar—Heart: A History [1]

8.2 Introduction

During heart development an intricate choreography of changes in cellular shape and cellular identity results in the formation of an architecture which rhythmically beats ~100,000 times a day. Perhaps unsurprising due to the heart’s complexity, congenital heart defects (CHDs) are relatively common occurring in ~1–3% of live births and ~10% of stillbirths [2, 3]. Identifying the molecular etiology of CHDs can help clinicians assess the risk of inheritance, provide accurate prognoses of disease progression, and ultimately facilitate the design of effective therapeutic strategies [4, 5]. Animal models, particularly zebrafish, have emerged as valuable tools in which to elucidate the etiology of CHDs. The accessibility of zebrafish embryos to both genetic manipulation and live imaging—facilitated by external fertilization, translucent embryos, and a robust community of resources—has allowed zebrafish researchers to identify molecular and cellular principles underlying cardiac development and disease. Since zebrafish display a strong molecular conservation to humans [6–8], these principles are likely applicable to studies of human health and disease. In this chapter we describe

R. Shrestha · J. Lieberth · S. Tillman · J. Natalizio · J. Bloomekatz (✉)
Department of Biology, University of Mississippi, Oxford, MS, USA
e-mail: rshrest4@go.olemiss.edu;
jclieber@go.olemiss.edu; sltillm1@go.olemiss.edu;
jdnatali@go.olemiss.edu; josh@olemiss.edu

the unique tools available to zebrafish researchers and highlight how those tools are being used to elucidate the molecular and cellular underpinnings of congenital heart defects. Since both genetic and environmental factors have been shown to cause CHDs [9] and a combination of environmental influences with genetic susceptibilities may account for a large proportion of CHDs [10], we have chosen as examples zebrafish studies that investigate both genetic causes of CHDs as well as studies that focus on the role of environmental perturbations on heart development. Due to space constraints, we were unable to review all zebrafish disease models of CHDs and we apologize in advance to our colleagues whose valuable work has been omitted. Readers interested in further reviews of these topics are directed to [11–18].

8.2.1 Zebrafish: A Model Organism for the Study of Heart Development

8.2.1.1 Anatomy and Physiology

Zebrafish possess an anatomy and physiology that is similar to mammals allowing findings from experiments in zebrafish to be easily adapted for translational research. In zebrafish blood enters the heart through the sinus venosus into the atrial chamber; it then passes through the atrioventricular valve into the ventricular chamber where it is expelled through the bulbus arteriosus to the body (Fig. 8.1g). Sequential contractions within the heart in both zebrafish and humans are regulated by ion channels within cardiomyocytes as well as specialized pacemaker cells located in the sinus venosus which coordinate

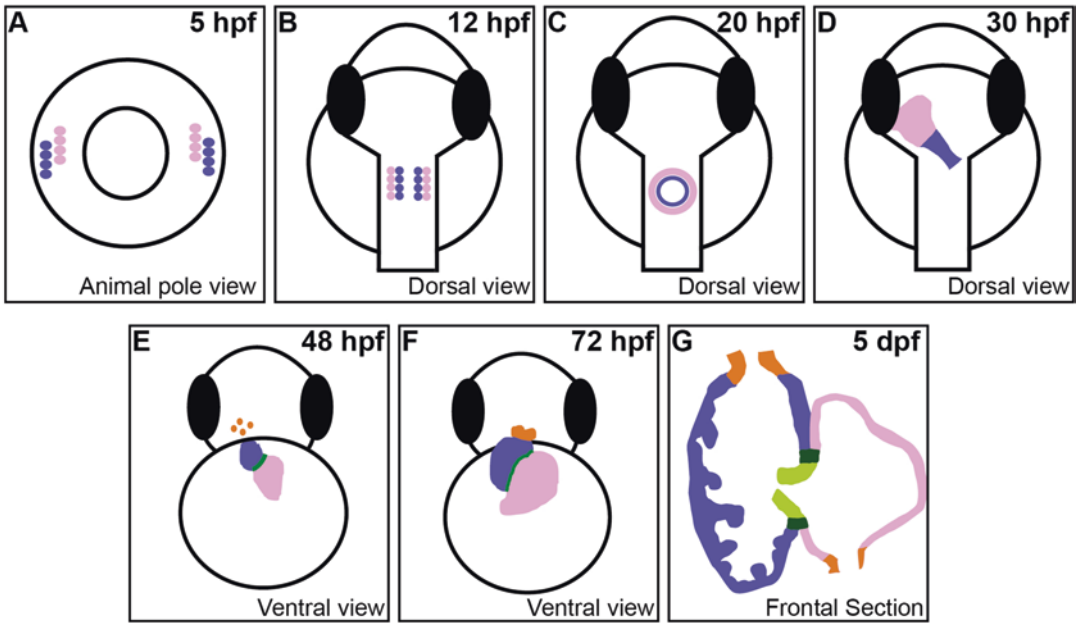


Fig. 8.1 Stages of cardiac development in zebrafish. (a) Schematic of a zebrafish embryo prior to gastrulation. Animal pole view is shown. Myocardial progenitors are located in bilateral marginal domains. Atrial (pink) and ventricular (purple) myocardial progenitors are located in distinct but overlapping domains. (b–d) Schematic of myocardial precursors in bilateral positions in the anterior lateral plate mesoderm (ALPM) at 12 hours post-fertilization (hpf). Dorsal view is shown. Ventricular precursors are found in slightly medial positions compared to atrial precursors (b). From these bilateral positions, myocardial precursors move toward the midline and merge into a single cardiac ring at

20 hpf (c). Myocardial cells then undergo rearrangements to form a primitive heart tube (d). (e–f) Schematic of the zebrafish heart at 48 hpf (e) and 72 hpf (f). Ventral view is shown. Cellular shape changes and the addition of late-differentiating cardiomyocytes (orange) results in morphologically distinct ventricular and atrial chambers as well as the outflow tract (orange). (g) Schematic of a 5-day post-fertilization (dpf) heart. A frontal section is shown. Trabeculating ventricular cardiomyocytes are shown (purple), along with the atrioventricular valves (green), atrial myocardium (pink), outflow tract/bulbus arteriosus, and inflow tract/sinus venosus (orange). (Adapted from [61, 72, 334])

and initiate contractions [19–21]. These specialized cells are regulated by innervating sympathetic and parasympathetic neurons that help the heart respond to changes in demand by up- or downregulating pacemaker activity [22].

The structural organization of cardiac tissue is also fundamentally similar between zebrafish and mammalian hearts. Cardiac chambers are composed of an inner endocardial lining, through which blood flows. This lining is surrounded by muscular myocardial tissue, which contracts to pump blood to the rest of the body. Myocardial tissue is perfused by a coronary artery system, which brings oxygenated blood to the heart. And the entire heart is covered by the epicardium, an outer protective layer [23, 24].

However, the cardiovascular system in zebrafish differs from humans in several distinct ways. Zebrafish lack a pulmonary system (gills are located immediately downstream of blood coming out of the ventricle) [25] with separate cardiac chambers pumping blood to and from the lungs. Furthermore, the ability of adult zebrafish cardiomyocytes to proliferate in response to long-term increases in oxygen demand [26] differs from humans and rodents where a large majority of postnatal cardiomyocytes undergo endoreplication, become binuclear, and cease proliferating [27, 28]. Additionally, unlike adult human and rodent hearts, adult zebrafish hearts can regenerate after injury [29, 30]. Several laboratories are focused on understanding and translating the principles of zebrafish cardiac regeneration to human hearts; reviews of these studies can be found here [31–35].

8.2.1.2 Cardiac Development

The molecular and cellular processes underlying the development of the heart, particularly during the early embryonic stages of cardiac development, are also remarkably well conserved between zebrafish and mammals [36]. In zebrafish, cardiac progenitors have been mapped to the first four rows of blastomeres adjacent to the margin just prior to gastrulation (beginning at 6 hours post-fertilization, hpf). These are some of the first cells to undergo an epithelial-to-mesoderm transition (EMT) and gastrulate [37, 38]. Further

studies have identified a spatial separation within this region between cells fated to become atrial and ventricular cardiomyocytes [39] (Fig. 8.1a). In mice cardiac progenitors are also one of the first mesodermal cell types to gastrulate [40, 41]. After gastrulation, cardiac precursors in zebrafish are found in bilateral locations within the anterior lateral plate mesoderm (ALPM) (Fig. 8.1b). At 16 hpf, cardiac cells move medially from these bilateral positions to the midline where they merge together to form a single cardiac ring [42–46] (Fig. 8.1c). This cardiac ring then undergoes cell rearrangements to become a bilayered primitive heart tube consisting of an inner endocardial layer that is surrounded by an outer myocardial layer [47] (Fig. 8.1d). In chicken and mouse embryos, the bilateral cardiac crescent undergoes similar medial movements and cell rearrangements to create a primitive heart tube [48–50].

After the primitive heart tube is formed, further remodeling occurs through cellular shape changes which create leftward looping and result in a kidney-shaped ventricular chamber and a cylindrical atrial chamber at 48 hpf in zebrafish (Fig. 8.1e). Leftward looping is driven by molecular signals that coordinate left-right asymmetry throughout the body. These signals originate from the coordinated rotation of motile cilia in Kupffer's vesicle, which is analogous in structure to the node which performs a similar function in mouse and chicken embryos [51, 52]. The formation and shape of the cardiac chambers emerge through cell shape changes [20, 53, 54] and the addition of late differentiating cardiomyocytes to the poles of the ventricular and atrial chambers (Fig. 8.1f). Late-differentiating cardiomyocytes contribute both to chamber formation and to the formation of the outflow and inflow tracts which ultimately become the bulbous arteriosus and the sinus venosus, respectively [55–57]. These late-differentiating cardiomyocytes are analogous to second heart field cells in mouse and chicken which are critical for the formation of cardiac chambers in these organisms as well [58–60]. As the heart matures, it supports the growth of the embryo by increasing its muscle mass. This increase in the muscle occurs through the proliferation and invagination of myocardial cells into

the lumen of the ventricle at 72 hpf, a process common to all vertebrates called trabeculation [61–64] (Fig. 8.1f, g).

Valves, which are essential in all vertebrates for unidirectional blood flow, form at the atrio-ventricular canal (AVC) and at the ventricular-bulbus arteriosus boundary in zebrafish [23]. Valve formation at the AVC starts at 36 hpf with the convergence of endocardial cells from the ventricular and atrial portions of the heart toward the AVC boundary. These cells constrict their apical surfaces to create a thickened area at the AVC boundary [16] and undergo endothelial-to-mesenchymal transitioning behaviors such as downregulating cell adhesions, extending protrusions, and asymmetrically moving into the extracellular matrix to form endocardial cushions [65–69]. Endocardial cushions continue to be remodeled and sculpted even during larval development forming mature valve leaflets by adulthood in zebrafish [70]. Valve formation occurs similarly in mouse and chicken embryos, where endothelial-to-mesenchymal transitioning behaviors have been shown to be instrumental in endocardial cushion formation [71].

The similarity between mammalian and zebrafish cardiac development is also reflected at the molecular level, where >90% of human cardiac genes are conserved in zebrafish [6]. These similarities along with the technical advantages of zebrafish (described below) make it a good model organism in which to elucidate the molecular mechanisms of cardiac development and model congenital heart defects. For further information regarding the molecular components underlying the aspects of zebrafish heart development described above, readers are directed to the following reviews [16, 18, 72–81].

8.2.2 Zebrafish Techniques

Zebrafish embryos have several technical advantages for elucidating molecular mechanisms during cardiac development including external development, small size, high fecundity, translucent embryos, and a large community of researchers. The external fertilization and development of

zebrafish embryos increase the accessibility of live-imaging techniques as well as embryonic manipulations such as injections and transplantations. Additionally, because they develop externally, zebrafish embryos can obtain much of their oxygen from passive diffusion until ~5 days post-fertilization (dpf), allowing investigators to observe cardiovascular defects and disease pathologies [82]. Comparatively, mouse embryos rely heavily on their cardiovascular system for oxygen due to their in utero development. Thus, cardiovascular defects in mouse embryos quickly lead to poor overall embryonic health and reabsorption [83]. The smaller size and high fecundity rate (100–300 embryos per mating pair on a weekly basis) of zebrafish also facilitates high-throughput experimental techniques such as genetic and small molecule screens, as well as the analysis of multiple mutant combinations. A smaller size, however, can be a disadvantage for biochemical techniques such as protein purification where a large amount of material is advantageous. Finally, a large community of zebrafish investigators who create and share transgenic and mutant resources has propelled the model organism regardless of the area of study into the forefront of scientific and biomedical research. Many of these community resources can be found at <http://zfin.org>, <http://www.zebrafish.org>, <http://ezrc.kit.edu>, <http://en.zfish.cn>, <http://zf-health.org>, and http://shigen.nig.ac.jp/zebra/index_en.html. These intrinsic advantages have facilitated the application of a myriad of genetic and cell biological techniques (see Tables 8.1 and 8.2) to questions of cardiac development and disease.

8.2.2.1 Forward Genetics: Genetic Techniques for the Unbiased Identification of Genes Important for Cardiac Development

A phenotype-based genetic screen is an unbiased way to identify genes important for a specific biological process such as cardiac development. This approach involves random mutagenesis, isolating mutations based on their phenotype and then mapping and identifying the genomic location of those mutations [84]. Instead of identifying a gene of interest and then asking what the phenotype

Table 8.1 Zebrafish genetic techniques used to identify genes and their functions

Approaches	Purpose	Techniques	Mechanism of action
Forward genetics	Discover genes involved in a biological process of interest	ENU	Generates point mutations at random sites in the genome
		Retrovirus/ gene-breaking transposon	Disrupts gene function by random integration into the genome
		Enhancer trap	Random integration of a reporter gene fused to a minimal promoter identifies tissue-specific enhancers
		Protein trap	Random integration of a reporter gene fused to a splice-acceptor and splice donor site identifies the subcellular localization of proteins
		Chemical library	Incubation of zebrafish embryos with small molecules during development in a high throughput fashion identifies chemicals that disrupt a targeted biological system
Reverse genetics	Identify the function of a specific gene	Morpholino	Impairment of gene function by complementary binding and blocking mRNA processing and/or translation
		CRISPR/Cas9; TALEN	Disruption of the reading frame of a specific gene resulting in its loss of function
		Transgene/mRNA injection	Overexpression of a gene
		Knock-in	Replacement of a wild-type allele with a disease allele

ENU *N*-ethyl *N*-nitrosourea, *CRISPR* clustered regularly interspaced short palindromic repeats, *TALEN* transcription activator-like effector nucleases

Table 8.2 Examples of zebrafish assays used to examine cardiac development

Biological processes affected	Properties examined	Approach
Heart size	Cell number	<ul style="list-style-type: none"> Initial assessment: mark nuclei with a transgenic reporter such as <i>Tg(myl7:H2A-mcherry)</i> and <i>Tg(myl7:nlskikGr)</i> to count myocardial cells Further analysis: perform cell proliferation, cell death, and cell-type specification assays
	Cell shape/size	<ul style="list-style-type: none"> Initial assessment: mark the outline of a cell with a transgenic reporter such as <i>Tg(myl7:mcherry-CAAX)</i> Further analysis: examine myofibrillar formation, actin-cytoskeleton, and cell polarity
Cardiac conduction and function	Calcium dynamics	Use a genetically encoded calcium reporter (GCaMP) to visualize Ca ²⁺ dynamics in vivo
	Action potentials	Record electrical impulses using a patch clamp
	Shear stress	Label endocardial membrane and individual blood cells with transgenic reporters and then combine with high-speed confocal imaging to visualize blood flow dynamics
	Physiological and structural measurements	Visualization of systolic and diastolic properties of the heart by utilizing echocardiography in vivo or ex vivo

is if that gene is mutated (a reverse genetic approach), this approach identifies the phenotype first and then asks what gene (or other genomic component such as a microRNA) is mutated to cause that phenotype. Building on the success of

forward genetic screens in *Drosophila melanogaster* to identify genes and networks important for segmentation and body plan polarity [85], this approach has been applied successfully in many model organisms, including zebrafish.

Two large chemical-based mutagenesis screens performed in the 1990s established zebrafish as a model system capable of revealing the genetic basis of developmental and disease processes, including processes related to the cardiovascular system [86, 87]. These original mutagenesis screens in zebrafish utilized *N*-ethyl *N*-nitrosourea (ENU) as a mutagen. ENU is an alkylating agent that creates point mutations at random sites in the genome [88]. This is the same mutagen used by mouse researchers to conduct forward genetic screens. Another approach for creating mutations is the use of retroviruses or gene-breaking transposons (GBT), which randomly integrate into the genome disrupting nearby gene function [89–92]. Modifications to retroviral or transposon vectors including addition of splice-acceptor and splice-donor sites and reporter genes such as GFP allow these vectors to act as enhancer or protein traps when they integrate into the genome. Enhancer traps allow investigators to unbiasedly identify genes that are expressed in a specific tissue, such as the heart [93–96], whereas protein traps allow investigators to visualize the subcellular localization of a protein into which the transposon has inserted [97].

Genetic screens in zebrafish generally involve a three-cross mating strategy for identifying recessive mutations (Fig. 8.2). Initially, mutagenized founders are outcrossed to create stable F1s. (After animals are exposed to a mutagen, random mutations are created in different cells, creating a mosaic animal. This includes the germline, where individual sperm cells can harbor different mutations.) This initial outcross creates heterozygous animals in which all cells in a particular animal contain the same mutation(s). F1 animals are then outcrossed a second time to create multiple heterozygous animals (F2). Intercrosses are then performed between F2 siblings, and embryos from the F2 intercrosses are then examined for cardiac phenotypes [98, 99].

Once a mutant phenotype is discovered and propagated, the location of the mutation is then identified. Traditionally, this has been accomplished by using polymorphisms to map meiotic recombination events, thereby identifying a rela-

tively narrow genomic interval containing the mutation that can be sequenced. However, the advent of cheap and quick sequencing has facilitated mutation identification via whole-genome sequencing [100–102]. The use of retroviral or transposons for mutagenesis also facilitates identification of the mutated gene by inverse PCR [103].

These screens are generally performed in a similar manner to those performed in mouse (see Chap. 1 by Garcia-Garcia) with minor differences in mating and mapping strategies. For example, to map meiotic recombination events without inbred lines in zebrafish, polymorphisms between the mutated and nonmutated DNA strands have to be identified in each mating pair. However, since a single mating pair can be used to generate hundreds of embryos, this is not a major obstacle. And in both zebrafish and mouse, the advent of cheap whole-genome sequencing has greatly reduced the need for the mapping of meiotic recombinants. In one example of how this unbiased approach is being used in models of CHDs, Ding et al. employed a GBT-mutagenesis strategy to unbiasedly identify genetic modifiers of doxorubicin- or anemic-triggered cardiomyopathy [104], thereby interrogating the interaction of environmental and genetic factors in heart disease.

More recently, forward genetic approaches in zebrafish have utilized the advantage of external fertilization to perform high-throughput screens of chemical libraries in order to identify small molecules that cause or modify cardiac phenotypes [105, 106]. These screens can be easily conducted due to the external development of zebrafish embryos and their small size, which means only a small amount of chemical is required. Chemical screens also have the advantage of being quick when compared to traditional mutagenesis screens because they do not require multiple generations before a cardiac phenotype can be assessed. Finally, these screens have the potential to identify small molecules that could be used in a translational or therapeutic setting. However, identification of the protein or proteins affected by a small molecule is not always straightforward [107, 108]. Using this approach,

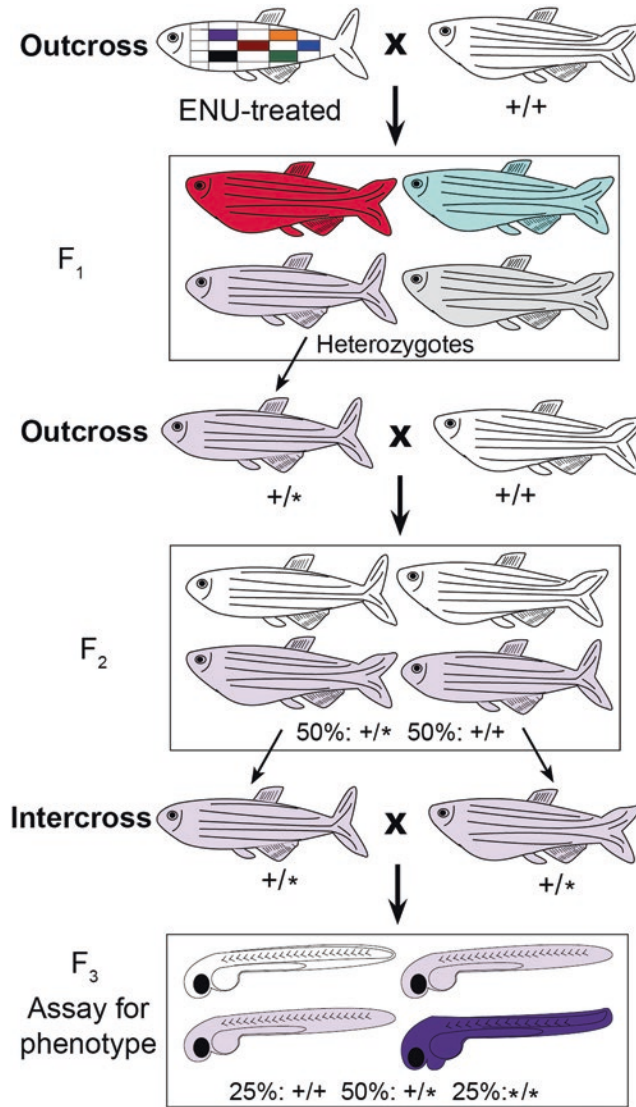


Fig. 8.2 Crossing scheme for an ENU-induced genetic screen for recessive mutants in zebrafish. (1) Male adult zebrafish are exposed to *N*-ethyl *N*-nitrosourea (ENU) to generate random germline point mutations (indicated by different dark colored boxes), creating a mosaic animal. (2) These mutagenized animals are then outcrossed to wild-type females to produce individual F₁ heterozygous animals. All cells within an animal produced from this cross will have the same genotype (shown as light color shading throughout the animal). (3) Individual F₁ heterozygotes are outcrossed to wild-type animals to produce more animals with the mutagenized genotype as the F₁.

This cross results in 50% heterozygous animals ($+/*$) (indicated by light purple shading) and 50% homozygous wild-type animals ($+/+$) (indicated by no shading). (4) F₂ siblings are then intercrossed to generate F₃ embryos which can be analyzed for mutant phenotypes. If two F₂ heterozygous animals are intercrossed, 25% of the resulting embryos (F₃) will be homozygous for the mutation (indicated by dark purple) and may show a phenotype in a specific assay, such as heart development. Since F₂ siblings contain both heterozygous and homozygous wild-type animals which are indistinguishable, there is a 25% chance that two heterozygous embryos will mate together

Ni et al. identified Cardionogen1–3, small molecules that when exposed to zebrafish embryos caused enlarged hearts by modifying the Wnt pathway [106]. Similarly, Saydmohammed et al.

used a transgenic reporter of FGF signaling [*Tg(dusp6:EGFP)*] to identify small molecules that hyperactivate FGF signaling and increase the pool of cardiac progenitors [109].

8.2.2.2 Reverse Genetics: Genetic Techniques for Identifying the Function of a Specific Gene

Zebrafish embryos are also amenable to reverse genetic approaches in which specific genes are targeted for mutation. The ability to target a specific gene is particularly useful when human studies identify genes possibly involved in congenital heart defects. In these studies, the role of research in a model organism like zebrafish would be to examine phenotypes resulting from mutations in that gene to confirm its role in cardiac development and to investigate the mechanism by which that gene facilitates cardiac development [110, 111].

Traditionally, morpholinos—antisense oligos that bind to and block mRNA function—have been used in zebrafish to inhibit a specific gene [112]. Morpholinos are chemically modified ribonucleotide oligos that are designed to be complementary to endogenous RNAs. These chemical modifications make the morpholino more stable by replacing the ribose ring characteristic of RNA oligos with a morpholine ring, leading to an uncharged phosphorodiamidate linkage rather than anionic phosphodiester linkage between nucleotides. By binding to endogenous RNAs, morpholinos sterically inhibit the ability of the targeted RNA to be translated or processed, leading to impaired gene function [113]. Although morpholinos bind specifically to the targeted RNA, they are also known to have nonspecific effects, including the triggering of the p53 and immune pathways [114, 115]. Additionally, recent direct comparisons of phenotypes generated by loss-of-function frameshift mutations or morpholino-mediated knockdown of the same gene have found that these phenotypes are not always similar. These differing phenotypes have further enhanced concerns regarding nonspecific morpholino effects [116, 117]. Due to these concerns, the zebrafish community has adopted a series of experimental guidelines, to ensure the specificity of a morpholino-mediated phenotype [118, 119]. These guidelines suggest that morphants should phenocopy genetic mutants, unless genetic compensation is thought to occur in the mutants.

A morpholino injected into an embryo homozygous for a null mutation or an allele lacking the morpholino-binding site should not display the morphant phenotype.

Fortunately, creating null mutations in zebrafish using CRISPR/Cas9 (clustered regularly interspaced short palindromic repeats) or TALEN (transcription activator-like effector nucleases) technologies is becoming routine, cheap, and accessible, allowing for a rigorous analysis of gene functionality [120–125]. These techniques target nucleases, Cas9 in the case of CRISPR/Cas9, or FokI in the case of TALENs, to specific DNA sequences where these nucleases make a double-strand break. This double-strand break is then repaired, usually by the nonhomologous end-joining (NHEJ) pathway which often inserts or deletes nucleotides, causing a mutation known as an indel. These indels may disrupt the reading frame of a gene (if they are not in multiples of 3) and thus can lead to a null mutation. The specificity of these technologies is very high because both CRISPR/Cas9 and TALEN require complementary nucleotide matches in order to recruit the nucleases to DNA. One difficulty encountered by zebrafish researchers is that small differences (polymorphisms) between the reference genome and zebrafish in a laboratory colony due to the lack of inbred lines can interfere with the targeting of nucleases. Thus, the targeted region is often sequenced prior to the design of CRISPR or TALEN strategies. Further information about the implementation of these technologies in zebrafish can be found in these references [120–125].

Although the analysis of null alleles, such as those generated by CRISPR/Cas9-mediated gene mutation, is important for the clear and unambiguous identification of gene function, disease alleles in human patients are not necessarily null alleles. To rigorously analyze the pathogenic mechanisms caused by a disease allele, the wild-type allele needs to be replaced with the disease allele (knock-in) [126, 127]. This strategy is preferable to the overexpression of a disease allele via transgene or mRNA injection. Overexpression experiments, despite injecting a wild-type allele as a control, differ from

knock-in experiments due to non-endogenous levels of gene expression as well as the existence of a dynamic mixture of wild-type and disease alleles. Several strategies have been designed to knock in exogenous DNA into a specific locus in zebrafish [128–131]. As these strategies become more routine, investigators will be able to precisely determine the specific dysfunction caused by a disease allele.

8.2.2.3 Assays to Investigate Cardiac Development

Multiple assays have been developed to elucidate the role of a specific gene or toxicant in cardiac development [72, 132] (see Table 8.2). Due to the anatomical location of the heart and the translucent quality of zebrafish embryos, many properties of the heart including size, shape, and physiology (rate of beating and rhythmicity) of the heart can initially be visualized by simple brightfield microscopy. Unfortunately, one of the easiest phenotypes to observe via brightfield microscopy, pericardial edema (the inflation of the space between the heart and the pericardial membrane due to increased fluid) is often not particularly diagnostic because a large number of cardiac and non-cardiac defects cause this phenotype. For example, along with defects in cardiac development, defects in the kidney and other organs that help to regulate extracellular fluid and blood pressure can also lead to pericardial edema [133–136]. It is also not easy to use pericardial edema to distinguish different cardiac mutations since defects in many of the processes of cardiac development including cardiac morphogenesis, cardiac specification, or cardiomyocyte function can cause similar looking pericardial edemas [79].

However, the ease of creating transgenic animals has allowed zebrafish cardiac researchers to develop sophisticated assays that examine different aspects of cardiac development. For example, there are multiple ways in which the size of the heart can be affected, including changes in the number of cardiac cells or changes in the size of cardiac cells. Cardiac cell number can be quantified using transgenes which mark nuclei, such as the *Tg(myl7:H2A-mcherry)* transgene in which the fluorescent protein mcherry is attached to his-

tone2A (H2A) and expressed in the myocardium via the *myosin light chain 7 (myl7)* promoter (Fig. 8.3a, b). Another transgene used to count myocardial cells is the *Tg(myl7:nlsKikGr)* transgene, in which a nuclear localization signal (nls) is attached to the photoconvertible protein Kikume green-red [43, 137]. These transgenes allow researchers to count myocardial cells at different developmental stages in vivo. After determining a change in cell number, further analysis can include assays that examine proliferation, cell death, and changes in the specification myocardial populations [72]. To measure changes in cell size and shape, transgenes such as *Tg(myl7:mkate-caax)*, which mark the outlines of cells by using the prenylation motif CAAX to localize mcherry to the membrane, can be used [138] (Fig. 8.3c, d). Then further analysis can be conducted into the biology underlying changes in cell size and shape such as examining defects in myofibrillar formation or changes in the actin cytoskeleton [138, 139].

Sophisticated assays have also been developed to interrogate defects in cardiac physiology. For example, calcium dynamics in cardiomyocytes, which is critical for triggering synchronous contractions, can be visualized in vivo by utilizing the genetically encoded calcium indicator, GCaMP [140, 141]. Furthermore, standard electrophysiology recordings of action potentials, which regulates calcium flux, can be performed on dissected whole zebrafish hearts or individual zebrafish cardiomyocytes [142–144]. Blood flow through the heart and the shear stress it creates can also be measured by combining high-speed confocal imaging with transgenic reporters that label the endocardial membrane and individual blood cells [66, 145, 146]. Finally in adult zebrafish, when the heart is no longer visible via brightfield microscopy, high-frequency echocardiography and ex vivo techniques have been used by multiple laboratories to visualize the systolic and diastolic properties of cardiac function [147–151]. In the following sections, we highlight several case studies in which zebrafish researchers have combined these cell biology assays with the genetic techniques outlined above to elucidate the mechanisms causing CHD.

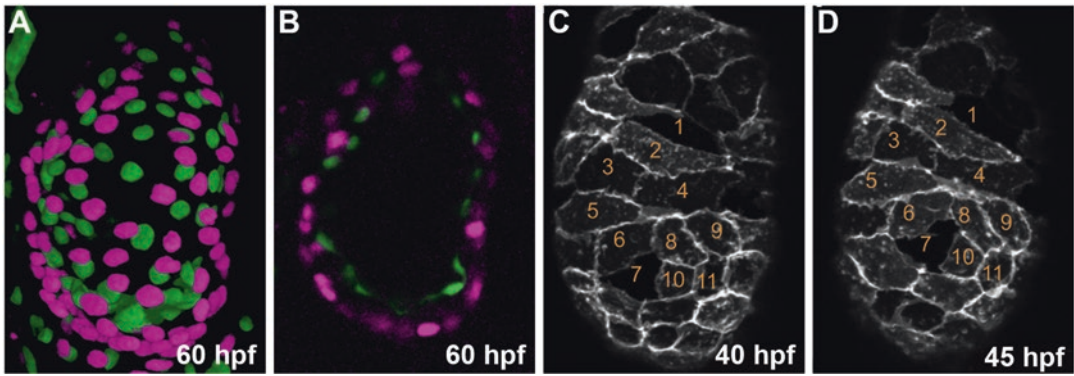


Fig. 8.3 Transgenes used for analyzing cardiac phenotypes in zebrafish. (a, b) Transgenes which label the nucleus can be used to assess whether changes in the size of the heart are due to changes in cardiac cell number. Myocardial nuclei (purple) are labeled with the *Tg(myl7:H2A-mcherry)^{sd12}* transgene [43]. Endocardial nuclei (green) are labeled with the *Tg(fli1a:neqfp)^{v7}* transgene [335]. A lateral view from a three-dimensional reconstruction of confocal slices (a) or a single confocal

slice (b) at 60 hpf is shown. (c, d) Transgenes which label the plasma membrane can be used to assess whether changes in the size of the heart are due to changes in cellular size or shape. The *Tg(myl7:mkate-caax)* transgene [138] was used to label the plasma membrane of myocardial cells in panels (c) and (d). A lateral view of the same heart is shown at 40 hpf (c) and 45 hpf (d). Numbers indicate specific individual cells. (Panels (a, b) are from [43]. Panels (c, d) are from [138])

8.3 Genetic Models of Cardiomyopathies in Zebrafish

The central function of the heart, as a pump that circulates blood throughout the body, is accomplished through the synchronized contractions of myocardial cells. Cardiomyopathies are a heterogeneous spectrum of cardiac disorders that originate in the disruption of this central function [5]. These defects encompass two major processes: defects in the contraction of myocardial cells (most often these defects are located in myofibril function) and defects in the synchronization of those contractions (cardiac conduction defects). Examples of these cardiomyopathies include hypertrophic cardiomyopathy (HCM) which is characterized by increases in the thickness of left ventricular myocardial wall, dilated cardiomyopathy (DCM) which is characterized by the enlargement of the left ventricular cavity and the thinning of the myocardial wall, and restrictive cardiomyopathy (RCM) which is characterized by a myocardium that is rigid and less elastic preventing sufficient filling of the ventricle [152–155]. Defects in myocardial con-

tractions are often due to aberrations in the structure and function of the myofibril, a subcellular organelle responsible for the contraction of myocardial cells. This is in contrast to cardiac conduction defects, such as long-QT syndrome or atrial fibrillation, which are often due to aberrations in the electrophysiological properties of the myocardial cell, which are responsible for determining the timing of a myocardial cell contractions. Defects in these properties result in arrhythmias that can compromise the ability of the heart to pump enough blood to the rest of the body. Studies elucidating how individual genes function in the mechanical and electrophysiological properties of a myocardial cell and how specific mutations disrupt these processes are essential for developing therapeutic and preventive interventions.

8.3.1 Cardiomyopathies and Sarcomeres

Underlying myocardial contractions are myofibrils, subcellular organelles that consist of repeating arrays of parallel actin and myosin filaments known as sarcomeres (Fig. 8.4). Myocardial

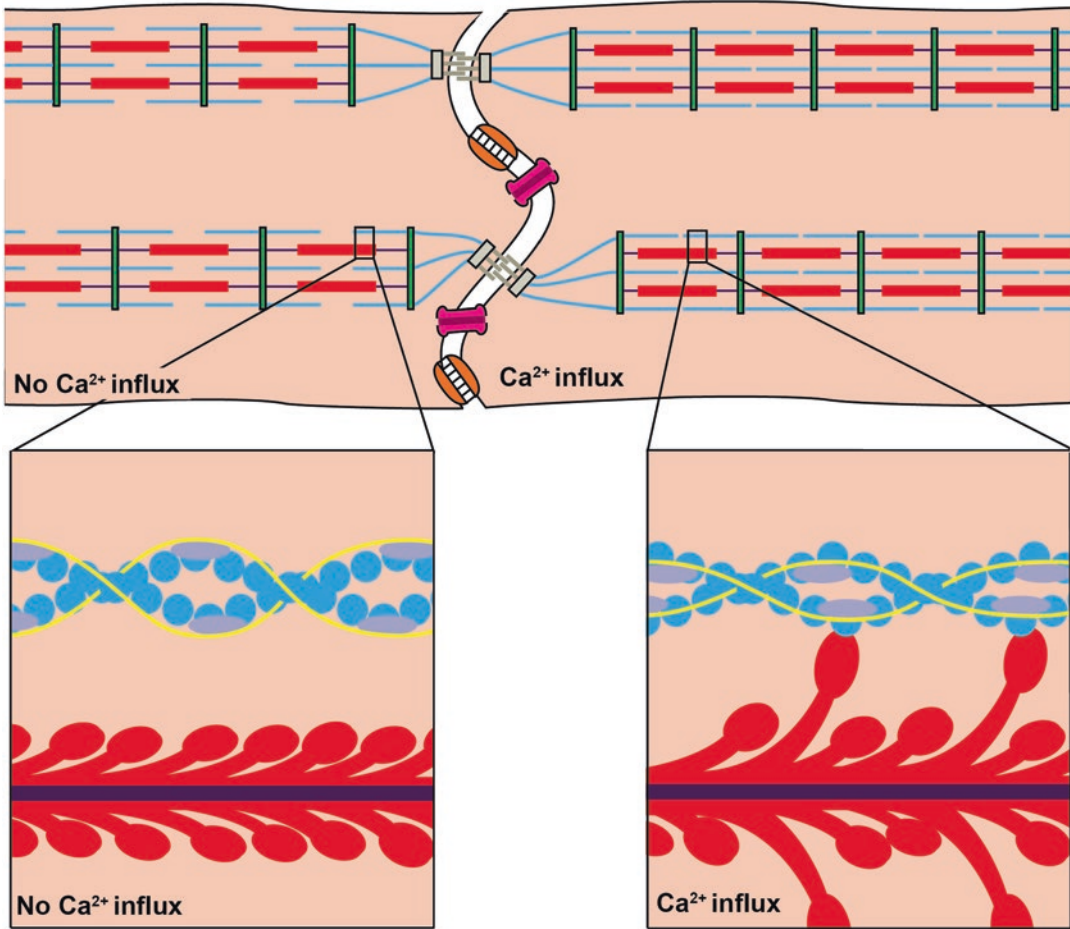


Fig. 8.4 Schematic of sarcomere dynamics. (Left cell and left inset) Without the influx of Ca²⁺ ions into the cytoplasm, tropomyosin prevents myosin from binding to actin (left inset), and sarcomeres do not shorten (left cell). (Right cell and right inset) However, when Ca²⁺ ions are in the cytoplasm, Ca²⁺ binding to Troponin C (light purple, inset) facilitates movement of tropomyosin (yellow) on the actin filament (blue) to expose binding sites for myosin (red). Myosin binding (right inset), contracting, and releasing of actin pull the actin filament, causing sarcomere shortening (right cell) and ultimately myocardial contraction. Actin

and myosin filaments within the sarcomere are anchored at the Z-discs (green). Titin, a large protein, extends from the Z-disc to the middle of the sarcomere where it binds to another titin molecule stretching from the other side of the sarcomere. Titin binds to and anchors the myosin filament at the Z-disc. Light blue, actin filament; red, myosin filament; dark purple, titin; green, Z-disc; yellow, tropomyosin; gray, adherens junction; purple, gap junction; orange, desmosomes. Altogether adherens junctions, gap junctions, and desmosomes make up the intercalated disc. (Figure based on [156, 336–338])

contractions are ultimately a result of myosin filaments binding to and pulling on the actin filaments within sarcomeres. This process is regulated by calcium ion (Ca²⁺)-dependent changes in the tropomyosin-troponin complex (composed of troponin I, troponin C, troponin T2, and tropomyosin) attached to the actin filament. Binding of Ca²⁺ to troponin C within the troponin complex facilitates the movement of tropomyosin on the

actin filament, allowing myosin to bind the actin filament and ultimately shorten the sarcomere [156] (Fig. 8.4).

Within individual sarcomeres the ends of the actin and myosin filaments are anchored in an electron dense region known as the Z-disc. Z-discs contain a myriad of proteins which help to connect individual sarcomeres together. Central to this function is α -Actinin, which cross-

links actin filaments between different sarcomeres [157]. Also attached to the Z-discs is titin (TTN), which forms a large homodimeric protein complex that stretches across the sarcomere binding myosin filaments and anchoring them to the Z-discs [158] (Fig. 8.4).

In zebrafish, sarcomere assembly in myocardial cells begins during the early stages of cardiac development [159]. Starting at ~15 hpf, before the fusion of the bilateral cardiac domains, myosin clusters form small disorganized rodlet structures, while actin filaments are found along the cortical ring. At 18 hpf, Z-discs as visualized by α -Actinin appear as irregular spaced dots between actin and myosin filaments. This stage resembles the premyofibril stage identified in skeletal myocytes. By 24 hpf, immediately after primitive heart tube formation, contractions begin indicating functional sarcomeres. Immunofluorescence studies at 24 hpf reveal nascent myofibrils, in which thin and thick filaments integrate with regularly spaced Z-discs. After their initial assembly, these nascent sarcomeres continue to mature, increasing in thickness and in distance between Z-discs [138, 139, 159–161].

Intriguingly, mutations in an array of different genes within the sarcomere can lead to similar primary cardiomyopathies [162, 163]. For example, mutations in MYH7, MYBPC3, TNNT2, TPM1, and ACTC1 have all been linked to HCM [163]. Conversely, disruptions in a specific gene can be associated with multiple different types of primary cardiomyopathies. For example, loss-of-function mutations in titin are associated with hypertrophic and dilated cardiomyopathy [158, 164]. Thus, studies in animal models such as zebrafish examining myofibril assembly and modeling cardiomyopathies are essential for elucidating the molecular mechanisms underlying myofibril assembly and the pathogenesis of cardiomyopathies.

8.3.2 Investigations into the Role of Titin (*ttn*) in Cardiac Development and Disease

Both forward and reverse genetic techniques have played significant roles in zebrafish studies investigating the role of *ttn* in cardiac development and in

CHD. Mutations in *ttn*, called *pickwick* (*pik*), were identified in the original zebrafish ENU-induced mutagenesis screens [86]. Indeed, because of its large size, *ttn* is often mutated in forward genetic screens [165]. These alleles were mapped to *ttn.2*, one of the two duplicated *ttn* genes in zebrafish. Particularly useful for cardiac studies, the m171 *pik* allele was identified as a missense mutation in the N2B domain of *ttn.2*, a domain only found in the cardiac specific *ttn* isoform. These loss-of-function alleles allowed researchers to investigate the role of *ttn* in cardiac development and function. *Pik* mutant hearts were found to have reduced systolic pressure, thin cardiomyocyte morphologies, and significantly disrupted sarcomere structures [166], phenotypes similar to those found in human patients with DCM [162]. Indeed, concomitantly with the discovery of *pik* alleles in zebrafish, mutations in human *TTN* were linked to the autosomal dominant inheritance of a familial form of DCM [167], revealing that *pik* mutations could function as a model of CHD.

Studies of *pik* mutations have revealed a role for *ttn* not only in sarcomere function but also in sarcomere assembly. These studies [168–171] complemented by studies in mice [172] and in vitro studies [173–175] reveal that titin is important during sarcomere assembly for the transition from the premyofibril to the myofibril state, as well as for myosin filament formation and for maintaining sarcomere integrity [169, 171, 176].

More recently, zebrafish investigators have used gene editing techniques to investigate an intriguing observation regarding *TTN* mutations; truncating *TTN* mutations (TTNtv) in patients with DCM are more likely to be found at the end of the gene (C-terminus) than at the beginning of the gene (N-terminal) [164, 177]. This is a counterintuitive result since TTNtv mutations at the N-terminus should result in less of the protein being translated and a more severe phenotype than TTNtv mutations at the C-terminus (Fig. 8.5). One hypothesis for this observation is that a C-terminal truncation could create a dominant-negative mutation [164, 178]. Using CRISPR/Cas9 and TALEN gene editing techniques, Zou et al. and Shih et al. modeled human C-terminal and N-terminal TTNtv mutations in zebrafish to analyze the mechanisms underlying

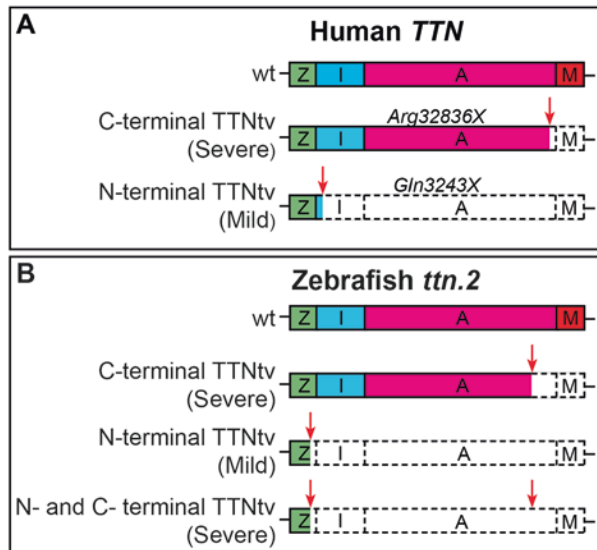


Fig. 8.5 Gene editing in zebrafish helps to identify mechanisms underlying phenotypic heterogeneity in titin truncating variants (TTNtv). (a, b) Schematic of the human and zebrafish titin proteins and corresponding truncating variants (TTNtv). Regions of titin are designated by their spatial location in the sarcomere. For example, the Z region (green) overlaps with the Z-disc, while the I (blue), A (purple), and M (red) regions overlap with the I-band, A-band, and M-band regions of the sarcomere, respectively. Arrows (red) indicate location of the truncation. Parentheses indicate phenotypic severity. (a) TTNtv mutations in patients with DCM are more often found in the C-terminus of the

protein [164]. Representative examples shown: A TTNtv (Arg32836X) from a patient with end-stage DCM [177] and a TTNtv (Gln3243X) from a healthy individual [180]. (b) To explore whether a C-terminal mutation results in a dominant-negative mutation, Shih et al. and Zou et al. used gene editing to recapitulate C-terminal and N-terminal human mutations and to make a double mutant containing both N- and C-terminal mutations. These double mutants have the same phenotype as C-terminal mutations suggesting that a dominant-negative mutation is not made in C-terminal mutations [171, 179]. Only mutations from [171] are shown

these differential severities [171, 179]. These mutations recapitulated the human data, with C-terminal truncations being more severe than N-terminal truncations. Additionally, they created a double N- and C-terminal truncation, with two mutations. These double mutants phenocopy the severe C-terminal truncating mutants, suggesting C-terminal TTNtvs are unlikely to act in a dominant-negative manner (Fig. 8.5). Another possible explanation is that an internal start site, identified by Zou et al., could create a shorter C-terminal peptide (named Cronos) that may partially rescue the N-terminal TTNtv alleles [179]. Alternatively, studies by Schafer et al. have found that TTNtv pathogenicity is also highly correlated to exon usage [180] and thus C-terminal TTNtv may simply be in exons with higher usage. This hypothesis is further supported by truncating mutations made by Shih et al. into highly

used exons [171], which display severe loss-of-function phenotypes. Future experiments, testing the functional nature of the Cronos peptide and the functionality of titin in cells with N-terminal TTNv alleles, will help to further elucidate the origin of these differing *ttn*-related pathologies.

8.3.3 Genetic Analysis of Troponin T and Other Sarcomere Proteins

Forward genetics has also played a large role in revealing other proteins within the sarcomere that are essential for cardiac development. A loss-of-function mutation in *troponin T type 2a* (*tnnt2a*), which facilitates attachment of the troponin complex to tropomyosin in order to regulate myosin-actin binding [181], was originally identified in a forward genetic screen. This mutation called

silent heart (sih) leads to a non-contractile heart with pericardial edema and sparse sarcomeres. These sarcomeres have unorganized thick filaments located near the cell membrane [182]. As this phenotype suggests, *tnnt2a* is required to continue sarcomere assembly beyond the initial stages of assembly but is not required for the early stages of thin filament assembly or for Z-disc formation [160, 183]. Several myosin filament proteins were also identified in forward genetic screens, including *half-hearted (haf)*, a nonsense mutation in *myosin heavy chain 7 (myh7)*, and *weak-atrium (wea^{m58})*, a nonsense mutation in *myosin heavy chain 6 (myh6)* [53, 86, 184]. Similar to chicken embryos, *myh7* and *myh6* in zebrafish are expressed specifically in the ventricular and atrial chambers, respectively [185, 186]. The ventricle in *myh7^{haf/haf}* mutants and the atrium in *myh6^{m58/m58}* mutants fail to contract, becoming enlarged and distended [53, 184]. Without myosin heavy chain, myofibrils are completely absent in the ventricle of *myh7^{haf/haf}* mutants and in the atrium of *myh6^{m58/m58}* mutants, revealing a role for myosin in both the function and assembly of these structures.

Human mutations in *TNNT2*, *MYH7*, and *MYH6* have also been associated with familial forms of HCM and DCM [187–190]. Mutations in *MYH7* and *TNNT2* are estimated to account for 40–50% and 15% of familial cases of HCM, respectively [191, 192], while mutations in *MYH6* have been associated with a spectrum of CHDs, including HCM and DCM [193]. The connection of these genes to HCM and DCM suggests that corresponding zebrafish mutants could be analyzed to understand HCM and DCM pathogenesis. For example, analysis of the zebrafish *myh6^{hu423}* missense mutation revealed that heterozygous mutants (*myh6^{hu423/+}*) are viable but display reduced atrial contractility, resulting in post-embryonic cardiac maturation and morphogenesis defects. Adult heterozygous *myh6^{hu423/+}* mutants have cardiac chambers that are more similar to a wild-type juvenile heart than an adult heart suggesting a failure of cardiac maturation [23]. Further analysis comparing these defects to the reactivation of fetal gene programs identified

in heart disease may help elucidate the mechanisms underlying CHD [194, 195].

Homozygous *tnnt2a^{sih/sih}*, *myh7^{haf/haf}*, and *myh6^{m58/m58}* mutants in zebrafish also provide a unique set of genetic tools with which to interrogate the role of contraction and hemodynamics in cardiac development. For example, by analyzing ventricular development in homozygous *myh6^{m58/m58}* mutants (in which atrial contraction is eliminated), ventricular maturation and morphogenesis were found to depend on proper blood flow [184]. Studies using these mutants have also found a role for proper hemodynamics in other aspects of cardiac development including in atrioventricular valve development, the process of ventricular trabeculation, the development of the epicardium, and the development of the cardiac conduction system [20, 196–200].

The complementary nature of human and zebrafish studies can also be seen in the identification of nexilin as a new component of the sarcomere involved in the pathogenesis of DCM. Studies in zebrafish found *nexilin*, a previously unknown gene, to be localized to the Z-disc and responsible for sarcomere maintenance and integrity [201]. Having identified a novel gene important for sarcomere biology, eight individuals from a cohort of patients with idiopathic DCM were found to carry heterozygous variants (a three-base pair deletion and two missense alleles) of *nexilin*. These variants were not found in wild-type SNP databases or in a large number of healthy control individuals suggesting that mutations in *nexilin* likely underlie DCM pathogenesis in some human patients. Zebrafish embryos were further used to analyze the role of these disease variants. mRNA injection of these variants had a dominant-negative effect on nexilin and Z-disc function compared to injection of wild-type *nexilin*, revealing a possible mechanism through which these heterozygous *nexilin* mutations could cause DCM. Similar studies using knockdown or overexpression experiments in zebrafish to verify the function of genes identified in human patients have revealed a role for *tcap*, *actc1a*, *myo18b*, *ilk*, *lama4*, *fbln7*, *tmem87b*, and *mybpc3* in congenital heart defects [202–208].

8.4 Models of Cardiac Conduction Defects

The rhythmicity of myocardial contraction is coordinated by electrical impulses that propagate through the heart regulating the flow of Ca^{2+} into and out of the myocardial cytoplasm. These electrical impulses originate in a specialized set of pacemaker cells located in the venous pole of the heart near the atrium [20–22, 78, 209]. In many respects zebrafish have a remarkably similar cardiac conduction system to humans. Rhythmic contractions in zebrafish occur approximately two beats every second [19, 210], which is similar to the human resting heart rate of 1–1.7 beats per second [211]. Comparatively, the resting heart rate of mice is approximately 5–14 beats per second [212, 213]. The action potential phases underlying cardiac conduction in zebrafish are also similar to those in humans. Ventricular action potentials initiate from a resting phase to quickly depolarize (fast depolarization), followed by a slow repolarizing plateau and a final fast repolarization phase (Fig. 8.6). Although an early repolarization phase is not as distinct in zebrafish ventricular cardiomyocytes as it is in humans, the long plateau during repolarization creates an action potential of similar morphology and duration to that of humans [19, 214]. This is particularly important because changes in repolarization

underlie a number of congenital conduction defects, such as long-QT syndrome [215].

Each action potential phase is regulated by a combination of different sodium, potassium, and calcium channels that regulate the flow of ions into and out of the cell. Mutations in these channels can result in abnormal action potentials and ultimately cardiac arrhythmias. Ventricular arrhythmias are one of the strongest contributors and indicators of sudden cardiac death [216], while atrial arrhythmias contribute to palpitations and stroke [217]. The similarities to human cardiac conduction make zebrafish a particularly suitable model organism in which to elucidate the mechanisms underlying cardiac conduction defects; several examples are highlighted below.

8.4.1 Defects in Repolarization: Changes in the QT Interval

On an electrocardiogram (ECG) of the heart, the duration of the ventricular action potential can be approximated by the QT interval, which is calculated by measuring the time from the beginning of the QRS complex to the end of the T wave (Fig. 8.6c). Both increases and decreases in ventricular action potential duration are associated with increased risk of arrhythmias in human

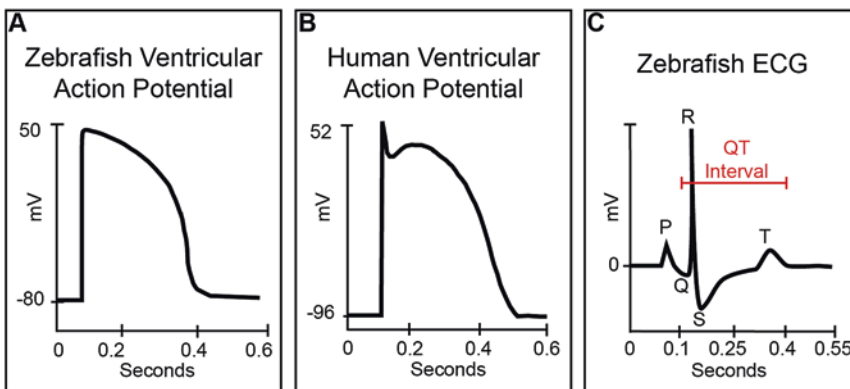


Fig. 8.6 Cardiac conduction is similar in zebrafish and humans. (a, b) Graph of a typical ventricular action potential in zebrafish (a) and humans (b). (c) Graph of a typical adult zebrafish heart electrocardiogram. The P, Q, R, S,

and T waves are labeled. The Q, R, and S waves together comprise the QRS complex. The QT interval (between the red lines) is measured from the start of the Q peak to the end of the T wave. (Graphs are adapted from [148, 339])

patients, which can cause the heart to be hemodynamically compromised. In order to use human QT intervals to identify aberrations in ventricular action potential duration, it must be normalized for heart rate and gender (QTc) which affect the QT interval in predictable patterns [218].

Increases in the QTc interval (>480 ms), a critical component of long-QT syndrome (LQTS) [219], are often due to an abnormally long slow repolarization phase. This phase is dependent on a balance between inward depolarizing channels and outward repolarizing channels [220]. One of the genes responsible for the repolarizing current in myocardial cells is *KCNH2*, which is often found to be mutated in long-QT syndrome patients [221]. *kcnh6a*, a member of the *kcnh2* voltage-gated potassium channel family [222], plays a crucial role in the repolarization of cardiac cells in zebrafish [87, 140]. In homozygous loss-of-function *kcnh6a*^{s213} mutants, which originated in a forward genetic screen [223], the ventricle fails to contract, yet the atrium exhibits normal morphology and contraction. Further cellular analysis of these mutant hearts using electrophysiological techniques reveals a compromised ventricular repolarization phase leading to a failure of conduction between the atrial and ventricular chambers (AV block) and loss of ventricular action potentials. Atrial action potentials are also abnormal, displaying increased duration and a longer refractory period. These studies reveal the physiological result of loss of *kcnh6a*, illuminating the differential effects loss of *kcnh6a* has on ventricular and atrial chambers.

Cellular studies in zebrafish have also begun to examine how *Kcnh2* channels are regulated. These studies show that intracellular trafficking to the membrane is likely a critical point of regulation [224]. One possible partner regulating *Kcnh2* trafficking is the RING finger protein *Rnf207*. Variants in *RNF207* were originally identified in a genome-wide association study (GWAS) of prolonged QT intervals. Furthermore, morpholino-mediated knockdown of *rnf207* in zebrafish results in action potential prolongation, occasional 2:1 AV block (two atrial contractions for every ventricular contraction), and slower than normal heartbeat (bradycardia). And *Rnf207* modulates membrane

localization of *Kcnh2* as well as colocalizes and binds to *Kcnh2* in vitro [225].

Complete loss of *kcnh6a* is helpful in the unambiguous identification of *kcnh6a* function; however, this phenotype is more severe than the QT prolongation that patients with *KCNH2* mutations experience [140, 222]. Hypomorphic alleles such as *kcnh6a*^{bre} which displays a 2:1 AV block [222] are likely to more accurately mirror disease pathogenesis. Similarly, heterozygous *kcnh6a*^{s213} zebrafish mutants may display phenotypes similar to the symptoms of patients with long-QT syndrome, which in humans is most often inherited in a dominant manner [226]. Heterozygous *kcnh6a* zebrafish mutant hearts display QT prolongation at the cellular level but are morphologically indistinguishable when compared to wild-type embryos [140]. Furthermore, heterozygous *kcnh6a* mutant zebrafish embryos also display an increased sensitivity to drugs that block inward-rectifying K⁺ ion currents (I_{Kr}), such as terfenadine. At concentrations that do not affect wild-type animals, heterozygous *kcnh6a*^{s213} mutants incubated in terfenadine develop a 2:1 AV block [140]. These phenotypes match theories of human CHD progression, in which a secondary environmental insult on top of a hidden genetic defect can cause heart disease.

Mutations in human *KCNH2* have also been found to cause short-QT syndrome as well as long-QT syndrome. Short-QT syndrome (SQTS), associated with a QTc ≤340 ms, although rarer than long-QT syndrome, can also result in atrial fibrillations, syncope, and cardiac arrest [227, 228]. These mutations are gain-of-function mutations in *kcnh2* family members that can lead to premature channel activation and ultimately a short-QT interval [229]. In zebrafish, short-QT syndrome is modeled using the *kcnh6a*^{reggae} mutation. The *reggae* mutation causes a gain-of-function L499P change within the voltage-sensing fourth transmembrane domain of the *Kcnh6a* potassium channel [230]. Analysis of the homologous L532P mutation in the human *KCNH2* channel reveals that the shorter QT interval is a result of a lower voltage-gated activation threshold, faster channel activation, and faster recovery from inactivation [231]. Gross phenotypic analysis

of homozygous *kcnh6a^{reggae}* mutants found no coordinated myocardial contractions at 24 hpf. *kcnh6a^{reggae}* mutants display a complete sinoatrial block, in which pacemaker cells at the base of the atrium contract, but the electrical pulse is not propagated to the atrial myocardium, interspersed with occasional uncoordinated atrial electrical and contractile activity (atrial fibrillation) and occasional normal sinus rhythm [230].

Several groups have taken advantage of the zebrafish models of long- and short-QT syndromes to examine the roles of different *kcnh6a* variants on cardiac conduction and to perform high-throughput screens for drugs and genes that can rescue QT prolongation. For example, Jou et al. found that by overexpressing different *kcnh6a* variants using mRNA injection in *kcnh6a*-morphant embryos, they could determine the benign or pathogenic nature of that variant [232], verifying zebrafish as a useful model of CHDs. To discover genes that are important for regulating repolarization, Milan et al. conducted a forward genetic screen using GBT to identify insertional mutants that either confer resistance to or sensitize the embryo to drug (dofetilide)-induced arrhythmia. Dofetilide slows cardiac repolarization [233]. They found that mutations in *gins3* conferred resistance to dofetilide-induced 2:1 AV block. Intriguingly, *GINS3* is also contained within a GWAS-associated genome region that correlates with QT interval variation [234]. *Gins3* is a subunit of a heterotetrameric complex important for initiation of DNA replication [235, 236]. Future studies into the mechanism of how *gins3* modifies dofetilide-induced arrhythmia are likely to further our understanding of how repolarization is regulated. Similarly, Peal et al. used the hypomorphic *kcnh6a^{bre}* mutants to screen for small molecule compounds that could rescue the 2:1 AV block. They identified flurandrenolide, which likely works through glucocorticoid signaling, and 2-methoxy-*N*-(4-methylphenyl) benzamide (2-MMB) as compounds that can suppress the long-QT phenotype in *kcnh6a^{bre}* mutant embryos [237].

KCNQ1, another voltage-gated potassium channel involved in cardiac repolarization, mediates the late repolarizing I_{Ks} -current and is also

mutated in a large percentage of long-QT syndrome patients [238–240]. Recent zebrafish studies into the regulation of *kcnq1* expression have begun elucidating how the balance in expression between inward depolarizing and outward repolarizing channels is maintained. In this study, Benz et al. sought to examine the function of *mir19b*, a microRNA whose expression is reduced in diseased myocardium, such as DCM. Using reverse genetic techniques including morpholino-mediated knockdown and CRISPR/Cas9 mutation, Benz et al. found that loss of *mir19b* function results in bradycardia, AV block, and action potential prolongation. Further examination identified *scn1b*, *scn4b*, *kcnk4*, and *kcnj2*, which are genes involved in sodium and potassium voltage-gated channels, as direct targets of *mir19b*. In particular, *Kcnk4* is a modulatory β -subunit of *Kcnq1*, which is upregulated in *mir19b*-morphants suggesting *mir19b* may help to maintain the proper expression of voltage-gated channels. Benz et al. speculate that loss of *mir19b* expression in DCM could contribute to the conduction problems observed in these patients [241].

8.4.2 Zebrafish Studies of Calcium Ion Flux in the Heart

Electrical impulses in the heart coordinate calcium ion (Ca^{2+}) fluctuations which in turn regulate myocardial contraction and relaxation. Extracellular Ca^{2+} enters the cell upon depolarization through L-type calcium channels, which triggers more Ca^{2+} release from the sarcoplasmic reticulum via ryanodine receptors to initiate sarcomere contraction. Relaxation is then accomplished through extrusion of Ca^{2+} back into the sarcoplasmic reticulum via SERCA2 or into the intercellular space via the Na^+ - Ca^{2+} exchanger NCX1 [156, 242]. Genetic analysis in zebrafish of both Ca^{2+} influx (*cacnalc*) and Ca^{2+} extrusion (*ncx1*) has revealed interconnections between cardiac conduction and myofibril assembly.

For example, ventricular cardiomyocytes in *cacnalc* mutants called *island beat (isl)* are smaller than in wild-type embryos and do not

beat, while atrial cardiomyocytes exhibit unsynchronized fibrillations; however the heart tube and myofibrils form normally [243]. These studies reveal that proper Ca^{2+} influx is not required for sarcomere assembly. However, the smaller ventricle in *cacna1c^{isl}* mutants reveals a role for Ca^{2+} in developmental cardiac hypertrophy. Indeed, further studies using small molecules that inhibit or activate L-type calcium channels confirm that increasing Ca^{2+} influx can enhance ventricular hypertrophy and that calcineurin may mediate this effect [244].

In *ncx1* mutants called *tremblor* (*tre*), in which extrusion of Ca^{2+} is compromised resulting in Ca^{2+} overload, ventricular contraction is also absent and atrial rhythm is disrupted, phenotypes similar to those found in *cacna1c^{isl}* mutants. However, ventricular sarcomeres are sparse, randomly oriented, and rarely connected in *ncx1^{tre}* mutants at 48 hpf [245, 246], suggesting that Ca^{2+} overload can affect sarcomere assembly. Comparisons between wild-type hearts and *ncx1* mutant hearts revealed that the E3 ligase *murfl* is upregulated in *ncx1^{tre}* mutants, suggesting that ectopic *murfl* may mediate *ncx1^{tre}* mutant phenotypes. Transgenic overexpression and morpholino-mediated knockdown experiments confirmed that *murfl* mediates the Ca^{2+} -overload phenotype [247]. Patterning of the atrial-ventricular canal (AVC) is also disrupted in *ncx1^{tre}* mutants. Genes normally expressed in a small medial location at the presumptive site of the AVC have broader expression domains in *ncx1^{tre}* mutants, suggesting that Ca^{2+} overload also affects AVC patterning. Intriguingly, in a screen for small molecules that can rescue the *ncx1^{tre}* mutant phenotype, Shimizu et al. identified the small molecule efsevin, an agonist of voltage-dependent anion-selective channel 2 (VDAC2) function. VDAC2 is a voltage-dependent anion channel in the mitochondria [248]. Efsevin rescues the *ncx1^{tre}* mutant phenotype by increasing mitochondrial outer membrane permeability to Ca^{2+} via VDAC2 and thus normalizing cytosolic Ca^{2+} oscillations and ventricular contractions [141]. Together, these studies reveal mechanistic and physiological roles for Ca^{2+} channels and transporters in cardiac excitation as

well as in sarcomere assembly and cardiomyocyte size. Indeed, along with *cacna1c*'s role in ventricular hypertrophy [244], *cacna1c* has also been shown to be important for establishing the electrical gradient within the ventricle, ensuring sequential contraction from the apex to base [249]. Developmental studies investigating the role of Ca^{2+} channels along the course of cardiac development in mouse [250] also reveal that individual Ca^{2+} channels are likely to have differential roles in interconnecting Ca^{2+} signaling to myofibril assembly and integrity. Future studies, similar to those above, that combine the high-throughput unbiased screening advantages of zebrafish with disease modeling are likely to elucidate fundamental mechanisms of cardiac conduction, identify small molecules for therapeutic studies, and reveal the mechanisms by which different physiological and developmental systems in the heart are interlinked.

8.4.3 Myofibril Assembly and Cardiac Conduction Crosstalk

At the intersection of sarcomere function and cardiac conduction are intercalated discs (Fig. 8.4). Intercalated discs consist of desmosomes, which mechanically couple adjoining cardiomyocytes; gap junctions, which electrochemically couple adjoining cardiomyocytes; and fascia adherens junctions, where myofibrils attach to the cell membrane [211]. Mutations in genes involved in intercalated disc formation, particularly those important for desmosome function, have been found in arrhythmogenic cardiomyopathies (ACM) [251]. The best-known subtype of ACM is arrhythmogenic right ventricular cardiomyopathy (ARVC), which is characterized by both conduction defects including ventricular arrhythmias and structural defects including fibrofatty replacement of the myocardium [252]. The association between ACM and mutations in desmosome genes suggests that a failure in mechanical coupling of myocardial cells underlies the pathologic electrical and structural characteristics of ACM. For example,

plakoglobin, an adaptor protein important for intercalated disc formation, is mutated in Naxos disease, a systemic disease that includes ARVC [253]. Loss of *plakoglobin* leads to thin, sparse intercellular junctions that are weakly connected to intermediate filaments [254]. To elucidate the pathology underlying ACM, Asimaki et al. created a transgene to express a mutated version of the human *plakoglobin* (2057del2) gene found in patients with Naxos disease [253] in the zebrafish myocardium [255]. Larvae expressing the *plakoglobin* (2057del2) mutation in the myocardium initially display bradycardia and decreased stroke volume at 48 hpf. By 3 weeks post-fertilization, the electrophysiological properties of these mutant embryos are severely perturbed, with prolonged action potentials, higher resting membrane potential, and decreased I_{na} -current. These aberrant conduction properties are followed by sarcomere disarray, cardiomegaly, and thinning of the atrial and ventricular walls and significantly reduced survival by 4–6 weeks post-fertilization.

After creating a zebrafish model of ACM, Asimaki et al. utilized a forward genetic approach (see Table 8.1) to unbiasedly identify small molecules that could rescue the physiological and structural defects found when plakoglobin (2057del2) is overexpressed in the myocardium of zebrafish embryos. SB216763, a canonical Wnt activator, was found to normalize cardiac action potentials in these mutant embryos. Intriguingly, exposure to SB216763, even after embryos had developed heart defects, was able to remediate those phenotypes. Mechanistic studies revealed that SB216763 rescues abnormally low levels of SAP97, a protein important for trafficking sodium and potassium channel components to the plasma membrane, thereby suggesting a possible function for plakoglobin mutations in ACM pathogenesis [255].

Connections between sarcomere function and cardiac conduction have also been examined in a zebrafish model of atrial fibrillation (AF), in which atrial myocardial cells contract asynchronously [256]. AF is the most common type of cardiac arrhythmia and is highly associated with increased morbidity and mortality [217].

Based on familial pedigrees with AF, mutations in sodium or potassium channels were initially identified as underlying AF [256, 257]. However, multiple studies suggest that AF can also have a molecular etiology that is not directly related to the cardiac conduction system. For example, titin-truncating variants (TTNtv) and mutant *nppa* isoforms have been identified in AF patients [258, 259]. Recently, Orr et al. discovered a familial pedigree with AF that is associated with a heterozygous mutation (E11K) in the atrial-specific myosin light chain (*MYL4*) gene. To create a disease model of this mutation, Orr et al. created a transgene that specifically expressed *myl4*(E17K) in the myocardium of zebrafish hearts. Expressing *myl4*(E17K) in the myocardium leads to atrial enlargement and malformed sarcomeres—with absent Z-discs. These mutants also display electrical abnormalities that include irregular sinoatrial impulses, slow atrial conduction, and overall bradycardia, recapitulating aspects of AF [260]. Future studies examining how myosin mutants and malformed sarcomeres affect cardiac conduction will not only help to reveal the fundamental mechanisms by which these processes are interlinked but are also likely provide insight to the pathology of AF.

8.5 Zebrafish Studies of Environmental Toxicants and Their Possible Contributions to Heart Defects

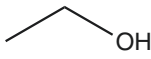
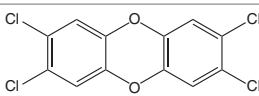
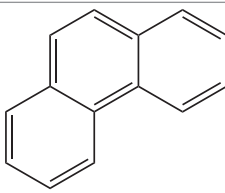
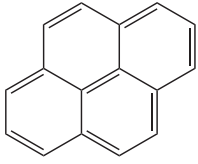
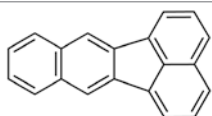
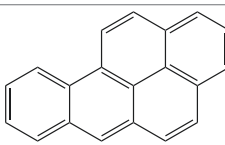
Along with genetic changes, environmental stressors are also known contributors to congenital heart defects [261–263]. Environmental stress can be caused by the loss of essential external elements such as oxygen (hypoxia), or it can be caused by exposure to toxicants, pharmaceuticals, or even alcohol and sugar [264–268]. Due to its external development as well as its small size, zebrafish are used by a wide array of investigators to examine the influence of environmental factors on cardiac development. For example, zebrafish are being used to investigate the mechanisms of compensation to changes in oxygen

concentration [269]. Zebrafish embryos are also being used to identify chemotherapeutics that are cardiotoxic [270, 271] and to identify drugs that might suppress those cardiotoxic side effects [272]. Additionally, zebrafish have been used to identify compounds found in personal care products (e.g., alpha-bisabolol), flame retardants (e.g., triphenyl phosphate), cigarette smoke, and insecticides (e.g. deltamethrin) that cause defects in cardiac development [273–276]. Here we briefly highlight a few studies (see Table 8.3) investigating the mechanisms by which toxicants can adversely affect zebrafish cardiac development.

8.5.1 Zebrafish Models of Fetal Alcohol Spectrum Disorders

Prenatal ethanol exposure was only clinically identified as a factor in causing birth defects in the late twentieth century [277]. Despite educational efforts, birth defects caused by alcohol exposure, referred to as fetal alcohol spectrum disorders (FASD), are estimated to be as high as 1:100 births in the United States [278]. Contributing factors to the high incidence of FASD is the widespread societal consumption of ethanol and the large percentage of pregnancies

Table 8.3 Environmental toxicants highlighted in this chapter

Name	Chemical structure	Cardiac phenotype	Origin	
Ethanol		Pericardial edema	Alcoholic beverages	[286, 340]
		Reduced heart size		
		Reduced ventricular thickness		
		Abnormal heart looping		
		Cardia bifida		
Tetrachlorodibenzo- <i>para</i> -dioxin (TCDD)		Pericardial edema	By-product of incomplete combustion	[299, 341]
		Bradycardia		
		Decrease in heart size		
		Defects in AV valve		
		Epicardial defects		
Phenanthrene		Pericardial edema	Burning of fossil fuels, oil, wood, and organic matter	[342]
		Tachycardia		
		Abnormal heart looping		
		Enlarged ventricle		
		Thin ventricular wall		
Pyrene		Pericardial edema	Incomplete combustion of crude oil and coal	[321, 343]
		Abnormal heart looping		
		Abnormal heart rate		
		Decreased stroke volume		
Benzo-k-fluoranthene		Pericardial edema	Incomplete combustion found in gasoline exhaust, cigarette smoke, motor oil	[322]
		Atrial chamber dilation		
		Bradycardia		
Benzo-a-pyrene		Pericardial edema	Forest fires, volcanic eruptions, oil spills, automobile emissions	[331, 344, 345]
		Bradycardia		
		Abnormal heart looping		
		Smaller ventricle and thinner atria		

which are unplanned (~50%) [279–282]. An array of developmental defects occur upon fetal alcohol exposure including defects in craniofacial, neural, ocular, and cardiac development [283].

Studies in zebrafish have provided important insights into the mechanisms of ethanol teratogenicity in the heart. Exposure of 0.6–0.9% ethanol (recent analysis has found that levels of ethanol in zebrafish tissues are ~33% of those in the surrounding media [284, 285]) from 2–20 hpf causes pericardial edema, aberrant looping, reduced ventricular chamber size, a wider atrioventricular canal, and uneven ventricular wall thickness at 48 hpf [286, 287]. Using transgenes to reveal the location of endocardial and myocardial cells, further analysis revealed that endocardial and myocardial movements during cardiac fusion (see Fig. 8.1c) are disrupted resulting in two separate cardiac domains, a phenotype known as cardia bifida. Further analysis of why ventricular size in ethanol-exposed zebrafish embryos is reduced (as revealed by counting myocardial nuclei; see Table 8.2) revealed decreases in the specification of both the second and first heart fields [288]. Intriguingly, many of these ethanol-induced developmental defects are partially or completely rescued by the addition of retinoic acid (RA) or folic acid [289]. Folic acid is a supplement taken by pregnant women to reduce birth defects, particularly neural tube defects [290]. Its role as an antagonist of ethanol toxicity suggests it may have other benefits as well. Future work deciphering the interactions between the folic and retinoic pathways and the pathways disrupted by ethanol will likely lead to a better understanding of the etiology of ethanol teratogenesis and may reveal potential therapeutic interventions.

8.5.2 2,3,7,8-Tetrachlorodibenzo-*p*-dioxin

Dioxins are lipophilic, persistent environmental contaminants that bioaccumulate due to their high chemical stability and absorption by fat tissues [291]. Commonly found in the air and soil, dioxins are created as by-products of incomplete

waste incineration and industrial processes such as smelting, chlorine bleaching and manufacturing of herbicides [292]. One of the most toxic dioxins, 2,3,7,8-tetrachlorodibenzo-*p*-dioxin (TCDD), is well known due to its presence as a by-product contaminant in the herbicide Agent Orange [293] and as a cause of blue sac syndrome in fish [294, 295]. Blue sac syndrome is found in wild fish that have been exposed to environmental toxicants resulting in pericardial edema, hemorrhaging, craniofacial abnormalities, and mortality during larval development [296]. TCDD is studied as a prototypic dioxin, used to understand the adverse outcome pathway of all dioxins. As one of the most potent dioxins, TCDD also acts as a reference for calculating the toxic equivalency factor (TEF) of other dioxins and quantitatively assessing the risk of dioxin mixtures discovered in the environment [297].

In zebrafish, embryonic exposure to TCDD (≤ 1 part per billion (ppb)) at ~6 hpf for 1 h results in large changes in cardiac morphology after 48 hpf [298, 299]. (TCDD-exposed embryos are indistinguishable from DMSO-exposed siblings until 48 hpf.) Starting at 72 hpf, gross morphological cardiac defects include pericardial edema, blood regurgitation, altered looping, compact ventricles, and enlarged atria. At 96 hpf, ventricular contraction is compromised with complete cessation occurring by 120 hpf. Further analysis, using a transgene that labels myocardial nuclei, has found that a decrease in cardiomyocyte number likely accounts for the decrease in cardiac size [299]. Histological and gene-expression analysis also found that epicardial development is inhibited in TCDD-exposed embryos [300]. Cardiotoxic effects of TCDD, however, are restricted to embryonic and larval development (<14 dpf). After 30 dpf TCDD exposure fails to induce gross morphological changes in the heart [301]. These studies indicate that the early embryo is exquisitely sensitive to TCDD exposure.

Molecular analysis of TCDD-mediated phenotypes identified aberrant activation of the aryl hydrocarbon receptor (AHR) pathway as the likely cause of the adverse cardiac phenotypes. These findings are based on studies which found that inhibition of *ahr2* or aryl hydrocarbon receptor nuclear

translocator 1 (*arnt1*), by morpholino-mediated knockdown, dominant-negative constructs and mutants, ameliorates phenotypes caused by TCDD exposure [302–307]. *ahr2* morphants alone do not display defects in early cardiac development, although *Ahr* mutant adult mice display cardiomyopathy [308]. *Cyp1a* expression, a target of the AHR pathway, is also increased in TCDD-exposed embryos [309–311], although *cyp1a* expression is not cardioprotective in TCDD-exposed embryos [312]. Additionally, expression of a constitutively active version of *ahr2* in the myocardium recapitulates phenotypic aspects of TCDD exposure including pericardial edema, elongated heart morphology, and epicardial absence [313]. Mammalian and cell culture studies have also found that TCDD exposure affects the size of the developing heart and the ability of cardiomyocytes to differentiate [314, 315], paralleling many of the zebrafish findings.

How AHR pathway activation disrupts normal cardiac development is an area of active investigation. Recent studies suggest that changes in the regulation of the transcription factor *sox9b* and the long noncoding RNA (lncRNA) *slincR* may at least partially mediate the effects of TCDD exposure. *Sox9b*, a transcription factor important for cranial-pharyngeal and cardiac development, is downregulated upon TCDD exposure [316]. Furthermore, expression of a dominant-negative form of *sox9b* in cardiomyocytes phenocopies many TCDD-mediated phenotypes, including decreased cardiomyocyte numbers and impaired epicardial development [317]. Conversely, *slincR*, which is intragenic to *sox9b*, is upregulated in an AHR-dependent manner when embryos are exposed to TCDD. And *slincR* is enriched at the 5'UTR of *sox9b* [318, 319]. These studies thus suggest a model in which activation of the AHR pathway by TCDD triggers an increase in *slincR* expression and a subsequent decrease in *sox9b* causing myocardial and epicardial defects during development. Future experimentation into the mechanisms by which cardiac development is disrupted by TCDD and how specific pathways are altered is likely to further elucidate the mechanisms underlying TCDD toxicity. Additionally, these future studies will also likely lead to an understanding of the robust and vulnerable aspects of cardiac development.

8.5.3 Polycyclic Aromatic Hydrocarbons

Polycyclic aromatic hydrocarbons (PAHs) originate largely from petroleum-based products and are ubiquitous contaminants in water environments, particularly those close to urban locations [320]. In these environments PAHs exist in complex mixtures. Studies in zebrafish have been used to identify the role of individual PAHs within these mixtures. Zebrafish embryos exposed from 6 to 96 hpf to individual PAHs can display a wide array of cardiac defects, including bradycardia, arrhythmia, reduction of contractility, and edema. Three-ring PAHs such as dibenzothiophene and phenanthrene cause reduced circulation, bradycardia, and 2:1 AV block. Cardiac chambers were also found to be dilated and had thinner walls in embryos exposed to three-ring PAHs, while exposure to pyrene, a four-ring PAH, caused less severe phenotypes including bradycardia at 80 hpf and anemia [321]. Five-ring PAHs have differential effects on zebrafish cardiac development, depending on the particular molecule. For example, zebrafish embryos exposed to benzo[k]fluoranthene (BkF) (40 μ M) from 4 to 48 hpf display pericardial edema, atrial chamber dilation, and bradycardia. However, exposure to benzo[a]pyrene (BaP) (40 μ M) during the same timeframe causes less severe pericardial edema, only occurring in ~40% of exposed embryos [322]. These five-ring PAHs also display differential AHR dependence and tissue induction of *cyp1a* [323]. BaP exposure induces *cyp1a* expression in vascular tissues including the endocardium. *Cyp1a* expression in response to BaP is *ahr2* dependent. Studies of the role of *cyp1a*, a BaP-hydroxylase, in BaP toxicity have found that it is both cardioprotective and produces toxic by-products [323, 324]. This is in contrast to BkF exposure, which induces *cyp1a* expression strongly in the epidermis and very weakly in the endocardium. BkF exposure also induces pericardial edema in *ahr2* morphants, even though *cyp1a* induction is reduced, revealing an *ahr2*-independent mechanism for BkF-mediated pericardial edema [322].

As a mixture, PAHs have synergistic effects on cardiac development [325]. Future studies

building on the study of individual PAHs to investigate the mechanisms underlying the synergistic phenotypes of complex PAH mixtures on cardiac development are likely to provide insight into both adaptive and maladaptive responses to PAHs. In one study of complex PAH mixtures, bluefin tuna cardiomyocytes were exposed in vitro to water samples from the Deepwater Horizon oil spill disaster. These samples caused increases in the QT interval and the duration of the ventricular action potential due to defects in membrane repolarization (see section 8.4). The I_{Ca} current was also decreased upon exposure [326]. Thus, PAHs affect both structural and functional aspects of cardiac development.

8.5.4 Endocrine Disruptors

Endocrine disruptors are a diverse class of toxicants, which also show effects on cardiac development. In one study of the role of estradiol, Romano et al. found that acute 17β -estradiol (E2) exposure results in increased heart rate due to the G-protein-coupled estrogen receptor (GPER) rather than the nuclear receptors ($ER\alpha$ or $ER\beta$). Activation of GPER in E2-exposed embryos triggers increases in thyroid hormone levels (triiodothyronine, T3), which is a known regulator of heart rate [327]. Conversely, a decrease in E2 levels leads to pericardial edema, bradycardia, and decreased heart size [328]. Similar phenotypes to decreased E2 levels are found in BaP-exposed embryos [329]. This corresponds with BaP's known role inhibiting aromatase (*cyp19*), which converts androgens to estrogens [330]. Indeed, addition of E2 rescues BaP-induced pericardial edema [331]. Future investigations into the crosstalk between E2 disruption and AHR-mediated induction in BaP-exposed embryos will likely reveal the pathogenic nature of BaP in cardiac development. By elucidating complex intertissue physiological effects of toxicant exposure, these studies reveal the power of using zebrafish as a model organism for toxicology studies as opposed to a simple cell culture system. Furthermore, due to the similar molecular pathways in zebrafish and human cardiac development, continued toxicology studies using

zebrafish are likely to reveal both mechanisms of how environmental contaminants affect fish populations and how toxicant contamination can affect human development.

8.6 Conclusion

Zebrafish is a powerful model for investigations into the molecular principles underlying cardiac development. The studies highlighted in this chapter reveal how the intrinsic advantages of zebrafish as a model organism (similarity to human development, external fertilization, ease of genetic manipulation, and accessibility to high throughput approaches) have made zebrafish integral to studies of the etiology of congenital heart defects. Zebrafish models do have their limitations, for example, a lack of a pulmonary system. The relevance of zebrafish to modeling CHD thus relies on an experimental design that minimizes these limitations and maximizes its advantages. For example, recent advances in genome editing which facilitate knock-in approaches are now allowing for a comprehensive examination of disease alleles in a physiologically relevant context.

One exciting avenue of future research in zebrafish will be investigations which consider the multifaceted nature of congenital heart defects. For example, significant crosstalk occurs between different cardiac systems such as between systems underlying myocardial contraction and conduction [260] or between hemodynamics and gene expression [146]. Understanding the connections between these processes will be crucial to understanding disease progression. Additionally, the limited number of patients whose congenital heart defects can be explained by individual factors [2, 332] suggests that the etiology of the majority of CHDs may be multidimensional. For example, while a single disease allele may not be enough to cause a change to heart development, the combination of multiple subphenotypic disease alleles may lead to CHDs [333]. Due to its high fecundity, zebrafish is an ideal model organism in which to examine multi-allelic interactions. Finally, zebrafish is an excellent model organism in which to examine the

interaction between genetic and environmental factors underlying CHDs. Similar to the multi-genic hypothesis, the interaction of environmental and genetic variables may help to explain both the origin of CHDs and the variable outcomes of inherited forms of CHD. In the long term, the use of zebrafish to elucidate the molecular and cellular etiology of CHDs is likely to be invaluable to our understanding of cardiac development and disease pathogenesis and to preclinical drug discovery for therapeutic interventions and diagnostics.

Acknowledgments We would like to thank members of the Bloomekatz and Willett laboratories, as well as M. Jekabsons, N. Chi, A. Houk, E. Perens, K. Willett, and our reviewers for valuable feedback. We apologize to the authors whose papers we could not reference due to space constraints.

Competing Interests: Authors declare no conflicts of interest.

Funding: J. Bloomekatz is supported by an American Heart Association Grant (18CDA34080195).

References

- Jauhar S. Heart: a history, first edit. New York: Farrar, Straus and Giroux; 2018.
- Pierpont ME, Brueckner M, Chung WK, et al. Genetic basis for congenital heart disease: revisited: a scientific statement from the American Heart Association. *Circulation*. 2018;138:e653–711.
- Hoffman JIE, Kaplan S. The incidence of congenital heart disease. *J Am Coll Cardiol*. 2002;39:1890–900.
- Chaix MA, Andelfinger G, Khairy P. Genetic testing in congenital heart disease: a clinical approach. *World J Cardiol*. 2016;8:180.
- McKenna WJ, Maron BJ, Thiene G. Classification, epidemiology, and global burden of cardiomyopathies. *Circul Res*. 2017;121:722–30.
- Shih Y-H, Zhang Y, Ding Y, Ross CA, Li H, Olson TM, Xu X. Cardiac transcriptome and dilated cardiomyopathy genes in zebrafish. *Circul Cardiovasc Genet*. 2015;8:261–9.
- Barbazuk WB, Korf I, Kadavi C, Heyen J, Tate S, Wun E, Bedell JA, McPherson JD, Johnson SL. The syntenic relationship of the zebrafish and human genomes. *Genome Res*. 2000;10:1351–8.
- Howe K, Clark MD, Torroja CF, et al. The zebrafish reference genome sequence and its relationship to the human genome. *Nature*. 2013;496:498–503.
- Jenkins KJ, Correa A, Feinstein JA, Botto L, Britt AE, Daniels SR, Elixson M, Warnes CA, Webb CL. Noninherited risk factors and congenital cardiovascular defects: current knowledge a scientific statement from the American Heart Association Council on Cardiovascular Disease in the Young. *Circulation*. 2007;115:2995–3014.
- Moreau JLM, Kesteven S, Martin EMMA, et al. Gene-environment interaction impacts on heart development and embryo survival. *Development*. 2019;146:dev172957.
- Peal DS, Lynch SN, Milan DJ. Patterning and development of the atrioventricular canal in zebrafish. *J Cardiovasc Transl Res*. 2011;4:720–6.
- Dvornikov AV, de Tombe PP, Xu X. Phenotyping cardiomyopathy in adult zebrafish. *Prog Biophys Mol Biol*. 2018;138:116–25.
- Gut P, Reischauer S, Stainier DYR, Arnaout R. Little fish, big data: zebrafish as a model for cardiovascular and metabolic disease. *Physiol Rev*. 2017;97:889–938.
- Grant MG, Patterson VL, Grimes DT, Burdine RD. Modeling syndromic congenital heart defects in zebrafish. *Curr Top Dev Biol*. 2017;127:1–40.
- Giardoglou P, Beis D. On zebrafish disease models and matters of the heart. *Biomedicines*. 2019;7:15.
- Paolini A, Abdelilah-Seyfried S. The mechanobiology of zebrafish cardiac valve leaflet formation. *Curr Opin Cell Biol*. 2018;55:52–8.
- Sarmah S, Marrs J. Zebrafish as a vertebrate model system to evaluate effects of environmental toxicants on cardiac development and function. *Int J Mol Sci*. 2016;17:2123.
- Tu S, Chi NC. Zebrafish models in cardiac development and congenital heart birth defects. *Differentiation*. 2012;84:4–16.
- Vornanen M, Hassinen M. Zebrafish heart as a model for human cardiac electrophysiology. *Channels*. 2016;10:101–10.
- Chi NC, Shaw RM, Jungblut B, et al. Genetic and physiologic dissection of the vertebrate cardiac conduction system. *PLoS Biol*. 2008;6:e109.
- Arrenberg AB, Stainier DYR, Baier H, Huysken J. Optogenetic control of cardiac function. *Science*. 2010;330:971–4.
- Stoyek MR, Croll RP, Smith FM. Intrinsic and extrinsic innervation of the heart in zebrafish (*Danio rerio*). *J Comp Neurol*. 2015;523:1683–700.
- Singleman C, Holtzman NG. Analysis of postembryonic heart development and maturation in the zebrafish, *Danio rerio*. *Dev Dyn*. 2012;241:1993–2004.
- Hu N, Sedmera D, Yost HJ, Clark EB. Structure and function of the developing zebrafish heart. *Anat Rec*. 2000;260:148–57.
- Menke AL, Spitsbergen JM, Wolterbeek APM, Woutersen RA. Normal anatomy and histology of the adult zebrafish. *Toxicol Pathol*. 2011;39:759–75.
- Wills AA, Holdway JE, Major RJ, Poss KD. Regulated addition of new myocardial and epicardial cells fosters homeostatic cardiac growth and maintenance in adult zebrafish. *Development*. 2008;135:183–92.
- Bergmann O, Zdunek S, Felker A, et al. Dynamics of cell generation and turnover in the human heart. *Cell*. 2015;161:1566–75.

28. Walsh S, Pontén A, Fleischmann BK, Jovinge S. Cardiomyocyte cell cycle control and growth estimation in vivo—an analysis based on cardiomyocyte nuclei. *Cardiovasc Res.* 2010;86:365–73.
29. Poss KD, Wilson LG, Keating MT. Heart regeneration in zebrafish. *Science.* 2002;298:2188–90.
30. Porrello ER, Mahmoud AI, Simpson E, Hill JA, Richardson JA, Olson EN, Sadek HA. Transient regenerative potential of the neonatal mouse heart. *Science.* 2011;331:1078–80.
31. Tzahor E, Poss KD. Cardiac regeneration strategies: staying young at heart. *Science.* 2017;356:1035–9.
32. Chen C-H, Poss KD. Regeneration genetics. *Annu Rev Genet.* 2017;51:63–82.
33. González-Rosa JM, Burns CE, Burns CG. Zebrafish heart regeneration: 15 years of discoveries. *Regeneration.* 2017;4:105–23.
34. Rubin N, Harrison MR, Krainock M, Kim R, Lien C-L. Recent advancements in understanding endogenous heart regeneration—insights from adult zebrafish and neonatal mice. *Semin Cell Dev Biol.* 2016;58:34–40.
35. Kikuchi K. Dedifferentiation, transdifferentiation, and proliferation: mechanisms underlying cardiac muscle regeneration in zebrafish. *Curr Pathobiol Rep.* 2015;3:81–8.
36. Evans SM, Yelon D, Conlon FL, Kirby ML. Myocardial lineage development. *Circul Res.* 2010;107:1428–44.
37. Stainier DY, Lee RK, Fishman MC. Cardiovascular development in the zebrafish. I. Myocardial fate map and heart tube formation. *Development.* 1993;119:31–40.
38. Warga RM, Nüsslein-Volhard C. Origin and development of the zebrafish endoderm. *Development.* 1999;126:827–38.
39. Keegan BR, Meyer D, Yelon D. Organization of cardiac chamber progenitors in the zebrafish blastula. *Development.* 2004;131:3081–91.
40. Parameswaran M, Tam PPL. Regionalisation of cell fate and morphogenetic movement of the mesoderm during mouse gastrulation. *Dev Genet.* 1995;17:16–28.
41. Tam PP, Parameswaran M, Kinder SJ, Weinberger RP. The allocation of epiblast cells to the embryonic heart and other mesodermal lineages: the role of ingression and tissue movement during gastrulation. *Development.* 1997;124:1631–42.
42. Bloomekatz J, Singh R, Prall OW, Dunn AC, Vaughan M, Loo C-S, Harvey RP, Yelon D. Platelet-derived growth factor (PDGF) signaling directs cardiomyocyte movement toward the midline during heart tube assembly. *eLife.* 2017;6:e21172.
43. Schumacher JA, Bloomekatz J, Garavito-Aguilar ZV, Yelon D. *tal1* regulates the formation of intercellular junctions and the maintenance of identity in the endocardium. *Dev Biol.* 2013;383:214–26.
44. Holtzman NG, Schoenebeck JJ, Tsai H-J, Yelon D. Endocardium is necessary for cardiomyocyte movement during heart tube assembly. *Development.* 2007;134:2379–86.
45. Bussmann J, Bakkens J, Schulte-Merker S. Early endocardial morphogenesis requires *Scf/Tal1*. *PLoS Genet.* 2007;3:e140.
46. Kupperman E, An S, Osborne N, Waldron S, Stainier DYR. A sphingosine-1-phosphate receptor regulates cell migration during vertebrate heart development. *Nature.* 2000;406:192–5.
47. Rohr S, Otten C, Abdelilah-Seyfried S. Asymmetric involution of the myocardial field drives heart tube formation in zebrafish. *Circul Res.* 2008;102(2):e12–9.
48. Cui C, Chevront TJ, Lansford RD, Moreno-Rodriguez RA, Schultheiss TM, Rongish BJ. Dynamic positional fate map of the primary heart-forming region. *Dev Biol.* 2009;332:212–22.
49. Van Vliet P, Wu SM, Zaffran S, Puceat M. Early cardiac development: a view from stem cells to embryos. *Cardiovasc Res.* 2012;96:352–62.
50. Ivanovitch K, Temiño S, Torres M. Live imaging of heart tube development in mouse reveals alternating phases of cardiac differentiation and morphogenesis. *eLife.* 2017;6:e30668.
51. Desgrange A, Le Garrec J-F, Meilhac SM. Left-right asymmetry in heart development and disease: forming the right loop. *Development.* 2018;145:dev162776.
52. Baker K, Holtzman NG, Burdine RD. Direct and indirect roles for Nodal signaling in two axis conversions during asymmetric morphogenesis of the zebrafish heart. *Proc Natl Acad Sci U S A.* 2008;105:13924–9.
53. Auman HJ, Coleman H, Riley HE, Olale F, Tsai H-J, Yelon D. Functional modulation of cardiac form through regionally confined cell shape changes. *PLoS Biol.* 2007;5:e53.
54. Dietrich A-C, Lombardo VA, Veerkamp J, Priller F, Abdelilah-Seyfried S. Blood flow and *bmp* signaling control endocardial chamber morphogenesis. *Dev Cell.* 2014;30:367–77.
55. de Pater E, Clijsters L, Marques SR, Lin Y-F, Garavito-Aguilar ZV, Yelon D, Bakkens J. Distinct phases of cardiomyocyte differentiation regulate growth of the zebrafish heart. *Development.* 2009;136:1633–41.
56. Zhou Y, Cashman TJ, Nevis KR, et al. Latent TGF- β binding protein 3 identifies a second heart field in zebrafish. *Nature.* 2011;474:645–8.
57. Hami D, Grimes AC, Tsai H-J, Kirby ML. Zebrafish cardiac development requires a conserved secondary heart field. *Development.* 2011;138:2389–98.
58. Waldo KL, Kumiski DH, Wallis KT, Stadt HA, Hutson MR, Platt DH, Kirby ML. Conotruncal myocardium arises from a secondary heart field. *Development.* 2001;128:3179–88.
59. Mjaatvedt CH, Nakaoka T, Moreno-Rodriguez R, Norris RA, Kern MJ, Eisenberg CA, Turner D, Markwald RR. The outflow tract of the heart is

- recruited from a novel heart-forming field. *Dev Biol.* 2001;238:97–109.
60. Kelly RG, Brown NA, Buckingham ME. The arterial pole of the mouse heart forms from Fgf10-expressing cells in pharyngeal mesoderm. *Dev Cell.* 2001;1:435–40.
 61. Liu J, Bressan M, Hassel D, Huisken J, Staudt D, Kikuchi K, Poss KD, Mikawa T, Stainier DYR. A dual role for ErbB2 signaling in cardiac trabeculation. *Development.* 2010;137:3867–75.
 62. Samsa LA, Yang B, Liu J. Embryonic cardiac chamber maturation: trabeculation, conduction, and cardiomyocyte proliferation. *Am J Med Genet C Semin Med Genet.* 2013;163:157–68.
 63. Ben-Shachar G, Arcilla RA, Lucas RV, Manasek FJ. Ventricular trabeculations in the chick embryo heart and their contribution to ventricular and muscular septal development. *Circul Res.* 1985;57:759–66.
 64. Han P, Bloomekatz J, Ren J, Zhang R, Grinstein JD, Zhao L, Burns CG, Burns CE, Anderson RM, Chi NC. Coordinating cardiomyocyte interactions to direct ventricular chamber morphogenesis. *Nature.* 2016;534:700–4.
 65. Steed E, Faggianelli N, Roth S, Rampsacher C, Concordet JP, Vermot J. Klf2a couples mechanotransduction and zebrafish valve morphogenesis through fibronectin synthesis. *Nat Commun.* 2016;7:11646.
 66. Boselli F, Steed E, Freund JB, Vermot J. Anisotropic shear stress patterns predict the orientation of convergent tissue movements in the embryonic heart. *Development.* 2017;144:4322–7.
 67. Gunawan F, Gentile A, Fukuda R, Tsegede AT, Jiménez-Amilburu V, Ramadass R, Iida A, Sehara-Fujisawa A, Stainier DYR. Focal adhesions are essential to drive zebrafish heart valve morphogenesis. *J Cell Biol.* 2019. jcb.201807175.
 68. Pestel J, Ramadass R, Gauvrit S, Helker C, Herzog W, Stainier DYR. Real-time 3D visualization of cellular rearrangements during cardiac valve formation. *Development.* 2016;143:2217–27.
 69. Chi NC, Shaw RM, De Val S, Kang G, Jan LY, Black BL, Stainier DYR. Foxn4 directly regulates tbx2b expression and atrioventricular canal formation. *Genes Dev.* 2008;22:734–9.
 70. Martin RT, Bartman T. Analysis of heart valve development in larval zebrafish. *Dev Dyn.* 2009; 238:1796–802.
 71. Combs MD, Yutzey KE. Heart valve development: regulatory networks in development and disease. *Circul Res.* 2009;105:408–21.
 72. Houk AR, Yelon D. Strategies for analyzing cardiac phenotypes in the zebrafish embryo. *Methods Cell Biol.* 2016;134:335–68.
 73. Liu J, Stainier DYR. Zebrafish in the study of early cardiac development. *Circul Res.* 2012;110:870–4.
 74. Sidhwani P, Yelon D. Fluid forces shape the embryonic heart: insights from zebrafish. *Curr Top Dev Biol.* 2019;132:395–416.
 75. Cao Y, Cao J. Covering and re-covering the heart: development and regeneration of the epicardium. *J Cardiovasc Dev Dis.* 2018;6:3.
 76. Kapuria S, Yoshida T, Lien C-L. Coronary vasculature in cardiac development and regeneration. *J Cardiovasc Dev Dis.* 2018;5:59.
 77. Knight HG, Yelon D. Utilizing zebrafish to understand second heart field development. In: Nakanishi T, Markwald RR, Baldwin HS, Keller BB, Srivastava D, Yamagishi H, eds. *Etiology and Morphogenesis of Congenital Heart Disease: From Gene Function and Cellular Interaction to Morphology.* Tokyo: Springer; 2016. p.193–9.
 78. Burkhard S, van Eif V, Garric L, Christoffels V, Bakkens J. On the evolution of the cardiac pacemaker. *J Cardiovasc Dev Dis.* 2017;4:4.
 79. Collins MM, Stainier DYR. Organ function as a modulator of organ formation. *Curr Top Dev Biol.* 2016;117:417–33.
 80. Foglia MJ, Poss KD. Building and re-building the heart by cardiomyocyte proliferation. *Development.* 2016;143:729–40.
 81. Steed E, Boselli F, Vermot J. Hemodynamics driven cardiac valve morphogenesis. *Biochim Biophys Acta.* 2016;1863:1760–6.
 82. Pelster B, Burggren WW. Disruption of hemoglobin oxygen transport does not impact oxygen-dependent physiological processes in developing embryos of zebra fish (*Danio rerio*). *Circul Res.* 1996;79:358–62.
 83. Papaioannou VE, Behringer RR. Early embryonic lethality in genetically engineered mice: diagnosis and phenotypic analysis. *Vet Pathol.* 2012;49:64–70.
 84. Fuentes R, Letelier J, Tajer B, Valdivia LE, Mullins MC. Fishing forward and reverse: advances in zebrafish phenomics. *Mech Dev.* 2018;154:296–308.
 85. Nüsslein-Volhard C, Wieschaus E. Mutations affecting segment number and polarity in *Drosophila*. *Nature.* 1980;287:795–801.
 86. Stainier DY, Fouquet B, Chen JN, et al. Mutations affecting the formation and function of the cardiovascular system in the zebrafish embryo. *Development.* 1996;123:285–92.
 87. Chen JN, Haffter P, Odenthal J, et al. Mutations affecting the cardiovascular system and other internal organs in zebrafish. *Development.* 1996;123:293–302.
 88. Knapik EW. ENU mutagenesis in zebrafish—from genes to complex diseases. *Mamm Genome.* 2000;11:511–9.
 89. Lin S, Gaiano N, Culp P, Burns JC, Friedmann T, Yee JK, Hopkins N. Integration and germ-line transmission of a pseudotyped retroviral vector in zebrafish. *Science.* 1994;265:666–9.
 90. Sivasubbu S, Balciunas D, Davidson AE, Pickart MA, Hermanson SB, Wangenstein KJ, Wolbrink DC, Ekker SC. Gene-breaking transposon mutagenesis reveals an essential role for histone H2afza in zebrafish larval development. *Mech Dev.* 2006;123:513–29.

91. Davidson AE, Balciunas D, Mohn D, Shaffer J, Hermanson S, Sivasubbu S, Cliff MP, Hackett PB, Ekker SC. Efficient gene delivery and gene expression in zebrafish using the Sleeping Beauty transposon. *Dev Biol.* 2003;263:191–202.
92. Gaiano N, Allende M, Amsterdam A, Kawakami K, Hopkins N. Highly efficient germ-line transmission of proviral insertions in zebrafish. *Proc Natl Acad Sci U S A.* 1996;93:7777–82.
93. Kawakami K, Takeda H, Kawakami N, Kobayashi M, Matsuda N, Mishina M. A transposon-mediated gene trap approach identifies developmentally regulated genes in zebrafish. *Dev Cell.* 2004;7:133–44.
94. Clark KJ, Argue DP, Petzold AM, Ekker SC. *zfishbook: connecting you to a world of zebrafish revertible mutants.* *Nucleic Acids Res.* 2012;40:D907–11.
95. Distel M, Wullimann MF, Koster RW. Optimized Gal4 genetics for permanent gene expression mapping in zebrafish. *Proc Natl Acad Sci U S A.* 2009;106:13365–70.
96. Ding Y, Liu W, Deng Y, et al. Trapping cardiac recessive mutants via expression-based insertional mutagenesis screening. *Circul Res.* 2013;112:606–17.
97. Trinh LA, Hochgreb T, Graham M, et al. A versatile gene trap to visualize and interrogate the function of the vertebrate proteome. *Genes Dev.* 2011;25:2306–20.
98. Patton EE, Zon LI. The art and design of genetic screens: zebrafish. *Nat Rev Genet.* 2001;2:956–66.
99. Stainier DYR. Zebrafish genetics and vertebrate heart formation. *Nat Rev Genet.* 2001;2:39–48.
100. Pan L, Shah AN, Phelps IG, Doherty D, Johnson EA, Moens CB. Rapid identification and recovery of ENU-induced mutations with next-generation sequencing and paired-end low-error analysis. *BMC Genomics.* 2015;16:83.
101. Obholzer N, Swinburne IA, Schwab E, Nechiporuk AV, Nicolson T, Megason SG. Rapid positional cloning of zebrafish mutations by linkage and homozygosity mapping using whole-genome sequencing. *Development.* 2012;139:4280–90.
102. Bowen ME, Henke K, Siegfried KR, Warman ML, Harris MP. Efficient mapping and cloning of mutations in zebrafish by low-coverage whole-genome sequencing. *Genetics.* 2012;190:1017–24.
103. Gaiano N, Amsterdam A, Kawakami K, Allende M, Becker T, Hopkins N. Insertional mutagenesis and rapid cloning of essential genes in zebrafish. *Nature.* 1996;383:829–32.
104. Ding Y, Long PA, Bos JM, et al. A modifier screen identifies DNAJB6 as a cardiomyopathy susceptibility gene. *JCI Insight.* 2016;2(8).
105. Pott A, Shahid M, Köhler D, Pylatiuk C, Weinmann K, Just S, Rottbauer W. Therapeutic chemical screen identifies phosphatase inhibitors to reconstitute PKB phosphorylation and cardiac contractility in ILK-deficient zebrafish. *Biomolecules.* 2018;8:153.
106. Ni TT, Rellinger EJ, Mukherjee A, et al. Discovering small molecules that promote cardiomyocyte generation by modulating Wnt signaling. *Chem Biol.* 2011;18:1658–68.
107. Peterson RT, Fishman MC. Designing zebrafish chemical screens. *Methods Cell Biol.* 2011;105:525–41.
108. Wiley DS, Redfield SE, Zon LI. Chemical screening in zebrafish for novel biological and therapeutic discovery. *Methods Cell Biol.* 2017;138:651–79.
109. Saydmohammed M, Vollmer L, Onuoha E, Maskrey T, Gibson G, Watkins S, Wipf P, Vogt A, Tsang M. A high-content screen reveals new small-molecule enhancers of Ras/Mapk signaling as probes for zebrafish heart development. *Molecules.* 2018;23:1691.
110. Liu LY, Fox CS, North TE, Goessling W. Functional validation of GWAS gene candidates for abnormal liver function during zebrafish liver development. *Dis Model Mech.* 2013;6:1271–8.
111. van Rooij FJA, Qayyum R, Smith AV, et al. Genome-wide trans-ethnic meta-analysis identifies seven genetic loci influencing erythrocyte traits and a role for RBPMS in erythropoiesis. *Am J Hum Genet.* 2017;100:51–63.
112. Eisen JS, Smith JC. Controlling morpholino experiments: don't stop making antisense. *Development.* 2008;135:1735–43.
113. Summerton J, Weller D. Morpholino antisense oligomers: design, preparation, and properties. *Antisense Nucleic Acid Drug Dev.* 1997;7:187–95.
114. Robu ME, Larson JD, Nasevicius A, Beiraghi S, Brenner C, Farber SA, Ekker SC. p53 Activation by knockdown technologies. *PLoS Genet.* 2007;3:e78.
115. Lai JKH, Galalova KK, Kuenne C, El-Brolosy MA, Stainier DYR. Induction of interferon-stimulated genes and cellular stress pathways by morpholinos in zebrafish. *Dev Biol.* 2019;454(1):21–8.
116. Kok FO, Shin M, Ni C-W, et al. Reverse genetic screening reveals poor correlation between morpholino-induced and mutant phenotypes in zebrafish. *Dev Cell.* 2015;32:97–108.
117. Hermkens DMA, van Impel A, Urasaki A, Bussmann J, Duckers HJ, Schulte-Merker S. Sox7 controls arterial specification in conjunction with hey2 and efnb2 function. *Development.* 2015;142:1695–704.
118. Stainier DYR, Raz E, Lawson ND, et al. Guidelines for morpholino use in zebrafish. *PLOS Genet.* 2017;13:e1007000.
119. Schulte-Merker S, Stainier DYR. Out with the old, in with the new: reassessing morpholino knockdowns in light of genome editing technology. *Development.* 2014;141:3103–4.
120. Gagnon JA, Valen E, Thyme SB, et al. Efficient mutagenesis by Cas9 protein-mediated oligonucleotide insertion and large-scale assessment of single-guide RNAs. *PLoS One.* 2014;9:e98186.
121. Burger A, Lindsay H, Felker A, et al. Maximizing mutagenesis with solubilized CRISPR-Cas9 ribonucleoprotein complexes. *Development.* 2016;143:2025–37.

122. Wu RS, Lam II, Clay H, Duong DN, Deo RC, Coughlin SR. A rapid method for directed gene knockout for screening in G0 zebrafish. *Dev Cell*. 2018;46:112–125.e4.
123. Hwang WY, Fu Y, Reyon D, Maeder ML, Tsai SQ, Sander JD, Peterson RT, Yeh J-RJ, Joung JK. Efficient genome editing in zebrafish using a CRISPR-Cas system. *Nat Biotechnol*. 2013;31:227–9.
124. Dahlem TJ, Hoshijima K, Juryneć MJ, Gunther D, Starker CG, Locke AS, Weis AM, Voytas DF, Grunwald DJ. Simple methods for generating and detecting locus-specific mutations induced with TALENs in the zebrafish genome. *PLoS Genet*. 2012;8:e1002861.
125. Huang P, Xiao A, Zhou M, Zhu Z, Lin S, Zhang B. Heritable gene targeting in zebrafish using customized TALENs. *Nat Biotechnol*. 2011;29:699–700.
126. Farr GH, Imani K, Pouy D, Maves L. Functional testing of a human PBX3 variant in zebrafish reveals a potential modifier role in congenital heart defects. *Dis Model Mech*. 2018;11:dmm035972.
127. Tessadori F, Roessler HI, Savelberg SMC, Chocron S, Kamel SM, Duran KJ, van Haelst MM, van Haften G, Bakkens J. Effective CRISPR/Cas9-based nucleotide editing in zebrafish to model human genetic cardiovascular disorders. *Dis Model Mech*. 2018;11:dmm035469.
128. Hoshijima K, Juryneć MJ, Grunwald DJ. Precise editing of the zebrafish genome made simple and efficient. *Dev Cell*. 2016;36:654–67.
129. Shin J, Chen J, Solnica-Krezel L. Efficient homologous recombination-mediated genome engineering in zebrafish using TALE nucleases. *Development*. 2014;141:3807–18.
130. Kimura Y, Hisano Y, Kawahara A, Higashijima S. Efficient generation of knock-in transgenic zebrafish carrying reporter/driver genes by CRISPR/Cas9-mediated genome engineering. *Sci Rep*. 2015;4:6545.
131. Auer TO, Durore K, De Cian A, Concordet J-P, Del Bene F. Highly efficient CRISPR/Cas9-mediated knock-in in zebrafish by homology-independent DNA repair. *Genome Res*. 2014;24:142–53.
132. Miura GI, Yelon D. A guide to analysis of cardiac phenotypes in the zebrafish embryo. *Methods Cell Biol*. 2011;101:161–80.
133. Siekmann AF, Standley C, Fogarty KE, Wolfe SA, Lawson ND. Chemokine signaling guides regional patterning of the first embryonic artery. *Genes Dev*. 2009;23:2272–7.
134. Kramer-Zucker AG, Wiessner S, Jensen AM, Drummond IA. Organization of the pronephric filtration apparatus in zebrafish requires Nephhrin, Podocin and the FERM domain protein Mosaic eyes. *Dev Biol*. 2005;285:316–29.
135. Incardona JP, Scholz NL. The influence of heart developmental anatomy on cardiotoxicity-based adverse outcome pathways in fish. *Aquat Toxicol*. 2016;177:515–25.
136. Sun Y, Wang Q, Fang Y, Wu C, Lu G, Chen Z. Activation of the Nkx2.5–Calr–p53 signaling pathway by hyperglycemia induces cardiac remodeling and dysfunction in adult zebrafish. *Dis Model Mech*. 2017;10:1217–27.
137. Lazic S, Scott IC. Mef2cb regulates late myocardial cell addition from a second heart field-like population of progenitors in zebrafish. *Dev Biol*. 2011;354:123–33.
138. Lin Y-F, Swinburne I, Yelon D. Multiple influences of blood flow on cardiomyocyte hypertrophy in the embryonic zebrafish heart. *Dev Biol*. 2012;362:242–53.
139. Reischauer S, Arnaout R, Ramadass R, Stainier DYR. Actin binding GFP allows 4D in vivo imaging of myofilament dynamics in the zebrafish heart and the identification of ErBB2 signaling as a remodeling factor of myofibrillar architecture. *Circul Res*. 2014;115:845–56.
140. Arnaout R, Ferrer T, Huisken J, Spitzer K, Stainier DYR, Tristani-Firouzi M, Chi NC. Zebrafish model for human long QT syndrome. *Proc Natl Acad Sci U S A*. 2007;104:11316–21.
141. Shimizu H, Schredelseker J, Huang J, et al. Mitochondrial Ca²⁺ uptake by the voltage-dependent anion channel 2 regulates cardiac rhythmicity. *eLife*. 2015;4:e04801.
142. Tsai C-T, Hsieh C-S, Chang S-N, et al. Genome-wide screening identifies a KCNIP1 copy number variant as a genetic predictor for atrial fibrillation. *Nat Commun*. 2016;7:10190.
143. Tucker NR, Dolmatova EV, Lin H, et al. Diminished *PRRX1* expression is associated with increased risk of atrial fibrillation and shortening of the cardiac action potential. *Circul Cardiovasc Genet*. 2017;10(5).
144. Tanaka Y, Hayashi K, Fujino N, et al. Functional analysis of *KCNH2* gene mutations of type 2 long QT syndrome in larval zebrafish using microscopy and electrocardiography. *Heart Vessels*. 2019;34:159–66.
145. Boselli F, Vermot J. Live imaging and modeling for shear stress quantification in the embryonic zebrafish heart. *Methods*. 2016;94:129–34.
146. Vermot J, Forouhar AS, Liebling M, Wu D, Plummer D, Gharib M, Fraser SE. Reversing blood flows act through *klf2a* to ensure normal valvulogenesis in the developing heart. *PLoS Biol*. 2009;7:e1000246.
147. Stoyek MR, Quinn TA, Croll RP, Smith FM. Zebrafish heart as a model to study the integrative autonomic control of pacemaker function. *Am J Physiol Heart Circ Physiol*. 2016;311:H676–88.
148. Liu CC, Li L, Lam YW, Siu CW, Cheng SH. Improvement of surface ECG recording in adult zebrafish reveals that the value of this model exceeds our expectation. *Sci Rep*. 2016;6:25073.
149. Wang LW, Huttner IG, Santiago CF, Kesteven SH, Yu Z-Y, Feneley MP, Fatkin D. Standardized echocardiographic assessment of cardiac function in normal adult zebrafish and heart disease models. *Dis Model Mech*. 2017;10:63–76.
150. Zhang H, Dvornikov AV, Huttner IG, Ma X, Santiago CF, Fatkin D, Xu X. A Langendorff-like system to

- quantify cardiac pump function in adult zebrafish. *Dis Model Mech*. 2018;11:dmm034819.
151. Lenning M, Fortunato J, Le T, et al. Real-time monitoring and analysis of zebrafish electrocardiogram with anomaly detection. *Sensors*. 2017;18:61.
 152. Japp AG, Gulati A, Cook SA, Cowie MR, Prasad SK. The diagnosis and evaluation of dilated cardiomyopathy. *J Am Coll Cardiol*. 2016;67:2996–3010.
 153. Maron BJ, Towbin JA, Thiene G, et al. Contemporary definitions and classification of the cardiomyopathies. *Circulation*. 2006;113:1807–16.
 154. Elliott P, Andersson B, Arbustini E, et al. Classification of the cardiomyopathies: a position statement from the European Society of Cardiology working group on myocardial and pericardial diseases. *Eur Heart J*. 2007;29:270–6.
 155. Muchtar E, Blauwet LA, Gertz MA. Restrictive cardiomyopathy: genetics, pathogenesis, clinical manifestations, diagnosis, and therapy. *Circ Res*. 2017;121:819–37.
 156. Bers D, Borlaug B. Mechanisms of cardiac contraction and relaxation. In: Zipes D, Libby P, Bonow R, Mann D, Tomaselli G, Braunwald E, editors. *Braunwald's heart disease: a textbook of cardiovascular medicine*. 11th ed. Philadelphia: Elsevier; 2019. p. 418–40.
 157. Pyle WG, Solaro RJ. At the crossroads of myocardial signaling. *Circ Res*. 2004;94:296–305.
 158. Linke WA, Hamdani N. Gigantic business. *Circ Res*. 2014;114:1052–68.
 159. Yang J, Shih Y, Xu X. Understanding cardiac sarcomere assembly with zebrafish genetics. *Anat Rec*. 2014;297:1681–93.
 160. Huang W, Zhang R, Xu X. Myofibrillogenesis in the developing zebrafish heart: a functional study of *tnnt2*. *Dev Biol*. 2009;331:237–49.
 161. Wanga J, Eckberg WR, Anderson WA. Ultrastructural differentiation of cardiomyocytes of the zebrafish during the 8–26-somite stages. *J Submicrosc Cytol Pathol*. 2001;33:275–87.
 162. McNally EM, Mestroni L. Dilated cardiomyopathy. *Circ Res*. 2017;121:731–48.
 163. Marian AJ, Braunwald E. Hypertrophic cardiomyopathy. *Circ Res*. 2017;121:749–70.
 164. Herman DS, Lam L, Taylor MRG, et al. Truncations of titin causing dilated cardiomyopathy. *N Engl J Med*. 2012;366:619–28.
 165. ZFIN. 99 ENU induced-alleles were reported to the Zebrafish Information Network (ZFIN). 2019. <http://zfin.org/>. Accessed 1 May 2019.
 166. Xu X, Meiler SE, Zhong TP, Mohideen M, Crossley DA, Burggren WW, Fishman MC. Cardiomyopathy in zebrafish due to mutation in an alternatively spliced exon of titin. *Nat Genet*. 2002;30(2):205–9.
 167. Gerull B, Gramlich M, Atherton J, et al. Mutations of *TTN*, encoding the giant muscle filament titin, cause familial dilated cardiomyopathy. *Nat Genet*. 2002;30:201–4.
 168. Seeley M, Huang W, Chen Z, Wolff WO, Lin X, Xu X. Depletion of zebrafish titin reduces cardiac contractility by disrupting the assembly of Z-discs and A-bands. *Circ Res*. 2007;100:238–45.
 169. Myhre JL, Hills JA, Prill K, Wohlgemuth SL, Pilgrim DB. The titin A-band rod domain is dispensable for initial thick filament assembly in zebrafish. *Dev Biol*. 2014;387:93–108.
 170. Steffen LS, Guyon JR, Vogel ED, Howell MH, Zhou Y, Weber GJ, Zon LI, Kunkel LM. The zebrafish *runzel* muscular dystrophy is linked to the titin gene. *Dev Biol*. 2007;309:180–92.
 171. Shih Y-H, Dvornikov AV, Zhu P, Ma X, Kim M, Ding Y, Xu X. Exon-and contraction-dependent functions of titin in sarcomere assembly. *Development*. 2016;143(24):4713–22.
 172. Weinert S, Bergmann N, Luo X, Erdmann B, Gotthardt M. M line-deficient titin causes cardiac lethality through impaired maturation of the sarcomere. *J Cell Biol*. 2006;173:559–70.
 173. Person V, Kostin S, Suzuki K, Labeit S, Schaper J. Antisense oligonucleotide experiments elucidate the essential role of titin in sarcomerogenesis in adult rat cardiomyocytes in long-term culture. *J Cell Sci*. 2000;113(Pt 21):3851–9.
 174. White J, Barro MV, Makarenkova HP, Sanger JW, Sanger JM. Localization of sarcomeric proteins during myofibril assembly in cultured mouse primary skeletal myotubes. *Anat Rec*. 2014;297:1571–84.
 175. Du A, Sanger JM, Linask KK, Sanger JW. Myofibrillogenesis in the first cardiomyocytes formed from isolated quail precardiac mesoderm. *Dev Biol*. 2003;257:382–94.
 176. Myhre JL, Pilgrim D. A titan but not necessarily a ruler: assessing the role of titin during thick filament patterning and assembly. *Anat Rec*. 2014;297:1604–14.
 177. Roberts AM, Ware JS, Herman DS, et al. Integrated allelic, transcriptional, and phenomic dissection of the cardiac effects of titin truncations in health and disease. *Sci Transl Med*. 2015;7:270ra6.
 178. Hinson JT, Chopra A, Nafissi N, et al. Titin mutations in iPS cells define sarcomere insufficiency as a cause of dilated cardiomyopathy. *Science*. 2015;349:982–6.
 179. Zou J, Tran D, Baalbaki M, et al. An internal promoter underlies the difference in disease severity between N- and C-terminal truncation mutations of titin in zebrafish. *eLife*. 2015;4:e09406.
 180. Schafer S, de Marvao A, Adami E, et al. Titin-truncating variants affect heart function in disease cohorts and the general population. *Nat Genet*. 2017;49:46–53.
 181. Wei B, Jin J-P. *TNNT1*, *TNNT2*, and *TNNT3*: isoform genes, regulation, and structure–function relationships. *Gene*. 2016;582:1–13.
 182. Sehnert AJ, Huq A, Weinstein BM, Walker C, Fishman M, Stainier DYR. Cardiac troponin T is essential in sarcomere assembly and cardiac contractility. *Nat Genet*. 2002;31:106–10.
 183. Becker JR, Deo RC, Werdich AA, Panáková D, Coy S, MacRae CA. Human cardiomyopathy mutations

- induce myocyte hyperplasia and activate hypertrophic pathways during cardiogenesis in zebrafish. *Dis Model Mech.* 2011;4:400–10.
184. Berdougou E, Coleman H, Lee DH, Stainier DYR, Yelon D. Mutation of weak atrium/atrial myosin heavy chain disrupts atrial function and influences ventricular morphogenesis in zebrafish. *Development.* 2003;130:6121–9.
 185. Somi S, Klein ATJ, Houweling AC, Ruijter JM, Buffing AAM, Moorman AFM, van den Hoff MJB. Atrial and ventricular myosin heavy-chain expression in the developing chicken heart: strengths and limitations of non-radioactive in situ hybridization. *J Histochem Cytochem.* 2006;54:649–64.
 186. Yelon D, Horne SA, Stainier DYR. Restricted expression of cardiac myosin genes reveals regulated aspects of heart tube assembly in zebrafish. *Dev Biol.* 1999;214:23–37.
 187. Kamisago M, Sharma SD, DePalma SR, et al. Mutations in sarcomere protein genes as a cause of dilated cardiomyopathy. *N Engl J Med.* 2000;343:1688–96.
 188. Thierfelder L, Watkins H, MacRae C, Lamas R, McKenna W, Vosberg HP, Seidman JG, Seidman CE. Alpha-tropomyosin and cardiac troponin T mutations cause familial hypertrophic cardiomyopathy: a disease of the sarcomere. *Cell.* 1994;77:701–12.
 189. Klaassen S, Probst S, Oechslin E, et al. Mutations in sarcomere protein genes in left ventricular noncompaction. *Circulation.* 2008;117:2893–901.
 190. Bainbridge MN, Davis EE, Choi W-Y, et al. Loss of function mutations in *NNT* are associated with left ventricular noncompaction. *Circ Cardiovasc Genet.* 2015;8:544–52.
 191. McKenna WJ. Hypertrophic cardiomyopathy: an update. *Cardiologia.* 1993;38:277–81.
 192. Watkins H, McKenna WJ, Thierfelder L, et al. Mutations in the genes for cardiac troponin T and α -tropomyosin in hypertrophic cardiomyopathy. *N Engl J Med.* 1995;332:1058–65.
 193. Carniel E, Taylor MRG, Sinagra G, et al. α -Myosin heavy chain: a sarcomeric gene associated with dilated and hypertrophic phenotypes of cardiomyopathy. *Circulation.* 2005;112:54–9.
 194. Bloomekatz J, Galvez-Santisteban M, Chi NC. Myocardial plasticity: cardiac development, regeneration and disease. *Curr Opin Genet Dev.* 2016;40:120–30.
 195. Szibor M, Pöling J, Warnecke H, Kubin T, Braun T. Remodeling and dedifferentiation of adult cardiomyocytes during disease and regeneration. *Cell Mol Life Sci.* 2014;71:1907–16.
 196. Peshkovsky C, Totong R, Yelon D. Dependence of cardiac trabeculation on neuregulin signaling and blood flow in zebrafish. *Dev Dyn.* 2011;240:446–56.
 197. Samsa LA, Givens C, Tzima E, Stainier DYR, Qian L, Liu J. Cardiac contraction activates endocardial Notch signaling to modulate chamber maturation in zebrafish. *Development.* 2015;142:4080–91.
 198. Bartman T, Walsh EC, Wen K-K, McKane M, Ren J, Alexander J, Rubenstein PA, Stainier DYR. Early myocardial function affects endocardial cushion development in zebrafish. *PLoS Biol.* 2004;2:e129.
 199. Hove JR, Köster RW, Forouhar AS, Acevedo-Bolton G, Fraser SE, Gharib M. Intracardiac fluid forces are an essential epigenetic factor for embryonic cardiogenesis. *Nature.* 2003;421:172–7.
 200. Peralta M, Steed E, Harlepp S, et al. Heartbeat-driven pericardiac fluid forces contribute to epicardium morphogenesis. *Curr Biol.* 2013;23:1726–35.
 201. Hassel D, Dahme T, Erdmann J, et al. Nexilin mutations destabilize cardiac Z-disks and lead to dilated cardiomyopathy. *Nat Med.* 2009;15:1281–8.
 202. Dhandapany PS, Razzaque MA, Muthusami U, et al. RAF1 mutations in childhood-onset dilated cardiomyopathy. *Nat Genet.* 2014;46:635–9.
 203. Schönberger J, Wang L, Shin JT, et al. Mutation in the transcriptional coactivator EYA4 causes dilated cardiomyopathy and sensorineural hearing loss. *Nat Genet.* 2005;37(4):418–22.
 204. Zhang R, Yang J, Zhu J, Xu X. Depletion of zebrafish Tcap leads to muscular dystrophy via disrupting sarcomere-membrane interaction, not sarcomere assembly. *Hum Mol Genet.* 2009;18:4130–40.
 205. Glenn NO, McKane M, Kohli V, Wen K-K, Rubenstein PA, Bartman T, Sumanas S. The W-loop of alpha-cardiac actin is critical for heart function and endocardial cushion morphogenesis in zebrafish. *Mol Cell Biol.* 2012;32(17):3527–40.
 206. Knöll R, Postel R, Wang J, et al. Laminin-4 and integrin-linked kinase mutations cause human cardiomyopathy via simultaneous defects in cardiomyocytes and endothelial cells. *Circulation.* 2007;116(5):515–25.
 207. Hodatsu A, Konno T, Hayashi K, Funada A, Fujita T, Nagata Y, Fujino N, Kawashiri M-A, Yamagishi M. Compound heterozygosity deteriorates phenotypes of hypertrophic cardiomyopathy with founder MYBPC3 mutation: evidence from patients and zebrafish models. *Am J Physiol Heart Circ Physiol.* 2014;307:1594–604.
 208. Russell MW, Raeker MO, Geisler SB, Thomas PE, Simmons TA, Bernat JA, Thorsson T, Innis JW. Functional analysis of candidate genes in 2q13 deletion syndrome implicates FBLN7 and TMEM87B deficiency in congenital heart defects and FBLN7 in craniofacial malformations. *Hum Mol Genet.* 2014;23:4272–84.
 209. van Weerd JH, Christoffels VM. The formation and function of the cardiac conduction system. *Development.* 2016;143:197–210.
 210. Sedmera D, Reckova M, deAlmeida A, et al. Functional and morphological evidence for a ventricular conduction system in zebrafish and *Xenopus* hearts. *Am J Physiol Heart Circ Physiol.* 2003;284:H1152–60.
 211. Guyton A, Hall J. *Textbook of medical physiology.* 11th ed. Philadelphia: Elsevier; 2006.

212. Bernstein S. *Biology of the laboratory mouse*. 2nd ed. New York: Dover Publications; 1966.
213. Bogue MA, Grubb SC, Walton DO, et al. Mouse Phenome Database: an integrative database and analysis suite for curated empirical phenotype data from laboratory mice. *Nucleic Acids Res*. 2018;46:D843–50.
214. Brette F, Luxan G, Cros C, Dixey H, Wilson C, Shiels HA. Characterization of isolated ventricular myocytes from adult zebrafish (*Danio rerio*). *Biochem Biophys Res Commun*. 2008;374:143–6.
215. Tse G, Chan YWF, Keung W, Yan BP. Electrophysiological mechanisms of long and short QT syndromes. *IJC Heart Vascul*. 2017;14:8–13.
216. Marsman RF, Tan HL, Bezzina CR. Genetics of sudden cardiac death caused by ventricular arrhythmias. *Nat Rev Cardiol*. 2014;11:96–111.
217. Ball J, Carrington MJ, McMurray JJV, Stewart S. Atrial fibrillation: profile and burden of an evolving epidemic in the 21st century. *Int J Cardiol*. 2013;167:1807–24.
218. Rautaharju PM, Surawicz B, Gettes LS, et al. AHA/ACCF/HRS recommendations for the standardization and interpretation of the electrocardiogram. *J Am Coll Cardiol*. 2009;53:982–91.
219. Schwartz PJ, Stramba-Badiale M, Crotti L, et al. Prevalence of the congenital long-QT syndrome. *Circulation*. 2009;120:1761–7.
220. Grant AO. Cardiac ion channels. *Circ Arrhythm Electrophysiol*. 2009;2:185–94.
221. Splawski I, Shen J, Timothy KW, et al. Spectrum of mutations in long-QT syndrome genes. *Circulation*. 2000;102:1178–85.
222. Langheinrich U, Vacun G, Wagner T. Zebrafish embryos express an orthologue of HERG and are sensitive toward a range of QT-prolonging drugs inducing severe arrhythmia. *Toxicol Appl Pharmacol*. 2003;193:370–82.
223. Beis D, Bartman T, Jin S-W, et al. Genetic and cellular analyses of zebrafish atrioventricular cushion and valve development. *Development*. 2005;132:4193–204.
224. Meder B, Scholz EP, Hassel D, Wolff C, Just S, Berger IM, Patzel E, Karle C, Katus HA, Rottbauer W. Reconstitution of defective protein trafficking rescues long-QT syndrome in zebrafish. *Biochem Biophys Res Commun*. 2011;408:218–24.
225. Roder K, Werdich AA, Li W, et al. RING finger protein RNF207, a novel regulator of cardiac excitation. *J Biol Chem*. 2014;289:33730–40.
226. Nakano Y, Shimizu W. Genetics of long-QT syndrome. *J Hum Genet*. 2016;61:51–5.
227. Mazzanti A, Kanthan A, Monteforte N, et al. Novel insight into the natural history of short QT syndrome. *J Am Coll Cardiol*. 2014;63:1300–8.
228. Rudic B, Schimpf R, Borggrefe M. Short QT syndrome—review of diagnosis and treatment. *Arrhythm Electrophysiol Rev*. 2014;3:76.
229. Brugada R, Hong K, Dumaine R, et al. Sudden death associated with short-QT syndrome linked to mutations in HERG. *Circulation*. 2004;109:30–5.
230. Hassel D, Scholz EP, Trano N, et al. Deficient zebrafish ether-à-go-go-related gene channel gating causes short-QT syndrome in zebrafish *reggae* mutants. *Circulation*. 2008;117:866–75.
231. Zhang YH, Colenso CK, Sessions RB, Dempsey CE, Hancox JC. The hERG K(+) channel S4 domain L532P mutation: characterization at 37°C. *Biochim Biophys Acta*. 2011;1808:2477–87.
232. Jou CJ, Barnett SM, Bian J-T, Weng HC, Sheng X, Tristani-Firouzi M. An in vivo cardiac assay to determine the functional consequences of putative long QT syndrome mutations. *Circ Res*. 2013;112:826–30.
233. Jaiswal A, Goldbarg S. Dofetilide induced torsade de pointes: mechanism, risk factors and management strategies. *Indian Heart J*. 2014;66:640–8.
234. Milan DJ, Kim AM, Winterfield JR, et al. Drug-sensitized zebrafish screen identifies multiple genes, including GINS3, as regulators of myocardial repolarization. *Circulation*. 2009;120:553–9.
235. Chang YP, Wang G, Bermudez V, Hurwitz J, Chen XS. Crystal structure of the GINS complex and functional insights into its role in DNA replication. *Proc Natl Acad Sci U S A*. 2007;104:12685–90.
236. De Falco M, Ferrari E, De Felice M, Rossi M, Hübscher U, Pisani FM. The human GINS complex binds to and specifically stimulates human DNA polymerase α -primase. *EMBO Rep*. 2007;8:99–103.
237. Peal DS, Mills RW, Lynch SN, Mosley JM, Lim E, Ellinor PT, January CT, Peterson RT, Milan DJ. Novel chemical suppressors of long QT syndrome identified by an in vivo functional screen. *Circulation*. 2011;123:23–30.
238. Sanguinetti MC, Curran ME, Zou A, Shen J, Specter PS, Atkinson DL, Keating MT. Coassembly of KVLQT1 and minK (IsK) proteins to form cardiac IKs potassium channel. *Nature*. 1996;384:80–3.
239. Hedley PL, Jørgensen P, Schlamowitz S, Wangari R, Moolman-Smook J, Brink PA, Kanters JK, Corfield VA, Christiansen M. The genetic basis of long QT and short QT syndromes: a mutation update. *Hum Mutat*. 2009;30:1486–511.
240. Barhanin J, Lesage F, Guillemare E, Fink M, Lazdunski M, Romey G. KvLQT1 and IsK (minK) proteins associate to form the IKs cardiac potassium current. *Nature*. 1996;384:78–80.
241. Benz A, Kossack M, Auth D, Seyler C, Zitron E, Juergensen L, Katus HA, Hassel D. miR-19b regulates ventricular action potential duration in zebrafish. *Sci Rep*. 2016;6:36033.
242. Eisner D, Bode E, Venetucci L, Trafford A. Calcium flux balance in the heart. *J Mol Cell Cardiol*. 2013;58:110–7.
243. Rottbauer W, Baker K, Wo ZG, Mohideen M-APK, Cantiello HF, Fishman MC. Growth and function of the embryonic heart depend upon the cardiac-

- specific L-type calcium channel $\alpha 1$ subunit. *Dev Cell*. 2001;1:265–75.
244. Andersen ND, Ramachandran KV, Bao MM, Kirby ML, Pitt GS, Hutson MR. Calcium signaling regulates ventricular hypertrophy during development independent of contraction or blood flow. *J Mol Cell Cardiol*. 2015;80:1–9.
 245. Langenbacher AD, Dong Y, Shu X, Choi J, Nicoll DA, Goldhaber JI, Philipson KD, Chen J-N. Mutation in sodium-calcium exchanger 1 (NCX1) causes cardiac fibrillation in zebrafish. *Proc Natl Acad Sci U S A*. 2005;102:17699–704.
 246. Ebert AM, Hume GL, Warren KS, Cook NP, Burns CG, Mohideen MA, Siegal G, Yelon D, Fishman MC, Garrity DM. Calcium extrusion is critical for cardiac morphogenesis and rhythm in embryonic zebrafish hearts. *Proc Natl Acad Sci U S A*. 2005;102:17705–10.
 247. Shimizu H, Langenbacher AD, Huang J, Wang K, Otto G, Geisler R, Wang Y, Chen J-N. The Calcineurin-FoxO-MuRF1 signaling pathway regulates myofibril integrity in cardiomyocytes. *eLife*. 2017;6:e27955.
 248. Naghdi S, Hajnóczky G. VDAC2-specific cellular functions and the underlying structure. *Biochim Biophys Acta*. 2016;1863:2503–14.
 249. Panáková D, Werdich AA, Macrae CA. Wnt11 patterns a myocardial electrical gradient through regulation of the L-type Ca(2+) channel. *Nature*. 2010;466:874–8.
 250. Tysler RC, Miranda AM, Chen C, Davidson SM, Srinivas S, Riley PR. Calcium handling precedes cardiac differentiation to initiate the first heartbeat. *eLife*. 2016;5:e17113.
 251. Corrado D, Link MS, Calkins H. Arrhythmogenic right ventricular cardiomyopathy. *N Engl J Med*. 2017;376:61–72.
 252. Bennett RG, Haqqani HM, Berruezo A, Della Bella P, Marchlinski FE, Hsu C-J, Kumar S. Arrhythmogenic cardiomyopathy in 2018–2019: ARVC/ALVC or both? *Heart Lung Circ*. 2019;28:164–77.
 253. McKoy G, Protonotarios N, Crosby A, Tsatsopoulou A, Anastasakis A, Coonar A, Norman M, Baboonian C, Jeffery S, McKenna WJ. Identification of a deletion in plakoglobin in arrhythmogenic right ventricular cardiomyopathy with palmoplantar keratoderma and woolly hair (Naxos disease). *Lancet*. 2000;355:2119–24.
 254. Acehan D, Petzold C, Gumper I, Sabatini DD, Müller EJ, Cowin P, Stokes DL. Plakoglobin is required for effective intermediate filament anchorage to desmosomes. *J Invest Dermatol*. 2008;128:2665–75.
 255. Asimaki A, Kapoor S, Plovie E, et al. Identification of a new modulator of the intercalated disc in a zebrafish model of arrhythmogenic cardiomyopathy. *Sci Transl Med*. 2014;6:240ra74.
 256. Christophersen IE, Ellinor PT. Genetics of atrial fibrillation: from families to genomes. *J Hum Genet*. 2016;61:61–70.
 257. Chen Y-H, Xu S-J, Bendahhou S, et al. KCNQ1 gain-of-function mutation in familial atrial fibrillation. *Science*. 2003;299:251–4.
 258. Ahlberg G, Refsgaard L, Lundegaard PR, et al. Rare truncating variants in the sarcomeric protein titin associate with familial and early-onset atrial fibrillation. *Nat Commun*. 2018;9:4316.
 259. Hodgson-Zingman DM, Karst ML, Zingman LV, Heublein DM, Darbar D, Herron KJ, Ballew JD, de Andrade M, Burnett JC, Olson TM. Atrial natriuretic peptide frameshift mutation in familial atrial fibrillation. *N Engl J Med*. 2008;359:158–65.
 260. Orr N, Arnaout R, Gula LJ, et al. A mutation in the atrial-specific myosin light chain gene (MYL4) causes familial atrial fibrillation. *Nat Commun*. 2016;7:11303.
 261. Baldacci S, Gorini F, Santoro M, Pierini A, Minichilli F, Bianchi F. Environmental and individual exposure and the risk of congenital anomalies: a review of recent epidemiological evidence. *Epidemiol Prev*. 2018;42:1–34.
 262. Oster ME, Riehle-Colarusso T, Simeone RM, Gurvitz M, Kaltman JR, McConnell M, Rosenthal GL, Honein MA. Public health science agenda for congenital heart defects: report from a Centers for Disease Control and Prevention experts meeting. *J Am Heart Assoc*. 2013;2(5):e000256.
 263. Nicoll R, Nicoll R. Environmental contaminants and congenital heart defects: a re-evaluation of the evidence. *Int J Environ Res Public Health*. 2018;15:2096.
 264. Simeone RM, Devine OJ, Marcinkevage JA, Gilboa SM, Razzaghi H, Bardenheier BH, Sharma AJ, Honein MA. Diabetes and congenital heart defects: a systematic review, meta-analysis, and modeling project. *Am J Prev Med*. 2015;48:195–204.
 265. Stingone JA, Luben TJ, Daniels JL, et al. Maternal exposure to criteria air pollutants and congenital heart defects in offspring: results from the national birth defects prevention study. *Environ Health Perspect*. 2014;122:863–72.
 266. Browne ML, Van Zutphen AR, Botto LD, Louik C, Richardson S, Druschel CM. Maternal butalbital use and selected defects in the national birth defects prevention study. *Headache*. 2014;54:54–66.
 267. Dunwoodie SL. The role of hypoxia in development of the mammalian embryo. *Dev Cell*. 2009;17:755–73.
 268. Caputo C, Wood E, Jabbour L. Impact of fetal alcohol exposure on body systems: a systematic review. *Birth Defects Res C Embryo Today*. 2016;108:174–80.
 269. Manchenkov T, Pasillas MP, Haddad GG, Imam FB. Novel genes critical for hypoxic preconditioning in zebrafish are regulators of insulin and glucose metabolism. *G3*. 2015;5:1107–16.
 270. Fleming A, Alderton W. Zebrafish in pharmaceutical industry research: finding the best fit. *Drug Discovery Today Dis Model*. 2013;10:e43–50.

271. MacRae CA, Peterson RT. Zebrafish as tools for drug discovery. *Nat Rev Drug Discov.* 2015;14:721–31.
272. Liu Y, Asnani A, Zou L, et al. Visnagin protects against doxorubicin-induced cardiomyopathy through modulation of mitochondrial malate dehydrogenase. *Sci Transl Med.* 2014;6:266ra170.
273. Jin M, Xiao Z, Zhang S, Men X, Li X, Zhang B, Zhou T, Hsiao C-D, Liu K. Possible involvement of Fas/FasL-dependent apoptotic pathway in α -bisabolol induced cardiotoxicity in zebrafish embryos. *Chemosphere.* 2019;219:557–66.
274. McGee SP, Konstantinov A, Stapleton HM, Volz DC. Aryl phosphate esters within a major PentaBDE replacement product induce cardiotoxicity in developing zebrafish embryos: potential role of the aryl hydrocarbon receptor. *Toxicol Sci.* 2013;133:144–56.
275. Palpant NJ, Hofsteen P, Pabon L, Reinecke H, Murry CE. Cardiac development in zebrafish and human embryonic stem cells is inhibited by exposure to tobacco cigarettes and e-cigarettes. *PLoS One.* 2015;10:e0126259.
276. Li M, Liu X, Feng X. Cardiovascular toxicity and anxiety-like behavior induced by deltamethrin in zebrafish (*Danio rerio*) larvae. *Chemosphere.* 2019;219:155–64.
277. Ben LC, Fernandes Y, Eberhart JK. Fishing for fetal alcohol spectrum disorders: zebrafish as a model for ethanol teratogenesis. *Zebrafish.* 2016;13:391–8.
278. May PA, Gossage JP, Kalberg WO, Robinson LK, Buckley D, Manning M, Hoyme HE. Prevalence and epidemiologic characteristics of FASD from various research methods with an emphasis on recent in-school studies. *Dev Disabil Res Rev.* 2009;15:176–92.
279. Finer LB, Zolna MR. Declines in unintended pregnancy in the United States, 2008–2011. *N Engl J Med.* 2016;374:843–52.
280. Popova S, Lange S, Probst C, Parunashvili N, Rehm J. Prevalence of alcohol consumption during pregnancy and fetal alcohol spectrum disorders among the general and aboriginal populations in Canada and the United States. *Eur J Med Genet.* 2017;60:32–48.
281. Popova S, Lange S, Probst C, Gmel G, Rehm J. Estimation of national, regional, and global prevalence of alcohol use during pregnancy and fetal alcohol syndrome: a systematic review and meta-analysis. *Lancet Global Health.* 2017;5:e290–9.
282. Dawson DA, Goldstein RB, Saha TD, Grant BF. Changes in alcohol consumption: United States, 2001–2002 to 2012–2013. *Drug Alcohol Depend.* 2015;148:56–61.
283. Fernandes Y, Buckley DM, Eberhart JK. Diving into the world of alcohol teratogenesis: a review of zebrafish models of fetal alcohol spectrum disorder. *Biochem Cell Biol.* 2018;96:88–97.
284. Ben LC, Nobles RD, Eberhart JK. Developmental age strengthens barriers to ethanol accumulation in zebrafish. *Alcohol.* 2014;48:595–602.
285. Flentke GR, Klingler RH, Tanguay RL, Carvan MJ, Smith SM. An evolutionarily conserved mechanism of calcium-dependent neurotoxicity in a zebrafish model of fetal alcohol spectrum disorders. *Alcohol Clin Exp Res.* 2014;38:1255–65.
286. Sarmah S, Muralidharan P, Curtis CL, et al. Ethanol exposure disrupts extraembryonic microtubule cytoskeleton and embryonic blastomere cell adhesion, producing epiboly and gastrulation defects. *Biol Open.* 2013;2:1013–21.
287. Sarmah S, Muralidharan P, Marris JA. Embryonic ethanol exposure dysregulates BMP and Notch signaling, leading to persistent atrio-ventricular valve defects in zebrafish. *PLoS One.* 2016;11:e0161205.
288. Sarmah S, Marris JA. Embryonic ethanol exposure affects early- and late-added cardiac precursors and produces long-lasting heart chamber defects in zebrafish. *Toxics.* 2017;5:35.
289. Sarmah S, Marris JA. Complex cardiac defects after ethanol exposure during discrete cardiogenic events in zebrafish: prevention with folic acid. *Dev Dyn.* 2013;242:1184–201.
290. Bibbins-Domingo K, Grossman DC, Curry SJ, et al. Folic acid supplementation for the prevention of neural tube defects. *JAMA.* 2017;317:183.
291. Mandal PK. Dioxin: a review of its environmental effects and its aryl hydrocarbon receptor biology. *J Comp Physiol B.* 2005;175:221–30.
292. World Health Organization. Dioxins and their effects upon human health. Geneva: World Health Organization; 2014. <http://www.who.int/mediacentre/factsheets/fs225/en/>.
293. Schecter A, Birnbaum L, Ryan JJ, Constable JD. Dioxins: an overview. *Environ Res.* 2006;101:419–28.
294. Symula J, Meade J, Skea JC, Cummings L, Colquhoun JR, Dean HJ, Miccoli J. Blue-sac disease in lake ontario lake trout. *J Great Lakes Res.* 1990;16:41–52.
295. King-Heiden TC, Mehta V, Xiong KM, Lanham KA, Antkiewicz DS, Ganser A, Heideman W, Peterson RE. Reproductive and developmental toxicity of dioxin in fish. *Mol Cell Endocrinol.* 2012;354:121–38.
296. Brzuzan P, Woźny M, Dobosz S, Kuźmiński H, Luczyński MK, Góra M. Blue sac disease in larval whitefish, *Coregonus lavaretus* (L.): pathological changes in mRNA levels of CYP1A, ERalpha, and p53. *J Fish Dis.* 2007;30:169–73.
297. Van den Berg M, Birnbaum LS, Denison M, et al. The 2005 World Health Organization reevaluation of human and mammalian toxic equivalency factors for dioxins and dioxin-like compounds. *Toxicol Sci.* 2006;93:223–41.
298. Henry TR, Spitsbergen JM, Hornung MW, Abnet CC, Peterson RE. Early life stage toxicity of 2,3,7,8-tetrachlorodibenzo-p-dioxin in zebrafish (*Danio rerio*). New York: Academic Press; 1997.
299. Antkiewicz DS, Burns CG, Carney SA, Peterson RE, Heideman W. Heart malformation is an early

- response to TCDD in embryonic zebrafish. *Toxicol Sci.* 2005;84:368–77.
300. Plavicki J, Hofsteen P, Peterson RE, Heideman W. Dioxin inhibits zebrafish epicardium and pro-epicardium development. *Toxicol Sci.* 2012;131:558–67.
 301. Lanham KA, Peterson RE, Heideman W. Sensitivity to dioxin decreases as zebrafish mature. *Toxicol Sci.* 2012;127:360–70.
 302. Lanham KA, Prasch AL, Weina KM, Peterson RE, Heideman W. A dominant negative zebrafish Ahr2 partially protects developing zebrafish from dioxin toxicity. *PLoS One.* 2011;6:28020.
 303. Prasch AL, Teraoka H, Carney SA, Dong W, Hiraga T, Stegeman JJ, Heideman W, Peterson RE. Aryl hydrocarbon receptor 2 mediates 2,3,7,8-tetrachlorodibenzo-p-dioxin developmental toxicity in zebrafish. *Toxicol Sci.* 2003;76(1):138–50.
 304. Antkiewicz DS, Peterson RE, Heideman W. Blocking expression of AHR2 and ARNT1 in zebrafish larvae protects against cardiac toxicity of 2,3,7,8-tetrachlorodibenzo-p-dioxin. *Toxicol Sci.* 2006;94:175–82.
 305. Souder JP, Gorelick DA. *ahr2*, but not *ahr1a* or *ahr1b*, is required for craniofacial and fin development and TCDD-dependent cardiotoxicity in zebrafish. *Toxicol Sci.* 2019;170:25–44.
 306. Garcia GR, Bugel SM, Truong L, Spagnoli S, Tanguay RL. AHR2 required for normal behavioral responses and proper development of the skeletal and reproductive systems in zebrafish. *PLoS One.* 2018;13:e0193484.
 307. Goodale BC, La Du JK, Bisson WH, Janszen DB, Waters KM, Tanguay RL. AHR2 mutant reveals functional diversity of aryl hydrocarbon receptors in zebrafish. *PLoS One.* 2012;7:e29346.
 308. Fernandez-Salguero PM, Ward JM, Sundberg JP, Gonzalez FJ. Lesions of aryl-hydrocarbon receptor-deficient mice. *Vet Pathol.* 1997;34:605–14.
 309. Andreasen EA, Spitsbergen JM, Tanguay RL, Stegeman JJ, Heideman W, Peterson RE. Tissue-specific expression of AHR2, ARNT2, and CYP1A in zebrafish embryos and larvae: effects of developmental stage and 2,3,7,8-tetrachlorodibenzo-p-dioxin exposure. *Toxicol Sci.* 2002;68:403–19.
 310. Troxel CM, Buhler DR, Hendricks JD, Bailey GS. CYP1A induction by beta-naphthoflavone, Aroclor 1254, and 2,3,7,8-tetrachlorodibenzo-p-dioxin and its influence on aflatoxin B1 metabolism and DNA adduction in zebrafish. *Toxicol Appl Pharmacol.* 1997;146:69–78.
 311. Shen C, Zhou Y, Ruan J, Chuang Y-J, Wang C, Zuo Z. Generation of a Tg(*cyp1a*-12DRE:EGFP) transgenic zebrafish line as a rapid in vivo model for detecting dioxin-like compounds. *Aquat Toxicol.* 2018;205:174–81.
 312. Carney SA, Peterson RE, Heideman W. 2,3,7,8-Tetrachlorodibenzo-p-dioxin activation of the aryl hydrocarbon receptor/aryl hydrocarbon receptor nuclear translocator pathway causes developmental toxicity through a CYP1A-independent mechanism in zebrafish. *Mol Pharmacol.* 2004;66:512–21.
 313. Lanham KA, Plavicki J, Peterson RE, Heideman W. Cardiac myocyte-specific AHR activation phenocopies TCDD-induced toxicity in zebrafish. *Toxicol Sci.* 2014;141:141–54.
 314. Wang Q, Kurita H, Carreira V, Ko C-I, Fan Y, Zhang X, Biesiada J, Medvedovic M, Puga A. Ah receptor activation by dioxin disrupts activin, BMP, and WNT signals during the early differentiation of mouse embryonic stem cells and inhibits cardiomyocyte functions. *Toxicol Sci.* 2016;149:346–57.
 315. Thackaberry EA, Nunez BA, Ivnitcki-Steele ID, Friggins M, Walker MK. Effect of 2,3,7,8-tetrachlorodibenzo-p-dioxin on murine heart development: alteration in fetal and postnatal cardiac growth, and postnatal cardiac chronotropy. *Toxicol Sci.* 2005;88:242–9.
 316. Hofsteen P, Plavicki J, Johnson SD, Peterson RE, Heideman W. Sox9b is required for epicardium formation and plays a role in TCDD-induced heart malformation in zebrafish. *Mol Pharmacol.* 2013;84:353–60.
 317. Gawdzik JC, Yue MS, Martin NR, Elemans LMH, Lanham KA, Heideman W, Rezendes R, Baker TR, Taylor MR, Plavicki JS. *sox9b* is required in cardiomyocytes for cardiac morphogenesis and function. *Sci Rep.* 2018;8:13906.
 318. Garcia GR, Shankar P, Dunham CL, Garcia A, La Du JK, Truong L, Tilton SC, Tanguay RL. Signaling events downstream of AHR activation that contribute to toxic responses: the functional role of an AHR-dependent long noncoding RNA (*slincR*) using the zebrafish model. *Environ Health Perspect.* 2018;126:117002.
 319. Garcia GR, Goodale BC, Wiley MW, La Du JK, Hendrix DA, Tanguay RL. In vivo characterization of an AHR-dependent long noncoding RNA required for proper *Sox9b* expression. *Mol Pharmacol.* 2017;91:609–19.
 320. Poster DL, Schantz MM, Sander LC, Wise SA. Analysis of polycyclic aromatic hydrocarbons (PAHs) in environmental samples: a critical review of gas chromatographic (GC) methods. *Anal Bioanal Chem.* 2006;386:859–81.
 321. Incardona JP, Collier TK, Scholz NL. Defects in cardiac function precede morphological abnormalities in fish embryos exposed to polycyclic aromatic hydrocarbons. *Toxicol Appl Pharmacol.* 2004;196:191–205.
 322. Incardona JP, Linbo TL, Scholz NL. Cardiac toxicity of 5-ring polycyclic aromatic hydrocarbons is differentially dependent on the aryl hydrocarbon receptor 2 isoform during zebrafish development. *Toxicol Appl Pharmacol.* 2011;257(2):242–9.
 323. Nebert DW, Dalton TP, Okey AB, Gonzalez FJ. Role of aryl hydrocarbon receptor-mediated induction of the CYP1 enzymes in environmental toxicity and cancer. *J Biol Chem.* 2004;279:23847–50.

324. Jayasundara N, Van Tiem Garner L, Meyer JN, Erwin KN, Di Giulio RT. AHR2-mediated transcriptomic responses underlying the synergistic cardiac developmental toxicity of PAHs. *Toxicol Sci.* 2015;143:469–81.
325. Billiard SM, Meyer JN, Wassenberg DM, Hodson PV, Di Giulio RT. Nonadditive effects of PAHs on early vertebrate development: mechanisms and implications for risk assessment. *Toxicol Sci.* 2008;105:5–23.
326. Brette F, Machado B, Cros C, Incardona JP, Scholz NL, Block BA. Crude oil impairs cardiac excitation-contraction coupling in fish. *Science.* 2014;343:772–6.
327. Romano SN, Edwards HE, Souder JP, Ryan KJ, Cui X, Gorelick DA. G protein-coupled estrogen receptor regulates embryonic heart rate in zebrafish. *PLoS Genet.* 2017;13:e1007069.
328. Allgood OE, Hamad A, Fox J, et al. Estrogen prevents cardiac and vascular failure in the 'listless' zebrafish (*Danio rerio*) developmental model. *Gen Comp Endocrinol.* 2013;189:33–42.
329. Bugiak BJ, Weber LP. Phenotypic anchoring of gene expression after developmental exposure to aryl hydrocarbon receptor ligands in zebrafish. *Aquat Toxicol.* 2010;99:423–37.
330. Dong W, Wang L, Thornton C, Scheffler BE, Willett KL. Benzo(a)pyrene decreases brain and ovarian aromatase mRNA expression in *Fundulus heteroclitus*. *Aquat Toxicol.* 2008;88:289–300.
331. Alharthy KM, Albaqami FF, Thornton C, Corrales J, Willett KL. Mechanistic evaluation of Benzo[a]pyrene's developmental toxicities mediated by reduced Cyp19a1b activity. *Toxicol Sci.* 2017;155:135–47.
332. Cowan JR, Ware SM. Genetics and genetic testing in congenital heart disease. *Clin Perinatol.* 2015;42:373–93.
333. Deacon DC, Happe CL, Chen C, et al. Combinatorial interactions of genetic variants in human cardiomyopathy. *Nat Biomed Eng.* 2019;3:147–57.
334. Staudt D, Stainier D. Uncovering the molecular and cellular mechanisms of heart development using the zebrafish. *Annu Rev Genet.* 2012;46:397–418.
335. Roman BL, Pham VN, Lawson ND, et al. Disruption of *acvr11* increases endothelial cell number in zebrafish cranial vessels. *Development.* 2002;129:3009–19.
336. Harvey PA, Leinwand LA. The cell biology of disease: cellular mechanisms of cardiomyopathy. *J Cell Biol.* 2011;194:355–65.
337. Al-Khayat HA. Three-dimensional structure of the human myosin thick filament: clinical implications. *Glob Cardiol Sci Pract.* 2013;2013:280–302.
338. Estigoy CB, Pontén F, Odeberg J, Herbert B, Guilhaus M, Charlestone M, Ho JWK, Cameron D, dos Remedios CG. Intercalated discs: multiple proteins perform multiple functions in non-failing and failing human hearts. *Biophys Rev.* 2009;1:43–9.
339. Poon KL, Brand T. The zebrafish model system in cardiovascular research: a tiny fish with mighty prospects. *Glob Cardiol Sci Pract.* 2013;2013:9–28.
340. Dlugos CA, Rabin RA. Structural and functional effects of developmental exposure to ethanol on the zebrafish heart. *Alcohol Clin Exp Res.* 2010;34:1013–21.
341. Carney SA, Prasch AL, Heideman W, Peterson RE. Understanding dioxin developmental toxicity using the zebrafish model. *Birth Defects Res A Clin Mol Teratol.* 2006;76:7–18.
342. Zhang Y, Huang L, Wang C, Gao D, Zuo Z. Phenanthrene exposure produces cardiac defects during embryo development of zebrafish (*Danio rerio*) through activation of MMP-9. *Chemosphere.* 2013;93:1168–75.
343. Zhang Y, Wang C, Huang L, Chen R, Chen Y, Zuo Z. Low-level pyrene exposure causes cardiac toxicity in zebrafish (*Danio rerio*) embryos. *Aquat Toxicol.* 2012;114–115:119–24.
344. Huang L, Wang C, Zhang Y, Li J, Zhong Y, Zhou Y, Chen Y, Zuo Z. Benzo[a]pyrene exposure influences the cardiac development and the expression of cardiovascular relative genes in zebrafish (*Danio rerio*) embryos. *Chemosphere.* 2012;87(4):369–75.
345. Gerger CJ, Weber LP. Comparison of the acute effects of benzo-a-pyrene on adult zebrafish (*Danio rerio*) cardiorespiratory function following intraperitoneal injection versus aqueous exposure. *Aquat Toxicol.* 2015;165:19–30.

Animal Model Contributions to Congenital Metabolic Disease

9

Corinna A. Moro and Wendy Hanna-Rose

Abbreviations

BH ₄	Tetrahydrobiopterin	HEXS	Refers to the enzymatic activity of the hexosaminidase α dimers
CMD	Congenital metabolic disorder	HPRT, <i>HPRT</i>	Human hypoxanthine-guanine phosphoribosyltransferase protein and gene, respectively
ENU	Ethyl nitrosurea	Hprt, <i>Hprt</i>	Rodent hypoxanthine-guanine phosphoribosyltransferase protein and gene, respectively
ES	Embryonic stem cell	IEM	Inborn error of metabolism
GM2	G represents gangliosides, M indicates monosialic, and 2 indicates second monosialic ganglioside discovered	iPS	Induced pluripotent stem cells
HEXA, <i>HEXA</i>	Human acetylhexosaminidase α subunit protein and gene, respectively. HEXA also refers to the enzymatic activity of the hexosaminidase α/β dimer	LNS	Lesch-Nyhan syndrome
Hexa, <i>Hexa</i>	Mouse acetylhexosaminidase α subunit protein and gene, respectively	PAH, <i>PAH</i>	Human phenylalanine hydroxylase protein and gene, respectively
HEXB, <i>HEXB</i>	Human acetylhexosaminidase β subunit protein and gene, respectively. HEXB also refers to the enzymatic activity of the hexosaminidase β dimers	Pah, <i>Pah</i>	Rodent phenylalanine hydroxylase protein and gene, respectively
Hexb, <i>Hexb</i>	Mouse acetylhexosaminidase β subunit protein and gene, respectively	PAL	Phenylalanine ammonia lyase
		PEG	Polyethylene glycol
		PKU	Phenylketonuria
		SD	Sandhoff disease
		THBD	Tetrahydrobiopterin deficiency
		TSD	Tay-Sachs disease

9.1 Overview

Genetic model systems allow researchers to probe and decipher aspects of human disease, and animal models of disease are frequently specifically engineered and have been identified serendipitously as

C. A. Moro · W. Hanna-Rose (✉)
Department of Biochemistry and Molecular Biology,
The Pennsylvania State University,
University Park, PA, USA
e-mail: cam6183@psu.edu; wxx21@psu.edu

well. Animal models are useful for probing the etiology and pathophysiology of disease and are critical for effective discovery and development of novel therapeutics for rare diseases. Here we review the impact of animal model organism research in three examples of congenital metabolic disorders to highlight distinct advantages of model system research. First, we discuss phenylketonuria research where a wide variety of research fields and models came together to make impressive progress and where a nearly ideal mouse model has been central to therapeutic advancements. Second, we review advancements in Lesch-Nyhan syndrome research to illustrate the role of models that do not perfectly recapitulate human disease as well as the need for multiple models of the same disease to fully investigate human disease aspects. Finally, we highlight research on the GM2 gangliosidosis Tay-Sachs and Sandhoff disease to illustrate the important role of both engineered traditional laboratory animal models and serendipitously identified atypical models in congenital metabolic disorder research. We close with perspectives for the future for animal model research in congenital metabolic disorders.

9.2 Introduction

The history of eukaryotic cellular metabolism research is rich and the output has been fruitful. We understand core metabolism in significant detail; individual steps of metabolic pathways are elucidated and ordered, the genes encoding the required enzymatic activities are known, and those enzymatic reactions are frequently well-studied and understood biochemically and biophysically. Moreover, we have a systems-level understanding of how these core pathways operate within a vast network of highly interconnected activities. Links in this network remain unrecognized, and surprises are undoubtedly to be discovered. Nevertheless, our understanding of the vast complex of cellular metabolic reactions is extensive. In contrast, our knowledge of how perturbations in core metabolic pathways impact human development, function, and health is much more limited.

Given that life is dependent on the extensive and complicated cellular metabolic network, it is not surprising that mutations in a vast number of genes that encode metabolic enzymes cause congenital metabolic disorders (CMDs), originally coined as inborn errors of metabolism (IEM) in 1908 [1]. Recognition of the metabolic basis of disease also has a rich history. It has been almost 120 years since the first time a disease was noted to follow a Mendelian inheritance pattern [2]. Identification of the heritable material was still 50 years away and the first genetic lesion causative of a disease of Mendelian inheritance was not identified for several more decades.

CMDs arise from the absence or low residual levels of enzymatic activity, leading to buildup of substrates and decreased production of important products, which each contributes to phenotypic outcome. CMDs are individually rare but collectively common, encompassing over 1400 types of diagnoses and affecting as many as 1 in 1000 newborns, with higher incidence in some populations that have reduced genetic diversity [3]. Newborns are routinely screened for a selection of CMDs in technologically advanced countries, resulting in timely early diagnoses of most individuals in the United States with phenylketonuria (PKU) and a selection of other CMDs [4]. In contrast other CMDs are ultra-rare and are diagnosed only after genetic sequencing of patients with unique syndromes and, thus, only in a few patients worldwide [5, 6]. Many CMDs are also thought to be underdiagnosed because they often present clinically as syndromes with a wide array of symptoms in a variety of tissue and organ systems making diagnoses difficult [7, 8].

The study of congenital metabolic disease can be approached on a variety of levels. It is relatively straightforward to elucidate the effects of a mutation in an enzyme on its catalytic activity. Our mechanistic understanding of enzyme function is quite exhaustive in some cases, even permitting engineering of new activities. It is more difficult to predict network-wide metabolic effects from loss or reduction of activity in one reaction. However, advances in NMR and mass spectrometry techniques that allow simultaneous monitoring

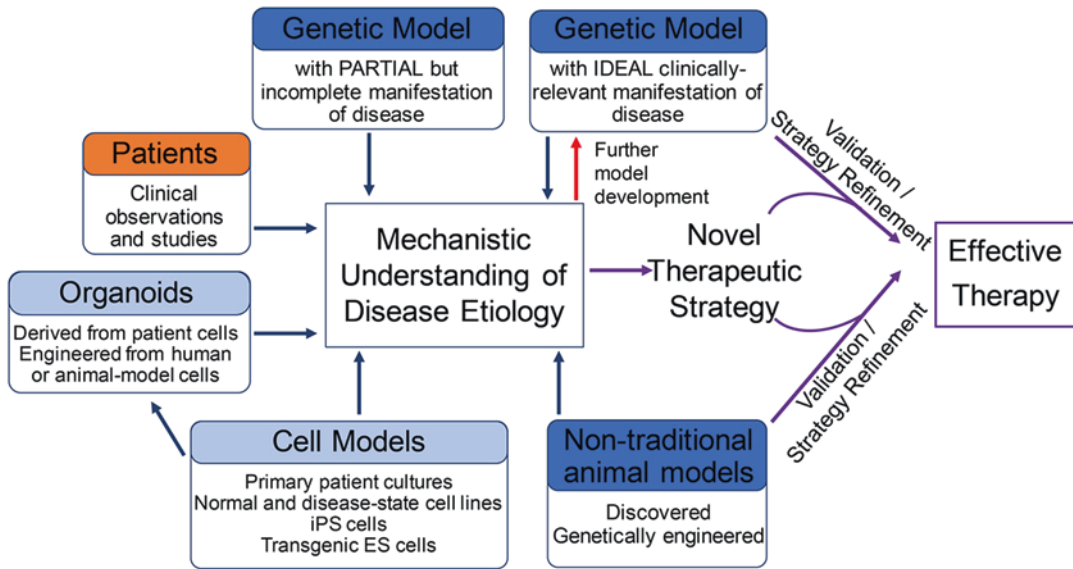


Fig. 9.1 The role of animal models in elucidating etiology and developing therapies of congenital metabolic disorders. Animal models (highlighted in dark blue) are developed in different ways, including using traditional forward genetics, standard transgenic approaches, and novel genome-editing technologies. Genome editing is facilitating development of animal models in nontraditional laboratory animals. Some model animals also arise among animals outside of laboratory environments as a result of founder mutations and reduced genetic diversity stemming from human domestica-

tion. Animal models ideally mimic human disease but often only partially recapitulate biochemical and/or phenotypic aspects of human disease. Each is useful for probing disease etiology. Research involving cell and in vitro models (highlighted in light blue) and human clinical studies (highlighted in orange) are combined with insights gained in animal models to both elucidate mechanisms of disease etiology and enhance model development (red arrow). An ideal animal model is an extremely powerful tool (purple arrows) for advanced therapeutic development

of both steady state and relative fluctuations of metabolites system-wide have made elucidation of such effects possible [9]. It is even more difficult to explain or predict the effects of a mutation in a metabolic gene in terms of phenotypic outcome in a multicellular organism where certain tissues or processes may be hypersensitive to loss of activity or specifically sensitive to toxicity of a substrate that accumulates abnormally. In fact, metabolic mutations frequently result in syndromes with a suite of seemingly unrelated phenotypes. Further confounding diagnoses and study is that environmental factors, diet in particular, may have effects on outcomes and progression and presentation of symptoms.

We have prepared a perspective to discuss examples of how the most complicated of models, both research model organisms such as mice and rats and less common models such as primates, and even domesticated animals, are contributing to the

elucidation of the etiology of clinical phenotypes and to implementation of effective therapeutic interventions for CMDs (Fig. 9.1).

9.3 Phenylketonuria

We start with a discussion of phenylketonuria (PKU, OMIM 261600). PKU is one of the most common CMDs [10]. Left untreated, it results in profound and irreversible brain damage. Dietary intervention for PKU via restriction of phenylalanine in the diet was developed in 1954, and by 1966 routine newborn screening for PKU and dietary intervention for affected infants was being implemented [11, 12]. This has led to great success in reducing the impact of PKU on patient outcomes [13]. While PKU dietary treatment is effective, it is a difficult regimen for patients and lack of compliance is common [14]. Avoiding

phenylalanine equates to avoiding protein, and patients must supplement with a phenylalanine-free protein formula to provide healthy nutritional requirements. Unfortunately, because many children and adults find the necessary formula supplement unpalatable and because dietary management is onerous for families, this treatment is less than ideal in practice.

We chose to highlight PKU because an excellent animal model was developed for PKU in the early 1990s and this model has facilitated impressive progress in development of therapies to help patients manage PKU more effectively, even allowing lenience in dietary management. PKU research already represents a major success story for the contribution of animal models to congenital metabolic disease management. Moreover, additional therapeutic options that will continue to improve the life of patients are under development with the animal model in a central role. Another reason we chose to highlight PKU is to illustrate how models beyond animals contribute to human disease research in conjunction with animal models. From genetic screens in mice, to discovery of an alternative enzymatic pathway in plants, fungi, and cyanobacteria, to investigations in nontraditional animal models, and finally, to treatments that employ prokaryotic systems, the PKU community has benefited from a wide swath of research models over many years with the mouse model as the key to many of the successes.

9.3.1 History and Prevalence

PKU is an autosomal recessive metabolic disorder characterized by high plasma levels of phenylalanine. It arises as a result of mutations in the gene encoding the enzyme phenylalanine hydroxylase (PAH), which converts phenylalanine to tyrosine [15–17]. PKU was first described by the Norwegian doctor Asbjørn Følling in 1934 [18]. A mother reported that her two children had a musty urine odor. The doctor performed a ketone test, which requires acidification of a urine sample with ferric chloride, and discovered that the children's urine turned green instead of producing the

typical reddish color. After further chemical analysis, he concluded that the green color was produced by phenylpyruvic acid, a phenylketone by-product derived from phenylalanine. PKU is found in 1 in 10,000–15,000 Caucasian births, but prevalence varies in other populations [19].

9.3.2 Clinical and Molecular Phenotypes and Alleles

PKU can manifest across a wide spectrum of severity. However, untreated classical PKU results in symptoms affecting the nervous system, including severe cognitive disability, seizures, and neurobehavioral problems. The skin is also affected with reduced levels of pigmentation and susceptibility to eczema and other skin conditions [20].

Phenylalanine is an essential amino acid that comes from dietary intake. PAH functions in the liver to metabolize phenylalanine to tyrosine. In the absence of PAH, the excessive plasma phenylalanine is transported across the blood-brain barrier, where it is neurotoxic. Additionally, the inability to produce tyrosine from phenylalanine results in a deficit of other metabolites, such as catecholamine neurotransmitters and melanin [15, 21]. Patients with PKU often have fair skin, blue eyes, and blond hair due to the inability to make melanin [21]. High levels of transport of the phenylalanine across the blood-brain barrier can also hinder the transport of other important amino acids, which likely contributes to phenotypic outcome [22].

PKU patients may seem normal at birth. However, developmental delays become evident around 3–6 months of age if left untreated. Due to the prevalence of PKU and our ability to effect positive outcomes with a dietary intervention, newborns in the United States have been routinely screened since the 1960s. Long-term neurological consequences can be avoided with a strict low phenylalanine diet. Dietary adherence must be maintained for the lifetime to limit the irreversible brain damage and manage PKU. Phenylalanine application to neural cell cultures limits neurite outgrowth and high levels of phenylalanine in

patients and model organisms are associated with decreased white matter and fewer synapses suggesting that phenylalanine is directly toxic to neurons [23, 24].

Phenylalanine is a potent teratogen [25]. Thus, control of phenylalanine levels is extremely important during pregnancy. Maternal PKU syndrome is caused by unmanaged elevated phenylalanine levels in pregnant PKU patients. Maternal PKU is associated with congenital heart disease, microcephaly, intrauterine growth retardation, and spontaneous abortion, regardless of the fetus' genetic PKU status [26].

The *PAH* gene was cloned in both humans [27] and mice [28] in the 1980s. More than 950 mutations have been associated with PKU and many categorized according to residual enzyme activity which negatively correlates with phenotypic severity [29]. Mutations in the *PAH* gene include missense mutations (62%), deletions (13%), splicing defects (11%), silent polymorphisms (6%), nonsense mutations (5%), and insertions (2%) [15], and a frequent mechanism of reduced enzymatic function appears to be protein destabilization [30, 31].

9.3.3 Animal Models

The first mouse model for PKU was purposefully generated in a forward genetic screen. After germline ethylnitrosourea (ENU) mutagenesis in mice, animals were screened for hyperphenylalaninemia and three mutants were identified [32, 33]. The three alleles, *Pah^{enu1}*, *Pah^{enu2}*, and *Pah^{enu3}*, were associated with varying degrees of hyperphenylalaninemia. *Pah^{enu1}* mice have a moderate elevation in serum phenylalanine concentration and urinary ketones, whereas *Pah^{enu2}* and *Pah^{enu3}* mice are severely elevated for both.

These animals were quickly appreciated as an ideal model in terms of their recapitulation of the molecular and pathological aspects of PKU. These mutants have provided an excellent model for unraveling differential effects of mutations in *PAH* on clinical outcome because the three alleles differ in severity of phenotype, amount of residual protein activity, and type of

molecular lesion in the gene [32–35]. Moreover, as strong model for the human disease, they have served as surrogates both in investigating etiology of disease and in testing of potential therapies. Here we focus on how the animal models have been useful for advancing therapeutic-focused research in conjunction with studies in multiple other systems from prokaryotes to plants.

9.3.4 Therapeutics

The concept of enzyme replacement therapy has heavily influenced PKU treatment research, even though significant challenges had to be overcome to make this a success story. *PAH* normally functions in the hepatocyte cytoplasm and requires the nonprotein cofactor tetrahydrobiopterin (BH_4) for activity. In fact, depletion of BH_4 , which can arise from mutations in enzymes in its biosynthetic pathway, reduces *PAH* activity and results in hyperphenylalaninemia and syndromes that overlap to some degree with PKU [36]. The need for the BH_4 cofactor and the liver localization of the normal protein complicates implementation of replacement enzyme therapy using *PAH* itself, as do issues with stability of the *PAH* enzyme [37]. However, the same cofactor requirement attribute has been exploited to implement a distinct therapeutic for PKU.

Some patients with mild PKU benefit from administration of BH_4 [38]. A synthetic form of BH_4 called sapropterin dihydrochloride (trade name KuvanTM) was the first therapeutic approved for PKU treatment [39, 40]. Studies in the *Pah^{enu1}* model revealed the molecular mechanisms underlying BH_4 function. BH_4 stabilized the *Pah* protein in this model, acting as a chaperone to promote proper protein folding and prevent the aggregation and degradation that lead to low enzymatic activity [39]. Patients who have destabilizing mutations in *PAH* can benefit from this therapy. Thus, the cofactor itself has led to an effective therapeutic, but attempts to bypass the cofactor entirely would also be beneficial for additional patients. It was research in a distinct field combined with academic scientists

who communicated across disciplines and with industry researchers that led to a breakthrough on this front.

Researchers studying lignin biosynthesis in plants in the 1950s determined that metabolites of phenylalanine were important to lignin synthesis and then subsequently identified the enzyme phenylalanine ammonia lyase (PAL) as a key player in lignin biosynthesis [41]. Phenylalanine ammonia lyase is found in plants as well as fungi and converts phenylalanine to *trans*-cinnamic acid and ammonia [41].

John Hoskins was an organic chemist who serendipitously shared lab space with a PKU diagnostics lab in the 1970s and became interested in the disease [42]. His interest eventually led him to join forces with Dr. Henry Wade who knew that depletion of phenylalanine was important in treatment of PKU and had access to PAL enzyme. Together they implemented formulations to test the effect of PAL in humans, in both normal test subjects after a high protein meal and on the high levels of phenylalanine in PKU patients [42, 43]. Their work provided proof of principle for an effective therapeutic but years of research to develop a safe product lay ahead.

PAL is not a mammalian protein and its introduction in mammals leads to an immunogenic response, making it unsuitable as a therapeutic. Immunogenicity issues are not uncommon in molecular therapeutics, and PKU researchers employed a common technique to mask the immunogenic protein from the host [44]. They used PEGylation, involving modification of the protein with polyethylene glycol, to try to limit the antigenicity and immunogenicity of the protein with some limited but insufficient success. In an academic/pharmaceutical collaborative effort in 2008, researchers turned to a selection of cyanobacteria, fungi, and plants as sources of diverse PAL proteins to try to identify a suitable candidate for enzyme replacement therapy.

PEGylated PAL proteins from *Anabaena variabilis*, *Nostoc punctiforme*, *Petroselinum crispum*, and *Rhodospiridium toruloides* were tested for therapeutic effect in the *Pah^{enu2}* mice [45]. High doses of protein followed by smaller, secondary doses decreased plasma and brain phenylalanine,

with the *Anabaena variabilis* (Av) protein showing the most favorable results in terms of thermal stability, proteolytic resistance, and optimal pH sensitivity. In addition to the decrease in phenylalanine levels, the characteristic hypopigmentation, due the lack of conversion of tyrosine to melanin, was also ameliorated [45]. The effects of enzyme treatment were reversible once treatments were halted.

A modified and optimized version of PAL from *Anabaena variabilis* was chosen as a candidate for Phase I clinical trials conducted by BioMarin as a therapeutic treatment for classical PKU due to the success found in the *Pah^{enu2}* mice. During human clinical trials, 60.7% of patients had a blood phenylalanine level below the recommended guidelines within 24 months of starting treatment [46]. Thus, the second therapeutic drug (trade name PalyzinqTM) and the first enzyme substitution therapy for PKU was approved by the FDA. This therapy no longer requires the onerous dietary restrictions associated with standard treatment.

9.3.5 Maternal PKU Models

Avian, rodent, and primate models for maternal PKU have been explored with emphasis on elucidating the etiology of the cardiac malformations associated with high phenylalanine during pregnancy [47–50]. Again, the *Pah^{enu2}* mouse model is a relevant model for what is observed in humans. *Pah^{enu2}* females produce offspring with structural defects in the cardiovascular system, although the structural problems reported in humans and mouse differ [47]. Gene expression analysis in chick and *Pah^{enu2}* reveal changes in genes relevant to cardiac development and function including cardiac troponin and myosin [48, 51].

9.3.6 The *Pah^{enu2}* Model and the Future

PKU research benefits from the fact that it is less rare than many CMDs. As a result, many advances in therapeutics and disease etiology have come

from insights gained in patients. Moreover, the mouse model for PKU is perhaps as close to ideal as can be expected between species. The future of PKU research will see *Pah^{enu2}* in a central role. Two recent advances illustrate the continued relevancy of this model for exciting future therapy development.

Our relatively recent realization of the importance of the gut microbiome and its interdependence with human metabolism has led to increased interest in probiotics as therapeutics [52]. An engineered probiotic for PKU treatment is a reasonable approach given that oral administration of recombinant PAL enzyme was shown to lower serum phenylalanine levels in the *Pah^{enu}* mouse models [53]. A *Lactobacillus* strain engineered to express *Anabaena variabilis*-derived PAL was tested in the *Pah^{enu2}* model, resulting in a reduction in serum phenylalanine levels [54]. Two other groups have engineered an *E. coli* Nissle strain to express phenylalanine-degrading enzymes and tested responses in the *Pah^{enu2}* model with positive outcomes [55, 56]. Isabella et al. produced an intricately engineered strain that expresses two phenylalanine-degrading enzymes: cytoplasmic PAL and a membrane-bound, periplasmic-localized L-amino acid deaminase (LAAD) that converts phenylalanine to phenylpyruvate [56]. Both enzymes are under inducible promoters to limit enzyme production until the final stages of manufacturing of the probiotic in the case of LAAD and until exposure to the microaerobic or anaerobic regions of the gut in the case of PAL. This strain was engineered with adherence to FDA guidelines regarding live biotherapeutic organisms with the goal of extending its use directly to clinical trials.

In the modern age of genome manipulation, it is now possible to consider editing of molecular lesions in patients. Again, *Pah^{enu2}* has provided the conditions for proof of principle for such experiments. In 2018, Villiger et al. reported use of a base editing CRISPR-Cas9 system [57, 58] to revert the *enu2* allele in cells of the mouse liver [59]. The edited mice had reduced blood phenylalanine levels, increased PAH activity, and a reversion of the mutant hypopigmentation.

In summary, 25 years of research with the *Pah* mouse model as a tool has already reaped benefits and is poised to promote additional progress for patients. This field is a success story. PKU is a great illustration where discoveries in animal models, combined with knowledge gleaned from multiple other systems from plants to bacteria, led to the discovery of a therapy that efficiently clears the neurotoxic effects in people that suffer from this rare, metabolic disease.

9.4 Lesch-Nyhan Syndrome

While it may be tempting to define an ideal disease model, as we discussed with PKU, as one that recapitulates the entirety of the disorder seen in humans, e.g., genetically, biochemically, histopathologically, and phenotypically, models that demonstrate one facet of the disease have been useful in advancing our understanding of CMDs. Research into the inborn error of purine metabolism called Lesch-Nyhan syndrome highlights the utility of establishing multiple animal models for a single CMD.

9.4.1 History and Prevalence

Lesch-Nyhan syndrome (LNS, OMIM 300322) is an X-linked recessive metabolic disorder of purine metabolism caused by mutations in the hypoxanthine-guanine phosphoribosyltransferase (*HPRT*) gene. It was first fully described by Michael Lesch and William Nyhan in 1964 [60]. They reported on two young male patients, ages 3 and 5, at Johns Hopkins Hospital who presented with severe motor dysfunction, involuntary movements and muscle contractions, and crystals in the urine. Both patients also displayed compulsive self-injury involving biting of lips and digits. In 1967, Seegmiller et al. demonstrated that cells of patients with LNS lack hypoxanthine-guanine phosphoribosyltransferase (*HPRT*) activity [61]. The *HPRT* gene was cloned and sequenced in 1983 [62, 63]. LNS prevalence is estimated at 1 in 380,000 live

births [64]. The recognition and description of LNS marked a milestone in that it was a first metabolic disturbance in purine metabolism linked to a neurobehavioral disease [60].

9.4.2 Clinical and Molecular Phenotypes and Alleles

LNS patients have a diversity of clinical phenotypes, including hyperuricemia resulting in gouty arthritis and renal disease, aberrant motor function, reduced gastrointestinal motility, and cognitive and behavioral problems [65–67]. The syndrome presents on a continuum. Patients with the highest levels of residual enzyme activity present with gouty arthritis without neurological involvement. This milder clinical manifestation has been alternatively called Lesch-Nyhan variant and Kelley-Seegmiller syndrome (OMIM 300323). In contrast, patients with little to no residual enzyme activity are severely affected with motor dysfunction and the neurobehavioral issues in addition to the hyperuricemia. The most striking behavioral symptom is that these individuals are typically auto-aggressive, causing self-injury usually via biting of lips, tongues, and digits.

As a result of a severe reduction or absence of HPRT enzymatic activity, individuals with LNS are unable to salvage purines to resynthesize nucleotides. Instead, the purines are degraded to uric acid, and purine biosynthesis is increased in a compensatory response, exacerbating the hyperuricemia [68]. The excess uric acid crystallizes in various tissues and organs, causing acute arthritis in the joints and stones and renal disease in the kidneys [66, 67, 69]. Uric acid production can be reduced in patients using drugs such as allopurinol, a xanthine oxidase inhibitor that prevents breakdown of hypoxanthine to uric acid, and this ameliorates the gouty aspects of the disease [66]. However, allopurinol has no effect on the neurological and motor manifestations.

The self-injurious behavior has been a topic of intense study. Self-injuries are not due to the lack of sensation. They are believed to be associated

with the dysfunction of dopaminergic pathways in the basal ganglia. Post-mortem tissue analyses revealed low HPRT enzymatic activity and a marked decrease in dopamine in the basal ganglia [70], as well as a decrease in markers of dopaminergic neurons [71, 72].

Patients with this disorder usually require restraints to attempt to stop the neurobehavioral issues. Treatments such as mild tranquilizers (e.g., benzodiazepine) and anticonvulsants (e.g., carbamazepine) have been used to help with the behavioral issues [73, 74]. However, in extreme cases, dental extractions are recommended [67, 75]. There are currently no treatments for motor deficits.

The official website of the Lesch-Nyhan Study Group lists 615 mutations in *HPRT* that are associated with LNS, in which 381 are single point mutations (61.9%). Previously, several mutational hot spots in the *HPRT* gene were found and the most predominant one included 12 unrelated individuals with a C to T mutation changing arginine to a stop codon in a CpG motif [76].

9.4.3 Models

9.4.3.1 Cells

The first efforts to analyze the molecular etiology of LNS were carried out in cell models. The specific lack of HPRT activity in patients was demonstrated using erythrocytes and fibroblasts collected from patients [61]. Such models have added to our understanding of the cellular biochemistry of purines as well. For example, these HPRT-deficient cell lines revealed alterations in de novo purine synthesis flux that occur upon loss of HPRT as well as changes in energetics as revealed by GTP:GDP ratios [77, 78]. Subsequently, cells engineered to lack HPRT activity, including human fibroblasts and dopaminergic neuroblastoma cell lines [79] and mouse dopaminergic neuroblastoma cell lines [80], have been used to address questions about the neurological biochemistry and functional ability of cells that lack HPRT activity. For example, recent application of genomics methods to examine gene expression in HPRT-deficient

human fibroblasts and neuroblastoma cells reveals downregulation of *Lmx1a* and *Engrailed 1*, transcription factors required for development and function of dopaminergic neurons, dysregulation of canonical Wnt signaling, aberrant pre-nilin expression [79], and disrupted miR181a expression, which subsequently regulates important dopaminergic cell developmental pathways [81]. Each finding from these cell models generates new hypotheses about the possible link between HPRT and neural function and dysfunction. Moreover, cell lines have provided a platform to demonstrate proof of principle for enzyme replacement therapies at least in terms of correction of the biochemical deficits, if not the behavioral ones [82].

9.4.3.2 Rodents

LNS was the first human congenital disease for which a genetically engineered mouse model was created [83, 84]. There were high hopes for modeling the human disease in mice because the rarity of the syndrome presents added challenges beyond those already inherent in research involving patients. *Hprt1*-deficient mice lack HPRT enzymatic activity and were experimentally demonstrated to be unable to salvage purines, suggesting a strong biochemical correlate of LNS in this model [85]. The brains of these mice also have reduced dopamine levels [86, 87], similar to the findings in the post-mortem brains of LNS patients. Overall, the mouse model has been useful for validating and probing the neurochemical changes that arise when HPRT1 activity is compromised. However, the neurobehavioral aspects of the disease were not reproduced in the knockout mice. There was one hopeful report that the self-injurious behaviors could be induced in the *Hprt1*-deficient mice upon inhibition of adenine phosphoribosyltransferase [88]. However, this result has not been reproducible [89, 90], and thus, the mouse model is not suitable for investigation into causal relationships between the neurochemical signatures shared by mice and humans and the behavioral outputs observed only in humans.

Because rats often provide a model system physiologically and behaviorally more similar to

humans than mice [91], rat models for LNS have also been explored. There were expectations of success in recapitulating the behavioral issues observed in patients via knockout of *Hprt* in rats because studies in rats, aimed at other purposes, serendipitously produced a model for the self-injurious behavior in LNS. Perinatal treatment of rats with 6-hydroxydopamine, which selectively kills dopaminergic and adrenergic neurons [92], results in a reduction of dopamine [93, 94]. Animals with this neural damage surprisingly exhibit self-mutilation of the limbs and abdomen when administered L-dopamine as adults [93, 94]. Similar outcomes are not observed when the 6-hydroxydopamine treatment is applied to adult animals. These studies lend support to the hypothesis that dopamine perturbations are causative of self-injurious behaviors and highlight the complicated etiology in terms of how changes in metabolite levels intersect with developmental events to produce the behaviors. Dopaminergic deficiencies have been directly observed using positron emission tomography in patients independent of age, again suggesting that the dopaminergic deficiencies arise from developmental as opposed to neurodegenerative processes [72].

The engineering of an *Hprt* knockout rat was reported in 2016 [95]. The neurochemical changes observed in humans and mice are also recapitulated in these rats. However, the behavioral phenotype was once again not observed. Thus, while there is substantial evidence supporting the role of dopamine deficiencies in the neurobehavioral aspects of LNS, the link between loss of HPRT activity and the perturbations to dopaminergic signaling remain unclear.

While less than ideal for studying intriguing aspects of neurobehavior, the rodent models have been useful to shed light on the underlying etiology of other adverse symptoms seen in LNS patients, specifically gastrointestinal motility issues that result in vomiting, dysphagia, and constipation [96]. The HPRT-deficient model mice have an overall decrease in gastrointestinal motility that is correlated with dysfunction in dopaminergic neurons of the gastrointestinal tract [65]. Moreover, gastrointestinal motility issues are not due to impairment of cholinergic or

nitrgic systems [65]. Thus, the mouse model did prove to be important for shedding light on the changes seen in gastrointestinal motility, illustrating significant benefit of a model that may be considered less than ideal on another front.

9.4.3.3 Back to Cells and the Future

The future of disease modeling is sure to include increased use of stem cells, including both induced pluripotent stem (iPS) cells and embryonic stem (ES) cells. Such modern models are being used for the study of HPRT activity in neural development and function. Knockdown of HPRT expression in human iPS and ES cells results in lower expression of the P2Y1 purinergic signaling receptor and impaired downstream signaling [97]. Gene and protein expression profiles across a timeline of dopaminergic neural development in mouse ES cells deficient for HPRT activity suggested that the cells are inhibited in neural differentiation in favor of glial differentiation [98]. Moreover, dysregulation in a wide swath of cell functions was suggested by the gene expression changes observed, suggesting that HPRT may have roles in neural differentiation beyond what would be expected if considered only a purine biosynthetic mutant. In short, much biology remains to be uncovered.

9.4.4 Conclusions

LNS is a complex, multifaceted disease that is associated with varied pathophysiology. The rat and mouse models were first deemed only partial successes, due to the lack of the neurobehavioral issues seen in humans. However, the mouse model has effectively provided insight into the neurochemical and gastrointestinal issues. Given the success of the models in recapitulating the biochemical changes seen in LNS patients and the recent results of experiments examining neural development in these models, it is likely that the rodent models will still provide the clues needed to make a breakthrough in the neurobehavioral puzzle.

LNS is a particularly rare disease, making it more difficult to glean information from clinical

studies. Because of the lack of a perfect model for assessing the most distressing clinical aspects of LNS, therapeutic research has received less emphasis relative to phenylketonuria as noted above. Instead a major thrust in LNS research has been efforts to develop the appropriate models and studying the etiology of the perturbations in the current models, both genetic and chemically induced, that will eventually advance therapeutic studies. This field highlights the usefulness of less than ideal models at the same time as illustrating the need for additional model development (Fig. 9.1).

9.5 Tay-Sachs and Sandhoff Disease

In the examples above, we discussed forward genetic and transgenic approaches to deliberately engineer genetic model systems. In this example, some of the engineered animal models do not perfectly reflect clinical aspects of the human disease. Researchers have instead made great use of serendipitous discoveries of useful models among domesticated animals. These animals are better suited to advance the types of effective therapeutic research we saw illustrated above for PKU.

9.5.1 History and Frequency

Tay-Sachs disease (TSD, OMIM 272800) and Sandhoff disease (SD, OMIM 268800) are rare, autosomal recessive neurodegenerative disorders that develop as a result of mutations reducing hexosaminidase activities. They are clinically indistinguishable and manifest as mental and motor deficits that progressively worsen. Both are classified as lysosomal storage disorders and characterized by an accumulation of GM2 gangliosides in the lysosome.

Tay-Sachs was first described in a single patient by British doctor Warren Tay in 1881 [99], who subsequently recognized the same syndrome in additional patients. In 1887, the American doctor Bernard Sachs, unaware of the work of William Tay, submitted a paper about a case in a girl of German descent [100], and in 1892, E.C. Kingdon

reported a case and reviewed the reports of both Tay and Sachs. Kingdon subsequently identified additional patients and the syndrome became known as Tay-Sachs [101, 102].

The American College of Medical Genetics and Genomics and American College of Obstetricians and Gynecologists recommend that people of Ashkenazi Jewish descent screen for TSD, as the carrier frequency in that population is 1 in 31 [3]. The carrier frequency in eastern French Canadians is 1 in 14 [103]. Other small founder populations, including Louisiana Cajuns, Irish, and Brazilian populations, also have an increased carrier frequency [102, 104]. Due to prescreening for carrier status in the Ashkenazi Jewish population, TSD incidence decreased 90% between 1970 and 1993 in North America [102].

Sandhoff disease was described in 1968 [105] as a variant of Tay-Sachs with a distinct enzymatic activity profile (see below). Like TSD, SD is fatal, and the patient normally exhibits progressive neurodegeneration [106]. SD prevalence is estimated to be 1 in 422,000, with a carrier rate of 1 in 310 [107]. Some isolated communities with high consanguinity have higher incidence rates. For example, northern Saskatchewan is home to isolated Métis communities where the population is mixed French Canadian and aboriginal and has a carrier frequency of 1 in 27 [108].

9.5.2 Clinical and Molecular Phenotypes and Alleles

TSD and SD are classified clinically into multiple forms: infantile, juvenile, and late-onset [102]. The infantile form is typically associated with acute symptoms of mental and motor dysfunction and is usually diagnosed by 6 months of age [109]. Catastrophic progressive neurodegeneration leads to hypotension, inability to sit or to hold up the head, eye abnormalities, and dysphagia. Patients diagnosed with infantile forms typically do not survive past the age of 3 or 4 years [110].

The juvenile form is characteristically diagnosed between the ages of 3 and 10 years [109]. There is more diversity in clinical manifestations

in the adolescents with juvenile forms. However, patients usually exhibit ataxia, slowed and slurred speech (dysarthria), dysphagia, hypotension, and seizures. Patients diagnosed with juvenile forms typically do not survive past the age of 15 years due to the progressive nature of the disorder.

The late-onset form is often diagnosed in adolescence, but the symptoms can also appear as late as the third decade of life. Recognition of previously undiagnosed mild neurodegenerative symptoms may be a characteristic of late-onset disease; patients in one study recalled previous clumsiness and motor skill issues prior to diagnoses [111]. Furthermore, the same study showed that patients with the late-onset form did not get properly diagnosed, on average, for about 8 years from onset of symptoms. Clinical manifestations include a gradual reduction in motor, cerebral, and spinocerebellar activity.

SD is also associated with some distinct organ pathologies relative to TSD. Both hepatosplenomegaly and cardiac involvement have been described in SD patients [112–114].

TSD and Sandhoff are caused by mutations that inhibit β -N-acetylhexosaminidase (Hex) activity. Hex enzymes are homodimers or heterodimers of α and β subunits, encoded by the genes HEXA and HEXB, respectively. HexA enzyme is a heterodimer of an α and a β subunit. HexB enzyme is a homodimer of two β subunits, and HexS enzyme is a homodimer of two α subunits. Mutations in the HEXA gene disrupt HexA and HexS enzyme function and cause TSD. Mutations in the HEXB gene disrupt HexA and HexB enzyme function and cause SD. SD was first differentiated from TSD because of the observation that a patient lacked both HexA and HexB activity [105], whereas TSD patients retain HexB activity. Note that a third disorder with TSD and SD symptoms arises from mutations in a Hex enzyme activator [115].

The loss of HexA results in a defect in hydrolysis of GM2 gangliosides in the lysosome. The resulting accumulation of GM2 gangliosides inside the lysosomes of neurons causes neural toxicity. TSD is one of multiple pathologies dubbed GM2 gangliosidoses, as mutations in other enzymes in the pathway can lead to similar molecular and clinical phenotypes [116].

TSD severity is negatively correlated with HexA activity; patients with the infantile form have the most pronounced depletion of enzyme activity, whereas adult-onset patients may retain 5% to as much as 20% of normal enzyme activity [117]. The wide diversity of clinical phenotypes is also reflective of the large number of specific disease-causing genetic lesions [116].

9.5.3 Models

Mouse models of TSD and SD were created via targeted deletion of the *Hexa* and *Hexb* genes [118–121]. The *Hexa* mice recapitulate the biochemical aspects of TSD and histopathological aspects in some regions of the brain. However, clinical symptoms similar to TSD were not observed at first. As these animals age past 1 year, they do show clinical signs similar to late-onset TSD [122], but they offer a less than ideal model for studying TSD etiology or for exploring therapeutic approaches to the most severe forms of TSD. The difference between human and mouse phenotypes upon mutation of the *Hexa* gene appears to be due to sialidase activities in mice that can metabolize the GM2 gangliosides in combination with the residual HexB enzymatic activity when HexA enzymatic activity is absent [123, 124]. A HexA-deficient mouse model in which NEU3 sialidase activity is also compromised displays a severe phenotype more characteristic of TSD [125].

In contrast, the *Hexb* mutant mice have progressive neurological phenotypes that parallel TSD and SD in humans, including a severely shortened life span [118]. The *Hexb* mutant mice have an 8-week asymptomatic period following birth. This is followed by 8 weeks of rapid progression of the disease to the point of death [118]. This model has been used effectively to study the etiology of the neurodegenerative events. During the asymptomatic period, accumulation of GM2 gangliosides damages neurons and impairs their survival. Subsequent inflammatory responses trigger reactive astrogliosis, further death, and neurodegeneration [126, 127]. Defects in neurite outgrowth of hippocampal neurons from early embryos was observed in culture [128], and there

are defects in differentiation that favor astrocytes at the expense of neurons in *Hexb* neural stem cells as well as *Hexb* mutant iPSCs [129].

Hexb deficiency has also been engineered in zebrafish using a CRISPR-Cas9 system to study the earliest stages of neural development [130]. This model is very useful for the ability to image early development in live animals, and Kuil et al. observed enlarged lysosomes and increased lysosomal numbers in glia as early as 3 days post-fertilization. The mutant animals also displayed reduced locomotor activity. Together, these results suggest early SD neurodegeneration is recapitulated in zebrafish, creating a powerful model for cell biological analysis of SD that will likely contribute significantly to the field. Interestingly, adult zebrafish are viable and do not show behavioral deficits [130], likely because zebrafish can make new neurons throughout its life [131].

TSD and SD have each been observed to arise spontaneously in domestic animal species (cats, dogs and pigs) and animal species kept in captivity (deer and flamingoes) [132–140]. Feline colony models of SD have been maintained and studied in the laboratory for decades and have been used to explore therapeutics for GM2 gangliosidosis [141–143]. The size and complexity of the cat brain relative to the mouse provide a superior model for humans, and approaches using viral vectors to reintroduce missing gene activities in cats have demonstrated proof-of-principle for such approaches [141–143].

Intriguingly, a promising model that recapitulates human TSD phenotypically and offers an exciting model for therapeutics-focused investigations has been found in a rare breed of primitive sheep called Jacob sheep. Multiple lambs from a single flock in the United States displayed progressive neurological symptoms, and evaluation revealed histological changes in the nervous system, including enlarged neurons, a decrease in white matter, and abnormalities in the retina. Hex enzyme activity was decreased in brain tissue and a mutation was found in the *Hexa* gene [144, 145]. The disease has also been identified in the population of British Jacob sheep from which the North American flock originated [146], and breeding populations have been established for research.

This model is being used to explore therapeutic approaches and, again, because of brain size and complexity is an excellent model for exploring therapeutics to benefit children with Tay-Sachs. In 2018, Gray-Edwards et al. reported significant success using intracranial administration of an adenovirus vector to introduce the *Hexa* gene or copies of both *Hexa* and *Hexb*. Experimental animals all showed delay of symptom onset [147].

These adenovirus-mediated gene therapies offer great promise as proof of principle for gene replacement therapies. However, adenovirus-mediated gene therapies have proven dangerous in humans and significant hurdles remain to be overcome to develop an efficacious strategy to reintroduce the missing enzymatic function in neural tissue. The cat and the sheep models offer great promise for testing engineered therapies to achieve the types of success achieved in PKU research.

9.5.4 Organoid Model: A Step into Patient-Oriented Models

While there is no substitute for animal models in the realm of probing neurobehavior, modern technologies offer options for modeling that will reap benefits for patients. Pluripotent cells can be both induced and then coaxed into formation of a variety of different organoids [148]. These organoids are complex structures that recapitulate aspects of cell differentiation and organ development, morphology, and function. Organoids formed from the cells of patients with specific genetic lesions are a step toward personalized medicine for rare CMDs. Cerebral organoids for Sandhoff disease have been produced and examined [149]. Fibroblasts were obtained from an infant with SD and used to produce iPS cells. The researchers also used a CRISPR-Cas9 system to edit the genetic lesion of the patient's cells, correcting one copy of the *HEXB* gene and used the original and edited, isogenic control cells to generate cerebral organoids. The SD organoids were larger than the isogenic control organoids and produced GM2 gangliosides, similar to what was seen in the brain of SD patients [149]. They were able to ameliorate GM2 accumulation using a gene replacement therapy

approach. Whole transcriptome analysis of these organoids revealed the reduced expression of an intriguing set of genes related to neural development in the mutant organoids.

9.6 Conclusions

CMDs are rare diseases. Thus, the number of patients affected is low and gaining extensive information clinically is challenging. As a result, the development of animal models has been critical and will continue to play a role in CMD research and therapeutic advances for patients with CMDs. We have only discussed a handful of CMDs. However, these diseases illustrate two major principles in our research enterprise. First, a model that recapitulates human clinical symptoms is a tremendously powerful tool for facilitating therapeutic development. Second, models that do not recapitulate all clinical symptoms of a disease have significant value as well (Fig. 9.1). They play a critical role in elucidating disease etiology which leads to new ideas and research pathways for therapeutic development as well as new ideas for further model development. Modeling rare disease is primarily aimed at helping patients. However, the impact is much broader because we have fundamental gaps in our understanding of the biology of disease phenotypic manifestation that will be addressed in these studies. For example, the catastrophic neural degeneration observed and investigated in Tay-Sachs models is likely to unravel aspects of immune responses in the brain that are novel.

Use of animal models is necessary to generate the knowledge to ameliorate quality of life issues for patients and families. For disorders where great models have already been established, we expect the current era of genome manipulation to lead to human disease models more sophisticated than gene deletion. The *Pah^{enu}* models, which are point mutations generated in forward screens, have been incredibly useful. As we move to the future, we also expect to see more frequent use of designer models engineered to carry specific human disease mutations. Advances in iPS and organoid technology will also be used to create patient-specific models

more frequently. As model-making in atypical clinically based research animals, such as pigs and cows, becomes possible because of advances in genome engineering [150], we also expect to see more complicated models for disorders. We are confident that each direction will result in eventual realization of truly designer treatments.

PKU is a rare disease, and LNS, TSD, and SD are even rarer, yet all are heavily studied. There are many other CMDs that are ultra-rare, with fewer than 100 patients identified worldwide, and these CMDs are understudied. While animal models can be engineered for such diseases, there is no a priori guarantee that the expense and research effort will produce a model for clinical aspects of disease and the research enterprise is simply not vast enough for an effective focus on each of these disorders. The community should also embrace genetic model systems such as zebrafish and invertebrates such as *Drosophila* and *C. elegans* for these diseases because these models are cheap and fast and bring the power of forward unbiased genetics to the table, which can be less expensive and yet quite effective in generating therapeutic ideas.

Glossary

Ataxia is a lack of voluntary coordination of muscle movements.

Dysphagia is difficulty swallowing.

Hyperphenylalaninemia refers to elevated concentrations of the amino acid phenylalanine in the blood.

Hyperuricemia refers to elevated uric acid levels in the blood.

PEGylated refers to covalent and noncovalent modification of a protein with PEG.

References

1. Harthan AA. An introduction to pharmacotherapy for inborn errors of metabolism. *J Pediatr Pharmacol Ther.* 2018;23(6):432–46.
2. Garrod AE. The incidence of alkaptonuria: a study in chemical individuality. 1902. *Mol Med.* 1996;2(3):274–82. [cited 2019 Sep 13]. <http://www.ncbi.nlm.nih.gov/pubmed/8784780>.

3. Kruszka P, Regier D. Inborn errors of metabolism: transition from childhood to adulthood. *Am Fam Physician.* 2019;99(1):25–32.
4. Kanungo S, Patel DR, Neelakantan M, Ryali B. Newborn screening and changing face of inborn errors of metabolism in the United States. *Ann Transl Med.* 2018;6(24):468. AME Publications. [cited 2019 Sep 13]. <http://www.ncbi.nlm.nih.gov/pubmed/30740399>.
5. Bick D, Jones M, Taylor SL, Taft RJ, Belmont J. Case for genome sequencing in infants and children with rare, undiagnosed or genetic diseases. *J Med Genet.* 2019. [cited 2019 Sep 13]; [jmedgenet-2019-106111](http://www.ncbi.nlm.nih.gov/pubmed/31023718). <http://www.ncbi.nlm.nih.gov/pubmed/31023718>.
6. Heimer G, Kerätär JM, Riley LG, Balasubramaniam S, Eyal E, Pietikäinen LP, et al. MECR mutations cause childhood-onset dystonia and optic atrophy, a mitochondrial fatty acid synthesis disorder. *Am J Hum Genet.* 2016;99(6):1229–44.
7. Wertheim-Tysarowska K, Gos M, Sykut-Cegielska J, Bal J. Genetic analysis in inherited metabolic disorders—from diagnosis to treatment. Own experience, current state of knowledge and perspectives. *Dev Period Med.* 2019;19(4):413–31. [cited 2019 Sep 13]. <http://www.ncbi.nlm.nih.gov/pubmed/26982749>.
8. Ezgu F. Inborn errors of metabolism. In: *Advances in clinical chemistry*; 2016. p. 195–250. [cited 2019 Sep 13]. <http://www.ncbi.nlm.nih.gov/pubmed/26975974>
9. Argmann CA, Houten SM, Zhu J, Schadt EE. A next generation multiscale view of inborn errors of metabolism. *Cell Metab.* 2016;23(1):13–26. NIH Public Access. [cited 2019 Aug 1]. <http://www.ncbi.nlm.nih.gov/pubmed/26712461>.
10. Sirrs S, Hollak C, Merkel M, Sechi A, Glamuzina E, Janssen MC, et al. The frequencies of different inborn errors of metabolism in adult metabolic centres: report from the SSIEM adult metabolic physicians group. In: *JIMD reports*. Wiley-Blackwell; 2015. p. 85–91. [cited 2019 Sep 15]. <http://www.ncbi.nlm.nih.gov/pubmed/26450566>.
11. Bickel H, Gerrard J, Hickmans EM. The influence of phenylalanine intake on the chemistry and behaviour of a phenylketonuria child. *Acta Paediatr.* 1954;43(1):64–77. John Wiley & Sons, Ltd (10.1111). [cited 2019 Sep 15]. <http://doi.wiley.com/10.1111/j.1651-2227.1954.tb04000.x>.
12. Bhattacharya K, Wotton T, Wiley V. The evolution of blood-spot newborn screening. *Transl Pediatr.* 2014;3(2):63–70. AME Publications. [cited 2019 Sep 15]. <http://www.ncbi.nlm.nih.gov/pubmed/26835325>.
13. Burlina AP, Lachmann RH, Manara R, Cazzorla C, Celato A, van Spronsen FJ, et al. The neurological and psychological phenotype of adult patients with early-treated phenylketonuria: a systematic review. *J Inher Metab Dis.* 2019;42(2):209–19. John Wiley & Sons, Ltd. [cited 2019 Sep 15]. <https://onlinelibrary.wiley.com/doi/abs/10.1002/jimd.12065>.

14. Brown CS, Lichter-Konecki U. Phenylketonuria (PKU): a problem solved? *Mol Genet Metab Rep*. 2016;6:8–12. Elsevier. [cited 2019 Sep 15]. <http://www.ncbi.nlm.nih.gov/pubmed/27014571>.
15. Williams RA, Mamotte CDS, Burnett JR. Phenylketonuria: an inborn error of phenylalanine metabolism. *Clin Biochem*. 2008;49:31–41.
16. Centerwall SA, Centerwall WR. The discovery of phenylketonuria: the story of a young couple, two retarded children, and a scientist. *Pediatrics*. 2000;105(1):89–103.
17. Blau N. Genetics of phenylketonuria: then and now. *Hum Mutat*. 2016;37(6):508–15.
18. Christ SE. Asbjørn Følling and the discovery of phenylketonuria. *J Hist Neurosci*. 2003;12(1):44–54. [cited 2019 Sep 7]. <http://www.ncbi.nlm.nih.gov/pubmed/12785112>.
19. Mitchell JJ, Trakadis YJ, Scriver CR. Phenylalanine hydroxylase deficiency. *Genet Med*. 2011;13(8):697–707. Nature Publishing Group. [cited 2019 Sep 7]. <http://content.wkhealth.com/linkback/openurl?sid=WKPTLP:landingpage&an=00125817-201108000-00002>.
20. Nova MP, Kaufman M, Halperin A. Scleroderma-like skin indurations in a child with phenylketonuria: a clinicopathologic correlation and review of the literature. *J Am Acad Dermatol*. 1992;26(2):329–33. Mosby. [cited 2019 Sep 15]. <https://www.sciencedirect.com.ezaccess.libraries.psu.edu/science/article/pii/S10967229270048K?via%3Dihub>.
21. Van Vliet D, Van Wegberg AMJ, Ahring K, Bik-Multanowski M, Blau N, Bulut FD, et al. Can untreated PKU patients escape from intellectual disability? A systematic review. *Orphanet J Rare Dis*. 2018;13(1):1–6.
22. Van Vliet D, Bruinenberg VM, Mazzola PN, Van Faassen MHJR, De Blaauw P, Pascucci T, et al. Therapeutic brain modulation with targeted large neutral amino acid supplements in the Pah-enu2 phenylketonuria mouse model. *Am J Clin Nutr*. 2016;104(5):1292–300.
23. Pietz J. Neurological aspects of adult phenylketonuria. *Curr Opin Neurol*. 1998;11(6):679–88.
24. Anderson PJ, Wood SJ, Francis DE, Coleman L, Anderson V, Boneh A. Are neuropsychological impairments in children with early-treated phenylketonuria (PKU) related to white matter abnormalities or elevated phenylalanine levels? *Dev Neuropsychol*. 2007;32(2):645–68.
25. Krishnamoorthy U, Dickson M. Maternal phenylketonuria in pregnancy. *Obstet Gynaecol*. 2005;7(1):28–33.
26. Lenke RR, Levy HL. Maternal phenylketonuria and hyperphenylalaninemia. *N Engl J Med*. 1980;303(21):1202–8.
27. Woo SLC, Lidsky AS, Güttler F, Chandra T, Robson KJH. Cloned human phenylalanine hydroxylase gene allows prenatal diagnosis and carrier detection of classical phenylketonuria. *Nature*. 1983;306:151–5.
28. Kwok SCM, Ledley FD, DiLella AG, Robson KJH, Woo SLC. Nucleotide sequence of a full-length complementary DNA clone and amino acid sequence of human phenylalanine hydroxylase. *Biochemistry*. 1985;24(3):556–61.
29. Romani C, Palermo L, MacDonald A, Limback E, Hall SK, Geberhiwot T. The impact of phenylalanine levels on cognitive outcomes in adults with phenylketonuria: effects across tasks and developmental stages. *Neuropsychology*. 2017;31(3):242–54.
30. Shi Z, Sellers J, Moulton J. Protein stability and in vivo concentration of missense mutations in phenylalanine hydroxylase. *Proteins*. 2012;80(1):61–70. NIH Public Access. [cited 2019 Sep 11]. <http://www.ncbi.nlm.nih.gov/pubmed/21953985>.
31. Gersting SW, Kemter KF, Staudigl M, Messing DD, Danecka MK, Lagler FB, et al. Loss of function in phenylketonuria is caused by impaired molecular motions and conformational instability. *Am J Hum Genet*. 2008;83(1):5–17. Cell Press. [cited 2019 Sep 11]. <https://www.sciencedirect.com.ezaccess.libraries.psu.edu/science/article/pii/S0002929708003224?via%3Dihub>.
32. Shedlovsky A, McDonald JD, Symula D, Dove WF. Mouse models of human phenylketonuria. *Genetics*. 1993;134(4):1205–10.
33. McDonald JDD, Bode VC, Dove WFF, Shedlovsky A, Vernon C, Dove WFF, et al. Pahhph-5: a mouse mutant deficient in phenylalanine hydroxylase. *Proc Natl Acad Sci U S A*. 1990;87(5):1965–7.
34. Haefele MJ, White G, McDonald JD. Characterization of the mouse phenylalanine hydroxylase mutation Pahenu3. *Mol Genet Metab*. 2001;72(1):27–30. Academic Press. [cited 2019 Sep 11]. <https://www.sciencedirect.com/science/article/pii/S1096719200931044?via%3Dihub>.
35. McDonald JD, Charlton CK. Characterization of mutations at the mouse phenylalanine hydroxylase locus. *Genomics*. 1997;39(3):402–5.
36. Blau N, Thöny B, Heizmann CW, Dhondt JL. Tetrahydrobiopterin deficiency: from phenotype to genotype. *Pteridines*. 1993;4(1):1–10.
37. Fitzpatrick PF. Allosteric regulation of phenylalanine hydroxylase. *Arch Biochem Biophys*. 2012;519(2):194–201.
38. Muntau AC, Roschinger W, Habich M, Demmelmair H, Hoffmann B, Sommerhoff CP, et al. Tetrahydrobiopterin as an Alternative Treatment for Mild Phenylketonuria. *N Engl J Med*. 2002;347(26):2122–32.
39. Gersting SW, Lagler FB, Eichinger A, Kemter KF, Danecka MK, Messing DD, et al. Pahenu1 is a mouse model for tetrahydrobiopterin-responsive phenylalanine hydroxylase deficiency and promotes analysis of the pharmacological chaperone mechanism in vivo. *Hum Mol Genet*. 2010;19(10):2039–49. Narnia. [cited 2019 Sep 11]. <https://academic.oup.com/hmg/article-lookup/doi/10.1093/hmg/ddq085>.
40. Cederbaum S. Tetrahydrobiopterin and PKU: into the future. *J Pediatr*. 2011;158(3):351–3. Mosby, Inc.

41. Koukol J, Conn EE. The metabolism of aromatic compounds in higher plants. *J Biol Chem.* 1961;236(10):2692–8.
42. Levy HL, Sarkissian CN, Scriver CR. Phenylalanine ammonia lyase (PAL): from discovery to enzyme substitution therapy for phenylketonuria. *Mol Genet Metab.* 2018;124(4):223–9. [cited 2019 Sep 16]. <http://www.ncbi.nlm.nih.gov/pubmed/29941359>.
43. Hoskins JA, Jack G, Wade HE, Peiris RJD, Wright EC, Starr DJT, et al. Enzymatic control of phenylalanine intake in phenylketonuria. *Lancet.* 1980;1(8165):392–4.
44. Taipa MÁ, Fernandes P, de Carvalho CCCR. Production and purification of therapeutic enzymes. In: *Advances in experimental medicine and biology.* 2019. p. 1–24. [cited 2019 Sep 16]. <http://www.ncbi.nlm.nih.gov/pubmed/31482492>.
45. Sarkissian CN, Gamez A, Wang L, Charbonneau M, Fitzpatrick P, Lemontt JF, et al. Preclinical evaluation of multiple species of PEGylated recombinant phenylalanine ammonia lyase for the treatment of phenylketonuria. *Proc Natl Acad Sci U S A.* 2008;105(52):20894–9.
46. Mahan KC, Gandhi MA, Anand S. Pegvaliase: a novel treatment option for adults with phenylketonuria. *Curr Med Res Opin.* 2019;35(4):647–51.
47. McDonald JD, Dyer CA, Gailis L, Kirby ML. Cardiovascular defects among the progeny of mouse phenylketonuria females. *Pediatr Res.* 1997;42(1):103–7. [cited 2019 Sep 11]. <http://www.ncbi.nlm.nih.gov/pubmed/9212044>.
48. Watson JN, Seagraves NJ. RNA-Seq analysis in an avian model of maternal phenylketonuria. *Mol Genet Metab.* 2019;126(1):23–9. Academic Press. [cited 2019 Sep 1]. <https://www.sciencedirect.com/science/article/pii/S1096719218302567?via%3Dihub>.
49. Brass CA, Isaacs CE, McChesney R, Greencard O. The effects of hyperphenylalaninemia on fetal development: a new animal model of maternal phenylketonuria. *Pediatr Res.* 1982;16(5):388–94.
50. Kerr GR, Chamove AS, Harlow HF, Waisman HA. “Fetal PKU:” the effect of maternal hyperphenylalaninemia during pregnancy in the rhesus monkey (*Macaca Mulatta*). *Pediatrics.* 1968;42(1):27–36.
51. Matalon R, Surendran S, McDonald JDD, Okorodudu AOO, Tying SKK, Michals-Matalon K, et al. Abnormal expression of genes associated with development and inflammation in the heart of mouse maternal phenylketonuria offspring. *Int J Immunopathol Pharmacol.* 2005;18(3):557–65. London: SAGE Publications. [cited 2019 Sep 11]. <http://journals.sagepub.com/doi/10.1177/039463200501800316>.
52. Le Barz M, Anhê FF, Varin TV, Desjardins Y, Levy E, Roy D, et al. Probiotics as complementary treatment for metabolic disorders. *Diabetes Metab J.* 2015;39(4):291–303. Korean Diabetes Association. [cited 2019 Sep 16]. <http://www.ncbi.nlm.nih.gov/pubmed/26301190>.
53. Sarkissian CN, Shao Z, Blain F, Peevers R, Su H, Heft R, et al. A different approach to treatment of phenylketonuria: phenylalanine degradation with recombinant phenylalanine ammonia lyase. *Proc Natl Acad Sci U S A.* 1999;96(5):2339–44. [cited 2019 Sep 7]. <http://www.ncbi.nlm.nih.gov/pubmed/10051643>.
54. Durrer KE, Allen MS, Hunt von Herbing I. Genetically engineered probiotic for the treatment of phenylketonuria (PKU); assessment of a novel treatment in vitro and in the PAHenu2 mouse model of PKU. *PLoS One.* 2017;12(5):e0176286. Wilson BA, editor. [cited 2019 Sep 11]. <http://www.ncbi.nlm.nih.gov/pubmed/28520731>.
55. Crook N, Ferreiro A, Gasparrini AJ, Pesesky MW, Gibson MK, Wang B, et al. Adaptive strategies of the candidate probiotic *E. coli* Nissle in the mammalian gut. *Cell Host Microbe.* 2019;25(4):499–512. Elsevier Inc.
56. Isabella VM, Ha BN, Castillo MJ, Lubkowitz DJ, Rowe SE, Millet YA, et al. Development of a synthetic live bacterial therapeutic for the human metabolic disease phenylketonuria. *Nat Biotechnol.* 2018;36(9):857–64. Nature Publishing Group. [cited 2019 Sep 10]. <http://www.nature.com/articles/nbt.4222>.
57. Gaudelli NM, Komor AC, Rees HA, Packer MS, Badran AH, Bryson DI, et al. Programmable base editing of T to G C in genomic DNA without DNA cleavage. *Nature.* 2017;551(7681):464–71. Nature Publishing Group.
58. Komor AC, Kim YB, Packer MS, Zuris JA, Liu DR. Programmable editing of a target base in genomic DNA without double-stranded DNA cleavage. *Nature.* 2016;533(7603):420–4. Nature Publishing Group. [cited 2019 Sep 11]. <http://www.nature.com/articles/nature17946>.
59. Villiger L, Grisch-Chan HM, Lindsay H, Ringnald F, Pogliano CB, Allegri G, et al. Treatment of a metabolic liver disease by in vivo genome base editing in adult mice. *Nat Med.* 2018;24(10):1519–25. Nature Publishing Group. [cited 2019 Sep 11]. <http://www.nature.com/articles/s41591-018-0209-1>.
60. Lesch M, Nyhan WL. A familial disorder of uric acid metabolism and central nervous system function. *Am J Med.* 1964;36(4):561–70. Elsevier. [cited 2019 Sep 2]. [https://www.sciencedirect.com/ezaccess.libraries.psu.edu/science/article/pii/0002934364901044?via%3Dihub](https://www.sciencedirect.com/ezaccess/libraries.psu.edu/science/article/pii/0002934364901044?via%3Dihub).
61. Seegmiller JE, Rosenbloom FM, Kelley WN. Enzyme defect associated with a sex-linked human neurological disorder and excessive purine synthesis. *Science.* 1967;155(3770):1682–4. American Association for the Advancement of Science. [cited 2019 Sep 2]. <http://www.ncbi.nlm.nih.gov/pubmed/6020292>.
62. Jolly DJ, Okayama H, Berg P, Esty AC, Filpula D, Bohlen P, et al. Isolation and characterization of a full-length expressible cDNA for human hypoxanthine phosphoribosyl transferase. *Proc Natl Acad*

- Sci U S A. 1983;80(2):477–81. [cited 2019 Sep 10]. <http://www.ncbi.nlm.nih.gov/pubmed/6300847>.
63. Nyhan WL. Lesch-Nyhan disease. *J Hist Neurosci*. 2005;14:1–10.
 64. Crawhall JC, Henderson JF, Kelley WN. Diagnosis and treatment of the Lesch-Nyhan syndrome. *Pediatr Res*. 1972;6(5):504–13. [cited 2019 Sep 2]. <http://www.ncbi.nlm.nih.gov/pubmed/4558815>.
 65. Zizzo MG, Frinchi M, Nuzzo D, Jinnah HA, Mudò G, Condorelli DF, et al. Altered gastrointestinal motility in an animal model of Lesch-Nyhan disease. *Auton Neurosci*. 2018;210:55–64. Elsevier. [cited 2019 Sep 2]. <https://www.sciencedirect.com/ezaccess/libraries/psu.edu/science/article/pii/S1566070217302692?via%3Dihub>.
 66. Torres RJ, Puig JG. Hypoxanthine-guanine phosphoribosyltransferase (HPRT) deficiency: Lesch-Nyhan syndrome. *Orphanet J Rare Dis*. 2007;2(1):48. [cited 2019 Sep 10]. <http://www.ncbi.nlm.nih.gov/pubmed/18067674>.
 67. Jinnah HA. Lesch-Nyhan disease: from mechanism to model and back again. *Dis Model Mech*. 2009;2(3–4):116–21. [cited 2019 Sep 10]. <http://dmm.biologists.org/cgi/doi/10.1242/dmm.002543>.
 68. Fu R, Sutcliffe D, Zhao H, Huang X, Schretlen DJ, Benkovic S, et al. Clinical severity in Lesch–Nyhan disease: the role of residual enzyme and compensatory pathways. *Mol Genet Metab*. 2015;114(1):55–61. Academic Press. [cited 2019 Sep 10]. <https://www.sciencedirect.com/science/article/pii/S1096719214003461?via%3Dihub>.
 69. Bell S, Kolobova I, Crapper L, Ernst C. Lesch-Nyhan syndrome: models, theories, and therapies. *Mol Syndromol*. 2016;7(6):302–11.
 70. Lloyd KG, Hornykiewicz O, Davidson L, Shannak K, Farley I, Goldstein M, et al. Biochemical Evidence of Dysfunction of Brain Neurotransmitters in the Lesch-Nyhan Syndrome. *N Engl J Med*. 1981;305(19):1106–11
 71. Ernst M, Zametkin AJ, Matochik JA, Pascualvaca D, Jons PH, Hardy K, et al. Presynaptic dopaminergic deficits in Lesch–Nyhan disease. *N Engl J Med*. 1996;334(24):1568–72. Massachusetts Medical Society. [cited 2019 Sep 10]. <http://www.nejm.org/doi/abs/10.1056/NEJM199606133342403>.
 72. Wong DF, Harris JC, Naidu S, Yokoi F, Marengo S, Dannals RF, et al. Dopamine transporters are markedly reduced in Lesch-Nyhan disease in vivo. *Proc Natl Acad Sci U S A*. 1996;93(11):5539–43. National Academy of Sciences. [cited 2019 Sep 10]. <http://www.ncbi.nlm.nih.gov/pubmed/8643611>.
 73. Roach ES, Delgado M, Anderson L, Iannaccone ST, Bums DK. Carbamazepine trial for Lesch-Nyhan self-mutilation. *J Child Neurol*. 1996;11(6):476–8. [cited 2019 Sep 16]. <http://www.ncbi.nlm.nih.gov/pubmed/9120227>.
 74. Pozzi M, Piccinini L, Gallo M, Motta F, Radice S, Clementi E. Treatment of motor and behavioural symptoms in three Lesch-Nyhan patients with intrathecal baclofen. *Orphanet J Rare Dis*. 2014;9(1):208. [cited 2019 Sep 16]. <http://ojrd.biomedcentral.com/articles/10.1186/s13023-014-0208-3>.
 75. Goodman EM, Torres RJ, Puig JG, Jinnah HA. Consequences of delayed dental extraction in Lesch-Nyhan disease. *Mov Disord Clin Pract*. 2014;1(3):225–9. [cited 2019 Sep 10]. <http://www.ncbi.nlm.nih.gov/pubmed/25419535>.
 76. Jinnah HA, De Gregorio L, Harris JC, Nyhan WL, O’Neill JP. The spectrum of inherited mutations causing HPRT deficiency: 75 new cases and a review of 196 previously reported cases. *Mutat Res*. 2000;463(3):309–26. [cited 2019 Sep 10]. <http://www.ncbi.nlm.nih.gov/pubmed/11018746>.
 77. Zoref-Shani E, Bromberg Y, Brosh S, Sidi Y, Sperling O. Characterization of the alterations in purine nucleotide metabolism in hypoxanthine-guanine phosphoribosyltransferase-deficient rat neuroma cell line. *J Neurochem*. 2006;61(2):457–63. John Wiley & Sons, Ltd (10.1111). [cited 2019 Sep 2]. <http://doi.wiley.com/10.1111/j.1471-4159.1993.tb02146.x>.
 78. Shirley TL, Lewers JC, Egami K, Majumdar A, Kelly M, Ceballos-Picot I, et al. A human neuronal tissue culture model for Lesch-Nyhan disease. *J Neurochem*. 2007;101(3):841–53. [cited 2015 Jun 14]. <http://www.ncbi.nlm.nih.gov/pubmed/17448149>.
 79. Kang TH, Guibinga G-H, Jinnah HA, Friedmann T. HPRT deficiency coordinately dysregulates canonical Wnt and presenilin-1 signaling: a neurodevelopmental regulatory role for a housekeeping gene? *PLoS One*. 2011;6(1):e16572. Public Library of Science. [cited 2019 Sep 10]. <http://www.ncbi.nlm.nih.gov/pubmed/21305049>.
 80. Ceballos-Picot I, Mockel L, Potier M-C, Dauphinaut L, Shirley TL, Torero-Ibad R, et al. Hypoxanthine-guanine phosphoribosyl transferase regulates early developmental programming of dopamine neurons: implications for Lesch-Nyhan disease pathogenesis. *Hum Mol Genet*. 2009;18(13):2317–27. Oxford University Press. [cited 2019 Sep 10]. <http://www.ncbi.nlm.nih.gov/pubmed/19342420>.
 81. Guibinga G-H, Hrustanovic G, Bouic K, Jinnah HA, Friedmann T. MicroRNA-mediated dysregulation of neural developmental genes in HPRT deficiency: clues for Lesch-Nyhan disease? *Hum Mol Genet*. 2012;21(3):609–22. Oxford University Press. [cited 2019 Sep 10]. <http://www.ncbi.nlm.nih.gov/pubmed/22042773>.
 82. Wade-Martins R, White RE, Kimura H, Cook PR, James MR. Stable correction of a genetic deficiency in human cells by an episome carrying a 115 kb genomic transgene. *Nat Biotechnol*. 2000;18(12):1311–4. [cited 2019 Sep 2]. http://www.nature.com/articles/nbt1200_1311.
 83. Hooper M, Hardy K, Handyside A, Hunter S, Monk M. HPRT-deficient (Lesch–Nyhan) mouse embryos derived from germline colonization by cultured cells. *Nature*. 1987;326(6110):292–5. [cited 2019 Sep 2]. <http://www.ncbi.nlm.nih.gov/pubmed/3821905>.

84. Kuehn MR, Bradley A, Robertson EJ, Evans MJ. A potential animal model for Lesch–Nyhan syndrome through introduction of HPRT mutations into mice. *Nature*. 1987;326(6110):295–8. [cited 2019 Sep 2]. <http://www.ncbi.nlm.nih.gov/pubmed/3029599>.
85. Jinnah HA, Page T, Friedmann T. Brain purines in a genetic mouse model of Lesch–Nyhan disease. *J Neurochem*. 1993;60(6):2036–45.
86. Jinnah HA, Wojcik BE, Hunt M, Narang N, Lee KY, Goldstein M, et al. Dopamine deficiency in a genetic mouse model of Lesch–Nyhan disease. *J Neurosci*. 1994;14(3):1164–75.
87. Finger S, Heavens RP, Sirinathsinghji DJS, Kuehn MR, Dunnett SB. Behavioral and neurochemical evaluation of a transgenic mouse model of Lesch–Nyhan syndrome. *J Neurol Sci*. 1988;86:203–13.
88. Wu C-L, Melton DW. Production of a model for Lesch–Nyhan syndrome in hypoxanthine phosphoribosyltransferase-deficient mice. *Nat Genet*. 1993;3(3):235–40. Nature Publishing Group. [cited 2019 Sep 4]. <http://www.nature.com/articles/ng0393-235>.
89. Edamura K, Sasai H. No self-injurious behavior was found in HPRT-deficient mice treated with 9-ethyladenine. *Pharmacol Biochem Behav*. 1998;61(2):175–9. Elsevier. [cited 2019 Sep 4]. <https://www.sciencedirect.com/science/article/pii/S0091305798000951?via%3Dihub#BIB18>.
90. Engle S, Womer DE, Davies PM, Boivin G, Sahota A, Simmonds HA, et al. HPRT-APRT-deficient mice are not a model for Lesch–Nyhan syndrome. *Hum Mol Genet*. 1996;5(10):1607–10. Narnia. [cited 2019 Sep 4]. <https://academic.oup.com/hmg/article-lookup/doi/10.1093/hmg/5.10.1607>.
91. Ellenbroek B, Youn J. Rodent models in neuroscience research: is it a rat race? *Dis Model Mech*. 2016;9(10):1079–87. Company of Biologists. [cited 2019 Sep 11]. <http://www.ncbi.nlm.nih.gov/pubmed/27736744>.
92. Breese GR, Traylor TD. Developmental characteristics of brain catecholamines and tyrosine hydroxylase in the rat: effects of 6-hydroxydopamine. *Br J Pharmacol*. 1972;44(2):210–22. John Wiley & Sons, Ltd (10.1111). [cited 2019 Sep 10]. <http://doi.wiley.com/10.1111/j.1476-5381.1972.tb07257.x>.
93. Breese GR, Baumeister AA, McCown TJ, Emerick SG, Frye GD, Mueller RA. Neonatal-6-hydroxydopamine treatment: model of susceptibility for self-mutilation in the Lesch–Nyhan syndrome. *Pharmacol Biochem Behav*. 1984;21(3):459–61. Elsevier. [cited 2019 Sep 10]. <https://www.sciencedirect.com.ezaccess.libraries.psu.edu/science/article/pii/S0091305784801100>.
94. Knapp DJ, Breese GR. The use of perinatal 6-hydroxydopamine to produce a rodent model of Lesch–Nyhan disease. In: *Current topics in behavioral neurosciences*; 2016. p. 265–77. [cited 2019 Sep 2]. <http://www.ncbi.nlm.nih.gov/pubmed/27029809>.
95. Meek S, Thomson AJ, Sutherland L, Sharp MGF, Thomson J, Bishop V, et al. Reduced levels of dopamine and altered metabolism in brains of HPRT knock-out rats: a new rodent model of Lesch–Nyhan disease. *Sci Rep*. 2016;6:25592. Nature Publishing Group. [cited 2019 Sep 2]. <http://www.ncbi.nlm.nih.gov/pubmed/27185277>.
96. Visser JE, Harris JC, Barabas G, Edey GE, Jinnah HA. The motor disorder of classic Lesch–Nyhan disease. *Nucleosides Nucleotides Nucleic Acids*. 2004;23(8–9):1161–4. [cited 2019 Sep 10]. <http://www.tandfonline.com/doi/abs/10.1081/NCN-200027432>.
97. Mastrangelo L, Kim J-E, Miyanohara A, Kang TH, Friedmann T. Purinergic signaling in human pluripotent stem cells is regulated by the housekeeping gene encoding hypoxanthine guanine phosphoribosyltransferase. *Proc Natl Acad Sci U S A*. 2012;109(9):3377–82. [cited 2019 Sep 10]. <http://www.pnas.org/cgi/doi/10.1073/pnas.1118067109>.
98. Kang TH, Park Y, Bader JS, Friedmann T. The housekeeping gene hypoxanthine guanine phosphoribosyltransferase (HPRT) regulates multiple developmental and metabolic pathways of murine embryonic stem cell neuronal differentiation. *PLoS One*. 2013;8(10):e74967. Cooney AJ, editor. Public Library of Science. [cited 2019 Sep 10]. <https://dx.plos.org/10.1371/journal.pone.0074967>.
99. Tay W. Symmetrical changes in the region of the yellow spot in each eye of an infant. *Arch Neurol*. 1969;20(1):104–5.
100. Sachs B. Arrested cerebral development with special reference to its cortical pathology. *J Nerv Ment Dis*. 1887;14(9):541–3.
101. Kingdon EC, Russell JS. Infantile cerebral degeneration with symmetrical changes at the macula. *Med Chir Trans*. 1897;80:87–118.5. Royal Society of Medicine Press. [cited 2019 Sep 12]. <http://www.ncbi.nlm.nih.gov/pubmed/20896909>.
102. Fernandes Filho JA, Shapiro BE. Tay–Sachs disease. *JAMA Neurol*. 2004;61(9):1466–8.
103. Maegawa GHB, Stockley T, Tropak M, Banwell B, Blaser S, Kok F, et al. The natural history of juvenile or subacute GM2 gangliosidosis: 21 new cases and literature review of 134 previously reported. *Pediatrics*. 2006;118(5):e1550–62.
104. Ferreira CR, Gahl WA. Lysosomal storage diseases. *Metab Dis Found Clin Manag Genet Pathol*. 2017;2:367–440.
105. Sandhoff K, Andreae U, Jatzkewitz H. Deficient hexosaminidase activity in an exceptional case of Tay–Sachs disease with additional storage of kidney globoside in visceral organs. *Life Sci*. 1968;7(6):283–8.
106. Hadfield MG, Mamunes P, David RB. The Pathology of Sandhoff’s Disease. *J Pathol*. 1977;123(3):137–44.
107. Meikle PJ, Hopwood JJ, Clague AE, Carey WF. Prevalence of lysosomal storage disorders. *J Am Med Assoc*. 1999;281(3):249–54.
108. Fitterer B, Hall P, Antonishyn N, Desikan R, Gelb M, Lehotay D. Incidence and carrier frequency of Sandhoff disease in Saskatchewan determined using

- a novel substrate with detection by tandem mass spectrometry and molecular genetic analysis. *Mol Genet Metab*. 2014;111(3):382–9.
109. Solovyeva VV, Shaimardanova AA, Chulpanova DS, Kitaeva KV, Chakrabarti L, Rizvanov AA. New approaches to Tay-Sachs disease therapy. *Front Physiol*. 2018;9:1–11.
 110. Bley AE, Giannikopoulos OA, Hayden D, Kubilus K, Tiftt CJ, Eichler FS. Natural history of infantile GM2 gangliosidosis. *Pediatrics*. 2011;128(5):1233–41.
 111. Neudorfer O, Pastores GM, Zeng BJ, Gianutsos J, Zaroff CM, Kolodny EH. Late-onset Tay-Sachs disease: phenotypic characterization and genotypic correlation in 21 affected patients. *Genet Med*. 2005;7(2):119–23.
 112. Venugopalan P, Joshi S. Cardiac involvement in infantile Sandhoff disease. *J Paediatr Child Health*. 2002;38(1):98–100. [cited 2019 Sep 16]. <http://www.ncbi.nlm.nih.gov/pubmed/11869411>.
 113. Sakpichaisakul K, Taeranawich P, Nitiapinyasakul A, Sirisopikun T. Identification of Sandhoff disease in a Thai family: clinical and biochemical characterization. *J Med Assoc Thai*. 2010;93(9):1088–92. [cited 2019 Sep 16]. <http://www.ncbi.nlm.nih.gov/pubmed/20873083>.
 114. Lee H-F, Chi C-S, Tsai C-R. Early cardiac involvement in an infantile Sandhoff disease case with novel mutations. *Brain Dev*. 2017;39(2):171–6. [cited 2019 Sep 16]. <http://www.ncbi.nlm.nih.gov/pubmed/27697305>.
 115. Klima H, Tanaka A, Schnabel D, Nakano T, Schröder M, Suzuki K, et al. Characterization of full-length cDNAs and the gene coding for the human GM2 activator protein. *FEBS Lett*. 1991;289(2):260–4.
 116. Cachon-Gonzalez MB, Zaccariotto E, Cox TM. Genetics and therapies for GM2 gangliosidosis. *Curr Gene Ther*. 2018;18(2):68–89. Bentham Science Publishers. [cited 2019 Sep 13]. <http://www.ncbi.nlm.nih.gov/pubmed/29618308>.
 117. Lawson CA, Martin DR. Animal models of GM2 gangliosidosis: utility and limitations. *Appl Clin Genet*. 2016;9:111–20. Dove Press. [cited 2019 Sep 1]. <http://www.ncbi.nlm.nih.gov/pubmed/27499644>.
 118. Phaneuf D, Wakamatsu N, Huang JQ, Borowski A, Peterson AC, Fortunato SR, et al. Dramatically different phenotypes in mouse models of human Tay-Sachs and Sandhoff diseases. *Hum Mol Genet*. 1996;5(1):1–14.
 119. Yamanaka S, Johnson MD, Grinberg A, Westphal H, Crawley JN, Taniike M, et al. Targeted disruption of the Hexa gene results in mice with biochemical and pathologic features of Tay-Sachs disease. *Proc Natl Acad Sci U S A*. 1994;91(21):9975–9.
 120. Sango K, Yamanaka S, Hoffmann A, Okuda Y, Sandhoff K, Suzuki K, et al. Mouse models of Tay-Sachs and neurologic phenotype and. *Nature*. 1995;11(2):170–6.
 121. Taniike M, Yamanaka S, Proia RLL, Langaman C, Bone-Turrentine T, Suzuki K. Neuropathology of mice with targeted disruption of Hexa gene, a model of Tay-Sachs disease. *Acta Neuropathol*. 1995;89(4):296–304. [cited 2019 Sep 12]. <http://www.ncbi.nlm.nih.gov/pubmed/7610760>.
 122. Miklyaeva EI, Dong W, Bureau A, Fattahie R, Xu Y, Su M, et al. Late onset Tay-Sachs disease in mice with targeted disruption of the Hexa gene: behavioral changes and pathology of the central nervous system. *Brain Res*. 2004;1001(1–2):37–50. [cited 2019 Sep 12]. <http://www.ncbi.nlm.nih.gov/pubmed/14972652>.
 123. Yuziuk JA, Bertoni C, Beccari T, Orlacchio A, Wu YY, Li SC, et al. Specificity of mouse GM2 activator protein and beta-N-acetylhexosaminidases A and B. Similarities and differences with their human counterparts in the catabolism of GM2. *J Biol Chem*. 1998;273(1):66–72. [cited 2019 Sep 12]. <http://www.ncbi.nlm.nih.gov/pubmed/9417048>.
 124. Bertoni C, Li YT, Li SC. Catabolism of asialo-GM2 in man and mouse. Specificity of human/mouse chimeric GM2 activator proteins. *J Biol Chem*. 1999;274(40):28612–8. [cited 2019 Sep 12]. <http://www.ncbi.nlm.nih.gov/pubmed/10497228>.
 125. Seyrantepe V, Demir SA, Timur ZK, Von Gerichten J, Marsching C, Erdemli E, et al. Murine Sialidase Neu3 facilitates GM2 degradation and bypass in mouse model of Tay-Sachs disease. *Exp Neurol*. 2018;299(Pt A):26–41. [cited 2019 Sep 12]. <http://www.ncbi.nlm.nih.gov/pubmed/28974375>.
 126. Wada R, Tiftt CJ, Proia RL. Microglial activation precedes acute neurodegeneration in Sandhoff disease and is suppressed by bone marrow transplantation. *Proc Natl Acad Sci U S A*. 2000;97(20):10954–9. [cited 2019 Sep 13]. <http://www.ncbi.nlm.nih.gov/pubmed/11005868>.
 127. Jeyakumar M, Thomas R, Elliot-Smith E, Smith DA, van der Spoel AC, d’Azzo A, et al. Central nervous system inflammation is a hallmark of pathogenesis in mouse models of GM1 and GM2 gangliosidosis. *Brain*. 2003;126(4):974–87. [cited 2019 Sep 13]. <http://www.ncbi.nlm.nih.gov/pubmed/12615653>.
 128. Pelled D, Riebeling C, van Echten-Deckert G, Sandhoff K, Futerman AH. Reduced rates of axonal and dendritic growth in embryonic hippocampal neurones cultured from a mouse model of Sandhoff disease. *Neuropathol Appl Neurobiol*. 2003;29(4):341–9. [cited 2019 Sep 13]. <http://www.ncbi.nlm.nih.gov/pubmed/12887594>.
 129. Ogawa Y, Kaizu K, Yanagi Y, Takada S, Sakuraba H, Oishi K. Abnormal differentiation of Sandhoff disease model mouse-derived multipotent stem cells toward a neural lineage. *PLoS One*. 2017;12(6):e0178978. Kerkis I, editor. <https://dx.plos.org/10.1371/journal.pone.0178978>.
 130. Kuil LEE, López Martí A, Carreras Mascaró A, van den Bosch JC, van den Berg P, van der Linde HC, et al. Hexb enzyme deficiency leads to lysosomal abnormalities in radial glia and microglia in zebrafish brain development. *Glia*. 2019;67(9):1705–18. John Wiley & Sons, Ltd. [cited 2019 Sep 11]. <https://onlinelibrary.wiley.com/doi/abs/10.1002/glia.23641>.

131. Becker CG, Becker T. Adult zebrafish as a model for successful central nervous system regeneration. *Restor Neurol Neurosci*. 2008;26(2–3):71–80.
132. Cork L, Munnell J, Lorenz M, Murphy J, Baker H, Rattazzi M. GM2 ganglioside lysosomal storage disease in cats with beta-hexosaminidase deficiency. *Science*. 1977;196(4293):1014–7. [cited 2019 Sep 13]. <http://www.ncbi.nlm.nih.gov/pubmed/404709>.
133. Kanae Y, Endoh D, Yamato O, Hayashi D, Matsunaga S, Ogawa H, et al. Nonsense mutation of feline β -hexosaminidase β -subunit (HEXB) gene causing Sandhoff disease in a family of Japanese domestic cats. *Res Vet Sci*. 2007;82(1):54–60. [cited 2019 Sep 13]. <http://www.ncbi.nlm.nih.gov/pubmed/16872651>.
134. Kolichski A, Johnson GS, Villani NA, O'Brien DP, Mhlanga-Mutangadura T, Wenger DA, et al. GM2 gangliosidosis in Shiba Inu dogs with an in-frame deletion in *HEXB*. *J Vet Intern Med*. 2017;31(5):1520–6. [cited 2019 Sep 13]. <http://doi.wiley.com/10.1111/jvim.14794>.
135. Martin DR, Krum BK, Varadarajan GS, Hathcock TL, Smith BF, Baker HJ. An inversion of 25 base pairs causes feline GM2 gangliosidosis variant 0. *Exp Neurol*. 2004;187(1):30–7. [cited 2019 Sep 13]. <http://www.ncbi.nlm.nih.gov/pubmed/15081585>.
136. Rahman MM, Chang H-S, Mizukami K, Hossain MA, Yabuki A, Tamura S, et al. A frameshift mutation in the canine HEXB gene in toy poodles with GM2 gangliosidosis variant 0 (Sandhoff disease). *Vet J*. 2012;194(3):412–6. [cited 2019 Sep 13]. <https://linkinghub.elsevier.com/retrieve/pii/S1090023312002237>.
137. Pepinsky RB, Zeng C, Wen D, Rayhorn P, Baker DP, Williams KP, et al. Identification of a palmitic acid-modified form of human Sonic hedgehog. *J Biol Chem*. 1998;273(22):14037–45. http://www.ncbi.nlm.nih.gov/entrez/query.fcgi?cmd=Retrieve&db=PubMed&dopt=Citation&list_uids=9593755.
138. Zeng BJ, Torres PA, Viner TC, Wang ZH, Raghavan SS, Alroy J, et al. Spontaneous appearance of Tay–Sachs disease in an animal model. *Mol Genet Metab*. 2008;95(1–2):59–65. Academic Press. [cited 2019 Sep 13]. <https://www.sciencedirect.com.ezaccess.libraries.psu.edu/science/article/pii/S1096719208001716?via%3Dihub>.
139. Fox J, Li YT, Dawson G, Alleman A, Johnsrude J, Schumacher J, et al. Naturally occurring GM2 gangliosidosis in two Muntjak deer with pathological and biochemical features of human classical Tay–Sachs disease (type B GM2 gangliosidosis). *Acta Neuropathol*. 1999;97(1):57–62. [cited 2019 Sep 13]. <http://link.springer.com/10.1007/s004010050955>.
140. Kosanke SD, Pierce KR, Bay WW. Clinical and biochemical abnormalities in porcine GM2-gangliosidosis. *Vet Pathol*. 1978;15(6):685–99. [cited 2019 Sep 13]. <http://journals.sagepub.com/doi/10.1177/030098587801500601>.
141. Rockwell HE, McCurdy VJ, Eaton SC, Wilson DU, Johnson AK, Randle AN, et al. AAV-mediated gene delivery in a feline model of Sandhoff disease corrects lysosomal storage in the central nervous system. *ASN Neuro*. 2015;7(2):175909141556990. [cited 2019 Sep 13]. <http://journals.sagepub.com/doi/10.1177/1759091415569908>.
142. McCurdy VJ, Rockwell HE, Arthur JR, Bradbury AM, Johnson AK, Randle AN, et al. Widespread correction of central nervous system disease after intracranial gene therapy in a feline model of Sandhoff disease. *Gene Ther*. 2015;22(2):181–9. [cited 2019 Sep 13]. <http://www.nature.com/articles/gt2014108>.
143. Bradbury AM, Cochran JN, McCurdy VJ, Johnson AK, Brunson BL, Gray-Edwards H, et al. Therapeutic response in feline Sandhoff disease despite immunity to intracranial gene therapy. *Moll Ther*. 2013;21(7):1306–15. [cited 2019 Sep 13]. <http://www.ncbi.nlm.nih.gov/pubmed/23689599>.
144. Torres PA, Zeng BJ, Porter BF, Alroy J, Horak F, Horak J, et al. Tay–Sachs disease in Jacob sheep. *Mol Genet Metab*. 2010;101(4):357–63. [cited 2019 Sep 12]. <http://www.ncbi.nlm.nih.gov/pubmed/20817517>.
145. Porter BF, Lewis BC, Edwards JF, Alroy J, Zeng BJ, Torres PA, et al. Pathology of GM2 gangliosidosis in Jacob sheep. *Vet Pathol*. 2011;48(4):807–13.
146. Wessels ME, Holmes JP, Jeffrey M, Jackson M, Mackintosh A, Kolodny EH, et al. GM2 gangliosidosis in British Jacob sheep. *J Comp Pathol*. 2014;150(2–3):253–7. [cited 2019 Sep 13]. <http://www.ncbi.nlm.nih.gov/pubmed/24309906>.
147. Gray-Edwards HL, Randle AN, Maitland SA, Benatti HR, Hubbard SM, Canning PF, et al. Adeno-associated virus gene therapy in a sheep model of Tay–Sachs disease. *Hum Gene Ther*. 2018;29(3):312–26. [cited 2019 Sep 13]. <http://www.ncbi.nlm.nih.gov/pubmed/28922945>.
148. Shi Y, Inoue H, Wu JC, Yamanaka S. Induced pluripotent stem cell technology: a decade of progress. *Nat Rev Drug Discov*. 2017;16(2):115–30. [cited 2019 Sep 16]. <http://www.ncbi.nlm.nih.gov/pubmed/27980341>.
149. Allende ML, Cook EK, Larman BC, Nugent A, Brady JM, Golebiowski D, et al. Cerebral organoids derived from Sandhoff disease-induced pluripotent stem cells exhibit impaired neurodifferentiation. *J Lipid Res*. 2018;59(3):550–63. <http://www.jlr.org/lookup/doi/10.1194/jlr.M081323>.
150. Tu Z, Yang W, Yan S, Guo X, Li X-J. CRISPR/Cas9: a powerful genetic engineering tool for establishing large animal models of neurodegenerative diseases. *Mol Neurodegener*. 2015;10(1):35. *BioMed Central*. [cited 2019 Sep 15]. <http://www.molecularneurodegeneration.com/content/10/1/35>.